

This item was submitted to Loughborough University as a PhD thesis by the author and is made available in the Institutional Repository (<https://dspace.lboro.ac.uk/>) under the following Creative Commons Licence conditions.



For the full text of this licence, please go to:
<http://creativecommons.org/licenses/by-nc-nd/2.5/>

BLL ID NO. - D 468-3/83

LOUGHBOROUGH
UNIVERSITY OF TECHNOLOGY
LIBRARY

AUTHOR/FILING TITLE	
SANDOVER, J	
ACCESSION/COPY NO.	
000771/02	
VOL. NO.	CLASS MARK
	LOAN COPY
- 1 JUL 1994	
13 NOV 1994	27 JUN 1997
13 NOV 1994	26 JUN 1998
28 JUN 1996	

000 0771 02



MEASUREMENT OF THE FREQUENCY RESPONSE
CHARACTERISTICS OF MAN EXPOSED TO VIBRATION

by

Jack Sandover

A Doctoral Thesis submitted in partial fulfilment of the
requirements for the award of Doctor of Philosophy of the
Loughborough University of Technology.

October 1982



by Jack Sandover 1982.

Loughborough University	
of Technology Library	
Date	June 83
Class	
Acc. No.	000771/02

Measurement of the frequency response characteristics of man exposed to vibration

Abstract

Despite much research into human response to whole-body vibration, there exists only a limited basic understanding - insufficient for any reliable prediction of response to a particular vibrational environment. It is argued that a viable explanation of human response to vibration is dependent on an adequate understanding of the complex biomechanical behaviour of the body. Further, knowledge of the degree of linearity of biomechanical frequency response is important if behaviour is to be understood and capable of prediction or application to system design. The aim of the research was to investigate the linearity of response and develop a reliable technique for the investigation of biomechanical response to vibration, the technique being simple and safe to apply to individuals in a variety of postures and eliciting results relevant to practical situations. A further aim was to investigate how far posture might modify the biomechanical behaviour.

A variety of stimuli, response functions and analysis techniques were investigated, and a pilot study used to test their relative values. The method which was developed made use of a random vibration stimulus and linear transfer-function analysis applicable to stochastic signals. The method proved to be very suitable for practical application - a 51 sec. exposure giving reliable results. Data analysis took into account the frequency dependent characteristics of the measurement-chain, from transducer to computer.

It was found that the 'apparent mass' frequency response function gave reliable results, so that for short periods of exposure the human system could be considered linear and time invariant with observed coherence function values in most cases greater than 0.95 between 0.4 Hz and 25 Hz, and 99% confidence limits for response magnitudes of the order of 0.2 dB. Transmission of vibration to the head was also investigated. This was found to be less reliable due to the nodding motion of the head, however, this could be improved by judicious transducer placement on each individual.

Although the response of an individual in a particular situation changed little, changes with posture were observed. Inter-subject variability was high and no general pattern of response allied to posture could be detected. It was considered that an important parameter was the detailed configuration of the lumbar spine, this being very difficult to measure or control.

The simplicity of the technique, the relevance of the apparent mass function to the lumbar spine and the linearity of response at normal vibration levels have important implications. Changes in spinal loading during long periods of exposure can be examined; linear predictions of severity and simple weighting methods are vindicated; tissue characteristics are normally linear and non-linearity can be used as an indicator of damage risk.

INDEX

	page
1. Introduction and aims	1
2. A review of the relevant literature	4
2.1 Human response to whole body vibration.	4
2.2 Previous work on the biodynamic frequency response.	8
2.3 Problems in measurement and interpretation of biodynamic responses.	10
2.4 Modelling biodynamic responses.	14
3. Development of the approach.	18
3.1 Aim.	18
3.2 Choice of method of analysis and type of stimulus.	19
3.3 Choice of measurements.	22
3.4 Choice of vibration level.	27
3.5 Conclusions	29
4. Pilot studies	30
4.1 Aims	30
4.2 Individual studies and results	30
4.2.1 Series 1	30
4.2.2 Series 2	31
4.2.3 Series 3	31
4.2.4 Series 4.	34
4.3 Conclusions.	37
5. The use of a random stimulus for estimation of system transfer functions - theory and computation.	39
5.1 Theory	39
5.1.1 The power spectrum	40
5.1.2 The system transfer function	41
5.1.3 The coherence function	43
5.1.4 Fourier transforms in digital computation	44
5.1.5 Windowing	46
5.1.6 The probability density function.	48

5.2	Errors	49
5.2.1	Data collection and recording	50
5.2.2	Digitisation	50
5.2.3	Data qualification	53
5.2.4	Data analysis	54
5.2.5	Estimated accuracy for this study.	59
5.3	Computation	65
5.3.1	Standard keyboard functions	66
5.3.2	Derived functions	67
5.3.3	Special functions	69
5.3.4	Routine for computations.	73
6.	Experiments to validate the random stimulus technique.	76
6.1	Introduction	76
6.2	General description of the experiments	77
6.3	Equipment	77
6.3.1	The vibration facility	77
6.3.2	Instrumentation	77
6.3.3	Force and acceleration measuring cell	78
6.3.4	Head harness	79
6.3.5	Foot measurement unit	79
6.3.6	Recording system	79
6.4	Subjects	81
6.5	Postures and constraints	81
6.6	Experiment 1	84
6.7	Experiment 2	86
6.8	Experiment 3	86
6.9	Experiment 4.	87
7.	Results of experiments 1 to 4.	89
7.1	Results of experiment 1	89
7.2	Results of experiment 2	90
7.3	Results of experiment 3	91
7.4	Results of experiment 4.	91a
8.	Discussion of results of experiments 1 to 4.	92
8.1	Experiment 1	92
8.2	Experiment 2	94
8.3	Experiment 3	95
8.4	Experiment 4	97

9.	The apparent mass function	100
9.1	The buttocks and thighs	102
9.2	The abdominal tissues	104
9.3	The spine	106
9.4	The pectoral girdle	107
9.5	The head and neck	108
9.6	General considerations	108
9.7	Conclusions	109
10.	The random stimulus technique and its application - general discussion	110
10.1	The measurement technique	110
10.2	Future work	114
10.2.1	Refinement of analysis	115
10.2.2	Non linear techniques	116
10.2.3	Trunk dynamics	117
10.2.4	Adaptation and fatigue.	120
11.	Conclusions.	121
12.	Acknowledgements.	122
13.	References.	123
14.	Figures.	139

Appendices

1. Glossary of symbols.
2. Behaviour of single degree of freedom linear system.
3. Head movements during z vibration.
4. Vibration facility.
5. Equipment specifications.
6. Flutter unit.
7. Anti-aliasing filters.
8. Electrical analogue.
9. Validation data for experiment 4.

1. INTRODUCTION AND AIMS

Serious consideration of human responses to whole body vibration stems from research carried out some four decades ago (Reiher & Meister 1931, Meister 1935, von Békésy 1939, Müller 1939, Coermann 1940). From the outset it was clear that many effects were frequency dependent. It was apparent too that body mechanics had an important influence, and attempts were made to measure the frequency dependent biomechanical characteristics to explain human responses - Dieckmann 1957. Unfortunately attempts to relate subjective responses directly to single measures of biomechanical response proved less than adequate (Coermann 1961) and most research now relates to direct measurements of subjective response or performance change as related to vibration amplitude and frequency.

The vibration receptors are many, non-specific and spread about the body. Conduction of the vibratory stimulus to the receptors is dependent on complex biomechanical pathways, as are the movements of the parts of the body relevant to task performance. Thus, one would expect and does obtain significant individual differences in subjective response and performance - Allen 1971. To understand these responses fully, we need a better understanding of the biomechanical behaviour of the body when exposed to vibration. Osborne 1978 demonstrated markedly different individual patterns of frequency dependent subjective responses and emphasized the need to study the individual (rather than the mean response of a group) if we are to derive a viable theory of human response to vibration. This certainly applies also to biomechanical behaviour.

Thus, it can be argued that further studies of the biomechanical behaviour of man exposed to vibration are warranted on the basis of a need for a better general understanding of individual responses to vibration. However, such work should also be beneficial in terms of the provision of data for optimal attenuation of vibration reaching the body in practical situations, for the design of human analogues or dummies for field testing of isolation systems, and for the prediction of human behaviour in new situations. A better insight into body biomechanics may, in addition, be the only viable means of tackling the problem of quantifying the vibratory environment as a cause of ill health, particularly as applied to situations where the levels of vibration and exposure time vary considerably during the working day.

It is well recognised that the human biomechanical system is extremely complex, involving non-linear tissue characteristics, complex movements and active control of responses. In practical situations, however, the vibratory stimulus may be of a random nature and not at a particularly high level, so that active control may not be so significant and human tissues may (like many mechanical structures under normal loading conditions) exhibit near linear characteristics. If indeed the biomechanical system approximates to a passive linear system, then the scope for linear techniques of prediction and modelling increases and may be of 'sufficient accuracy to describe and interpret our still meagre experimental biological data' (von Gierke 1964). The method developed in this thesis relies upon the use of linear analysis techniques. The evidence in the literature for or against the human biomechanical system being well behaved will be shown to be equivocal. The use of linear techniques, although dependent on system linearity, offers an opportunity to study the bases for human response to vibration that would probably not occur otherwise. It is considered that the rejection of linear techniques on the grounds of supposed system non-linearities, without first investigating the extent of them, would be counter productive.

Bearing in mind the expected variability in behaviour between individuals, it is clear that investigatory methods should allow attention to be paid to the individual and the actual sources of variability. Therefore, there is a need to develop techniques that are simple and quick to apply, yet reliable. It may not be necessary to have a high degree of accuracy, but to investigate variability the accuracy needs to be known and sufficient to detect differences in behaviour. A degree of non-linear behaviour is expected and the use of a vibratory environment far removed from normality is likely to exaggerate such behaviour. The investigatory techniques therefore need to be applicable to vibrations experienced in practical situations.

The aim of the research described here was to develop a reliable technique for the investigation of biomechanical responses to vibration. The technique being simple and safe to apply to a variety of individuals holding a variety of postures whilst carrying out a variety of tasks. Ideally the method would give satisfactory results from short term measurements (so that temporal changes could be recognised and subject exposure minimised) or over a long period of exposure. The technique would be tested by using it to explore some of the obvious non-linearities

resulting from body geometry, to explore the extent of unknown non-linearities under typical vibratory conditions and to investigate some of the postural variables which probably contribute significantly to the observed individual differences in response.

Linearity is usually taken to relate only to geometrical and mechanical properties. However, the dynamic equations of coupled systems can include product terms of variables (as for the model in Appendix 3) or system characteristics may change during measurement as a result of active feedback mechanisms or adaptation. In this thesis such behaviour is also referred to as non-linear.

2. A REVIEW OF THE RELEVANT LITERATURE

2.1 Human response to whole-body vibration

In many vehicles vibration is a significant component of the environment experienced by operators and passengers (see Table 2.1). Very often the individual is seated and unable to realize the potential attenuation properties of the legs. Vibration then has to be absorbed in the upper body with discomfort, reduced performance capacity and poor health as possible consequences - see reviews of Guignard & Guignard 1970, Guignard & King 1972, Frolov & Potemkin 1975.

Although little is known of the role of vibration discomfort as regards choice of mode of transport, vehicle 'ride' clearly concerns transport system designers (see Conference 1975) and numerous research groups have attempted to quantify its frequency-dependent characteristics - Osborne 1976. It is often suggested (although the epidemiological evidence is still not fully convincing) that people subjected to significant levels of vibration as part of their job may be at increased risk of spinal disorders, digestive and cardio-vascular problems - Hasan 1970, Vihko & Hasan 1970, Kohl 1975, Wickstrom 1978, Heide 1979, Pope et al 1980. As regards task performance, vibration can affect visual acuity (Griffin & Lewis 1978) and manual control (Lewis & Griffin 1978), and deterioration in tracking performance as a result of low-level flight buffetting in military aircraft was the stimulus for much of the early research into the effects of vibration on man. Evidence on the effects of whole-body vibration on cognitive performance is inconclusive, but it has been suggested (Poulton 1976) that vibration can act as an arousing stimulus.

Vibration can reach the upper body of the seated person via the seat pan, the seat back, the arms or the legs and the biomechanics of the vibration pathways within the body, together with the location of the relevant receptors, are important as regards human responses.

Compared with (say) the auditory receptor system the mechanical receptor system is diffuse in location and action. The tactile receptors, the proprioceptive system and the pain system probably all offer information on the vibration stimulus. The receptors are located cutaneously and sub-cutaneously; at the muscles and joints; in the utricle, saccule and semi-circular canals; and in the fascia, tendons and

Vertical Vibration ConditionsVertical Vibration Measure-

<u>Device</u>	<u>Activity</u>	<u>*Acceler- ometer Place- ment</u>	<u>ments</u>	
			<u>Peak Fre- quency (Hz)</u>	<u>Acceler- ation at Peak Fre- quency (m/s²)</u>
Train	26.8 m/s	SE	6.00	.884
Light Truck	8.9 m/s, local streets-	SE	3.75	2.166
" "	8.9 m/s, " "	BB	4.25	3.892
" "	22.4 m/s, on highway	SE	6.00	2.532
" "	on dirt	SE	3.75	2.345
" "	on dirt, seated	BB	4.25	7.609
Bus	8.9 m/s, local streets	SE	6.00	3.787
"	8.9 m/s, local streets	BB	4.25	1.709
Jeep	4.5 m/s, on dirt	SE	4.50	6.037
Motorcycle	15.6 m/s, local streets	SE	4.00	.677
Jackhammer	21.7 blows/s, standing	BB	6.00	1.411
"	21.7 blows/s, standing	BB	5.25	1.131
Tractor	6.7 m/s, on dirt	SE	3.75	4.433
Backhoe	2.2 m/s, on dirt	SE	5.50	2.973
"	working with bucket	SE	6.00	3.070
Concrete Truck	unloaded, local streets	SE	7.50	3.678
" "	unloaded, on dirt roads	SE	4.50	1.288
" "	loaded, local streets	SE	6.50	3.617
" "	loaded, on dirt roads	SE	5.25	6.343
Bucket Loader	2.2 m/s, on dirt roads	SE	3.50	25.641
" "	working with bucket	SE	4.00	10.753
Bulldozer	2.2 m/s, on dirt roads	SE	5.00	5.249
"	working with blade	SE	3.75	10.035
Ferry	Captain's deck	SE	6.00	4.227
"	Captain's deck seated	BB	4.25	6.642
"	Captain's deck	ST	4.25	2.051
"	Captain's deck standing	BB	6.00	2.227
"	Engine Room seated	SE	4.75	1.039
"	Engine Room	ST	5.25	1.362
Motorboat	3.1 m/s	SE	5.25	.709
"	8.9 m/s	SE	3.50	1.815
"	13.4 m/s	SE	5.50	1.260
"	13.4 m/s, hitting waves	SE	3.25	1.411

Horizontal Vibration ConditionsHorizontal Vibration
Measurements

Motorcycle	15.6 m/s, local streets	SE	3.50	.994
Jackhammer	21.7 blows/s, standing	BB	4.75	1.002
Ferry	Captain's Deck	SE	5.25	3.022
"	Captain's Deck seated	BB	8.50	11.575
"	Captain's Deck Standing	ST	3.50	3.493
"	Captain's Deck Standing	BB	4.25	10.138
Motorboat	3.1 m/s	SE	4.00	.945
"	8.9 m/s	SE	5.25	1.168
"	13.4 m/s	SE	4.25	.956
"	13.4 m/s, hitting waves	SE	3.50	1.788

*SE = accelerometer placed between seat and buttocks

ST = accelerometer placed between feet and floor

BB = accelerometer placed on bitebar

Table 2.1 Some typical vibration environments (After Pope et al 1980)

connective tissues of the viscera - Corso 1967. However, in addition, each receptor has its own threshold of stimulation and its own dynamic characteristics - Frolov & Potemkin 1975.

Very often, vibrations in the z direction predominate, e.g. Hansson & Kjellberg 1981, and the bulk of laboratory research has used z stimuli. In the case of the seated person subjected to z vibration, the spine and its associated musculature clearly play an important role in the distribution of mechanical forces. A typical configuration of the spine and pelvis for a seated person is illustrated in fig 2.1. The individual vertebrae are free to move in all directions, subject to the constraints of a variety of ligaments and muscles connecting adjacent vertebrae and groups of vertebrae and direct constraint at the two apophyseal joints. The thoracic vertebrae are subject to significant constraint due to rib connections, whilst the lumbar vertebrae are responsible for the considerable mobility of the trunk in flexion and extension. The sacral vertebrae are usually fused together to form the sacrum. The sacrum and innominate bones are joined at the two sacro-iliac joints together with the symphysis pubis with very strong ligaments to form a relatively rigid structure - the pelvis. The lumbar vertebrae usually present a marked lordosis (backward curve) during standing, although this may be reduced to a greater or lesser extent during sitting. The supportive action, during vibration, of the trunk musculature and the intra-abdominal pressure may be significant, but they are not well understood - Sandover 1981. However abdominal muscle activity has certainly been observed to change in a phasic manner with a sinusoidal stimulus - Cursiter & Harding 1974, Dupuis 1969, so that active responses must be considered possible. The viscera, shoulders and arms, and head are significant anatomical structures which probably influence force transmission through the upper body. An idea of their relative masses is given in table 2.2.

	kg (values rounded)	% (values rounded)
Head and neck	6.3	9.0
Both shoulders	7.4	10.6
Thorax (less shoulders)	8.1	11.6
Abdomen and pelvis	19.7	28.1
(Hence, Trunk minus limbs)	(41.5)	(59.3)
Upper extremities	7.0	10.0
Upper legs	13.9	19.8
Lower legs and feet	8.7	12.4
Total	71.1 kg	100.4%

ARMS
29.7
3:1

Table 2.2 Typical weights of body components
(Values after data of Dempster 1955 and Barter 1957)

The variety of sensations elicited by exposure to vibration is illustrated in table 2.3. Magid et al. 1960 (also in Ziegenruecker & Magid 1959) vibrated subjects at levels to the maximum voluntarily tolerated and questioned subjects closely as to the location and type of pain experienced. They found that the following were of major importance in terms of limiting tolerance for very short exposures:

Chest pain (precordial)	5 - 7 Hz
Dyspnea (actual air hunger)	1 - 3 Hz
Abdominal pain (peri-umbilical or lower mid-quadrant)	4.5 - 10 Hz
Testicular pain (groin)	7/10 Hz
Head symptoms (pain and/or congested sensation)	13 - 20 Hz
Anxiety	
General discomfort (summation of all symptoms in terms of discomfort)	4.5 - 9 Hz

Under slightly less severe conditions they recorded:

Speech, pharynx and jaw sensations	6 - 20 Hz
Urges to micturate and defecate	10 - 18 Hz
Muscular effects	13 - 20 Hz
Attempts at muscular control	4.5 - 9 Hz
Valsalva manoeuvre	4.5 - 10 Hz
Lumbosacral pain	8 - 12 Hz
Respiration difficulties	4 - 8 Hz

Subjects experienced a "sensation of displacement of the body and its parts" and the authors explained many of the symptoms by reference to stretching and deformation of body tissues. For instance, abdominal pain was believed to be caused by 'stretching and deformation of the terminal ileum, cecum, hepatic flexure and transverse colon and of their supporting mesenteries'.

Knowledge of the basic structures of the body and the types of pain experienced have lead to a number of simple linear mechanical models to explain the effects of vibration, probably the best known being that of von Gierke 1964 illustrated in fig. 2.2. The actual behaviour is, however, much more complex. For instance, although Krause 1963 and Lange & Coermann 1965 demonstrated relative motion between individual lumbar vertebrae, the data of Christ & Dupius 1966 show that some of the

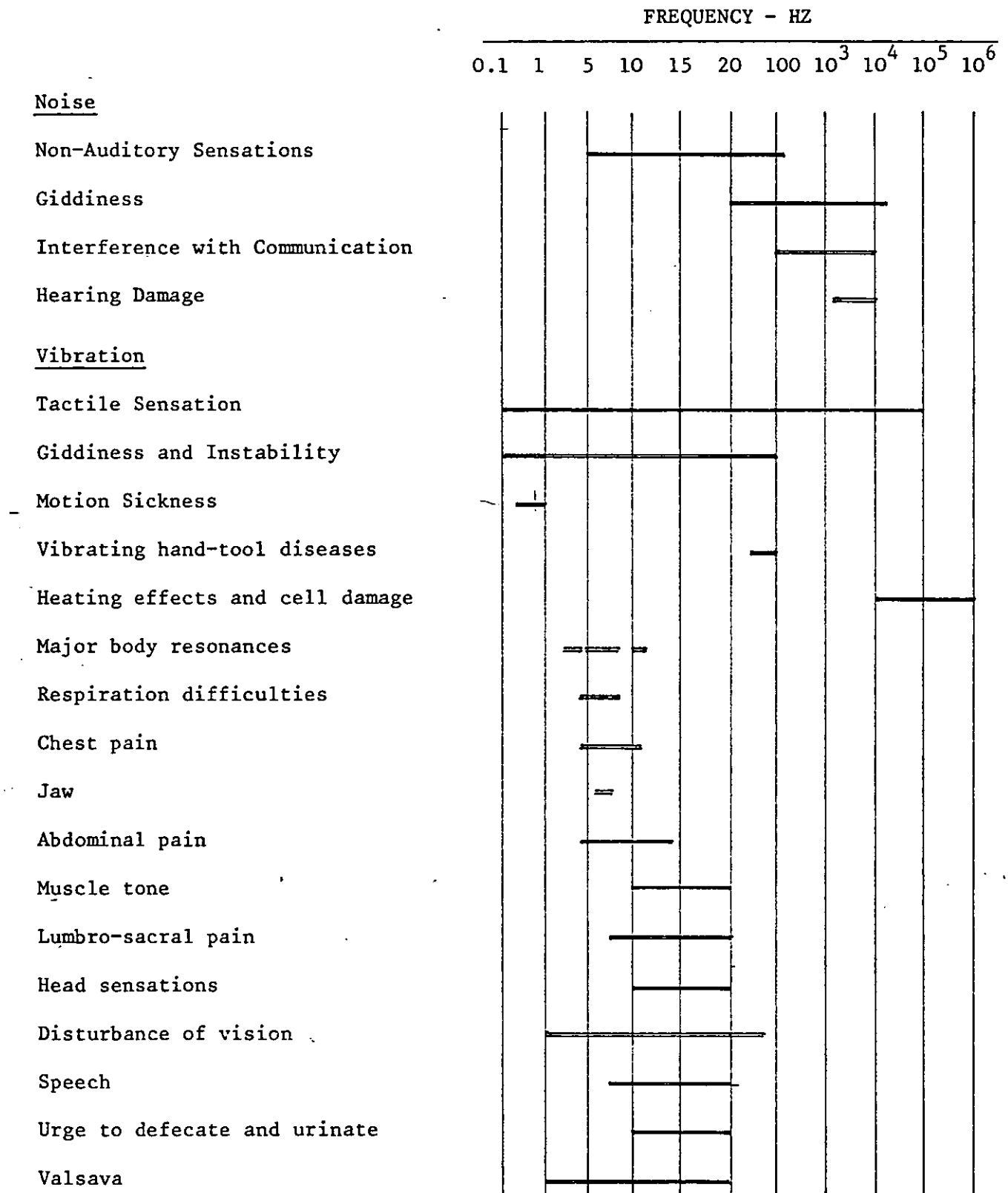


Table 2.3 Vibration sensations observed in the literature
(adapted from Guignard & King, 1972).

relative motion arises from relative angular rotation. There is probably some coupling between motions, so that a stimulus in one direction may lead to the movement of parts of the body in other directions - Dieckman 1958, Barnes & Rance 1974.

Thus, to understand human responses completely, one has to consider movements in three dimensions, expect conscious or unconscious efforts to control the vibration and consider a number of target organs and receptors. However, if the assumptions are recognised, simple conceptual models may lead to a better understanding of human responses to vibration. Complex models face the risk of becoming too mechanistic and ignoring the wide differences between individuals.

Due to the predominance of stimuli in the z direction compared with other directions, a common simplification is to consider only z stimuli. This approach is followed in this thesis. However, vibration stimuli in only one direction still need representation in two dimensions - amplitude and frequency. Reiher & Meister 1931 mapped zones of equal subjective response on a frequency-amplitude graph. Subsequently, the majority of investigators have expressed their results in terms of some form of equal response 'contour' on an acceleration amplitude-frequency graph. The inherent assumption being that the human system is linear and that the contour can be used as a weighting function to apply data from studies with sinusoidal vibration to situations where the stimulus is not purely sinusoidal.

Contours of equal subjective magnitude (often misinterpreted as 'equal comfort contours') typically show differences in shape at different basic intensity levels and increased sensitivity at about 5 Hz (fig. 2.3). The experiments of Magid et al 1960 related to very high vibration intensities and their contour shows a well pronounced area of maximum sensitivity between about 4 Hz and 8 Hz (fig. 2.4). Task performance during vibration is very much task-dependent, and a variety of equal performance contours can be found in the literature. However, increased sensitivity at about 5 Hz is a common feature and "it has generally been found that increases in tracking error due to low frequency, whole body vibration are highly correlated with the transmission of vibration to the shoulder and head" (Lewis & Griffin 1978). This tendency towards increased sensitivity over a small range of frequencies (also shown in table 2.3) coincides with relatively frequent occurrence of low frequency

vibration in vehicles - see table 2.4. The importance of this phenomenon coupled with the possible link with biomechanical behaviour has lead to a number of studies of frequency dependent biomechanical effects during vibration.

2.2 Previous work on the biodynamic frequency response

The dynamic behaviour of any system can be considered in terms of an 'across' frequency response function - where stimulus and response are of the same type (e.g. acceleration) but measured at two points remote from each other, or an 'input' frequency response function - where stimulus and response are measured at the same point but are of different types (e.g. force and acceleration). In the literature one can find examples of the application of both types of approach to human biomechanical responses to vibration. The commonest approach is to measure the transmissibility, where acceleration at the head is compared with the acceleration at the seat (an 'across' function). The usual 'input' function measured is the mechanical impedance - a term coined by von Békésy as the mechanical equivalent of electrical impedance, where the force at the seat is related to the velocity at the seat. Both transmissibility and impedance are essentially complex ratios of response to stimulus, and one can make use of transient stimuli - Macduff 1969, Sandover & Cole 1971, or random stimuli - Pradko 1964, Frolov 1970. However, if stimulus and response are sinusoidal, then the complex ratio can be obtained by simply measuring the amplitude ratio and phase shift between the two sinusoids. If the system is linear then transmissibilities in terms of displacement, velocity or acceleration are identical. If the system is linear and known, then impedance and transmissibility can be related. Early workers such as Muller 1939 and Coermann 1940 had to cope with purpose-built displacement measuring devices to measure transmissibility. They were able to observe resonance phenomena and changes with posture. However, von Békésy 1939 measured whole-body impedance using a piezo-quartz force cell with integral mass cancellation. His technique included the use of Lissajou figures and impedance difference methods to increase sensitivity, and his force cell was sufficiently sensitive to reveal body sway and the ballistocardiogram. Dieckman 1957 measured both transmissibility and impedance, using improved (strain gauge based) instrumentation. Using modelling techniques, Dieckmann developed the 'K value' approach to tolerance criteria. This widely accepted method assumed that tolerance is acceleration-dependent below 5 Hz, velocity-dependent between 5 & 40 Hz,

SOURCE

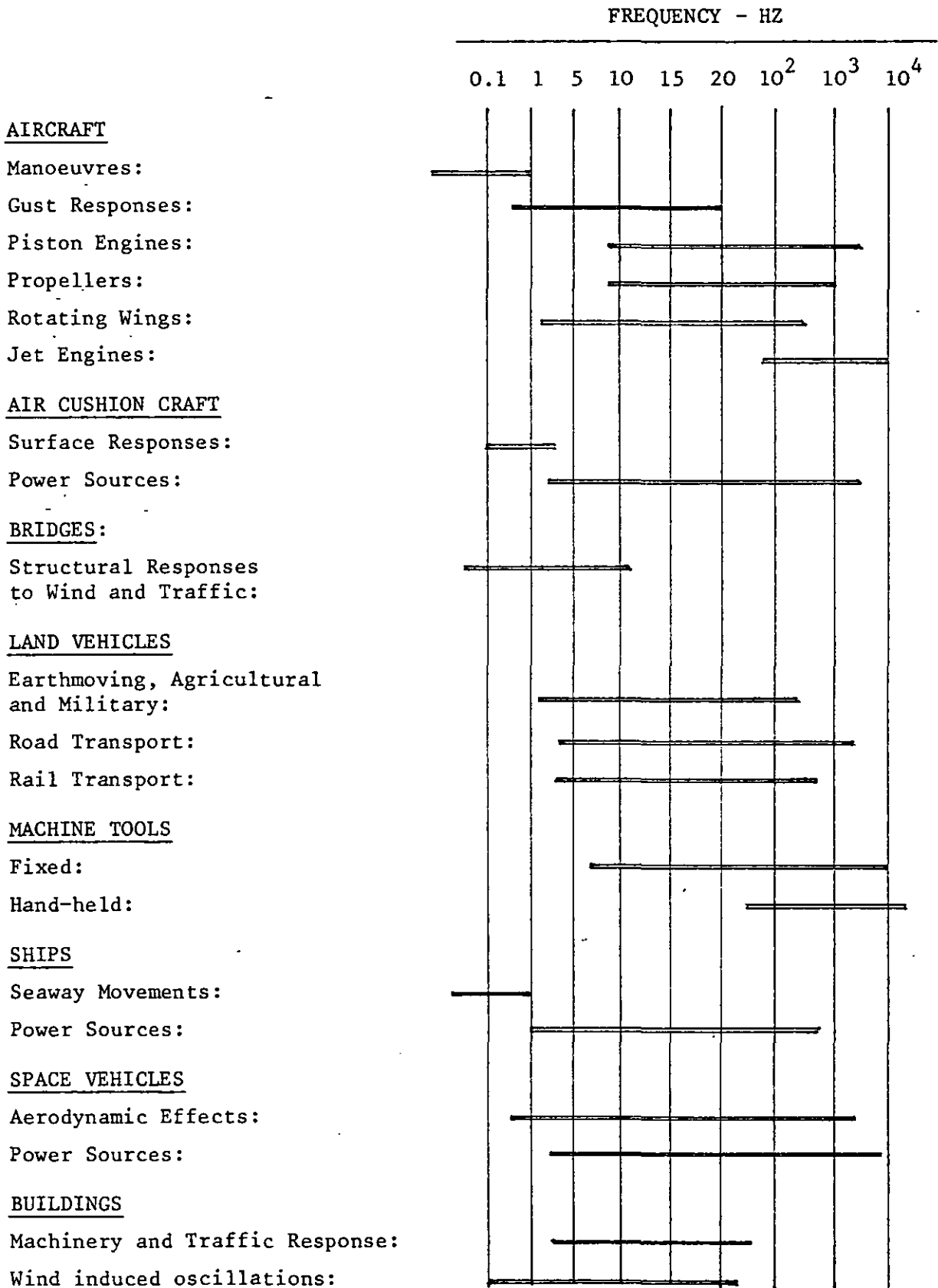


Table 2.4 Approximate frequency ranges of disturbing vibration from various sources (after Guignard & King, 1972).

and displacement-dependent between 40 and 100 Hz. The work of Coermann 1961 (also 1962) can be regarded as the classic in this area. Coermann developed impedance measuring techniques with emphasis on accuracy and theoretical understanding. He measured the mechanical impedance of subjects in different postures and also with various forms of restraint, in an attempt to investigate the influence of the soft tissues of the body. His measures also included transmissibility to different parts of the body. Coermann and his colleagues (Coermann et al 1960) clearly considered body biodynamics as a "first step toward the explanation of the physiologic or pathologic effects" of the mechanical environment. They considered the thorax-abdomen system of importance in regard to human tolerance to vibration, the peak in the impedance curve at 5 Hz being attributed to resonant motion of the mass of the upper torso. Coermann attempted to relate the behaviour of a simple single degree of freedom model (derived from his impedance measurements) to subjective responses. However, the correlation was poor unless a more complex model was assumed. His concept of tolerance being related to the motion of two or three body parts was developed to give a 'composite tolerance' curve relating to spine-abdomen, lumbosacral and head 'tolerance curves' (von Gierke & Coermann 1963). An alternative approach put forward by Pradko (Pradko, Lee & Kaluza 1966, Lee & Pradko 1968) assumed that subjective responses are related to the 'absorbed power' arising from exposure to vibration.

Unfortunately, although a number of authors have measured transmissibility or impedance it is difficult to compare their results. Different methods of measurement and a variety of postures have been used. The problem is exacerbated by the variety of units and graphical presentations used. To alleviate some of these problems the essential experimental details of a number of studies of the physical responses of seated subjects are listed in table 2.5 and the data are reproduced to a common format in figs 2.5 to 2.28. The impedance data have been converted to apparent mass data (see section 3) so that they can be compared more easily with the transmissibility data and the results given in this thesis.

There appears to be less variability between authors for the apparent mass data than for the transmissibility data. This is probably as a result of the inherent difficulties in measuring transmissibility arising from location of the head accelerometer (e.g. Dieckmann 1957 used a hand-held accelerometer) and the effects of posture (figs 2.25 to 2.27).

Table 2.5: Summary of experimental details of transfer function experiments (in chronological order)
T indicates transmissibility
I indicates impedance

Name		Measurement	Stimulus	Subjects	Fig.
V. Bekesy	1939	I	Z,Y sinusoidal 0.5-100 Hz	2S body wt 60 kg sitting and standing	2.5
Muller	1939	Head T	Z sinusoidal 0-20 Hz 0.8 to 16 mm	3S standing and sitting	2.19
Coermann	1940	Head T	Z sinusoidal 15-140 Hz 50 μ	10S sitting and standing	
Dieckman	1957	I, T Head, Hip & Shoulders	Z sinusoidal 1-40 Hz	10S sitting and standing hand-held accelerometer	2.6, 2.20
Latham	1957	Head T	Z sinusoidal 0-20 Hz 4 & 9 mm	Subjects sitting on ejection seat fixed to trolley	2.21
Guignard & Irving	1960	Head, hip, shoulder T	Z sinusoidal 2-15 Hz 2.5 m/s ²	10S sitting on hard seat with sight tube (no back rest) feet fixed. Accel. head harness	2.22
Coermann et al	1960	Soft tissue movement	Z sinusoidal 1-20 Hz	Subjects supine	
Coermann	1961	I, Head T	Z sinusoidal 1-20 Hz up to 5 m/s ²	8S sitting (feet free) standing Accel. head harness	2.7-2.9, 2.23
Weis et al	1963	I	Transient, various directions		
Coermann & Okada	1964	I, Head T	Z sinusoidal 2-13 Hz ± 3 m/s ²	5S reclining chair at different back angles	2.26
Edwards & Lange	1964	I	Z sinusoidal 1-20 Hz 2 to 5 m/s ² peak accel.	2S supine and standing	2.34

Table 2.5 (cont.)

Name	Measurement	Stimulus	Subjects	Fig.
Pradko et al 1966	Head T	Z Random and sinus 1-60 Hz	3S in plywood seat	2.24
Woods 1967	Shoulder & thigh T	Z,Y sinusoidal 1-10 Hz 0.7 to 2.1 m/s ² r.m.s.		
Wittman & Phillips 1969	I	Z transients 60 to 140 m/s ² @ 120 ms	Sitting	2.33
Vogt 1968	I & Head T	Z sinusoidal 5 m/s ² + up to 30 m/s ² Z constant 2-20 Hz	10S, sitting and supine	2.30
Vykukal 1968	I	Z sinusoidal (± 4 m/s ²) + 10 to 40 m/s ² Z constant 2-20 Hz	Semi-supine	2.31
Suggs et al 1969	I	Z sinusoidal 1-10 Hz	11S Natural upright posture feet vibrated	2.15
Frolov 1970	Head T	Z random 3-250 Hz	Sitting upright, knees up, arms up. Changes with time	2.25
Sandover & Cole 1971	I	Z transient	Sitting upright and slumped feet supported	
Rowlands 1972	Head transmissibility	Z,Y sinusoidal with harmonics 1-10 Hz 4 m/s ² r.m.s.	7S in ejector seat, restraints Head harness for accelerometer	
Lawes 1974	I	Z swept sine 3-30 Hz ± 2.5 m/s ²	14S standing, sitting erect and relaxed and at task. feet supported	2.16

Table 2.5 (cont.)

Name		Measurement	Stimulus		Subjects	Fig.
Miwa	1975	I	Z sinusoidal, slow sweep 10 m/s ² (rms?)	3-200 Hz	20S Various sitting postures	2.10-2.14
Griffin	1975	Head T	Z sinusoidal 0.2 to 4 m/s ² r.m.s.	7-75 Hz	Least and most "severe" postures. Bite bar	
Rowlands	1977	Head and Shoulder T	Z transient swept sine ±2 to 4 m/s ²	0-25 Hz	6S sitting in various postures and back rests	2.27
Griffin et al	1978	Head T	Z sinusoidal (and other)	1-100 Hz	Sitting in various postures Dental bite. Feet free	
Mertens	1978	I, Head T	Z sinusoidal (4 m/s ² rms) + 10-40 m/s ² Z constant	2-20 Hz	9S sitting	2.32
Guignard et al	1979	Head T (True Z)	Z sinusoidal	2-32 Hz	Well controlled posture, feet moving. Full head acc. harness	2.28
ISO	1979				Accumulation of values from the literature	2.18
Donati	1980	I, Chest T	Z sinusoidal and random	1.5-10 Hz	15S Tractor seat	2.17

Apparent mass data from studies carried out under similar conditions have been plotted together in fig. 2.29. This shows a nearly flat response at low frequencies, a peak at 4 to 6 Hz, and then a rapid fall off at about 12 dB/octave. The difference between the six sets of data is not a great deal more than the variability expected between subjects (figs 2.7a and 2.11a). The phase angle curves tend to be well behaved with a smooth roll-off from about 2Hz, and a point of inflection (at 45° -phase angle) at about 5Hz. The transmissibility curves also tend to reach a maximum at 4 to 6 Hz. At low frequencies, the body behaves as a pure mass, and any differences in supported weight are evident. Thus the weight of the subject (fig. 2.11) and the weight taken by leg supports (fig 2.13) lead to predictable changes in the apparent mass curve at low frequencies. Type of stimulus, body posture and restraint appear to have an effect, although this is small, and there is no clear pattern.

2.3 Problems in measurement and interpretation of biodynamic response

The objective nature of measurements of transmissibility and mechanical impedance is attractive. However, both the basic approach and the methods that have been used are open to criticism.

A number of extrinsic and intrinsic factors are known to, or can be reasonably expected to influence biodynamic response to vibration:-

Body size, build and weight: Heavy subjects tend to have lower transmissibility values at resonance (Guignard & Irving 1960, Griffin et al 1978). Body weight is the main controlling factor for impedance values at low frequencies ^{where} the body behaves like a pure mass (Coermann 1961).

Sex and age: Some differences (Griffin et al 1978) but these may be related to the above.

Posture: A very erect posture tends to increase transmissibility and impedance, especially at higher frequencies (Coermann 1961, Frolov 1969, 1970, 1973, Griffin et al 1978). Indeed, there is a marked subjective intensity/posture/transmissibility inter relationship (Griffin 1975), and seat back/posture/transmissibility inter relationship (Rowlands 1977). Leg and arm position can have a significant effect on transmissibility (Rowlands 1977, Frolov 1969, 1970, 1973). Posture as regards the low back may be of particular significance, as spinal curvature (Frolov 1969) and the sacroiliac

joint (Pope et al 1980) may be important controlling factors for biomechanical responses to vibration. Definition and control of low back posture is particularly difficult.

Muscle tone: Tensing the muscles of the trunk and legs tends to raise the resonant frequency (of transmissibility) but may reduce the amplitude at resonance (Guignard & Irving 1960), although increased transmissibility has also been observed (Griffin et al 1978). This may appear as a raised impedance at the same resonant frequency on an impedance plot (Edwards & Lange 1964).

Seating, restraints and clothing: These seat-man interface characteristics clearly influence the characteristics of the stimulus perceived by the individual. They have been shown to have a marked effect on transmissibility (Rowlands 1977, Coermann & Okade 1964). In some situations, seat design may not affect impedance strongly (Coermann & Okade 1964). Restriction of normally free movement of soft body tissues may have marked effects (Coermann 1961). Some biomechanical experiments have been carried out with the feet of the seated subject hanging free, others with the feet supported. This clearly influences the gross posture of the subject, and the vibration transmitted to the body via the legs.

The experimental design of some biomechanical studies is rightly criticised as such factors as the above have been disregarded or glossed over. The marked inter-subject variability (much of which may, in reality, be intra-subject variability) that follows from the above has led to grave problems of interpretation.

Most investigators simply consider each frequency in isolation and make use of simple statistics on the transmissibility or impedance values at that frequency - the median, 20th and 80th percentile curves of Coermann 1961 are a typical example. However, the biomechanical frequency response needs to be considered in both amplitude and frequency dimensions. Fig 2.30 illustrates this problem. Five simple systems having identical characteristics apart from their resonant frequencies are represented. If one needs to characterise the system responses, then the above approach would suggest taking the mean value at each frequency. However, the resulting curve suggests much greater damping (taking the mean value is a 'smoothing' operation) than either of the individual systems possess. A more characteristic curve would be simply the central one of the individual curves. Biodynamic modelling tends to encourage a

simplistic approach to experimental data, with some 'average response' being used as the starting point for a model and individual responses being disregarded (and often not published). In this way, the characteristic peaks and troughs of individual responses are lost and an untypical smooth response curve results (Griffin et al 1978). This problem is often exacerbated by the unscientific procedure of extrapolating between measured data points so that a smooth curve results. Rowlands 1977 attempted to overcome such problems by considering only values at the resonance points, Garg & Ross 1976 by shifting the spectrum to make the resonance points coincide.

The practical value of biodynamic measurements is sometimes questioned. Gross whole-body biodynamic measures are unlikely to relate to subjective responses at low vibration levels (where the surface receptors may be the most relevant) and are too simplistic for consideration of the effects of vibration on task performance. To simplify analysis, measurements are often carried out under sinusoidal conditions which may not be representative of the vibration environments to which people are exposed. The investigator in this field has to accept these criticisms. However, he can counter them by pointing out that current biodynamic knowledge and techniques are but the first steps towards explanation of human response to vibration, and without them it will continue to be necessary to take the costly ad-hoc approach to practical problems.

Probably the gravest criticism of transmissibility and impedance techniques relates to the assumption that the human system is linear and passive. The techniques are inherently dependent on the system being linear, as otherwise the system is essentially different at each instant in time as the stimulus varies instantaneously in intensity. If a system is linear over a narrow stimulus intensity band but not over a wider band, then the techniques are acceptable, but of no use in predicting behaviour under different conditions. The experiments of Griffin 1975 indicated that man can adapt his posture to minimise vibration effects, and Allen 1978 used the ocular pursuit reflex as an example of active control up to significant vibration frequencies (3 to 4 Hz).

However, the extent of such adaptation and active control under realistic (e.g. random) vibration conditions is, as yet, unknown - although it may be expected to be less than under sinusoidal conditions.

If the duration of exposure is significant, muscle fatigue (Broderick & von Gierke 1971) may have a significant influence on such behaviour whilst experiments described by Frolov & Potemkin 1975 suggest that man 'detunes' himself over a period of time so that body resonant frequencies move away from the main frequency components of the stimulus.

The experimental evidence as regards linearity in transmissibility and impedance measurements is equivocal. If measurements are obtained under identical conditions apart from the characteristics of the stimulus, then it follows from the theory of superposition that the results should be identical if the system is linear. Bearing in mind all the factors affecting biodynamic responses it is clearly difficult to maintain identical experimental conditions but the literature contains the results of a number of attempts to do this. One possibility is to superimpose a steady acceleration on the vibratory stimulus by simulating changes in the gravitational field on a centrifuge. This method was first attempted by Vogt et al 1968, and subsequently extended by Vyukal 1968, Vogt et al 1973 and Mertens 1978 (Figs. 2.31-2.33). Under the conditions pertaining (static acceleration up to 40 m/s^2) the human system exhibited a clear non-linear behaviour (stiffening with increased static acceleration). If the system is linear, responses obtained during transient stimulation should be identical to those during vibration, and for low intensity transients Sandover & Cole 1974 found this to be so. However, for high intensity transients (i.e. relatively high acceleration levels or long durations) both Sandover & Cole 1974 and Wittmann & Phillips 1969 (Fig. 2.34) found evidence of non-linearity. When less extreme vibration conditions are considered, the evidence is not clear. Krause & Lange 1963, Edwards & Lange 1964 and Lange & Edwards 1970 were able to demonstrate marked differences in the biodynamic responses of supine men as the stimulus vibration changed from '0.2G' to '0.5G' (Fig. 2.35). By considering harmonic generation, Rowlands 1972 found evidence of non-linearity. Rowlands & Maslen 1973 found that doubling the stimulus from 1 to $2 \text{ m/s}^2 \text{ r.m.s.}$ had a slight effect on transmissibility whilst Rowlands 1977 found only small differences in transmissibility between 2 and 4 m/s^2 . From experiments with a random stimulus varying in intensity from 0.35 to 2 'G p-p', Pradko et al 1966 concluded that the human system was sufficiently linear for determination of transfer functions, and Frolov 1969 came to a similar conclusion - although later (Frolov 1973) he considered that non-linear mechanical models were necessary to explain responses if the stimulus amplitude exceeded 0.3 mm. Griffin 1975 found

small but significant differences in transmissibility as the stimulus intensity varied between 0.2 and 4 m/s² r.m.s. However, in another situation (swept sine stimulus) Griffin et al 1978 found the differences to be minimal. The general conclusions of Rowlands 1977 and Griffin et al 1978, that any non-linear effects are minimal compared with inter- and intra- subject variability, are significant here.

As a result of the nodding action of the head a number of problems arise when one attempts to obtain a reliable measure of seat to head transmissibility. These are dealt with in more detail in section 3.3. Rarely have these problems been recognised by investigators and much of the available data must be regarded as suspect, particularly if trunk characteristics are of interest. Impedance techniques, on the other hand, are "precise, and at the same time the most satisfying from a scientific point of view" (Payne 1965). However, the latter are limited in that the impedance of elements remote from the driving point tends to be swamped by the effects of elements nearest to the driving point (Payne 1969). This does not apply, however, if the remote elements are in parallel with the near elements.

Clearly, investigations of transmissibility and impedance should take into account the intervening variables and criticisms discussed above. However, if such factors affect biodynamic responses to any significant degree then it is most likely that they also pertain to subjective reactions, task performance changes, physiological and pathological effects. For instance, Osborne 1978 has highlighted the need to consider individual equal sensation contours rather than the average for a group of subjects.

2.4 Modelling biodynamic responses

A common consequence of a transmissibility or impedance work is to attempt to formulate some form of biodynamic model, and the modelling approach will be used to a small extent in this thesis in attempts to explain some of the variability in response arising from different conditions and subjects. A small number of representative models and some areas of concern are reviewed briefly below.

As well as aiding the interpretation and explanation of experimental findings, models can be useful in explaining physiological and

pathological findings, in predicting responses to force environments not yet experienced and for protection engineering - von Gierke 1964. They should tempt one to ask more intelligent questions - von Gierke 1978. A model may also be a useful format for experimental design, for stating experimental conclusions and for manipulating experimental variables - Mohr 1978. Models may be 'analytic' or 'conceptual' - that is, based on analysis of human responses or on a synthesis of elements related to the known anatomy of the body and available data on tissue characteristics. The modelling process, in practice, usually involves elements of both approaches and the ideal model satisfies both analytic data and the known tissue characteristic and anatomy of the body.

Simple, mass-spring-damper models were used by Latham 1957 and Dieckmann 1958 to explain known human responses to impact and vibration. Since then, many lumped and distributed parameter models, some including non-linearities, have been developed to simulate human responses to impact or vibration - see reviews by Roberts et al 1966, Sandover 1971 and the special publications, Conference 1970, 1977, 1978.

Coermann 1961 developed a two degree of freedom model which matched his impedance data in his attempts to link biomechanical responses to subjective reaction to vibration. Suggs et al 1969 and Tomlinson & Kyle 1971 used, respectively, impedance and seat transmissibility data to generate two degree of freedom models which were translated into mechanical hardware for tractor seat testing. Payne 1970 drew together data from a variety of sources in order to generate a complex, non-linear model to predict human responses to impact. The models mentioned above have related to the z direction only. Payne's model is perhaps typical of attempts to relate to known anatomical information whilst the others were essentially analytic. Probably the best known in this area is that of von Gierke 1964 (Fig. 2.2). Von Gierke attempted to relate experimental data from a variety of studies to the human anatomy. Of particular importance was his attempt to link acoustic, blast and vibration information in one model. Muksian & Nash 1974 and 1976 developed a complex model which (although still restricted to z motion) included non-linearities in elasticity and damping, coulomb friction and ballistocardiographic and diaphragm muscle forces as well as attempting to relate to the anatomy. It is interesting to note that they only found it necessary to introduce non-linearities for responses at greater than 5Hz, whereas Allen 1978

argued that one would expect non-linearities most at frequencies below 5Hz.

In the field of aircraft ejection research, distributed parameter and multidirectional models have been developed to predict the loads imposed on the spine. Vulkan & King 1970 developed a four degree of freedom model which included flexion and compression at the lumbar and cervical regions of the spine. The model was validated by comparison with stresses measured in cadaveric spines during simulated ejection. Orne & Liu 1971, developed a discrete parameter representation of a curved spine using available data on disc characteristics. This model was used to calibrate the importance of bending in the spine, the time history of the impact, and the importance of horizontal force components. Cramer et al 1976, used a continuum model of a curved spine with inertial loading to consider ejection problems.

With increases in available computing power, more complex models can be considered. Begeman et al 1973, and Prasad & King 1974, developed extremely complicated, discrete element models closely related to the anatomy of the spine. These included the facets; the natural curvature of the spine; flexion, extension and head and neck motions; and eccentric loading. The approach was developed further (Belytschko et al 1973, 1976, 1978, Schultz et al 1973, Belytschko & Privitzer 1978a, 1978b) to include all the skeletal components of the trunk and movements in all directions. A number of models are available to predict gross head, trunk and limb movements during impact - Frisch et al 1976.

In contrast, probably the most practically useful model for impact research has been the simplest - the linear, single degree of freedom model used as the basis for the 'Dynamic Response Index'. The approach, developed by Payne, has been used for the assessment of ejection seat acceleration profiles (see Brinkley 1968 and 1969, Brinkley & Shaffer 1971) in terms of the probability that injury might occur.

If a model is to satisfy both the conceptual and the analytic approaches, ideally it should take into account adaptive responses and muscle activity, mechanical coupling between skeletal components and movements in several directions. It should not exclude the possibility of the unexpected - for instance, Huijgens 1977 has shown that transverse standing waves in the spine can explain the observed low frequency

resonances. Analytic validation should include consideration of both magnitude and phase angle (Wittman & Phillips 1969 showed that a non-linear model can be confused with a linear one if phase angle is neglected) although this makes modelling more difficult (see, for example, Schmid 1976). Likewise, both input and through transfer functions should be satisfied if a model is to be acceptable - Vogt et al 1978.

Thus, the modeller is hedged in by a number of points he should take into account, whilst at the same time subject to two severe practical problems - the availability of good experimental, in vivo, data and the cost of operating a complex model. Consequently, shortcomings are all too easy to be found. For instance, the complex model of Muksian & Nash 1974, 1976 is validated only against transmissibility data without consideration of phase. Unfortunately, much of the available data on frequency response is in terms of group means. If the modeller uses such data (and this is usually the case) then very pronounced resonant characteristics are likely to be omitted - Griffin et al 1978. Avoidance of the group mean leads to a need for consideration of methods of scaling so that responses of a range of individuals can be predicted. Although difficult, the scaling processes are not beyond reason - they have been used successfully in the impact field to make use of animal data (e.g. Kaleps et al 1970). An associated factor is knowledge of the contribution of individual components to the overall response. For instance, it would be quite reasonable to accept a rough estimate from a single trial for damping in the intervertebral disc if it were known that considerable variation would lead only to minor changes in seat to head transmissibility.

If a model is to be for general predictive use then it must satisfy the potential users - it needs to be based on appropriate stimuli and response criteria (Allen 1978), it needs to be able to give information on the probability of (say) injury arising in a particular population and it needs to be simple. Those involved in the modelling process need to be aware that it is unlikely that a single 'final' model is attainable but that a whole hierarchy may be needed (von Gierke 1978) and (perhaps most important of all) that a model is only a simplified representation of a system - not the system itself (Mohr 1978).

3. DEVELOPMENT OF THE APPROACH

3.1 Aim

As stated in section 1, the aim was to develop a technique which was reliable; simple and safe to apply; gave satisfactory results with short exposures, yet could be applied to long term exposure; could be applied to systems not completely linear whilst at the same time giving information on the extent of any non-linearity.

Reliability is required to avoid unnecessary repeat exposure of subjects and demands clear, uncorrupted signals, the use of a minimal amount of instrumentation at the experiment and no reliance on human judgement (as is often the case when estimating values from chart records). Accuracy is, of course, also important. However, marked inter- and intra-subject variability is to be expected so that a high level of accuracy is not necessary. More important is a known level of accuracy, significantly better than the variability expected, so that differences can be confidently attributed to situational changes rather than measurement error.

Subject safety demands that the stimulus be at as low a level as possible and well understood, so that risk is minimal. Likewise, the exposure time necessary to give reliable results needs to be minimal. One aim was to investigate changes in response related to postural change. This demands that the time required to obtain a reliable spectrum over the relevant frequency range be sufficiently short that one can be confident that posture has not changed during the measurement. Clearly, posture is likely to be in a continual state of change, but it was considered that with subject instruction posture might not change significantly over a period of about a minute.

The literature indicated that some degree of non-linearity in response was to be expected, although it might not be great. Non-linearities might be related to non-linear material properties of body tissues, the existence of active feed-back mechanisms in postural control or to non-linear geometry of body movements, and ideally the approach should be able to differentiate between these.

3.2 Choice of method of analysis and type of stimulus

Most techniques relate to derivation of the frequency response function and choice of technique relates to available technology rather than the technique itself. Frequency analysis can be carried out simply by analogue or digital filtering, although the response function derived is then only in terms of magnitude. The full frequency response function may be obtained via the Fourier Transform (also Laplace Transform - Kandianis 1971) of the Correlation Function using analogue or digital techniques. The function may also be obtained directly from the Fourier Integral of the time series using analogue or digital techniques (Harris & Crede pp23-32, Sandover & Cole 1971) although the method is very time-consuming. However, the Cooley Tukey Fast Fourier Transform (FFT) coupled with digital computation offers an efficient and relatively fast technique which is now the most used.

One drawback of the frequency response function approach is that it applies only to time-invariant, linear systems. To cope with non-linear systems, one has to make use of more complex approaches such as use of the Wiener series (Marmarelis & Marmarelis 1978), or direct comparison of system input and output signals with those of a non-linear analogue whose characteristics are varied (Yeager et al 1969), although a great deal of information about simple non-linearities can be obtained from simple sinusoidal responses (Broch 1963).

For a system to be linear its output response must be directly proportional to the input stimulus. It then also satisfies the principal of superposition. However, rarely is a practical system truly linear. Although a system may be linear or approximately linear under normal loading conditions, most become non-linear under extreme loading conditions (e.g. elastic beams - Eringen 1952), failure being an obvious case of non-linearity. If system (or signal) noise is present then obviously the system is (or appears to be) non-linear. Thus true linearity is uncommon in practical systems. However, if the non-linearity can be expected to be small and the system properties time invariant, then an acceptable approach might be to use linear techniques in the first instance in order to obtain a linear approximation to the system behaviour and to estimate the degree of non-linearity present.

Simple sinusoidal stimulation and measurement of the input and output sinusoids is a viable method although it is laborious, and as regards phase-angle at high frequencies, not always accurate. Lawes 1974 used a small analogue computer to speed up the analysis when using a sinusoid whose frequency changed slowly. However, a good sinusoidal stimulus (without harmonics) is difficult to obtain on an hydraulic vibrator, and this approach was discarded. The frequency response function approach appeared the most reasonable for the work described here, as it was known that the human system could exhibit near linear behaviour and the method could be applied to a variety of deterministic and stochastic stimuli. In particular, the Fast Fourier Transform (FFT) technique was chosen because of its availability. The FFT had already been applied to physiological systems. French & Holden 1971a & b developed an FFT package for neurophysiological data, and Stein et al 1972 and Mannard & Stein 1973 applied the package to the analysis of motor function using impulse trains as stimuli.

Provided that the time signals begin and end at zero amplitude, the FFT can be applied to a variety of deterministic signals - a pure sinusoid or a periodic signal, a slow swept sine (or quasi steady-state) signal, a transient signal (including the swept-sine transient - see below) or a series of 'warble tones'. The FFT can also be applied to a random stimulus or a real life stimulus. However, in this case the frequency response function obtained is only viable if the signal properties do not change with time. In addition, the resulting function is only an estimate of the true response.

The laborious nature of the sine and slow swept sine techniques has already been mentioned. Another drawback is the possibility of active control of human response to vibration. If active control were to occur, then it would appear likely to be most pronounced when the stimulus is the easily anticipated sinusoid, whereas the vibration encountered in practical situations might not allow much anticipation and active control.

The transient stimulus or impulse offers the advantage of speed - a single transient gives the frequency response over a spectrum of frequencies - and anticipation is less likely (Weis et al 1963). However, Sandover & Cole 1971, 1973 found that anticipation could lead to difficulties in some situations, and the transient needed to be very short and of high intensity if there were to be sufficient power at high

frequencies to give a reliable frequency response function (they developed an ad-hoc criterion of 20dB signal to noise ratio for acceptability at any particular frequency). The latter problem may be overcome by using a 'swept-sine transient' which has equal energy over a range of frequencies. The method was first applied to engineering structures by White 1969 and was used by Rowlands 1977 to measure human vibration transmissibility. The use of a stochastic stimulus to measure human responses is quite feasible. However, only Pradko et al 1966 and Frolov & Potemkin (Potemkin & Frolov 1971, Frolov & Potemkin 1975) have done so, and neither made full use of the frequency response function.

Broch 1975 compared a variety of methods and concluded that whilst sinusoidal and slow-sweep sinusoidal stimuli led to the best dynamic range, the procedure was very slow. The use of a random stimulus reduced the exposure but reduced the dynamic range also. He found that the swept-sine transient required a shorter exposure and gave a better dynamic range than a random stimulus. Rowlands 1977 chose to use the swept-sine transient in preference to a random stimulus for transmissibility studies as the exposure time required for reliable data was much shorter. However, his total exposure time per condition was eventually 70sec whereas it will be shown in section 6 that a 50sec exposure time should be sufficient when using a random stimulus under practical conditions. Rowlands pointed out that although only a sinusoidal stimulus is theoretically compatible with the analysis of non-linear systems, in practice harmonic distortion makes it suspect.

The possibility of some non-linearity occurring is important as regards choice of stimulus. Bendat & Piersol (1971) have shown (pp197) that if the frequency response function technique is applied to a non-linear system, then the result is the best linear approximation to the true response under the specific input conditions. Thus, if linear techniques are to be used, then the stimulus should be as close as possible as that encountered in practice. Frolov & Potemkin 1975 pointed out that strictly speaking there cannot be any purely deterministic processes in practice, although in fact one frequently encounters random, stationary vibration. However, whilst Jones 1979 considered the use of quasi-sinusoidal stimuli suspect, he also criticised a Gaussian vibration as being subjectively featureless because the occasional large bump is not encountered as is the case in real situations. On the other hand, a vibration stimulus which is too bumpy (or at too high a level) could lead

to undue tissue stress and introduce non-linearities not arising in practice. In human vibration work, the use of a practical stimulus has the advantage that subjects would probably use the same adaptive measures as they would use in practice so that the results are more likely to be representative, particularly if changes over long periods of exposure are suspected. In addition, a continuous random stimulus has the advantage that the biomechanical responses of subjects can be measured with the subject carrying out some task. Indeed, the subject need not be aware that biomechanical measurements are being taken. However, if linear analysis techniques are to be used, then the stimulus must be Gaussian and stationary. A useful stimulus for electrical networks is a pseudo random stimulus whose spectral lines coincide with the FFT lines. This leads to rapid elimination of noise in the averaging process, so that exposure time is short. However, the method is less reliable if non-linearities are expected and, moreover, could not be used here as the vibrator system characteristics would inevitably result in a normal random signal by the time it reached the point of measurement.

To summarize. The use of a sinusoidal stimulus leads to long exposures, may over-emphasise active responses and may suffer from harmonic distortion. A swept-sine transient approach reduces subject exposure, and probably avoids active responses. If some non-linearities are suspected then a random stimulus, kept as close as possible to known operational levels and conditions has a distinct advantage. In practice, Griffin et al 1978 and Weis et al 1964 showed that the differences in human frequency response as related to the stimulus used may not be great. The response measured with a random stimulus is theoretically only an estimate of the true response. However, it will be shown that the estimate can be a good one, and the use of random analysis techniques focusses attention on the effects of signal distortion (in terms of stimulus and measurement noise and changes with time) that inevitably arise in practice even when deterministic stimuli are used.

3.3 Choice of measurements

The basic model building block - the simple, single degree of freedom, linear system, fig. 3.1 (overleaf) - is first considered. It is assumed that the system is excited at its base by a known acceleration time function y (velocity v) which leads to an acceleration of the mass m of y_1 , and a force time function at the base of f .

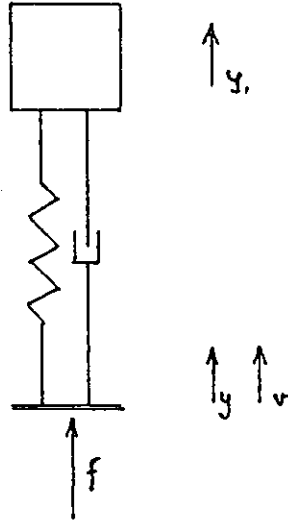


Fig. 3-2. Simple, single degree of Freedom system.

The various frequency response functions are defined in terms of the complex ratios of the response of the system to a stimulus. The complex values at a given frequency ω of the above time functions are denoted as $Y(\omega)$, $V(\omega)$, $Y_1(\omega)$ and $F(\omega)$.

The across frequency response function considered is the transmissibility, given by $\frac{Y_1(\omega)}{Y(\omega)}$.

A number of input, or driving point, frequency response functions are available (Church 1963) although only four are relevant here:

The driving point mechanical impedance, given by $\frac{F(\omega)}{V(\omega)}$

The mechanical mobility, given by $\frac{V(\omega)}{F(\omega)}$

The apparent mass, given by $\frac{F(\omega)}{Y(\omega)}$

A further possibility is the transfer impedance, given by $\frac{F(\omega)}{V_1(\omega)}$

(where $V_1(\omega)$ relates to the velocity of the mass) $V_1(\omega)$

In the case of the simple system, the force at the base is also that which accelerates the mass so that $f = m \cdot y_1$. The complex velocities can be transformed to complex accelerations by dividing by $j\omega$. Thus the frequency response function can be expressed as follows:

$$\text{Transmissibility} = \frac{Y_1(\omega)}{Y(\omega)}$$

$$\text{Mechanical impedance} = \frac{F(\omega)}{V(\omega)} = \frac{m \cdot Y_1(\omega)}{(Y(\omega)/j\omega)} = j\omega m \cdot \left(\frac{Y_1(\omega)}{Y(\omega)} \right)$$

$$\text{Mechanical mobility} = \frac{Y(\omega)}{F(\omega)} = \frac{1}{j\omega m} \cdot \left(\frac{Y(\omega)}{Y_1(\omega)} \right)$$

$$\text{Apparent mass} = \frac{F(\omega)}{Y(\omega)} = m \cdot \left(\frac{Y_1(\omega)}{Y(\omega)} \right)$$

$$\text{Transfer impedance} = \frac{F(\omega)}{V_1(\omega)} = \frac{m \cdot Y_1(\omega)}{(Y_1(\omega)/j\omega)} = j\omega m$$

Thus, for the simple system, the transmissibility and apparent mass spectra are similar, but the impedance and mobility have a $j\omega m$ term in their relationship to transmissibility. The latter is apparent in the characteristic sloping 'mass-line' of impedance curves. The transfer impedance gives no information on the spring and damper characteristics of the system. Weis & Primiano 1964 have shown that for a distributed-mass linear system, the measured impedance can be used to obtain the acceleration of the centre of gravity of the system. Thus, if y_{cg} is this acceleration, then (using the above nomenclature)

$$\frac{Y_{cg}(\omega)}{Y(\omega)} = \frac{\text{Impedance } (\omega)}{j\omega \text{ times mass of body}}$$

In apparent mass terms, this relationship is very simple:

$$\frac{Y_{cg}(\omega)}{Y(\omega)} = \frac{\text{Apparent mass } (\omega)}{\text{Mass of body}}$$

If several simple systems are in series or in parallel, then the sum-total frequency response function can be calculated from the component values as for electrical circuits, although the component systems must be massless for simple calculation in the series situation. The mobility concept has some advantages in this respect, as addition is similar to that for addition of electrical resistances.

Weis et al 1964 have shown that the power transferred during vibration is given by the product of impedance and power spectral density of input velocity. Likewise it may be shown that the power is given by the product of apparent mass and power spectral density of input acceleration divided by $j\omega$.

Thus, the input frequency response functions give information on the energy transfer relationship and forces involved and the general behaviour of the system (in terms of centre of gravity movement and input behaviour). The functions can be applied directly to the design of protection systems - Weis et al 1963. However, input frequency response function measurements can hide the existence of resonances of parts of the body of low mass, remote from the measurement point - Payne & Band 1971, although this is less so if the component systems are in parallel. If a known critical part of the body is to be investigated, then the relevant transmissibility function will give a clearer picture of its behaviour. However, the input frequency response function can give information in the behaviour of body parts where transducers cannot be fitted and may even bring to notice resonances not expected from one's conceptual model of the body.

A number of practical problems arise when one attempts to measure the frequency response functions of the seated human. Three basic measurements are involved: the movement at the input interface, the force at the input interface and the movement of some remote part (usually the head). At the input, the basic problem is definition of the interface. In the normal situation, the person is seated on a flexible cushion surface and the forces vary continuously over the surface. To overcome this problem it is usual to make use of a flat or contoured, rigid ^a set surface and to measure the forces at the seat surface/substrate interface. For input acceleration measurements, it is usually assumed that the pelvis is the main structural component being excited, and accelerometers are fitted to a bar or pad inserted between the ischial tuberosities and the seat surface. For the resulting frequency response function to be relevant, then both stimulus and response need to be in the same direction (usually Z), and this is not easy to control with the acceleration bar or pad in conjunction with a soft cushion.

However, the input measurement problems are minimal compared with those of measurement of head acceleration. If the skull is taken to be

the relevant skeletal structure then the measurement problems relate to transducer fixation and the geometry of head motion. If a transducer is strapped to the head, then the intervening soft tissues mean that the transducer motion may not be representative of skull motion. To alleviate this problem it is usual to strap the transducer to the head as tightly as possible (to the point of giving pain), or to use a bite-bar to obtain nearly direct transducer-skull contact. Most designs of bite-bar are such that muscular forces are used to hold the transducer firmly in position - this gives rise to the possibility that increased action of neck and shoulder muscles, modifies the transmission of vibration to the head. However, Sandover 1974 and Sandover & Soames 1975 have shown that errors arising from lack of knowledge of motion geometry may be much greater than those arising from problems of transducer fixation.

The transfer function is on the basis of input and output being in the same direction (in this case, Z). However, the accelerometer is a direction dependent device with the signal giving no indication of the direction of the measured acceleration as related to (say) the earth's gravitational field. Early workers in this field assumed that the head moved only in the Z direction. However, the data of Dieckmann 1958 and Barnes & Rance 1974 indicate that coupling is involved so that the head moves in more than one direction, even though the input to the body is only in the Z direction. The problem is dealt with in detail in appendix 3. In general there is evidence to suggest that as a result of Z vibration at the seat, the head rotates in the sagittal plane about an axis of rotation somewhere in the region of the occipital condyles. This rotation may be subject to resonance phenomena and lead to a non-linear transfer relationship. This suggests that transducers mounted at some distance from the vertical plane through the occipital condyles (e.g. forward on a dental bite) will give a poorer representation of the Z vibration imposed on the head than transducers mounted close to the plane.

To summarize, the input frequency response functions are of value if energy transfer, protection and general behaviour are of interest, whilst transmissibility is more useful if an understanding of individual body part behaviour is required. Input frequency response function measurements are generally more reliable than transmissibility measurements which must remain questionable until one has a good understanding of the geometry of motion of the head.

The line of biomechanical research being followed related more to low-back stresses and input characteristics (which governs other responses anyhow), and less to head or extremity behaviour. For this reason it was felt that application initially to the input frequency response functions was most relevant. It was considered that transmissibility data might give useful supportive information but could not be relied upon sufficiently for definitive information until the geometric behaviour of the head-neck system was better understood. Choice of the actual input frequency response function offers few problems, as all are based on essentially the same data and it is possible to convert from one to the other. As force and acceleration transducers were to be used the apparent mass function could be obtained with minimal computation. One important factor in favour of the apparent mass function is its direct relationship to the transmissibility function for single degree of freedom systems. In practice, it had been found that the biomechanical response to vibration approximated to such a system so that the apparent mass spectra and transmissibility spectra were similar. This proved to be a great advantage in data interpretation, and the apparent mass function has been used throughout this thesis.

3.4 Choice of vibration level.

Although the use of a random stimulus had many attractions, it was considered that other stimuli should be used in a pilot study to investigate the practicality of the various stimuli and techniques. Also, an important consideration from the outset was to consider the viability of the assumption that human mechanical response to vibration was near linear. To investigate the latter, the responses to a variety of stimuli characteristics and levels were to be compared. It was decided that the stimuli should be at levels to be expected in many transportation systems, with levels in the approximate ratio 1:2:3 being compared.

However, problems arise when deciding on the equivalent levels across a variety of stimuli. For instance, if we wished to obtain transfer functions using a sinusoidal stimulus at different frequencies, one might use stimuli of the same acceleration amplitude at each frequency, or the same displacement amplitude - both approaches appear in the literature. However, feasible alternatives are the same velocity, the same subjective intensity, levels that lead to the same decrement in performance or levels equivalent to those of some practical vibration environment. If non-

linearity is expected to be a problem then it would appear best to use either stimuli that lead to the same stress levels at the body parts which influence the biomechanical response or stimulus levels representative of those met in a range of practical situations. The former is impossible to specify until the body characteristics are understood, but as a first approximation one could assume a simple single degree of freedom model and aim for stimuli giving the same spring compression. In this case the stimulus acceleration amplitude would reduce to minimal at the resonance frequencies and increase ($\text{@ } 12\text{dB/octave}$) at higher frequencies (see Appendix 2, fig. A2.1). Choice of a stimulus representative of field situations is also difficult as measured acceleration spectra (at the man/seat interface) vary considerably. Road vehicles and similar wheeled vehicles often exhibit peaks in the spectrum at frequencies between 1Hz and 15Hz, with a rapid fall off at high frequencies (-6dB/octave to -12dB/octave) - Bonnardel 1975, Boulanger et al 1976, Stikeleather et al. 1972 (one third octave spectra converted approximately to linear frequency spectra by subtracting 3dB/octave). However, they can also exhibit nearly flat spectra (Stikeleather et al.), and other vehicles may have nearly flat spectra (tracked vehicle, excavator - Boulanger), or increasing spectra $\text{@ } +6\text{dB/octave}$ (railway - Bonnardel), or with very rapidly decreasing spectra $\text{@ } -20\text{dB/octave}$ from 3Hz (tractor - Bonnardel). Clearly much depends on the vehicle suspension and track surface. Rao et al. 1975 argued that a 'constant velocity' spectrum is most representative of road surface inputs to vehicles and to simulate this used an acceleration spectrum increasing by 6dB/octave from approx. 0.5Hz to 25Hz. However, to this one needs to add vehicle suspension and seat effects, which together would tend to increase acceleration $\text{@ } 1$ to 3Hz, and reduce them by something of the order of 12dB/octave at higher frequencies, so that the resultant to be expected at the seat is an increase in power spectral density to 1 to 3Hz. with a 6dB/octave decrease at higher frequencies. In general then, to obtain constant stress one should use an increasing spectrum from about 5Hz, whilst to simulate a road vehicle one should use a decreasing spectrum from about 1 to 3Hz., whereas individual spectra between these extremes can be found in practice.

The remaining problem is choice of equivalent levels between stimuli. No information is available on the equivalence of transient stimuli to the others, but some research has been directed towards the relative effects of sinusoidal and random vibration. For the same rms level, a random

stimulus will lead to greater extremes of stress in body tissues and this, together with the fact that one is less likely to be able to anticipate change, would suggest that a random vibration should be subjectively more intense than a sinusoidal vibration of the same rms level. However, this might be offset if a sinusoidal stimulus were to maintain resonances. Some studies of subjective equivalence (Pradko et al. 1966, Dupuis et al. 1971, Donati et al.) tend to support the prediction that random stimuli are subjectively more intense. However, Woods 1967 found random vibration to be subjectively less intense. As regards performance, Weisz et al. 1965 and Shoenberger 1972 considered random and sinusoidal vibration to have similar effects at the same rms level. Over a number of biological measures Bastek et al. 1977 found little real difference between the effects of random and sinusoidal vibration, although there were indications that random vibration might have a greater effect in some situations. Studies where the ISO weighted rms value has been used for comparison (Shoenberger 1978, Griffin 1976) indicate that the weighted rms is a useful measure of the subjective equivalence of sinusoidal and random vibration. This too suggests that man is more sensitive to random vibration on a simple rms basis.

As one might expect, the vibration levels met in practice vary considerably. Bonnardel's review covers a_z rms levels from 0.5 to 4 m/s^2 , whilst the data of Boulanger et al. (3 vehicles) from 0.35 to 1.65 m/s^2 .

Thus, the available information does not direct the researcher to a significant degree. Use of the same acceleration levels at each frequency and comparison by means of simple rms values would seem to be a reasonable compromise, with levels of the order of 1 or 2 m/s^2 being representative of many transport situations.

3.5 Conclusions

Use of a random vibration stimulus coupled with the correct analysis techniques and use of the 'apparent mass' input frequency response function should give best results. However, the other techniques and frequency response functions should also be investigated further. Vibration levels of the order of 1 or 2 m/s^2 rms at all frequencies gives the best compromise stimulus level to compare techniques.

4. PILOT STUDIES

To investigate the viability of the various techniques, a number of pilot studies were carried out. These studies were in essence a continuous development of methods and understanding of subject responses. Instrumentation and analysis were also under development, but they were similar to those described in sections 5 and 6 and only the minimum of detail is given here. The responses given in this section are therefore reasonably accurate, but should be considered as essentially illustrative. Four series of pilot studies are described below, the majority based on the input frequency response function.

4.1 Aims

The primary aims of the pilot studies were to consider further the assumption of linearity, and to compare the various stimuli in terms of ease of use and practical feasibility. In addition, the studies were used to investigate consistency of results (inter and intra-subject variability; changes with time); posture and postural control (at an initial level); the feasibility of transmissibility measurements; and the use of a zero attenuation cushion.

4.2 Individual studies and results

4.2.1 Series 1

Despite considerable experience with sinusoidal and vehicle vibration on the vibrator, and transient stimuli on an ejection simulator (Sandover and Cole 1971), there existed no experience with the presentation of swept-sine transient stimuli, impulses or random stimuli on the vibrator.

To generate a random signal, tape-recordings were made from equipment used at Birmingham University (see Rao et al. 1975). It was found that the vibrator responded satisfactorily and the single subject found the vibration stimulus acceptable.

A combination of two oscillators was used to generate impulses and swept-sine transients. For the former, a single half-sine (displacement) pulse was used. For the latter, a constant amplitude sine-wave, sweeping

from approx. 2Hz. to 20Hz. in 1s. was used. Provided that the vibrator table was already moving, it was found that with a 70kg. load, both table force and acceleration followed the swept-sine signal reasonably well (fig. 4.1).

4.2.2 Series 2

For this trial, one subject (47) was exposed to sinusoidal vibration, swept-sine transient stimuli, impulses and random vibration in succession. The frequency response function for the sinusoidal stimulus was calculated from the time record directly; for the other stimuli FFT analysis was used (10 averages).

The resulting spectra are illustrated in figs. 4.2 to 4.5. It is clear from the figures that the spectra for the swept-sine and random stimuli were similar and not far removed from those from the sinusoidal exposure. Considerable scatter was evident in the spectrum from the impulses.

Inspection of the input and output power spectra showed that the available energy fell off rapidly with increasing frequency for the transient stimuli. Using the simple criterion of Sandover & Cole 1973, that response data are suspect if input or output signal-to-noise-ratio is less than 10dB, all the impulse data at frequencies greater than 5.6Hz were suspect. It was assumed that this accounted for the scatter in this data. On the same basis, the data were suspect for frequencies greater than about 15Hz for the swept-sine stimuli and random stimuli, although only marginally so.

In general it was felt that the problems likely to arise from poor signal to noise ratio when using impulses, together with its clearly artificial nature, were sufficient to justify concentration on the other forms of stimulus in future trials.

4.2.3 Series 3

For this series, three subjects were exposed to swept-sine, sinusoidal and random vibrations. An attempt was made to make the three types of stimuli of similar relative magnitude, and for each stimulus different levels of vibration were used to investigate the linearity of

response. Likewise, the effects of stimuli of different spectral characteristics were considered. The effects of gross postural change were also investigated.

Three subjects of widely different body dimensions (roughly 5th to 95th percentile for stature, and 50th to 95th percentile for body weight) were chosen. Their dimensions are given below:

Subject	Weight (kg)		Height (cm)	
	Standing	Sitting	Standing	Sitting
80	93	79	188	-
76	90	71	179	92
75	69	54	169	88

The subjects were seated on a load cell mounted on the vibrating chair with the back supported by horizontal strips of flexible webbing only. A 'bead cushion' (Bolton 1966) was placed between the subject and load cell to distribute the load. Two postures were used, although posture was controlled only by instruction ("hands in lap, erect but not stiff" or "hands in lap, slumped"). The foot-rest was adjusted to make the upper surfaces of the thighs horizontal.

In an attempt to maintain similar stimulus intensities (see section 3.4) it was intended that the rms levels of the sinusoidal and random acceleration signals be the same, and the peak to peak acceleration amplitude of the sinusoidal and swept-sine signals be the same. The latter was relatively easy to control. However, no equipment was available to measure true rms levels for slowly moving signals. To overcome this, acceleration signals were recorded at slow speed on magnetic tape and later measured at high replay speed in a calibration trial. The final values depended to some extent on subject weight, but were approximately 1, 2 and 3 m/s² rms. These three levels were used to investigate the linearity of response. In addition, two types of random stimulus were used. The power of one (RA) increased slightly with frequency (approx. +2dB/octave on a one third octave basis), the power of the other (RB) decreased slightly with frequency (-2dB/octave).

All the data were analysed using FFT techniques (average of 10 samples). In the case of sinusoidal data, only the spectral frequencies corresponding to the stimulus frequencies were used - although at low

frequencies the energy spread sufficiently to estimate responses at adjacent frequencies. The swept-sine transients proved to have insufficient energy for reliability at frequencies below 2.4Hz.

The resulting spectra are shown in figs. 4.6 to 4.23. All figures are to the scales marked on fig. 4.6.

In general, the results showed no marked differences between the stimuli used. The magnitudes at and below resonance were somewhat higher with the sinusoidal stimulus for subject 76, and for subjects 76 and 80 there were more marked intensity effects for the swept-sine stimulus than for other stimuli. The differences between stimuli were otherwise of the same order as the other differences (e.g. between levels).

As regards linearity, the effects of stimulus intensity were variable. For the sinusoidal stimuli, apparent mass magnitudes generally decreased with increasing intensity at frequencies greater than resonance, otherwise no clear pattern existed. Despite wide variation between intensities, no pattern of change existed for the swept-sine stimuli. However, in the case of the random stimuli, the spectra were generally smoother and although the effects of stimulus intensity were small one could discern a pattern of decreasing 'resonant' frequency with increasing intensity. This was unexpected as it is equivalent to a 'softening spring' non-linearity, whereas a stiffening effect might rather be expected (see section 2). However, over the intensity range 1:3 the change in resonant frequency was only of the order of 1.2:1, which is equivalent to a change in stiffness of the order of 1.5:1. This was not considered sufficient to justify complete rejection of the use of linear techniques, as changes in posture (e.g. one might expect a tendency to slump at high intensity levels) and other effects might have contributed significantly to the differences.

The slumped posture tended to reduce the resonant frequency (for subjects 76 and 80) and increase the apparent damping (figs. 4.17 and 4.11). This was expected.

The lowest intensity random stimulus was found to be quite acceptable and roughly equivalent to normal transportation conditions. It was considered ethical to accept two children for this condition, and their apparent mass spectra are shown in fig. 4.24 along with those of the other

subjects. Unfortunately, the data for the children was unreliable at low frequencies as a result of poor signal-to-noise-ratio. However, an overall similarity between the five spectra was evident, the major difference being clearly related to subject mass.

4.2.4 Series 4

Series 4 related to a number of small trials to test specific problems.

To check the overall accuracy of the various methods, a 70 kg mass was vibrated. The resulting spectra are given in fig. 4.25. The results indicated minimal difference between stimuli apart from sinusoidal vibration (approx. 10% positive bias), and one of the four random signals (approx. 5% negative bias).

Closer inspection of some of the previous data with a swept-sine stimulus showed that below about 2Hz the responses suffered from poor coherence as a result of low signal levels, and an unfortunate carry-through of the oscillatory nature of the input power spectrum to the transfer function. It was recognised that the power of low frequencies could be increased by increasing the time at low frequencies (i.e. a non-linear frequency sweep - see White 1972). However, the exposure time would then be greater and negate the main advantage of swept-sine transients over random stimuli. In the case of random stimuli, it was found that if only a small number of samples (less than 10) were averaged then the resulting spectrum was 'noisy'. However, only 20 samples (exposure time \approx 50s) needed to be averaged to give a satisfactory, smooth response spectrum, and the resulting coherence functions (for apparent mass of subjects) were usually better than 0.9. The input power spectrum was nearly flat with a maximum at about 5Hz and the worst coherence values occurred above 5Hz as the input power dropped with increasing frequency. It was considered that some spectrum shaping would probably improve this situation without increasing exposure time. Two consecutive periods of 50s. were analysed for two subjects holding two postures. The spectra were found to differ by less than 1dB magnitude and 6 degrees phase - well less than the differences between subjects and postures.

It was felt that the realism of the random stimulus, coupled with very promising results as regards reliability gave it a significant advantage over the swept-sine stimulus. The following studies were concerned with practical usage of random stimuli.

As a precursor to possible transmissibility studies, three head accelerometer attachments were investigated (using one subject only) - with the accelerometer fitted to a 'bite-bar', at the crown of the head using a head harness, and at the nape of the neck using elastic webbing. The results from the accelerometer on the crown of the head appeared credible, but the others not. In the case of the accelerometer at the nape of the neck, large phase changes suggested a significant time delay.

Previous experiments had been carried out with the subject seated directly on a hard surface. However, it was recognised that buttock tissues might play a significant role in transmission and some form of cushion was needed to simulate normal conditions. An R.A.E. bead bag (Bolton 1966) had already been used for similar research and its ability to transmit vibration without distortion needed consideration. A fibre-glass moulding (of the same shape as the buttocks of a subject) was loaded with a 70kg mass and fitted with an accelerometer to measure the transfer of acceleration from table to buttock form. The system was excited with a random stimulus (with and without the bead bag). The relative sensitivity of the accelerometers was taken into account in a calibration run by taking readings with the buttock accelerometer fitted on the same metal structure as the table accelerometer. The resulting spectra are shown in fig. 4.26. The coherence values were all close to unity. Clearly, the errors involved were small, and the flexibility of the buttock form introduced as much error as the bead bag. It was considered that the bead bag was a practically useful tool and introduced only minor errors which could be further reduced by calibration with the bead bag in position.

To investigate postural effects and to gain further experience with use of a random stimulus, a number of trials were carried out with one subject (No. 75). In the first trial, only 10 samples were averaged for each posture but the data was calibrated for correct apparent mass. The results are shown in fig. 4.27. Firstly, the subject was tested in a normal posture with and without use of a 'bead bag' cushion. The results showed a marked difference and this was assumed to relate to the load taken by the muscle masses of the buttocks. An attempt was made to

investigate the effects of the buttocks further by asking the subject to tense them in a straining action. Unfortunately, this proved difficult for more than a few seconds, and only two samples could be averaged with consequent loss in reliability. However, the data was sufficient to suggest a marked stiffening effect. Finally, the subjects toes were held firmly to the footrest to change the leg characteristics, and the subject was asked to raise his arms above the head to consider the importance of arm position. The latter changed the apparent mass spectrum significantly. In the second trial 20 samples were averaged for each posture and the results are shown in fig. 4.28. The much smoother spectra resulting from greater averaging are immediately apparent. The subject was asked to hold a normally erect posture (thighs horizontal), then his upper legs were raised by 10 cm at the knee (to change the loading on the under-thigh). During the third run, a 20kg weight was carried on the subject's thighs - the intention being to separate spinal and buttock influences. In the final run, the subject was asked to assume a slumped posture. The similarity between the results of the first four runs suggested that the buttocks and thigh muscles (when relaxed) had little influence (if the simple additive effect of the 20kg is taken into account). Likewise, the effect of the slumped posture was less than anticipated.

The final pilot study related to the exposure of five subjects to random vibration whilst maintaining two simple postures - 'slumped' and 'erect'. The subject details are given below, and the resulting spectra in figs. 4.29 and 4.30.

Subject	Standing Weight (kg)	Standing Height (cm)
02	72	177
47	72	179
75	69	169
76	87	179
77	68	173

The aim in this case was to investigate the practicability of the approach and to gain some insight into inter subject differences. As regards the former, the method proved completely satisfactory - subjects

had no encumbrances such as transducer harness to annoy, and the environmental exposure was short and relevant to past experience. The main differences between subjects only occurred at frequencies up to resonance, and subject weight appeared important - as one would expect. However, apart from the heaviest subject, no clear pattern emerged. The more distinct differences between subjects in the slumped posture were probably due to the subjects' understanding of the posture required. In general, however, one observed lower resonant frequencies and more apparent damping in the slumped posture.

For all the trials in series 4, the coherence function values were of the order of 0.9 or better. In one trial the random vibration input was spectrally shaped to have slightly more energy at high frequencies. The coherence function values in this case were markedly improved, being of the order of 0.95 or better.

4.3 Conclusions

As regards changes in response with stimulus level and characteristic, no clear pattern of effects was apparent. Any differences were of the same order of magnitude as those resulting from small postural changes and might well have been related to the latter. There was certainly insufficient evidence to justify abandoning the use of linear techniques. Coherence function values of 0.9 and more supported the assumption of linearity.

The transient impulse stimulus (and to a lesser extent the swept sine transient) had two important drawbacks. The stimulus appeared artificial to the subject who tended to tense himself prior to the stimulus in preparation. The power available at some frequencies was insufficient for reliable results and spectrum shaping as a solution was not considered attractive as the problems arose mostly at low frequencies. In addition, with the particular vibrator used, some problems arose if the transient was applied when the vibrating table was completely at rest. Due to its similarity to vibrations met in many transport situations, the random stimulus was found to be acceptable and realistic to subjects, particularly at low stimulus intensities. In contradiction to some predictions, reliable results were found possible with quite short exposures (50s) to random vibration.

Trials with a zero attenuation cushion or 'bead bag' showed that it introduced only minor errors up to 25Hz. Trials with subjects suggested that such a cushion was necessary to simulate normal seating conditions. Transmission of vibration to the head could be measured during random vibration, but one could place little confidence in the results, particularly if the head accelerometer was mounted at the mouth or neck.

In general, inter and intra subject variation was not extreme and there existed no obvious pattern of change. At low frequencies, subject mass was an important variable, and for any one subject there was usually a clear difference between two well separated classes of posture ('erect' and slumped). Gross changes in arm position were observed to have a significant effect for the one subject investigated. It appeared that subjects might be able to control their response for short periods of time as consecutive analyses showed little change. It was considered that some of the inter-subject differences might relate to differences in posture, with definition and control of posture a problem.

Thus the pilot studies indicated the use of linear techniques. They also showed that the random stimulus approach could give accurate and reliable data as well as have practical advantages over other techniques. The technique and its application are developed further in the following pages.

5. THE USE OF A RANDOM STIMULUS FOR ESTIMATION OF SYSTEM TRANSFER FUNCTIONS - THEORY AND COMPUTATION

The use of a random stimulus has (almost by definition) a variety of traps for the unwary. Essentially, results are always an estimate of normal behaviour. The accuracy of this estimate is of vital importance and controls data collection and experimental procedures. Computation too can be involved. For this reason, background theory, estimation of accuracy and computational methods are considered in some detail here.

5.1 Theory

The processes involved in dealing with random signals are essentially the application of statistics to time series, although some of the nomenclature may differ.

Thus, the mean μ_x is given by

$$\mu_x = \lim_{T \rightarrow \infty} \frac{1}{T} \int_0^T x(t) \cdot dt \quad (\text{where } x(t) \text{ is a function of time, and } T \text{ is the sample duration}).$$

and the same raw estimate $\hat{\mu}_x$ of the mean is given by

$$\hat{\mu}_x = \frac{1}{T} \int_0^T x(t) \cdot dt$$

The mean square ψ_x^2 is given by

$$\psi_x^2 = \lim_{T \rightarrow \infty} \frac{1}{T} \int_0^T (x(t))^2 \cdot dt$$

and the raw estimate by

$$\hat{\psi}_x^2 = \frac{1}{T} \int_0^T (x(t))^2 \cdot dt$$

The variance σ_x^2 is given by

$$\sigma_x^2 = \lim_{T \rightarrow \infty} \frac{1}{T} \int_0^T (x(t) - \mu_x)^2 \cdot dt$$

and the raw estimate by

$$\hat{\sigma}_x^2 = \frac{1}{T} \int_0^T (x(t) - \hat{\mu}_x)^2 \cdot dt$$

Thus if $\mu_x = 0$, the mean square is equal to the variance σ_x^2 , and the root mean square (r m s) is equal to the standard deviation σ_x .
Also $\sigma_x^2 = \psi_x^2 - \mu_x^2$

It is to be emphasised that the values obtained in practice are estimates of behaviour, the true value only being found when the measurement time is infinite.

The theory of random signal processing is dealt with extensively in the literature, Bendat & Piersol 1971, Otnes & Enochson 1972, Beauchamp 1973, Newlands 1975, Beauchamp & Yuen 1979. Only the bare essentials of those functions required for this investigation are dealt with below. For treatment of the whole area with mathematical rigour, one is referred to Bendat & Piersol.

5.1.1 The Power Spectrum

In signal analysis it is common to work in the frequency domain, and in many respects the basic measure is the 'power spectrum' and in particular the 'power spectral density'. The power spectrum relates to the signal power as observed in the frequency domain, power being considered as the square of the signal amplitude. The observed amplitude or power is dependant on the bandwidth used, and the power spectral density relates to the power normalized to power per unit bandwidth, so that:-

$$\text{Power spectral density (PSD) } G_x(f) = \lim_{\Delta f \rightarrow 0} \frac{\psi_x^2(f, \Delta f)}{\Delta f}$$

(where f is the frequency of interest, and Δf is the bandwidth)

The PSD may also be referred to as the 'Normalized power spectrum', the 'normalized auto spectrum' or the 'auto spectral density'.

$$\text{Thus, } \psi_x^2 = \int_0^\infty G_x(f) \cdot df.$$

(i.e. the total area under the PSD graph extended to $f = \infty$).

On a digital computer, this may be approximated to by trapezoidal integration or integration using Simpson's rule followed by multiplication by the effective filter bandwidth.

It can also be shown that,

$$\psi_x = \left[\int_{0^-}^{0^+} G_x(f) \cdot df \right]^{\frac{1}{2}}$$

i.e. the square root of the Dirac function at $G_x(0)$

Thus in practice ($f \neq 0$) raw estimates \hat{M}_u^2 , $\hat{\Psi}_x^2$ and then \hat{G}_x^2 can be obtained from the PSD estimate.

The 'cross spectral density' $G_{xy}(f)$ is a measure of the relationship between two signals. It can be regarded as the complex product of two signals (in the frequency domain), its dimensions still being those of amplitude squared per unit bandwidth. The cross spectral density is also known as the normalized cross-spectrum.

To differentiate between auto spectra (PSD) and cross-spectra it is common to use the following abbreviations:-

Auto spectra:- $G_{xx}(f)$, $G_{yy}(f)$, $G_{nn}(f)$ etc.

Cross spectra:- $G_{xy}(f)$, $G_{xn}(f)$ etc.

This notation will be used below when clear differentiation between auto and cross-spectra is required, otherwise the simple expression for PSD (e.g. $G_x(f)$) will be used.

5.1.2 The system transfer function

If a linear system is subjected as a forcing function $X(f)$ and the measured response function is $Y(f)$, then the system 'transfer function' (or 'system function' or 'frequency response function') is given by

$$H(f) = \frac{Y(f)}{X(f)}$$

where $H(f)$, $X(f)$, and $Y(f)$ are complex functions at frequency f . (see Harris & Crede 1961 Ch. 23). In the use of a sinusoidal forcing function $X(f)$ and $Y(f)$ are obtained simply from the waveform amplitudes and relative phase angle. For other forcing functions $X(f)$ and $Y(f)$ are given by the relevant Fourier Transforms. Accurate values for $H(f)$ are clearly only obtained at frequencies where $X(f)$ and $Y(f)$ have a significant value.

The transfer function, like any complex frequency function is a three dimensional entity, requiring real, imaginary and frequency axes for complete representation. The Nyquist plot attempts to simulate the three dimensions by taking the projection on the real - imaginary plane and marking the frequency points along the line. The problem of representation may also be overcome by using two plots - in cartesian coordinates by taking the projections on the frequency - real and

frequency - imaginary planes, or by polar coordinates referred to the projection on the real-imaginary plane (phase angle relative to the real axis) and plotting magnitude and phase angle against frequency. The Nyquist plot is in many respects most informative. However, the magnitude/phase approach is most commonly used. So that the data can be compared with other data and for reasons of general understanding, this approach is used in this thesis.

In the case of the random stimulus, the transfer function can be obtained simply by the ratio of the power spectral densities:

$$|H(f)|^2 = \frac{G_y(f)}{G_x(f)}$$

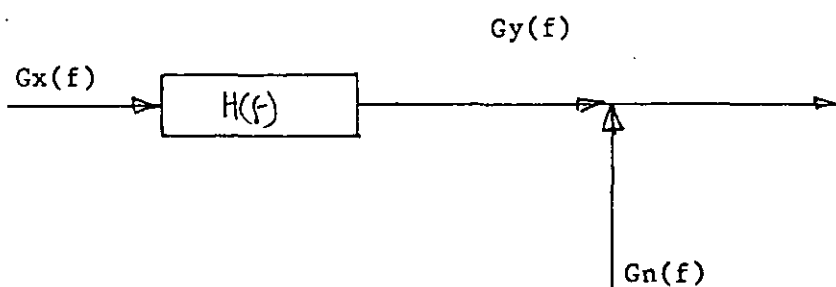
However, this gives only the magnitude information. This may be sufficient when the system gain only is required. However, phase information is vital if the system is to be understood.

An alternative is to take the ratio of the cross-spectrum to input spectrum:

$$H(f) = \frac{G_{xy}(f)}{G_{xx}(f)} \quad \left(= \frac{G_y(f) \cdot G_{xx}(f)}{G_x(f) \cdot G_x(f)} \right)$$

In this case both magnitude and phase information are retained. However, this approach has an important additional advantage in that averaging techniques may be used to make the result less sensitive to random noise in the signal.

Thus, if one considers a system with signal noise $G_n(f)$ superimposed on the output:



It can be shown that $G_{ny}(f) = G_{yy}(f) + G_{nn}(f)$
and $G_{nxy}(f) = G_{xy}(f) + G_{nx}(f)$

so that the first relationship becomes

$$\left| H(f) \right|^2 = \frac{G_{yy}(f)}{G_{xx}(f)} + \frac{G_{nn}(f)}{G_{xx}(f)}$$

(True value) (Effect of noise)

and the latter

$$H(f) = \frac{G_{xy}(f)}{G_{xx}(f)} + \frac{G_{nx}(f)}{G_{xx}(f)}$$

(True value) (Effect of noise)

If multiple averages are taken, then $G_{nn}(f)$ remains constant but $G_{nx}(f) \rightarrow 0$ as n and x are uncorrelated, so that in the latter case the measured $H(f)$ tends to the true value.

5.1.3 The coherence function

In addition, the viability of the transfer function can itself be estimated by the 'coherence function' given by

$$\gamma_{xy}^2(f) = \frac{|G_{xy}(f)|^2}{G_{xx}(f) \cdot G_{yy}(f)}$$

The coherence function can be considered as a measure of causality between output and input. The function is always between zero and unity. If $\gamma^2 = 1$, the output relates completely to the input. If $\gamma^2 = 0$, the output is independent of the input. Thus the coherence function gives an indication of the possible existence of undetected input signals, non-linearities in the system or noise in the measuring system.

It can also be shown that a signal/noise ratio given by

$$\frac{S(f)}{N(f)} = \frac{\gamma_{xy}^2(f)}{1 - \gamma_{xy}^2(f)}$$

is a measure of the fraction of the output signal attributable to the input signal at each frequency.

The coherence function may be regarded as the frequency domain counterpart of the square of the correlation coefficient, whilst the transfer function is analogous to the regression coefficient. The former

relates to degree of causality the latter to the actual relationship - Roth 1971.

5.1.4 Fourier transforms in digital computation

It is possible to obtain auto and cross power spectra by Fourier transformation of the time domain functions auto and cross correlations (e.g. Kandianis 1973). However, the advent of readily available digital computing systems and the fast Fourier transform (see below) has made direct calculation of the spectra a more viable proposition.

The discrete Fourier transform (DFT) is defined by

$$X_k = \frac{1}{N} \sum_{i=0}^{N-1} x_i \cdot e^{(-2\pi j i k/N)}$$

(Beauchamp & Yuen 1979)

Where X_k is the DFT (at the frequency point k) of the time function x_i and $i, k = 0, 1, \dots, N-1$.

Likewise the inverse DFT is given by

$$x_i = \sum_{k=0}^{N-1} X_k \cdot e^{(2\pi j i k/N)}$$

The latter expression is essentially the Fourier series, and this emphasises that the DFT relates to a series of harmonics rather than a continuous spectrum. The continuous Fourier integral (given by

$$X(f) = \int_0^T x(t) \cdot e^{(-2\pi j f t)} dt,$$

a formula subject to some qualifications for mathematical rigour - qualifications met in normal applications) may be obtained on an analogue computer but an excessive number of non-linear elements is required. It is possible to calculate the DFT directly on a digital computer and helpful tables are available (Harris & Crede 1961, Ch 23) but the process is very lengthy (e.g. Sandover & Cole 1971). To overcome the problem of computational load, the fast Fourier transform algorithm (FFT) has been developed - Cooley & Tukey 1965.

The FFT algorithm requires that the 'frame size' N is an integral power of 2, and involves $\frac{\log_2 N}{2N}$ times as many operations as the normal DFT

(Beauchamp & Yuen). Thus if $N = 256$, the calculation time is about $1/64$ of that for the DFT.

The FFT algorithm can operate in both time-frequency and frequency-time directions, taking two N size blocks of real and imaginary time data and replacing them by two N size blocks of real and imaginary frequency data or vice versa. However, the functions are symmetric, so that data for +ve and -ve frequencies are identical. This redundancy is often made use of to save computational time or computer memory. The former has been done by the author in preparation for 'on-line' analysis of human responses with a small general purpose computer. The latter approach is used in the Hewlett Packard computer used for this study. It is described below:

Normal time data (i.e. no imaginary) is held in a block of size N and the FFT replaces the time data by real and imaginary frequency data (no negative frequencies) such that the first point refers to the zero frequency component and this is followed by $N/2$ real and $N/2 - 1$ imaginary frequency data points.

The following then apply:

$$\Delta f = \frac{1}{N \cdot \Delta t} = \frac{1}{T}$$

$$T = N \cdot \Delta t$$

$$F_{\max} = \frac{1}{2} \cdot N \cdot \Delta f$$

where:

$1/\Delta t$ is digitising rate

N is block size (binary number)

T is time to digitise one data block

F_{\max} is highest frequency point

Δf is resolution bandwidth

Excepting for the zero frequency point, the resultant values need multiplication by two to take negative frequencies into account. A further multiplication by $1/\sqrt{2}$ is needed to obtain the rms value, as the spectrum normally relates to the peak value of the component sinusoids.

In terms of rms values then, the true value X_k is $\sqrt{2}$ times the value from the FFT. Dependent on the actual programme used, the returned X_k may or may not already be scaled by $\sqrt{2}$ and by $1/N$.

Assuming previous scaling by $1/N$, the power spectrum is given by $2(X_k)^2$, and the power spectral density by $S_x(k) = \frac{2(X_k)^2}{\Delta f} = 2 T (X_k)^2$

and the mean by

$$\mu^2 = T.(X_0)^2$$

$(X_k)^2$ is in fact usually obtained by conjugate multiplication of X_k by itself:-

$$(X_k)^2 = X_k \cdot X_k^*$$

$$(i.e. X_k \text{ real} + j \cdot X_k \text{ imaginary}) \cdot (X_k \text{ real} - j \cdot X_k \text{ imaginary})$$

Similarly, the cross spectrum is obtained from:-

$$G_{xy}(k) = 2 \cdot T \cdot X_k \cdot Y_k^*$$

To speed computation, the data are usually in "integer" format. To retain some of the accuracy lost thereby, the data are usually scaled so that the maximum value is the maximum integer size available. If the mean value is significant, X_0 can be very large and swamp other data values. In addition, during windowing (see below) side lobes from a significant X_0 component could mask values at other frequencies. Thus a number of problems indicate that the mean value (usually of little importance and often arising as a result of offset or drift in the signal conditioning system) be kept as small as possible in order to maintain accuracy. The accuracy problem is exacerbated by the fact that the power spectra relate to the squares of the time data values.

5.1.5 Windowing

The DFT assumes that the time data series of length N is one period of an harmonic signal. Therefore, a sine wave starting and finishing at zero in the length N is dealt with exactly. However, this is not usually the case and normally some smoothing in the time or frequency domain is required. This is explained in the time domain. If the first or last time data points have a significant value, then the DFT regards them as discontinuities so that high frequency components erroneously appear. This can be overcome by multiplying the time data block by a 'window' function so that early and late data points change slowly from zero to their actual values. In fact, the process is one of convolution. The data is convolved with the window. In the first case (with no apparent window) the window is a rectangular function and this leads to excessive

side lobes about the actual values in the frequency domain, whilst well designed windows reduce this effect. The windowing process is very important in most cases of digital frequency analysis, and is discussed extensively in the literature already referred to. A variety of window functions have been designed. However, the general conclusion one obtains from the literature is that for normal signal analysis, the exact function to be chosen is not vital as long as the rectangular function is avoided, although there is usually a trade-off between frequency resolution and amplitude accuracy (with the common Hanning window having good resolution and possible errors in amplitude of 0 to -1.5dB). Two commonly used functions are the Hanning and cosine taper functions described below.

The Hanning window is essentially a cosine bell given by

$$x = 0 \text{ for } t < 0, t > T$$

$$x = \frac{1}{2} \left(1 - \cos \frac{2\pi t}{T} \right) \text{ for } 0 \leq t \leq T$$

The cosine taper window may be regarded as a Hanning function applied to the first and last tenths of the window, so that

$$x = \frac{1}{2} \left(1 - \cos \frac{2\pi t}{T} \right) \quad 0 \leq t \leq \frac{T}{10}$$

$$x = \frac{1}{2} \left(1 + \cos \left[\frac{10\pi}{T} \left(t - \frac{9T}{10} \right) \right] \right) \quad \frac{9}{10}T \leq t \leq T$$

$$x = 1 \quad \frac{T}{10} < t < \frac{9}{10}T$$

$$x = 0 \quad t < 0, t > T$$

The windows (especially the Hanning, whose 'area' is half the rectangular window) attenuate the data, and a correction factor needs to be applied if the absolute value of the PSD is required. Clearly, the true correction depends on the relative amount of energy in the parts of the time block attenuated. However, it is usual to assume constant distribution of energy over the block, so that simple integration of the area under the window is sufficient. Thus for the Hanning window the correction factor based on power is given by:

$$T \div \int_0^T \left[\frac{1}{2} \left(1 - \cos \frac{2\pi t}{T} \right) \right]^2 dt \quad \text{i.e.} \quad 8/3 \quad (\sqrt{8/3} \text{ for rms})$$

Similarly the correction factor for the PSD obtained with a cosine taper window is $40/35 (\sqrt{40/35} \text{ for rms})$

For the work reported here, the simple Hanning function was used. Fig. 5.1 shows the smoother transfer function obtained with the Hanning window.

Windowing can, in fact, be carried out in the frequency domain. The Hanning function is particularly useful in this respect, as it is equivalent to the following algorithm.

$$\hat{G}(k) \text{ smoothed} = \frac{1}{4} |X_{k-1}|^2 + \frac{1}{2} |X_k|^2 + \frac{1}{4} |X_{k+1}|^2$$

The usual approach is to window in the time domain, but recently Beauchamp & Yuen have argued that frequency domain windowing has a number of advantages. It is also worth pointing out that in the time domain the window has to operate on each time sample of those averaged. In the frequency domain, the averaged sample only needs operation. Considerable computation savings may therefore arise.

Windowing also increases the effective bandwidth to be used for error estimation purposes. The effective bandwidth for the Hanning window is 1.3 times that of the rectangular window (Beauchamp & Yuen).

5.1.6 The probability density function

The probability density function (PDF) is used to establish a probabilistic description of the instantaneous values of the time function. However, it is also a useful tool for the detection of non-linearities (e.g. signal clipping) and the presence of harmonic data. During digital analysis, it is relatively easy to obtain a histogram of the number of data points within a certain amplitude class interval. For instance, in FORTRAN the following algorithm is sufficient:

```
DO 99 J = 1,N
  IDATA = DATA(J)/SCALE + OFST
  IHIST(IDATA) = IHIST(IDATA)+1
99 CONTINUE
```

where SCALE is the ratio of the A/D range to the number of class intervals of the histogram stored in IHIST; OFST is used to make all values positive; and N is the size of the time data block DATA. The simple histogram counts are scaled by $\frac{1}{Nw}$ (where w is the class interval dimension, and N is the total count) to give an estimate of the probability density function $\hat{p}(x)$. To compare with other data it is usual to work in terms of the 'standardised variable' $z = \frac{(x - \mu_x)}{\sigma_x}$. The values of μ_x and σ_x can be obtained directly from the PDF from

$$\mu_x = \int_{-\infty}^{\infty} x \cdot p(x) \cdot dx$$

$$\text{and } \psi_x^2 = \int_{-\infty}^{\infty} x^2 \cdot p(x) \cdot dx$$

Assuming $\mu_x=0$, the histogram amplitude dimensions (i.e. along the horizontal axis) are divided by σ_x , and the PDF values multiplied by σ_x . The resultant standardised variable PDF can then be compared directly with the Normal Distribution given by

$$p(z) = \frac{1}{\sqrt{2\pi}} \cdot e^{-\frac{z^2}{2}}$$

5.2 Errors

When considering errors of measurement, it is useful to differentiate between 'random' and 'systematic' errors. Systematic errors are those inherent in the measurement due to some 'flaw' (Cromer 1974) in the measuring system, whilst random errors are those related to the variability between repeated measurements. Random errors, being both positive and negative, will tend to cancel out if sufficient measurements are made, whilst systematic errors remain. Systematic errors are difficult to detect or eliminate, and must be minimised as far as possible by care in measurement and the use of calibration as close as possible to the data source.

The use of a random stimulus by definition introduces random errors. Estimation of these and other errors is of great importance in the design of the most effective data analysis procedure. Bendat & Piersol offer a wealth of advice for the analysis of random signals using digital computer techniques. They point out a number of steps in the process - data

collection and recording, digitisation, data qualification, and data analysis, and these are dealt with separately below.

5.2.1 Data Collection and Recording

The transducer and signal amplifier systems can lead to non-linearity together with gain and phase errors which vary with frequency. Fortunately, these errors tend to be small with the stiff cell and piezo-electric transducers used (see section 6). However, it is unwise to rely on transducer specifications, and the calibration technique described in section 5.3 was developed to minimize systematic errors in the measuring system. By measuring the transfer characteristics of a known system, it was possible to offset gain and phase differences between channels. The technique made it possible to do this to differing degrees at different frequencies if necessary. Piezo-electric transducer systems usually have good linearity and no attempt was made to evaluate non-linearities in dynamic measurements with different signal levels. However, the calibration was carried out at or near the range of interest (e.g. the use of 70 kg mass i.e. at the upper end of the expected range of sitting weights, for calibration) so that such non-linearity would be minimised.

The errors and their treatment described above also apply to the tape-recording system. However, the magnetic tape-recorder also introduces temporal changes between channels (skew), temporal changes due to variations in tape-speed and as a frequency modulation system is used, amplitude variations due to changes in tape-speed. To overcome these, as well as the use of flutter compensation (Appendix 6), force and acceleration signals were recorded on tape-recorder channels close to each other (e.g. channels 2 and 3 with channel 4 shunted for flutter compensation) to minimise the temporal effects of skew and speed variations. In the event, the specification for tape-recorder speed control was better than that of the oscillator used for the ^{digitising} square wave. However, both were more than adequate at 0.15% and 0.2% respectively, and the calibration method would minimize any systematic differences between channels.

5.2.2 Digitisation

Although the use of the discrete Fourier transform and a digital computer is necessary to make work of this nature a feasible proposition,

the digitisation of the analogue signal can introduce grave errors if procedures are lax. Although others occur, the main sources of error are known as quantisation, interpolation and aliasing errors.

Quantisation error (or quantisation noise) is introduced in the digitising process due to the rounding off of the sampled value to the nearest digital level (see fig. 5.2). The effect is similar to the introduction of noise to the signal and is dependent on the number of bits available in the analogue to digital conversion process.

It can be shown (Beauchamp 1973) that the rms level of this 'quantisation noise' is equal to $\frac{1}{\sqrt{12}}$ times the difference between levels used in the digitisation process. The machine used for this study had a 10 bit analogue to digital converter so that the number of levels was 1024. The quantisation noise therefore was $\frac{1}{1024\sqrt{12}}$ times the input voltage range. That is, the voltage range : rms quantisation noise ratio was 71 dB. For a sinusoidal signal therefore, the signal rms : noise rms ratio would be $71 \text{ dB} - 20 \log_{10} (2\sqrt{2}) = 62 \text{ dB}$, and for a random signal of crest factor 3, the signal rms : noise rms ratio would be 55 dB.

Interpolation errors arise from the time taken to sample the analogue signal, and can lead to phase and ratio errors between channels. Although the recorded square wave could have been used to minimise interpolation problems by sequential digitisation of force and acceleration, this would have led to gross increases in digitisation and computation time. For the machine used, there was a $13 \mu\text{s}$ time lag between sampling the two channels. This represents $\frac{1}{770}$ of the time between samples used ($\Delta t = 0.01\text{s}$), and was considered small enough to be neglected.

Probably the most significant source of digitising error is the appearance of high frequency components at lower frequencies - known as aliasing. The sampling theorem of communication theory states that "a function whose Fourier Transform $X(f)$ is zero for all frequencies f greater than some frequency w is uniquely described by its values at uniformly spaced instants t units apart, when $t \leq \frac{1}{2w}$ ". However, the sampling process introduces replicas of the original spectrum centred on harmonics of the sampling frequency $\frac{1}{t}$ as illustrated in fig. 5.3. Thus, the spectrum is 'folded back' on itself at a frequency of $\frac{1}{2t}$, known as the Nyquist or folding frequency. If w and $\frac{1}{2t}$ are not well separated,

then errors (aliasing errors) are introduced. In effect it is no longer possible to recover the original signal.

Aliasing errors can be reduced by increasing the sampling rate $\frac{1}{T}$ or low-pass filtering the signal. An often misused rule of thumb is that the sampling rate should be twice the highest frequency of interest; this assumes no energy at higher frequencies, and can lead to errors if the signal is noisy. To specify a data processing system fully, one has to take into account the expected signal spectrum and signal to noise ratio together with the frequency range to be investigated, and balance filter characteristics against digitising rate. Under the assumption of a signal to noise ratio of 60dB and a level signal spectrum, the derivation of suitable parameters is illustrated in fig. 5.4. Stacy & Waxman 1965 put this relationship in graphical form, as shown in fig. 5.5. By choosing high digitising rates one, in effect, wastes a quantity of data and this has to be balanced against the cost of filters having high cut-off rates. A reasonable balance was achieved by construction of a simple pair of filters with a 36 dB/octave cut-off, and rejection of data at frequencies above half the Nyquist frequency.

Pilot studies and the literature search indicated that the human response function fell off rapidly above 10 Hz, and it was considered that it would be sufficient to analyse only up to 25 Hz.

The measured -60 dB point of the filters was in fact ≈ 80 Hz, so that a Nyquist frequency of 50 Hz would only allow the use of data to 20 Hz. However, due to the characteristics of the vibrator and the human response, both force and acceleration signals were not at constant level but fell off rapidly at higher frequencies so that data analysis up to 25 Hz only required a Nyquist frequency of about 50 Hz.

Of course, the use of filters introduces significant gain and phase errors. However, the filters were designed to have near linear phase characteristics and were matched as far as possible (see Appendix 7). In addition to this, the calibration method included the filters, so that any gain and phase errors and mismatch had minimal effect.

5.2.3 Data Qualification

The basic theory used only applies to stationary, ergodic, random processes. Unfortunately, it is not easy to check that real data satisfy this condition. Bendat & Piersol suggest that it is most important that the data be stationary, normal, and exhibit no periodicities.

If the physical characteristics of the system producing the signals to be analysed can be expected to be time invariant, then it is reasonably safe to assume that the signal is stationary. A simple test, however, is to compute mean square values and test for trends using the 'run test' (Bendat & Piersol, pp 235). In this case, the original random signal was generated by a pseudo random binary sequence and consequently low pass filtered at several stages - at the signal generator, at the vibrator signal conditioning unit, and effectively at the electro-hydraulic vibrator itself (see section 6). A relatively well behaved signal was therefore to be expected. As part of the computation procedure, mean square values could be calculated for each of the 20 samples averaged in a measurement. This procedure was followed for a number of measurements chosen at random. The run test for a series of 20 values demands that there be between 6 and 15 'runs' above and below the mean value in sequence along the 20 values if the signal is to be considered stationary at the 0.05 confidence level. For the measurements chosen at random the number of runs were 11, 8, 8, 8, 12, 10, 8, 9, 9, 9 for the input (acceleration) signal and 10, 8, 10, 10, 11, 10, 14, 5, 10, 12 for the output (force) signal.

Bendat & Piersol consider that significant periodicities can be observed in the power spectrum (if the resolution bandwidth is small), or in the amplitude probability density function, whilst the data can only be tested for normality by considering the amplitude probability density function.

A visual check for periodicities and normality was made possible by plotting the probability density function together with a normal distribution for each measurement. These visual checks showed that the system was reasonably well behaved for the whole body transfer functions, but less so for the measurements at the feet.

In general, it was considered that assumptions of stationarity, randomness and normality were reasonable, and random theory could be applied.

5.2.4 Data Analysis

A number of statistical errors arise in the analysis of random data. The problem is dealt with fully in Bendat & Piersol (ch. 6), and summarised below.

The mean square error of an estimate of a function consists of a term related to the systematic errors involved ('bias error' squared), together with a term related to the random errors arising ('random error' squared or 'variance'). In general, one attempts to reduce bias errors as far as possible in the design of the experiment and choice of frequency resolution, and then one balances the need for reasonable record lengths against the predicted random errors (which increase with decreasing record length).

Estimates of the frequency response function are dependent on estimates of power spectra. A-priori choice of analysis parameters can be made to reduce errors in these spectral estimates to required levels, particularly if (as in this case) knowledge of the expected response function exists. Better estimates of the errors in the frequency response function are possible a-posteriori.

Bias errors

Bendat & Piersol list five possible sources of bias error:

- a) Bias inherent in the estimation procedure - usually insignificant compared with random errors.
- b) Bias arising from non-linear or time varying processes. Perhaps the most obvious possible source in experiments with people, and already discussed. However, it does again emphasize the need to keep sample lengths short.

c) Other correlated inputs which affect the output. This possibility arises if one considers inputs from the foot rest, arm rests and back rest. For this reason, inputs from the arm rests and back rests were eliminated. It was considered that elimination of input from the feet was not desirable, rather that this input should be itself considered in some detail.

d) Bias in the spectral estimates used. (Dealt with below).

e) Measurement noise at the input, that is, noise which does not pass through the system being studied (dealt with below).

Bias in the spectral estimates used:

This is primarily related to the resolution bandwidth Δf and the double differential of the spectrum at the frequency of interest. In the case of a second order system of natural frequency f_0 with excitation of relatively smooth spectrum, the effects of filter bandwidth have been investigated by Forlifer (1964). Bearing in mind the results of the pilot study, and human responses given in the literature, it is not unreasonable, for the purposes of bias error calculation, to make the assumption of second order system responses. Bendat & Piersol used Forlifer's approach to obtain fig. 5.6. For small values of damping ratio ζ , the half-power point bandwidth Δr is approximately equal to $2\zeta f_0$.

The envisaged values for the human system under consideration were (from the pilot study) $\zeta \simeq 0.25$ and $f_0 \simeq 5$ Hz so that $\Delta r \simeq 2.5$ Hz. The relationship $\Delta r = 2\zeta f_0$ is normally applied only to systems where ζ is much smaller, but the pilot study results indicated that Δr was of this order. Using fig. 5.6 a resolution bandwidth Δf of 0.2 Hz, and half-power point bandwidth Δr of 2.5 Hz lead to a bias error ξ_b of $\simeq 1\%$, and if $\Delta f = 0.4$ Hz, then $\xi_b \simeq 1.2\%$. Both are small errors compared with the expected random errors. The use of a 'Hanning' window (see below) increases these errors by a small amount, but they remain small (see table on page 58).

Noise at the input:

Bendat & Piersol show that this bias error is given by

$$1 + \epsilon_b = \left[1 + \frac{G_n(f)}{G_u(f)} \right]^{-1} = \frac{1 - \frac{G_n(f)}{G_u(f)}}{1 - \left(\frac{G_n(f)}{G_u(f)} \right)^2}$$

where $G_n(f)$ is the power spectral density of the noise at the input and $G_u(f)$ is the power spectral density function of the input.

Thus, for values of $G_n(f)$ less than about 10% of $G_u(f)$, the error ϵ_b is of the same order as the noise-signal ratio. The bias error ϵ_b is always negative, so that the estimate is always biased to be less than the true value.

In these studies, the system noise was reduced as far as possible, and noise - signal ratios better than -40dB (1%) can be expected over much of the frequency range. Thus, apart from bias errors arising from the basic experimental design (changes with posture and time, and uncorrelated input forces at the feet), the bias errors are each of the order of 1%. The expected random errors are much greater (see below) and as total error relates to the square of individual errors, these bias errors are insignificant.

Random Errors

The random errors which inevitably arise have to be reduced by some averaging or smoothing process operating on the spectral estimates. Both time and frequency averaging are possible, but the former is more efficient if the data is to be processed digitally, as was the case for this study. Time averaging consists of breaking the complete record of duration T into $n/2$ smaller records, calculating the spectrum for each, and then taking the mean value at each frequency point over the $n/2$ sample records.

The power spectrum obtained is statistically a parameter associated with the variance of the signal (average power at each frequency point). The choice of a suitable number of samples for the averaging process can be obtained via confidence limits. If the signal is assumed to have an amplitude distribution which is close to Gaussian, then as the variance of

a mean-square estimate of a Gaussian variable is distributed as Chi-squared, the sampling distribution of the smoothed power-spectral estimate is approximately Chi-square with n degrees of freedom.

Thus, if $G(f)$ is the power spectrum value at frequency f , and $\hat{G}(f)$ is the estimate of $G(f)$, then the sampling distribution is given by:

$$\frac{\hat{G}(f)}{G(f)} = \frac{\chi^2_n}{n}$$

$$\text{or} \quad \frac{n \hat{G}(f)}{\chi^2_{n; \frac{\alpha}{2}}} \leq G(f) \leq \frac{n \hat{G}(f)}{\chi^2_{n; 1 - \frac{\alpha}{2}}}$$

where $(1 - \alpha)$ is the confidence interval for $G(f)$ based on the estimate $\hat{G}(f)$; and $\chi^2_{n; \frac{\alpha}{2}}$, and $\chi^2_{n; 1 - \frac{\alpha}{2}}$ can be obtained from tables of the Chi-square distribution. An alternative to the use of tables is the graphical method illustrated in fig. 5.7, taken from Lowson 1972 (see also Jenkins & Watts 1969 fig. 3.10). Using these relationships, it is relatively easy to predict the number of degrees of freedom required to give the requisite accuracy and confidence interval.

For these studies, an error range of approximately $\pm 2\text{dB}$ with a confidence interval of approximately 80% would seem appropriate. Using the above relationships, 20 degrees of freedom lead to proportional errors of approximately +42%, -38% - i.e. +1.5dB and -2dB (Power) at the 90% and 10% confidence limits. This compares with $\pm 50\%$ for the 90% and 10% confidence limits predicted by use of the simple formula

$$\text{standard error of the mean} = \frac{1}{\sqrt{(\text{Degrees of freedom})}}$$

obtained from the Central Limit Theorem.

Application to this study

For the Fast Fourier Transform process commonly used on digital computers (where the block size is equivalent to the number of data points in the time-domain, and twice the number of frequency points), the duration of each sample record T is the inverse of the resolution bandwidth Δf . The number of degrees of freedom is given by $2B_e T$, where B_e is the effective bandwidth. If a rectangular data window is used, B_e is equal to Δf . However, in these studies, a 'Hanning' window was used, and this effectively increases the bandwidth by a factor of 1.3 (see

Beauchamp pp359) so that $B_e = 1.3\Delta f$. Thus, the number of degrees of freedom is given by $2 \times 1.3\Delta f \times T \times \text{no. of sample records} = 2.6 \times \text{No. of sample records}$.

Thus, the 20 degrees of freedom considered necessary above, requires 8 sample records, and a frequency resolution of 0.4Hz requires a sample record of duration 2.5s, so that the total time required would be 20s. This seemed to be a very short exposure, and one could expect conditions to remain unchanged for this period as well as expect subjects to hold the same posture, so that the resulting bias errors would be small.

In general, this a-priori analysis of bias and random errors indicated that reasonable accuracy could be obtained without requiring unreasonable constraints on the experimental design. Basically, the duration of the experimental exposure, and the requirements of random error and bias error reduction have to be balanced against each other.

Using the methods described above, a range of suitable conditions was drawn up. This is given in tabular form below:

A priori estimates of error for various conditions (assuming the use of a Hanning window)

Δf - Hz.	No. of Samples	Total time s.	Bias error in spectral estimate %	Random error (90% & 10%) limits	
				dB (Power)	%
0.2	10	50	1	+1.4 - 1.8	+37 - 34
0.2	20	100	1	+1.0 - 1.2	+26 - 25
0.4	10	25	1.5	+1.4 - 1.8	+37 - 34
0.4	20	50	1.5	+1.0 - 1.2	+26 - 25
0.4	50	125	1.5	+0.6 - 0.7	+15 - 15
0.8	10	12.5	5	+1.4 - 1.8	+37 - 34
0.8	20	25	5	+1.0 - 1.2	+26 - 25
0.8	50	62.5	5	+0.6 - 0.7	+15 - 15

The use of large resolution bandwidths to reduce the total record time would appear to be the most efficient as bias and random errors are then of the same order. However, the determination of the frequencies of specific occurrences (e.g. resonance points) are often as, if not more, important than the actual transfer-function value at that frequency and most of the impedance studies in the literature are based on $\frac{1}{2}$ Hz. resolution. These considerations, together with the fact that the random errors could be better assessed a-posteriori by the use of the coherence function (see below), indicated that a frequency resolution of 0.2Hz or 0.4Hz, together with averages over about 20 samples would probably be more suitable.

5.2.5 Estimated accuracy for this study

The types of error arising have been discussed and predictions made of the errors expected. Mention has already been made of a -posteriori methods of error estimation, and these were used to predict, from the pilot studies and a small number of special measurements, the errors to be expected. Model studies were also used to check the predictions.

A Posteriori estimation

The a-posteriori methods discussed by Bendat & Piersol determine the confidence intervals for the coherence function and the random errors in the frequency response function from the power spectral density and coherence function estimates obtained from the raw data.

Confidence limits for the coherence function:

From empirical studies, Enochson & Goodman 1965 found that if

$$0.35 \leq \gamma_{xy}^2(f) \leq 0.95$$

and there are $n \geq 20$ degrees of freedom, where $\gamma_{xy}^2(f)$ is the coherence function between x and y, then:-

$$\tanh[w(f) - \sigma_w - \sigma_w \cdot Z_{\alpha/2}] < \gamma_{xy}(f) \leq \tanh[w(f) - \sigma_w^2 + \sigma_w \cdot Z_{\alpha/2}] \dots \dots I$$

where $w(f) = \tanh^{-1}(\hat{\gamma}_{xy}(f))$
 $\sigma_w^2 = \frac{1}{(n-2)}$

n is the number of degrees of freedom

Z_{α} is the 100α percentage point of the standardized normal distribution (obtained from tables)

and $\hat{\gamma}_{xy}(f)$ is the positive square root of the coherence function estimate

The confidence limits for $\gamma_{xy}^2(f)$ are the square of the limits obtained above.

Benignus 1969 developed a more complex relationship which, however, extended its usefulness to include the full 0 to 1.0 range for $\gamma_{xy}(f)$, and down to eight degrees of freedom. However, it was not considered necessary to use this relationship for these studies.

Confidence limits for the frequency response function:

The response function is the ratio of two functions distributed as χ^2 and therefore has the F distribution (Hoel 1971 pp270).

If the true function is $H(f)$ and the estimate $\hat{H}(f)$, then

$$|\hat{H}(f) - H(f)|^2 \leq \hat{r}^2(f)$$

where $\hat{r}^2(f) = \left(\frac{2}{n-2} \right) \cdot F_{2, n-2, \alpha} [1 - \gamma_{xy}^2(f)] \cdot \frac{\hat{G}_x(f)}{\hat{G}_y(f)}$

(Bendat & Piersol)

where n is the number of degrees of freedom

$\hat{G}_x(f)$ is the power spectral estimate of the input

$\hat{G}_y(f)$ is the power spectral estimate of the output

$\gamma_{xy}^2(f)$ is the estimate of the coherence function

and $F_{2, n-2, \alpha}$ is the 100 α percentage point of the F distribution with $n_1 = 2$, and $n_2 = n-2$ degrees of freedom (obtained from tables).

The confidence limits can be represented as a circle of radius $\hat{r}(f)$ about each point on an Argand diagram.

$$\text{Thence, } |\hat{H}(f)| - \hat{r}(f) \leq |H(f)| \leq |\hat{H}(f)| + \hat{r}(f) \quad \text{--- II}$$

$$\text{and } \hat{\phi}(f) - \Delta\hat{\phi}(f) \leq \phi(f) \leq \hat{\phi}(f) + \Delta\hat{\phi}(f) \quad \text{--- III}$$

where $|H(f)|$ and $\phi(f)$ refer to modulus and phase.

$\hat{r}(f)$ is the positive square root of $\hat{r}^2(f)$.

$$\text{and } \Delta\hat{\phi}(f) = \sin^{-1} \left[\frac{\hat{r}(f)}{|\hat{H}(f)|} \right]$$

Using the above relationships (I, II, and III) the confidence limits for the transfer function and coherence function were obtained for the conditions which the pilot studies indicated should apply.

Thus the following 90% confidence limits were calculated for various estimates of the coherence function and number of samples:-

Coherence function estimate - $\hat{\gamma}_{xy}^2(f)$	No. Samples $(\frac{n}{2})$	Limits for the coherence function $\gamma_{xy}^2(f)$
0.90	10	$0.77 < \gamma_{xy}^2(f) \leq 0.95$
0.95	10	$0.88 < \gamma_{xy}^2(f) \leq 0.97$
0.90	20	$0.83 < \gamma_{xy}^2(f) \leq 0.94$
0.95	20	$0.91 < \gamma_{xy}^2(f) \leq 0.97$

To calculate typical errors in the frequency response function, values for $|\hat{H}(f)|$, $\hat{G}_x(f)$, $\hat{G}_y(f)$, and $\hat{\gamma}_{xy}^2(f)$ were taken from data obtained in the pilot studies. As might be expected, $\frac{\hat{G}_y(f)}{\hat{G}_x(f)}$ was nearly equal to

$|\hat{H}(f)|^2$. If they are assumed to be equal the following simple relationships apply:

$$|\hat{H}(f)| \cdot (1 - \hat{r}_1(f)) \leq |\hat{H}(f)| \leq |\hat{H}(f)| \cdot (1 + \hat{r}_1(f))$$

$$\text{and } \hat{r}_1(f) = \sin^{-1} \left[\hat{r}_1(f) \right]$$

where $\hat{r}_1(f)$ is the positive square root of $\frac{2}{n-2} F_{2, n-2, \alpha} \left[1 - \hat{\gamma}_{xy}^2(f) \right]$

Using these simple relationships, the following values were obtained for the 90% and 95% confidence limits for the frequency response function. (continued)

From measurements taken from actual data, it was estimated that the assumption that $|\hat{H}(f)|^2 = \frac{\hat{G}_{xy}(f)}{\hat{G}_x(f)}$ led to possible errors in the estimation of $\hat{r}(f)$ of 20% maximum. However, this would only vary the

Coherence function estimate - $\hat{\gamma}_{xy}^2(f)$	No. Samples	$\hat{r}_1(f)$	Limits for the frequency response function		
			Gain		Phase
			%	dB	
Upper and lower 90% confidence limits					
0.98	20	0.0509	± 5	+ 0.43 - 0.45	$\pm 2.9^\circ$
0.95	20	0.0805	± 8	+ 0.7 - 0.7	$\pm 4.6^\circ$
0.95	10	0.121	± 12	+ 1.0 - 1.1	$\pm 7.0^\circ$
0.95	5	0.198	± 20	+ 1.6 - 1.9	$\pm 11.4^\circ$
0.9	20	0.114	± 11	+ 0.9 - 1.1	$\pm 6.5^\circ$
0.9	10	0.171	± 17	+ 1.4 - 1.6	$\pm 9.8^\circ$
0.9	5	0.280	± 28	+ 2.1 - 2.8	$\pm 16.3^\circ$
Upper and lower 95% confidence limits					
0.98	20	0.058	± 6	+ 0.49 - 0.52	$\pm 3.3^\circ$
0.98	40	0.040	± 4	+ 0.34 - 0.35	$\pm 2.3^\circ$
0.95	40	0.063	± 6	+ 0.53 - 0.57	$\pm 3.6^\circ$
0.95	20	0.092	± 9	+ 0.8 - 0.8	$\pm 5.3^\circ$
0.95	10	0.1405	± 14	+ 1.1 - 1.3	$\pm 8.1^\circ$
0.95	5	0.236	± 24	+ 1.8 - 2.3	$\pm 13.7^\circ$
0.9	20	0.131	± 13	+ 1.1 - 1.2	$\pm 7.5^\circ$
0.9	10	0.198	± 20	+ 1.6 - 1.9	$\pm 11.4^\circ$
0.9	5	0.334	± 33	+ 2.5 - 3.5	$\pm 19.5^\circ$

above limits by a small amount.

Model Studies

The above predictions were checked by measuring the characteristics of a known system. The only mechanical system that could be designed to have accurately known characteristics and yet be easily constructed, was a simple mass. However, this has the disadvantage that no resonance characteristics are exhibited, and a mass was in any case to be used for calibration purposes. It was decided that it would be better to use a known electrical system and assume that the characteristics of the electro-mechanical transducers would not introduce any changes not eliminated by the calibration method.

A second order, single degree of freedom electrical analogue was constructed (see Appendix 8). It was set to have an undamped natural frequency of approximately 8Hz., with a damping factor of 0.25, characteristics similar to those expected for the human transfer-function. Accelerations at the seat had been recorded during the pilot studies. A typical tape recording of acceleration was used to give the input to the model. The input and response were measured as follows. The transducer outputs (electric charges) were simulated by putting the model input and output voltages across calibrated capacitors. These charges were amplified by the charge-amplifiers and recorded by the system used for human studies - fig. 5.8. Care was taken to ensure that voltage levels were of the same order as used in the experimental work, so that all the variants in the practical system would be simulated. The results were processed on the computer in the usual way.

To obtain the best estimate of the true model transfer function, it was obtained 'on line' at the computer. The charge-amplifiers and tape-recorder were not used, and a random signal with a nearly flat spectrum was used as the input signal. The anti-aliasing filters were used. Fig 5.9 illustrates the transfer-function obtained using 80 samples, each 2.5s long ($f = 0.4s$). Superimposed are the calculated values for $f_0 = 8Hz$, $\zeta = 0.25$, and values obtained by measuring input and response on a U.V. oscilloscope when the stimulus was a sinusoid. Clearly, the response is very close to the simple system with $f_0 = 8Hz$. and $\zeta = 0.25$, and the results better than those obtained by using a sinusoidal stimulus. This transfer-function was taken to be the true value for the following

discussion of error estimates.

Sufficient recorded data were available for the analysis of 40 samples each of duration 2.5s ($\Delta f = 0.4$ s). Figure 5.10 shows the transfer function obtained by averaging the 40 samples, whilst Fig. 5.11 shows the superimposed functions from 10 computations, each averaged over 4 samples, and Fig. 5.12 shows that for 2 computations averaged over 10 samples.

Compared with Fig. 5.9, Fig 5.10 exhibits a bias of approximately $+0.8$ dB and -2° at 20 Hz, with negligible values at resonance, whereas the expected bias errors for $\Delta f = 0.4$ Hz are ± 0.13 dB.

The predictions are therefore, of the right order, though those at 20 Hz were optimistic (where the large bias may have resulted from the low power values of the response).

The random error predictions were applied to the data at the resonance frequency and at 20 Hz - points where the coherence-function estimates were relatively low. The following values were obtained.

	Resonance Frequency			20 Hz		
	Coherence estimate	Mag.	Phase	Coherence estimate	Mag.	Phase
10 x 4 samples. Actual	0.96	± 0.7 dB	$\pm 2.5^\circ$	0.95	± 0.25 dB	$\pm 2^\circ$
{ 5 samples. Predicted	@ 0.95	+ 1.6 dB	$\pm 11.4^\circ$	@ 0.95	+ 1.6 dB	$\pm 11.4^\circ$
{ (90% Conf. Limit)		- 1.9 dB			- 1.9	
2 x 20 Actual	0.97	± 0.1 dB	$\pm 1^\circ$	0.92	± 0.15 dB	$\pm 0.5^\circ$
{ 20 Samples. Predicted	@ 0.95	+ 0.7 dB	$\pm 4.6^\circ$	@ 0.90	+ 0.90 dB	$\pm 6.5^\circ$
{ (90% Conf. Limit)		- 0.7 dB			- 1.1 dB	

Unfortunately, insufficient data were available to obtain 20 computations (the range of values would then approximate to the 90% confidence limits) of 5 or more samples, and useful estimates were not possible for less than 20 computations of less than 5 samples. However, the above values do indicate that the predictions were of the right order, possibly pessimistic.

As part of the model study, a comparison was made between three bandwidths in the range considered to be suitable. To keep the total analysis time constant, the number of samples averaged were increased with increasing bandwidth. The values used were $\Delta f = 0.2$ Hz (20 samples), $\Delta f = 0.4$ Hz (40 samples); and $\Delta f = 1.0$ Hz (100 samples). The resulting transfer functions were closely similar, although that for $\Delta f = 1.0$ Hz did indicate that this bandwidth was rather coarse for resonances of 8 Hz and below when the damping was of the order expected. This agrees with Griffin et al 1978 who found that resonances at about 2 Hz were equally well estimated with bandwidths of 0.125 and 0.25 Hz, with slightly less accuracy at 0.5 Hz, and were subject to increasing error as the bandwidth increased to 1 Hz and beyond.

Overall accuracy of the recording and analysis system

The model studies gave a good indication of the overall efficacy of the recording and analysis system. They were such that if 20 samples were averaged using a bandwidth of 0.4 Hz, one could expect coherence function estimates of about 0.97 at resonance and better than 0.95 over most of the frequency range (fig. 5.12). For a coherence function estimate of 0.95, the 90% confidence limits are then ± 0.7 dB, $\pm 4.6^\circ$, and the 95% confidence limits are ± 0.8 dB, $\pm 5.3^\circ$. The 90% confidence limits are then (on the scales used for the graphs) equivalent to ± 3.5 mm (magnitude) and ± 2.3 mm (phase). That is, approximately seven times and five times the line thickness used on the graph plotter. Bearing in mind that this is probably a pessimistic estimate for most of the frequency range, the use of 20 averages with a 0.4 Hz bandwidth would seem to be quite suitable and lead to minimal exposure for the subject. The signals used approximated to normal, stationary, random processes and digitisation and quantization errors appeared to be minimal. Errors in the transducer system could not be checked accurately, but any gross bias errors could be assumed eliminated by the calibration method used.

Practical results

The pilot studies with subjects resulted in coherence function estimates of about 0.9 or 0.95 when a bandwidth of 0.4 Hz was used and 20 samples averaged. The predicted 90% confidence limits in this case would be ± 0.9 , -1.1 dB modulus and $\pm 6.5^\circ$ phase ($\gamma^2 = 0.90$) and ± 0.7 dB modulus and $\pm 4.6^\circ$ phase ($\gamma^2 = 0.95$). The coherence function estimates for the model studies were greater than these, and one has to question the practical situation. However, the coherence function estimates obtained from the mass-calibration runs were close to unity. Although measurements with a mass have the disadvantage that no resonance phenomena exist (so that response signal levels near 20 Hz are good and little affected by noise), they do suggest that the transducer system does not introduce the reduction in coherence function estimates observed with subjects. One or two of the later pilot studies (with an improved shape input spectrum) showed that higher coherence values (e.g. 0.97 minimum) could be obtained with subjects. Thus it would seem safe to assume that the low coherence estimates found in some human runs could relate either to a poor input spectrum resulting in insufficient power for accuracy or to a genuine non-linearity in response, rather than failings in the measuring, recording and analysis procedures.

5.3 Computation

The computation of apparent mass etc. was carried-out on a Hewlett-Packard 5451A Fourier Analyser. The full system available offered, together with the Fourier Analyser, a two channel analogue to digital converter, digital magnetic-tape storage and a digital graph plotter. On this machine the signals are processed as blocks of data, and a number of data-block sizes and analogue to digital conversion rates are available. The Fourier Analyser uses a fast-fourier-transform algorithm together with conventional digital techniques to perform many of the operations useful in signal processing.

The programming language used is such that certain standard operations are called by depressing a key at a console. In addition to this, one can write a simple 'key-board programme' which simulates use of a number of keys in a pre-determined manner, or write 'user-programmes' (e.g. special graph-plotting routines) which can be called from the key-board. The computer may also be used with 'FORTRAN' and other languages.

Practical results

The pilot studies with subjects resulted in coherence function estimates of about 0.9 or 0.95 when a bandwidth of 0.4 Hz was used and 20 samples averaged. The predicted 90% confidence limits in this case would be ± 0.9 , -1.1 dB modulus and $\pm 6.5^\circ$ phase ($r^2 = 0.90$) and ± 0.7 dB modulus and $\pm 4.6^\circ$ phase ($r^2 = 0.95$). The coherence function estimates for the model studies were greater than these, and one has to question the practical situation. However, the coherence function estimates obtained from the mass-calibration runs were close to unity. Although measurements with a mass have the disadvantage that no resonance phenomena exist (so that response signal levels near 20 Hz are good and little affected by noise), they do suggest that the transducer system does not introduce the reduction in coherence function estimates observed with subjects. One or two of the later pilot studies (with an improved shape input spectrum) showed that higher coherence values (e.g. 0.97 minimum) could be obtained with subjects. Thus it would seem safe to assume that the low coherence estimates found in some human runs could relate either to a poor input spectrum resulting in insufficient power for accuracy or to a genuine non-linearity in response, rather than failings in the measuring, recording and analysis procedures.

5.3 Computation

The computation of apparent mass etc. was carried-out on a Hewlett-Packard 5451A Fourier Analyser. The full system available offered, together with the Fourier Analyser, a two channel analogue to digital converter, digital magnetic-tape storage and a digital graph plotter. On this machine the signals are processed as blocks of data, and a number of data-block sizes and analogue to digital conversion rates are available. The Fourier Analyser uses a fast-fourier-transform algorithm together with conventional digital techniques to perform many of the operations useful in signal processing.

The programming language used is such that certain standard operations are called by depressing a key at a console. In addition to this, one can write a simple to 'key-board programme' which simulates use of a number of keys in a pre-determined manner, or write 'user-programmes' (e.g. special graph-plotting routines) which can be called from the key-board. The computer may also be used with 'FORTRAN' and other languages.

5.3.1 Standard key-board functions

A variety of functions were available, those of importance for this study are described below.

Fourier transform:

The programme uses a fast-fourier-transform algorithm to obtain the discrete-fourier-transform of a block of data (in the time domain) whose dimension is a power of 2. The transformed data (now in the frequency domain) is held in the same block. Only positive frequency values are held. As the number of frequency points is half the block size, the block is able to hold both the real and imaginary values (or magnitude and phase values). This is a common procedure and results in the following common relationships -

$$\begin{aligned} \Delta f &= \frac{1}{N \cdot \Delta t} & \text{where } \Delta f & \text{ is the resolution bandwidth} \\ T &= N \cdot \Delta t & \frac{1}{\Delta t} & \text{ is the digitising rate} \\ F_{\max} &= \frac{1}{2} \cdot N \cdot \Delta f & N & \text{ is the block size} \\ & & T & \text{ is the time to digitise one block} \end{aligned}$$

As only the positive frequencies are held, the resulting spectrum is equal to half the amplitude spectrum related to the input voltage.

Power spectrum:

The programme conjugate multiplies the fourier transform by itself to obtain the power spectrum. Two fourier transforms may be operated upon, in which case both power-spectra are obtained together with the cross-power-spectrum. If the operation is repeated, the resulting values are summed. Again, as only the positive frequencies are held, the resulting spectrum is equal to only half of the spectrum values related to the input voltage.

Transfer function:

The programme operates on two power-spectra and the cross-spectrum (as obtained above) to obtain the transfer-function and coherence-function from

$$H(f) = \frac{G_{xy}(f)}{G_{xx}(f)}$$

$$\text{and } \gamma_{xy}^2(f) = \frac{|G_{xy}(f)|^2}{G_{xx}(f) \cdot G_{yy}(f)} \quad (\text{see section 6.1})$$

Hanning function:

Time data is operated upon by a 'Hanning' window. No account is taken of the necessary correction factor in the frequency domain.

Histogram: A block of data in the time-domain is operated upon to give an amplitude distribution histogram. The available positive and negative voltage amplitude (-V to +V) at the analogue to digital converter is divided into N bands, where N is the data block size. The histogram gives the number of counts in each band, scaled down by a factor of 32,767.

5.3.2 Derived functions

It was possible to derive a number of basic functions useful for this study by using small key-board programmes or FORTRAN based programmes. Their derivation is described below:

Power spectral density:

The FFT is computed on the analyser without reference to the sampling rate used, so that the result of the 'power spectrum' key-board function $(X_k)^2$ has to be multiplied by $2/\Delta f$ to obtain the power spectral density (see 6.1). To take into account the number of sample records (n_1) and use of the Hanning function, further multiplication by $\frac{8}{3n_1}$ is necessary. As n_1 and Δf are known constants, the overall effect is multiplication by a constant ; a simple key-board function.

Mean value:

The mean value is given by $\mu^2 = T(X_0)^2 = \frac{1}{\Delta f} \cdot (X_0)^2$ (see 5.1)

The same modifications as those above are necessary, although the Hanning correction is 2, so that $\mu^2 = \frac{2}{n_1 \Delta f} (X_0)^2$

In practice, despite attempts to keep mean-values small, on occasions the zero frequency component was sufficiently large compared with other components to alter scaling factors. For this reason the zero frequency component was usually set to zero if not required directly.

Standard deviation:

The standard deviation (σ_x , the positive square root of the variance σ_x^2) can be obtained from the relationship

$$\sigma_x^2 = \psi_x^2 - \mu_x^2 \quad (\text{section 6.1})$$

where the mean square value can be obtained from $\psi_x^2 = \int_0^\infty G_x(f) \cdot df$.

Thus, bearing in mind the correction factors given above and the fact that the frequency points are Δf apart, an estimate of the variance is given by

$$\sigma_x^2 = \frac{8}{3} \cdot \frac{2}{n_1} \cdot \int_1^{N/2} (X \cdot k)^2 \cdot dk$$

This was used initially, but it was found that errors arose if the mean value was large. To overcome this problem a slightly more cumbersome method was used.

The mean value can be obtained by integrating the time-domain histogram. Furthermore, if the count for each channel of the time-domain histogram is squared and the resulting histogram integrated, then the mean square can be obtained. The standard deviation is then obtained from

$$\sigma_x^2 = \psi_x^2 - \mu_x^2$$

Although simple, this involves more operations than the previous approach. However, it has the advantage that the values for σ_x and μ_x obtained are true values for the period of time sampled.

Probability density:

The standard histogram function is useful in checking that the data does not contain excessive harmonics, that amplifiers have not been overloaded and so on.

However, it is possible to obtain the probability density function from the histogram and this is of great value in checking that the data is approximately Gaussian. The standardized variable z is given by $z = \frac{x - \mu_x}{\sigma_x}$ where x refers to voltage amplitudes in this case. Also, it can be shown that for digitised data of zero mean (see Bendat & Piersol pp309), the probability density function can be estimated by

$$\hat{p}(x) = \frac{N_x}{N' \cdot W}$$

where N' is the total number of data points

W is a narrow interval centred at x

and N_x is the number of data points within the range $x \pm \frac{W}{2}$

Thus, if $\mu_x = 0$ the standardised values Z may be obtained by dividing the actual values x by the standard deviation σ_x .

The standard histogram function is such that the digitisation voltage range $-V$ to $+V$ is divided into N levels, where N is the data block size, and the range $2V$ is equivalent to $\frac{2V}{\sigma_x}$ standardized values. The graph-plotter user programmes are such that N levels are plotted over $\frac{Y}{100}$ inches (where Y is a keyed-in parameter). Thus, to obtain a graph where x cms is equivalent to 1 standardised value Z , X must be set to $\frac{2V}{2.54 \cdot \sigma_x} \cdot \frac{Y}{100}$.

The interval W is given by $\frac{2V}{N \sigma_x}$, so that $\hat{p}(x) = N_x \cdot \frac{\sigma_x}{2 n_1 V}$ (as $N' = n_1 \cdot N$) Thus, if the amplitude for each channel as given by the standard histogram function is scaled by $\frac{2.767 \sigma_x}{2 n_1 V}$ then the values are probability density estimates. The plotter parameter Y is given by $y \cdot yz \cdot \frac{100}{2.54}$ (where yz is max. value displayed on screen and y is number of cms per $\hat{p}(x)$ unit).

5.3.3 Special functions

Calculation of 99% confidence limits: It was shown in section 5.2.5 that the error function is given by

$$\hat{r}^2(f) = \left(\frac{2}{n-2} \right) \cdot F_{2, n-2, \alpha} [1 - \hat{\gamma}_{xy}^2(f)] \frac{\hat{G}_y(f)}{\hat{G}_x(f)}$$

and that the confidence limits can be represented as a circle of radius $\hat{r}(f)$ about $|H| \cdot \underline{\hat{f}}$. Thus the range of values about the estimates are given by

$$|\hat{H}(f)| \pm \hat{r}(f)$$

$$\text{and } \hat{\phi}(f) \pm \sin^{-1}\left(\frac{\hat{r}(f)}{|\hat{H}(f)|}\right)$$

For 99% confidence limits $\alpha = 0.01$, and for 20 sample records $n = 40$.

Hence from tables $F_{2, 38, 0.01} = 5.21$

$$\text{Thus } \hat{r}^2(f) = 0.2742 [1 - \hat{r}^2] \cdot \frac{\hat{G}_y(f)}{\hat{G}_x(f)}$$

where \hat{r}^2 , $\hat{G}_y(f)$, $\hat{G}_x(f)$ are all standard key-board functions.

If errors in \hat{r} are small, then $\sin^{-1}\left(\frac{\hat{r}(f)}{|\hat{H}(f)|}\right) \simeq \tan^{-1}\left(\frac{\hat{r}(f)}{|\hat{H}(f)|}\right)$
(if error $\leq 10^\circ$, the difference is less than 1.5%).

To obtain curves equivalent to the 99% confidence limits, the greatest magnitude and phase differences were used to obtain a confidence limit 'transfer function' which could be plotted along with the transfer function estimate. The confidence limit 'transfer functions' were obtained from

$$(|\hat{H}(f)| + \hat{r}(f)) \underline{\hat{\phi}(f) + \Delta\phi} = |\hat{H}(f)| \cdot \underline{\hat{\phi}(f)} \cdot \left(1 + \frac{\hat{r}(f)}{|\hat{H}(f)|}\right) \cdot \underline{0_j} \cdot 1 \cdot \underline{\Delta\phi}$$

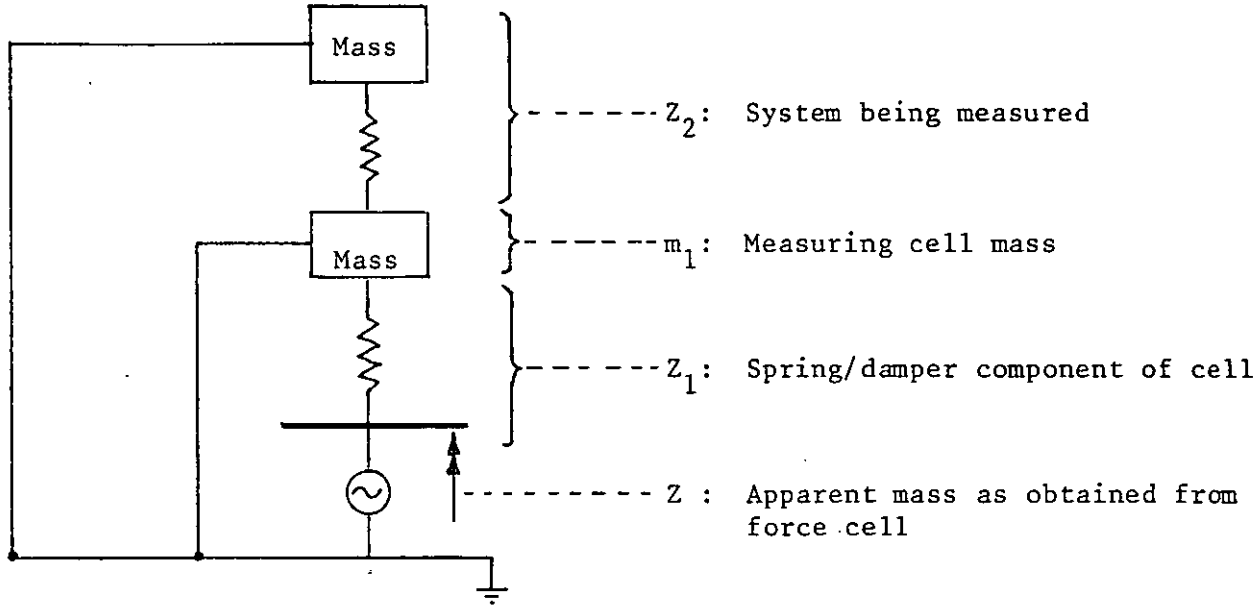
$$\text{and } (|\hat{H}(f)| - \hat{r}(f)) \underline{\hat{\phi}(f) - \Delta\phi} = |\hat{H}(f)| \cdot \underline{\hat{\phi}(f)} \cdot \left(1 - \frac{\hat{r}(f)}{|\hat{H}(f)|}\right) \cdot \underline{0_j} \cdot 1 \cdot \underline{\Delta\phi}$$

$$\text{where } \Delta\phi = \tan^{-1}\left(\frac{\hat{r}(f)}{|\hat{H}(f)|}\right) \text{ and } 1 \cdot \underline{\Delta\phi} = 1 \cdot \underline{\tan^{-1}\left(\frac{\hat{r}(f)}{|\hat{H}(f)|}\right)} = \frac{(|\hat{H}(f)| + j \cdot \hat{r}(f))}{\sqrt{(|\hat{H}(f)|^2 + \hat{r}^2(f))}}$$

All these calculations can be achieved by simple key-board programmes.

'Mass cancellation': Any force measuring system will have its own dynamic characteristics, which will affect the force values obtained. In impedance testing it is usual to carry out 'mass cancellation' by subtracting a fixed amount from the force analogue signal. However, it was possible to combine both calibration and consideration of system characteristics in the digital analysis.

Consider a measuring system assumed to have relatively simple mechanical characteristics:



In this case, $\frac{1}{Z} = \frac{1}{Z_1} + \frac{1}{(m_1 + Z_2)}$

i.e. $Z = \frac{Z_1(m_1 + Z_2)}{(Z_1 + m_1 + Z_2)}$

Thus, for maximum accuracy, Z_1 should be very large (or known very accurately) and m_1 very small (or known to the accuracy required for Z_2). However, some measurement error is involved (probably variable with frequency). This is assumed to be linear, so that:

$$Z = \frac{K \cdot Z_1 (m_1 + Z_2)}{(Z_1 + m_1 + Z_2)} \quad (K \text{ constant})$$

Now, if a normal test is carried out with the unknown system Z_2 replaced by a known mass M the measured value is:

$$Z_m = \frac{K \cdot Z_1 (m_1 + M)}{(Z_1 + m_1 + M)}$$

Hence

$$\frac{Z}{Z_m} = \frac{(m_1 + Z_2)(Z_1 + m_1 + M)}{(m_1 + M)(Z_1 + m_1 + Z_2)}$$

Thus, by calibration with a known mass M , we can eliminate the measurement error, but we still need to know m_1 and Z_1 .

By carrying out successive calibrations with different values of M (or, ideally, known elastic systems Z_m) these unknowns may be eliminated. However, a simpler expedient was followed - the force cell was made stiff and light ($Z_1 \rightarrow \infty$, $m_1 \rightarrow 0$), so that the following apply:

$$\frac{Z}{Z_m} \approx \frac{m_1 + Z_2}{m_1 + M}$$

and

$$Z_2 = (m_1 + M) \frac{Z}{Z_m} - m_1$$

Then it is only necessary to take the ratio of the measured spectrum and the calibration spectrum ($\frac{Z}{Z_m}$) and apply the corrections $x(m + M)$, $-m$ during the digital computation. This is essentially the same as the analogue 'correction factor' technique, but takes into account changes in system sensitivity (including amplifying, recording, and D/A conversion) with frequency, and good dynamic calibration is possible without the need for absolute calibration of both force and acceleration signals (time consuming operations for dynamic measurements).

In fact the lowest resonant frequency of the load cell with a 70 kg load was found to be of the order of 500 Hz. The maximum frequency used in analysis was 25 Hz (i.e. 1/20th) and it can be shown that in this case $Z \approx -3,400 m_1$. The mass of the cell m was 8.5 kg*, so that the maximum possible error in the assumption $Z_1 \rightarrow \infty$ is given by

$$\frac{Z_1 + m_1 + M}{Z_1 + m_1 + 0} = \frac{-3400 + 8.5 + 70}{-3400 + 8.5} \quad \text{i.e. about 2\% overestimate}$$

(and for much of the spectrum where Z_2 is of the same order as M , the error will be much less).

Cast iron plates weighing 20 kg were first designed for calibration. However, these were found to give some spurious acceleration signals and were replaced by a 70 kg lead weight for the calibration of all the data reported here. As a check on the system, several weights were measured, and fig. 5.13 shows that overall accuracy is maintained down to at least 20 kg apparent mass. The figure also illustrates the differences that occur with frequency.

*In most experiments a bead bag of 3.5 kg was used so that $m_1 = 12$ kg.

However, this was not included in the calculations of Z_2 .

Normalisation of spectra: It was shown in 3.3 that in the case of a linear single degree of freedom system, the apparent mass is given by the product of the transmissibility and the system mass. To a first approximation, the apparent mass data for subjects can be regarded as the response of a single degree of freedom system in parallel with an 'unsprung' mass; with the apparent mass values at the lowest frequencies equivalent to the total mass of the system, and the apparent mass at the highest frequencies equivalent to the unsprung mass.

The mean of the last ten frequency points of the apparent mass spectrum was taken as the unsprung mass, and the first frequency point as the total mass. The unsprung mass was then subtracted from the apparent mass spectrum, which was then normalised to unit mass.

This procedure was developed as the 'normalised' apparent mass could be better compared with subject transmissibility. Again, all calculations were possible with a simple key-board programme.

5.3.4 Routine for Computations

The two important elements of data treatment were data validation and data presentation. The data needed to be considered in terms of coherence function (and possibly confidence limits) to check the basic reliability, and in terms of available power to check that any loss in coherence was not simply a function of stimulus shortcomings. In addition, the probability density function was used to check that the time functions were normally distributed and included no significant periodicities. The time functions also needed to be checked for stationarity. Apart from stationarity checks, all the above used graphical presentation. The system transfer functions were again presented graphically. A log magnitude, linear phase against log frequency format was considered most suitable. The log log format for magnitude is the accepted format for engineering situations. It tends to emphasise significant changes at low values of magnitude and the information at low frequencies. It tends also to mask minor differences between spectra, which may at times be a disadvantage. The log log format also allows easy comparison of spectra where a proportional relationship is expected either in magnitude or frequency. Presentation of all data graphically is time consuming and the minimum of explanation was felt sufficient for the data validation graphs. For data presentation and comparison, the spectra were plotted complete

with annotated axes. The latter were generated in special purpose FORTRAN programs.

The computational routine demanded several passes on the analyser system, and is given briefly below:

Pass 1: Raw analogue data filtered and digitised. Digital (time domain) data stored on magnetic tape for later treatment. In each case, input and output data were interleaved and separate passes were required for apparent mass, transmissibility, and foot transfer function. Sufficient data for 20 (or 40 for calibration) sample records was collected).

Pass 2: Time data read from magnetic tape and power spectrum, coherence and transfer functions obtained, raw histograms of time data generated and viewed on an oscilloscope display. The first run related to system calibration (e.g. 70 kg mass for apparent mass) and the resulting information used to calibrate subsequent runs. Overall means and standard deviations calculated from histograms and printed out to allow user interaction to generate probability density functions. Raw spectra etc. stored on magnetic tape for further use.

Pass 3: Magnetic tape accessed, and raw data plotted. Normal distribution plotted from values previously calculated and stored. Confidence limits calculated and plotted (later runs only). With experience one generated a degree of confidence in the data and the system transfer function with 99% confidence limits and coherence function were considered sufficient. Only one in five runs were then given the full validation treatment.

Pass 4: Time data accessed on magnetic tape and each sample record analysed for mean and standard deviation. Values for 20 sample records printed out and 'run' test carried out manually. This treatment was used only occasionally.

Pass 5: Raw data on magnetic tape accessed and different conditions plotted for comparison on the same annotated axes.

Pass 6: Raw data on magnetic tape accessed, data normalised (as in 6.3.3) and different transfer functions plotted for comparison on the same annotated axes.

6. EXPERIMENTS TO VALIDATE THE RANDOM STIMULUS TECHNIQUE

6.1 Introduction

The input transfer function can be regarded as the fundamental one, as it describes the mode of transfer of energy to the body upon which the other transfer functions are dependent and it reflects the behaviour of the major dynamic components. However, in the case of man, its physical basis is not understood. In order to investigate further the viability of the random stimulus approach and, in particular, the credibility of the assumption of linearity, it was decided that the technique would be applied to the human apparent mass with the additional aim of exploring the physical basis of the human apparent mass function. Also, it was decided that transmissibility be explored further, both in its own right and to throw light on the physical basis of the apparent mass function. An opportunity arose to measure intra-abdominal pressures during vibration and the technique was applied to the pressure transmission also.

The conceptual model shown in fig. 6.1 was used as a basis for consideration of the apparent mass function. In the literature, particularly that relating to shock response (Sandover 1971), there is often an inherent assumption that the spine is the major load bearing structure in the trunk and responsible for much of the dynamic characteristics. However, Yeager et al 1969 took the view that a "major portion of the body's spring characteristics are to be found in the tissue of the buttocks...." (again in regard to impact). Clearly, if this is the case, one would expect the large muscle masses of the gluteus group at pelvis and thigh to be important, and in particular their state of tension. The viscera too may be expected to have a part to play as they are supported directly by the pelvis and spine. If these components control the measured apparent mass, then one can expect posture to be an important parameter. Changes in posture may lead to changes in spinal geometry (and thence its stiffness); changes in spinal, abdominal and buttock muscle tension; changes in the position of the pelvis and legs. The energy input from the feet and legs is an unknown and could conceivably have a significant contribution.

As regards the physical basis of the apparent mass function, the aim of these experiments was to identify those components contributing significantly to trunk behaviour by attempting to modify them through

judicious changes in posture or muscle tone, by adding masses to the body, or by constraining body tissues from their normal modes of vibration. It was considered that this would best be done with a small number of subjects investigated thoroughly. To make the results of more direct practical value, the extent of the variability in measured responses also needed consideration.

6.2 General description of the experiments

All the measurements were to be based on the random stimulus linear analysis approach as described in section 5. A considerable fall-off above 5Hz. in the power spectrum of the human response was expected, and to counteract this (for reasoning see section 3.4) the stimulus spectrum was shaped to give slightly more energy at the higher frequencies yet still sufficient at low frequencies to satisfy signal to noise ratio requirements. The stimulus level was of the order of either 1 or 2 m/s² r.m.s. (unweighted) and satisfied safety constraints (see 6.4). In all the experiments the apparent mass transfer function was obtained. Other measurements were transmissibility, apparent mass as measured at the feet and a transfer function relating input acceleration to intra-abdominal pressure:

6.3 Equipment

6.3.1 Vibration facility

The vibrator and its control system was developed over a number of years specifically for the exposure of human subjects to $\frac{1}{2}$ z vibration. Emphasis was placed on subject safety with other environmental factors unobtrusive and well controlled. The facility is described in detail in appendix 4.

6.3.2 Instrumentation

The experimental approach was based primarily on calculation of the transfer characteristics at the man-seat interface, which required measurement of force and acceleration at the interface. The data were recorded on analogue magnetic tape, prior to off-line digitisation and processing. Manufacturers specifications for the equipment used are given in appendix 5.

6.3.3 Force and acceleration measuring cell

The accurate measurement of the forces and accelerations envisaged required transducers with a frequency response from near D.C. to high frequencies and this requirement was satisfied by one make of piezo-electric transducer and charge amplifier. The transducers were mounted together in a measuring cell as one unit (Fig. 6.2). Three force transducers were mounted in a triangle such that two were situated approximately under the ischial tuberosities of the subject, with the third located centrally in front of them. The three were connected together in parallel so that the total force on the cell was given by the total charge from the parallel system. The accelerometer could be mounted in one of two positions, one located between the two load cells at the ischial tuberosities, the other slightly forward of this position. The transducers were mounted in the upper section of the unit. This consisted of a 50 mm slab of Duralumin which had been milled out to reduce weight yet maintain stiffness in a configuration related to the expected loading. The lower section of the unit consisted of a 13 mm plate of Duralumin which was attached to the upper section with seven small nylon bolts. In this way the two sections were held in contact and the load cells very slightly pre-loaded. Non load-bearing air tight seals ensured that transducers were not affected by damp or dust. However, the stiffness of the load cells was many orders of magnitude greater than that of the nylon bolts and seals, so that accurate measurement of loads was not affected.

Initially it was found that the static sensitivity of the cell was dependent on load position (presumably as a result of friction at these bolts) so that errors could arise as the subject's centre of gravity moved. The bolts were modified to have a narrow shank and sealed only at the bearing surface so that static friction was reduced to a minimum. Further static tests with up to 60kg showed the system to be linear within 2.7%, and 7% less sensitive than predicted from manufacturers specifications for each load cell. Variation in sensitivity across the cell (20kg load) was +6% to -5% about the total cell sensitivity. Friction can be expected to have reduced effects under dynamic loading and these errors were considered acceptable bearing in mind that the resulting transfer functions were in any case to be calibrated dynamically.

6.3.4 Head harness

For those experiments where head acceleration was measured, the head harness shown in fig. 6.3 was used. The basic framework of the harness was the nylon liner from a safety helmet. A piezo-resistive accelerometer was mounted on a stiff plate fixed to the centre of the nylon framework. Leather straps with 'velcro' fastening were used to hold the helmet firmly on the head. The arrangement allowed both circumferential and height adjustment. The straps were tightened sufficiently for the accelerometer plate to press firmly on the apex of the head. This mounting arrangement had been shown to be reliable by Sandover 1974 and the pressure exerted by the plate probably satisfied the criteria of Ziegert & Lewis 1979 for unit transfer of skull accelerations to the accelerometer. The apex location was deemed to be the best compromise for reliable measurements of head movements in the z direction (see Appendix 3).

6.3.5 Foot measurement unit

In some experiments the apparent mass was measured at the feet. Only one force transducer was available and this led to constraints on design. The unit consisted of a horizontal steel foot bar welded to a cylindrical steel hub which was free to move smoothly up and down a vertical steel bar attached to the vibration foot-rest. A piezo-electric force transducer was located under the hub, and a piezo-electric accelerometer was attached to the under surface of the foot bar. The foot bar could be adjusted vertically relative to the seat. The arrangement was somewhat clumsy, but offered no real problems to the subject.

6.3.6 Recording system

The outputs from the force and acceleration amplifiers were recorded on a seven channel F.M. tape-recorder (see Appendix 5) for subsequent off-line processing. The tape-recorder was such that record and replay can operate concurrently and the input signal was replayed (with a short delay) to a display oscilloscope. This was used as an immediate check that the experimental signals were satisfactory.

To obviate tape-recorder speed variations (although these were expected to be very low) a square wave signal of known frequency was recorded at the time of the experiment. During computation, this was used

to drive the analogue to digital convertor. It was anticipated that maximal signal to noise ratio would be required to obtain reliable transfer function data. The primary interfering noise was at low frequencies, arising from tape 'flutter'. A small flutter compensation unit was constructed so that the output from a tape-recorder channel that had been shorted during recording was subtracted from any signal channel during replay. The flutter compensation unit also contained provision for a T.T.L. output in step with the square wave signal from the tape-recorder. The unit is described fully in Appendix 6.

For reliable digitisation of the tape-recorded signals, aliasing errors have to be obviated (see section 6). Bearing in mind the cost of multi-purpose anti-aliasing filters, a simple pair of filters suitable for this particular study, was constructed. They are described in Appendix 7.

The complete recording and digitising system is outlined in Fig. 6.4.

The frequency characteristics of the system were as follows:

Tape recorder	: D.C. - 5 kHz \pm 0.5 dB
Charge amplifiers	: Time constant set to 1 sec (can be increased) with highest frequency 50 kHz (20 kHz \pm 1 dB).
Load cell accelerometer	: DC - 20 kHz.
Head accelerometer	: DC - 1.3 kHz
Force transducers	: DC - to calculated lowest resonant frequency of 1.7 kHz (with 100 kg load).

Accurate determination of the lowest resonant frequency of the complete measuring cell proved very difficult. With a 70 kg load, the lowest resonant frequency appeared to be about 1 kHz with a lower limit of about 500 Hz. (as indicated by applying a transient force and observing the system response).

The limitations on the complete system were therefore:

Lowest resonant frequency	: approx. 500 Hz.
Shortest time constant	: 1 sec.

6.4 Subjects

Due to the nature of the experiments, only a small pool of subjects was available. However, in experiment 4, subjects were chosen to represent a variety of statures and weights.

Strict attention was paid to subject safety. Each subject was asked to sign a written agreement to partake in the study and comply with laboratory rules as a means of emphasising the need to regard safety seriously. As part of the acceptance procedure the subject completed a medical questionnaire with the experimenter. This resulted, in effect, in a structured interview to investigate possible contra-indications to participation. The subject was made aware of the aims and dangers of the experiment and it was made clear that he could halt the experiment at any time without explanation. The subject held a 'halt button' to stop the vibration directly. At all times the facility was manned by the experimenter and a 'second operator'. One of the above worked at the control console, the other attended the subject with instructions to halt the experiment if he considered the subject to be in difficulty or if the subject asked for the experiment to be halted.

These procedures satisfied B.S. DD 23:1973. The vibration levels were kept below the I.S.O. "fatigue - decreased proficiency" level relevant to the estimated time of exposure for the experiment. (Again to satisfy DD 23).

The subjects were measured for weight and stature in the sitting and standing positions. Sitting weight is difficult to measure and the values must be considered approximate. The measured values are given with the details of each experiment.

6.5 Postures and constraints

In section 4.2 consideration of the effects of postural change and body constraints were mentioned. Here, an attempt was made to use repeatable conditions, and these are described below.

"Erect Posture": The subject sat on the load cell using the bead bag (see section 4.2.4). The cell was positioned so that with the subjects back touching the seat back, the ischial tuberosities were situated

approximately between the rear load transducers of the load cell. The subject was asked to position his feet comfortably but such that the back of the lower leg was approximately vertical. The foot rest was then adjusted in height so that the upper surface of the thigh was horizontal. The subject was asked to hold his hands loosely on the thighs or in the lap. The experimenter then squatted close to the chair so that the subject's back could be seen clearly in profile. He instructed the subject to hold his back reasonably erect but without undue muscle tensing. The experimenter then gave the subject further instructions until the back was indeed approximately vertical and lightly touching the seat-back webbing (this sometimes necessitated further adjustment of the load cell):

"Very Erect Posture": This posture was essentially the same as the 'erect' posture, but the subject was instructed to tense his back and trunk muscles significantly and attempt to "stretch" his head/neck from his trunk. This probably involved some change in pelvis and spine position and initially, at least, subjects tended to hold the breath in. Observation of the head accelerometer position (horizontal for 'erect' posture) showed that the head tilted back slightly (10° to 15°) in the 'very erect' posture.

"Slumped Posture": The leg position was unaltered from 'erect', but the subject was instructed to loosen his spine and shoulders and allow the head to droop forward slightly.

For all these postures, the subject was asked to hold them as constantly as possible during the time of exposure. The experimenter checked that visible changes did not occur.

"Abdominal restraint": A length of stiff, 50mm wide nylon webbing was wound tightly around the abdomen for several turns. The lower turns pressed down on the pelvis, the upper turns pressed on the lower ribs. The aim of the arrangement was to constrain the visceral tissues to move vertically. In the event, the constraint tended also to support the rib cage on the pelvis and offer a new route for vibration transmission.

"Buttock short circuit": Two hardwood blocks (50mm x 50mm x 33mm high) were machined to have a spherical indentation 8mm deep in the upper surface. The blocks were positioned, one under each ischial tuberosity. The

indentation ensured that the ischial tuberosities stayed in position on the blocks so that the rest of the buttocks lost contact with the load cell (bead bag removed). The aim of this arrangement was to transfer all the vibration energy (apart from that through the legs) via the small amount of tissue over the ischial tuberosities rather than the buttocks generally.

"Buttocks loaded": Instead of the bead bag, the subject sat on a piece of 25mm wood which was located well forward so that the body weight was carried on the gluteal muscles with the ischial tuberosities located behind the wood and taking no load. (In experiment 1, the subject sat on 25mm wood with two holes (approx. 50mm diameter) to locate and unload the ischial tuberosities) Lindan et al. 1965 showed that if the feet were allowed to hang free, or the subject leant forward, or cut-outs were made for the ischial tuberosities, then the load was distributed relatively evenly over the whole buttock and thigh area. With the feet supported to approx, 20% body weight, the load was concentrated about the ischial tuberosities and the rear portion of the buttocks.

"Driving position": The erect posture was held (i.e. legs not in pedal positions), excepting that the arms rested with the wrists supported on a framework such that the arms were in the same position as when holding a truck steering wheel. The posture was designed to avoid arm muscle activity and significant vibration input through the arms. The intention being to investigate arm position and the inertial effects of the arms only. The hand rest framework could be fitted to the chair and vibrated, or fixed in space.

"Arms restrained": Guignard & Irving 1960 contended that shoulder 'shrugging' was an important element of movement during vibration. An attempt was made to restrict this movement by crossing the arms over the chest of the subject (hands to collar bone) and enclosing the arms, upper chest and shoulders in a 165mm wide, tight fitting elasticated belt.

"Additional Weight": It appeared feasible that the response of certain parts of the body might be altered by adding mass. For instance, if the spine is the dominant structure in terms of elasticity, then addition of a load at the shoulders should lead to a lower resonant frequency, whereas a load at the waist should behave as an unsprung mass. To investigate this possibility, strips of lead were bound together to form a long flexible

mass that could be moulded to the body. Two weights, each of 5kg, were constructed. To add 10kg to the shoulders, one weight was moulded to rest vertically over each shoulder, close to the neck. To add 10kg to the pelvis, both weights were moulded to rest horizontally around the waist and on the pelvis.

6.6 Experiment 1

One subject (No. 83) was exposed to random vibration (power in spectrum falling off with frequency) at approx. 2.3 m/s^2 rms (unweighted) unless noted otherwise. Acceleration at the head was measured with the harness described in section 5.2.2 (care being taken that the accelerometer was positioned in the horizontal plane) and also with a dental bite arrangement. In the latter case the accelerometer was bolted to a thin aluminium plate shaped to fit the mouth and allow tongue movement. The plate carried a thick layer of hot setting dental wax. The unit was adapted to the subject by heating the plate in boiling water to soften the wax sufficiently for the subject to bite on to the unit and leave a dental impression. In this way the bite could be held firmly but comfortably by the subject's teeth during the experiment, so that there was effective contact between the plate and skull. The accelerometer was positioned approximately 2cm in front of the teeth.

The aim of the experiment was to investigate changes in apparent mass with posture and to compare the two common techniques of head acceleration measurement in transmissibility experiments.

The order of the postural conditions was as below. The exposure for each condition was approximately 1 min. This subject tended to hold a slightly rounded back in the 'erect' posture.

<u>Run No.</u>	<u>Condition</u>
83/05	Erect posture (low level stimulus $\approx 1\text{m/s}^2$)
83/06	Erect posture
83/07	Subject asked to assume most uncomfortable posture (w.r.t. vibration). He stiffened his back, which then lifted away from the backrest.
83/08	Subject asked to assume most comfortable posture. He slumped slightly and his head rotated forward a little.
83/09	Erect posture, but a sheet of hardboard was inserted between back and webbing backrest (to increase friction). Subject instructed to lean back into backrest.
83/10	Erect posture, but feet pulled forward on footrest so that lower legs at 30° to vertical.
83/11	Erect posture.
83/12	Erect posture with buttock short circuit.
83/13	Driving position - hand-rest vibrated.
83/14	Driving position - hand-rest fixed in space
83/15	Erect posture, hands held above head, arms slack
83/17	Erect posture, but foot rest raised by approx, 100mm so that knees lifted.
83/18	Erect posture, 10kg. on shoulders.
83/19	Erect posture.
83/20	Erect posture, 10kg on pelvis.
83/21	Erect, buttocks loaded, 10kg on shoulders.
83/22	Erect, buttock loaded only (as comparison with 83/21).
83/23	Erect
83/24	Erect with abdominal restraint
	Lunch
83/27	Erect posture normal vibration level - 2.3 m/s^2 rms
83/28	Erect posture low vibration level - 1.1 m/s^2 rms
83/29	Erect posture, stimulus spectrum shaped +6db/octave - 2.3m/s^2 rms
83/30	Erect posture, stimulus spectrum shaped + 6dB/octave - 1.1 m/s^2 rms

Subject Details:

	Weight (kg)		Height (cm)	
	Standing	Sitting	Standing	Sitting
Subject 83	77	59	173	90

6.7 Experiment 2

Two subjects (S1 and S2), partaking in a study of intra-abdominal pressure changes during impact - Cole 1978, were available with the measuring system. Each subject had swallowed an intra-abdominal pressure 'pill' some time prior to exposure and the pressure signal was transmitted via an aerial around the waist. It was estimated that at the time of exposure, the pill was located in the lower intestine.

The aim of the experiment was to investigate changes in abdominal pressure during vibration in order to give some information on visceral movements. The intra-abdominal pressure signal was treated in the same way as the cell force signal, so that the resulting transfer function relates pressure to seat acceleration. Dynamic calibration was not possible, and the results should be considered only in terms of relative pressure changes with frequency and posture.

The order of exposure was as below:

<u>Run No.</u>	<u>Condition</u>
S1/01	Erect posture
S1/02	Erect with buttock short circuit
S1/03	Erect posture
S2/01	Erect posture
S2/02	Erect with buttock short circuit
S2/03	Erect
S2/04	Erect with abdominal restraint

Subject details:

	Standing Weight (kg)	Standing Height (cm)
Subject S1	62	178
Subject S2	No details available	

6.8 Experiment 3

One subject (01) was exposed to random vibration at approx. 2 m/s^2 rms (unweighted). The apparent mass transfer function was measured at the feet using the foot rest described in Section 5.2.3. Calibration was carried out in the same way as for the normal measuring cell, using a

20kg. weight. The aim of the experiment was to explore further postural changes in preparation for experiment 4 and to attempt to find a posture where the input transfer function and transmissibility were identical (indicating a direct vibration transmission path). Runs 13 and 14 were to consider the possibility of active control of the situation with longer exposure and exposure to a simple stimulus. On several occasions the subject was asked to assume the erect posture with the aim of testing the repeatability of response in a simple posture.

The order of postural conditions was as below.

<u>Run No.</u>	<u>Condition</u>
01/01	Erect posture
01/02	Very erect
01/03	Slumped
01/04	Erect with buttock short circuit
01/05	Very erect with buttock short circuit
01/06	Erect, buttocks loaded
01/07	Erect
01/08	Erect with abdominal restraint
01/09	Erect
01/10	Erect with arms restrained
01/11	Erect with arms restrained and buttock short circuit
01/12	Very erect with arms restrained and buttock short circuit
01/13	Erect (5 min. exposure)
01/14	Erect 5Hz. sinusoidal stimulus, (5 min. exposure)

Subject details: see section 6.9.

6.9 Experiment 4

In this, the final experiment reported here, six subjects were exposed to random vibration at 1m/s^2 rms ($\pm 5\%$) (unweighted). The measures taken were apparent mass at seat and feet, and seat to head transmissibility (using the harness described in section 5.2.2). All followed the same programme of changes in posture, with the same aims as experiment 3 - to isolate the spinal transmission path and to consider how repeatable are the results when subjects are asked to assume the same posture on a number of occasions. Three orders of presentation were used, in case this affected the repeatability in the simple posture.

7. RESULTS OF EXPERIMENTS 1 TO 4

The results are presented in graphical format, despite the resulting problems in data comprehension. Rowlands 1974 attempted to reduce such data by using only the magnitude at the first two resonance points, and Lawes 1974 by using data from resonances and anti-resonances only, whilst Osborne 1978 used a curve-fitting approach to treat equal comfort contours. Such approaches were considered, but rejected as they were insufficient to truly represent each response, which involved amplitude, phase and frequency dimensions.

To reduce the volume of data presented, only group response spectra and some individual results are given here. A complete set of validation data for experiment 4 is presented in appendix 9. This may be regarded as a definitive set of results representative of all the experimental work.

The results of each experiment are presented separately below. The following coding is used:

E - Erect posture
 VE - Very erect posture
 Sl - Slumped posture
 Ab - Abdominal restraint
 Ar - Arms restrained
 Bs - Buttock short circuit
 Bl - Buttocks loaded
 Dr - Driving position
 Wt - Additional weight.

7.1 Results of experiment 1

Fig 7.1 Typical validation graphs.

Fig 7.2 Validation for run with improved spectral shaping.

Fig 7.3 Coherence functions for apparent mass and two measures of transmissibility.

Table of figures to compare conditions (see also section 6.6).

Conditions compared	Fig. No.		
	App. Mass	Trans. head	Trans. bite
Four consecutive measures holding E posture	7. 4	7. 6	
Five different runs (over @ 3 hrs): E posture	7. 5	7. 7	7. 8
E/Most uncomfortable/most comfortable	7. 9	7.10	7.11
With backrest/feet forward/E	7.12	7.13	7.14
Bs/E (2 runs)	7.15	7.16	
Bs/Bl/E	7.17	7.18	
Ab/E	7.19	7.20	
Wt shoulders/wt pelvis/E	7.21	7.22	
Bl, Wt shoulders/Bl/E	7.23	7.24	
E/Hands above head	7.25	7.26	
E/Dr hands vibrated/Dr hands fixed	7.27		
E, normal and low vibration levels, shaped and unshaped.	7.28		

Fig 7.029 Comparison of apparent mass, transmissibility to the head harness and to the dental bite.

7.2 Results of experiment 2

Table of figures to compare conditions.

Conditions compared	App. Mass	Transmissibility	Pressure function
S1: 2E/Bs	7.29	7.30	7.31
S2: 2E/Bs/Ab	7.32	7.33	7.34

Comparisons of the response functions apparent mass (transposed to unit gain), transmissibility, abdominal pressure transfer:

Fig 7.35 : Run S1/01 (E)

Fig 7.36 : Run S1/03 (E)

Fig 7.37 : Run S2/01 (E)

Fig 7.38 : Run S2/03 (E)

7.3 Results of experiment 3

Table of figures to compare conditions (see also section 6.8)

Conditions compared	Fig. No.		
	App. Mass	Transmissibility	App. M. Feet
Four different runs (E)	7.39	7.40	7.41
Mean E/VE/S1	7.42	7.43	7.44
Mean E/Bs/B1	7.45	7.46	7.47
Mean E/Ab	7.48	7.49	7.50
Mean E.Ar/Bs/Ar,Bs	7.51	7.52	7.53
Mean E/VE/VE,Bs/VE, Bs, Ar	7.54	7.55	7.56

Comparisons of the response functions - apparent mass (transposed to unit gain), transmissibility, and foot apparent mass:

- Fig 7.57 : Run 01/07 (E)
- Fig 7.58 : Run 01/02 (VE)
- Fig 7.59 : Run 01/10 (Ar)
- Fig 7.60 : Run 01/05 (VE, Bs)
- Fig 7.61 : Run 01/12 (VE, Bs, Ar)

7.4 Results of experiment 4

Table of figures to compare conditions

Conditions compared	Fig. No.					
	Subject 81	Subject 82	Subject 85	Subject 84	Subject 83	Subject 01
App. Mass: 4E	7.62	7.63	7.64	7.65	7.66	7.67
Transmissibility: 4E & mean	7.68	7.69	7.70	7.71	7.72	7.73
App. Mass: Dr/E @ 2 m/s ²	7.74	7.75	7.76	7.77	7.78	7.79
App. Mass: Bs/Ar/Ab	7.80	7.81	7.82	7.83	7.84	7.85
App. Mass: Bs/Bs,Ar/Bs,Ar,Ab	7.86	7.87	7.88	7.89	7.90	7.91
Transmissibility: Mean E/Bs,Ar/Bs,Ar,Ab	7.92	7.93	7.94	7.95	7.96	7.97
App. Mass: VE/VE,Bs,Ar/VE,Bs,Ar,Ab	7.98	7.99	7.100	7.101	7.102	7.103
Transmissibility: VE/VE,Bs,Ar/VE,Bs,Ar,Ab	7.104	7.105	7.106	7.107	7.108	7.109
Those below compare apparent mass with transmissibility (both converted to unit gain)						
Representative of E curves	7.110	7.111	7.112	7.113	7.114	7.115
VE	7.116	7.117	7.118	7.119	7.120	7.121
Bs	7.122	7.123	7.124	7.125	7.126	7.127
Ve,Bs,Ar,Ab	7.128	7.129	7.130	7.131	7.132	7.133
Those below compare all postural conditions against the range of values for the erect posture.						
Apparent Mass: Bs,Ab,Ar,/Bs,Ar/,VE,/VE, Bs,Ar/Dr	7.134	7.135	7.136	7.137	7.138	7.139
Transmissibility: Bs,Ab,Ar,/Bs,Ar/,VE,/VE,Bs, Ar	7.140	7.141	7.142	7.143	7.144	7.145

8. DISCUSSION OF RESULTS OF EXPERIMENTS 1 TO 4

8.1 Experiment 1

The validation graphs (e.g. fig 7.1) showed that with the random stimulus used, the vibration signals could be considered normally distributed with signal levels reasonably good over the frequency band. Coherence values were of the order of 0.9. The runs with the input spectrum shaped to give slightly more energy at high frequencies proved useful (fig 7.2). The coherence was much improved, apart from the lowest two frequency points (0.8 and 1.2 Hz) and values were mostly better than 0.95. It seemed reasonable to assume that only minor shaping was needed to lead to good coherence across the range of frequencies of interest.

However, the validation graphs for transmissibility showed the coherence values to be much lower. Fig 7.3 illustrates a typical set of coherence values for one run (i.e. simultaneous measurements). The signal levels were again good, apart from the 20-25 Hz region, and one must assume that the low coherence relates to true non-linearity. The pattern of very low values about 5Hz for transmission to the dental bite occurred on nearly all runs and coincided with marked changes in the response function (Fig 7.8).

In one condition the subject held the same erect posture for four minutes and the resulting apparent mass spectra were closely similar (Fig 7.4). During the experiment, the subject was asked to revert to the basic, erect, posture several times (over a period of nearly 3 hours, as lunch intervened). The resulting apparent mass spectra (Fig 7.5) differed slightly, in terms of magnitude rather than shape. As might be expected, the differences were greater than those between four continuous measurements. A similar pattern was evident for transmissibility, although variability was greater at the higher frequencies where the coherence was poor.

A secondary aim of this experiment was to investigate the postural differences noted by Griffin 1975, Rowlands 1977, and Frolov 1970. For uncomfortable and comfortable postures, Griffin 1975 observed a difference of the order of 2.5:1 (i.e. 8 dB) at 7Hz with increasing differences with increasing frequency. A similar, but less marked effect was found for transmission to the bite (Griffin used a bite bar) see Fig 7.11. However,

from Fig 7.11 it is apparent that the differences at lower frequencies are less. Indeed Figs 7.9 and 7.10 would suggest that the general differences in response are probably of no practical significance. Rowlands 1977 measured transmissibility with a head harness similar to that used in this experiment and observed a marked reduction in transmissibility between 7 and 20Hz if no backrest was used, and an increase at about 4Hz if the legs were pulled forward (with backrest). No marked effects were noted here (fig 7.13), although the use of a backrest clearly reduced the seat forces at low frequencies (fig 7.12). Frolov 1970 demonstrated large changes in transmission if the hands are held above the head. Figs 7.25 and 7.26 show that this was so in this experiment also, with a marked difference in both magnitude and resonant frequency for apparent mass and transmissibility. These comparisons serve to demonstrate that differences in transducer location and postural control can lead to markedly different results between authors.

Of the basic postural changes (Buttocks short circuited, buttocks loaded, abdominal restraint), the "short circuit" of the buttocks seemed to have the greatest effect - it tended to reduce the apparent mass and increase the resonant frequency from approx. 4Hz to 5Hz. This suggested that the buttocks do have a significant role in dynamic response. The use of an abdominal restraint led to emphasis of a 'resonance' at approx. 8Hz. However, the resonance effect at 8Hz apparent on the control run (83/23) is not a common feature of the other runs and may relate to some other postural change during this period of the experiment. The use of a 10kg mass to modify tissue characteristics proved inconclusive. Fig 7.21 shows an increase in apparent mass of about 10kg up to the resonance frequencies. This suggests that the system simply stiffens in reaction to the static load increase so that the overall dynamic characteristics (e.g. resonant frequency) do not change. Fig 7.27 indicated that a relaxed driving posture had little effect. Fig 7.28 confirmed previous results that the effect of changes in stimulus level and spectrum were of the same order as those to be expected from different runs with the same nominal posture i.e. posture of greater significance than non-linearity in response. In general, raising the arms above the head produced the greatest change in response with the buttock short circuit a close second.

A remarkable feature of figs 7.9 to 7.26 is the similarity between the apparent mass response function and the transmissibility function for the same condition, especially if expected changes in mass are taken into

account. Fig 7.29 shows that this only applied to transmission to the head harness. The increase in difference of phase angle with frequency could be explained by a time-lag between force at the seat and acceleration at the head.

The results were used to aid the design of later experiments by suggesting the following:

Further spectral shaping of the stimulus could lead to significant improvement in coherence as noise effects are reduced.

The transmissibility measured with a head harness might prove a useful adjunct to apparent mass measures, provided care was taken with accelerometer location, particularly so if coherence could be improved. The use of a dental-bite mounted accelerometer was not considered reliable (see also appendix 3).

The use of blocks under the ischial tuberosities changed the response function significantly. It appeared that the buttocks played an important part in the biomechanical response, yet their action could be by-passed by using the blocks. The use of such blocks might allow one to investigate spinal responses more directly.

8.2 Experiment 2

Unfortunately the results for intra-abdominal pressure were unreliable compared with the other transfer functions. The coherence function was of the order of 0.9 for the middle frequencies, but fell off rapidly at high and low frequencies. Only those parts of the response function where the coherence was of the order of 0.9 are shown in figs 7.35 to 7.38. The pressure response proved a good example of the value of the coherence function: breathing affects the intra-abdominal pressure so that one might expect breathing effects at about 0.2Hz. and perhaps slightly higher frequencies. Breathing, however, is an extraneous stimulus as regards the vibration so that the transfer function is non-linear. In this case, the low values of coherence function have indicated the presence of this non-linearity and the resulting erroneous data at low frequencies.

The validation data confirmed that further shaping of the stimulus

spectrum would lead to improved coherence for the apparent mass, values being often near unity. However, the transmissibility results did not improve, especially for subject S1. The transfer function curves showed a similar dip (@ 7Hz) as for the dental bite data in experiment 1. The coherence function likewise was low at about 5Hz.

The effects of the two constraints (buttock short circuit and abdominal restraint) were not so clear cut as in experiment 1. The abdominal restraint simply served to reduce the apparent mass at high frequencies (S2). The buttock short circuit had no significant effect on the apparent mass and indicated increased damping on the transmissibility. The abdominal restraint tended to increase the pressure transfer. This suggests that in the normal situation, some pressure is taken up in expansion of the abdominal walls.

Both subjects exhibited peaks in transmissibility in the region of 12 Hz although the apparent mass functions were generally similar to those for subject 83.

The pressure functions indicated resonance phenomena arising at the same frequencies as for the apparent mass and transmissibility. For subject S2, the character of the pressure function is remarkably similar to that of the other response functions.

8.3 Experiment 3

Experiment 3 focused on an attempt to measure the response at the feet, but was also regarded as preparation for experiment 4.

Measurements of the apparent mass at the feet proved possible and resonance phenomena at around 5Hz were observed. The validation curves demonstrated that near unit coherence could be obtained for the whole body apparent mass. However, the coherence functions for both transmissibility and foot response were also very good (@ 0.9) apart from some poor coherence at low frequencies for the foot response.

Experiment 3 included a further five minute exposure, and as in experiment 1 the response functions changed very little over that time (including feet) and this applied to the sinusoidal stimulus also. However, comparison of the four attempts to hold the erect posture showed

that the spectra for three runs were closely similar, whilst the fourth run (01/09) gave a different response for apparent mass and transmission Figs. 7.39, 7.40. Although no unusual behaviour had been observed during the run, it was assumed that the subject had changed his posture in some way. The results of the other three runs were considered sufficiently similar to justify taking a mean value at each frequency to give a representative curve for comparison with other conditions. In the case of the foot response (Fig. 7.41), the differences between the four runs were greater and run 01/09 was not significantly different so that the envelope was used for comparison with other conditions. The general form of the apparent mass function for Subject 01 was similar to that for subjects 83, S1 and S2. However, the transmissibility curves again showed a peak in the 12Hz region (as S1 and S2), not seen in subject 83.

The apparent mass measured at the feet showed that resonance phenomena did occur in the legs. The response function was similar to that for the whole body apparent mass with a peak at about 5Hz although it suggested greater damping and a greater unsprung mass relative to the total mass. There was little difference between the results for different conditions, suggesting that the reactions at the feet related little to the upper trunk condition. It was expected that the foot function could be used to inspect changes in trunk centre of gravity shift by comparison of the apparent masses at the lower frequencies. Unfortunately, this proved suspect. In most cases the total mass at the feet (as obtained from the apparent mass at low frequencies) was of the order of 22 kg, and of the trunk (from seat apparent mass) 58 kg. This would lead to a total mass of 80 kg compared with a measured standing weight of 70 kg. The measured sitting weight was 51 kg against the 58 kg obtained from the apparent mass. It was concluded that foot measurements be continued as they gave information on a possible additional input to the trunk (although the reverse might be the case!), but that their value as an indicator of centre of gravity shift was likely to be minimal.

The changes in response to the various constraints were again less apparent than for subject 83. Both buttock restraints had little effect, although of the two the 'buttocks loaded' condition had the greater effect (i.e. the reverse situation to subject 83) Figs. 7.45 - 7.47. The abdominal restraint again emphasised resonance at about 10Hz - Figs. 7.48, 7.49.

In an attempt to isolate spinal responses, the 'very erect' posture was included. In the normal situation this increased the apparent mass at high frequencies and led to a marked increase in transmissibility at the second resonance frequency (@ 12Hz) - Fig 7.42 and 7.43. When the buttocks were short circuited, (again in an attempt to isolate spinal responses) the change in response was small for both the 'erect' and 'very erect' postures. Restraining the arms - Figs. 7.51, 7.52 led to a similar result to that observed when subject 83 was asked to raise the arms above the head - generally increased damping effect and twin resonance peaks.

Comparison of the whole body apparent mass and transmissibility curves proved interesting. As in the case of subject 83, they were generally very similar, although only to about 8Hz (just beyond the first resonance peak). The transmissibility exhibited a clear second resonance in the 10-15Hz region, the magnitude of this peak being equal to or greater than that of the first.

8.4 Experiment 4

A complete set of validation curves for experiment 4 is in appendix 9. The coherence function for apparent mass proved to be consistently high at between 0.97 and unity. Only for the occasional run, and occasional frequency point did the coherence function fall to about 0.9. The coherence function for the transmissibility was usually of the order of 0.9 at high frequencies and better below about 7Hz. However, it was usually very low at the highest frequencies and occasionally across many frequencies. In general, the coherence values were higher than anticipated from experiment 1, but the transmissibility function still could not be considered fully reliable. The coherence values for the apparent mass measured at the feet did not live up to the expectations engendered by experiment 3. Although values close to unity could be observed, very low values also occurred, especially at low frequencies (possibly as a result of postural sway). This response function could not be considered reliable.

In general, the shape of the apparent mass function was similar between subjects and conditions. However, the shape of the foot response function and transmissibility varied a great deal between subjects and conditions.

Figures 7.62 to 7.67 show that the apparent mass changed little when the erect posture was assumed several times over the period of the experiment. However, the variation was greater than that seen in experiment 3, and the use of a simple mean was not considered justified. The variability in transmissibility (Figs. 7.68 to 7.73) was greater. For comparison between apparent mass and transmissibility, a run of the erect group was chosen whose apparent mass was representative of the four runs. For comparison of conditions, an overlay containing the curves for the four erect runs was prepared and compared with each condition. The following procedure was followed. If a marked digression from the four erect runs was observed, then all the curve was added to the overlay. If digression was observed in a combined situation (e.g. Bs,Ar) then the component curves were added, even if similar to the erect posture. The resulting diagrams are presented in Figs. 7.134 to 7.145.

The basic (i.e. E) apparent mass curves were similar in shape with a relatively clear resonance at about 5Hz and usually a point of inflexion between 9 and 12 Hz. The curves for subject 84 were clearly of two distinct types. Only the buttocks short circuit condition (Bs) led to changes of any consistency across the subject group, with reduction in magnitude and increase in phase angle at the higher frequencies. Only for one subject (84) did the very erect posture have a marked effect. In four cases (81, 82, 83, 01), a combination of postural changes led to a marked effect. This combination was the Bs,Ar position, with or without the V.E. posture. There seemed to be some dependence of Bs,Ar on the Bs effect, but no clear pattern was evident. On two occasions the driving posture led to low levels at low frequency, as though a reduction in upper body weight had occurred.

The transmissibility curves varied extensively, and despite the acceptance of only very marked changes a number were plotted. The general shape for the erect postures varied between subjects, some showed a clear maximum at about 5Hz, some a clear second maximum at about 12Hz. However, some (e.g. 85) showed little sign of either. The Bs, posture did not affect the curves significantly. The very erect posture usually led to a marked increase in magnitude at the high frequencies, often as an accentuation of the second resonance point. The combination posture Bs,Ar often led to marked changes with two or three resonance points quite different from the other conditions. The changes due to Bs,Ar did not appear to relate direction to the individual components Bs and Ar.

In general, the effects of postural change were disappointingly varied and did not live up to the expectations of the previous experiments.

Comparison of the apparent mass and transmissibility curves Figs. 7.110 to 7.133 again showed the two to be similar up to and including the first maximum. This applied to all of the four conditions studied (E/VE/Bs/VE,Bs,Ar,Ab). The transmissibility curves usually had a pronounced maximum at about 15Hz not evident on the apparent mass curve. At frequencies greater than the first resonance point, the phase angle curves showed a distinct separation for the erect posture, with apparent mass phase reducing (unsprung masses?) and transmissibility phase increasing. This was not so marked in the other postures.

9. THE APPARENT MASS FUNCTION

Knowledge of the apparent mass of man is useful in design for vibration attenuation. However, the known inter and intra subject variability reduces the value of the function until that variability is well understood. This suggests that a better understanding of the biomechanical source of the apparent mass function is required. However, the apparent mass (as compared with transmissibility) gives information on the forces involved so that the better understanding should lead to information on vibration as a possible source of pain and injury in the low back.

The two main characteristics of the human frequency response function were the first peak (or resonance) at about 5Hz, and a secondary peak or point of inflexion between 9 and 12Hz. The latter was more pronounced for transmissibility. The question posed is "what anatomical structures are primarily responsible for these characteristics?" The actual resonant behaviour of the anatomical structures is by no means well understood. Von Gierke 1964 and Von Gierke & Coermann 1963 suggested that the behaviour related to the motion of the mass of the upper torso supported by the elastic structure of the spine at 8Hz, and the motion of the abdominal mass restrained by the elasticity of the abdominal wall, diaphragm and lung plus thorax at 4-8Hz (see Fig. 2.2). As regards tolerance they separated three areas - spine, abdomen at 5Hz, lumbosacral at 10Hz and head at 30Hz. Guignard & Irving 1960 considered the 5Hz maximum in transmissibility to be due largely to resonance of the upper torso and shoulder girdle. They observed a "shrugging motion of the shoulders, with articulation at the sternoclavicular joints, nodding of the head and anteroposterior flexion of the upper spine" (Guignard & King 1972). They also noted that seat-shoulder transmissibility was greater than seat-head transmissibility. Guignard & King concluded that there was no simple explanation of the 4/5Hz resonance, it being probably due to a combination of thoraco-abdominal visceral motion and pectoral girdle motion. They considered the 11-14Hz resonance to be associated with axial compression of the torso, and controlled by the elastic properties of the spinal column and supporting musculature. Belytschko & Privitzer 1978 concluded from their modelling studies that the resonance seen at 5Hz results from a combination of three factors: compression at the buttocks or man/seat interface, flexural response of the spine, axial response of the viscera. They considered that the buttock resonance masked many of

the other resonances in impedance measurements and found that axial compression of the spine could lead only to resonances at much higher frequencies. They assumed the viscera to be incompressible, but restrained by elastic abdominal walls so that the end result was hydrodynamic behaviour. Frolov & Potemkin 1975 assumed the curved spinal column (especially the lumbar spine) to be a basic structural element, and Huijens 1977 demonstrated that transverse (but not longitudinal) standing waves at frequencies of the same order of magnitude as observed in practice would exist in the spine (his range of values were 0.4 to 12Hz). Pope et al 1980 suggested that the sacroiliac joint could act as a vibration absorber. From measurements with rhesus monkeys, Broderson & Von Gierke 1971 used stroboscopic techniques to observe resonances in the abdominal viscera and spine at 6 and 8Hz respectively. They also observed mass-like behaviour at high frequencies in the impedance function. This they attributed to the pelvis (or soft buttock tissues in man), and Belytschko & Prévitzer 1978 included a 16.2 kg mass-like pelvis in their model. Yeager et al 1969 contended that the buttocks were the primary source of resonance.

The apparent mass responses measured in this research were similar to those found in the literature. In Fig. 9.1 the results for the erect posture for the six subjects have been normalized for frequency and magnitude (see section 10). In Fig 9.2, the results shown in Fig. 9.1 have been shifted to normalize for subject weight and the boundaries superimposed on the results of other authors (Fig. 2.29). It is apparent that the results of this research are not markedly different so that it is safe to use them as a source of information to clarify understanding of the input frequency response.

As regards changes with posture, few authors have compared more than 'erect' and 'relaxed' (erect postures shifting the response spectrum slightly upwards in frequency). Only Miwa 1975 compared other postures. Those relevant here were the use of added weights and the difference between feet supported and free. In the latter he found an expected (unsprung mass) increase in apparent mass at low frequencies as the full body weight was supported by the measuring cell with the feet unsupported (Fig. 2.13). Thus, the position of the feet may be a source of difference between authors. For instance, subjects had their feet unsupported in Coerman's experiments, and a modification to the curve in Fig. 2.29 to take this into account would probably bring the Coerman curve

closer to the others. Coerman's research was in a military aircraft context, and the feet unsupported condition may have related well to the pilot restrained in an ejection seat. However, in most transport situations the feet are supported so that measurements with the feet unsupported are not representative and merely serve to add an unknown variable, as well as introduce postural changes in the low back and increase the proportion of load taken on the thighs. If we compare Figs. 7.21 and 4.28 with Miwa's results in Fig. 2.14, the effect of weights carried at the waist are clearly similar at frequencies beyond the major resonance. The lack of effect at low frequencies in Fig. 2.14 is unexpected. One would expect differences of 8, 16 and 24 kg as the total load carried by the cell increases by these amounts (as seen in Figs. 7.21 and 4.28). One has to question Miwa's data in this respect, but no explanation can be offered.

To facilitate discussion of the effects of the postural constraints used here, their expected effect on the body and the observed changes in response (including the pilot studies), are summarised in table 9.1.

These findings can be used to throw some light on question of the anatomical structures as sources of resonance. Clearly, several structures need consideration: the buttocks and thighs, the abdominal tissues, the spine, the pectoral girdle and the head and neck. These are dealt with separately below:

9.1 The buttocks and thighs

The contention of Yeager et al 1969, that the buttocks are the primary source of resonances must be placed in the context of their model with a 10Hz resonant frequency. An important piece of evidence in their argument was a graph of buttock compression v load. This was based on an experiment with an 80 kg man, and no details of the experiment were supplied. The graph shows increasing stiffness with load up to the maximum (80 kg) although a linear relationship appears to be developing at this level. A reliable estimate is difficult, but the stiffness at 80 kg load would appear to be between about 100 kN/m and 300 kN/m. Loaded with an 80 kg mass, a spring of 300 kN/m would have a resonant frequency of 9.75 Hz - hence the conclusion of Yeager et al.

Table 9.1. Summary of observed effects of posture

Posture	Description	Effect
V.E.	Spinal musculature tensed. Pelvis rotated forward. (Hence lumbar lordosis greater and more load on buttocks) Abdominal muscles tensed. Head back 10° to 15°	First resonant peak increased in frequency (1Hz) or amplitude (2dB). Phase angle beyond resonance greater. (3 obvious cases) Second resonance in transmissibility enhanced (3 cases)
Sl	Spine in flexion Muscles relaxed Head forward.	No significant effects
Ab	Abdomen pulled in. Abdominal walls supported Upper trunk supported.	Second resonance enhanced slightly. (Both apparent mass and transmissibility) (4 cases)
Bs	Trunk supported on thin layer of tissue at ischial tuberosities. No load on buttocks and thighs.	Change at higher frequencies as if reducing unsprung mass. No effect on transmissibility (5 cases)
B1	All load on buttocks and thighs.	No significant effects
Dr	Inertial effects of arms included.	No significant effects. (1 case only)
Ar	Reduce shrugging slightly and stiffen shoulder muscles	Effect in 2 cases, but contradictory.
Bs,Ar & Bs,Ar,VE	Combined situation	Introduced multiple resonances and/or increased values at higher frequencies. Both apparent mass and transmissibility. (3 cases)

However, their buttock deflection data (being the only available) merits further attention. If one takes the mass to be 55 kg (the mean sitting weight of the subjects in experiment 4), the two extreme stiffness values lead to resonant frequencies of 6.8Hz and 11.8Hz respectively. If the buttocks as a whole were important one would expect a marked difference in response between postures where body weight is spread over the buttocks, or concentrated on the ischial tuberosities. If one assumes that their buttock measurement was carried out under the same conditions as the main experiment (flat wooden seat, feet unsupported), then the above data can be taken to relate to the former condition and represent the lower extreme of resonant frequencies to be expected in these studies (feet supported, with bead bag).

Modelling studies of Chow & Odell 1978 suggest that as the ischial tuberosities take the full load (i.e. feet supported, hard seat) then the bone is separated from the seat surface by only some 2 mm of skin and tissue - with consequent marked change in compressive behaviour. At 1 m/s^2 rms 5Hz sinusoidal acceleration, the relative displacement is 2.8 mm peak to peak. Thus, if body resonances at 5Hz were solely due to buttock deflection, in postures where the ischial tuberosities take the whole trunk load then the movement would be of the same order as the 'spring' length - only acceptable as a possibility if accompanied by severe non-linearity.

All this suggests that if the buttock tissues are the prime source of resonance phenomena then: a) In postures where the load is spread over the buttocks, the resonant frequency would be somewhere between 6 and 12Hz.

b) In postures where the load is concentrated at the ischial tuberosities, the resonant frequencies would be much higher and the system non-linear.

The existence of such behaviour is not supported fully by the changes in response observed in the experiments reported here. The main effect was in the 'buttock short circuit' condition, but then the main resonances at about 5Hz were not affected and any changes were at the higher frequencies. Essentially, the Bs condition tended to reduce the unsprung mass (i.e. the high frequency apparent mass) - Figs. 7.134-139, whilst transmissibility was unaltered - Figs. 7.140-145 and the basic resonance at 5Hz remained the same. The Bs condition must approximate closely to a

position of maximum compression of the ischial tissues (condition (b) above) so that it seems unlikely that the main 5Hz resonance related to ischial tissue compression. There were minimal differences in the apparent mass 5Hz resonance or in transmissibility between the E and Bs postures, and this suggests that buttock tissue compression had no significant contribution in the E posture either. Finally, were the buttocks the primary source of resonances, then one would expect changes in the upper body (e/g. raising the arms, abdominal restraint, shoulder restraint) to have no effect at all on the response spectra - this was clearly not the case.

A simple alternative explanation is that in the normal position, the buttocks and thigh tissues rest directly on the load cell and behave as highly damped, near mass-like structures i.e. as an unsprung mass. In the Bs position, these tissues are removed from the load cell and hang from the thighs and pelvis with a dynamic behaviour similar to that of the whole body (although not sought for, or identified in these experiments, resonant behaviour in these tissues can often be observed during vibration).

The fact that there were no clear differences in response characteristics between the two subjects who tended to be endomorphic compared with the group and the two who tended to be ectomorphic (i.e. subjects 81 and 84 compared with 82 and 85), also suggests that the buttocks have minimal effect.

Thus, we can safely discard the buttocks and thighs as major sources of response behaviour, and consider tissues more remote from the vibration input.

9.2 The abdominal tissues

Noticeable visceral movements certainly occur during vibration and Magid et al 1960 related pain sensations in the abdomen to stretching of the supporting tissues. That resonance phenomena occur at 3, 4 or 5Hz is also clear - Cole 1978 cites several cases of resonance in abdominal or thoracic pressure and movement. White et al 1962 measured intra-colonic pressure during vibration and observed resonance at 4Hz, and Figs. 7.35-7.38 show that pressure in the lower intestine is maximum at 5 or 6Hz, the actual response characteristic being very similar to the apparent mass

function. The results of Coermann et al 1960 shown in Fig. 9.3 are of interest here. They suggest that the viscera move longitudinally and serve to expand and contract the abdominal and thoracic walls and to move the diaphragm with maximal effect at about 4Hz. However, with the abdominal walls restrained, movements are less and resonance appears at 7 or 8Hz. This would suggest that visceral resonances are primarily related to movements of the abdominal wall. This is supported by Coermann's measurements of impedance during vibration (Fig. 2.9) where (for the erect posture), the use of an abdominal restraint reduced the peak at 4Hz and introduced an inflexion at about 8Hz. However, although this effect was sometimes observed in these studies, it was then much less apparent and also appeared in the transmissibility function. In the one case where abdominal restraint was used in the intra-abdominal pressure measurements, the restraint led simply to a slight increase in pressure at all frequencies. The minimal effect of abdominal restraint observed in this research may have been simply as a result of the restraint design - it tended to support the ribs directly.

Thus there is plenty of evidence that resonance behaviour occurs in the abdominal viscera. However, its contribution to the apparent mass function is still unclear. Unfortunately the exact nature of the intra-abdominal pressure supportive action is not well understood (Sandover 1981). At least three possibilities can be suggested - inertial movements of the viscera combined with connective tissue and abdominal wall elasticity leads to resonance; muscle activity (e.g. transverse and oblique abdominis and rectus abdominis) fired by body resonances leads to changes in abdominal space and pressure; the viscera are compressed by pectoral and thoracic resonances. However, one can estimate the magnitude of the contribution to the apparent mass. Belytschko & Privitzer 1978 used cadaveric data to estimate the following proportions of the trunk mass -

Head	11.3% (5.6 kg)
Thorax (T10 to T1)	25.0% (12.4 kg)
Viscera (L5 to T11)	25.7% (12.8 kg)
Other abdominal tissues (mostly spinal) (L5 to T11)	5.5% (2.7 kg)
Pelvis (Arms excluded)	32.6% (16.2 kg)

The apparent mass at resonance is usually some 4dB (i.e. 60%) greater

than the subject sitting weight. If the viscera, at 25% of the sitting weight were wholly responsible for this increase then they would be moving at more than three times the input acceleration (equivalent to a damping factor of about 0.1). This seems hardly likely. However, their proportion of the total mass suggests that they could make a significant contribution.

At resonance, the measured intra-colonic pressures of White et al 1962 were approximately 750 Pa per m/s^2 of vibration acceleration. If one takes the visceral area to be 0.025 m^2 (Sandover 1981), then the dynamic force acting on the pelvis is equivalent to an apparent mass of the order of 19 kg. This is a 50% increase on the weight given in the table above, and in line with the general dynamic behaviour of the trunk.

Thus, the role of visceral motion is still unclear. A simple elastic balloon model may be sufficient, but some support of the upper torso is also possible. The influence on the apparent mass could be significant, but it is doubtful if the viscera are the sole source of resonance at 4 to 5Hz.

9.3 The spine

Although the spine is often considered as a single axially compressible element, the theoretical analyses mentioned at the beginning of section 9. suggest that the spine should be considered as three separate components - a relatively rigid thoracic spine (with thorax attached), a curved lumbar spine that bends in the sagittal plane and the lumbo-sacral junction.

Krause 1963, Lange & Coerman 1965, and Christ & Dupuis 1966 have all found evidence of resonance phenomena occurring in the lumbar spine. The data of Christ & Dupuis are probably the most reliable as they measured angular motion of the vertebrae and took this into account in estimating vertical and horizontal motion. Maximum motion relative to the seat (vertical, horizontal and angular) occurred at 4Hz. It is difficult to estimate accurately from their graphs the relative linear motion between vertebrae. However, at 4Hz, even L4 moved some 6 mm horizontally and vertically relative to the seat (whose input movement was 5 mm), as though the pelvis rocked about the ischial tuberosities. (This is in accord with the view of Branton 1969, that during sitting the pelvis is rotated

about the ischial tuberosities in dynamic postural control.) Relative angular movements between vertebrae (L4 to L2, L2 to T12) were of the order of 1° at 4Hz, with T12 rotating at about 4° relative to the seat - the summation of relative movements, sacrum to T12. Thus, complex bending and sacral movement may be sources of resonance phenomena at 4 to 5Hz in the apparent mass function.

If it is accepted that bending in the lumbar spine is an important factor, then the configuration of the lumbar spine is an important variable. In the model used by Belytschko & Privitzer 1978, the lumbar spine has a clear lordosis, but a photograph of the arrangement used by Christ & Dupuis 1966 suggests that the lordosis was minimal. The angular movements of Christ and Dupuis relate to lumbar flexion due to vibratory forces whilst in lordosis one would expect extension. The question then arises - do both occur? If this is the case, then in some postures one would expect minimal bending and higher resonant frequencies. Thus, a detailed understanding of the behaviour of the lumbar spine during vibration is of great importance, and the only good experimental data (of Christ & Dupuis) was from one subject only.

The complex nature of the movements makes it difficult to estimate spinal forces (and hence contribution to the apparent mass) from the above data. However, the upper thorax, head and spinal tissues contribute some 42% of the trunk mass. If the arms are included, over 50%. Therefore, unless the abdominal walls have a strong supportive action the contribution of spinal loads to the apparent mass must be significant.

The effects of the VE posture are of interest here. It tended to increase the resonant frequency or reduce damping (in terms of increased amplitude and phase angle). This could be attributed to stiffened spinal musculature, changes in the lumbar curve, or increased dependence on spinal support as abdominal support was less.

9.4 The pectoral girdle

Guignard & Irving 1960 observed articulation about the sternoclavicular joints, so that one can consider both shoulders and arms to be moving relative to the upper spine. These constitute some 20% of the trunk mass, so that this motion could contribute significantly to the apparent mass. However, it is doubtful if this motion is the main

contributor and as the apparent mass and transmissibility curves are similar at 4 to 5Hz, it follows that it is unlikely that the motion is the main source of transmissibility resonance. An alternative explanation to that of Guignard & Irving is simply that the upper spine is resonating (relative to the seat) at about 5Hz, and the pectoral girdle, attached loosely to the spine, follows this motion with inertia leading to phase lag. Unfortunately the arm restraints used here throw little light on the problem. They had minimal effect on the response functions, but neither was the restraint very effective. So much freedom exists in the pectoral area that longitudinal motion relative to the thoracic spine was still possible.

No conclusions can be drawn on the role of the pectoral girdle. However, casual observation suggests that the movement is very free and unlikely to have sufficient stiffness to be a source of resonance in the 4 to 5Hz region.

9.5 The head and neck

It can be argued that the head and neck contribute only some 9% of the trunk weight, and being remote from the measurement point, contribute little to the apparent mass. However, it is argued in appendix 3 that the nodding motion of the head contributes significantly to transmissibility resonances at about 10Hz. Thus, predictions of spinal resonance behaviour at about 10Hz are not necessarily supported by transmissibility resonances at those frequencies.

9.6 General considerations

Although the head accelerometer location was chosen to minimise head nodding effect, it is quite possible that resonances occurring at higher frequencies relate to nodding effects. However, at low frequencies the transmissibility probably approximates to transmissibility to the cervical spine. In this case the transmissibility may give clues on the anatomical sources of apparent mass.

In these studies, where apparent mass and transmissibility were measured at the same time, the two response functions are often very similar up to and just beyond the first resonance.

One clear difference between the curves is that the phase angles are progressively greater for the transmissibility. However, the apparent mass function probably includes effects of unsprung mass at the pelvis. Many apparent mass curves showed a tendency to constant magnitude and low phase angle at the highest frequencies, suggesting unsprung masses of some 10 kg - of the order that one would expect from the table of proportions given above. If the unsprung mass effect were removed, then the apparent mass and transmissibility curves would approximate more closely (as it does for the Bs and VE conditions). If, as this suggests, the apparent mass and transmissibility relate to the same basic resonance at 4 to 5Hz, then it must relate to relatively large masses at the thorax level supported on elastic tissues to give resonance relative to the seat. It would suggest that resonance in tissues not contributing motion to the head (e.g. the viscera, if they do not support the thorax) does not contribute significantly to the overall resonance phenomenon at 4 to 5Hz.

9.7 Conclusions

Taking into account all the possibilities discussed above, one can conclude the following.

a) Resonance effects due to buttock and thigh compression are probably minimal. Rocking actions of the pelvis may, however, be important.

b) The abdominal tissues exhibit resonance behaviour at 4 to 5Hz. However, it is unlikely that apparent mass maxima at 4 to 5Hz relate only to abdominal tissue resonance.

c) Bending occurs in the lumbar spine and resonant behaviour arises at 4 to 5Hz. This, possibly with rocking motion in the pelvis, is probably the major source of resonance behaviour at 4 to 5Hz in the apparent mass and in transmissibility.

10. THE RANDOM STIMULUS TECHNIQUE AND ITS APPLICATION - GENERAL DISCUSSION

10.1 The measurement technique and its application.

The aim of this research was to develop a reliable technique, simple and safe to apply in investigations of biomechanical responses to vibration. The initial assumption - that some responses were sufficiently linear in behaviour to justify linear techniques - proved sound as regards the basic input function of apparent mass. The use of a random stimulus and linear techniques allowed reliable measurements under conditions acceptable to subjects.

The acceptance of the Cooley & Tukey Fast Fourier Transform and rapid developments in digital computation led to extensive application of the random stimulus transfer function approach to well ordered (e.g. electrical) systems during the early part of the last decade. The practical application to human systems, the development of a measuring cell with across cell linearity, the development of dynamic calibration methods are novel and demanded the identification of possible sources of error and methods of assessing data reliability from a mass of theoretical literature. However it showed that good data could be obtained in situations more representative of real life than most previous work. The coherence function proved a valuable tool, both in terms of estimating the reliability of data and identifying artifacts and signal noise problems.

During exposure to vibration of similar pattern and level to that met in many forms of transportation, the apparent mass changed little as the vibration level and spectral character was changed by factors of the order of two or three, and in this respect the human response can be considered linear. The coherence function is a measure of signal noise, extraneous input and system linearity. If the former are small, then the function can be used directly as a measure of linearity (being increasingly pessimistic as signal noise or extraneous input increase). The experiments showed that, provided the stimulus was shaped to reduce signal noise to a minimum, then the coherence function for the apparent mass was usually between 0.97 and unity. Thus as regards the input, the human system can be said to be at least 97% linear. The major source of signal noise was the tape-recorder, so that it is probable that less signal

shaping would be needed if the tape recorder could be eliminated.

Despite the misgivings of many authors, these experiments showed that the use of random stimuli (and consequently parameter estimation) can give acceptable and reliable data - provided some care is taken. The 99% confidence limits for the apparent mass data were usually of the order of $\pm 0.13\text{dB}$, $\pm 2^\circ$ - much less than the variability in response to be expected (e.g. Figs 7.4, 7.62 - 7.67). With reliability of this order, the use of a random stimulus has a number of advantages over other stimuli - the vibration is similar to that met in practice, so that the effects of tissue non-linearities are neither over or under emphasised; the stimulus provides a realistic environment for the subject so that adaptation and active control can be expected to be normal; the approach forces the user to take account of possible sources of error (such as signal noise) and the coherence function helps detect them, whereas these errors are likely to be overlooked with deterministic stimuli.

The calibration method and the use of digital 'mass-cancellation' proved reliable and easy to operate. The approach has a considerable advantage over normal methods in that frequency dependent changes in the measuring system characteristics are taken into account. The approach assumes the measuring system to be linear over the range used. One problem is the mass of load cell structures between the transducers and the human interface. The method assumes these to be rigid and mass-like, and errors in measurement of the mass lead to similar errors in the apparent mass function. The latter can be important at high frequencies where the apparent mass is low. In the results presented here, the mass of the bead-bag was not taken into account, so that a slight positive bias can be expected in runs where the bead-bag was used.

The overall reliability and accuracy of the method as applied to the apparent mass was sufficient to detect, with confidence, minor changes in response supposedly due to changes in posture or some other variable controlled by the subject rather than the experimental method. The ease of application, short exposure time and minimal encumbrance of the subject make extensive study of inter and intra-subject changes a possibility. In addition, it will allow measurement of the apparent mass whilst the subject is carrying out a task and unaware that a biodynamic measurement is being made. Provided that the vibration stimulus is random, stationary and has sufficient energy at all frequencies to avoid signal

noise problems, then it is also feasible to use the method during full environmental simulation, or indeed under field conditions.

Provided care was taken to control the posture it was found that, in a normal posture, the apparent mass response function changed by only a small amount as a subject assumed the same posture on a number of occasions - magnitude and phase changes at 1dB and 10° respectively (over 4 runs). Differences in pattern and resonance frequency as well as amplitude are to be expected between subjects. To gain some insight into this situation the apparent mass curves for the six subjects of experiment 4 (Figs. 7.62 to 7.67) were superimposed but shifted in frequency till the resonance point coincided, and in magnitude till the curves coincided in the 1 to 3 Hz region (by visual inspection only). The result (Fig. 9.1) is surprising. The difference between curves being only of the order of 2 dB magnitude and 20° phase. The basic input transfer function for this simple posture was, for all six subjects, essentially of the same nature and therefore (one can hypothesise) dependent on similar anatomical structures. This suggests that one way of presenting large quantities of apparent mass data (e.g. for designers) might be to normalize for sitting weight and present a mean value with a statistic for frequency shift and a statistic for gain and phase variability.

Extension of the technique to measurement of transmissibility and to visceral and lower leg behaviour, proved feasible but less reliable. Measurements of apparent mass at the feet gave some idea of leg dynamics and interaction with trunk dynamics, but proved insufficiently reliable as a measure of postural change and trunk centre of gravity shift. Likewise measurements of intra-abdominal pressure gave an indication of visceral dynamics, but the results could not be used as absolute measures. With the head harness used, the coherence function for transmissibility followed a distinctive pattern. Apart from the lowest frequencies, the coherence function was constantly high for lower frequencies. However, in the region of the major resonance (@ 5Hz) the coherence values dropped suddenly and became more variable. At these higher frequencies the transmissibility could only be considered about 90% linear (and sometimes much less). Thus, the use of linear techniques for simple transmissibility must be considered with some reservations. A major source of difficulty was identified as the location of transducers on the head so that angular movements of the head are taken into account. In this research, the measurement of angular motion of the head was not

important, and it proved possible to locate a transducer to indicate vertical motion at the head/neck interface and minimise non-linearity. In general, the results of this research suggest that non-linearities arising from movements not in line with the assumed measurement axis (or lack of knowledge of such movements) are greater than tissue non-linearities.

The technique proved ideally suited to the investigation of differences in response arising from postural change. Despite this, no clear patterns could be identified. However, the postural studies indicate that the effects of thigh and buttock compression on vibration biodynamics are minimal and that the behaviour of the spine is more important than resonance in abdominal tissues. Bending in the lumbar spine and rocking of the pelvis are probably the main contributors. Thus the difficulty in identifying clear patterns of response in this and other studies is most likely to arise from the lack of suitable techniques to measure or control the configuration of the lumbar spine and pelvis. However, biodynamic dependence on posture in the lumbar spine has a positive value in that biodynamics responses can then be used in ad-hoc methods of reducing the load on the lumbar spine.

The unobtrusive nature of the method developed here makes it ideal for studies of man's long term reactions to the vibration environment. Some adaptation occurs and possibly active control of body mechanisms. The former might relate to changes in overall posture to minimise the stresses in certain parts of the body, the latter to active body movements or forces opposing those movements or forces generated by vibration (i.e. long and short term measures).

Cursiter & Harding 1974 and Dupuis 1977 have shown that muscle activity in the back follows a cyclic pattern in step with low frequency sinusoidal seat vibration. This could indicate active control. However, one would expect active control to lead to a non-linear response and this was not the case in these studies with random vibration. Unless e.m.g. behaviour simply relates to changes in muscle length arising from trunk movement, this suggests that sinusoidal behaviour is not representative as it allows active control not possible during exposure to complex vibration. The question also arises whether active muscle control can respond sufficiently at the 4 to 6 Hz frequencies of major concern.

The work reported here involved only a short period of exposure and limitations on subject posture. Were the subject to be exposed to long periods of vibration whilst performing a task (e.g. driving simulation) and the frequency response function obtained without the subject's knowledge, then it would seem probable that he would adopt the posture (or range of postures ; Branton 1969 found considerable posture change during travel) giving the least vibration effect - Griffin 1975. Some evidence is already available in this area over periods of two to four hours - Frolov & Potemkin 1975 observed shift in transmissibility resonance frequency away from the stimulus frequency (a detuning action), whilst Broderson & von Gierke 1971 (in 1 hr. exposures of rhesus monkeys) observed major reductions in impedance after about 10 mins. exposure. However, this adaptation may be at some cost - for instance muscle fatigue or indeed increased spinal loading. The practical implications, in terms of seat design and protective measures to minimise the risks of long term vibration exposure, are clear.

The linearity of response has implications too. These experiments have shown that if the subject is exposed to an environment where active control is minimised then, once obvious sources of non-linearity are accounted for, the body exhibits linear behaviour. This indicates that tissue characteristics are also linear. Taking the elastic behaviour of metals as a model one would expect linear behaviour under normal loading regimes, and non-linear behaviour (e.g. as found in impact or with constant acceleration) as indicative of risk of tissue damage. The close relationship between the apparent mass function and the lumbar spine, coupled with linear behaviour has further implications. Simple dose-response relationships for the effects of vibration on spinal health are acceptable - weighting methods can be used and an increase in vibration level can be taken to lead to a similar increase in spinal load.

10.2 Future work

It has been argued that the measurement and analysis technique is reliable and practicable, and knowledge of trunk dynamic behaviour (and the apparent mass function in particular) should lead to a better idea of spinal loading during vibration. Several lines of development in this research then need consideration.

10.2.1 Refinement of analysis

This research relied upon off-line analysis of tape-recorded data and this had two main drawbacks: the analogue tape-recorder was a major source of signal noise in a situation where minimal signal noise was vital; poor or unusual results were only detected much later (after the subject had been dismissed). Provided that the raw data was recorded as a back up, these drawbacks would be eliminated by on-line digitisation and simple data treatment as the experiment proceeded, followed by storage of the treated data for detailed analysis later. Provided that the computer had sufficient speed, this approach would also allow pre-treatment of data to eliminate geometric non-linearity and feedback of response spectra to the subject in investigation of active control (both dealt with in more detail below).

Data pre-treatment suggests the use of a general purpose computer. The Fast Fourier Transform on most general purpose computers is usually soft-ware based and consequently slow in execution compared with special-purpose machines (for instance, on a PDP11/10 machine used by the author, only two channel operation at digitisation rates to 100Hz was possible if 'real-time' frequency analysis with minimal data treatment was required). Moreover, the other main advantage of the dedicated machine - a flexible and easily understood set of signal analysis commands - becomes less important as the user gains experience of the analysis requirements for a particular situation.

Despite its efficiency, the FFT algorithm is usually the major limitation on the speed of frequency analysis. The FFT algorithm has reduced efficiency with time data, as it operates on the imaginary time data unnecessarily. However, for this research at least two channels of time data needed treatment, and processing efficiency can then be increased by nearly 100% by making use of the symmetry of the FFT and using the imaginary part of one time data channel for the real part of a second channel (Bendat & Piersol 1971 pp 308/9). In preparation for general purpose computation, a frequency analysis sub-routine was written in FORTRAN for the PDP11/10 mentioned above. By judicious programming to adapt the analysis to the particular needs of this research (e.g. elimination of zero frequency computations at the earliest stage) it was found that all three spectra needed (G_{xx} , G_{yy} , G_{xy}) could be obtained almost as quickly as one channel of Fourier transformation.

The Hanning function too tends to reduce computational efficiency as it reduces the contribution of the data at the beginning and end of the time sample. Were the data treated twice, with the second set of sample blocks overlapping the first, then the maximum Hanning attenuation of the first set of sample blocks can be made to coincide with the minimum of the second set and each time data point would make a full contribution. This approach would increase the degrees of freedom (by a factor of just less than two), and for a given exposure time increase the reliability of the response function. With a fast general purpose computer or off-line analysis and sufficient storage, this could be used to reduce exposure time whilst maintaining reliability.

The graphical presentation of the confidence limits proved useful, but rather rigid in operation. It would, however, be a valuable tool during an experiment - giving guidance on the value of the data being collected. An easily understood display, e.g. response curves being dotted where the confidence limits are too wide, would aid the user. The validation graphs (power spectra and histograms) had a decreasing value as experience with the system increased. It is considered that data checks on stationarity, normality, etc. are necessary, but user efficiency would be improved were they automatic with full graphical output only when tests indicate digression from the desired norm.

The comparison of response spectra needs attention. The simple visual method used here is time consuming, unreliable and does not lend itself to statistical evaluation. When the response characteristics are similar, then the approach suggested above (10.1) should prove helpful but cannot be considered a full solution to the problem. Certainly from the results presented here, on only a few occasions were the spectra sufficiently similar to allow simple averaging of values at each frequency.

10.2.2 Non linear techniques

Marmarelis & Marmarelis 1978 have developed the 'white-noise' method for the analysis of non linear physiological systems and this approach might well be adopted for vibration response. However, the results of these investigations suggest that the basic tissue behaviour is near linear - at least under conditions similar to those likely to be encountered in most practical situations. The development of a better

understanding of body biomechanics and subsequent isolation of, and correction for, obvious non-linearities arising from body geometry would seem a better long term strategy than hasty application of non-linear techniques.

10.2.3 Trunk dynamics

Knowledge of the dynamic behaviour of the trunk has two important practical applications. First, occupational exposure to vibration is a possible source of ill health, particularly as regards early onset of spinal disorders and to some extent as regards gastro-intestinal disorders (Sandover 1981). Knowledge of trunk dynamics would give insight into the stresses in the spine. Second, vision is an important variable in considerations of task performance during vibration, and our understanding of motion of the eye in response to seat vibration is still minimal.

Degeneration in the lumbar spine may relate to bending or direct compressive forces at the disc (Sandover 1981). It was argued above that spinal resonance is probably the main contributor to the apparent mass function. Thus, the apparent mass function, with appropriate modifications to take into account pelvic and other unsprung masses and visceral forces, would be a useful method of transposing the environmental measure (seat vibration) to the spinal stress measure - i.e. a 'weighting' function. However, this assumes that compressive force is the relevant stress criterion. If bending is the relevant criterion, then the apparent mass function would need modification - probably on the lines of reduced high frequency sensitivity inherent in an assumption of stress proportional to relative displacement (appendix 2). The influence of this approach on current methods is shown in fig 10.1. The I.S.O. weighting network is currently used for vibration analysis, the D.R.I. analogue for evaluation of ejection seat impacts. The apparent mass curve is representative of those in fig 9.1. If unsprung masses were taken into account or relative displacement used as a criterion, the apparent mass curve would approximate more to the D.R.I. curve and move further from the I.S.O. curve. However, the D.R.I. curve would appear to over emphasise resonance as well as emphasise 8Hz. rather than 5Hz. If, as Sandover 1981 suggests, peak values are more important than r.m.s. values, then phase needs consideration. The I.S.O. curve is a simple weighting network, and

phase relationships are not specified. The suggested modifications to the apparent mass curve would result in phase angles nearer to those of the D.R.I. curve.

The discussion in section 9. shows that research on trunk dynamics would benefit from a conceptual model closer to the actual trunk anatomy. It is suggested that fig 10.2 is more realistic than that of fig. 6.1. yet still relatively simple. The model highlights three problem areas which, until they are better understood, limit the gathering of useful biodynamic information relating to spinal stress and visual performance - the biodynamic behaviour in the lumbar and pelvic structures; the angular motion of the head resulting from Z seat excitation; and to a lesser extent, the interactions between visceral movement, abdominal muscle activity and visceral connections to thorax, spine and pelvis.

In retrospect it is apparent that the experiments described here suffered from inadequate measurement and control of the position of the pelvis and lumbar curvature. However, although photography and palpation are possible means of recording and control, they only give an approximate answer as well as being laborious. Correct postural control, such as the use of a sight tube (Guignard & Irving 1960) is an attractive proposition. However, this is unlikely to isolate the differences in postural strategy employed by different subjects. The use of instructions (e.g. the "very erect" posture used here) might be useful in delineating extreme conditions. Although there is some information on the normal configuration of the lumbar spine and pelvis in the standing person there is little information on the seated person. Both Åkerblom 1948 and Schoberth 1962 have measured significant pelvic rotation from the standing to the sitting position, so that the available information on standing configurations cannot be used to estimate sitting configurations. Thus there is no easy solution to the problem of measurement and control of pelvic position without resort to radiography or invasive techniques. Devices clamped to the pelvis would need to be large, and to obtain good contact with skeletal structures, attachment pressures might need to be so high as to be regarded as "invasive". If dynamic measurements of posture are to be successful (@ 1 to 20Hz) then these problems become greater and invasive methods (such as those of Christ & Dupuis, but making use of more sophisticated measurement and analysis techniques) may be the only solution.

The apparent mass gives information on centre of gravity motion in the direction of the stimulus. Sandover 1981 has suggested that horizontal movements of the centre of gravity of the upper trunk should give information on the bending and muscular loads on the intervertebral joints. Also, information on subject posture may be obtained from static foot force and trunk centre of gravity positions. Investigation of these aspects of centre of gravity shift would be possible with a modified load cell with four transducers, DC capability and reduced weight.

Biggs 1975 has shown that it is possible to mount a number of accelerometers rigidly about the head without making use of a dental bite or bite bar. Assuming planar motion, it is possible to calculate the motion of a rigid mass from the output of four linear accelerometers, Padgaonkar et al. 1975, Chou & Sinha 1976. This demands some computational power but would facilitate investigation in detail of the mode of motion of the head during vibration. Four lines of research are then suggested - calculation of the true Z motion of the head for transmissibility; calculation of the true angular motion at the eyes for visual performance research; consideration of the most suitable positions for single accelerometers to estimate Z and rotational motion of the head; investigation of the effects of muscular activity and the value of the dental bite as a transducer mount (it is hypothesised that the biting action increases muscle tension and changes head dynamics during vibration).

In this research a single attempt was made to measure intra-abdominal pressure changes and well calibrated measurements would give useful information on the effects of visceral movement on the apparent mass and more accurate estimation of spinal forces would follow. However, a more general study could throw light on the interactions between visceral movement, muscle activity, posture, etc. A simultaneous measurement of apparent mass, intra-abdominal pressure changes, muscle activity and centre of gravity shifts during exposure to vibration, would facilitate modelling that particular situation. This suggests closely controlled experiments with a small number of subjects investigated in detail in order to avoid the problems arising when modelling is based on mean values from a large group where variation between subjects is large and little understood.

10.2.4 Adaptation and fatigue

As the apparent mass function is an indicator of load on the lumbar spine, there is a good case for observing changes over long periods of exposure. The approach could also be used to investigate creep in the lumbar disc (Kazarian 1975). If modern methods of estimating fatigue in large muscles from e.m.g. spectra can be adapted to the muscles of the back during vibration, then this would be a valuable adjunct.

A much needed experiment is on-line measurement of the response function with the subject able to observe the result and encouraged to change the response by modifying posture or muscle tension. By overlapping sample blocks (see 10.2.1) it should be possible to obtain reliable response functions from exposures of the order of 20 s so that the effects of change are immediately clear to the subject. This might prove a more sensitive method of investigating postural change in the low back and the mode of transmission of vibration through the body, as well as giving information on the adaptive processes. Application to the problems of transmissibility and head motion would be particularly relevant. The possibility of active control during some types of vibration and not others is of concern to experimenters. Comparison of sinusoidal vibration (low and high frequencies) with random vibration in regard to linearity of response and muscle activity could offer some information. Use of the coherence function to evaluate causality between muscular response patterns to stimulus would be important.

The hypothesis that non-linearity in biodynamic response is indicative of tissue damage has great practical relevance. It is doubtful if epidemiological evidence will be adequate to define close-effect relationships - Sandover 1981. If the linearity of response (indicated directly by the coherence function) were observed whilst stimulus intensity was steadily increased, then changes could be used to define safe working intensities.

11. CONCLUSIONS

During exposure to vibration typical of many working environments, the body exhibits essentially linear biodynamic behaviour at the man-seat interface.

The measurement technique developed, based on use of a random stimulus and linear analysis, proved a reliable, simple and safe tool for consideration of biodynamic response to vibration. Frequency response estimates to an accuracy of $\pm 0.15\text{dB}$ Magnitude, $\pm 20^\circ$ phase are possible.

The apparent mass is a reliable function to measure and relates to loading in the lower spinal areas. For a single subject in a controlled posture, the function changes little over short periods of time. In general, changes with subject and posture are large. However, in the case of a normal upright posture, inter-subject differences need not be large if sitting weight and resonant frequency are normalised.

The measurement technique is applicable to transmission of vibration to the head and abdomen. However, geometric sources of non-linearity need to be taken into account for the data to be reliable. Simultaneous measurement of several functions, especially apparent mass and transmissibility, is a useful means of exploring biodynamic behaviour.

Postural effects are dependant on the configuration of the lumbar spine and pelvis which is difficult to measure or control. The configuration is probably a significant contributor to inter-subject differences.

The linearity of the basic input behaviour has important implications. Active control of behaviour is unlikely although adaptation is probable. The linearity of the apparent mass function (which suggests linear tissue characteristics) at ordinary exposure levels and the relationship between apparent mass and spinal load indicate that simple dose relationships are acceptable for considerations of spinal health. In particular, the use of weighting functions and assumptions of a proportional relationship between vibration level and spinal stress are reasonable.

12. ACKNOWLEDGEMENTS

I am indebted to a great number of friends with whom I have discussed the nature of biodynamic responses and a particular debt is owed to Professors Zarek and Floyd who first introduced me to the subject. I wish to acknowledge the friendly assistance of colleagues in the Department of Electrical Engineering as well as the use of their computing facilities.

This thesis would not have existed without the patience of Bron and Beryl in coping with me and the word-processor.

My greatest debt is to my family.

13) REFERENCES

- AKERBLOM, B. (1948)
Standing and sitting posture.
 A.B. Nordiska Bokhandeln, Stockholm.
- ALLEN, G.R. (1971)
 Human reaction to vibration.
Ann.Mtg.Inst.Environmental Sc. April 1971.
- ALLEN, G.R. (1978)
 A critical look at biodynamic modelling in relation to specifications for human tolerance of vibration and shock.
AGARD -CP.-253, Nov.1978.
- ASHLEY, C. (1970)
 Equal annoyance contours for the effects of sinusoidal vibration on man.
Human resp. to vibration mtg. Loughborough Univ.Tech. Sept. 1970.
- BARNES, G.R. & RANCE, B.H. (1974)
 Transmission of angular acceleration to the head in the seated human subject.
Aerosp.Med. 45(4), 411-416.
- BARTER, J.T. (1957)
 Estimation of the mass of body segments.
 WADC Tech. Rept. 57-260.
- BASTEK, R. et al (1977)
 Comparison of the effects of sinusoidal and stochastic octave-band-wide vibrations-a multi-disciplinary study.Pts.I & II.
Int.Arch.Occup.Env.Health 39, 143-164.
- BEAUCHAMP, K.G. (1973)
Signal processing.
 Allen & Unwin.
- BEAUCHAMP, K.G. & YUEN, C.K. (1979)
Digital methods for signal analysis.
 Allen & Unwin.
- BEGEMAN, P.C., KING, A.I. & PRASAD, P. (1973)
 Spinal loads resulting from -Gx acceleration.
17th Stapp Car Crash Conf.SAE, N.Y. Nov.1973, 343-360.
- BEKESY Von, G. (1939)
 Uber die Empfindlichkeit des stehenden und sitzenden Menschen gegen sinusformige Erschutterungen.
Akustische Zeitschrift 4, 360-369.
- BELYTSCHKO, T. & PRIVITZER, E. (1978a)
 A three dimensional discrete element dynamic model of the spine, head and torso.
AGARD-CP-253.

- BELYTSCHKO, T. & PRIVITZER, E. (1978b)
Refinement and validation of a three dimensional head-spine model.
AMRL-TR-78-7.
- BELYTSCHKO, T., ANDRIACCHI, T.P., SCHULTZ, A.B. & GALANTE, J.O. (1973)
Analog studies of forces in the human spine: computational techniques.
J. Biomechanics 6, 361-371.
- BELYTSCHKO, T., SCHWER, L. & PRIVITZER, E. (1978)
Theory and application of a three dimensional model of the human spine.
Av. Sp. Env. Med. 49(1), 158-167.
- BELYTSCHKO, T., SCHWER, L. & SCHULTZ, A. (1976)
A model for analytic investigation of three dimensional head-spine dynamics.
AMRL-TR-76-10.
- BENDAT, J.S. & PERSOL, A.G. (1971)
Random data: Analysis and measurement procedures.
Wiley - Interscience.
- BENIGNUS, V.A. (1969)
Estimation of the coherence spectrum and its confidence interval using the fast fourier transform.
IEEE Trans. Audio Electroacoustics. AU-17(2).
- BINGHAM, GODFREY & TUKEY (1967)
Modern techniques of power spectral estimation.
IEEE Trans. Audio & Electroacoustics , AU-15, (2), 56-66.
- BOLTON, C.B. (1966)
Proposal for ventile incompressible cushions.
RAE Tech. Memo ME350.
- BONNARDEL, G. (1975)
Environment vibratoire dans les vehicules de transport.
IRT Rept. No. 12, Dec. 1975.
- BOULANGER et al (1976)
Evaluation du degre d'exposition a des vibrations transmises a l'ensemble du corps.
INRS Rept. 245/RE, Oct. 1976 (RAE Trans. 1930, March 1978)
- BRANTON, P. (1969)
Behaviour, body mechanics and discomfort.
Ergonomics 12(2), 316-327.
- BRINKLEY, J.W. (1968)
Development of aerospace escape systems.
Air University Review 19(5), 34-49.
- BRINKLEY, J.W. (1969)
Evaluation of the effects of selected egress system design parameters during &Gz acceleration.
Paper at 40th Ann. Mtg. Aerosp. Med. Assn., San Fransisco, May 1969

- BRINKLEY, J.W. & SHAFFER, J.T. (1971)
Dynamic simulation techniques for the design of escape systems: Current applications and future Air Force requirements.
Symposium on biodynamic models and their applications.
AMRL-TR-71-29-2.
- BROCH, J.T. (1962)
On the use of warble tone and random noise for acoustic measurement purposes.
Brueel & Kjaer Tech. Rev. 4.
- BROCH, J.T. (1963)
Non-linear amplitude distortion in vibrating systems.
Brueel & Kjaer Tech. Rev. 4.
- BROCH, J.T. (1975)
On the measurement of frequency response functions.
Brueel & Kjaer Tech. Rev. 4.
- BRODERSON, A.B. & Von GIERKE, H.E. (1971)
Mechanical impedance and its variation in the restrained primate during prolonged vibration.
ASME Paper 71-WA/BHF-8.
- BRUMAGHIM, S.H. (1969)
Subjective response to commercial aircraft ride: passenger ride quality testing.
Int. Symp. Man Made Systems.
- BS.DD23:1973
Guide to the safety aspects of human vibration experiments.
British Standards Inst., June 1973.
- CHAPMAN, P. (1975)
Digital vibration control techniques.
In: Seminar on understanding digital control and analysis in vibration test systems. Pt. I. Shock & Vibr. Info. Center, Naval Res. Labs, Washington DC, May 1975.
- CHOU, C.C. & SINHA, S.C. (1976)
On the kinematics of the head using linear acceleration measurements.
J. Biomechanics 9, 607-613.
- CHOW, W.W. & ODELL, E.I. (1978)
Deformations and stresses in soft body tissues of a sitting person.
J. Biomech. Eng. (Trans. ASME), 100, 19-87.
- CHRIST, W. & DUPUIS, H. (1966)
Über die Beanspruchung der Wirbelsäule unter dem Einfluss sinusförmiger und stochastischer Schwingungen.
Int. Z. angew. Physiol. einschli. Arbeitsphysiol. 22, 258-278.
- CHURCH, A.H. (1963)
Mechanical vibrations.
Wiley.

- COERMANN, R.R. (1940)
 Untersuchungen über die Einwirkung von Schwingungen auf den menschlichen Organismus.
Luftfahrtmedizin 4(2), 73-117. (RAE Lib.Trans.217, Nov.1947)
- COERMANN, R.R. (1961)
 The mechanical impedance of the human body in sitting and standing position at low frequencies.
Aero.Systems Div.WPAFB.Ohio ASD Tech.Rept. 61-492.
- COERMANN, R.R. (1962)
 The mechanical impedance of the human body in sitting and standing position at low frequencies.
Human Factors 4, 227-253.
- COERMANN, R.R. & OKADA, A. (1964)
 Übertragung von Erschütterungen auf den Menschen bei verschiedener Anstellwinkeln der Rückenlehne.
Int.Z.angew.Physiol.einschl.Arbeitsphysiol. 20, 398-411.
- COERMANN, R.R., ZIEGENRUECKER, G.H., WITTWER, A.L. & Von GIERKE, H.E. (1960)
 The passive dynamic mechanical properties of the human thorax-abdomen system and of the whole body system.
Aerosp.Med. 31(6), 443-445.
- COLE, S.H. (1978)
 The vertical transmission of impulsive energy through the seated human.
Ph.D. Thesis, Dept.Human Sciences, University of Technology, Loughborough.
- CONFERENCE (1970)
 Symposium on biodynamic models and their applications. 26-28 Oct.1970
 AMRL-TR-71-29.
- CONFERENCE (1975)
 Symposium on ride quality.
 NASA TM X-3295 / DOT-TSC-OST-75-40.
- CONFERENCE (1977)
 Symposium on biodynamic models and their applications. 15-17 Feb.1977.
Av.Sp.Env.Med. 49, Jan 1978.
- CONFERENCE (1978)
 Models and analogues for the evaluation of human biodynamic response, performance and protection.
 AGARD-CP-253.
- COOLEY, J.W. & TUKEY, J.W. (1965)
 An algorithm for the machine calculation of complex Fourier Series.
Math.Comp. 19, 297-301.

CORSO, J.F. (1967)

The experimental psychology of sensory behaviour.
Holt Rinehard & Winston.

CRAMER, H.J., KING LIU, Y. & VON ROSENBERG, D.U. (1976)

A distributed parameter model of the inertially loaded human spine.

J. Biomechanics 9, 115-130.

CROMER, A.H. (1974)

Physics for the life sciences.

McGraw-Hill.

CURSITER, M.C. & HARDING, R.H. (1974)

Electromyographic recordings of shoulder and neck muscles of seated subjects exposed to vertical vibrations.

J. Physiol. 239, 117-118P.

DEMPSTER, W.T. (1955)

Space requirements of the seated operator.

WADC Tech. Rept. 55-159.

DIECKMANN, D. (1955)

The effect of mechanical vibration on man: a review and summary of research up to date.

Max-Planck Inst. Occ. Physiol. (Brit. Railw. Res. Dept. Trans.).

DIECKMANN, D. (1957)

Einfluss vertikaler mechanischer Schwingungen auf der Menschen.

Int. Z. angew. Physiol. einschl. Arbeitsphysiol. 16, 519-564.

DIECKMANN, D. (1958)

A study of the influence of vibration on man.

Ergonomics 1(4), 347-355.

DONATI, P. (1980)

Effets a court terme sur l'homme assis des vibrations transmises a l'ensemble du corps.

Doct. Ing. thesis. L'Institut. Nat. Polytechnique de Lorraine.

DONATI, P., GALMICHE, J.P., GROSJEAN, A., MISTROT, P. & ROURE, L.

Etude des equivalences subjectives entre les vibrations sinusoidales et les vibrations aleatoires transmises a l'ensemble du corps des individus.

Inst. Nat. de Rech. et Sec. Vandoeuvre.

DUPUIS, H. (1977)

Human response to vibration under different conditions.

Proc. Europ. Symp. on Life Sci. Res. in Space,
Cologne/Porz, 24-26 May, 1977.

DUPUIS, H. (1969)

Zur physiologischen Beanspruchung des Menschen durch mechanische Schwingungen.

VDI Fortschrittsberichte 11(7).

DUPUIS, H., HARTUNG, E. & LOUDA, L. (1971)

The effect of random vibrations of a limited frequency band compared with sinusoidal vibrations, on human beings.

RAE Lib. Trans. 1603.

EDWARDS, R.G. & LANGE, K.O. (1964)

A mechanical impedance investigation of human response to vibration.

WPAFB Ohio AMRL-TR-64-91.

ENOCHSON, L.D. & GOODMAN, N.R. (1965)

Gaussian approximations to the distribution of sample coherence.

Res. & Tech. Divn. AFSC, WPAFB, Ohio. AFFDL TR-65-57.

ERINGEN, A.C. (1952)

On the non-linear vibration of elastic bars.

Q.J. Appl. Maths. 9, 361-369.

FORLIFER, W.R. (1964)

The effects of filter bandwidth in spectrum analysis of random vibration.

Shock & Vibr. & Ass. Env. Bull. 33(II),

Dept. Defense, Washington D.C., Feb. 1964.

FRENCH, A.S. & HOLDEN, A.V. (1971a)

Frequency domain analysis of neurophysiological data.

Computer Programs in Biomed. 1, 219-234.

FRENCH, A.S. & HOLDEN, A.V. (1971b)

Semi-on-line implementation of an alias-free sampling system for neuronal signals.

Computer Programs in Biomed. 2, 1-7.

FRISCH, G.D., O'ROURKE, J. & D'AULERIO, L. (1976)

The effectiveness of mathematical models as a human analog.

SAE SP-412, 760774.

FROLOV, K.V. (1969)

Method of studying the reactions of a human operator considered as an oscillatory system to harmonic and random vibrational action.

NASA Trans. TT F-14, 289.

FROLOV, K.V. (1970)

Dependence on position of the dynamic characteristic of a human operator subjected to vibration.

ASME Winter Ann. Mtg. Dec. 1970 (Ed. N. Perrone), 146-150.

FROLOV, K.V. (1973)

Investigation of human body dynamic response to mechanical oscillations by methods of mechanics.

Strojnický Casopis XXIV(6), 556-561.

FROLOV, K.V. & POTEKIN, B.A. (1975)

Vibration as an artificially created human factor of the environment.

NASA Trans. TT-F-16475, July 1975.

GARG, D.P. & ROSS, M.A. (1976)
Vertical mode human body vibration transmissibility.
IEEE Trans. on Systems, Man & Cybernetics SMC-6(2), 102-112.

GIERKE Von, H.E. (1964)
Biodynamic response of the human body.
In: Third Int. Symp. on Bioastronautics and the exploration
of space. Brooks AFB, 16-18 Nov. 1964. 385-411.

GIERKE Von, H.E. (1978)
Technical evaluation report.
AGARD-CP-253.

GIERKE Von, H.E. & COERMANN, R.R. (1963)
The biodynamics of human response to vibration and impact.
Ind. Med. & Surg. 32(1), 30-32.

GRIFFIN, M.J. (1975)
Vertical vibration of seated subjects: Effects of
posture, vibration level and frequency.
Av. Sp. Env. Med. 46(3), 269-276.

GRIFFIN, M.J. (1976)
Subjective equivalence of sinusoidal and random whole-body
vibration.
J. Acoust. Soc. Amer. 60(5), 1140-1145.

GRIFFIN, M.J. & LEWIS, C.H. (1978)
A review of the effects of vibration on visual acuity and
continuous manual control. Pt. I: Visual acuity.
J. Sound & Vibr. 56(3), 383-413.

GRIFFIN, M.J., LEWIS, C.H., PARSONS, K.C. & WHITHAM, E.M. (1978)
The biodynamic response of the human body and its application
to standards.
AGARD-CP-253.

GUIGNARD, J.C. & GUIGNARD, E. (1970)
Human response to vibration: A critical survey of published
work.
ISVR Memo. 373.

GUIGNARD, J.C. & IRVING, A. (1960)
Effects of low-frequency vibration on man.
Engineering 190, 364-367.

GUIGNARD, J.C. & KING, P.F. (1972)
Aeromedical aspects of vibration and noise.
AGARD -AG-151.

GUIGNARD, J.C. et al (1979)
A method for studying human biodynamic responses to
whole-body z-axis vibration.
AGARD-CPP-267, Paper No. 10.

HANSSON, J.-E. & KJELLBERG, A. (1981)
Vibrationsexponering och upplevda besvar vid truckkorning pa
godsbangardar.
Arbetskyddsstyrelsen Work Rept. 1981:1.

HARRIS, C.M. & CREDE, C.E. (Eds) (1961)
Shock and vibration handbook.
 Mc Graw-Hill (3 vols.)

HASAN, J. (1970)
 Biomedical aspects of low frequency vibration-A selective review.
Work-Environment-Health 6(1), 19-45.

HEIDE, R. (1979)
 Zur Wirkung langzeitiger beruflicher
 Ganzkörpervibrationsexposition.
Zentralinstitut für Arbeitsmedizin der DDR Dr. Med. diss.
 Betr. Nr. 90-141-708.

HOEL, P.G. (1976)
Elementary statistics.
 Wiley (4th. Edn.)

HORNICK, R.J. & LEFRITZ, N.M. (1966)
 A study and review of human response to prolonged random vibration.
Human Factors 8(6), 481-491.

HUIJGENS, J.M.M. (1977)
 Bending vibrations in the human vertebral column.
J. Biomech. 10, 443-444.

I.S.O. DIS/5982
 Vibration and shock: Mechanical driving point impedance of the human body.
International Standard ISO/DIS 5982, 1979.

ISO 2631
 Guide for the evaluation of human exposure to whole-body vibration.
International Standard ISO 2631, 1978-01-15.

JENKINS, G.M. & WATTS, D.G. (1969)
Spectral analysis and its applications.
 Holden-Day.

JONES, J.G. (1979)
 Ride-bumpiness and the influence of active control systems.
 AGARD-CPP-267. Paper No. 1.

KALEPS, I., Von GIERKE, H.E., & WEIS, E.B. (1970)
 A five-degree-of-freedom mathematical model of the body.
 In: Conference (1970).

KANDIANIS, F. (1971)
 Frequency response of structures excited by transient or random forces using cross correlation and its Laplace Transform.
 ISVR Tech. Rept. 47.

- KANDIANIS, F. (1973)
Correlation techniques in the analysis of transient processes.
J.Sound & Vibr. 26(2), 161-172.
- KAZARIAN, L.E. (1975)
Creep characteristics of the human spinal column.
Orthop.Clin.N.Amer. 6(1), 3-18.
- KOHL, U. (1975)
Les dangers encourus par les conducteurs de tracteurs. (The hazards of tractor driving)
Arch.d.malad.prof. 36(3), 145-162.
- KRAUSE, H. (1963)
Das schwingungsmechanische Verhalten der Wirbelsäule.
Int.Z.angew.Physiol.einschl.Arbeitsphysiol. 20, 125-155.
- KRAUSE, H.E. & LANGE, K.O. (1963)
The non-linear behaviour of biomechanical systems.
ASME Paper No. 63-WA-278.
- LANGE, K.O. & EDWARDS, R.C. (1970)
Force input and thoraco-abdominal strain resulting from sinusoidal motion imposed on the human body.
Aerosp.Med. 41(5), 538-543.
- LANGE, W. (1975)
A review of biomechanical models for the evaluation of vibration stress.
AGARD. Vib. & Combined Stresses in Advan.Systems. Mar. 1975.
- LANGE, W. & COERMANN, R. (1965)
Relativbewegungen benachbarter Wirbel unter Schwingungsbelastung.
Int.Z.angew.Physiol.einschl.Arbeitsphysiol. 21, 326-334.
- LATHAM, F. (1957)
A study in body ballistics: seat ejection.
Proc.Roy.Soc. 147, 121-139.
- LAWES, C.E. (1974)
A study of the mechanical impedance of the human body at low frequency by continuous monitoring techniques.
Ph.D.Thesis, Loughborough Univ.Tech.
- LEE, R.A. & PRADKO, F. (1968)
Analytical analysis of human vibration.
SAE Rept. 680091.
- LEWIS, C.H. & GRIFFIN, M.J. (1978)
A review of the effects of vibration on visual acuity and continuous manual control. Pt.II. Continuous manual control.
J.Sound. & Vibr. 56(3), 415-457.
- LOWSON, M.V. (1972)
Estimation of power spectra.
In: Digital processing & analysis of signals. Short Course. Loughborough Univ.Tech. Nov. 1972.

MACDUFF, J.N. (1969)
Transient testing of man.
Sound & Vibration 3(8).

MACFARLANE, A.G.J. (1970)
Dynamical system models.
Harrap, London.

MAGID, E.B. & COERMANN, R.R. (1960)
The reaction of the human body to extreme vibrations.
Inst. Env. Sciences Conf. on Hyper-environments: Space
frontier., Los Angeles, April 1960.

MAGID, E.B., COERMANN, R.R. & ZIEGENRUECKER, G.H. (1960)
Human tolerance to whole body sinusoidal vibration.
Aerosp. Med. 31, 915-924.

MANNARD, A. & STEIN, R.B. (1973)
Determination of the frequency response of isometric soleus
muscle in the cat using random nerve stimulation.
J. Physiol. 229, 275-296.

MARMARELIS, P.Z. & MARMARELIS, V.Z. (1978)
Analysis of physiological systems
Plenum.

MEISTER, F.J. (1935)
Die Empfindlichkeit des Menschen gegen Erschutterungen.
Forschung 6(3), 116-120.

MERTENS, H. (1978)
Nonlinear behavior of sitting humans under increasing
gravity.
Av. Sp. Env. Med. 49(1), 287-298.

MIWA, T. (1969)
Evaluation methods for vibration effect. Pt. 8 The vibration
greatness of random waves.
Jap. Ind. Health. 7, 89-115.

MIWA, T. (1975)
Mechanical impedance of human body in various postures.
Ind. Health. 13(1), 1-22.

MOHR, G.C. (1978)
The case for models in biodynamics.
Av. Sp. Env. Med. 49(1), 111-113.

MUKSIAN, R. & NASH, C.D. (1974)
A model for the response of seated humans to sinusoidal
displacement of the seat.
J. Biomech. 7(5), 209-215..

MUKSIAN, R. & NASH, C.D. (1976)
On frequency-dependent damping coefficients in
lumped-parameter models of human beings.
J. Biomech. 9, 339-342.

MULLER, E.A. (1939)

Die Wirkung sinusformiger Vertikalschwingungen auf den
sitzenden und stehenden Menschen.
Arbeitsphysiol. 10(5), 459-476.

NEWLANDS, D.E. (1975)

An introduction to random vibrations and spectral analysis.
Longman.

OBORNE, D.J. (1976)

A critical assessment of studies relating whole-body
vibration to passenger comfort.
Ergonomics 19, 751-774.

OBORNE, D.J. (1978)

The stability of equal sensation contours for whole-body
vibration.
Ergonomics 21(8), 651-658.

ORNE, D. & LIU, Y.K. (1971)

A mathematical model of spinal response to impact.
J. Biomechanics 4, 49-71.

OTNES, R.K. & ENOCHSON, L. (1972)

Digital time series analysis.
Wiley.

PADGAONKAR, A.J., KRIEGER, K.W. & KING, A.I. (1975)

Measurement of angular acceleration of a rigid body using
linear accelerometers.
ASME J. Applied Mechanics, 552-556.

PAYNE, P.R. (1965)

Personnel restraint and support system dynamics.
Frost Eng. Devel. Corp., AMRL-TR-127, Oct. 1965.

PAYNE, P.R. (1969)

Injury potential of seat cushions.
J. Aircraft 6(3), 273-278.

PAYNE, P.R. (1970)

Biodynamic modeling for aircraft escape systems.
In: Conference 1970.

PAYNE, P.R. & BAND, E.G.U. (1971)

A four degree of freedom lumped parameter model of the seated
human body.
AMRL-TR-70-35

PERRONE, N. (Ed) (1970)

Dynamic response of biomechanical systems.

ASME Winter Ann. Mtg.

POPE, M.H., WILDER, D.G. & FRYMOYER, J.W. (1980)

Vibration as an aetiological factor in low back pain.
In: Conf. on Engineering aspects of the spine. May
1980. I. Mech. E. Publ. No. 1980-2

- POTEMKIN, B.A. & FROLOV, K.V. (1971)
Model representation of the biomechanical system of a human operator with random vibrations.
Doklady Akad. Nauk SSSR 197(6), 1284-1287.
- POULTON, E.C. (1976)
Arousing environmental stresses can improve performance, whatever people say.
Av. Sp. Env. Med. 47(11), 1193-1204.
- PRADKO, F. (1964)
Human vibration response.
In: Army Res. Off. 10th. Ann. Army Human Factors R&D Conf. Oct. 1964.
- PRADKO, F., LEE, R.A. & GREENE, J.D. (1965)
Human vibration-response theory.
ASME 65-WA/HUF-19. 1965.
- PRADKO, F., LEE, R.A. & KALUZA, V. (1966)
Theory of human vibration response.
ASME 66-WA/BHF-15.
- PRASAD, P. & KING, A.I. (1974)
An experimentally validated dynamic model of the spine.
ASME Trans. 41(3), 546-550.
- RAO, B.K.N., JONES, B. & ASHLEY, C. (1975)
Laboratory simulation of vibratory road surface inputs.
J. Sound & Vibration 41(1), 73-84.
- REIHER, H. & MEISTER, F.J. (1931)
Die Empfindlichkeit des Menschen gegen Erschütterungen.
Forschung a d G d Ingenieurwesens 2(11), 381-386.
- ROBERTS, V.L., TERRY, C.T. & STECH, E.L. (1966)
Review of mathematical models which describe human response to acceleration.
ASME 66-WA/BHF-13.
- ROTH, P.R. (1971a)
Effective measurements using digital signal analysis.
IEEE Spectrum 8(4), 62-70.
- ROTH, P.R. (1971b)
How to use the spectrum and coherence function.
Sound & Vibration 5(1), 10-14.
- ROWLANDS, G.F. (1972)
The transmission of harmonically distorted low frequency vibration to the head of the seated man.
RAE Tech. Rpt. 72080.
- ROWLANDS, G.F. (1974)
The transmission of vibration by the human body with special reference to the problems of measurement and analysis.
Loughborough Univ. Tech. Ph.D. Thesis, Dec. 1974.

ROWLANDS, G.F. (1977)

Transmission of vertical vibration to the head and shoulders of seated men.

RAE Tech.Rept. 77068.

ROWLANDS, G.F. & MASLEN, K.R. (1973)

Transmission of vertical vibration to the shoulder of the seated man.

RAE Tech.Memo EP 540, March 1973.

SANDOVER, J. (1971)

A study of human analogues. Part I. A survey of the literature.
Dept.Ergonomics & Cybernetics, Loughborough Univ..

SANDOVER, J. (1974)

Human self protective mechanisms against vibration. Final Rept.

Dept.Human Sc., Loughborough Univ.Tech. LUTERG Rpt.140, August 1974.

SANDOVER, J. (1981)

Vibration, posture and low-back disorders of professional drivers.

Dept.Human Sc., Loughborough Univ.Tech. Rpt.DHS 402. May 1981.

SANDOVER, J. & COLE, S.H. (1971)

Study of human analogues. Pt.2. Experimental programme.

Dept.Ergonomics & Cybernetics, Loughborough Univ.Tech., May 1971.

SANDOVER, J. & COLE, S.H. (1973)

Human response to impulsive forces. Interim Rept.: Errors arising from low signal levels.

Dept.Ergonomics & Cybernetics, Loughborough Univ.Tech. LUTERG 89, April 1973.

SANDOVER, J. & COLE, S.H. (1974)

Human response to impulsive forces. Final Rpt.V.

Dept.Human Sc., Loughborough Univ. LUTERG 143.

SANDOVER, J. & SOAMES, R.W. (1975)

Head movement during low frequency vibration.

J.Physiol. 247, 19-20.

SCHMID, W. (1976)

Zur mechanischen Impedanz des Menschen.

Automobil-Industrie 3/76, 2-11.

SCHOBERTH, H. (1962)

Sitzhaltung, sitzschaden, sitzmöbel.

Springer, Berlin.

SCHULTZ, A.B., BELYTSCHKO, T.B. & ANDRIACCHI, T.P. (1973)

Analog studies of forces in the human spine: mechanical properties and motion segment behavior.

J.Biomechanics 6, 373-383.

SHOENBERGER, R.W. (1972)
Human response to whole-body vibration.
Perceptual & Motor Skills 34, 127-160

SHOENBERGER, R.W. (1976)
A comparison of the perceived intensity of sinusoidal and multi-frequency wholebody vibration.
AMRL-TR-76-1.

SHOENBERGER, R.W. (1976)
Comparison of the subjective intensity of sinusoidal multifrequency, and random whole-body vibration.
Av.Sp.Env.Med. 47(8), 856-862.

SHOENBERGER, R.W. (1978)
Intensity judgements of non-sinusoidal vibrations: Support for the ISO weighting method.
Av.Sp.Env.Med. 49(11), 1327-1330.

STACY, R.W. & WAXMAN, B.D. (1965)
Computers in biomedical research.
Academic Press.

STALNAKER, R.L., McELHANEY, J.H. & ROBERTS, V.L. (1970)
A mechanical impedance model for head injury due to linear impacts.
In: Conference 1970.

STEIN, R.B., FRENCH, A.S., MANNARD, A. & YEMM, R. (1972)
New methods for analysing motor function in man and animals.
Brain Res. 40, 187-192.

STIKELEATHER, L.F., HALL, G.O. & RADKE, A.O. (1972)
A study of vehicle vibration spectra as related to seating dynamics.
SAE Paper No. 720001.

SUGGS, C.W., ABRAMS, C.F. & STIKELEATHER, L.F. (1969)
Application of damped spring-mass human vibration simulator in vibration testing of vehicle seats.
Ergonomics 12(1), 79-90.

TOMLINSON, R.W. & KYLE, D.J. (1971)
The development of a dynamic model of the seated human operator.
Nat.Inst.Agricultural Eng. Unpubl.Dept.Memo,

VIHKO, V. & HASAN, J. (1970)
Biomedical aspects of low frequency vibration.-A bibliography of references.
Work-Env.-Health 7(1), 91-107.

VOGT, H.L., COERMANN, R.R. & FUST, H.D. (1968)
Impedance of sitting human under sustained acceleration.
Aerosp.Med. July, 675-679.

VOGT, L., MERTENS, H. & KRAUSE, H.E. (1978)
Model of the supine human body and its reactions to external forces.
Av. Sp. Env. Med. 49(1), 270-278.

VOGT, L.H., KRAUSE, H.E., HOHLWECK, H. & MAY, E. (1973)
Mechanical impedance of supine humans under sustained acceleration.
Aerosp. Med. 44(2), 123-128.

VULCAN, A.P. & KING, A.I. (1970)
Forces and moments sustained by the lower vertebral column of a seated human being during seat to head acceleration.
ASME Winter Ann. Mtg. (Ed. N. Perrone), 84-100.

VYKUKAL, H.C. (1968)
Dynamic response of the human body to vibration when combined with various magnitudes of linear acceleration.
Aerosp. Med. Nov. 1968, 1163-1166.

WAMBOLD, J.C. & PARK, W.H. (1975)
A human model for measuring objective ride quality.
ASME 75-DET-6.

WEIS, E.B. & PRIMIANO, F.P. (1964)
The motion of the human center of mass and its relationship to the mechanical impedance.
AMRL, WPAFB, AMRL-TR-65-50.

WEIS, E.B., CLARKE, N.P. & Von GIERKE, H.E. (1963)
Mechanical impedance as a tool in biomechanics.
ASME 63-WA-280.

WEIS, E.B., CLARKE, N.P., BRINKLEY, J.W. & MARTIN, P.J. (1964)
Mechanical impedance as a tool in research on human response to acceleration.
Aerosp. Med. Oct. 1964, 945-950.

WEISZ, A.Z., GODDARD, C. & ALLEN, R.W. (1965)
Human performance under random and sinusoidal vibration.
AMRL-TR-65-209.

WHITE, G.H., LANGE, K.O. & COERMANN, R.R. (1962)
The effects of simulated buffeting on the internal pressure of man.
Human Factors 4, 275-290.

WHITE, R.G. (1969a)
Measurement of structural frequency response by transient excitation.
ISVR TR 12, Jan. 1969.

WHITE, R.G. (1969b)
Use of transient excitation in the dynamic analysis of structures.
J. Royal Aero. Soc. 73, 1047-1050.

- WHITE, R.G. (1972)
Spectrally shaped transient forcing functions for frequency response testing.
J.Sound & Vibration. 23(3), 307-318.
- WICKSTROM, G. (1978)
Effect of work on degenerative back disease. A review.
Scand.J.Work.Env.& Health 4 Suppl.1, 1-12.
- WITTMANN, T.J. & PHILLIPS, N.S. (1969)
Human body nonlinearity and mechanical impedance analyses.
J.Biomech. 2, 281-288.
- WOODS, A.G. (1967)
Human response to low frequency sinusoidal and random vibration.
Aircraft Engrg. 39, 6-4.
- YEAGER, R., MACHOWSKY, G.V. & SHANAHAN, R.J. (1969)
Development of a dynamic model of unrestrained seated man subjected to impact.
Technology Inc., NADC-AC-6902, March 1969.
- ZIEGENRUECKER, G.H. & MAGID, E.B. (1959)
Short time human tolerance to sinusoidal vibrations.
Aero.Med.Lab., WPAFB, WADC Tech.Rpt.59-391, July 1959.
- ZIEGERT, J.C. & LEWIS, J.L. (1978)
In vivo mechanical properties of soft tissue covering bony prominences.
J.Biomech.Eng.(Trans. ASME) 100, 195-201.
- ZIEGERT, J.C. & LEWIS, J.L. (1979)
The effect of soft tissue on measurements of vibrational bone motion by skin mounted accelerometers.
J.Biomech.Eng. (Trans.ASME) 101, 218-220.

14. FIGURES

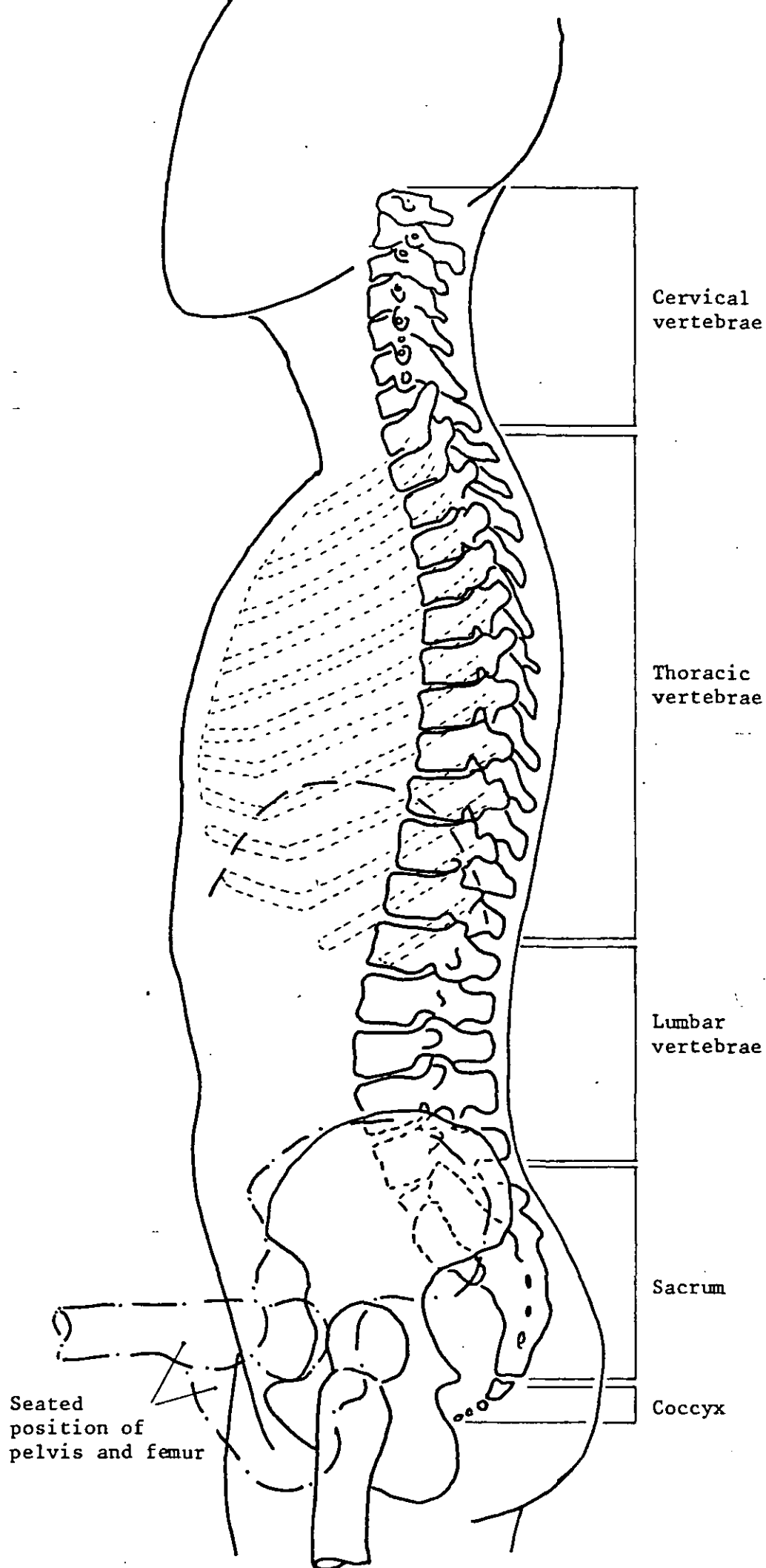


Fig. 2.1 Configuration of the spine (Standing subject)

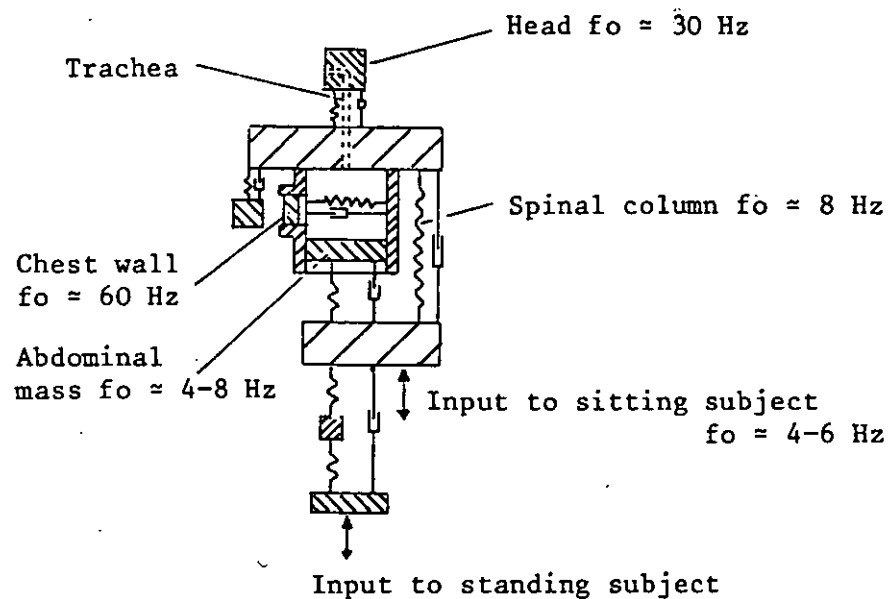


Fig. 2.2 Mechanical model, relevant for vibration, impact and external pressure (after von Gierke 1964)

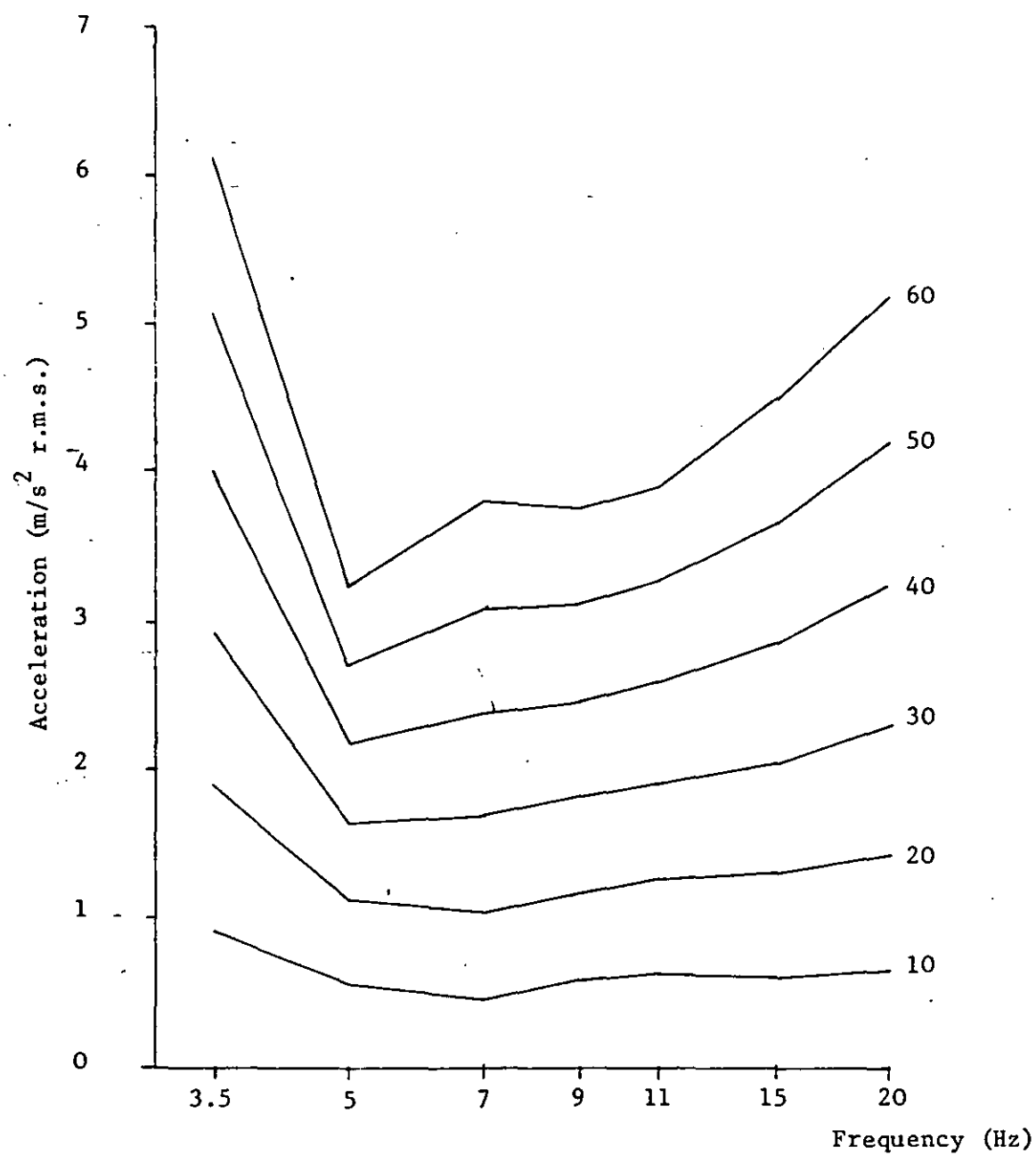


Fig. 2.3 Equal subjective magnitude curves (after Shoenberger & Harris 1971)

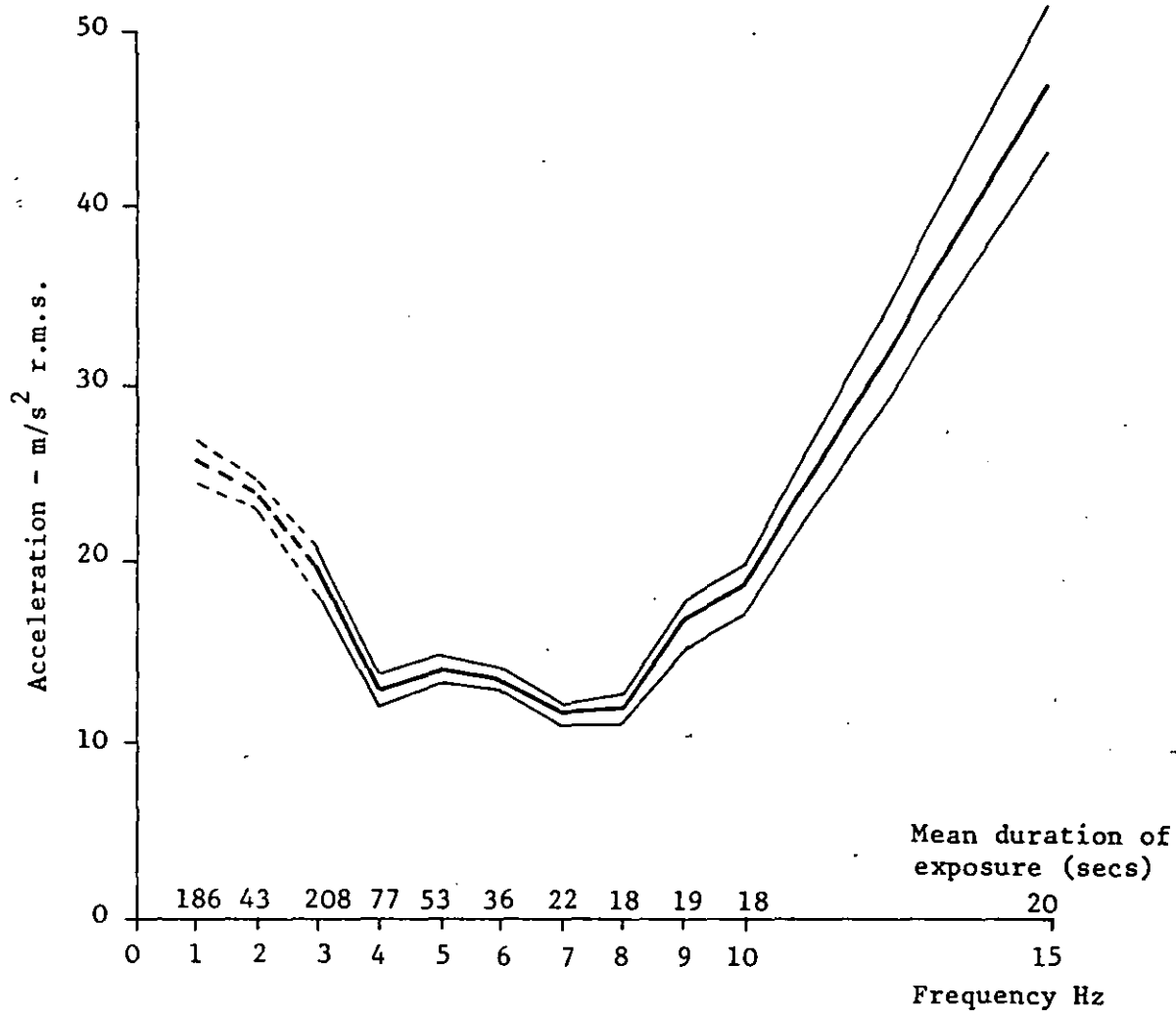


Fig. 2.4a Arithmetic mean ± 1 SD of tolerance (10 subjects)
(after Magid et al 1960)

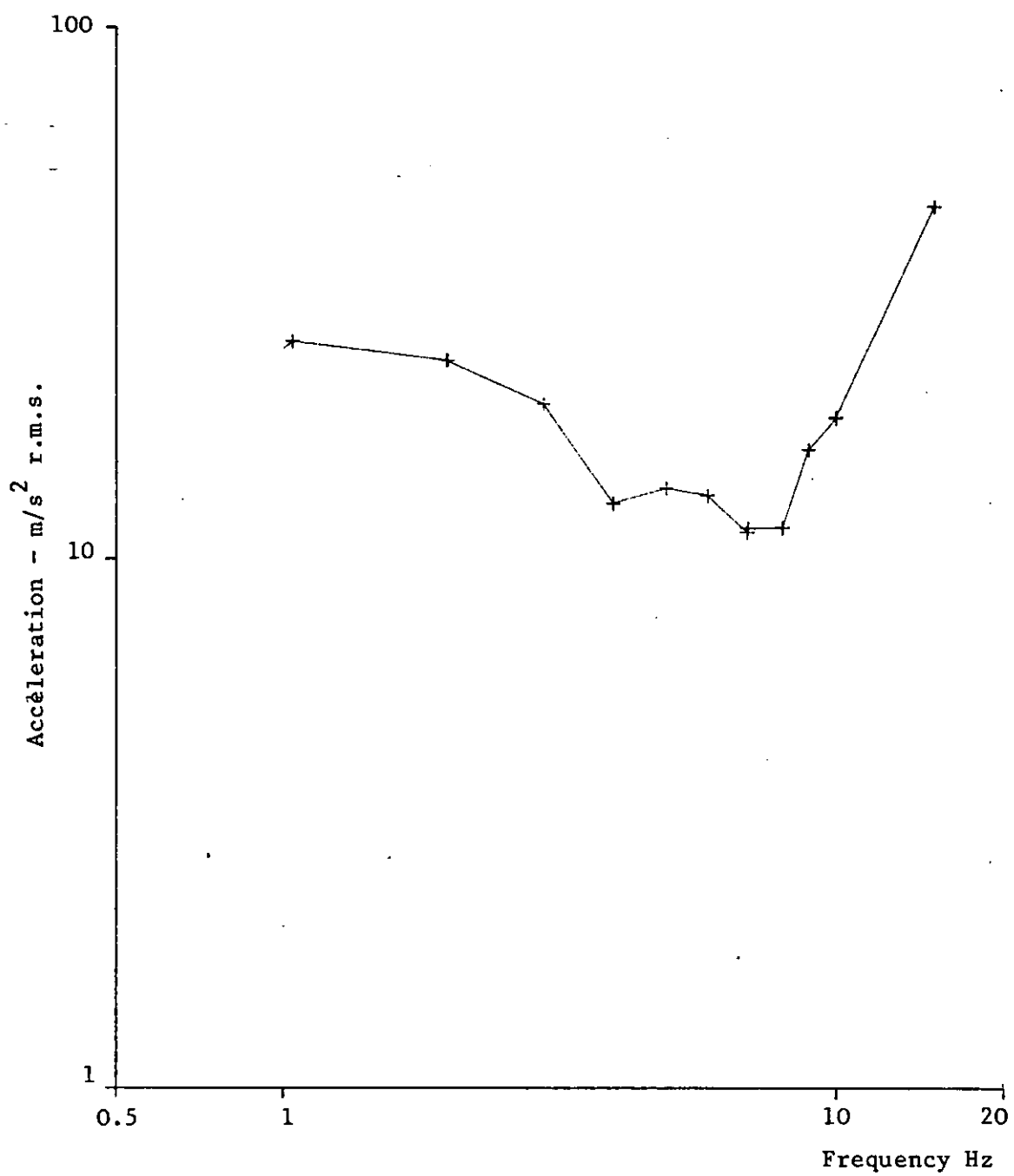


Fig. 2.4b Data of 2.4a plotted on a log/log graph to scale of figures 2.5 - 2.28

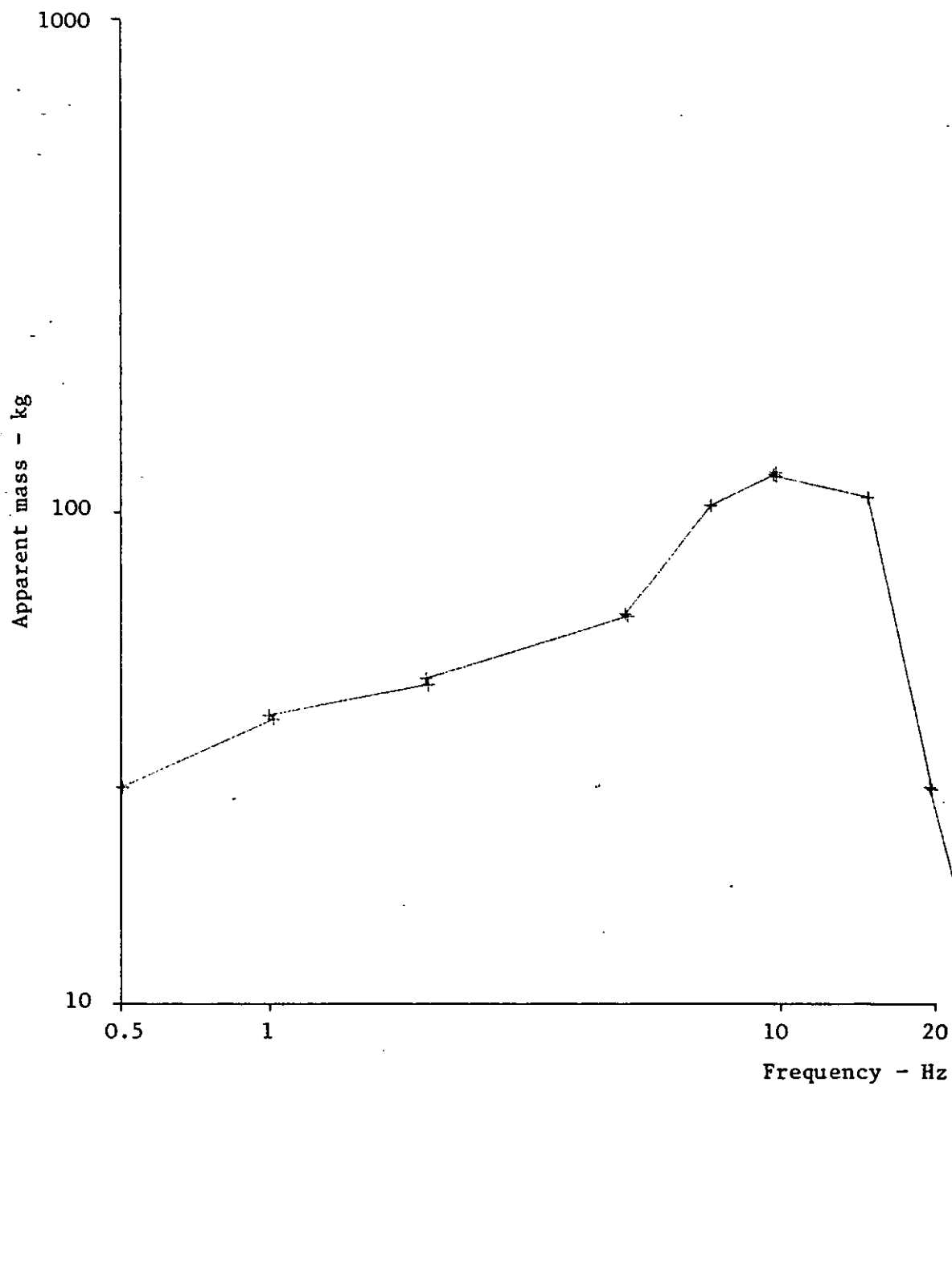


Fig. 2.5a Apparent mass of standing subjects (von Békésy 1934)
(60 kg subjects)

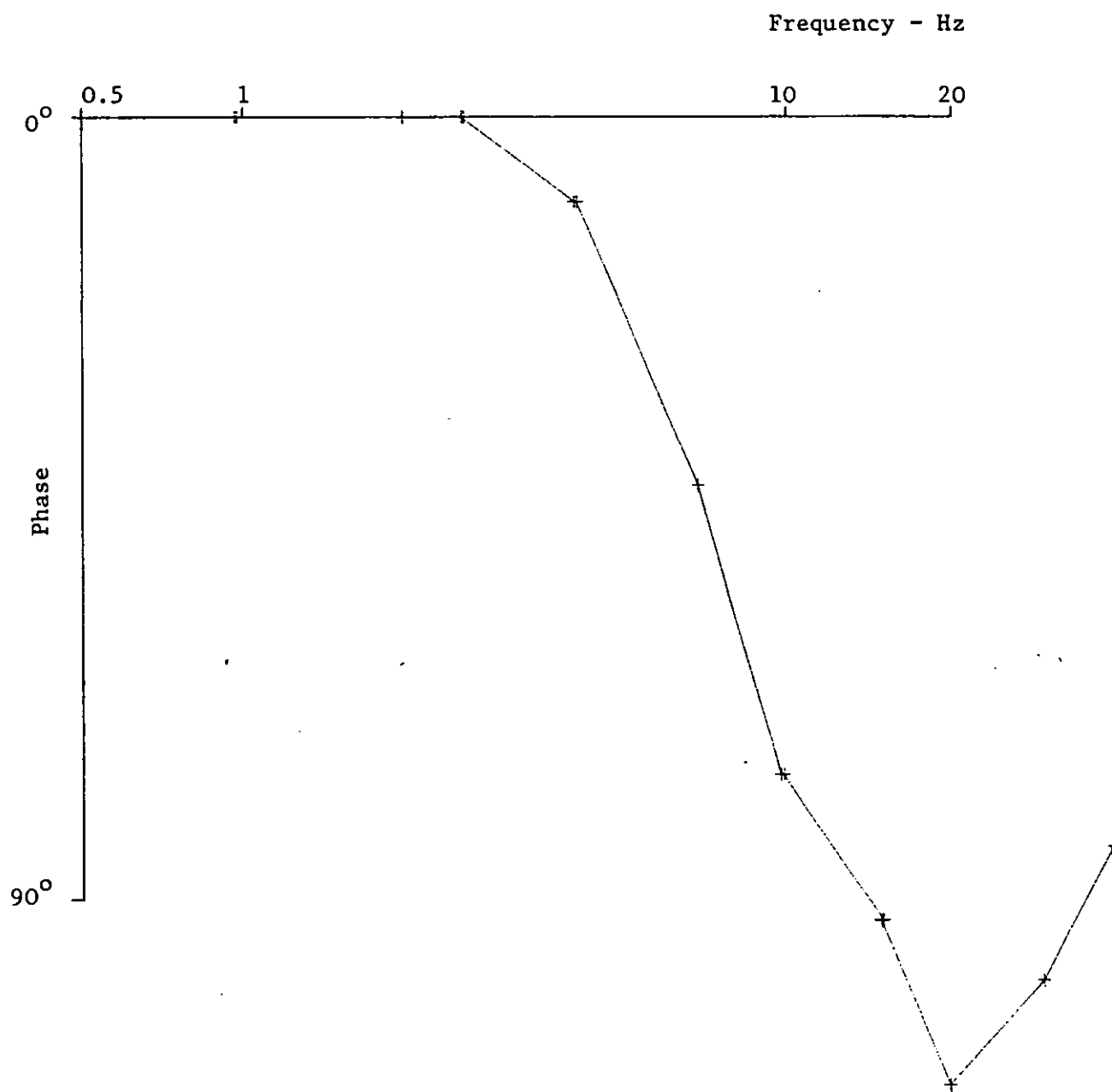


Fig. 2.5b Phase angles

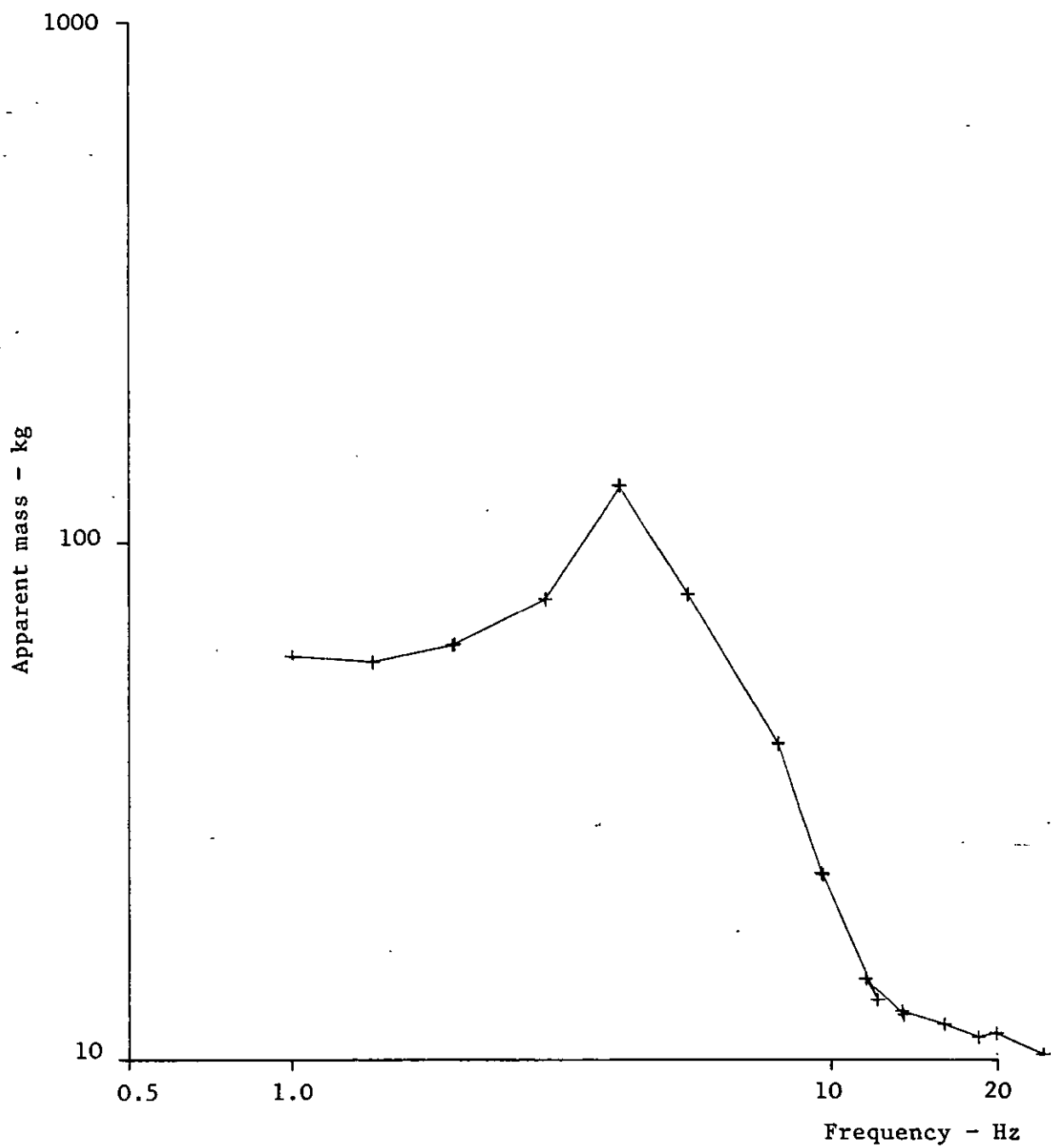


Fig. 2.6 Apparent mass of seated subject (Dieckmann 1957)

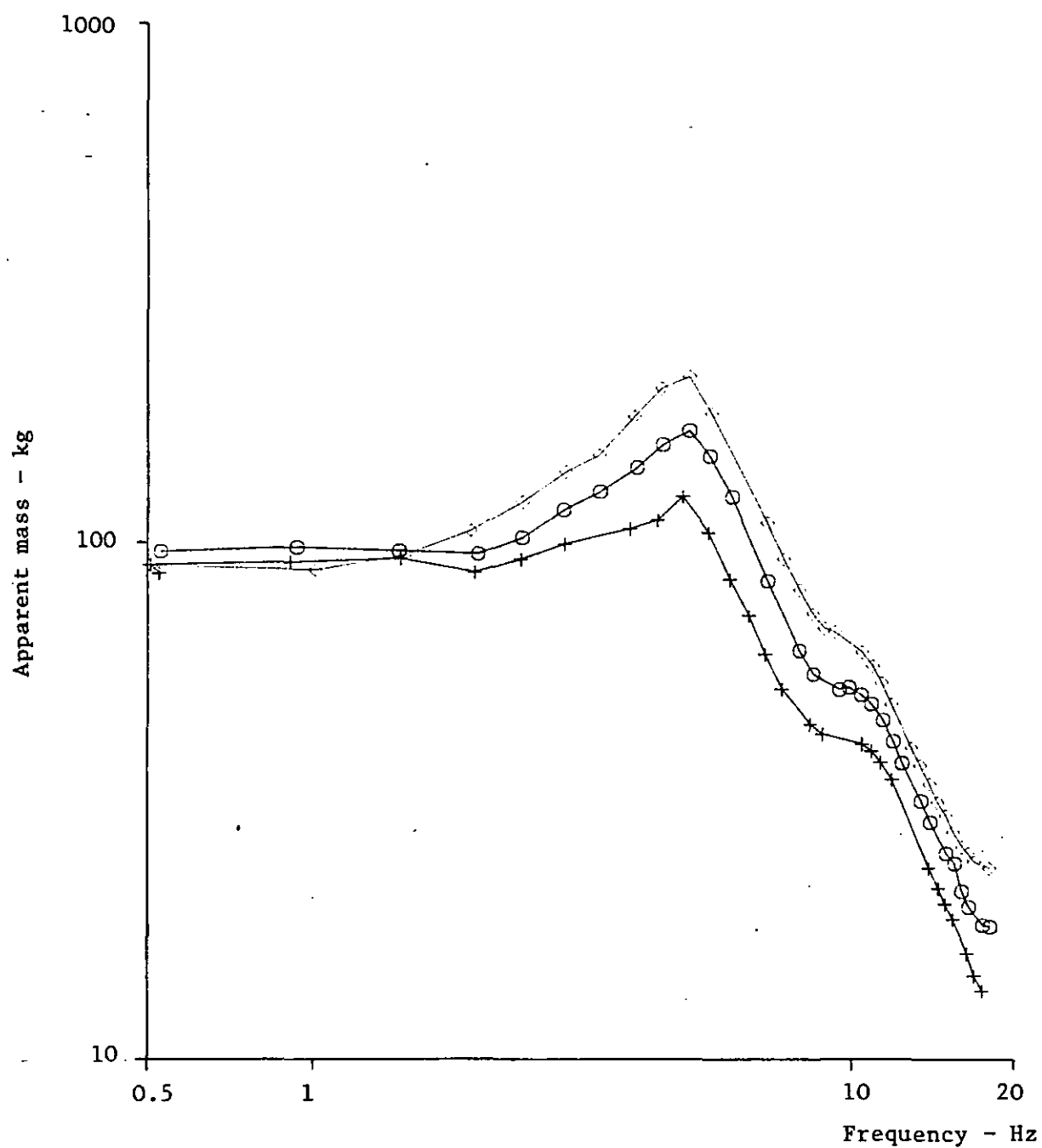


Fig. 2.7a Apparent mass of seated subjects (Coermann 1961)
(median, 20th and 80th percentiles for 8 subjects)

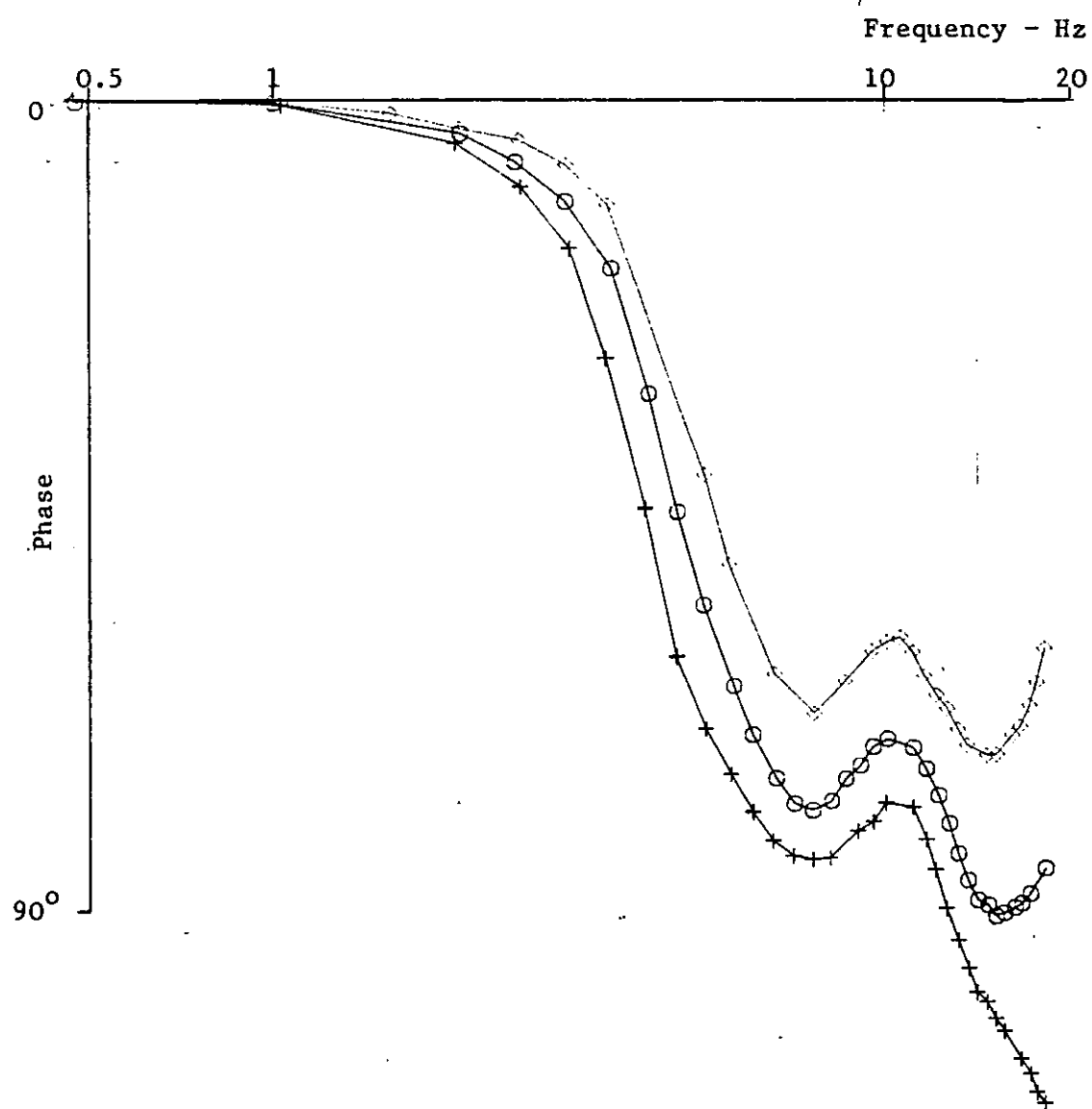


Fig. 2.7b · Phase angles

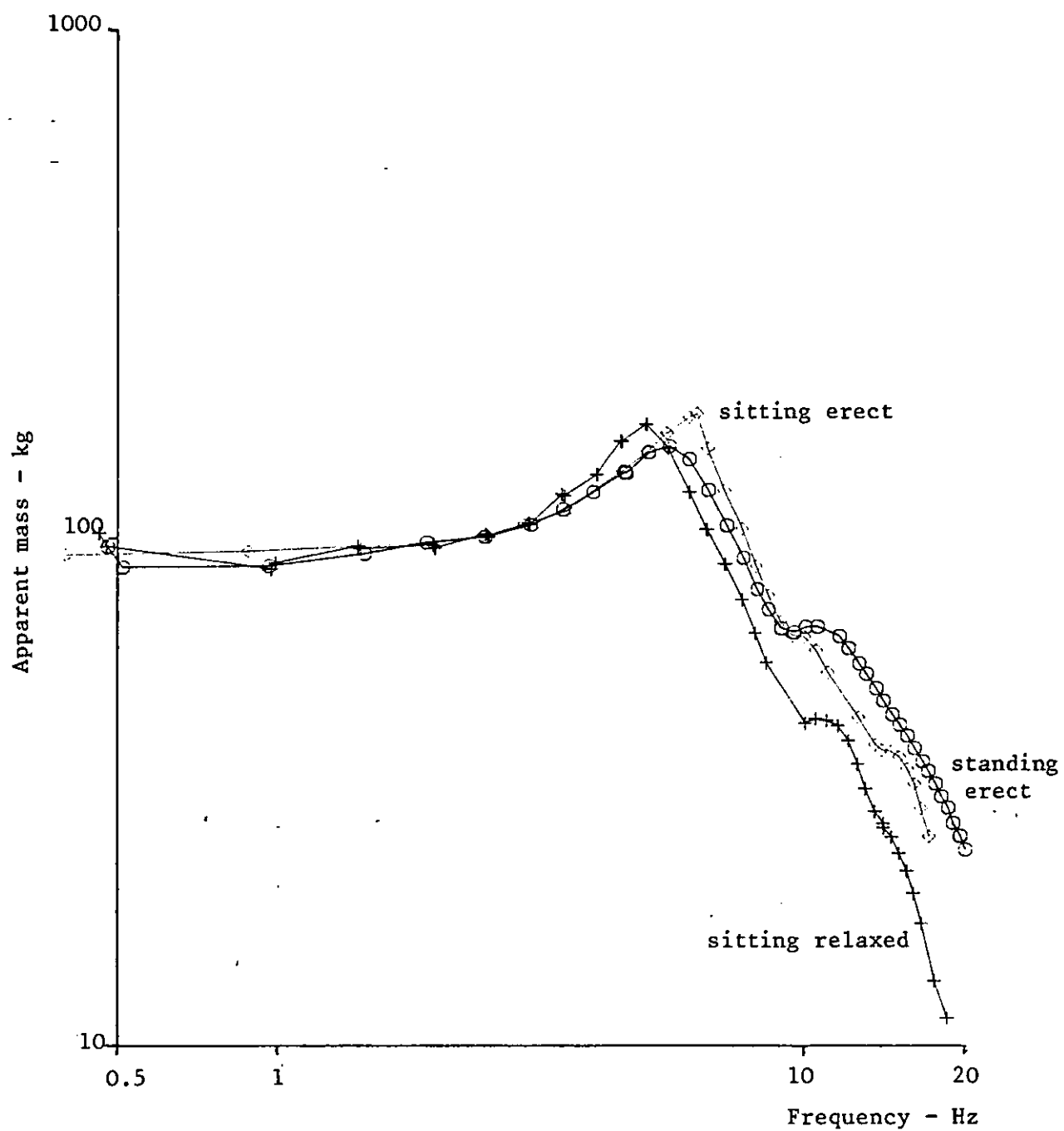


Fig. 2.8a Apparent mass of seated subjects (Coermann 1961)
(Effects of posture)

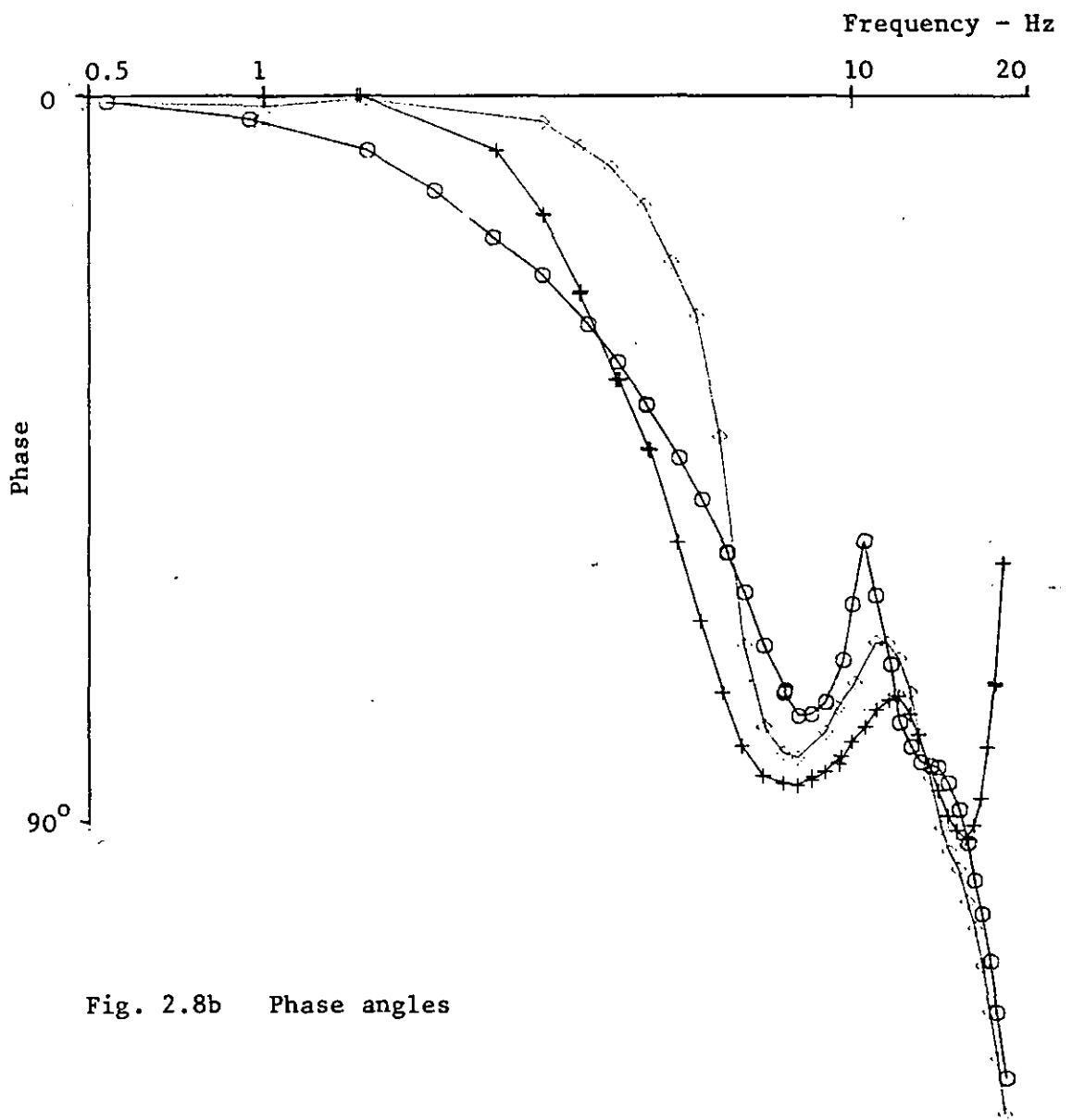


Fig. 2.8b Phase angles

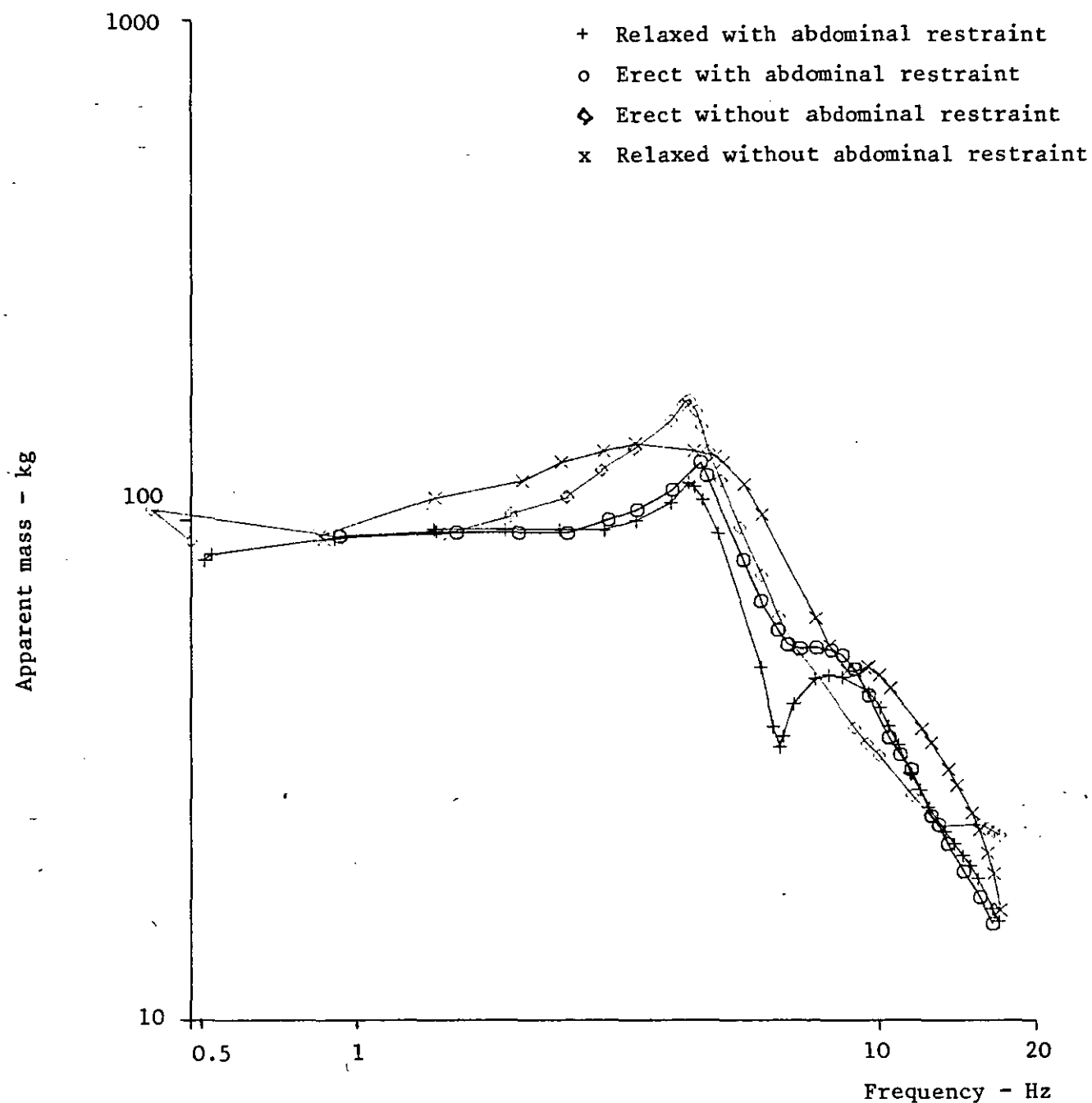


Fig. 2.9 Apparent mass of seated subject (Coermann 1961)
(Effects of restraints)

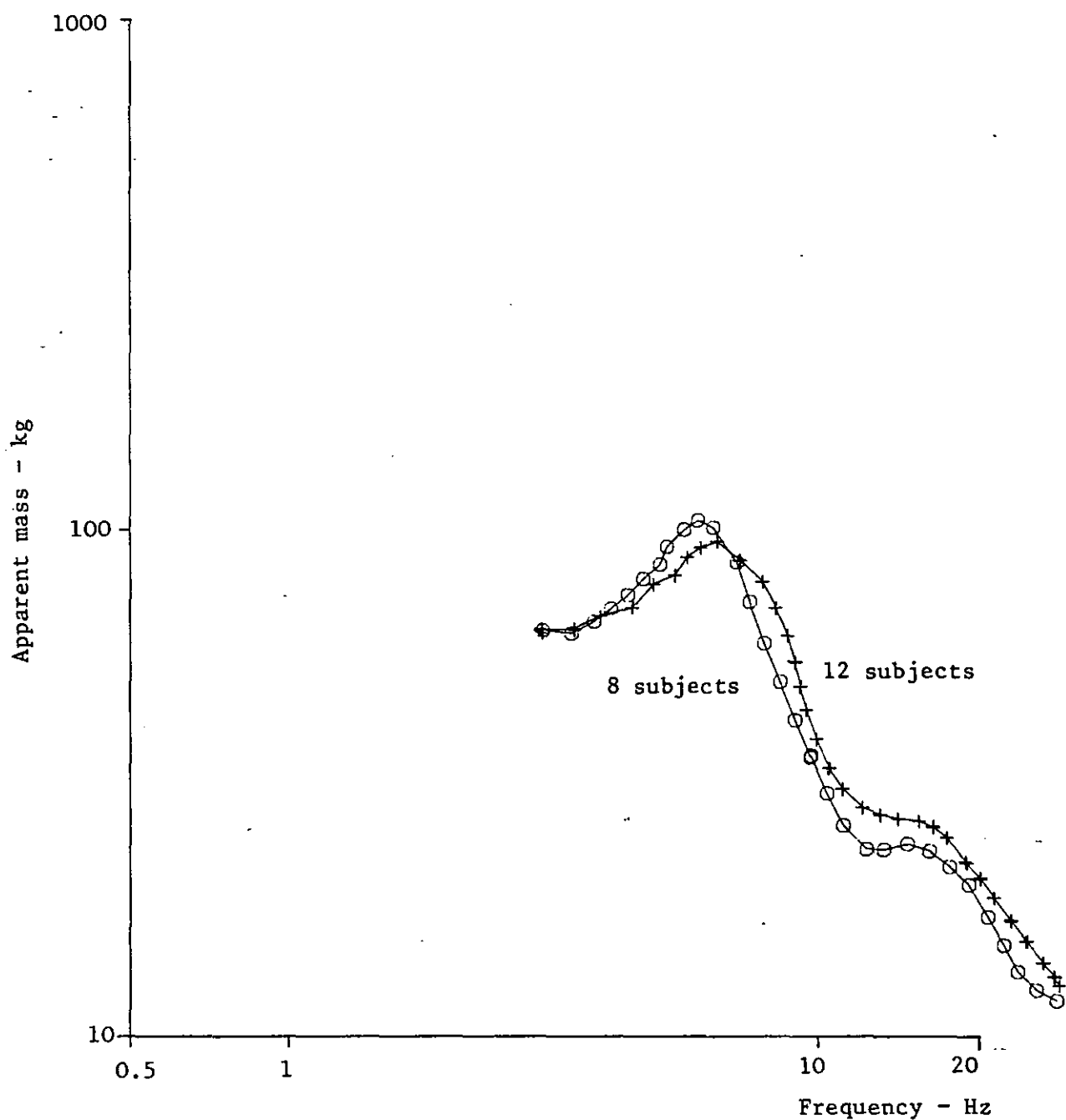


Fig. 2.10a Apparent mass of seated subject (Miwa 1975)
(inter subject variation - major divisions)

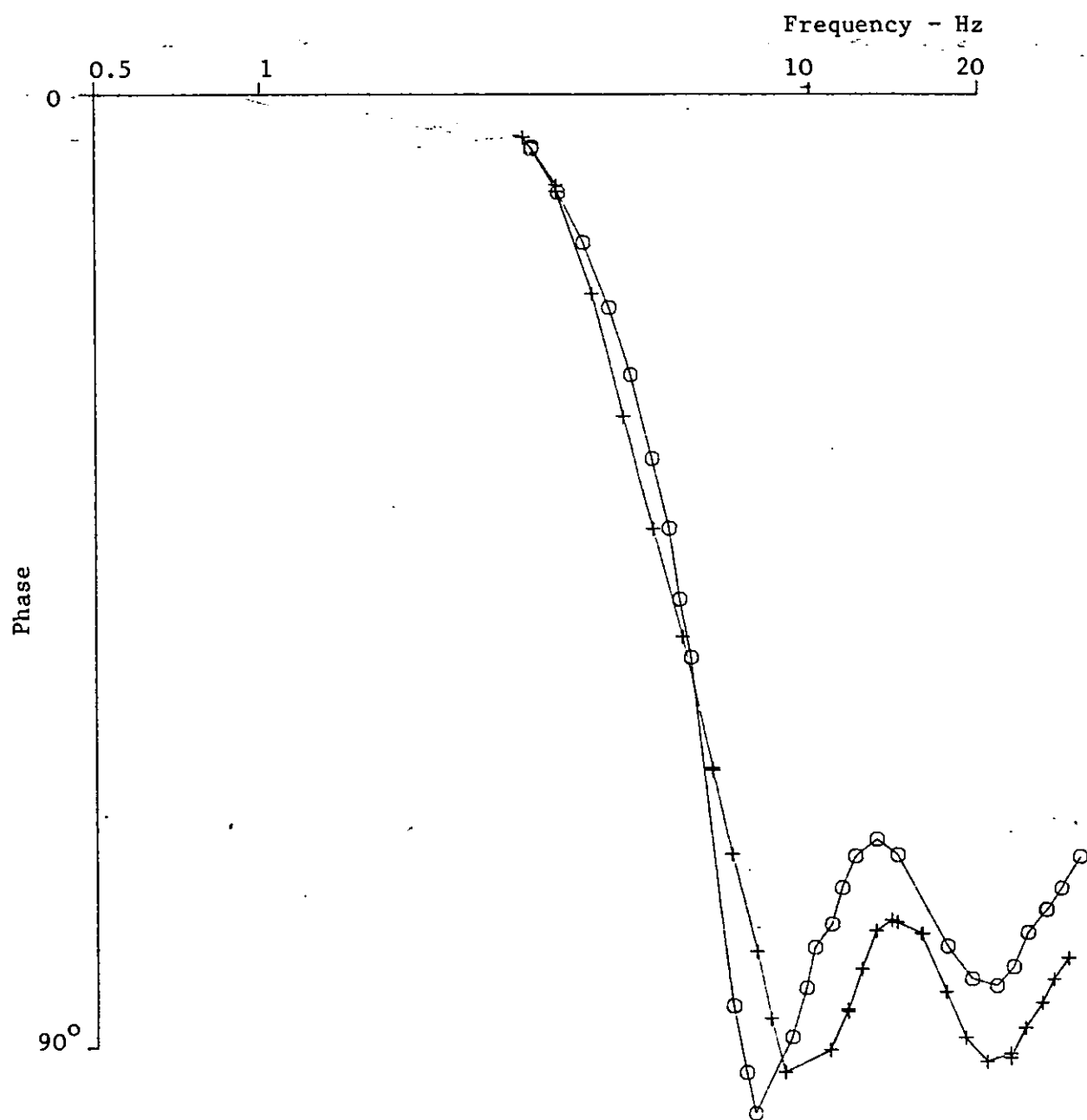


Fig. 2.10b Phase angles

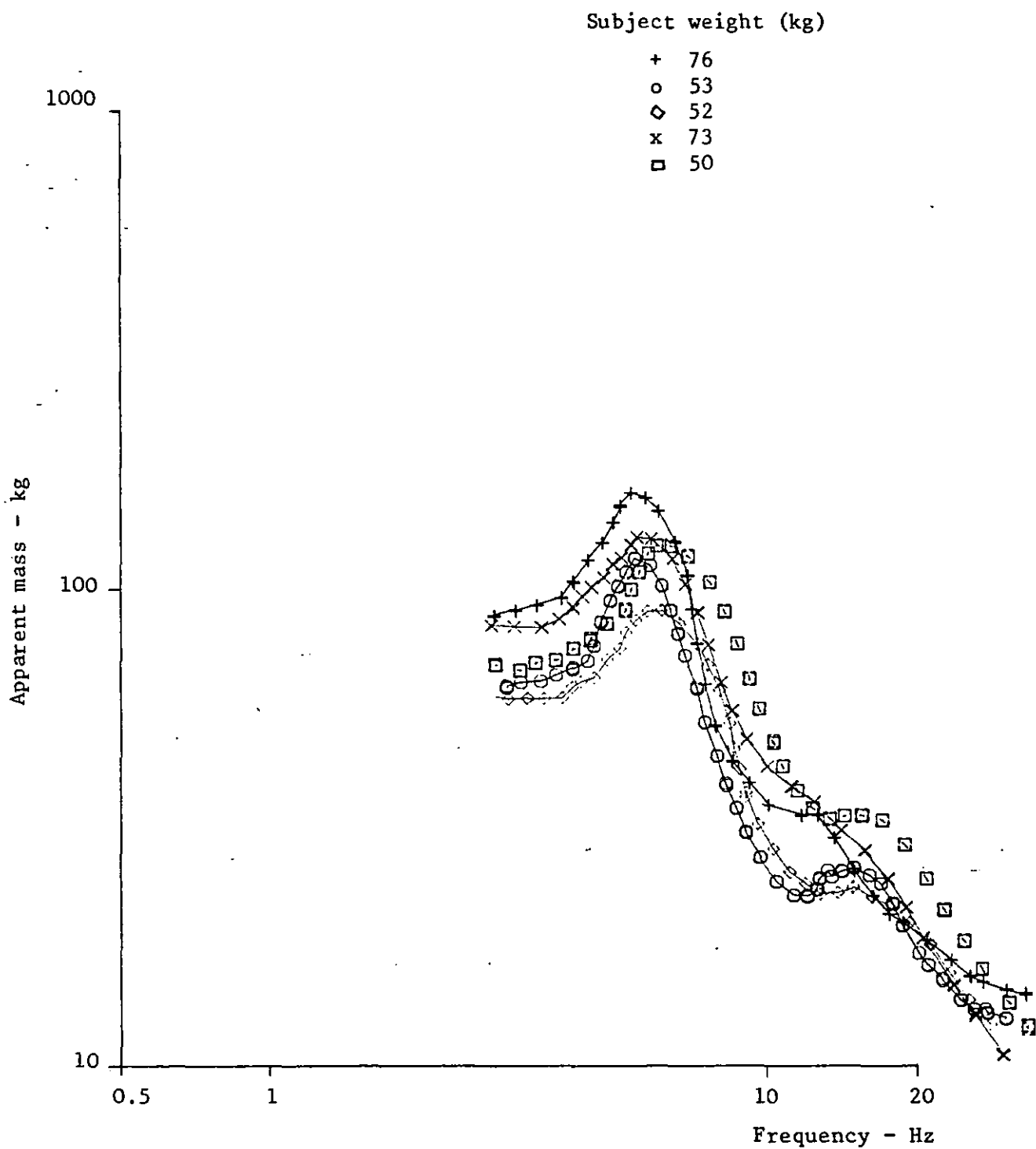


Fig. 2.11a Apparent mass of 5 seated subjects (Miwa 1975)

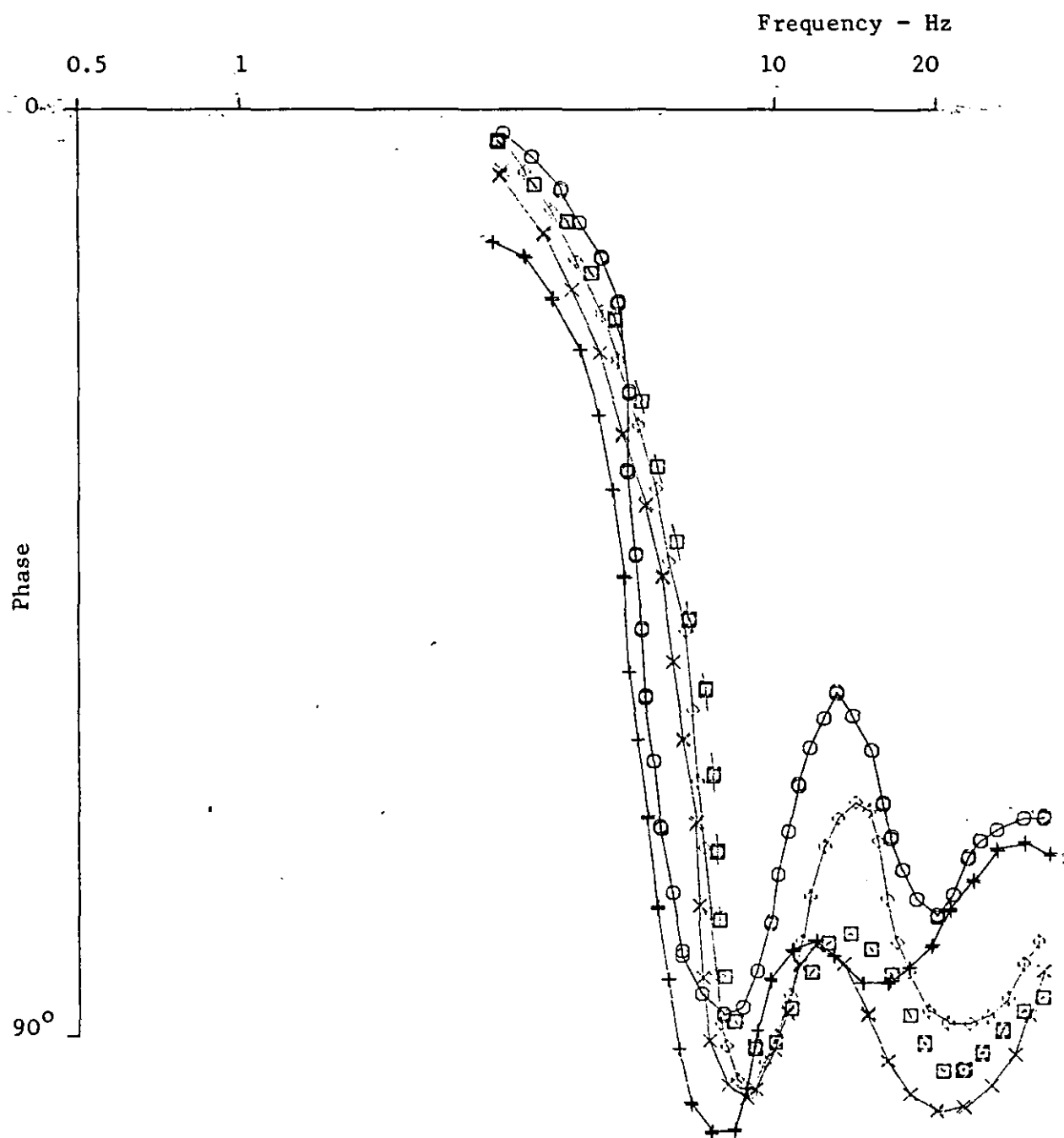


Fig. 2.11b Phase angles

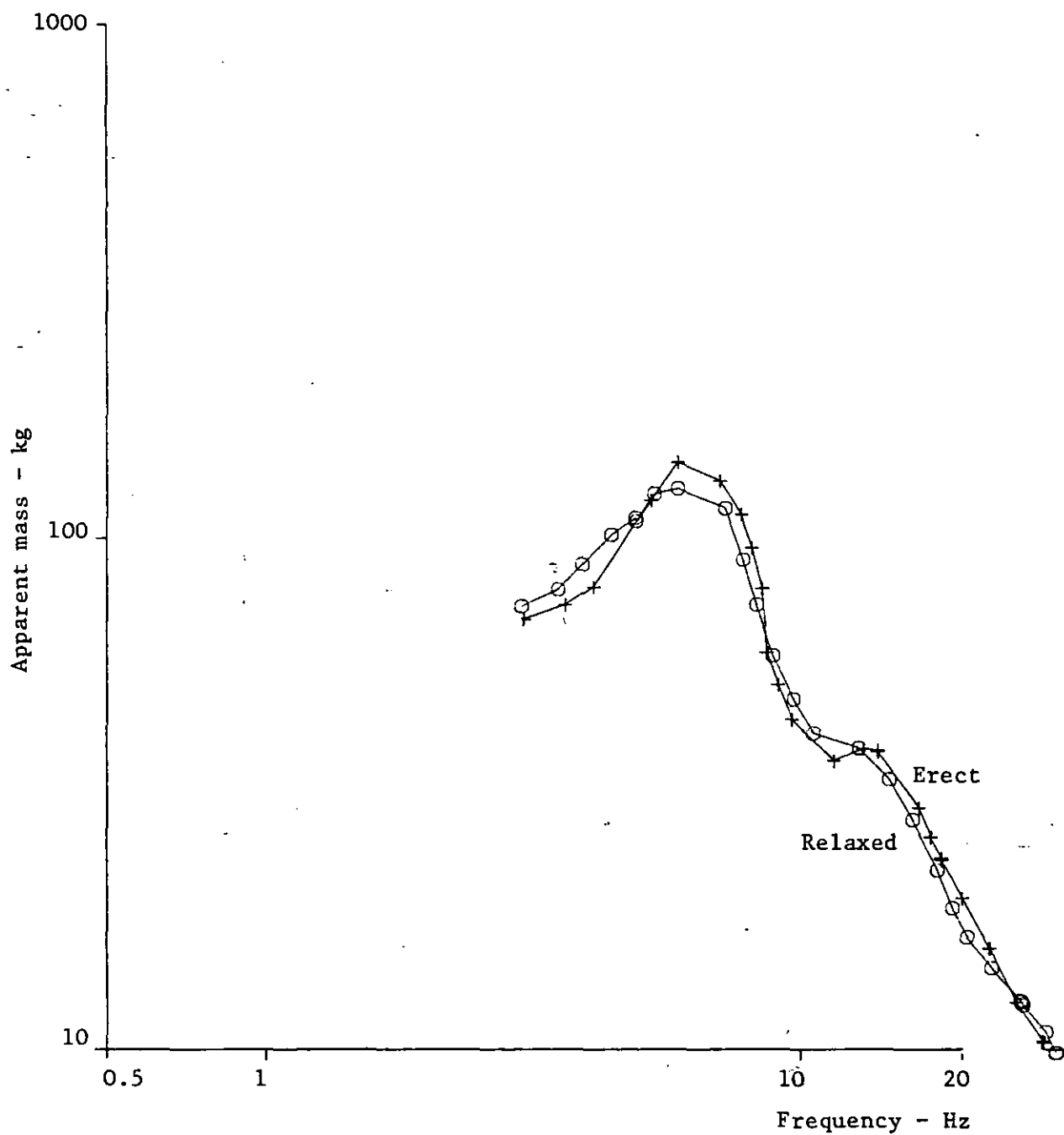


Fig. 2.12a Apparent mass of sitting subjects (Miwa 1975)
(Effects of posture)

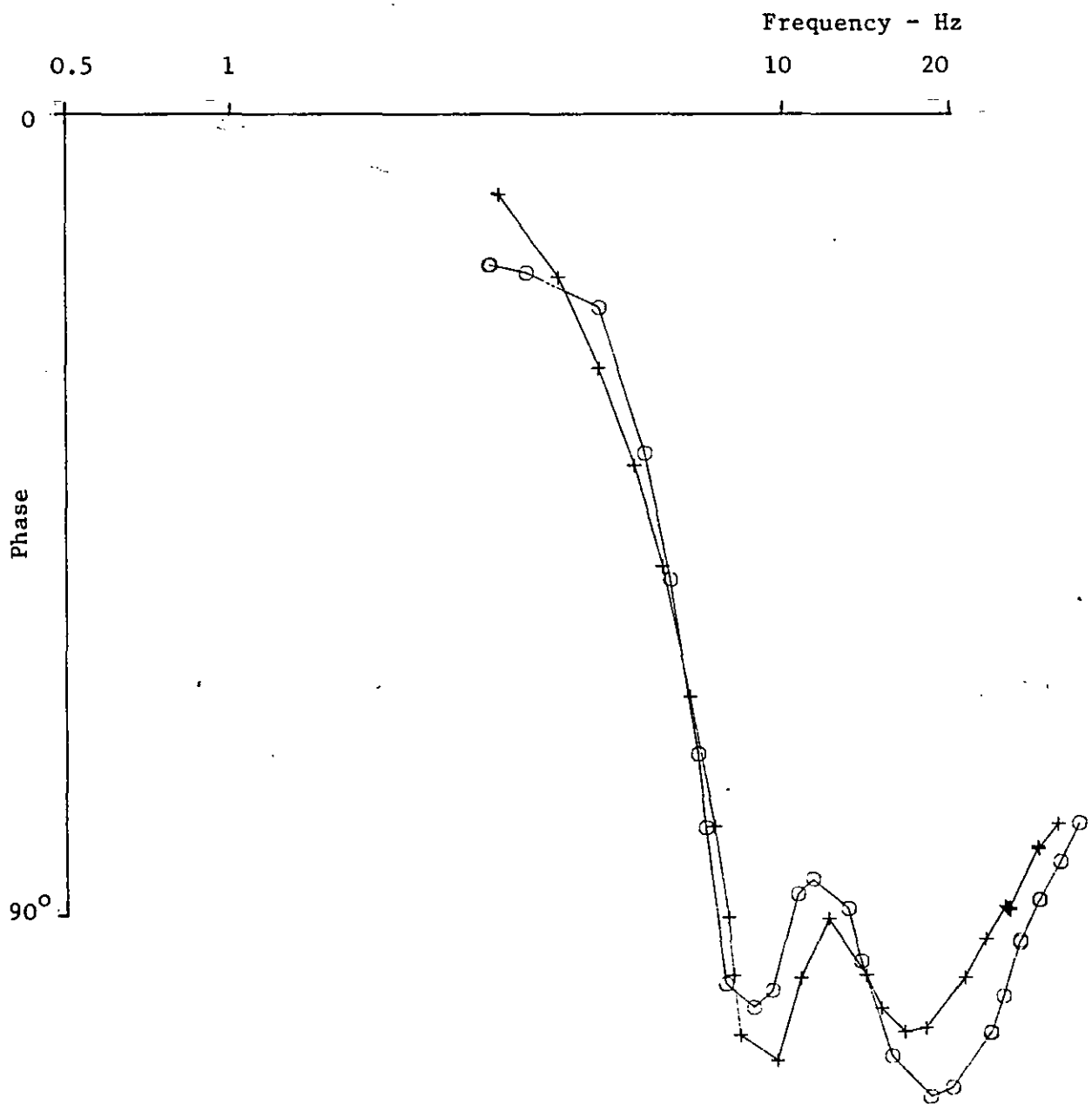


Fig. 2.12b Phase angles

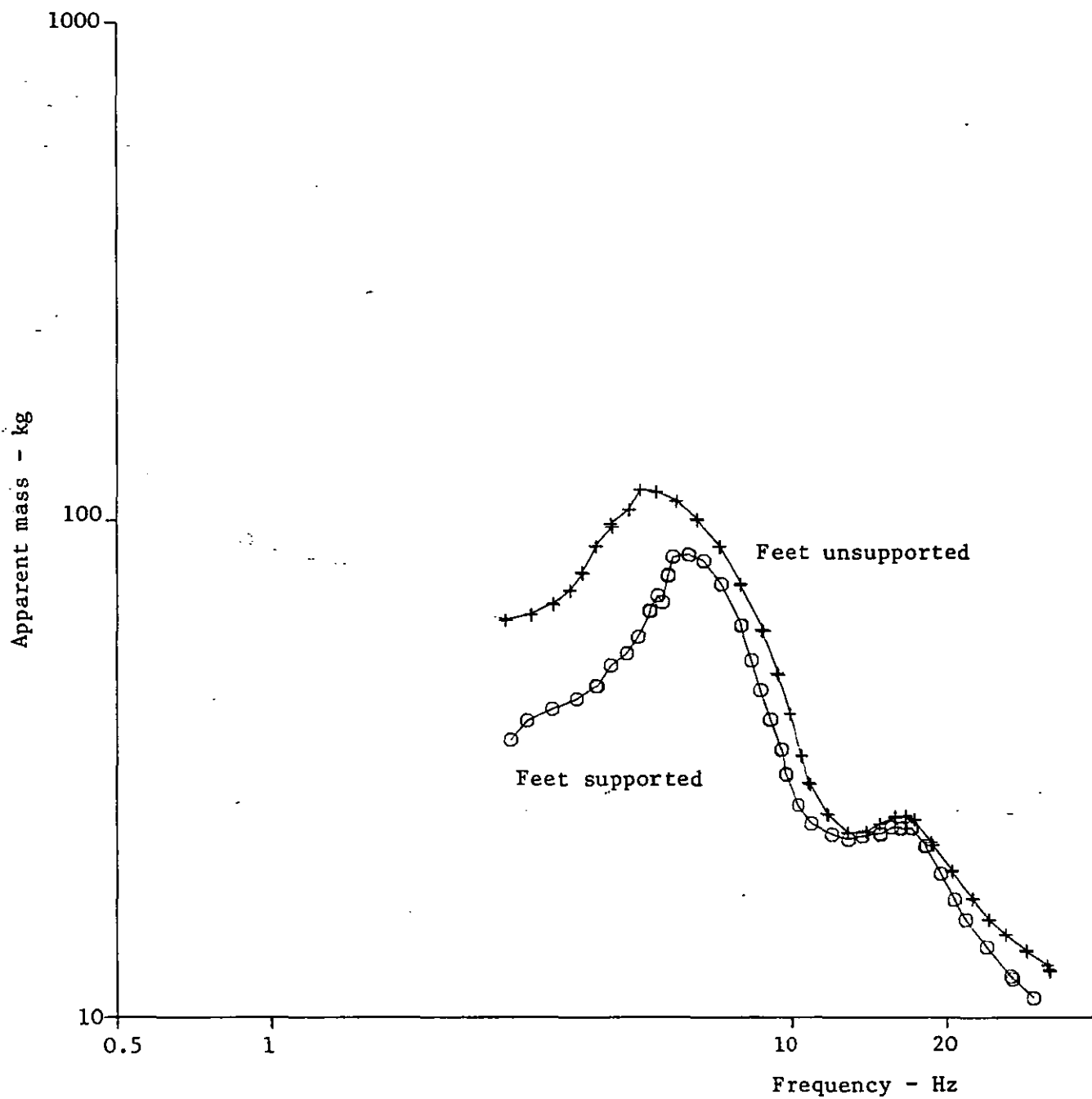


Fig. 2.13a Apparent mass of seated subjects (Miwa 1975)
(Effects of foot position)

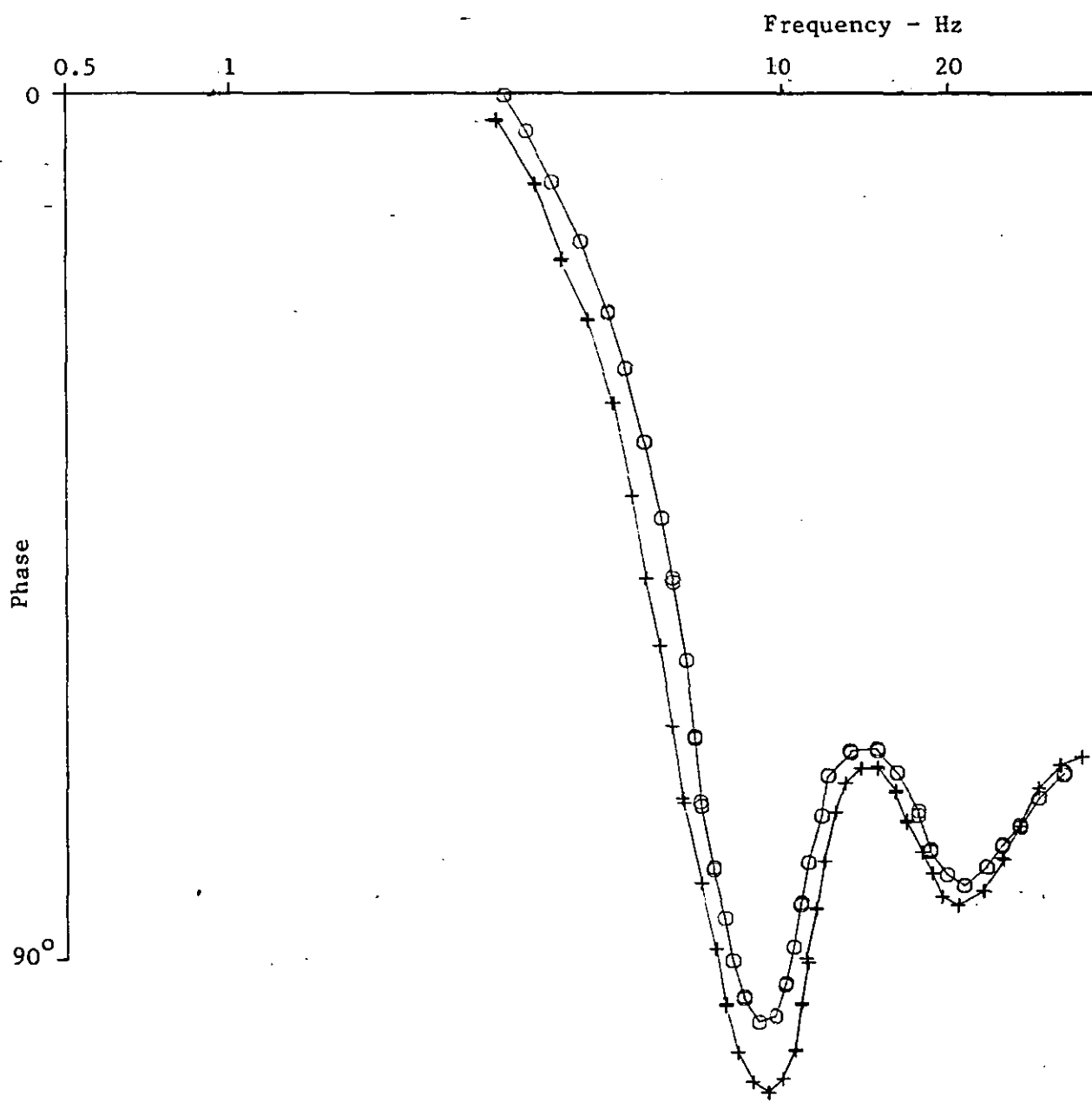


Fig. 2.13b Phase angles

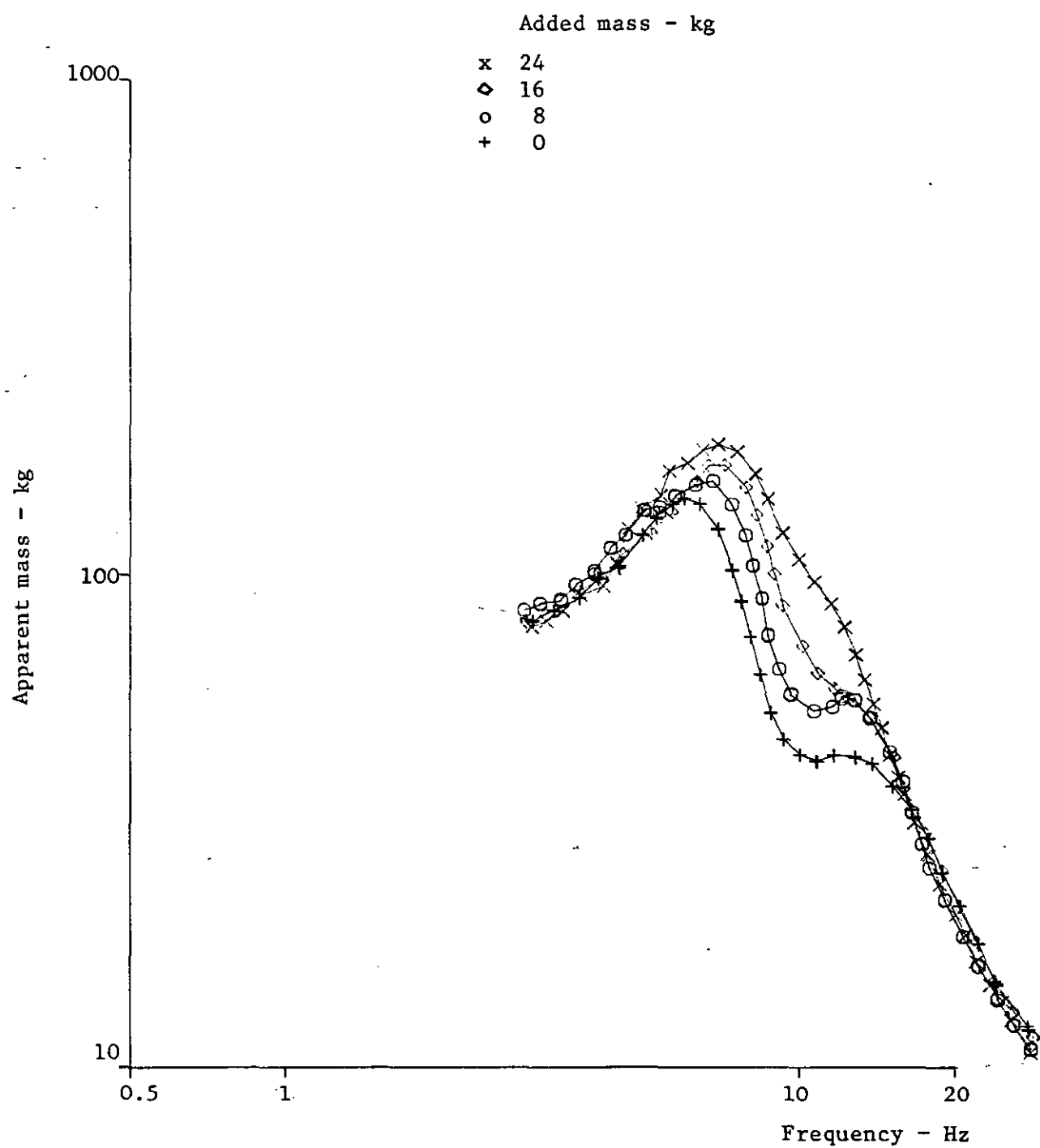


Fig. 2.14a Apparent mass of seated subjects (Miwa 1975)
(Effects of additional mass carried at waist -
subject mass 73 kg)

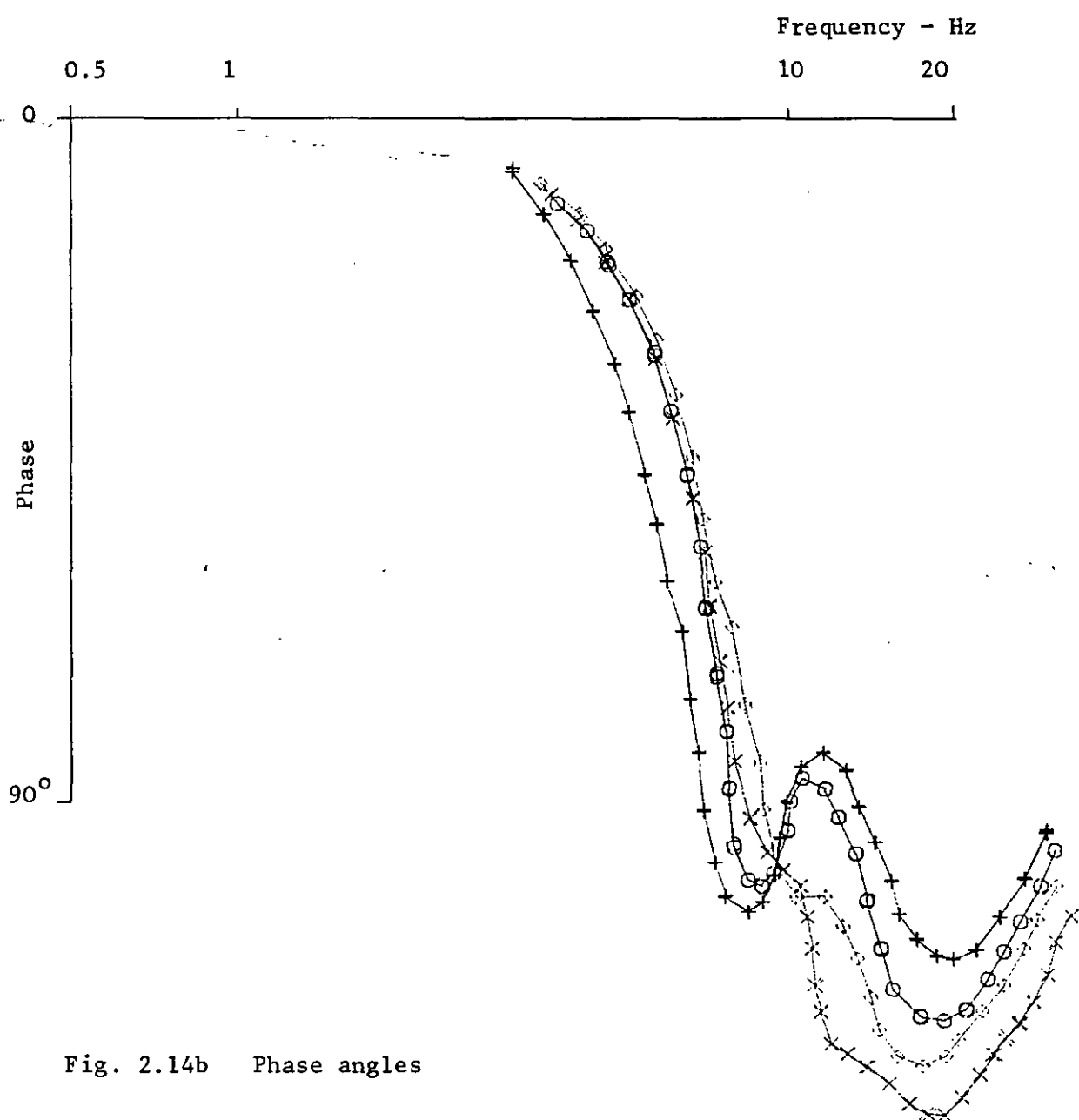


Fig. 2.14b Phase angles

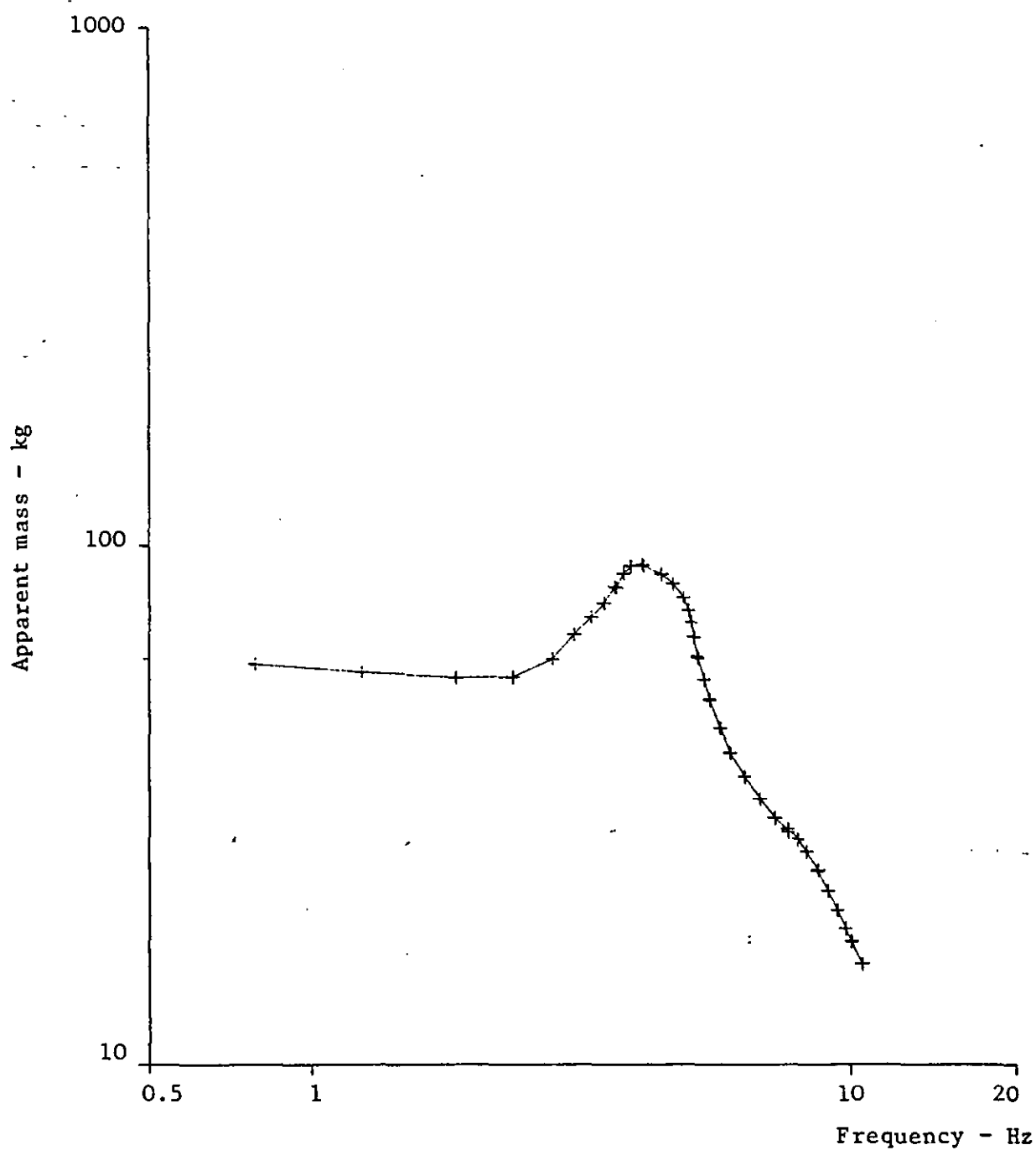


Fig. 2.15a Apparent mass of seated subjects (Suggs et al 1969)
(mean of 11 subjects)

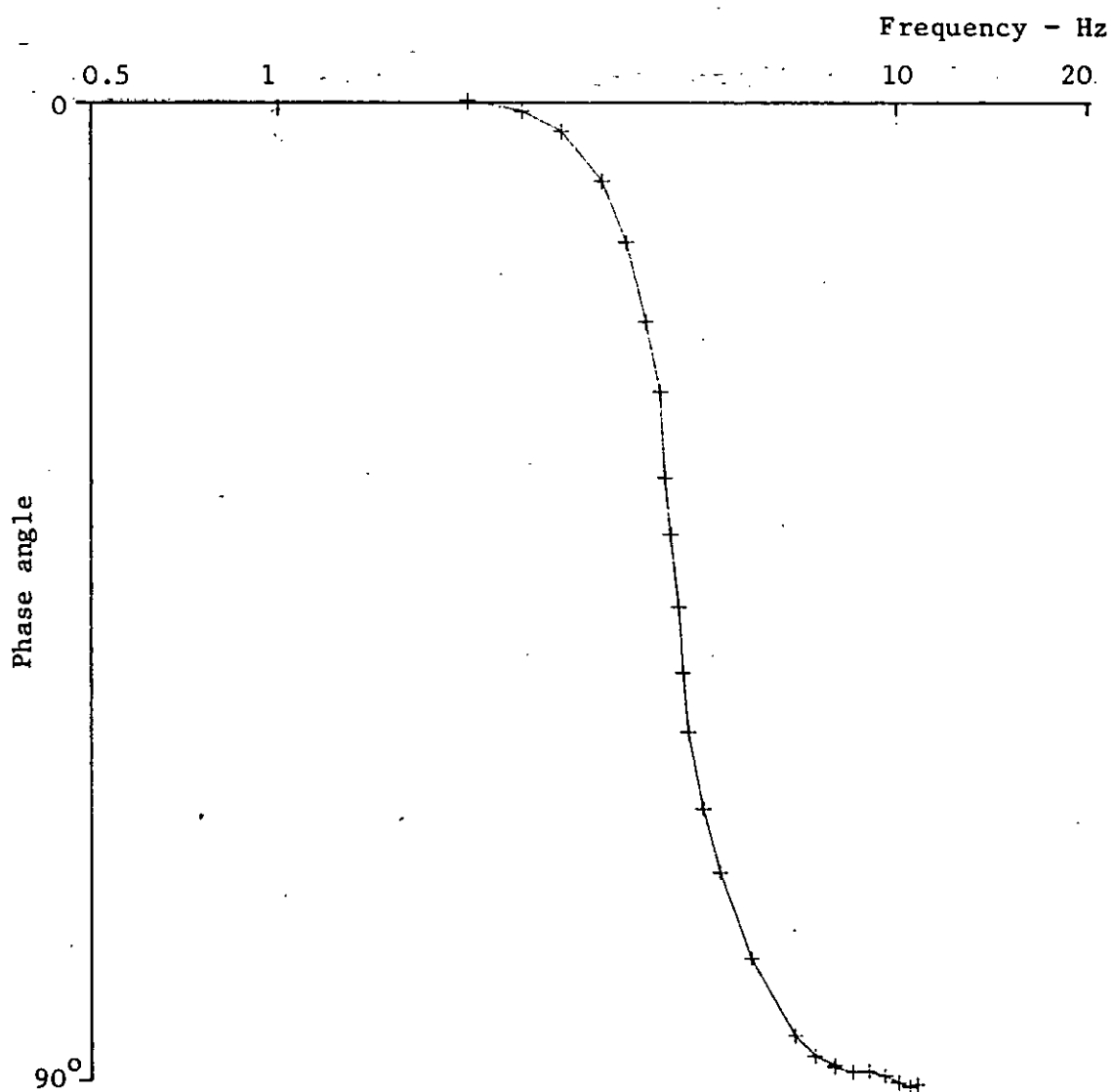


Fig. 2.15b Phase angles

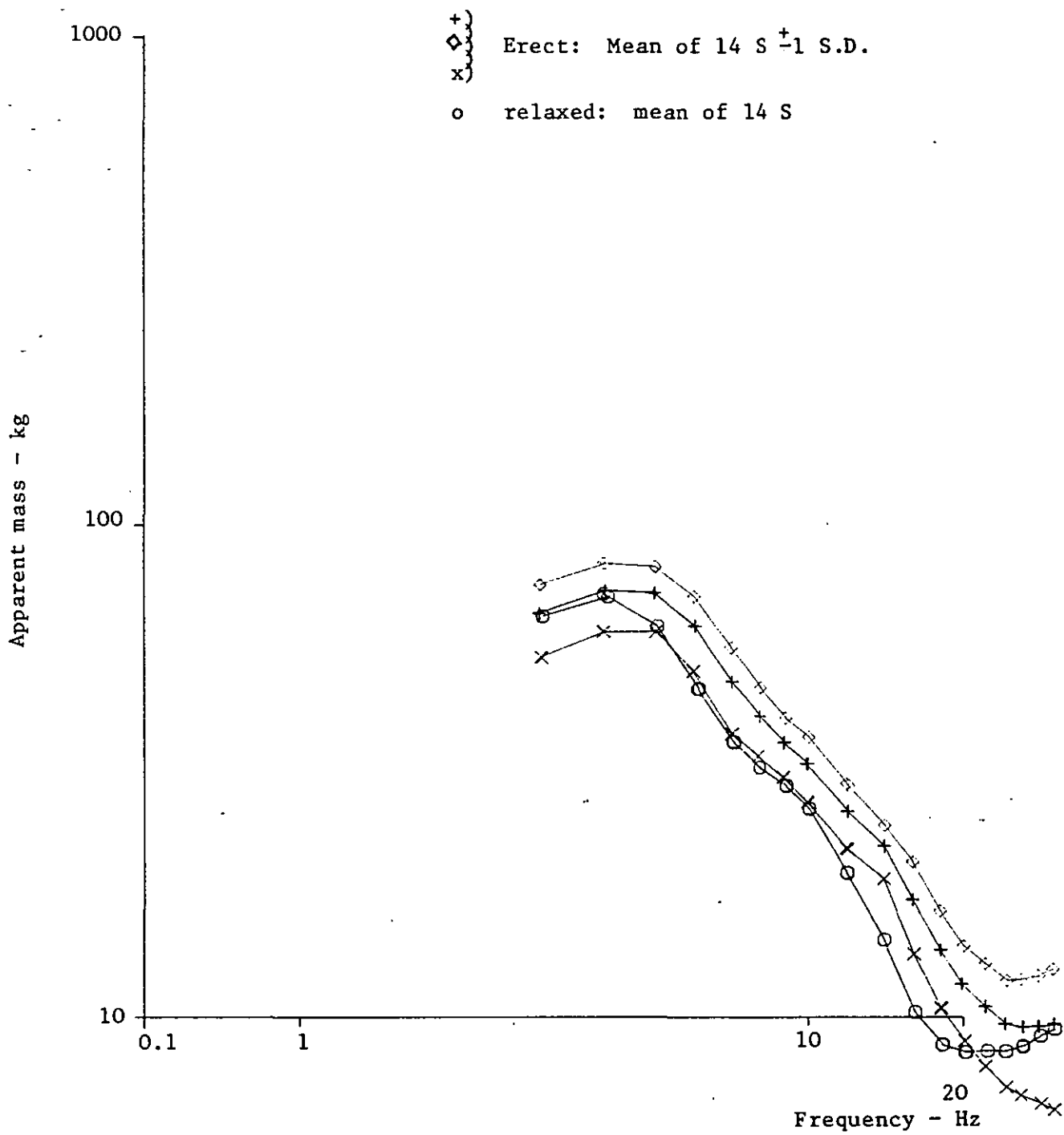


Fig. 2.16a Apparent mass of seated subjects (Lawes 1974)

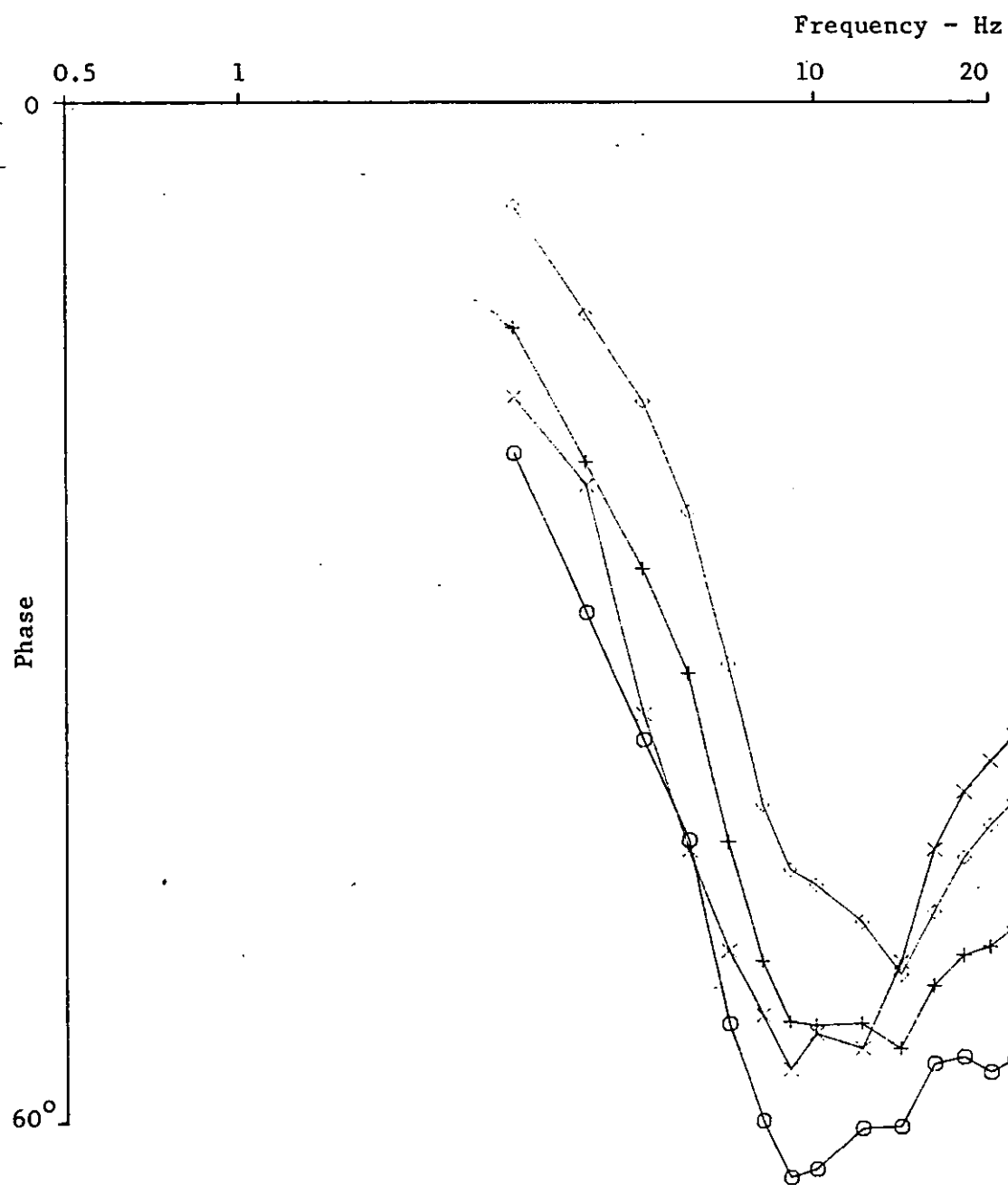


Fig. 2.16b Phase angles

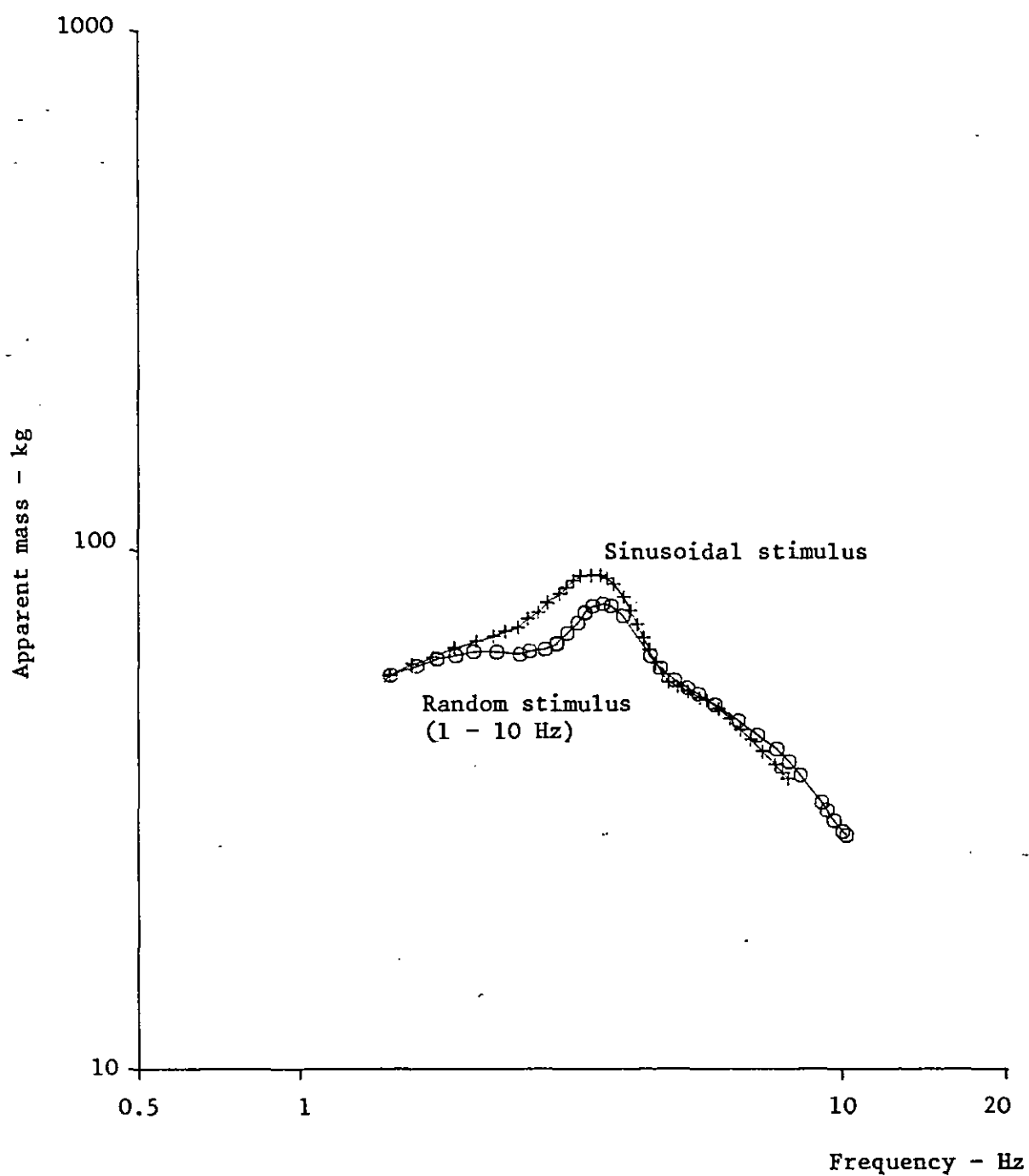


Fig. 2.17a Apparent mass of seated subjects (Donati, 1980)
(Effects of stimulus - mean of 15 S)

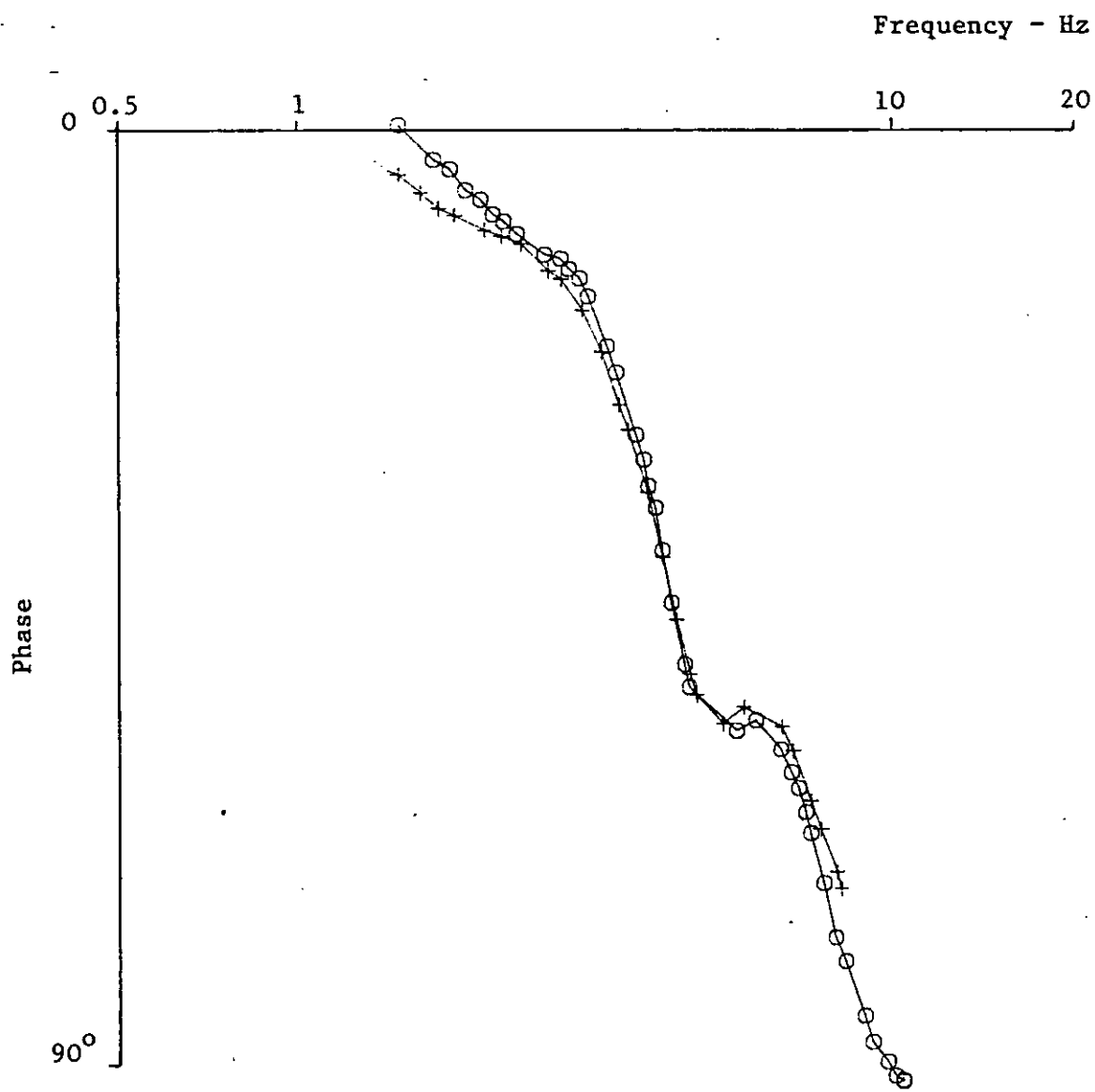


Fig. 2.17b Phase angle

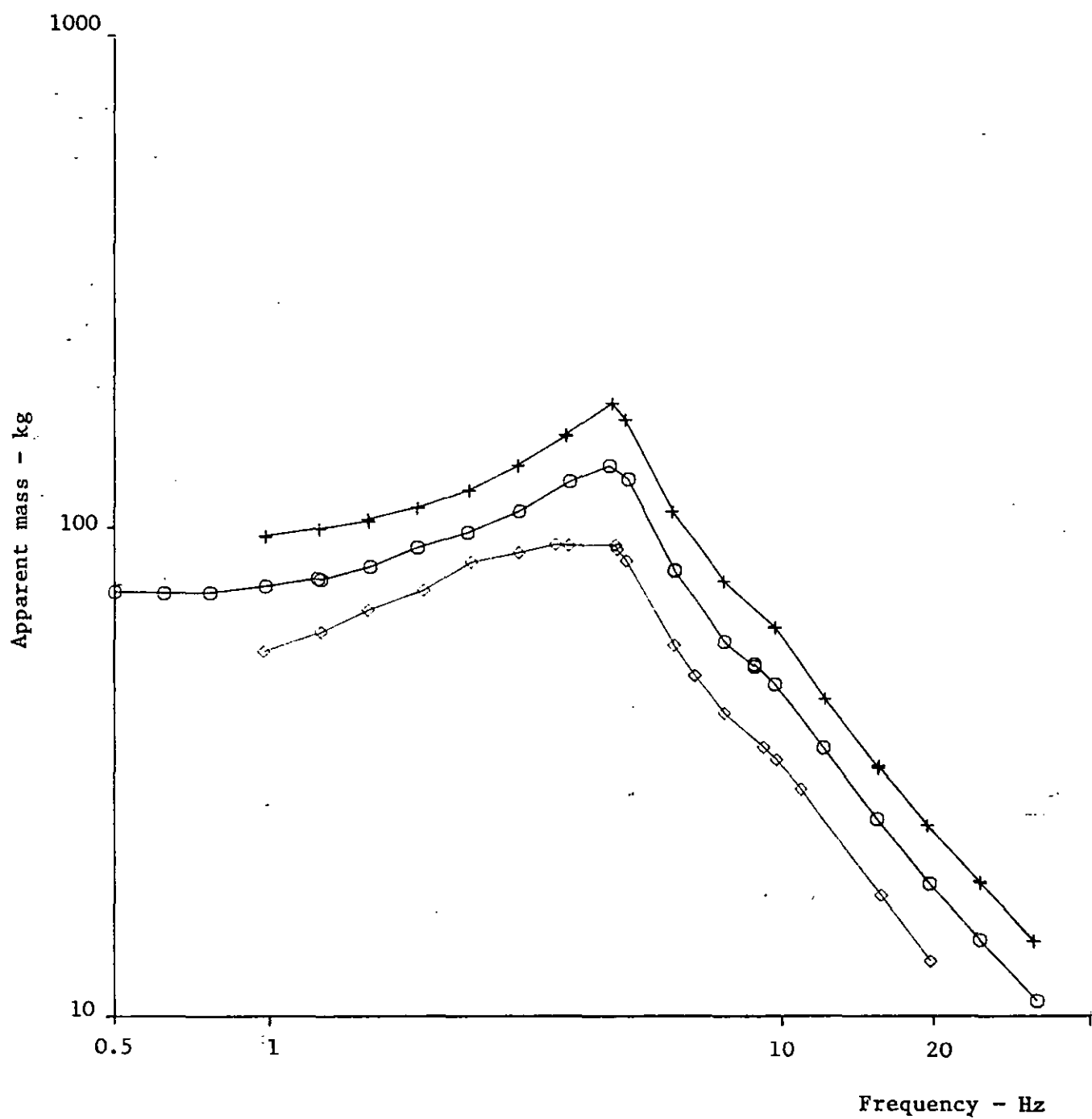


Fig. 2.18a Apparent mass of seated subjects (values of ISO/DIS 5982)

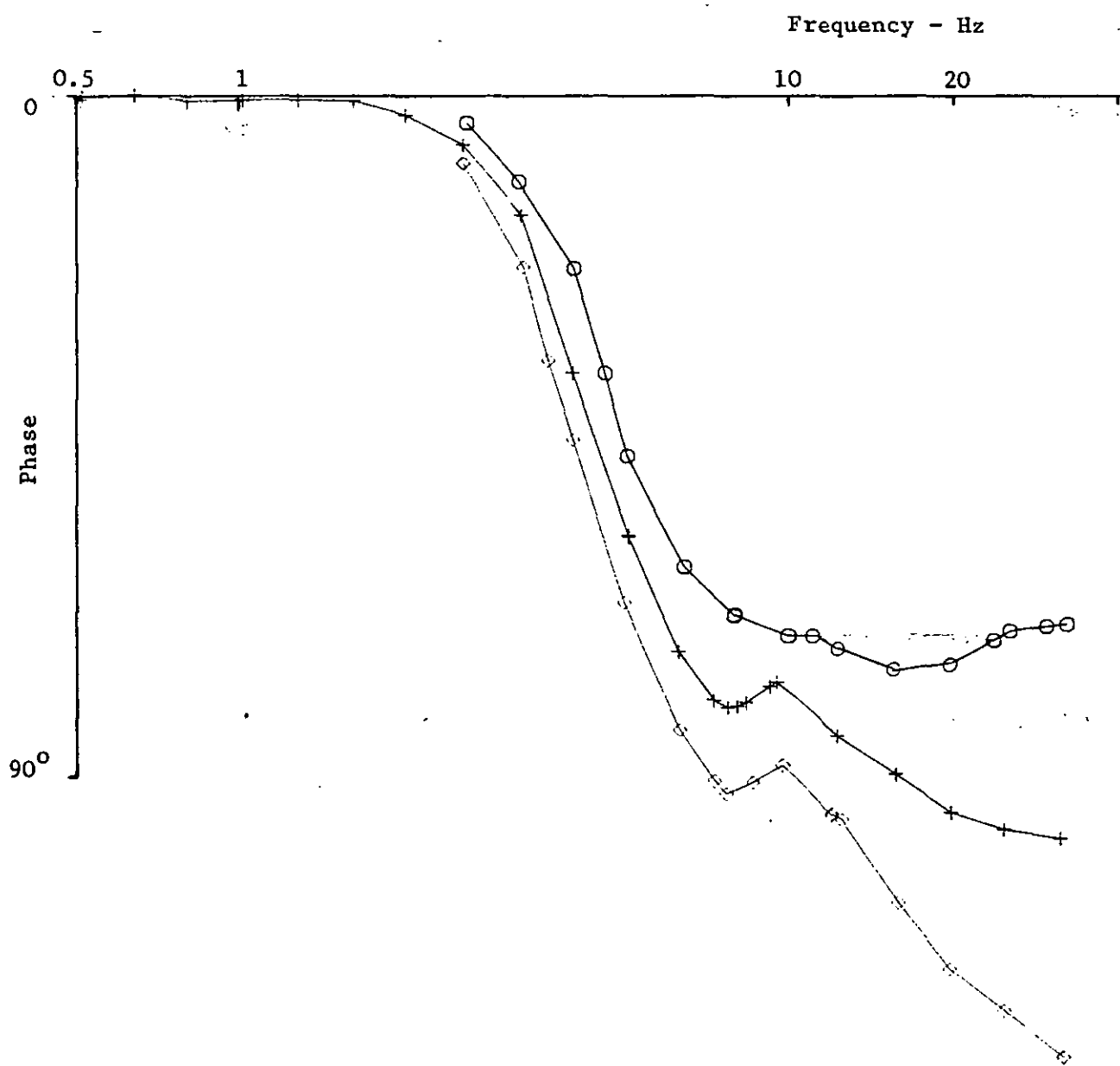


Fig. 2.18b Phase angles

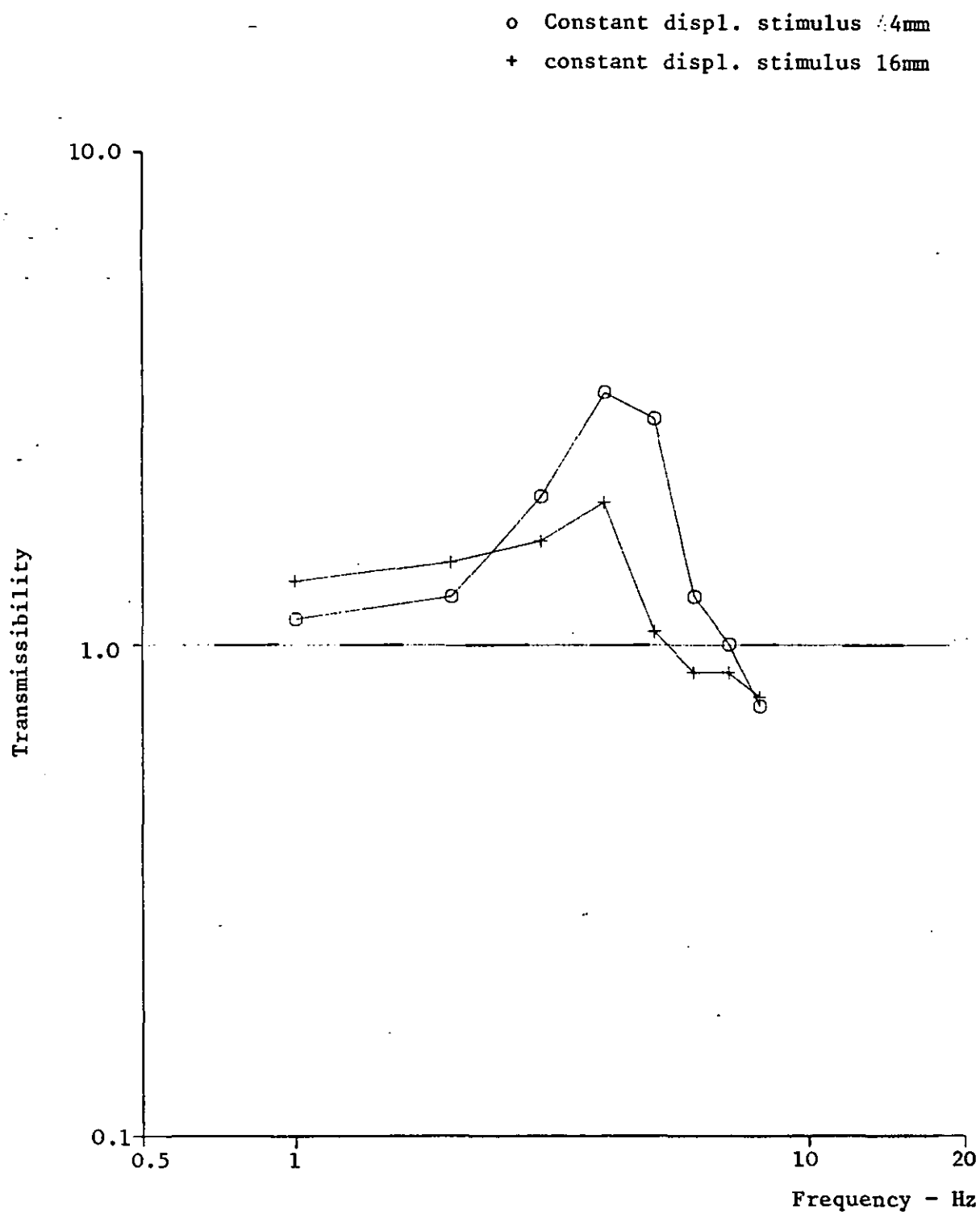


Fig. 2.19 Transmissibility of seated subject

(Müller 1939)

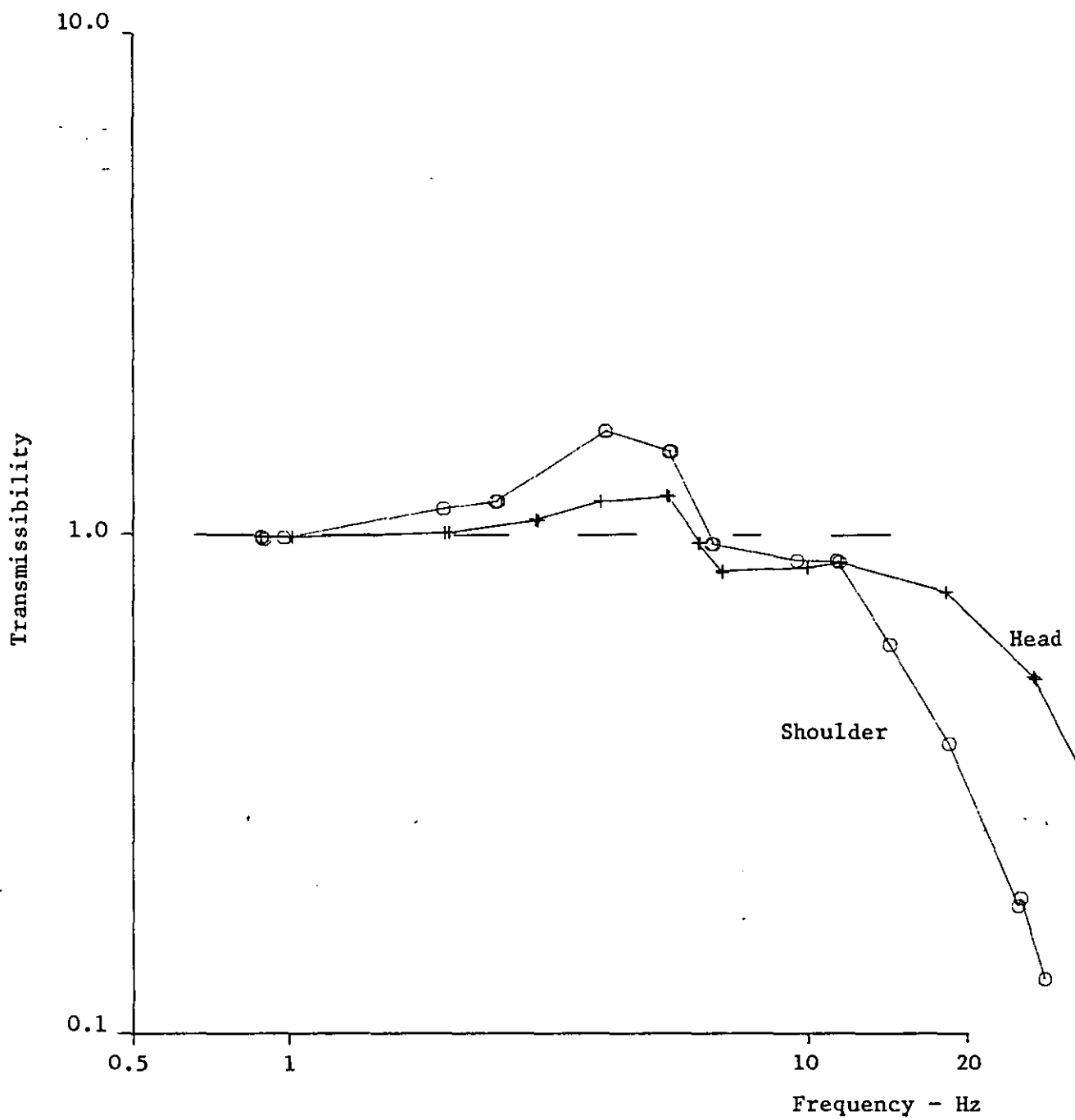


Fig. 2.20 Transmissibility of seated subject (Dieckmann 1957)

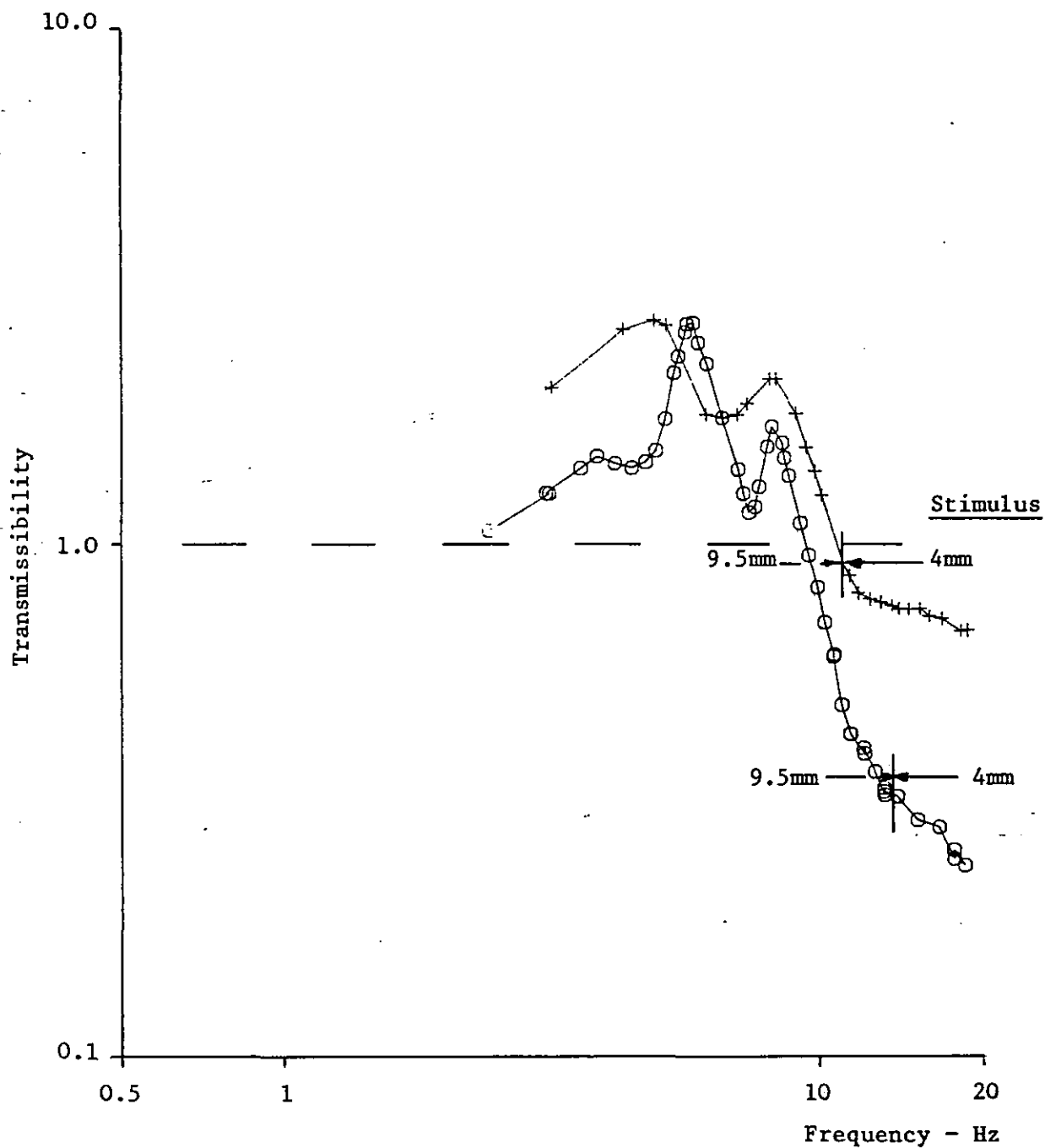


Fig. 2.21 Transmissibility of seated 2 subjects (Latham 1957)

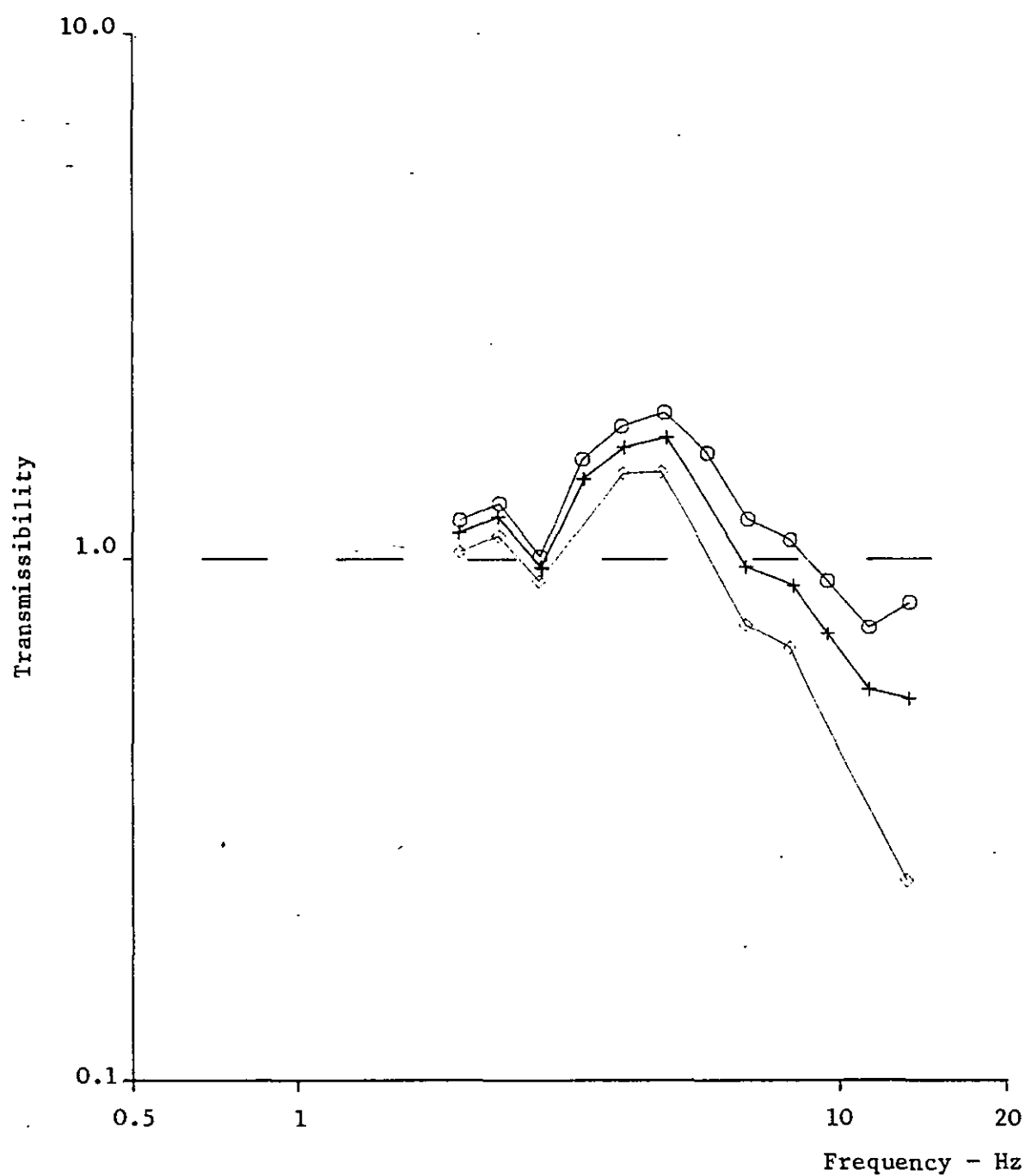


Fig. 2.22a Transmissibility of seated subjects (Guignard & Irving, 1960)
(mean ± 1 S.D. of 10 S)

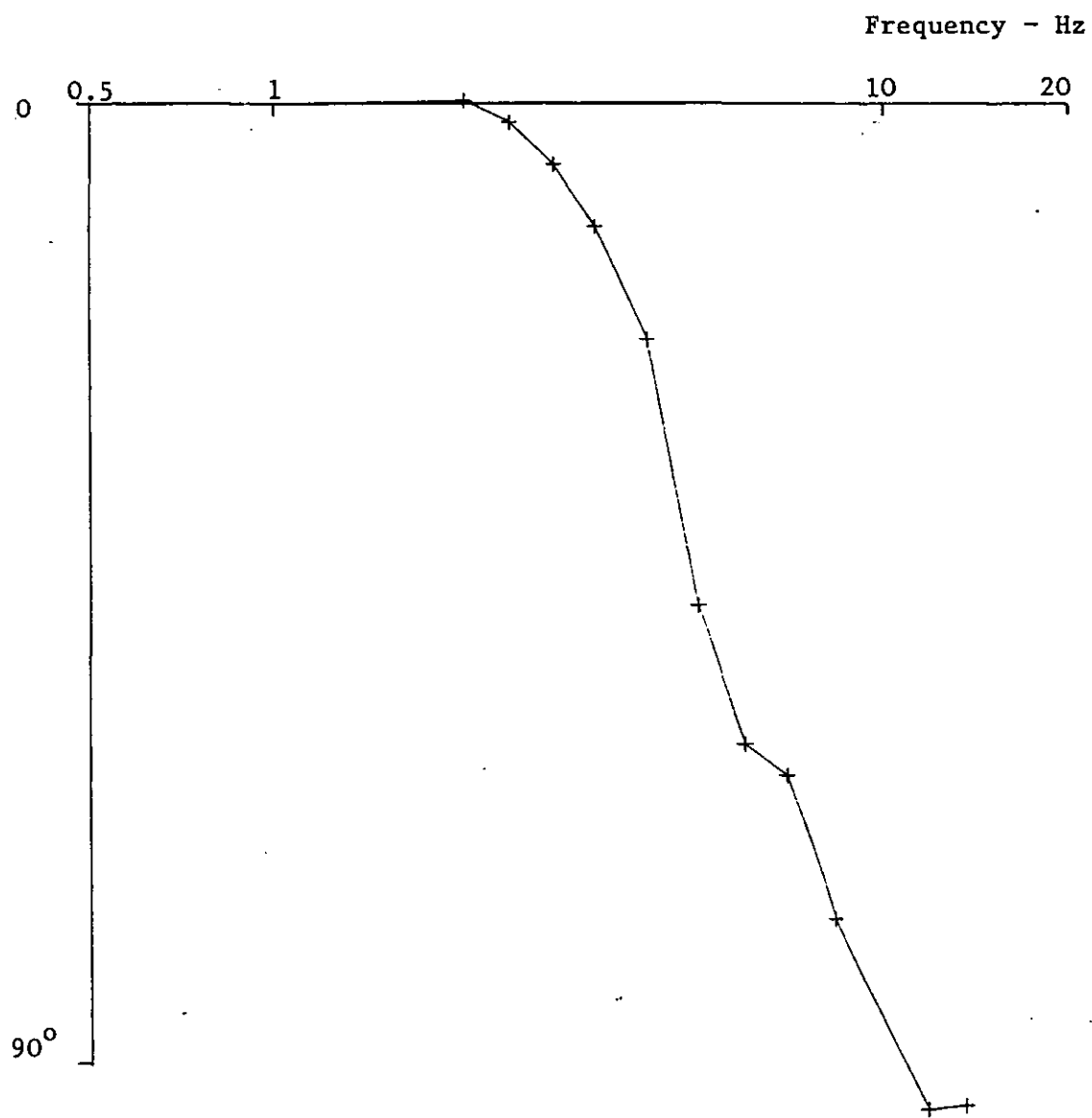


Fig. 2.22b Phase angle

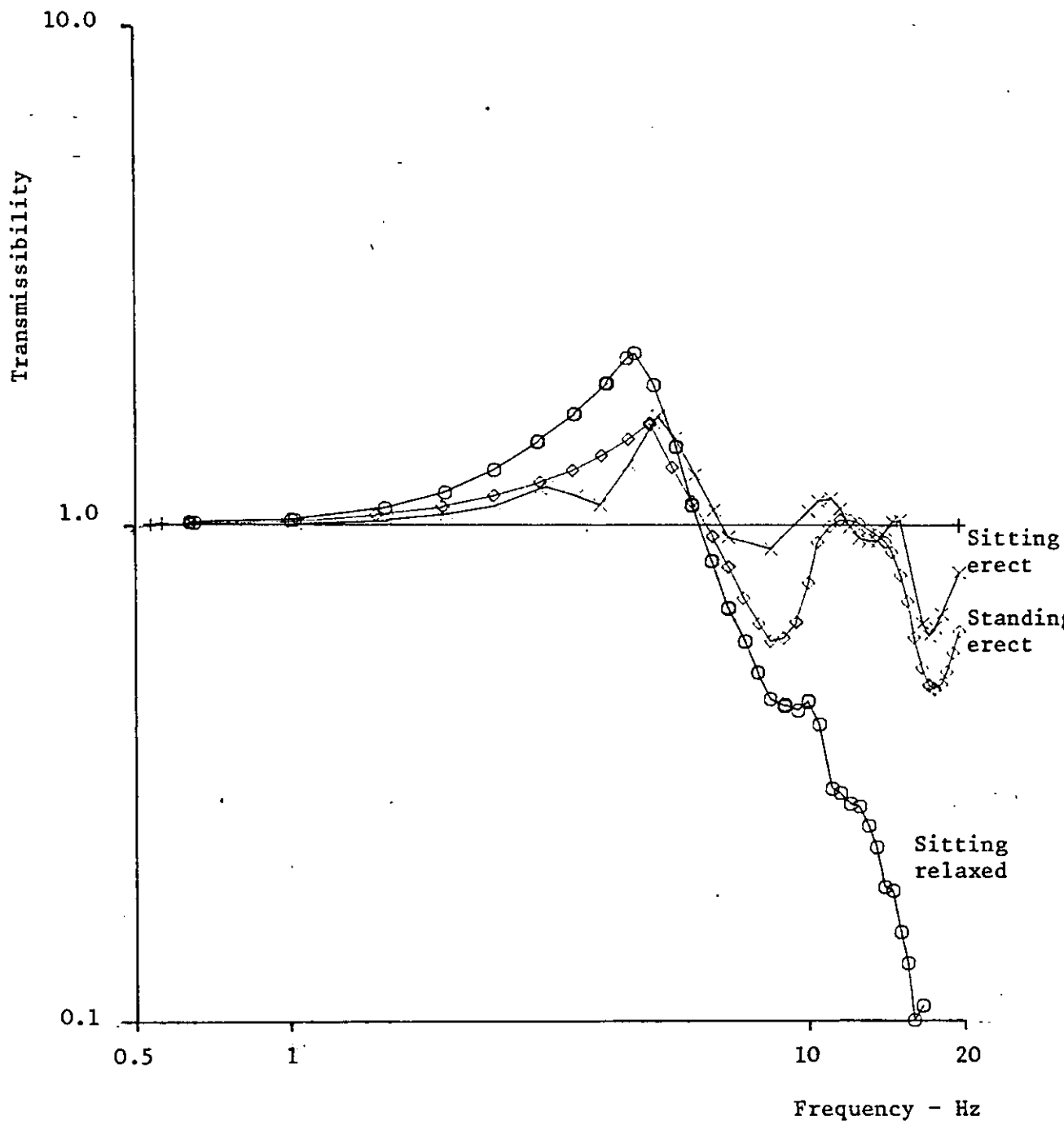


Fig. 2.23 Transmissibility of subject in various postures. (Coermann, 1961)

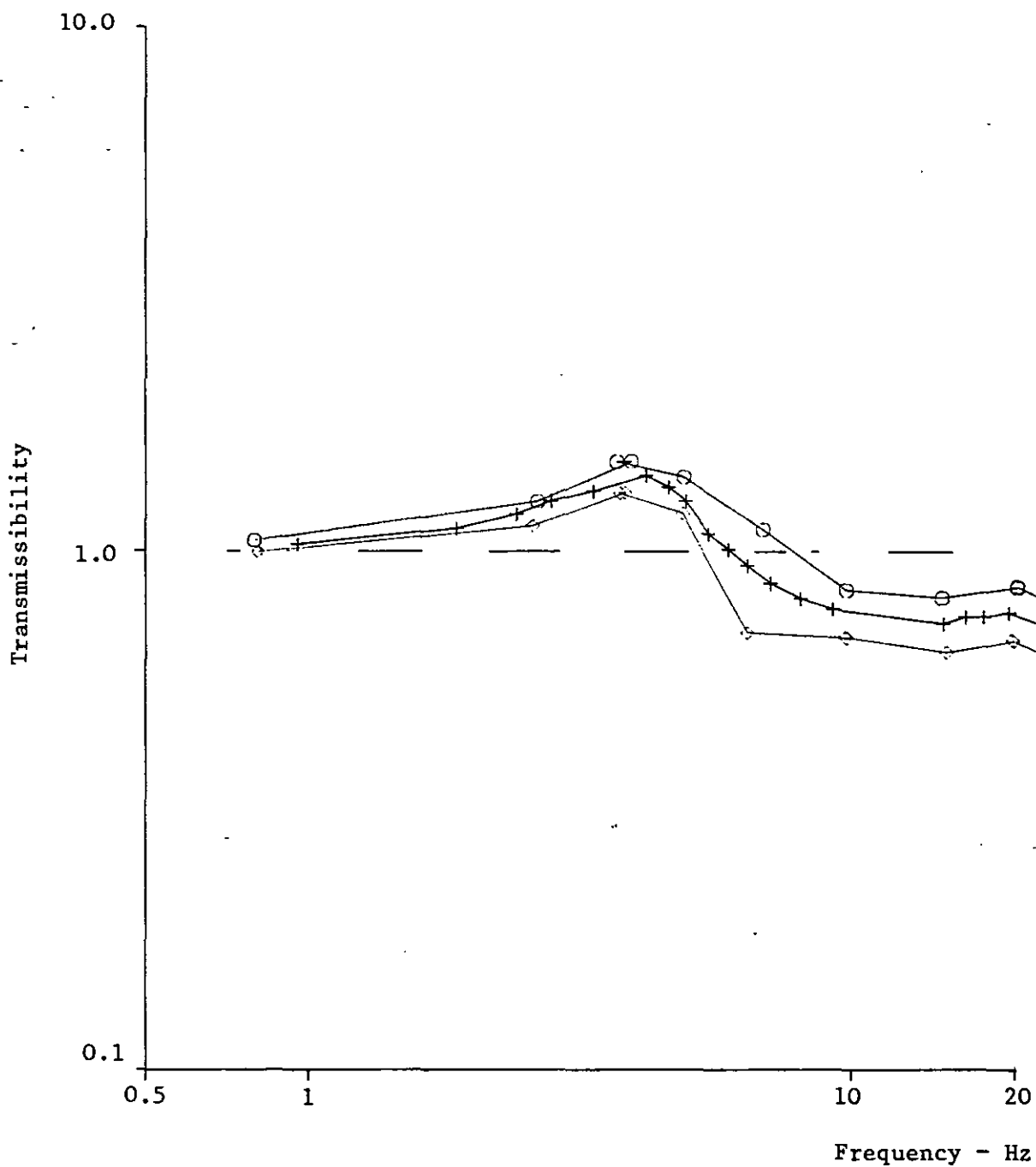


Fig. 2.24 Transmissibility of seated subjects (Pradko et al., 1966)
(10 S, 7 vibration intensities, mean
and 90% confidence limits illustrated)

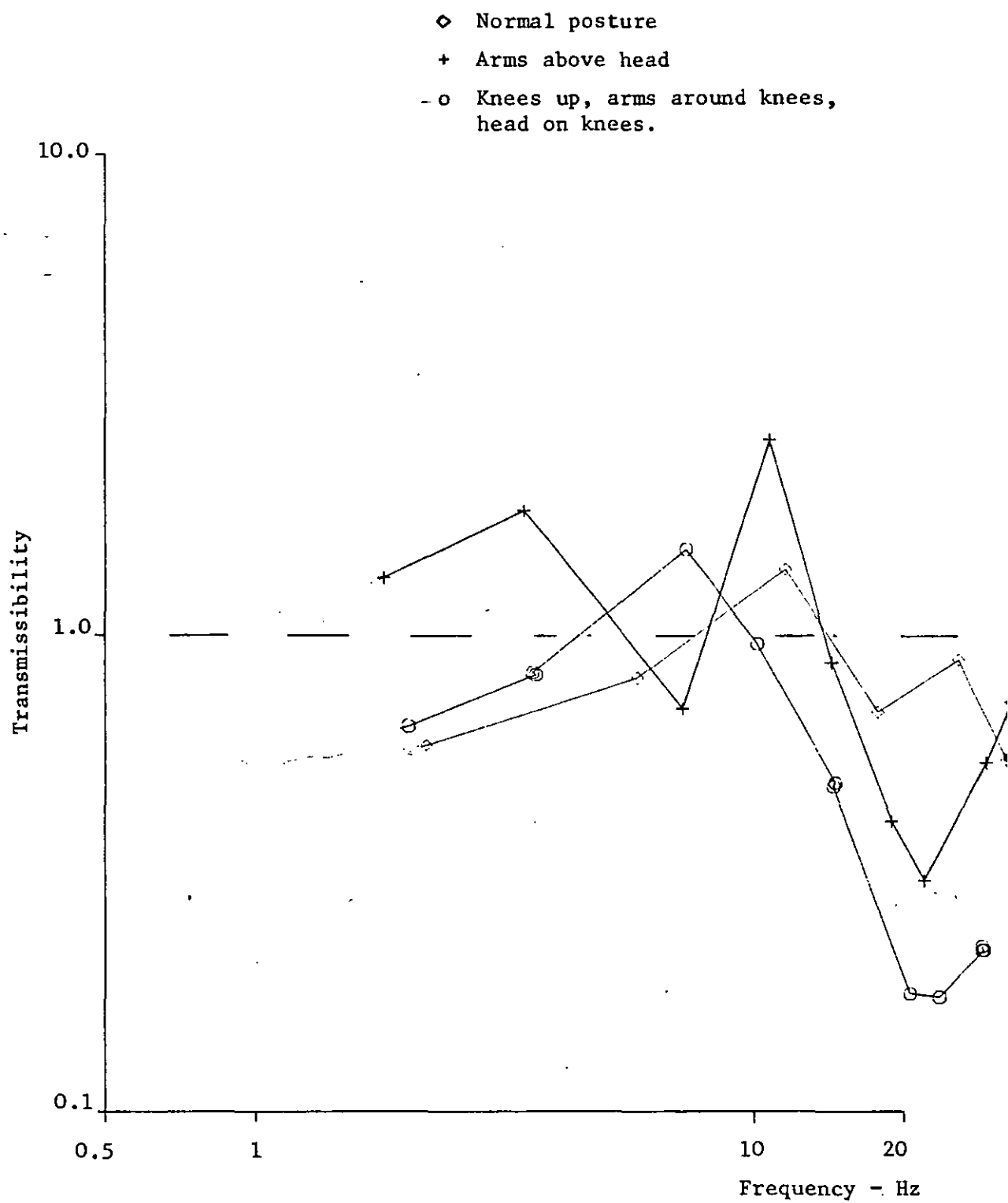


Fig. 2.25 Transmissibility of seated subject (Frolov, 1970)

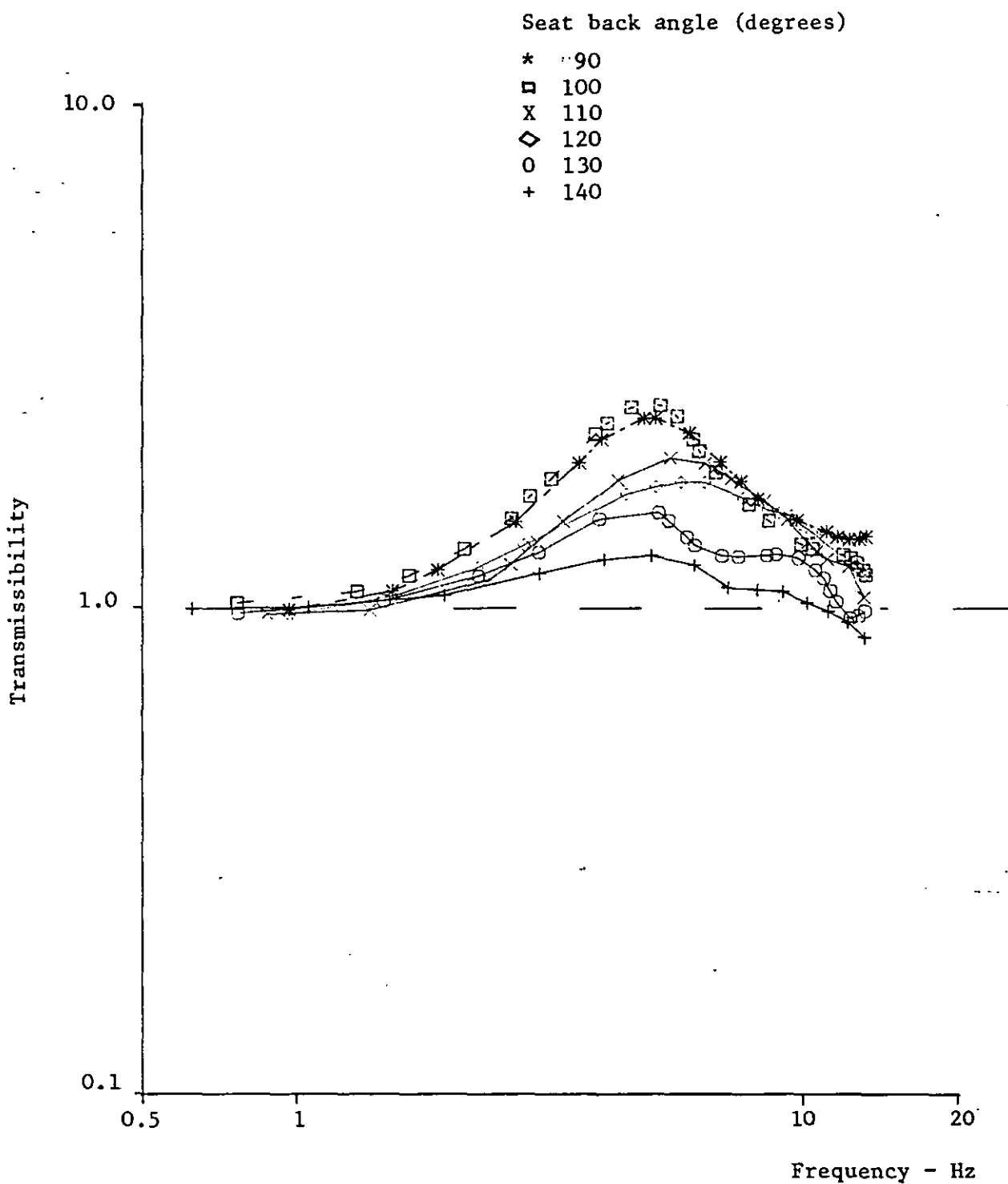


Fig. 2.26 Transmissibility of seated subjects (Coermann & Okada, 1964)
(effects of seat back - mean of 5 S)

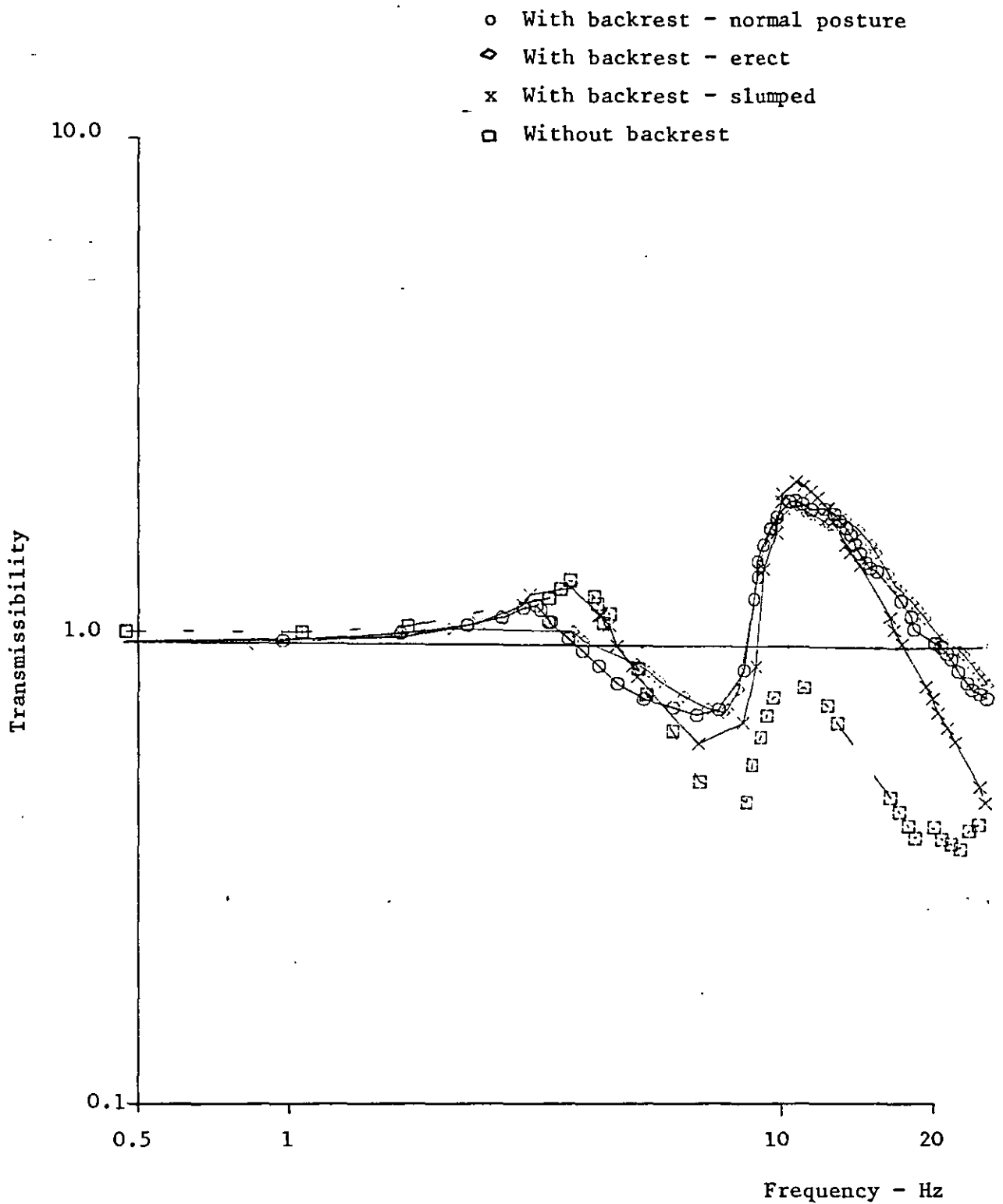


Fig. 2.27a Transmissibility of seated subject (Rowlands, 1977)

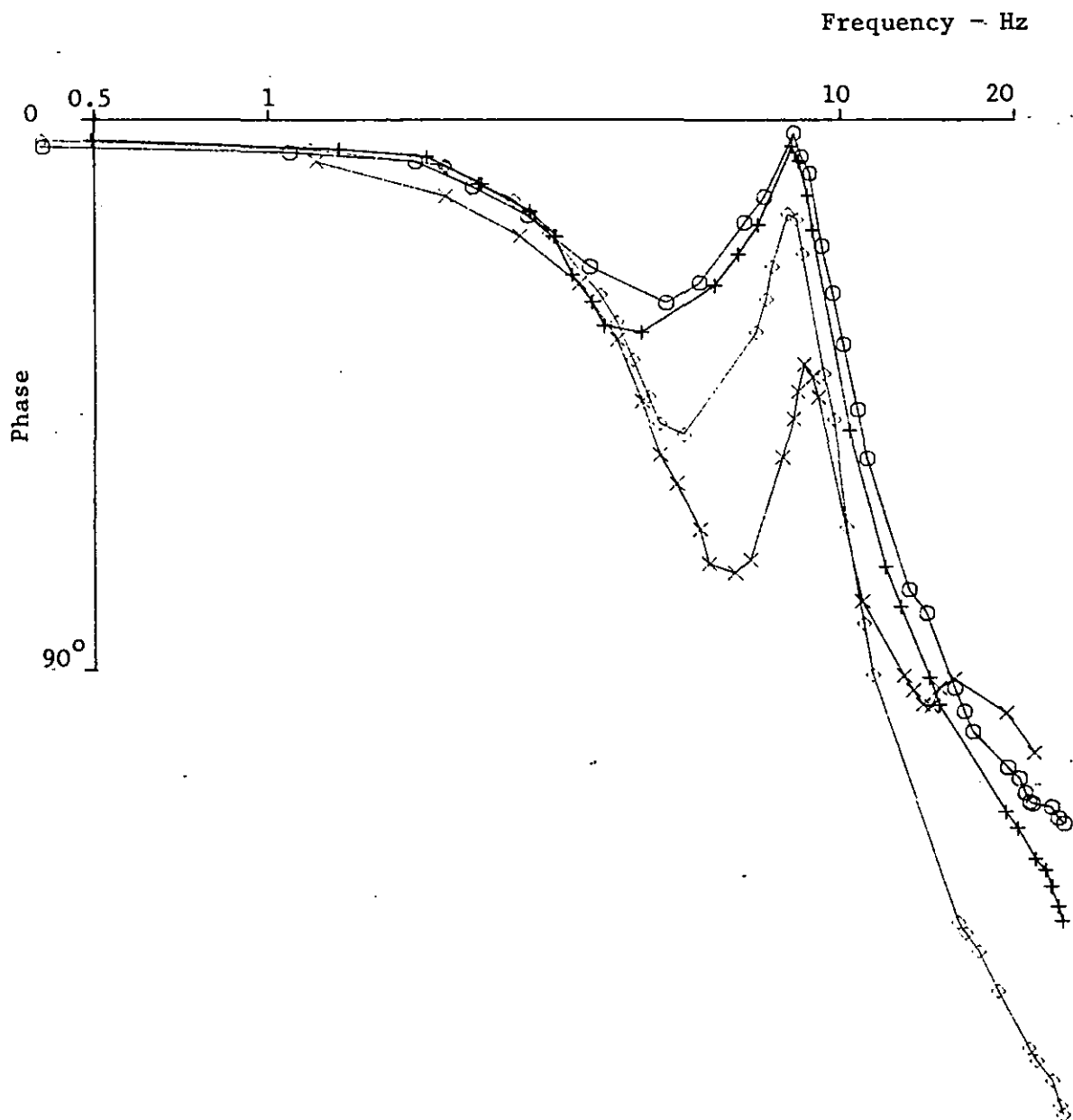


Fig. 2.27b Phase angles

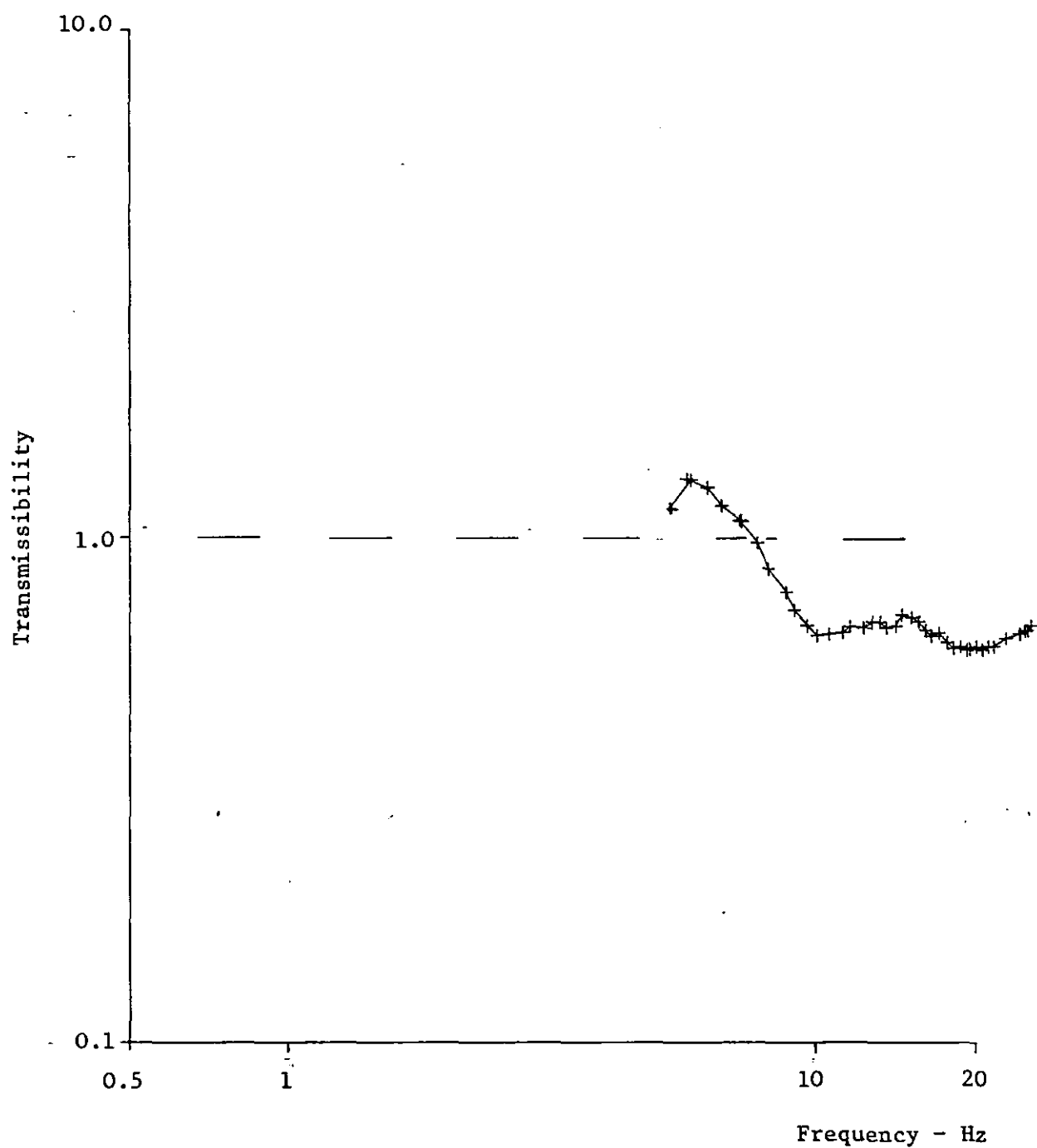


Fig. 2.28a Transmissibility of seated subject (Guignard et al., 1979)
(True (corrected) a_z transmission)

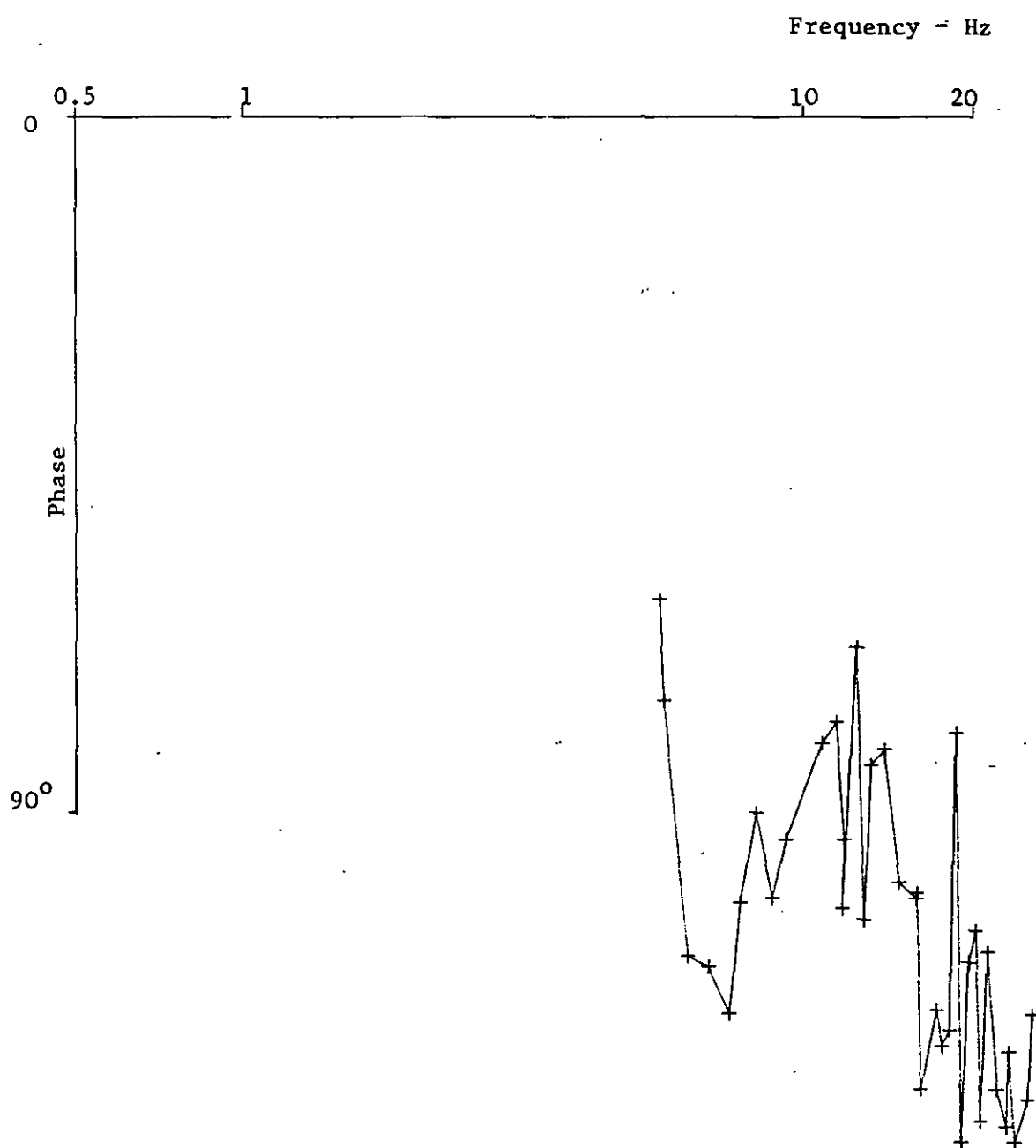


Fig. 2.28b Phase angle

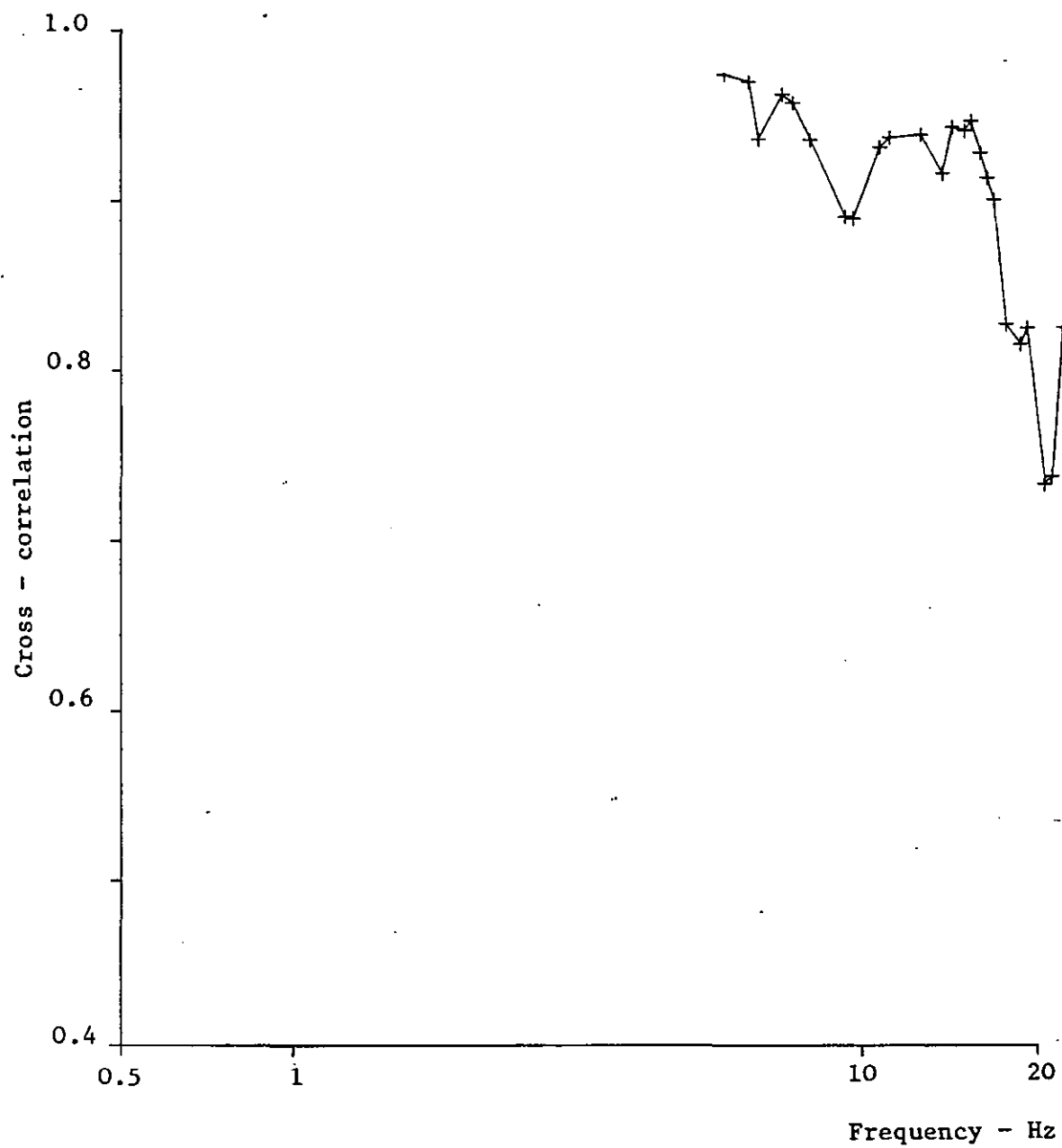


Fig. 2.28c Correlation of measurement

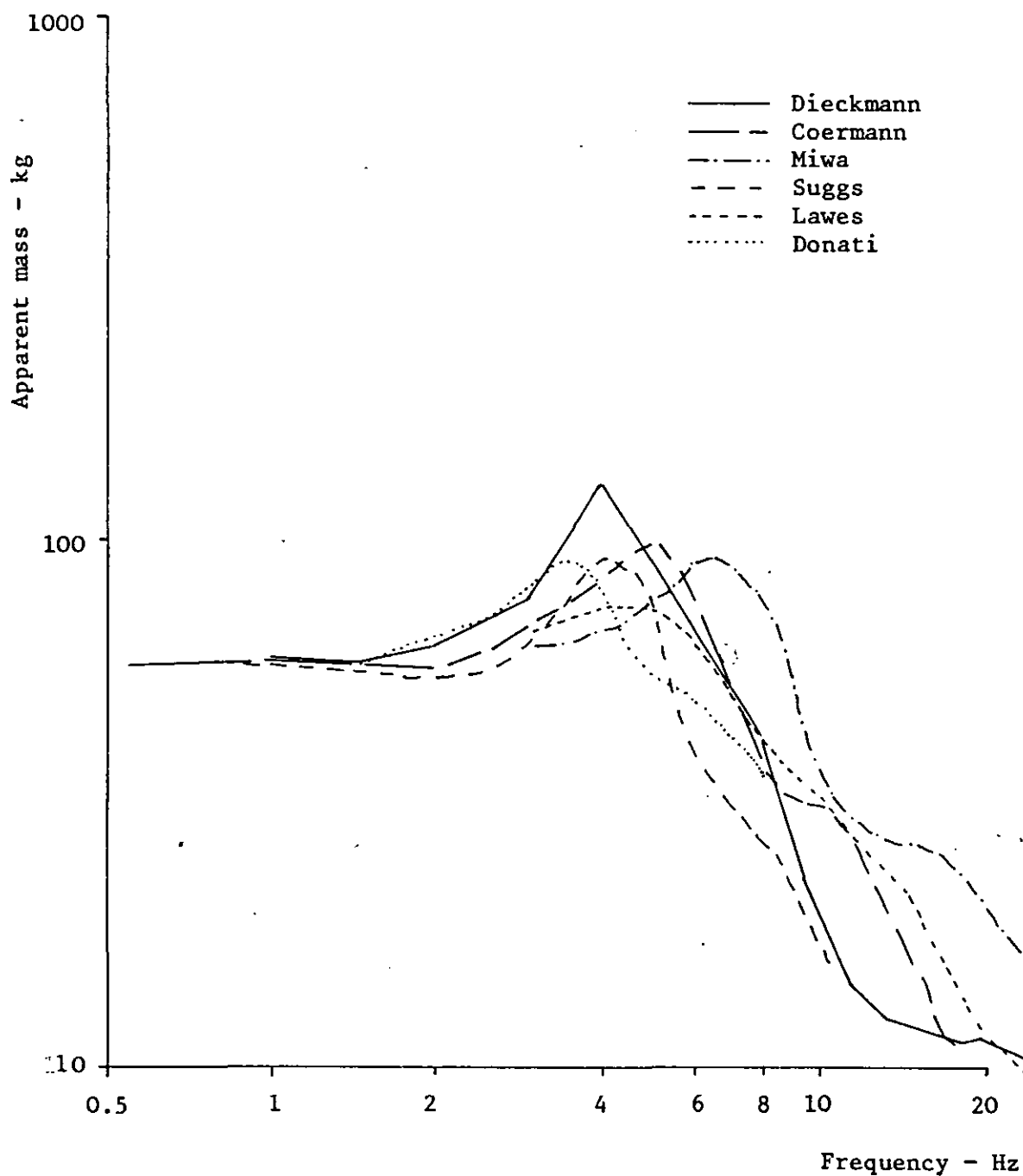


Fig. 2.29 Apparent mass data from various authors.
(Data of Coermann shifted to allow for subject mass)

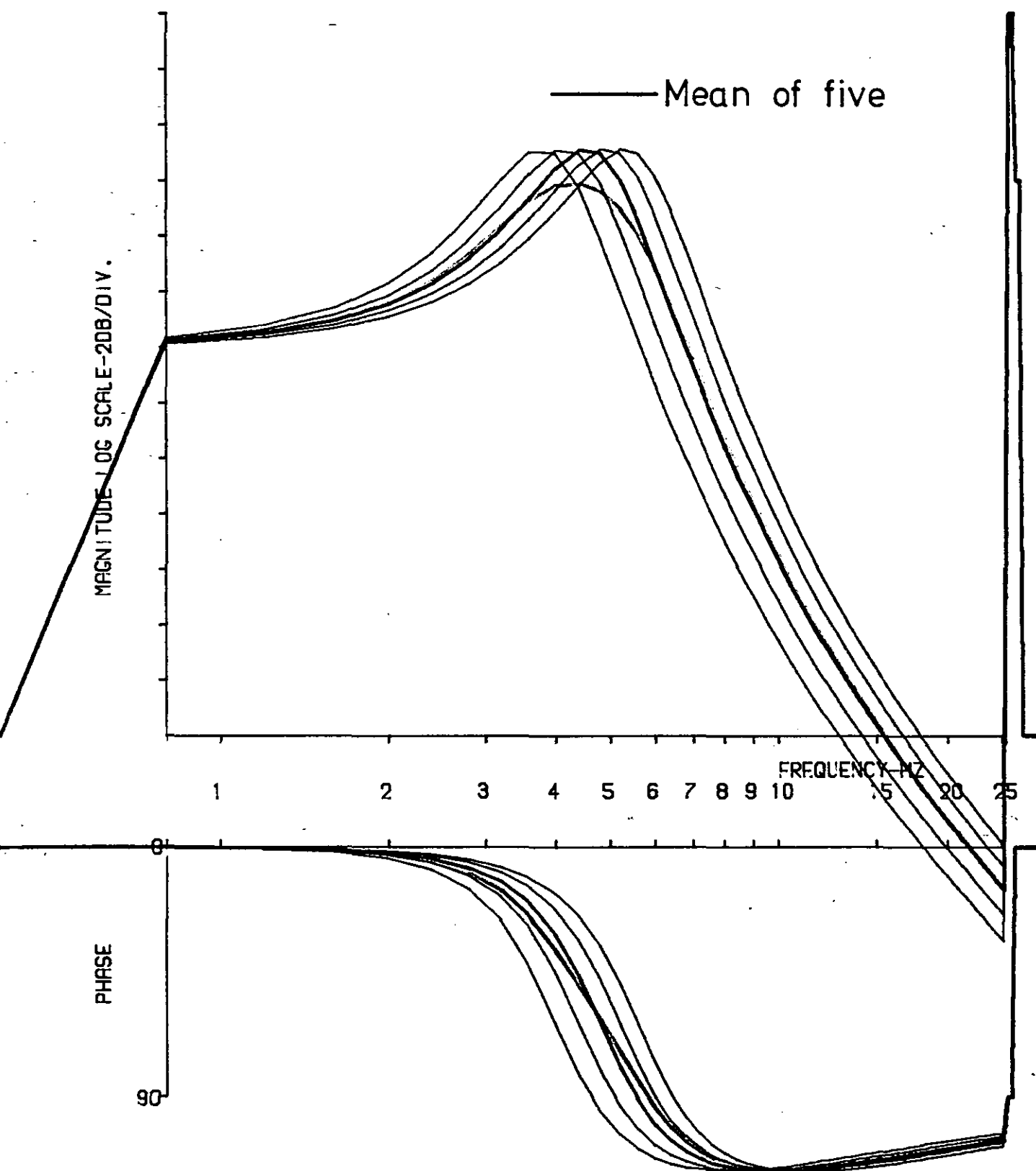


Fig. 2.30 An illustration of how the mean value can give misleading information

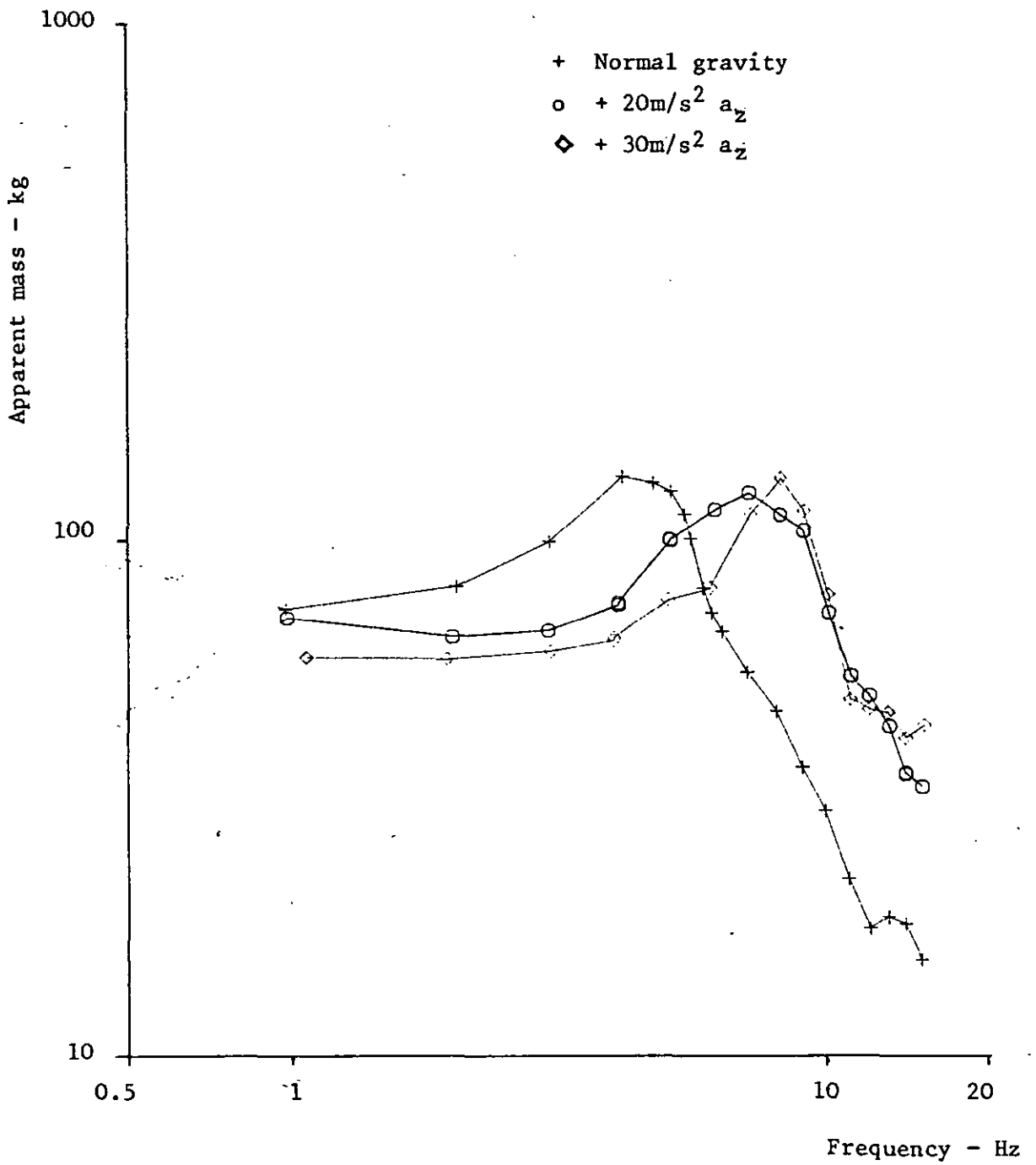


Fig. 2.31a Changes in apparent mass with sustained acceleration (Vogt et al., 1968)

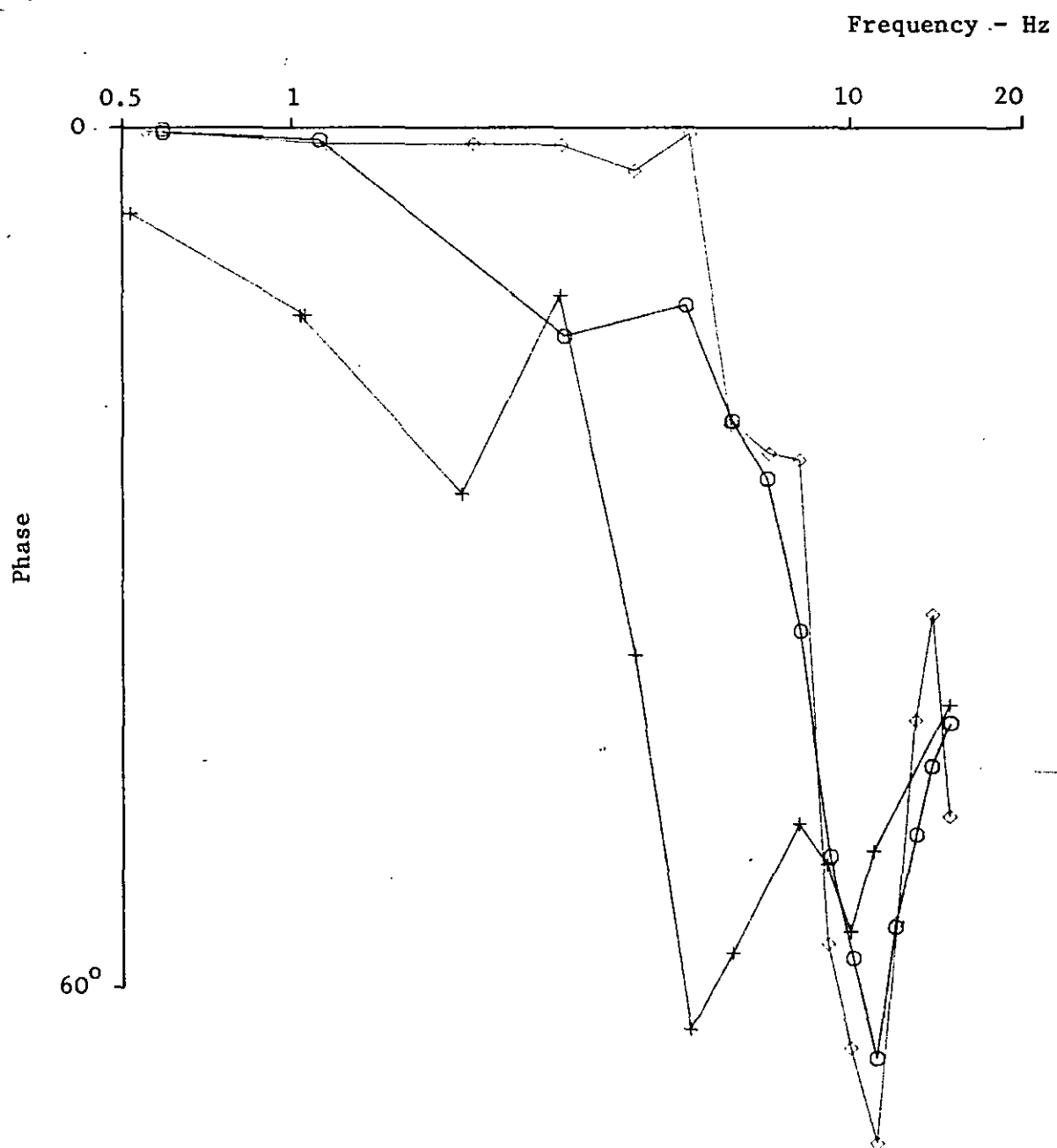


Fig. 2.31b Phase angles

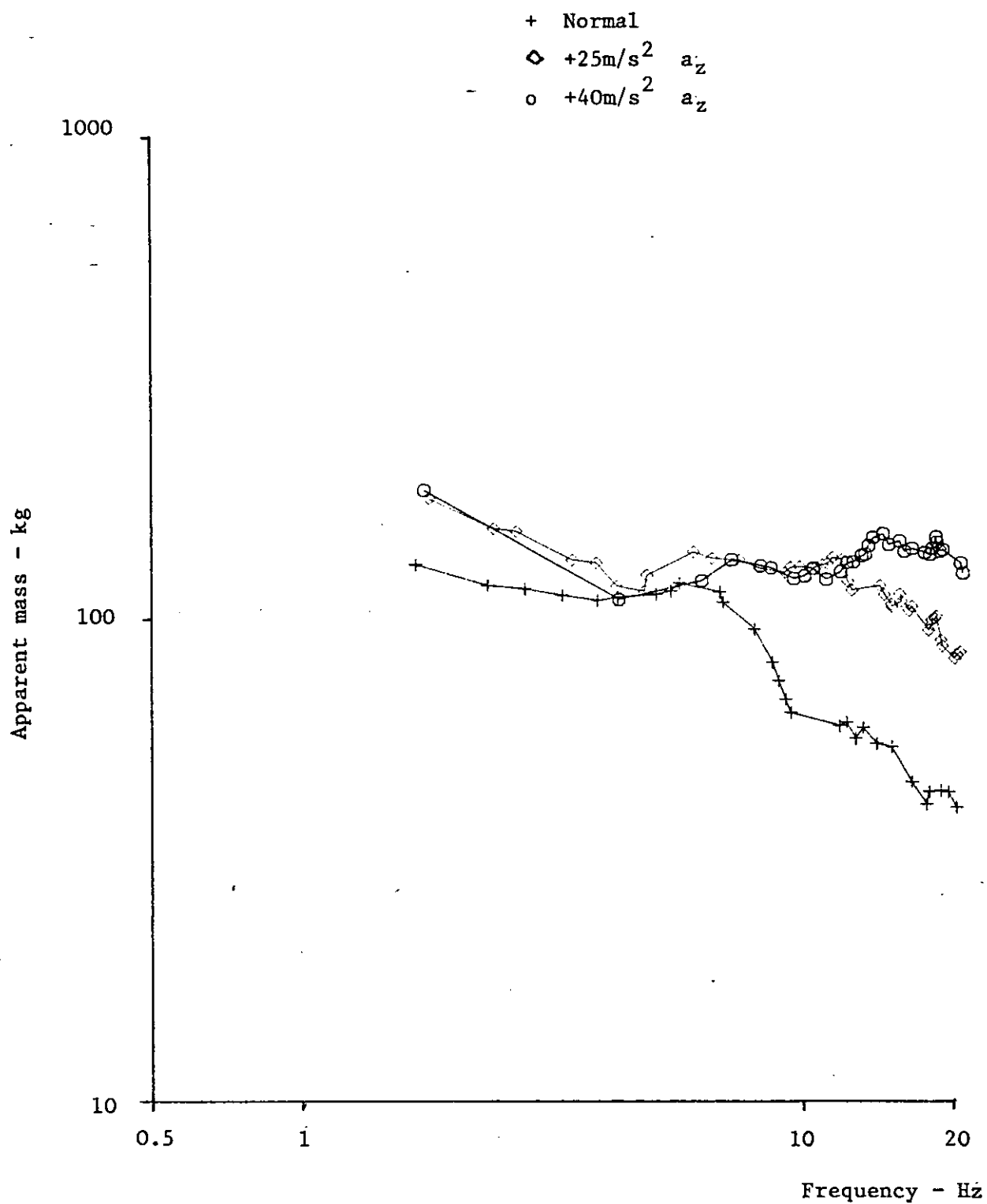


Fig. 2.32 Changes in apparent mass with sustained acceleration (Vyukal, 1968)

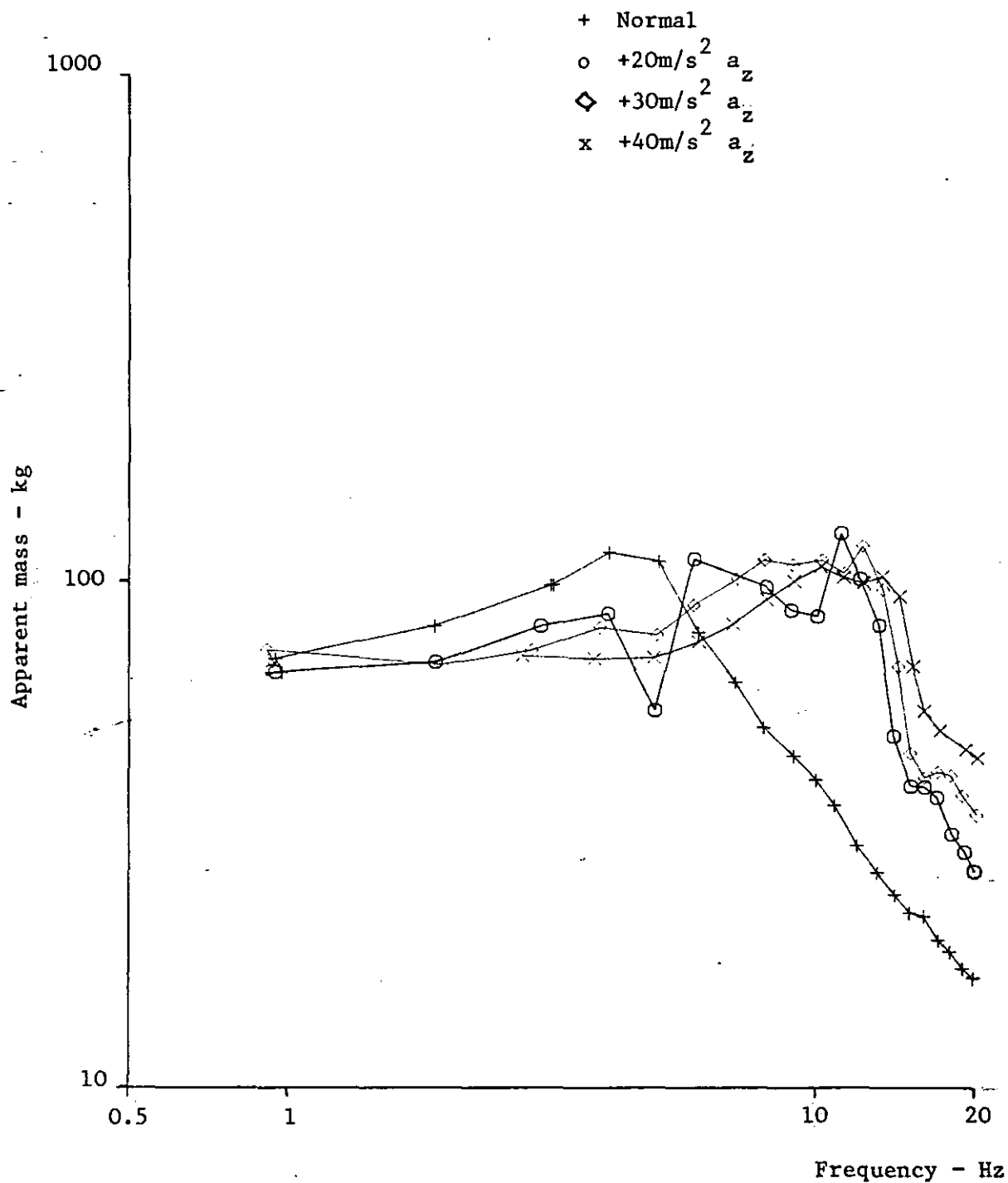


Fig. 2.33 Changes in apparent mass with sustained acceleration (Mertens, 1978)

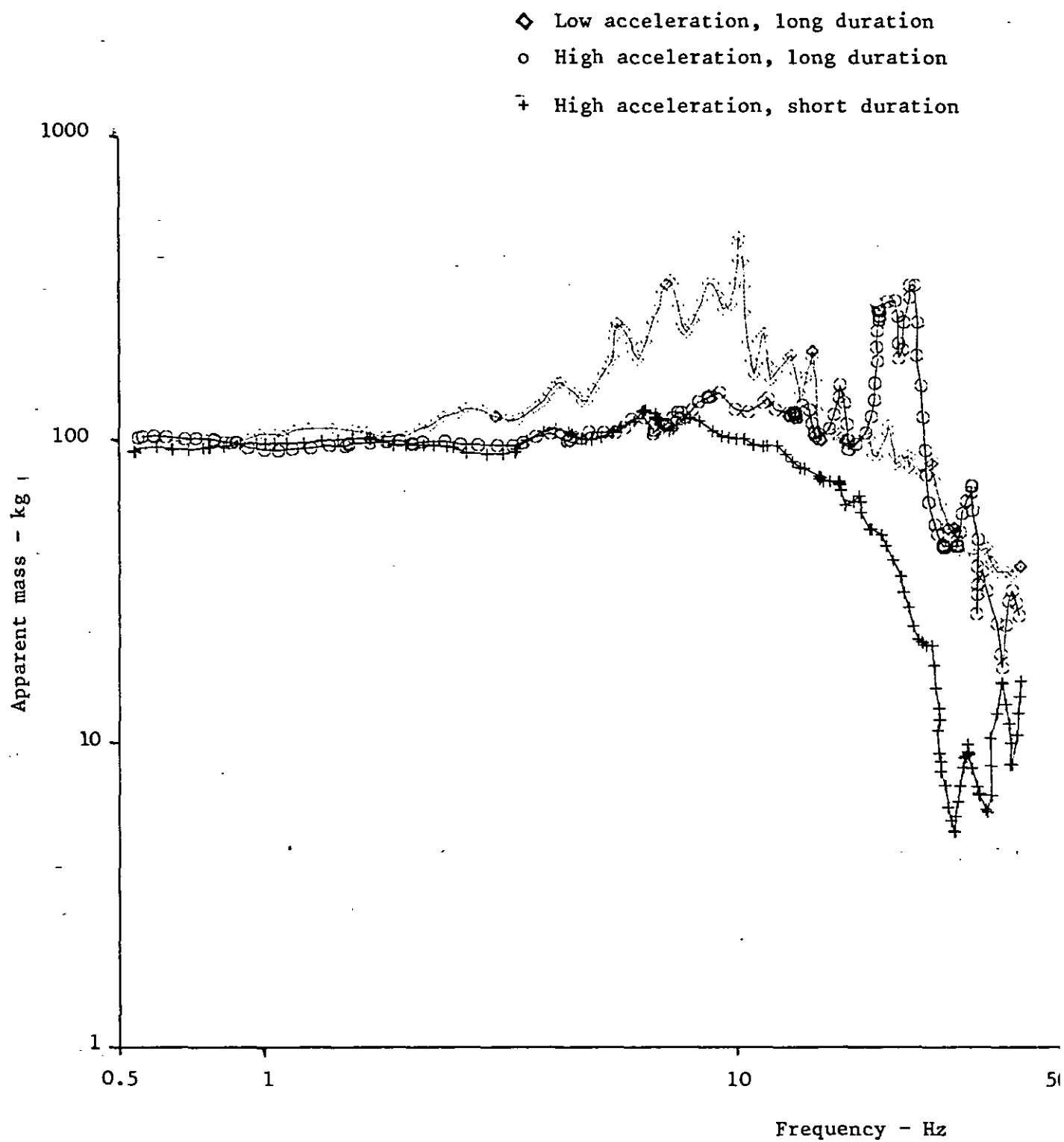


Fig. 2.34 Changes in apparent mass measured during impacts of different profile (Wittmann & Phillips, 1969).

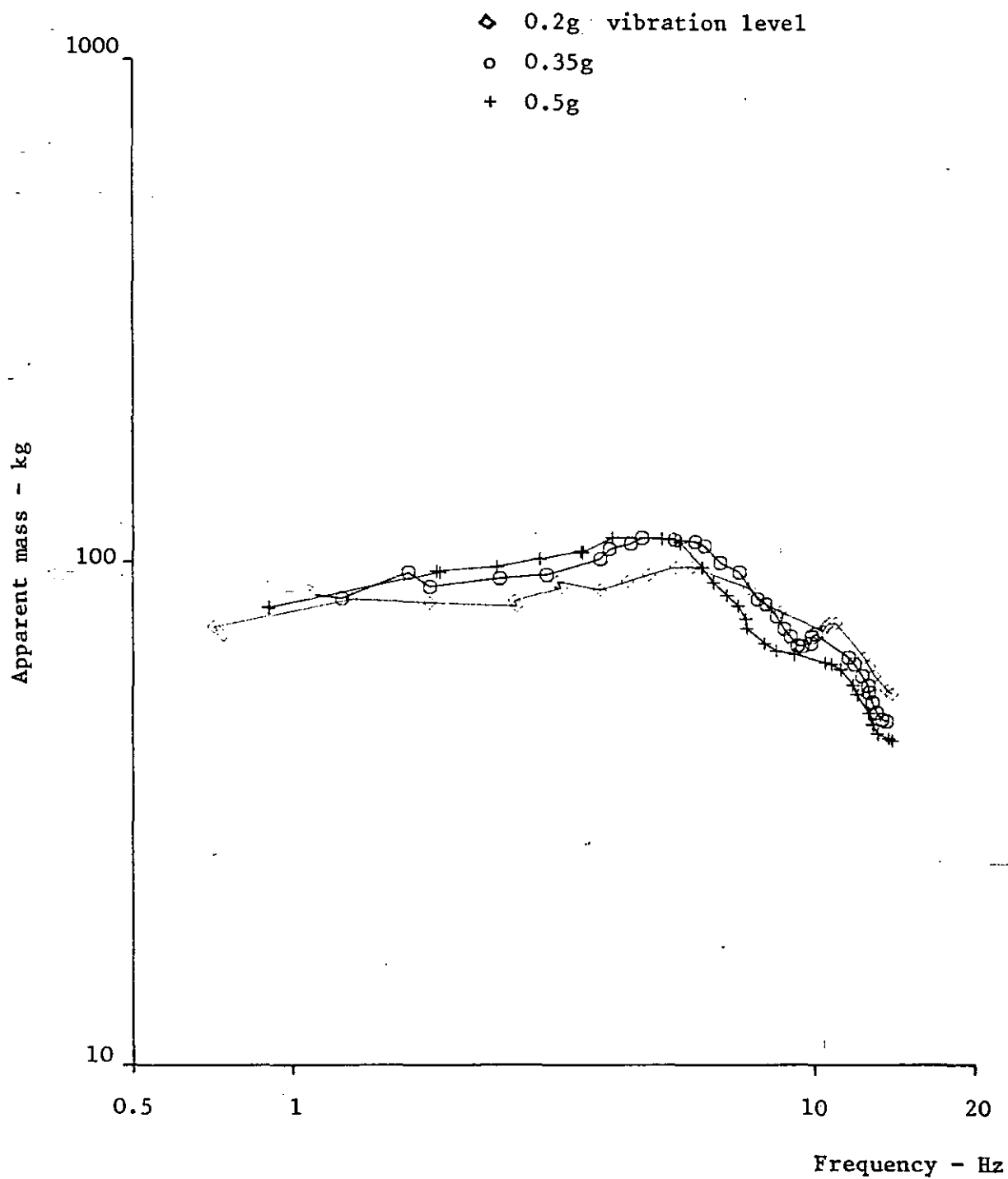


Fig. 2.35 Changes in apparent mass with vibration level (Edwards & Lange, 1964)
(subject supine, vibration a_z)

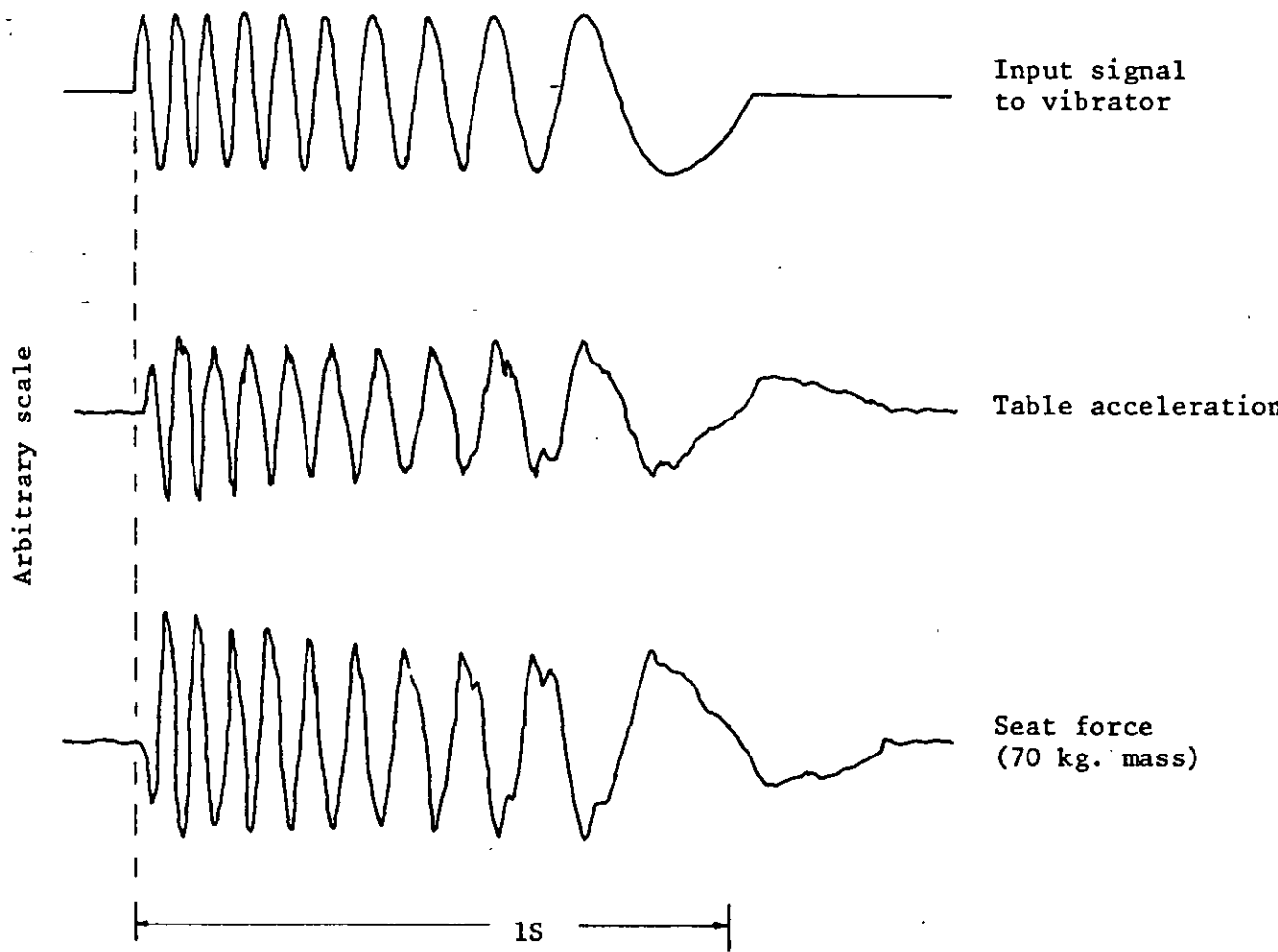
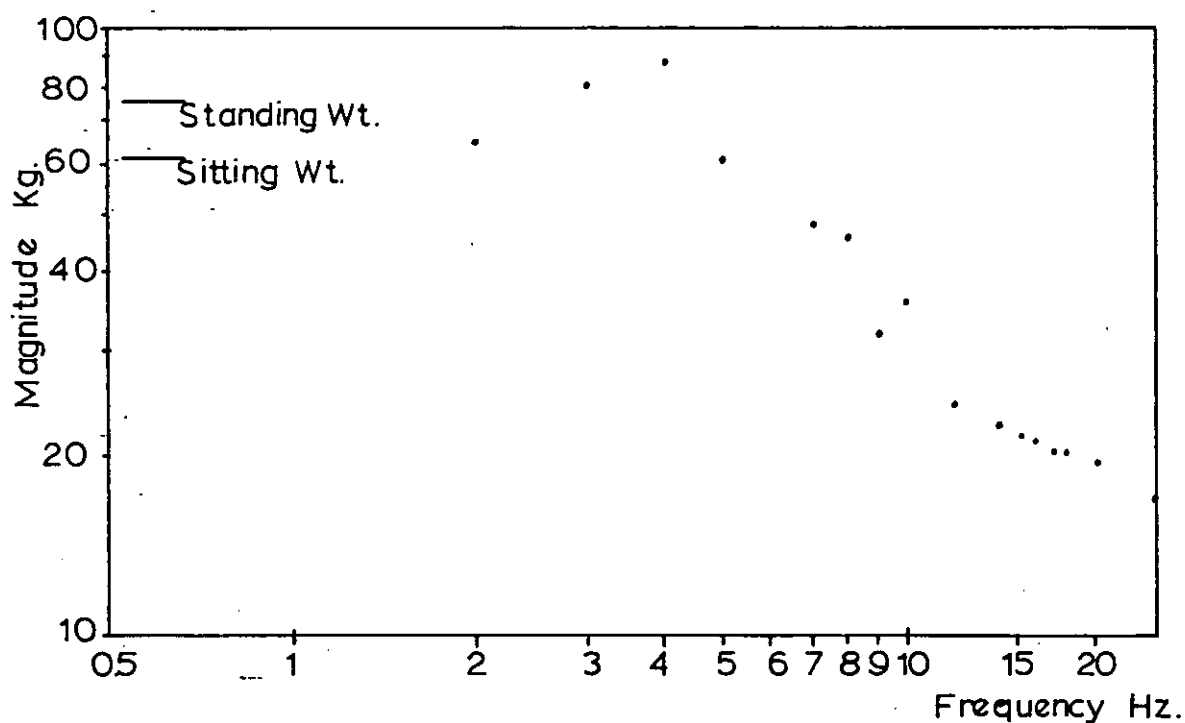


Fig. 4.1 Swept-sine transient



RESPONSE FUNCTION - SUBJECT 47 - SINUSOIDAL

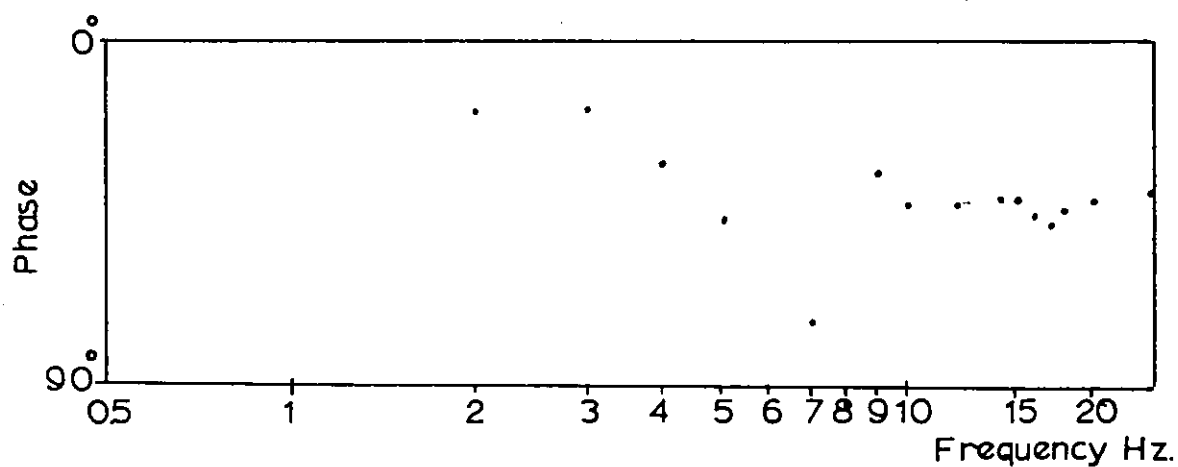
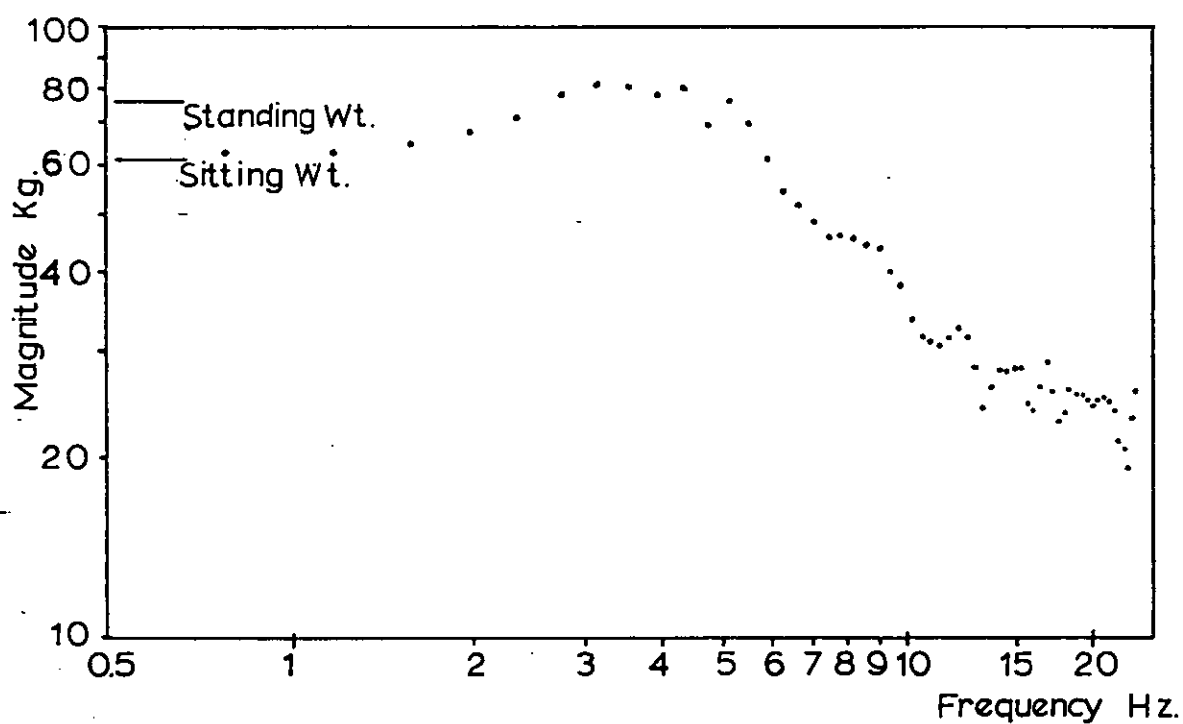


Fig. 4.2 Apparent mass - sinusoidal stimulus



RESPONSE FUNCTION - SUBJECT 47 - SWEPT SINE

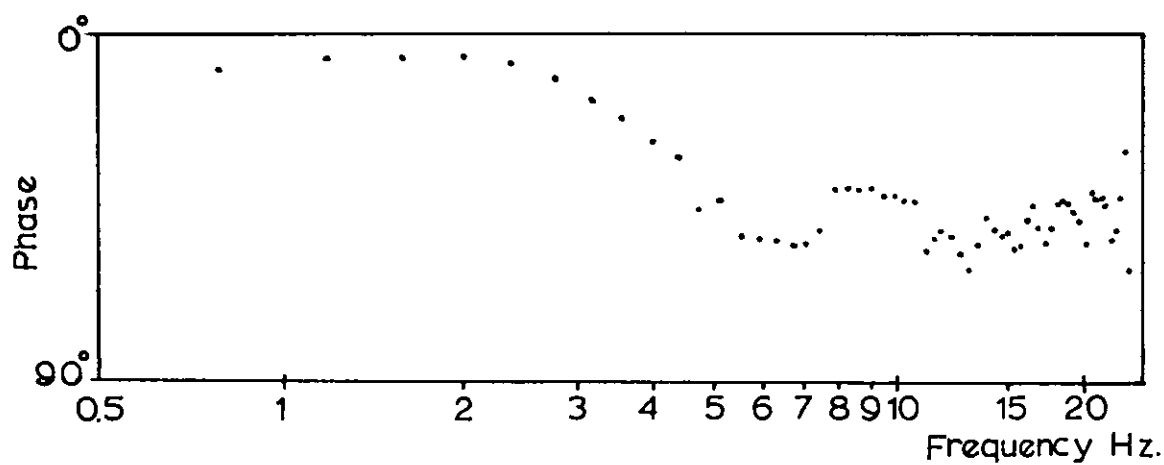
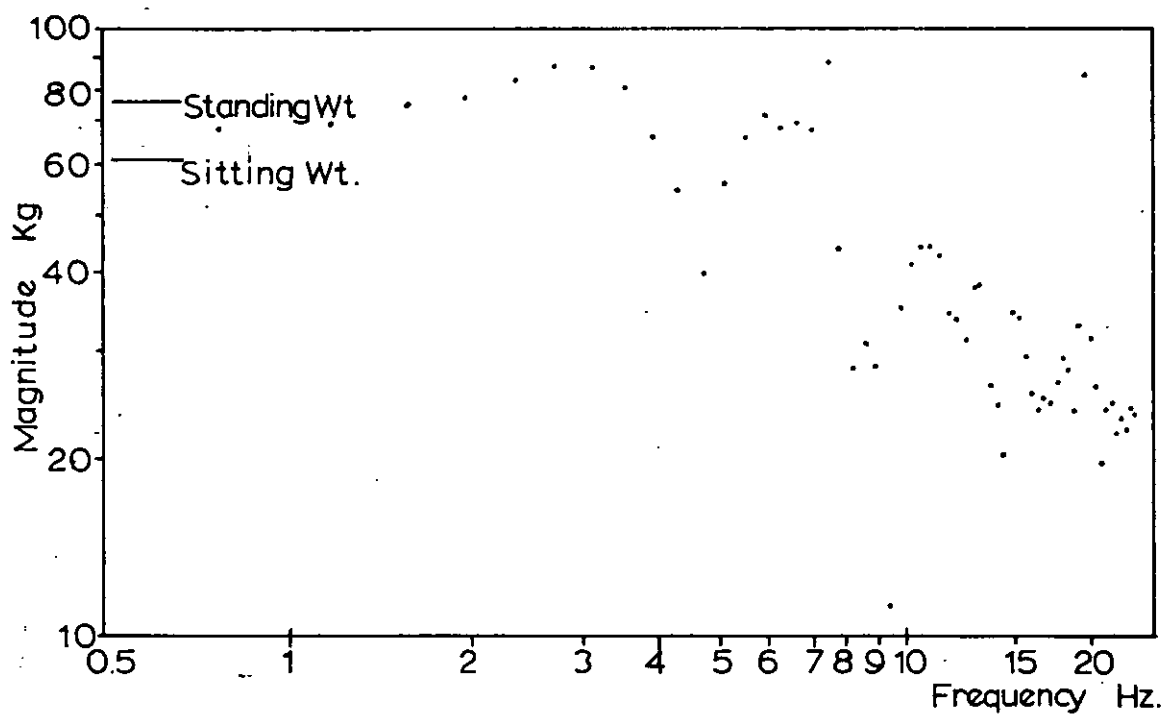


Fig. 4.3 Apparent mass - swept - sine transient



RESPONSE FUNCTION - SUBJECT 47 - TRANSIENT

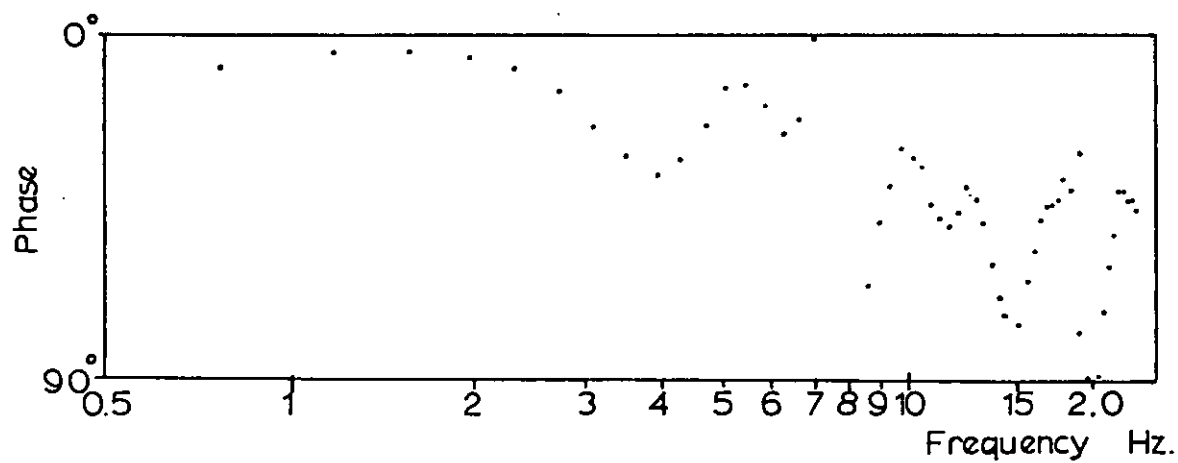
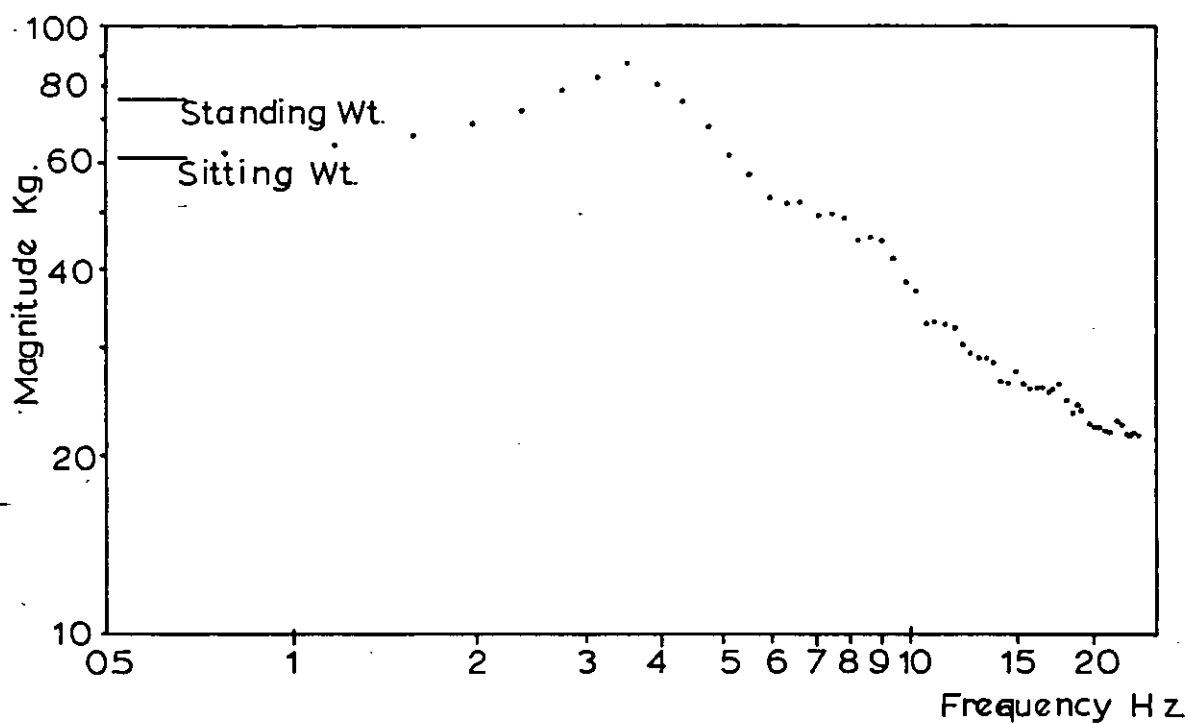


Fig. 4.4 Apparent mass - impulse stimulus



RESPONSE FUNCTION - SUBJECT 47 - RANDOM

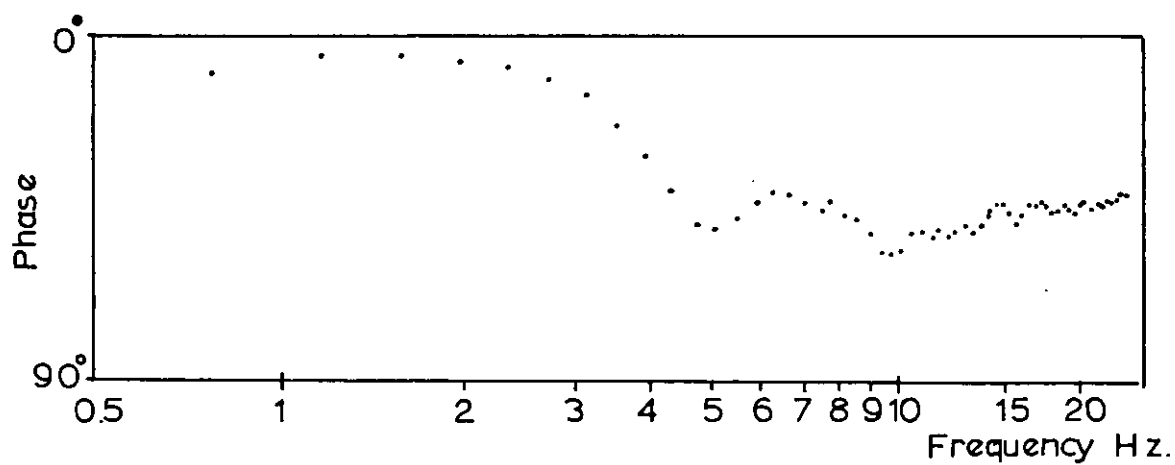


Fig. 4.5 Apparent mass - random stimulus

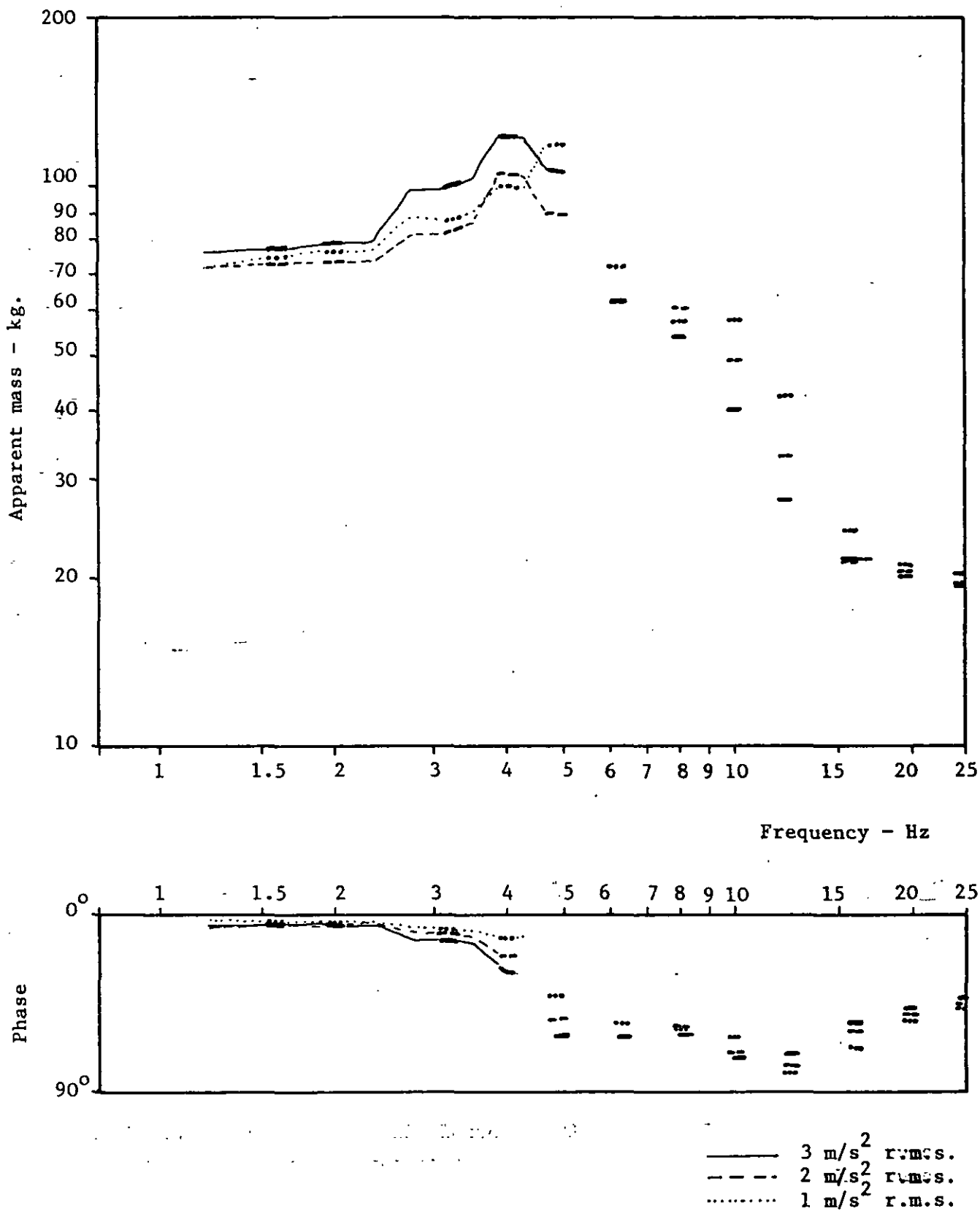


Fig. 4.6 Response to sinusoidal stimuli.

N.B. Figs. 4.7 - 4.30 are all plotted to the scales and axes of fig. 4.6

54 SSF

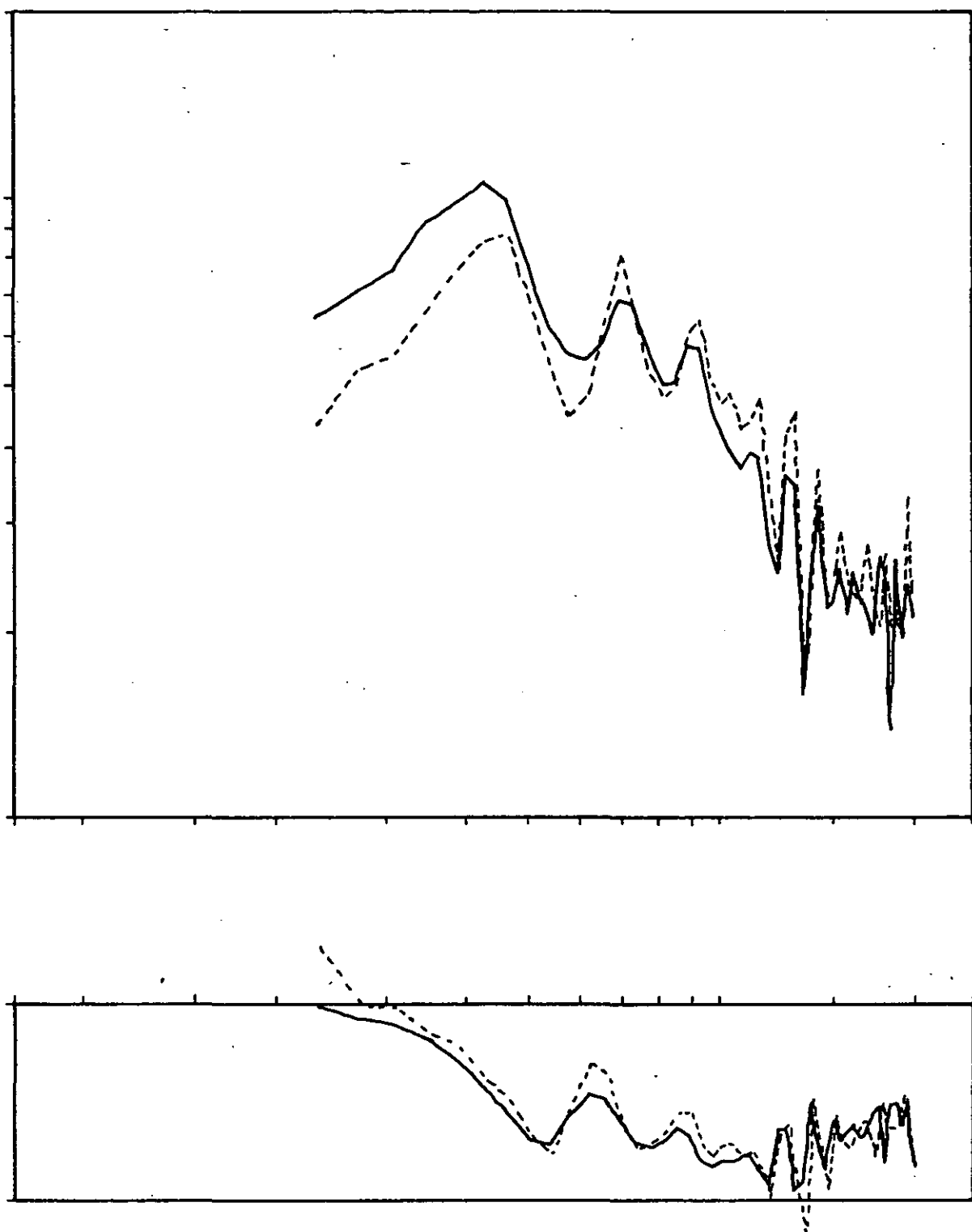


Fig. 4.7 Response to swept sine transients. Subject 80 erect.

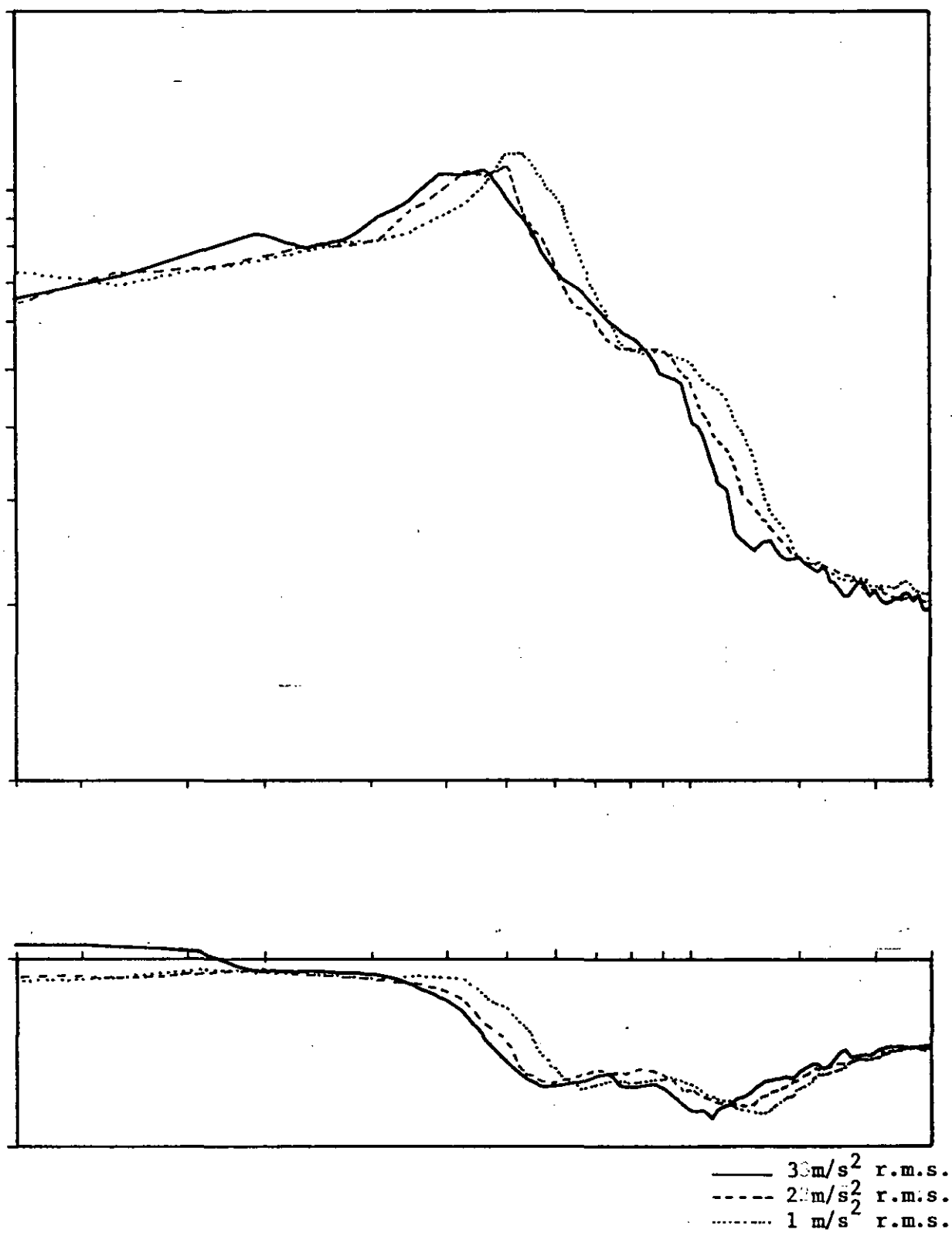


Fig. 4.8 Response to random stimuli (RA)
Subject 80. Erect

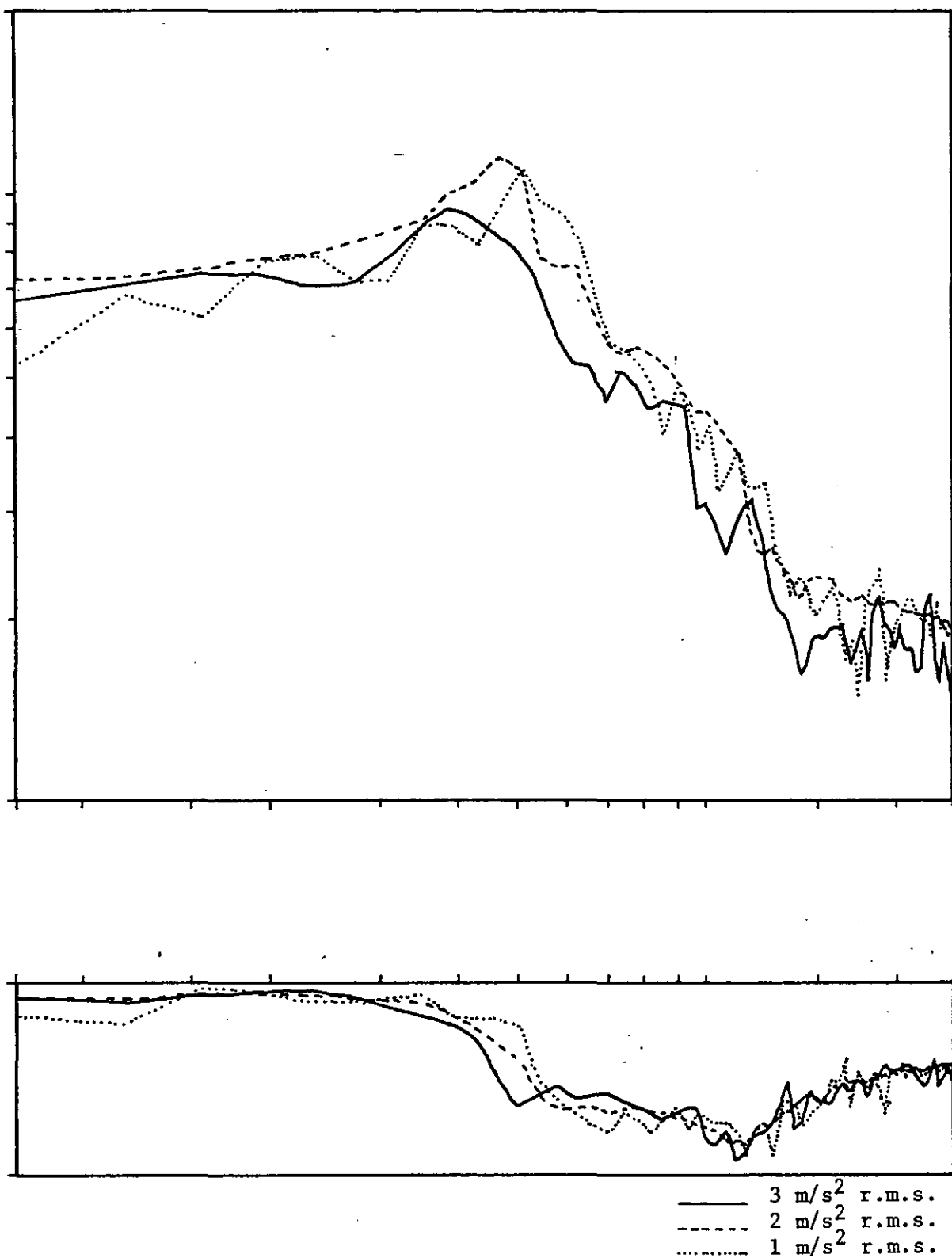


Fig. 4.9 Response to random stimuli (RD)
Subject 80. Erect.

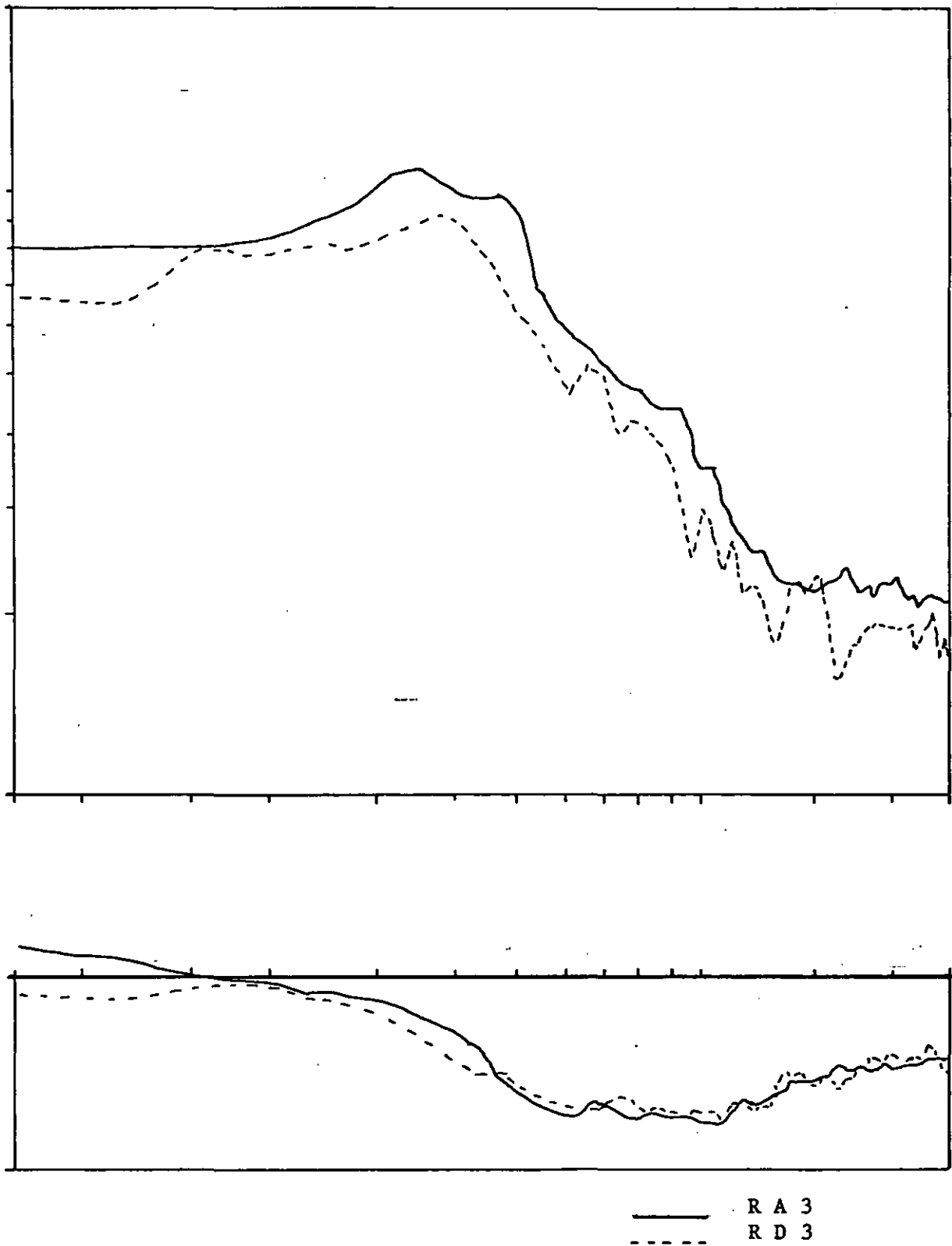


Fig. 4.10 Response to random stimuli
Subject 80. Slumped.

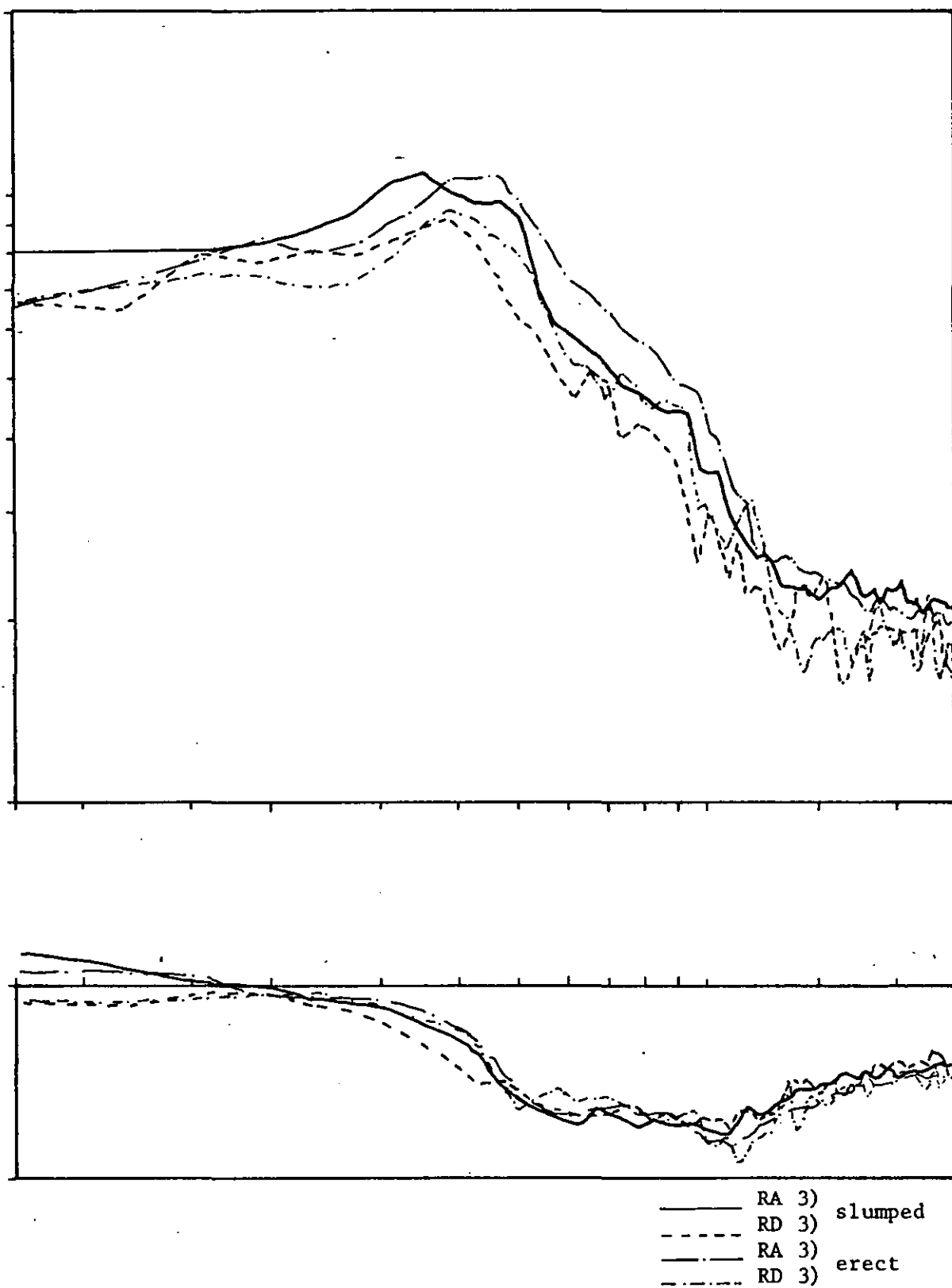


Fig. 4.11 Response to random stimuli.
Subject 80.

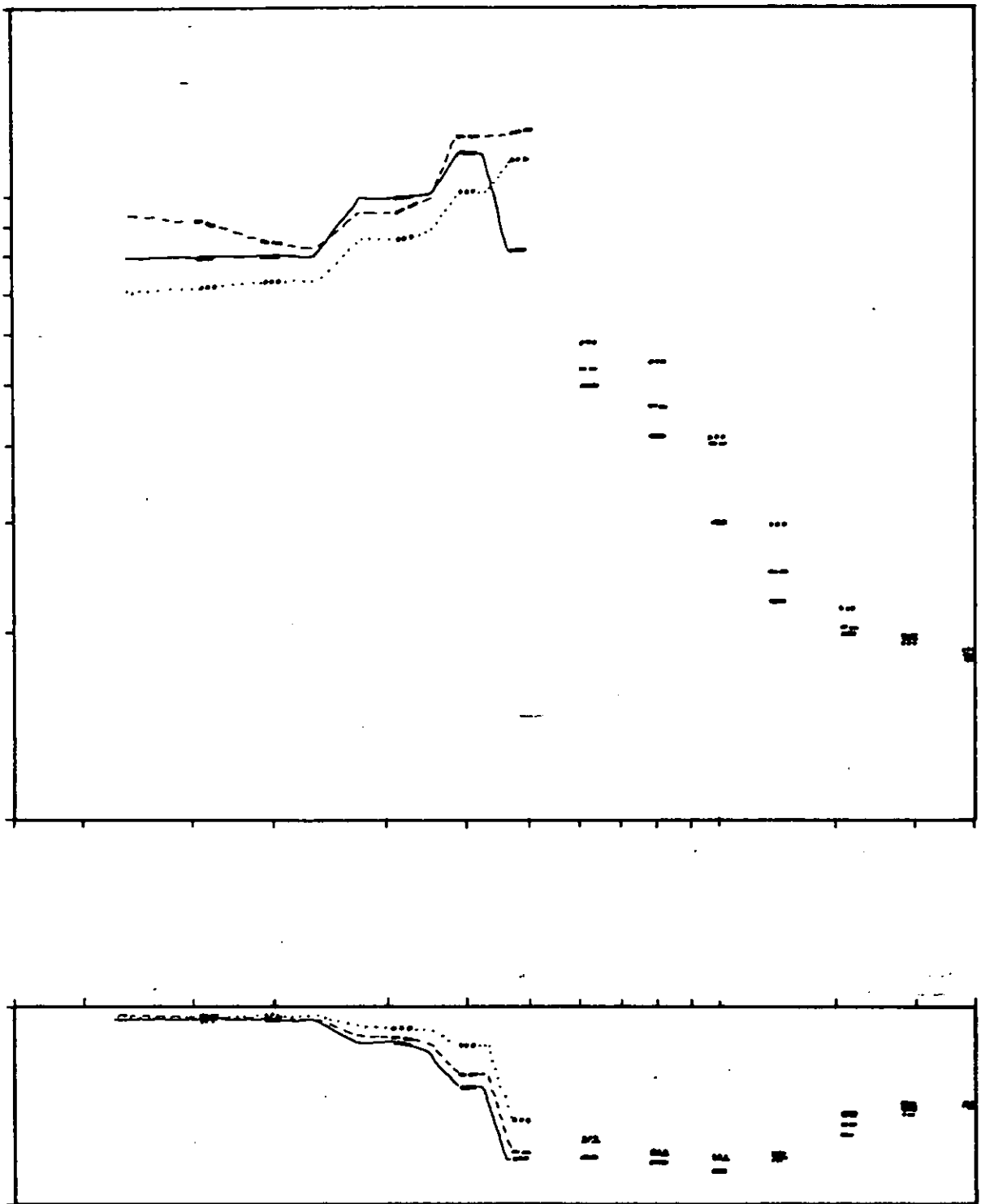


Fig. 4.12 Response to sinusoidal stimuli.
Subject 76. Erect.

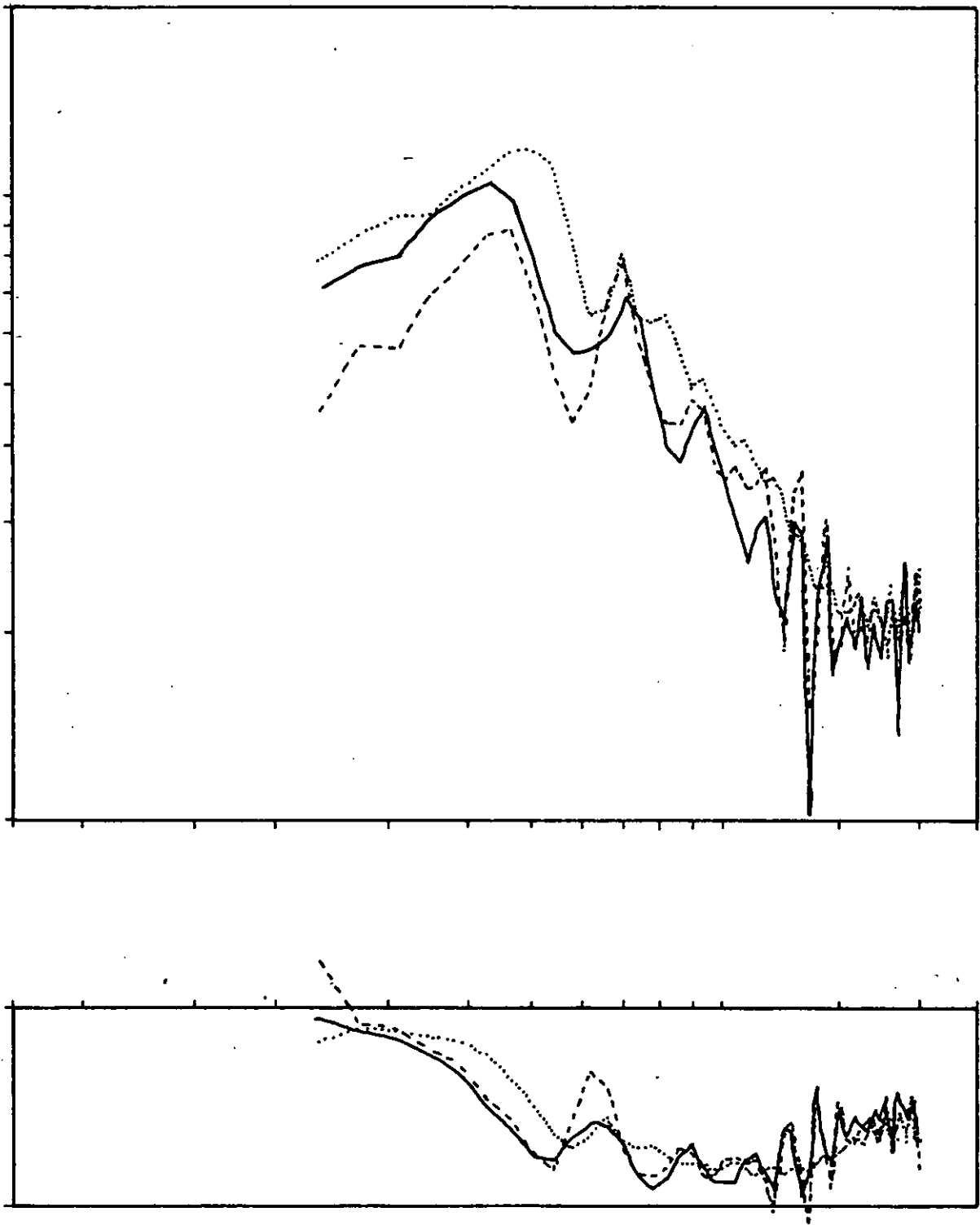


Fig. 4.13 Response to swept-sine transients.
Subject 76. Erect.

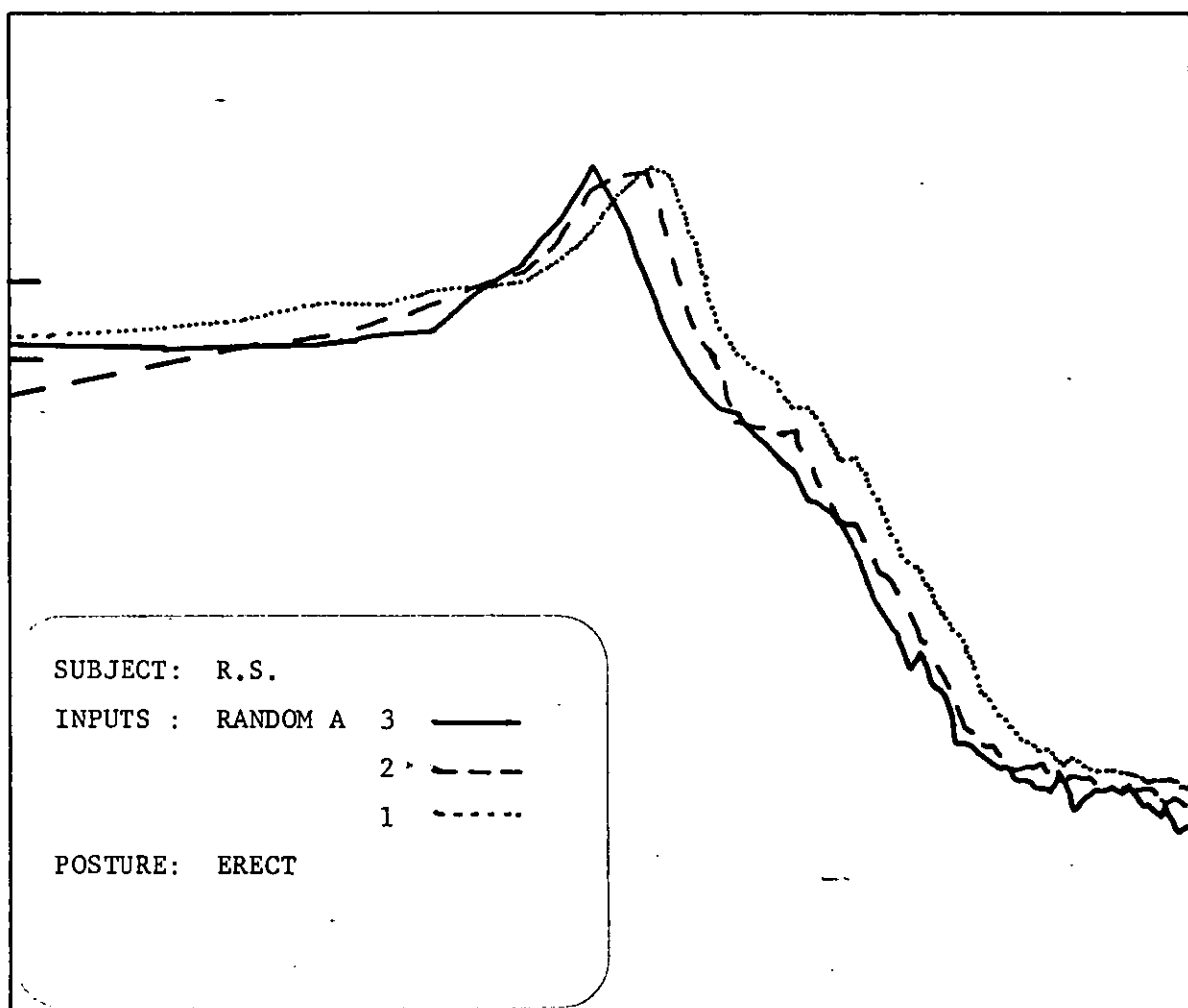


Fig. 4.14 Response to random stimuli (RA)
Subject 76. Erect.

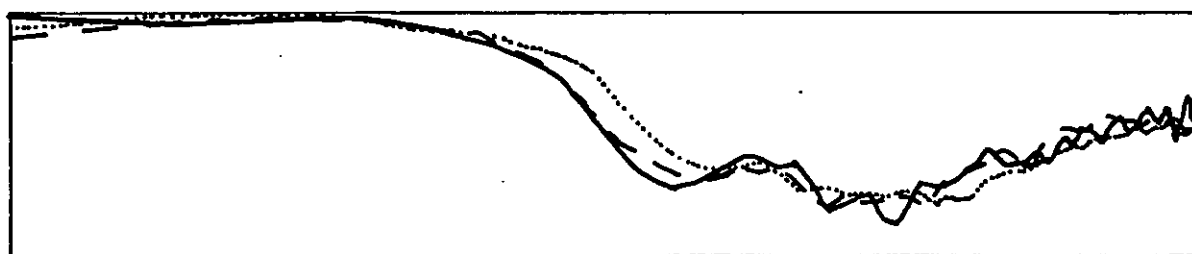
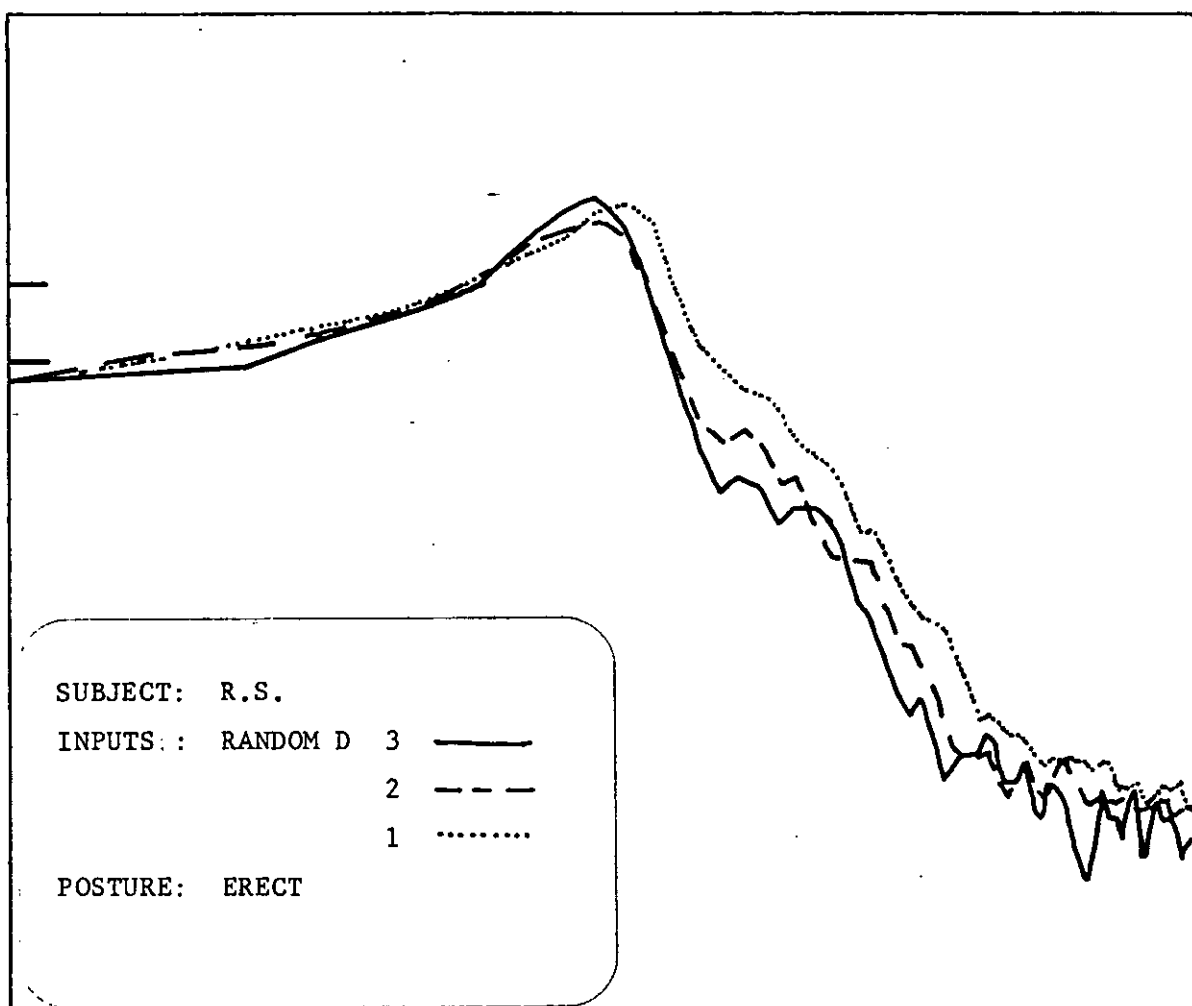


Fig. 4.15 Response to random stimuli (RD)
Subject 76. Erect.

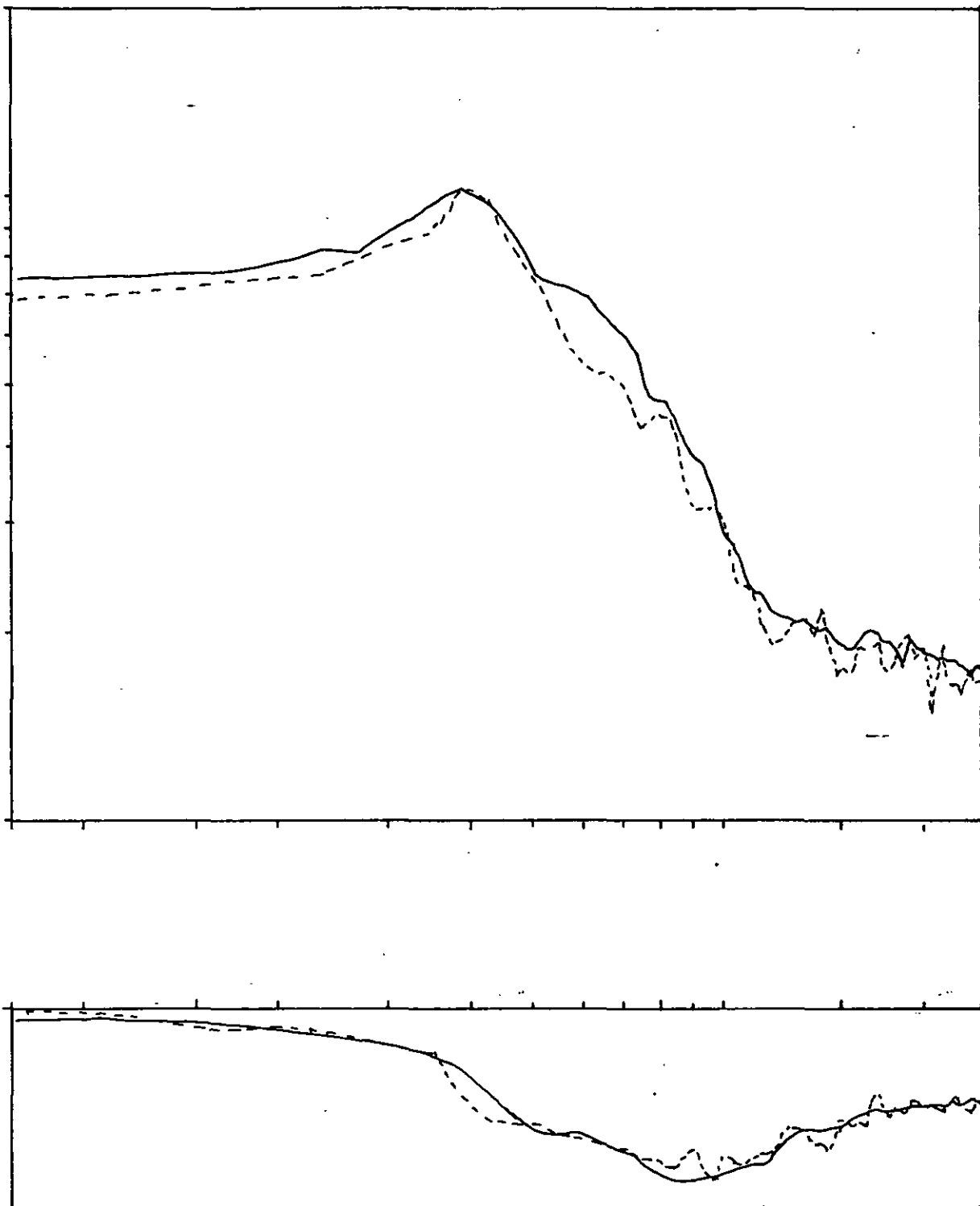


Fig. 4.16 Response to random stimuli.
Subject 76. Slumped.

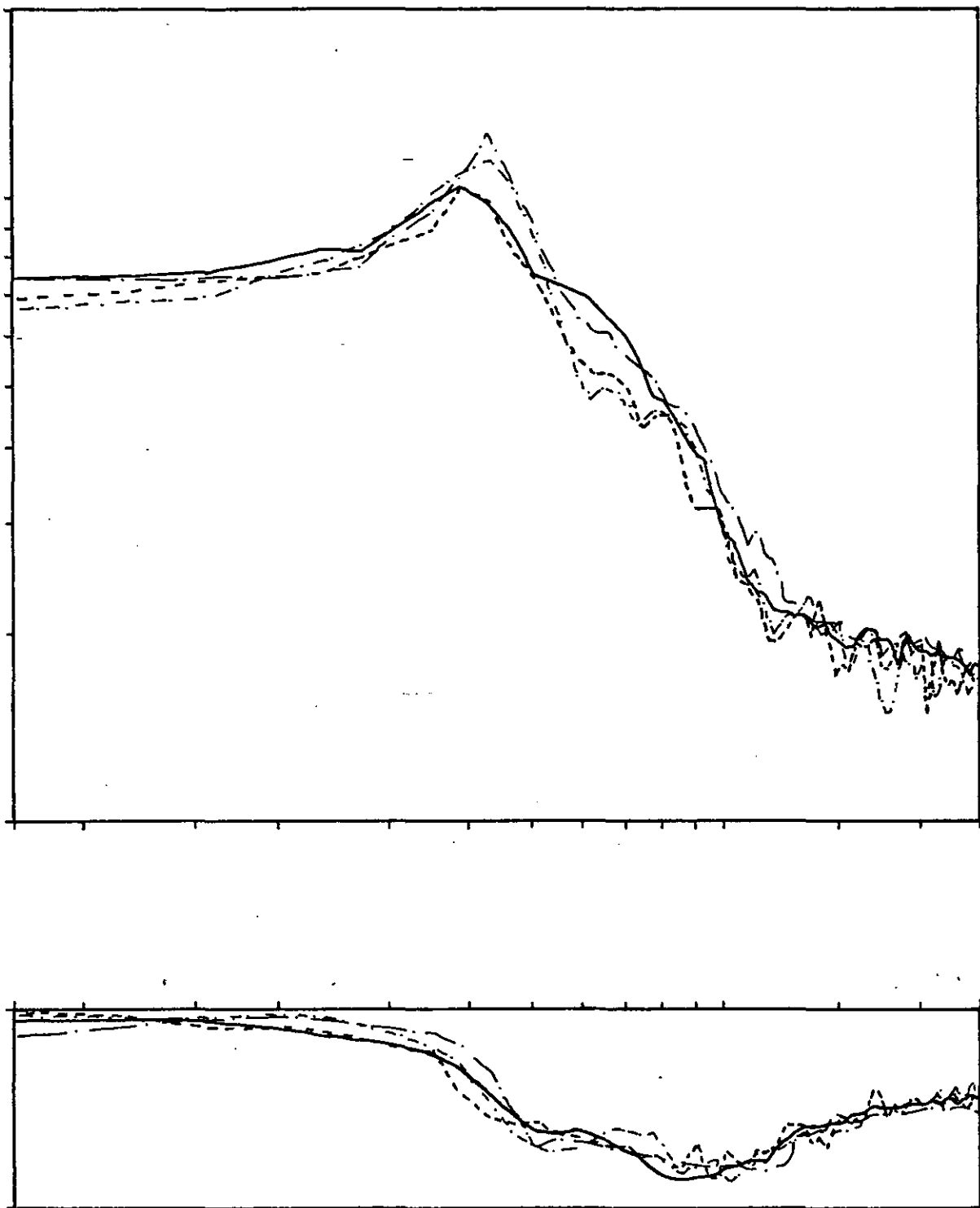


Fig. 4.17 Response to random stimuli.
Subject 76.

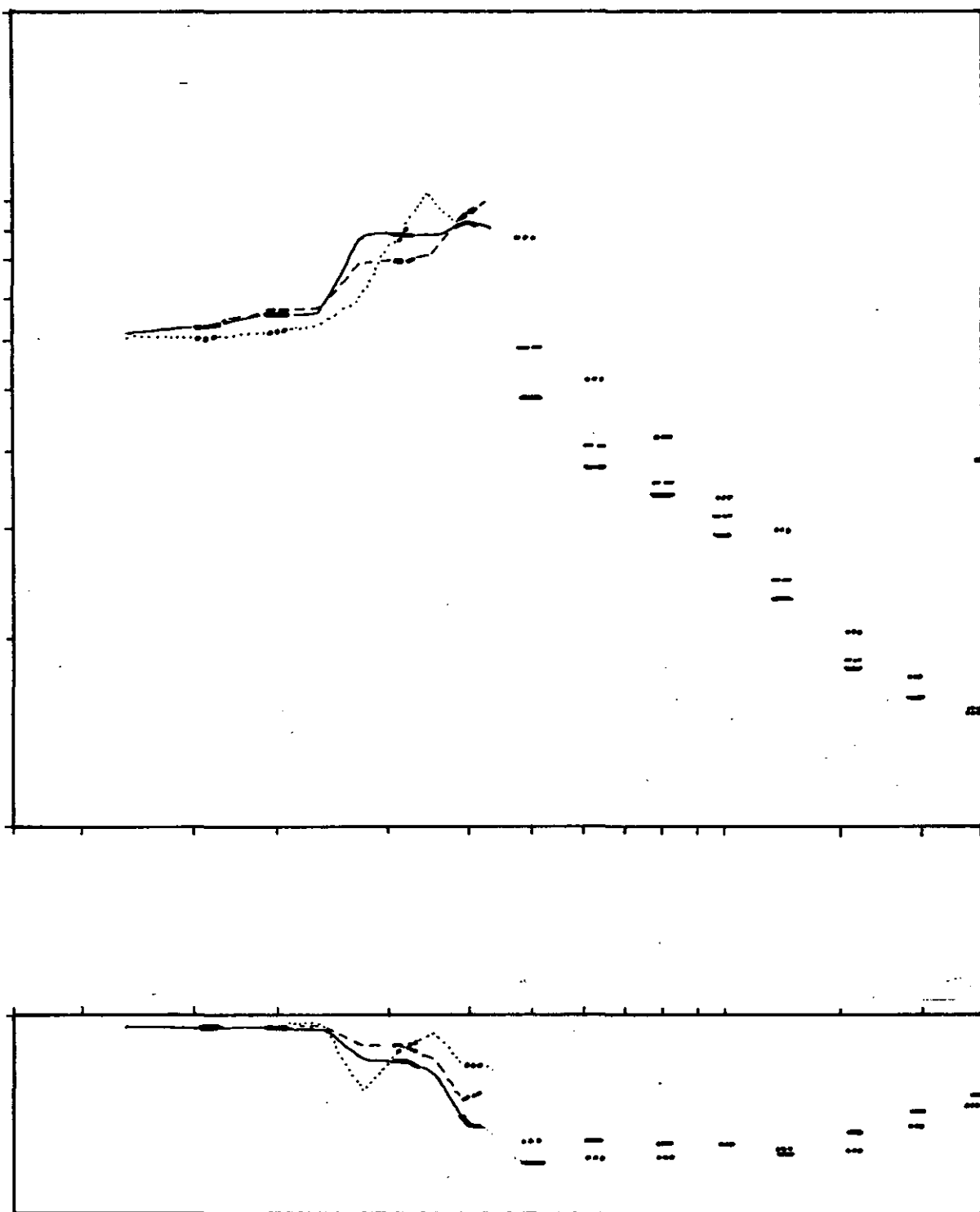


Fig. 4.18 Response to sinusoidal stimuli
Subject 75 Erect

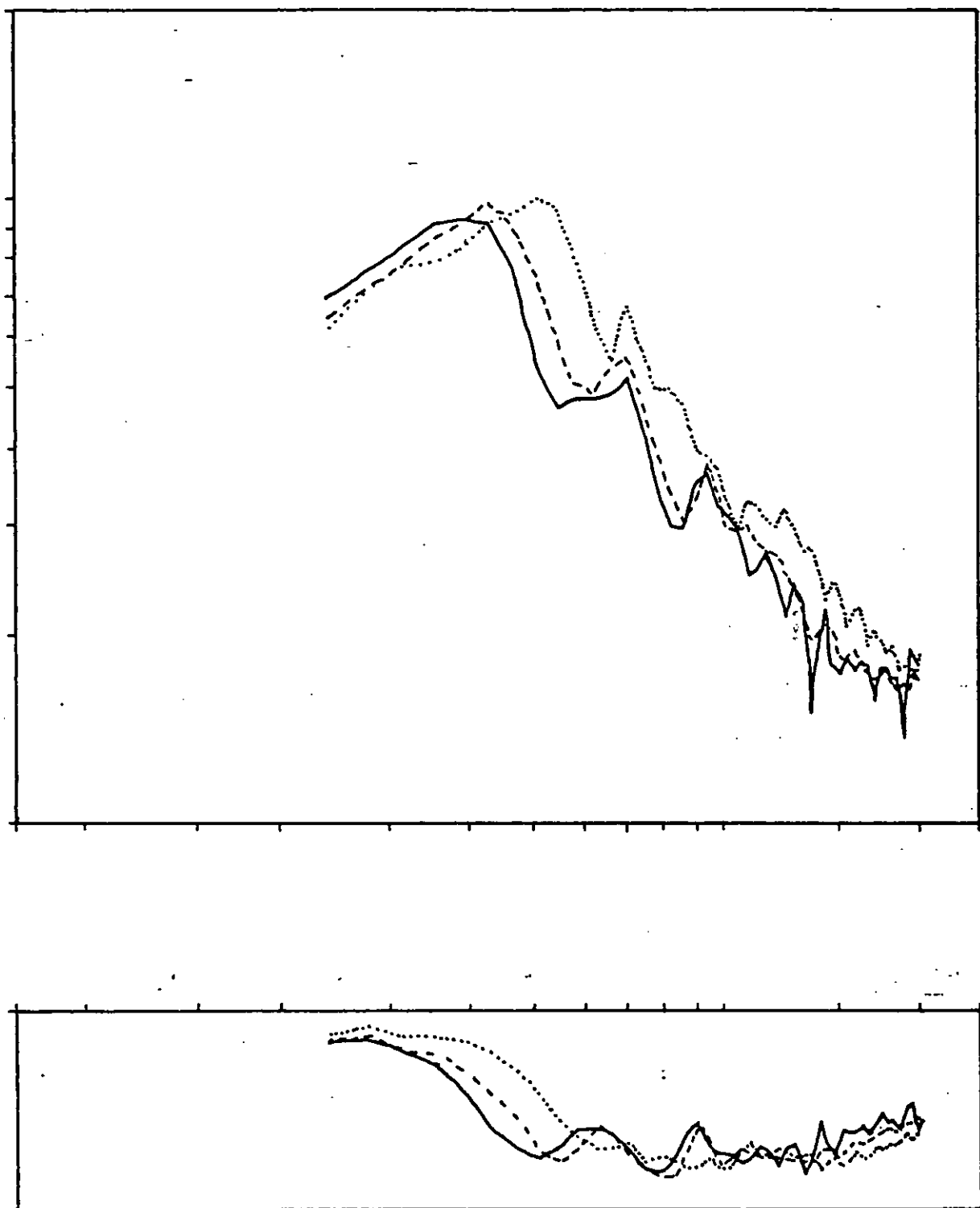


Fig. 4.19 Response to swift-sine transients
Subject 75 Erect

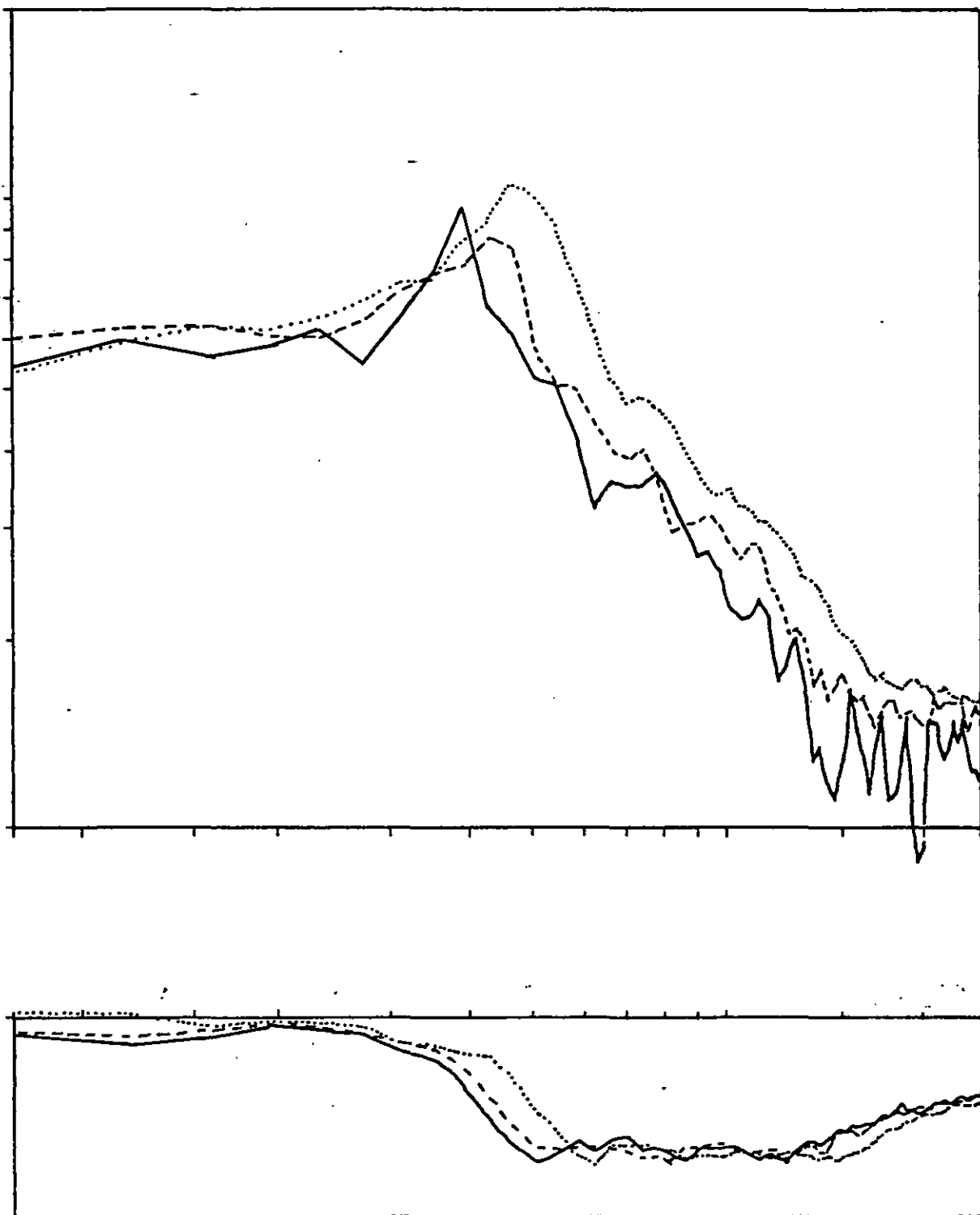


Fig. 4.20 Reponse to random stimuli (RA)
 Subject 75 Erect

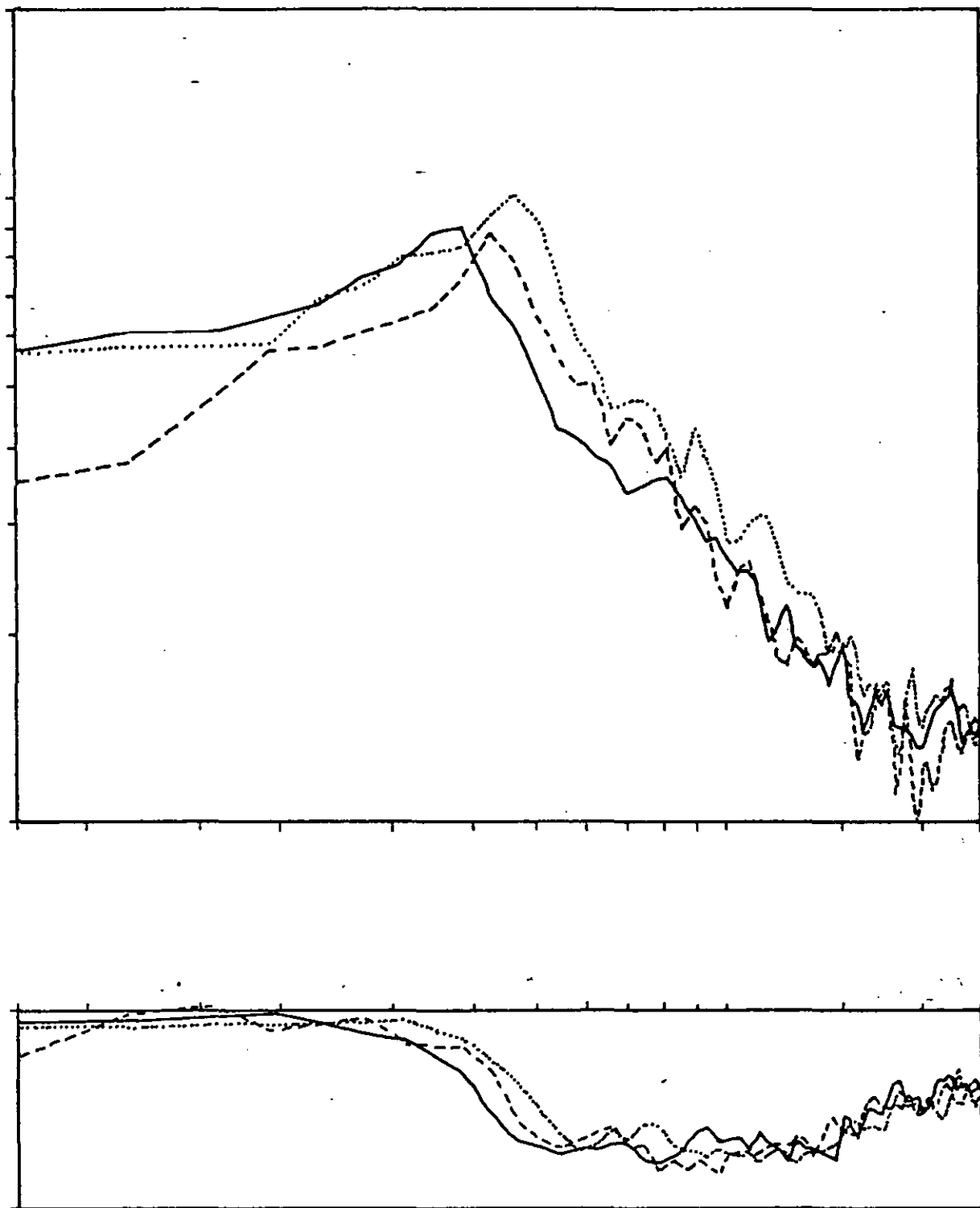


Fig. 4.21 Response to random stimuli (RD)
Subject 75 Erect

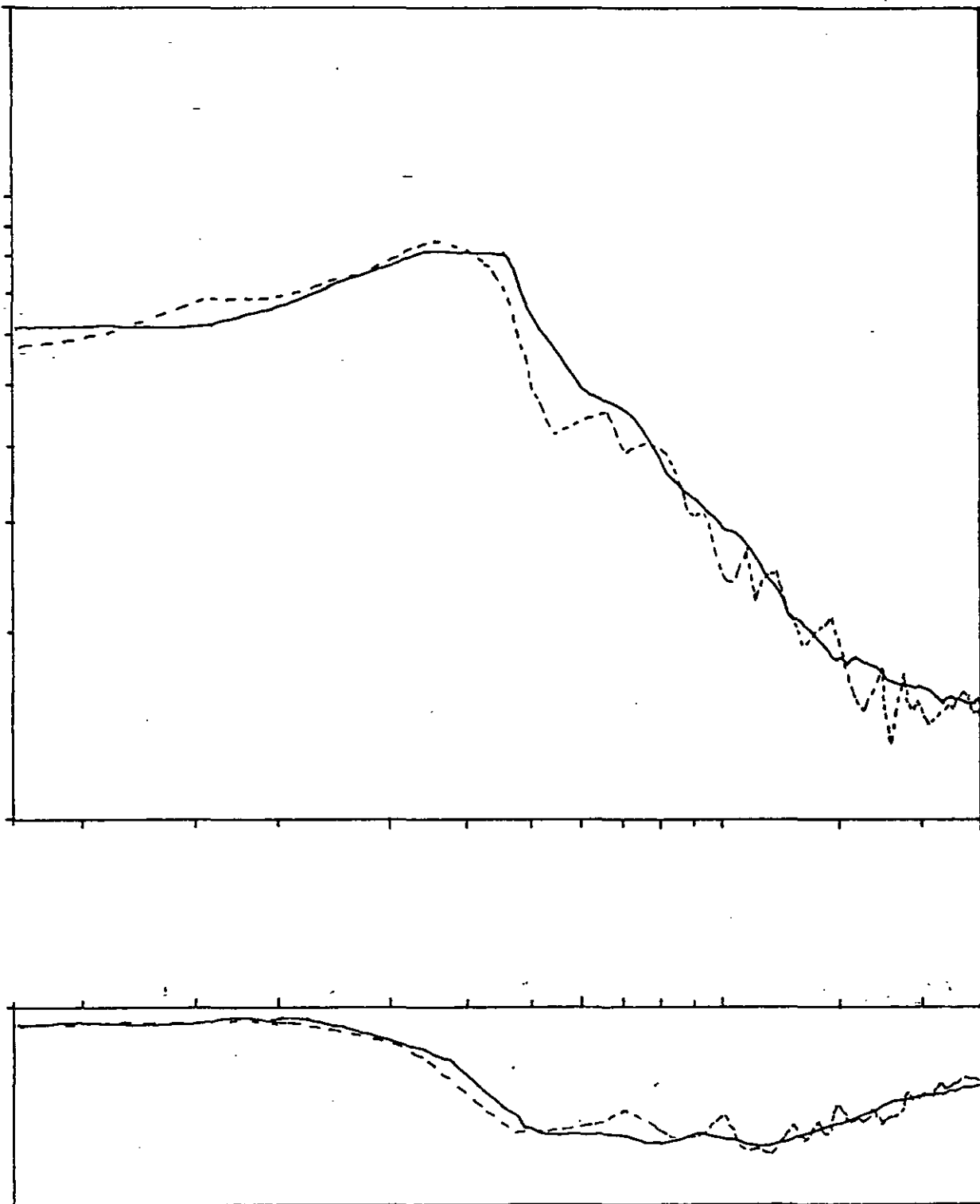


Fig. 4.22 Response to random stimuli
Subject 75 Slumped

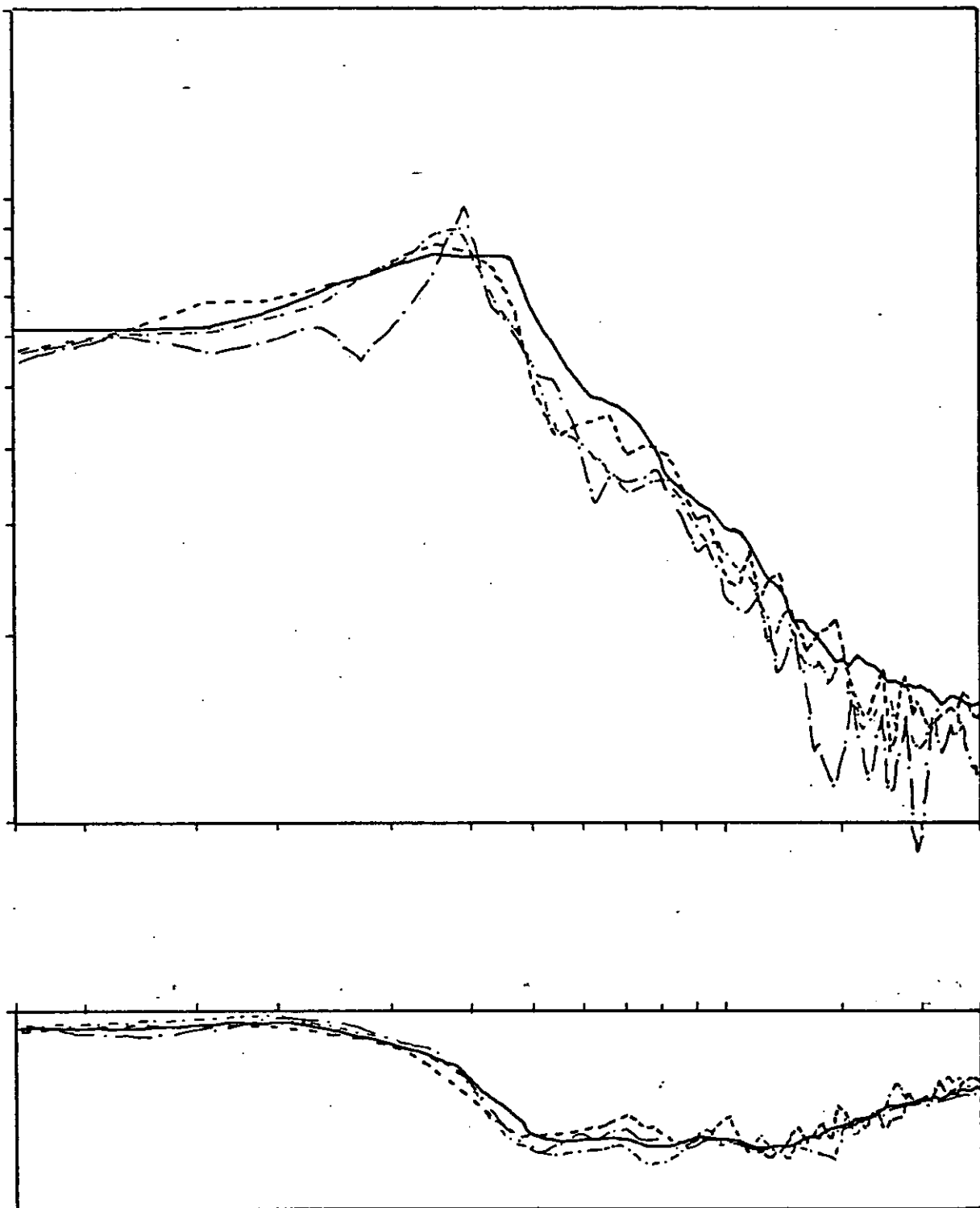


Fig. 4.23 Response to random stimuli
Subject 75

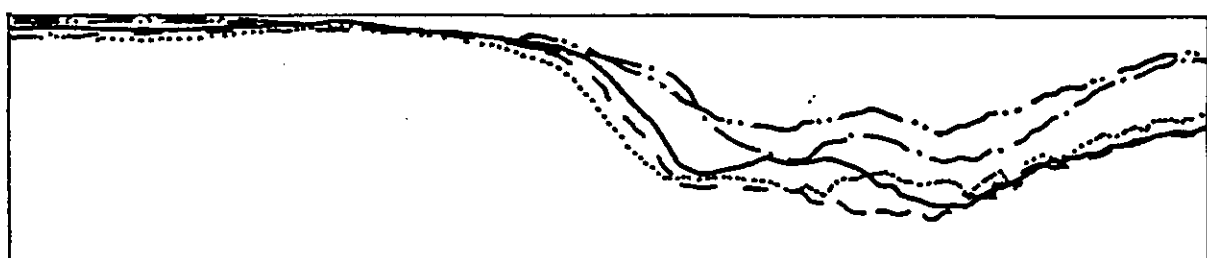
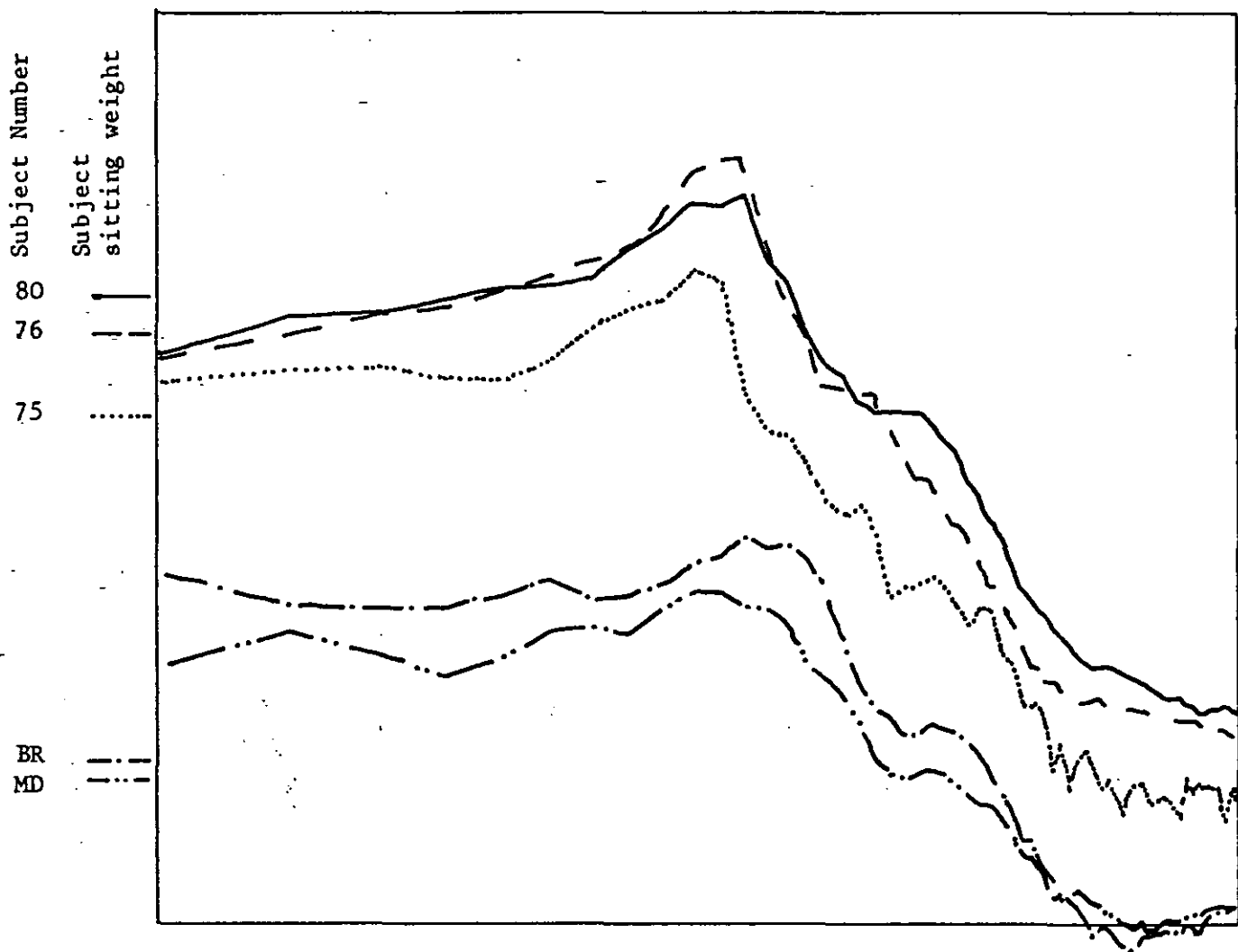


Fig. 4.24 Comparison of five subjects - Random Stimulus

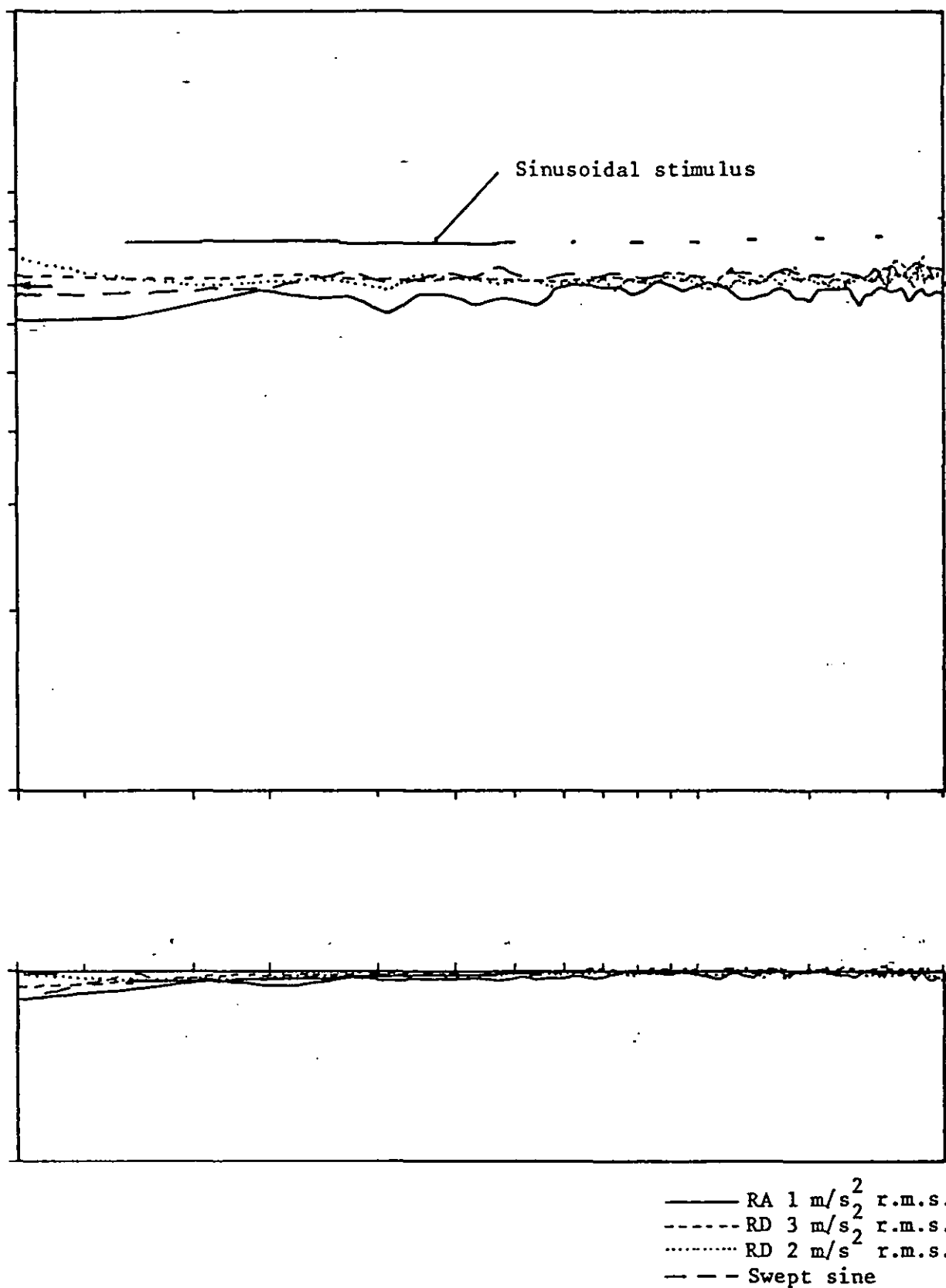
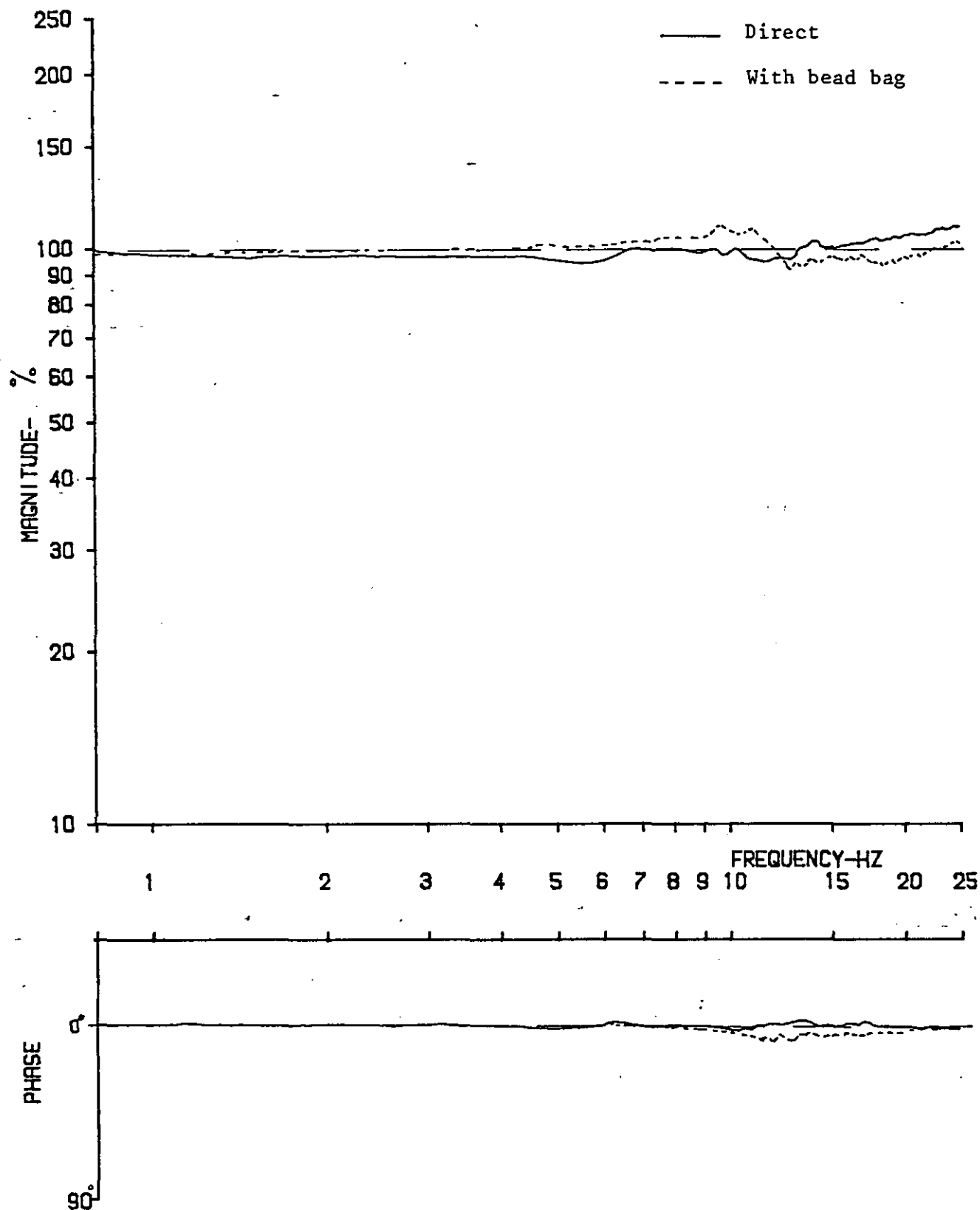


Fig. 4.25 Apparent mass of 70 kg weight using different stimuli



RUN NO.

Fig. 4.26 The effects of a 'bead bag' on the transmission of vibration to a buttock form

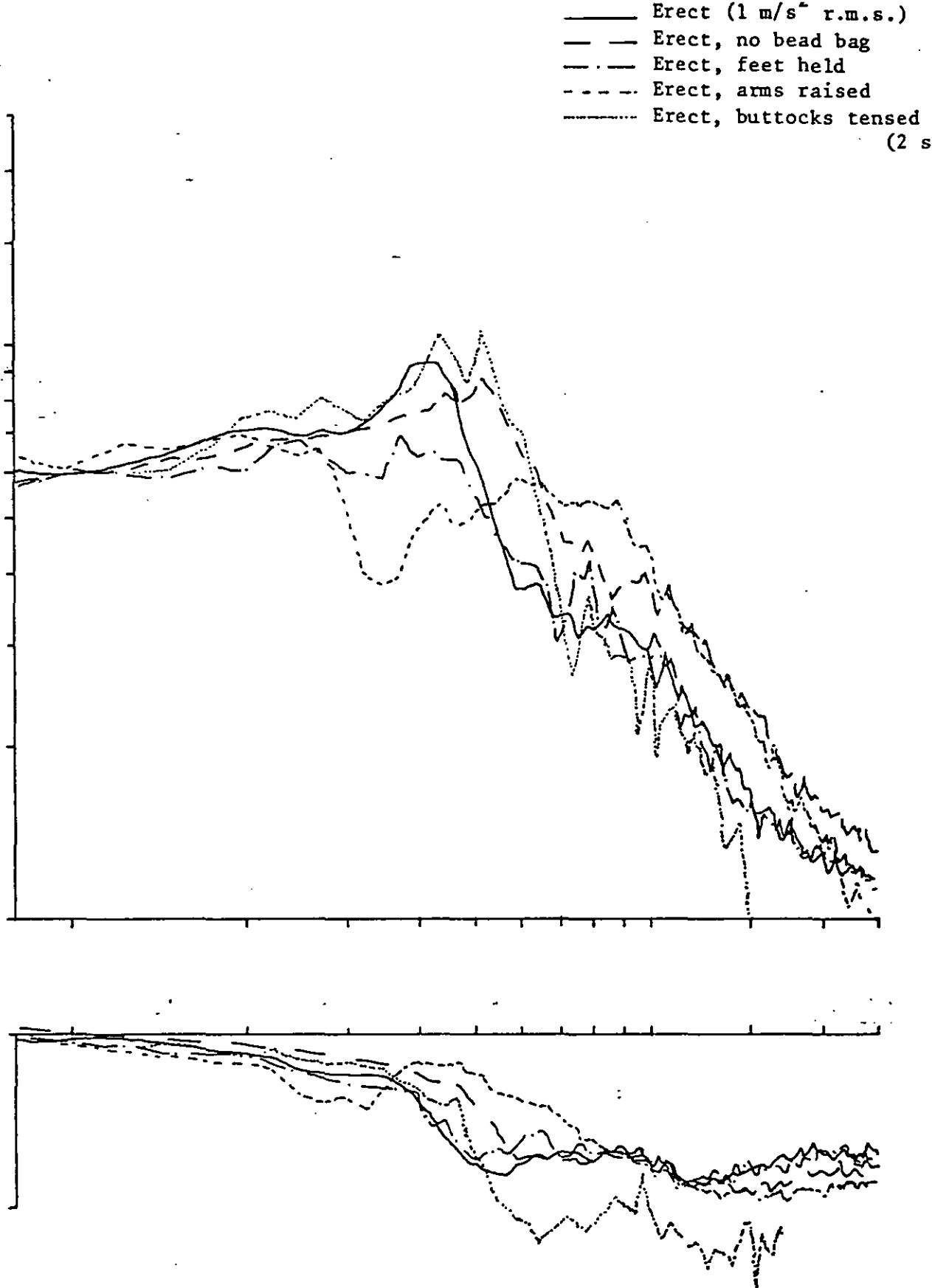


Fig. 4.27 The effects of different postures
 Random stimuli Subject 75

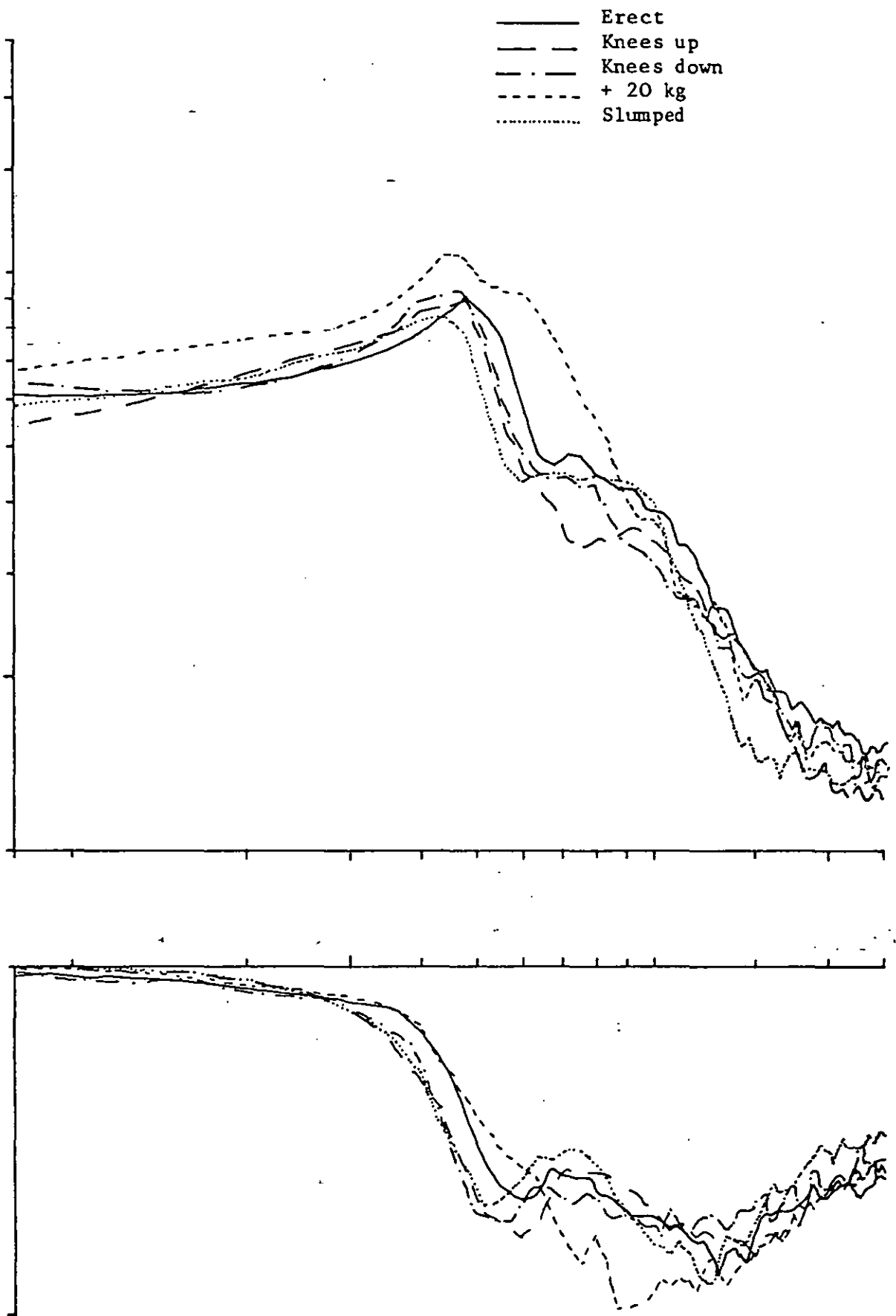


Fig. 4.28 The effects of different postures
Random stimulus Subject 75

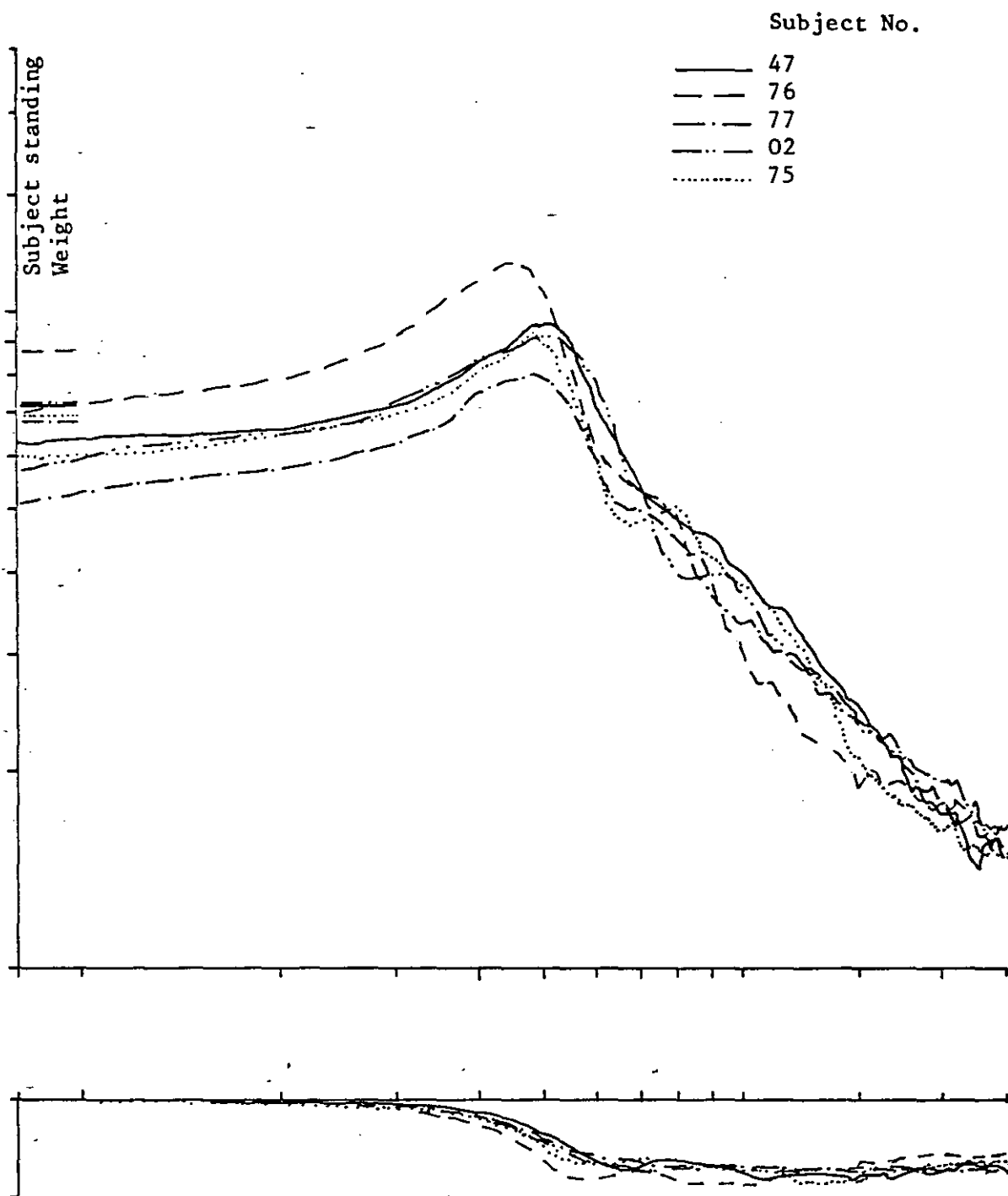


Fig. 4.29 Apparent mass of 5 subjects - erect

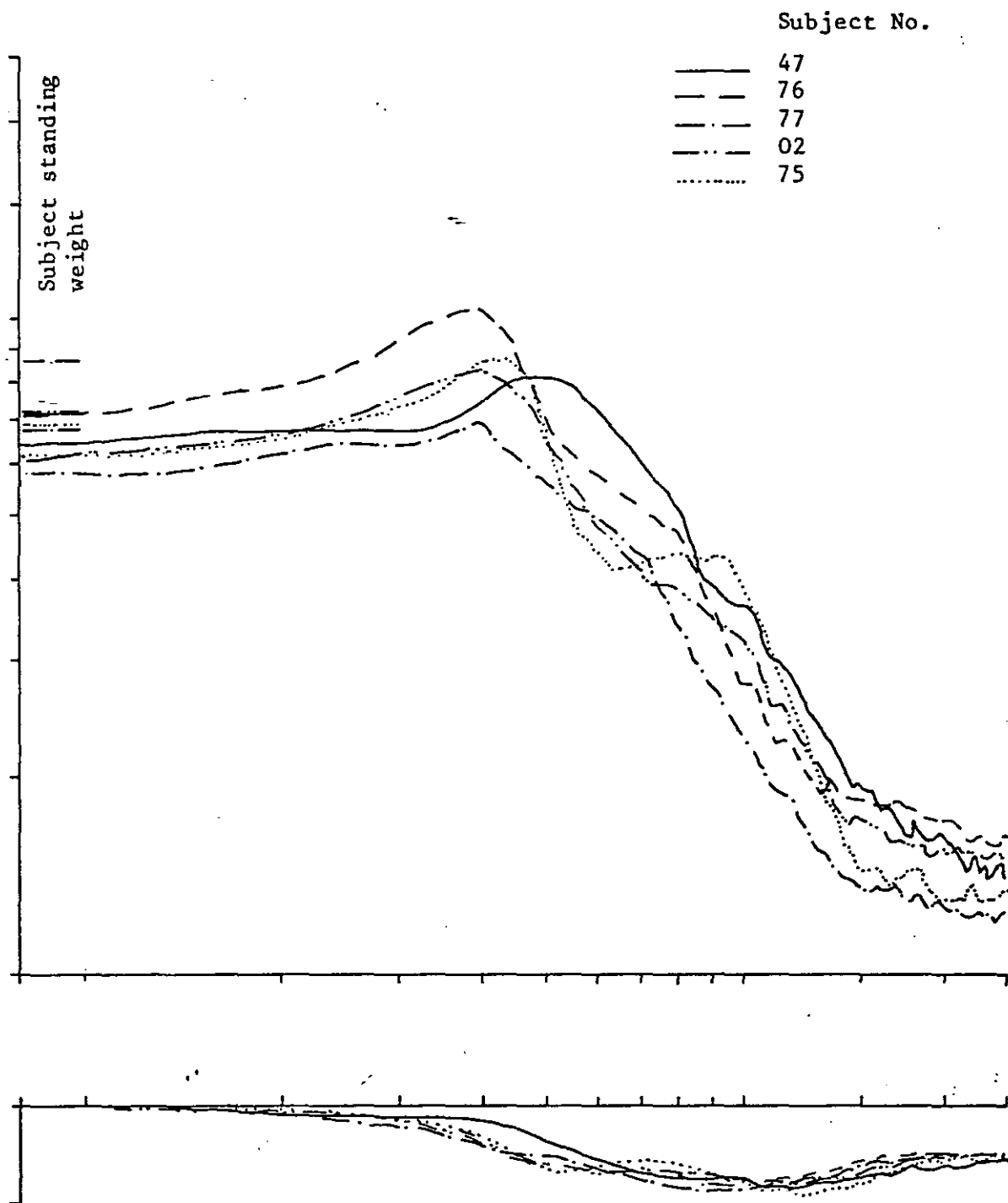


Fig. 4.30 Apparent mass of 5 subjects - slumped

Fig. 5.1 Illustration of the value of the Hanning function in estimation of the system response function.

- a) Response function of S.D.F. model using random stimulus, 20 samples averaged
- b) Ditto, excluding Hanning function
- c) & d) Relevant input and output P.S.D. functions and the coherence function.

Note reduced variability and increased coherence when Hanning used. Note also the poor coherence at frequencies where the P.S.D. is very low.

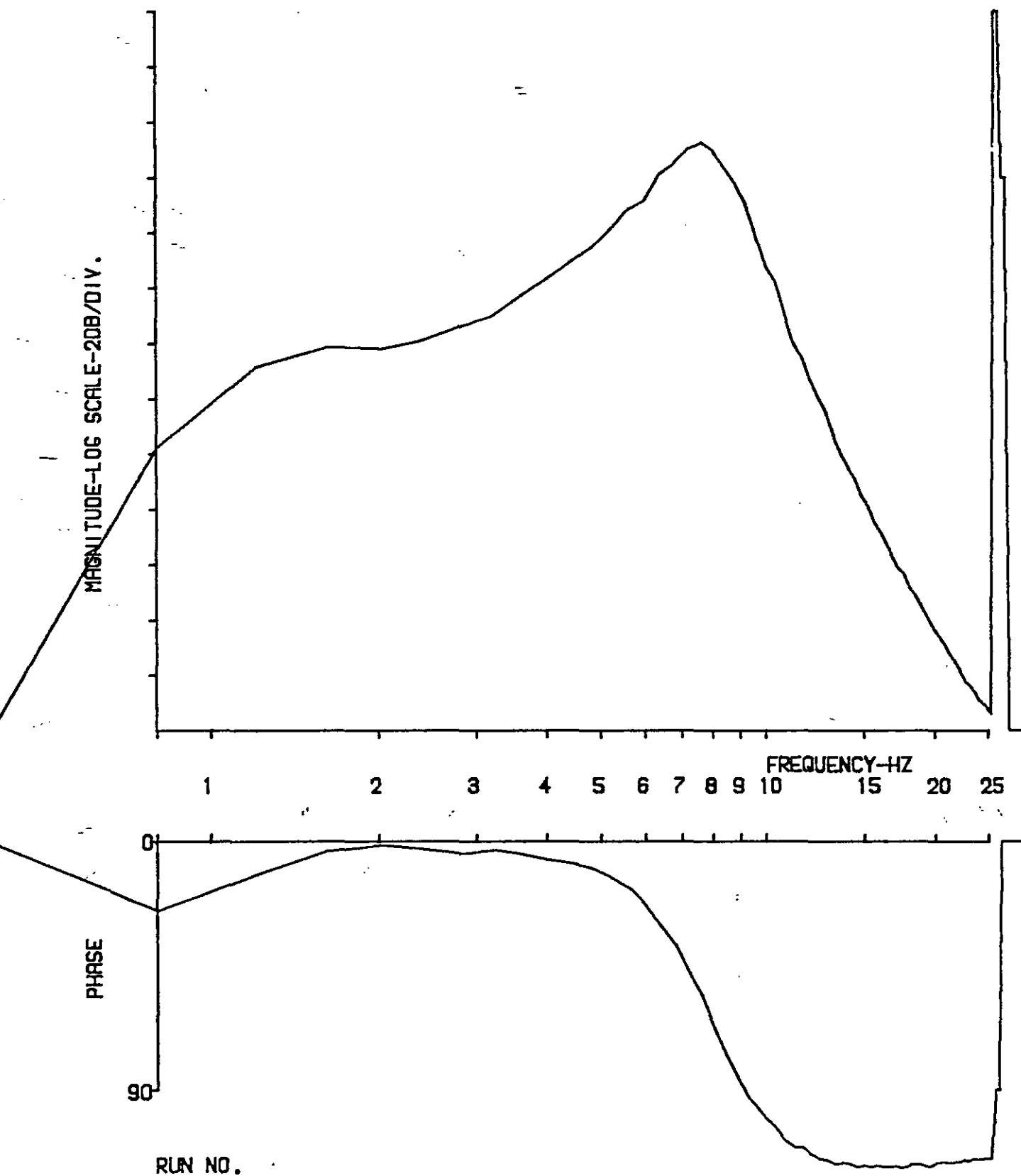


Figure 5.1a

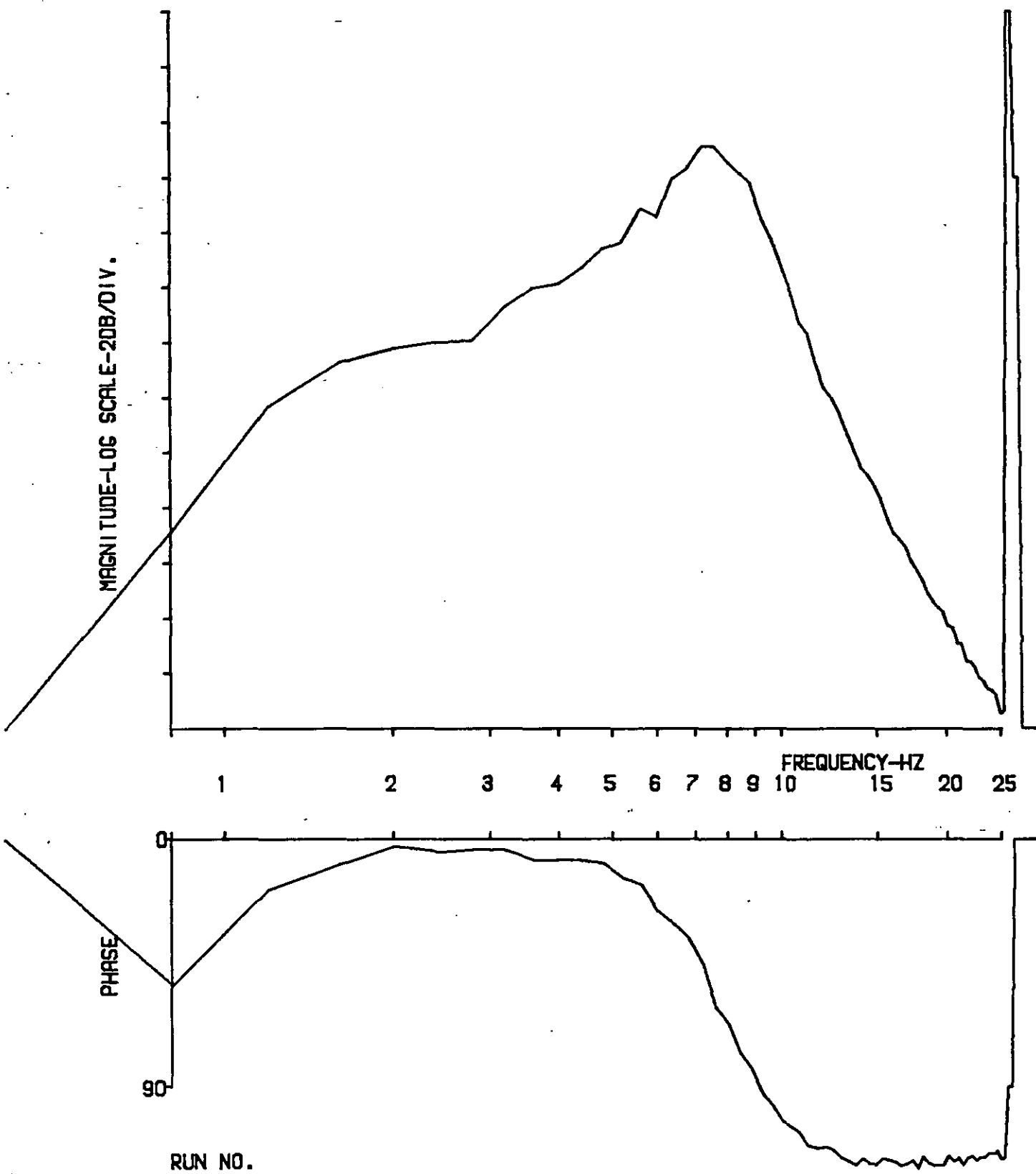
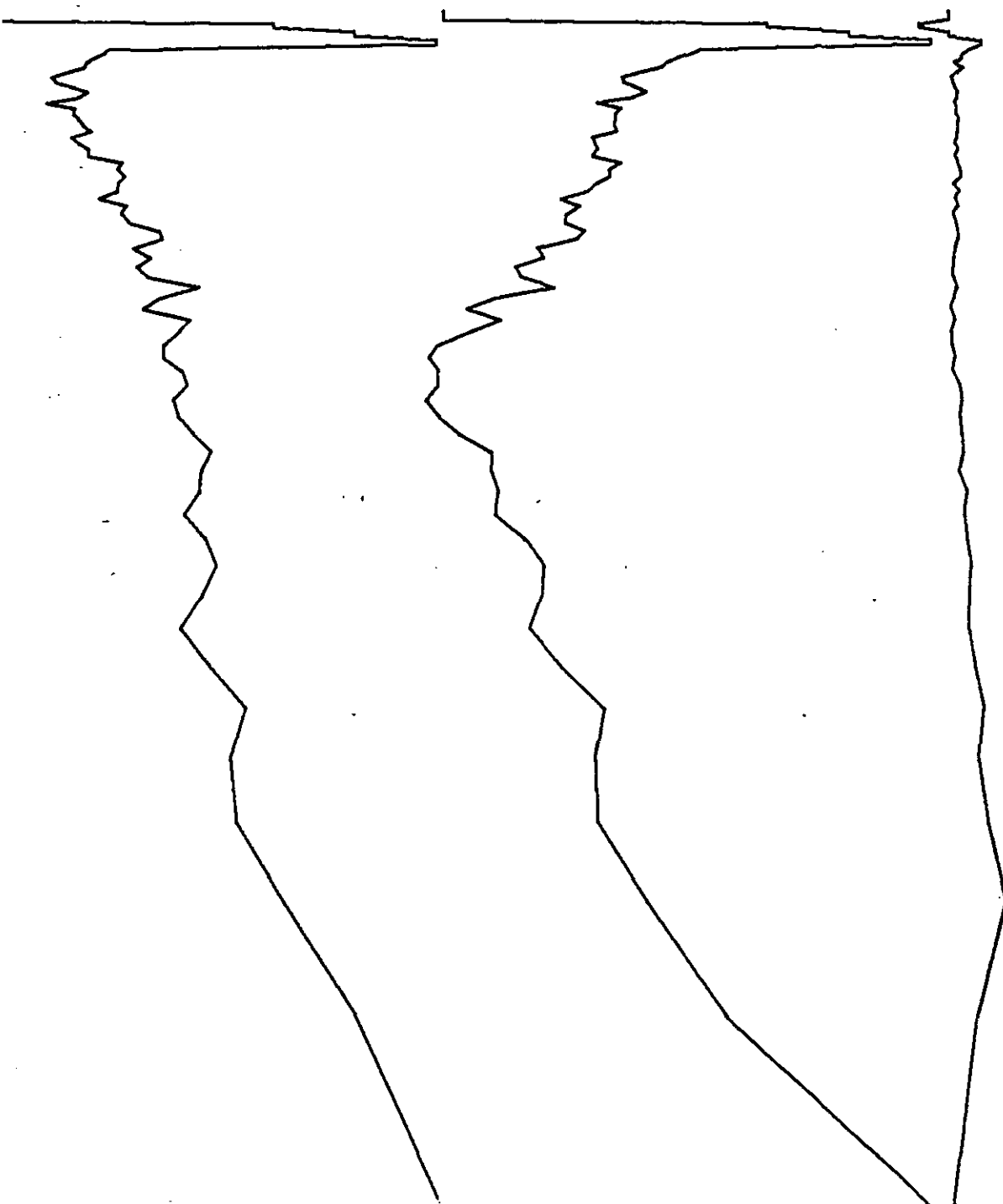


Figure 5.1b



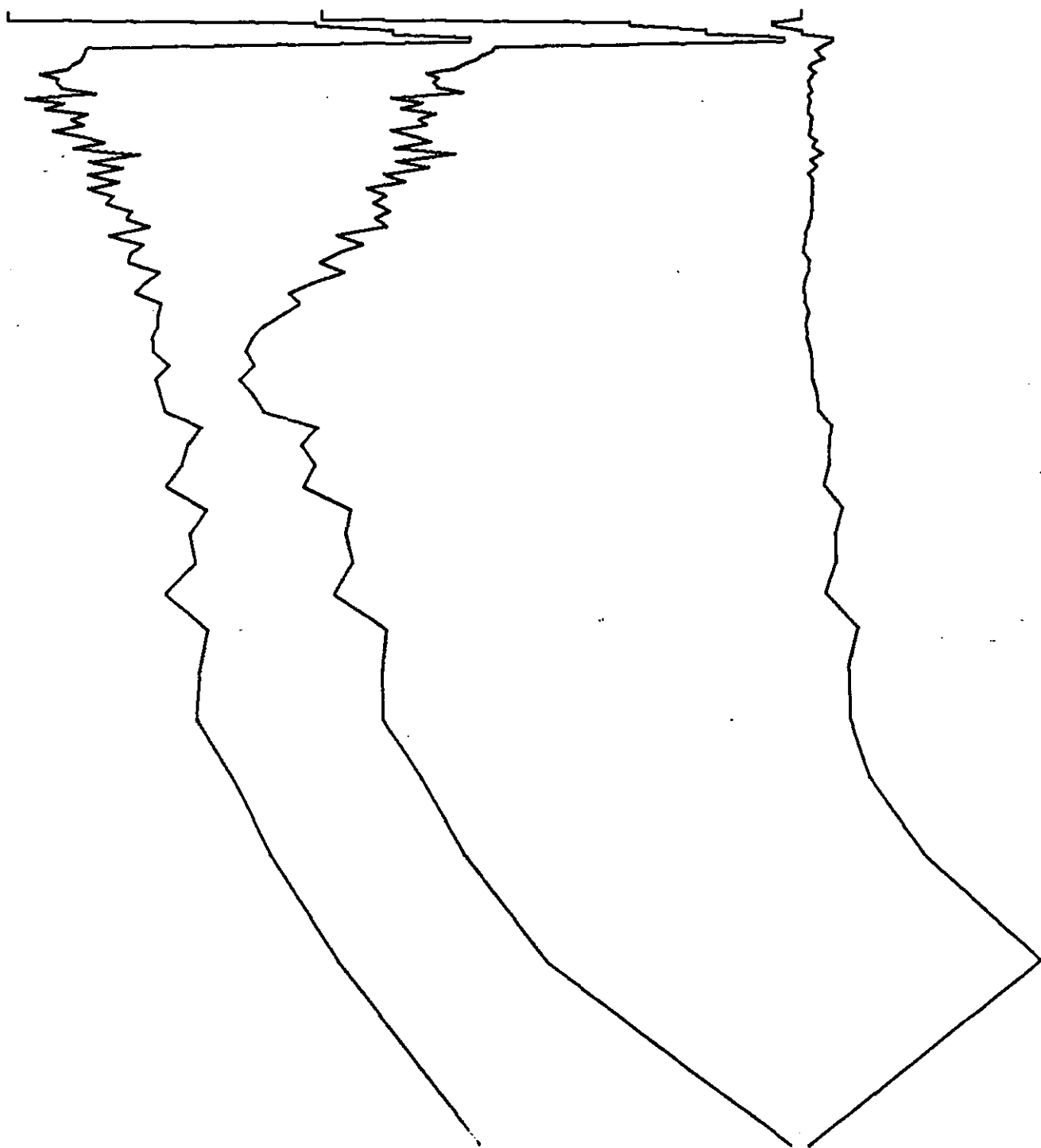
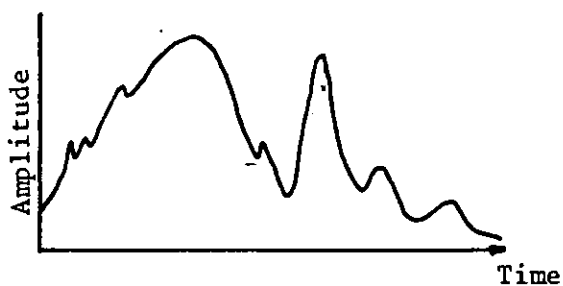


Figure 5.1d

Analogue signal



Digitised signal

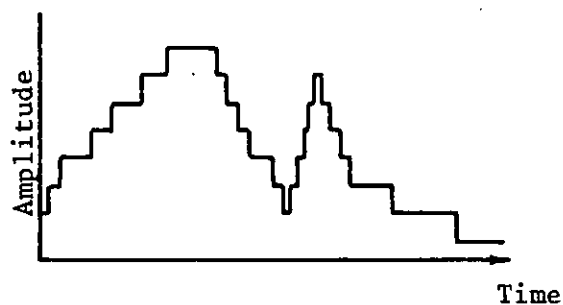


Fig. 5.2 Amplitude quantization

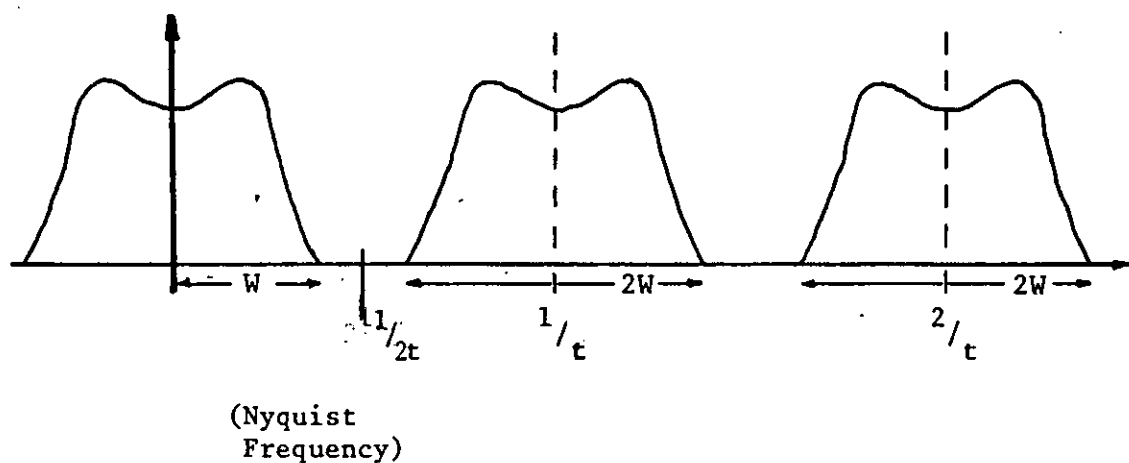


Fig. 5.3 Illustration of the 'images' of the original spectrum which lead to aliasing.

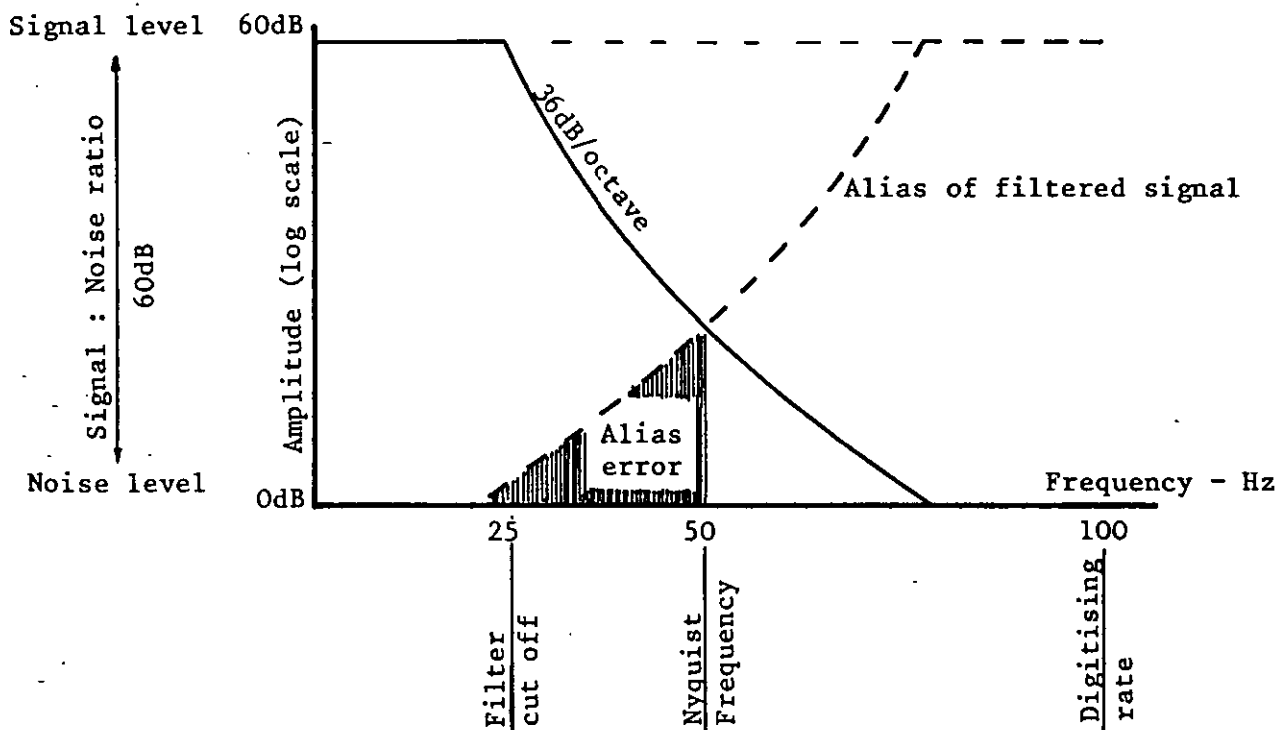


Fig. 5.4 Consideration of required filter characteristics

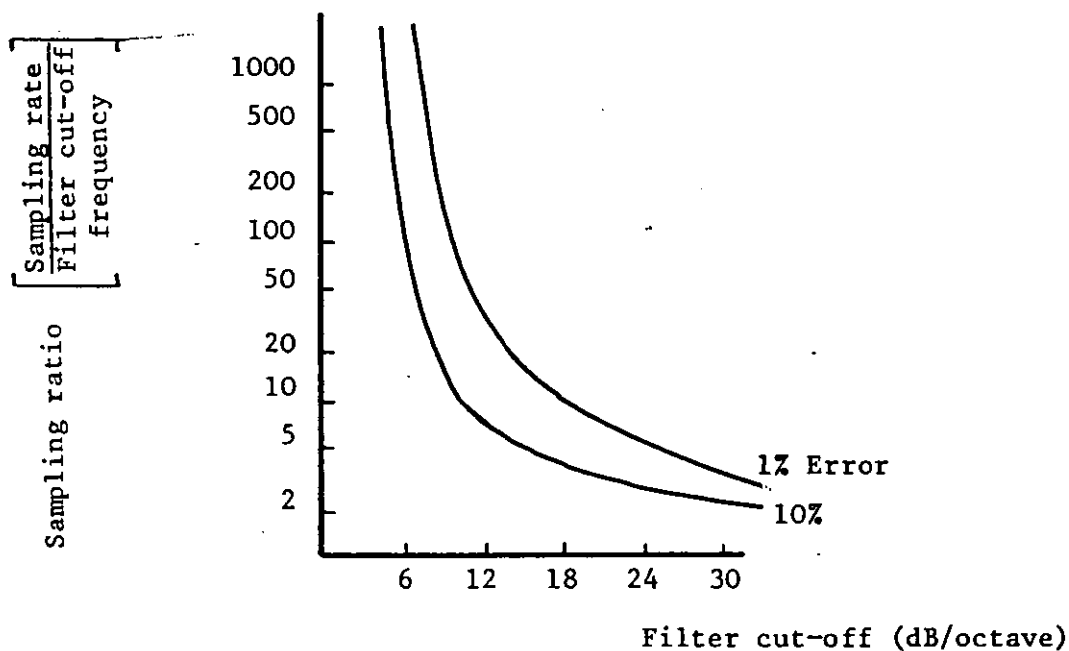


Fig. 5.5 Sampling rate required for given accuracy (after Stacy, R.W. & Waxman, B.D. (1965)).

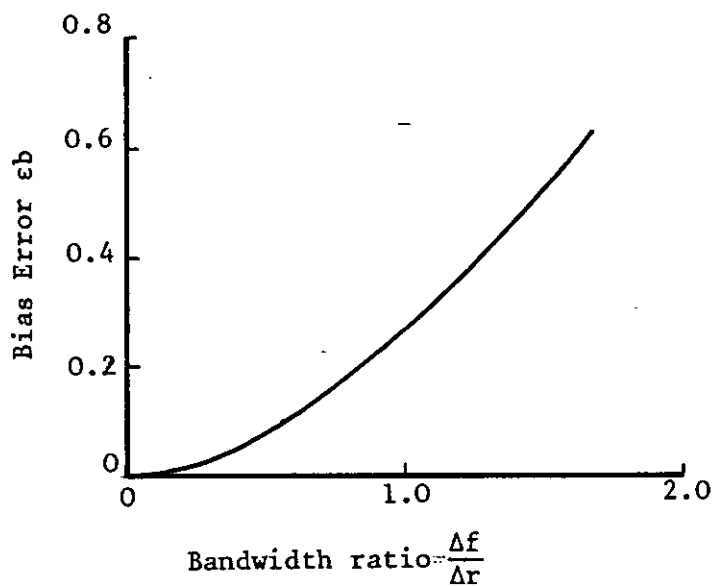


Fig. 5.6 Bias error for second order system response (after Bendat, J.S. & Piersol, A.G. (1971)).

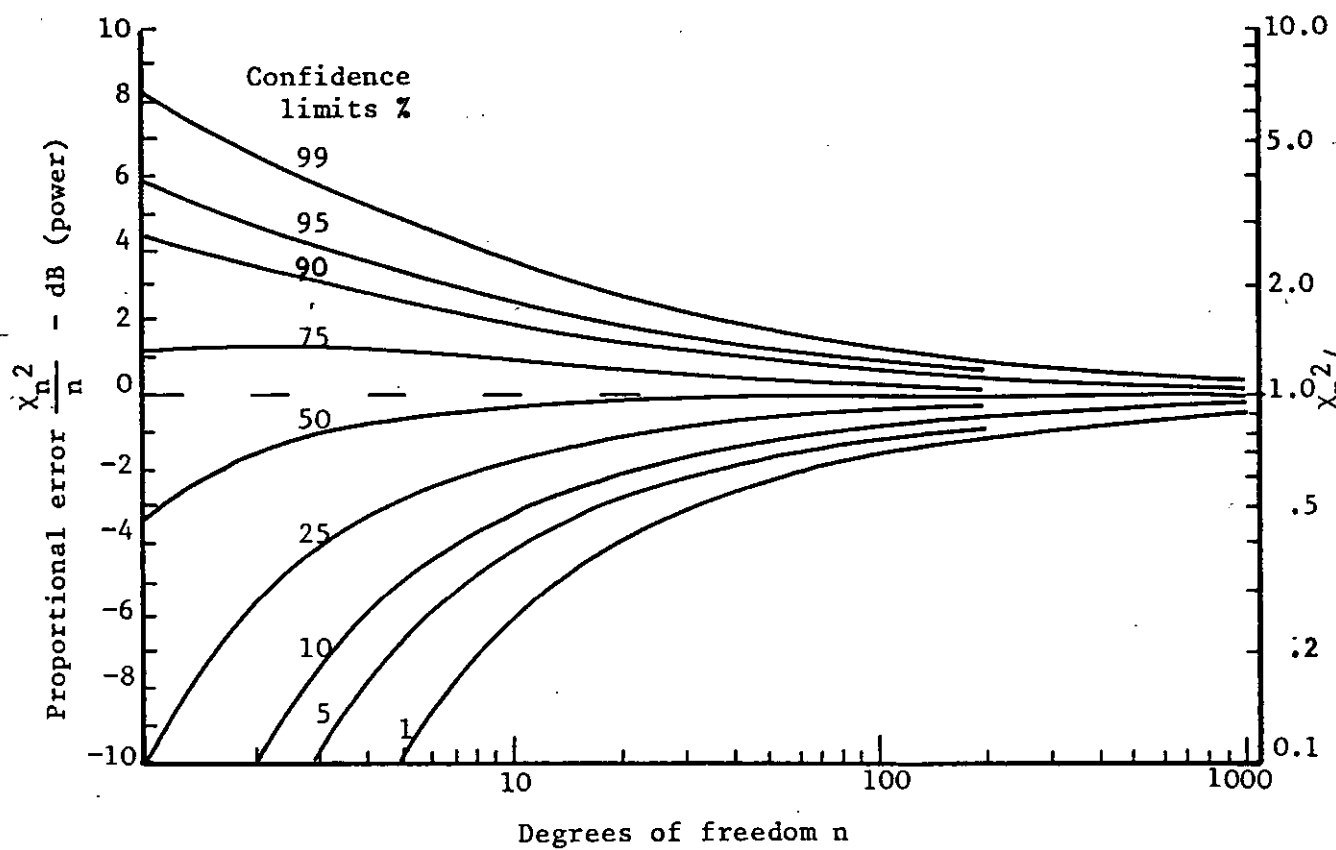


Fig. 5.7 Confidence limits for power spectra (after LOWSON, M.V. (1972))

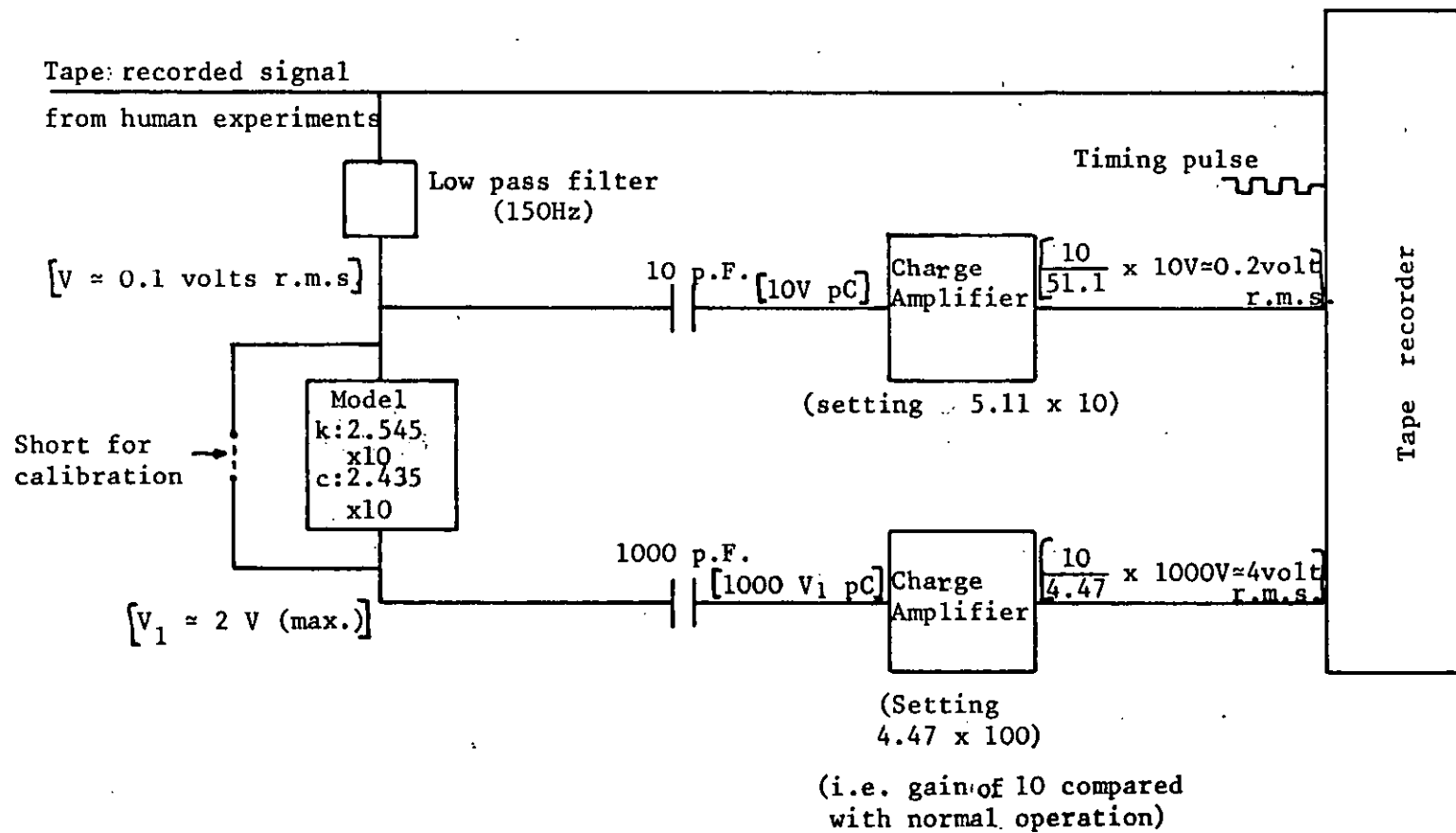


Fig. 5.8 System used to check error calculations

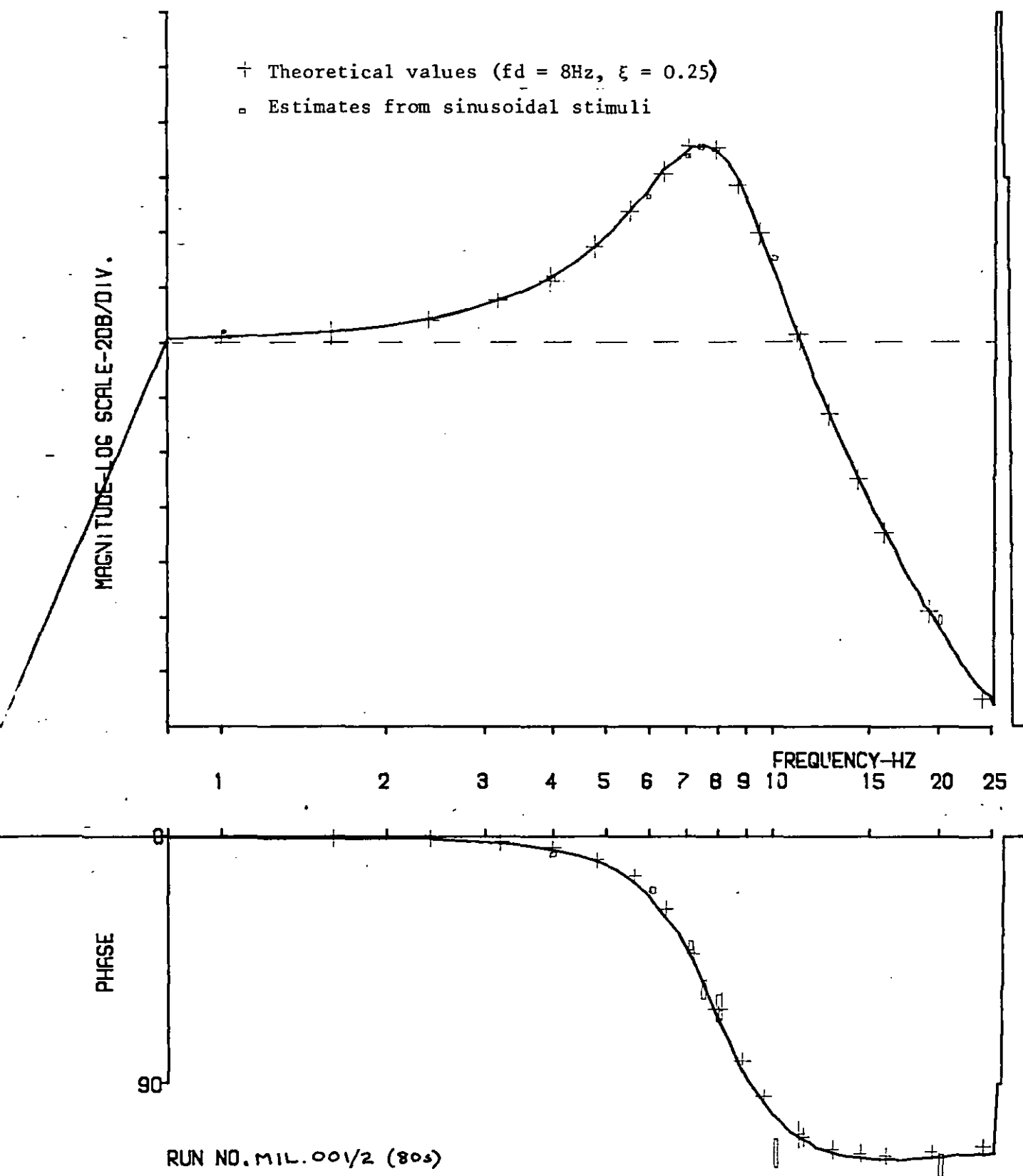


Fig. 5.9a Model response (80 samples, on-line)

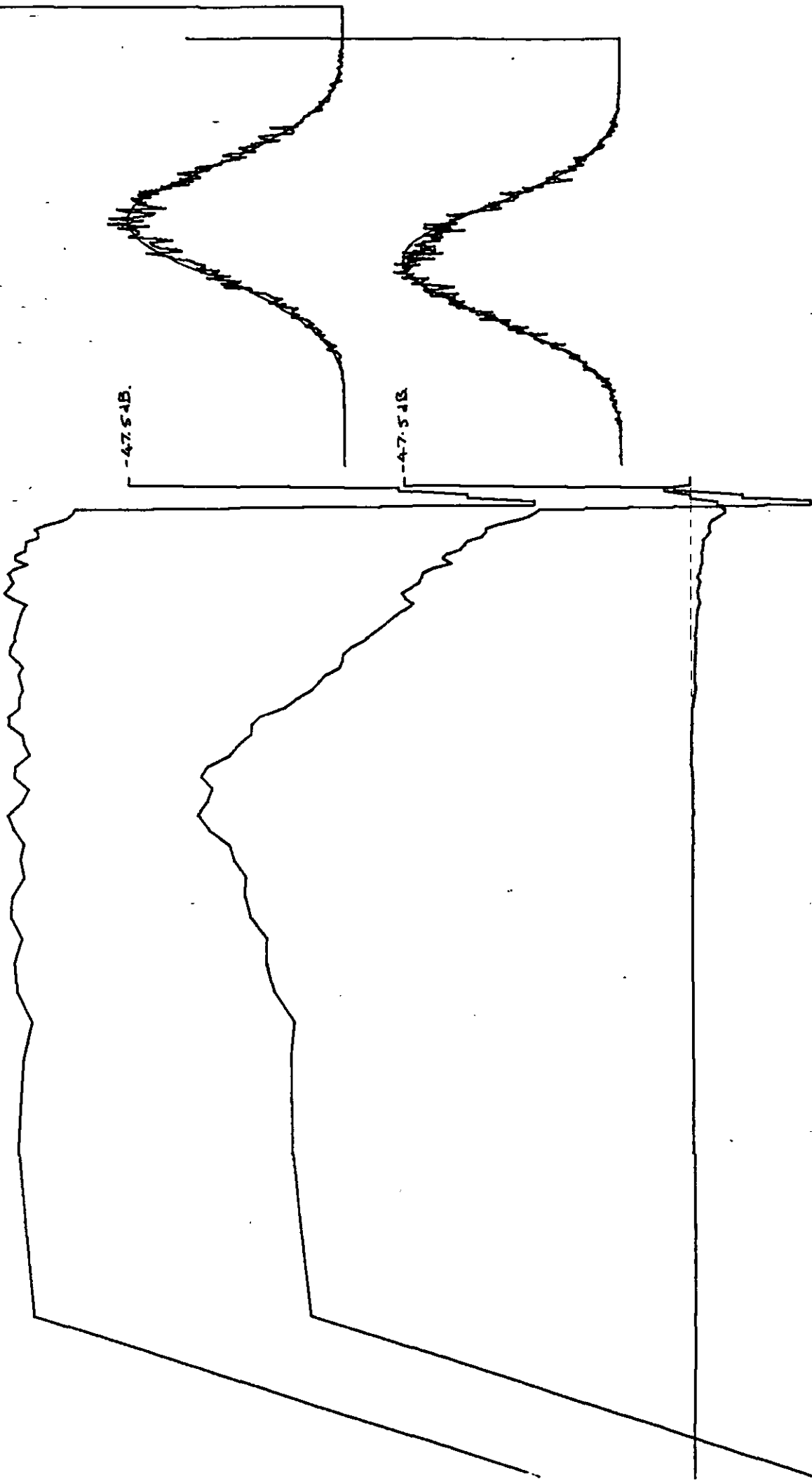


Fig. 5.9b

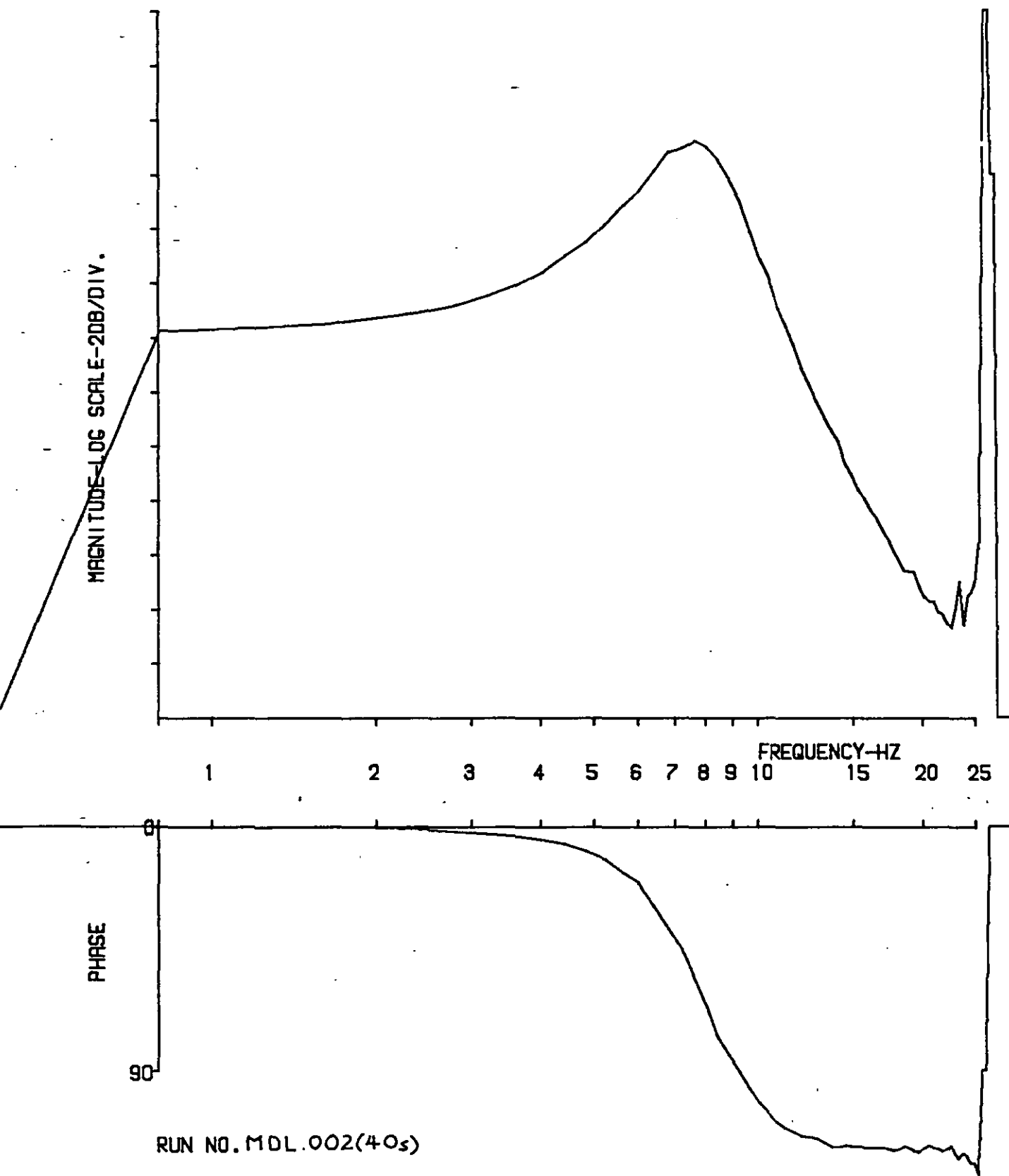


Fig. 5.10a Model response (40 samples)

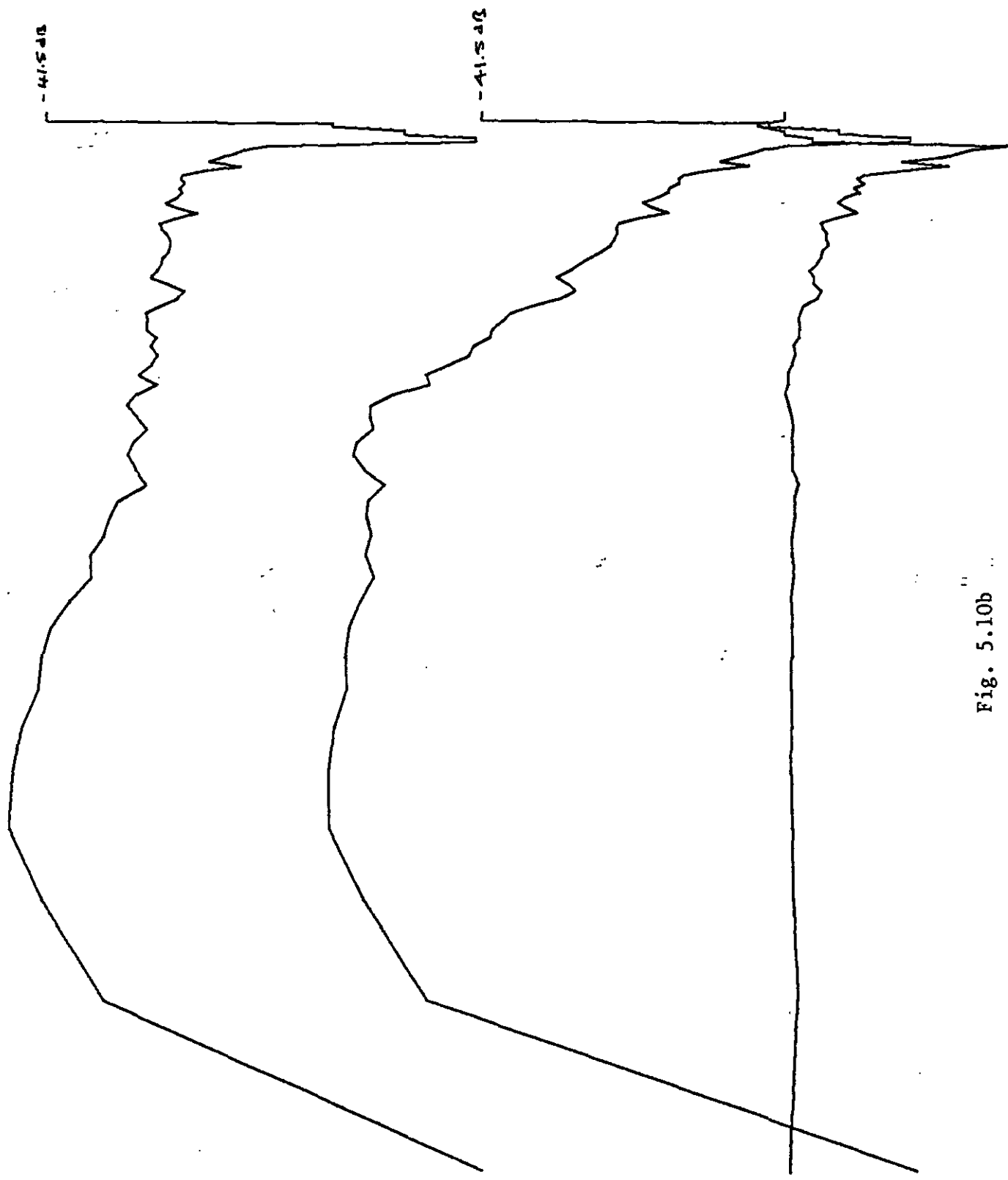


Fig. 5.10b

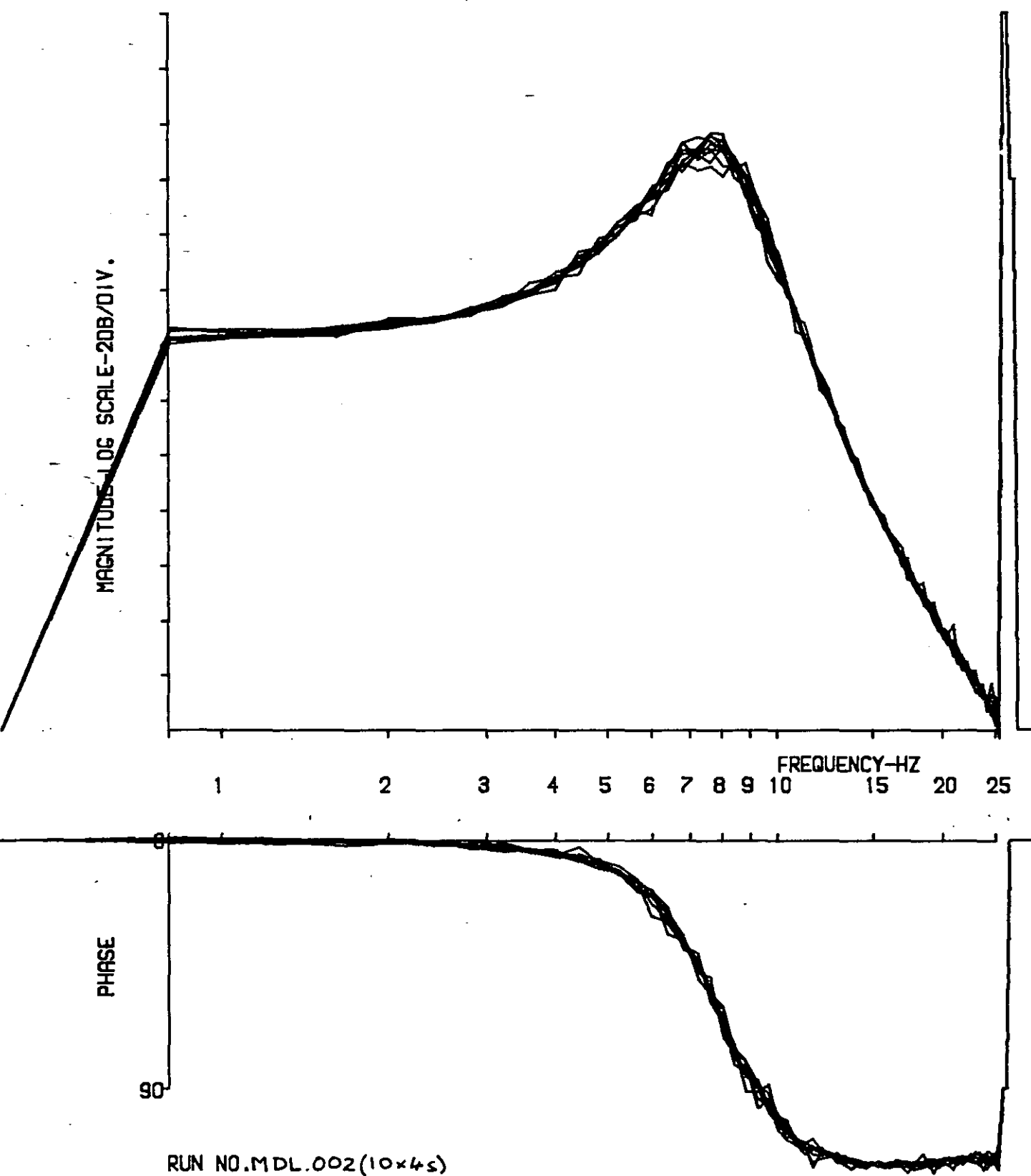


Fig. 5.11a Model response (10 plots, each 4 samples)

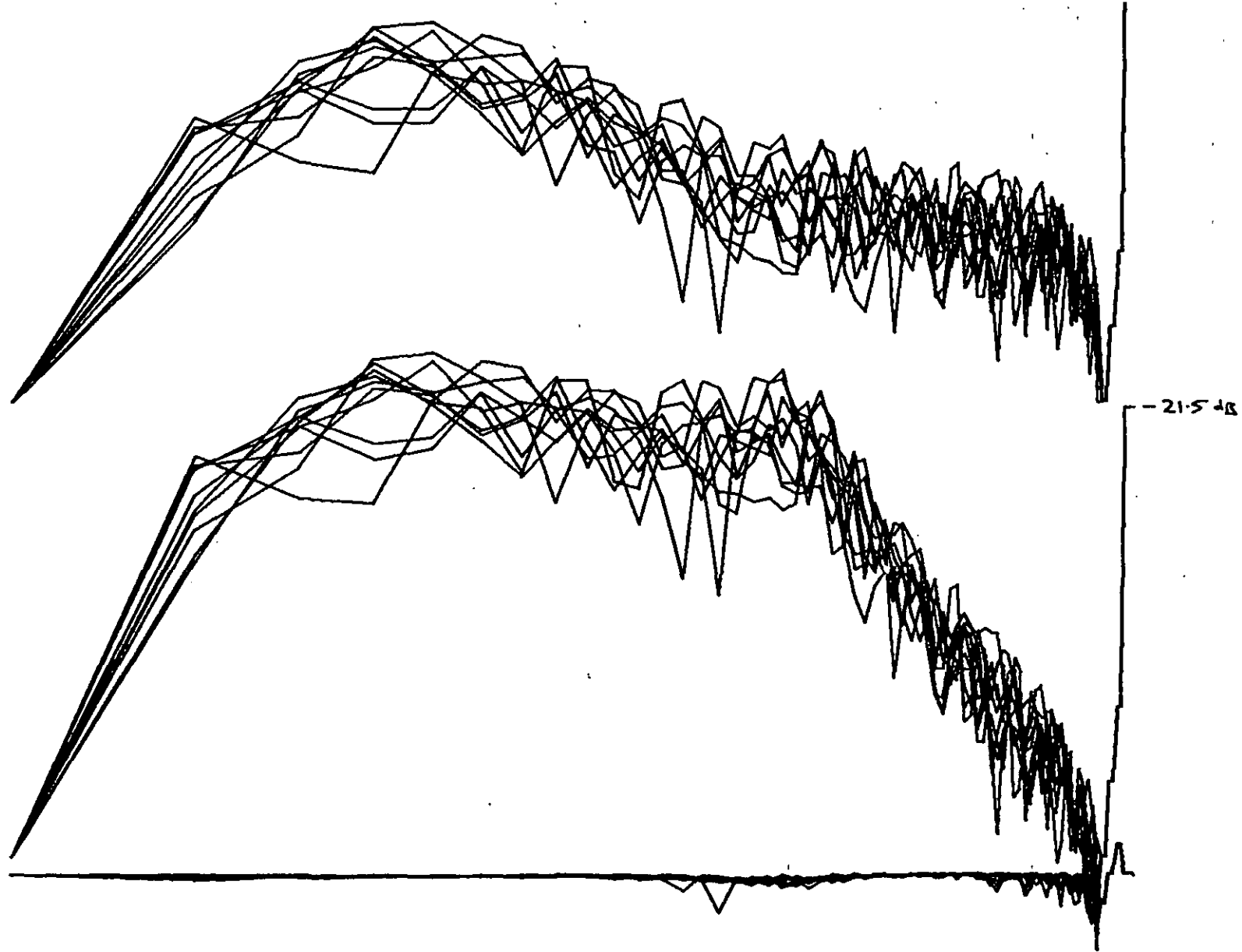


Fig. 5.11b

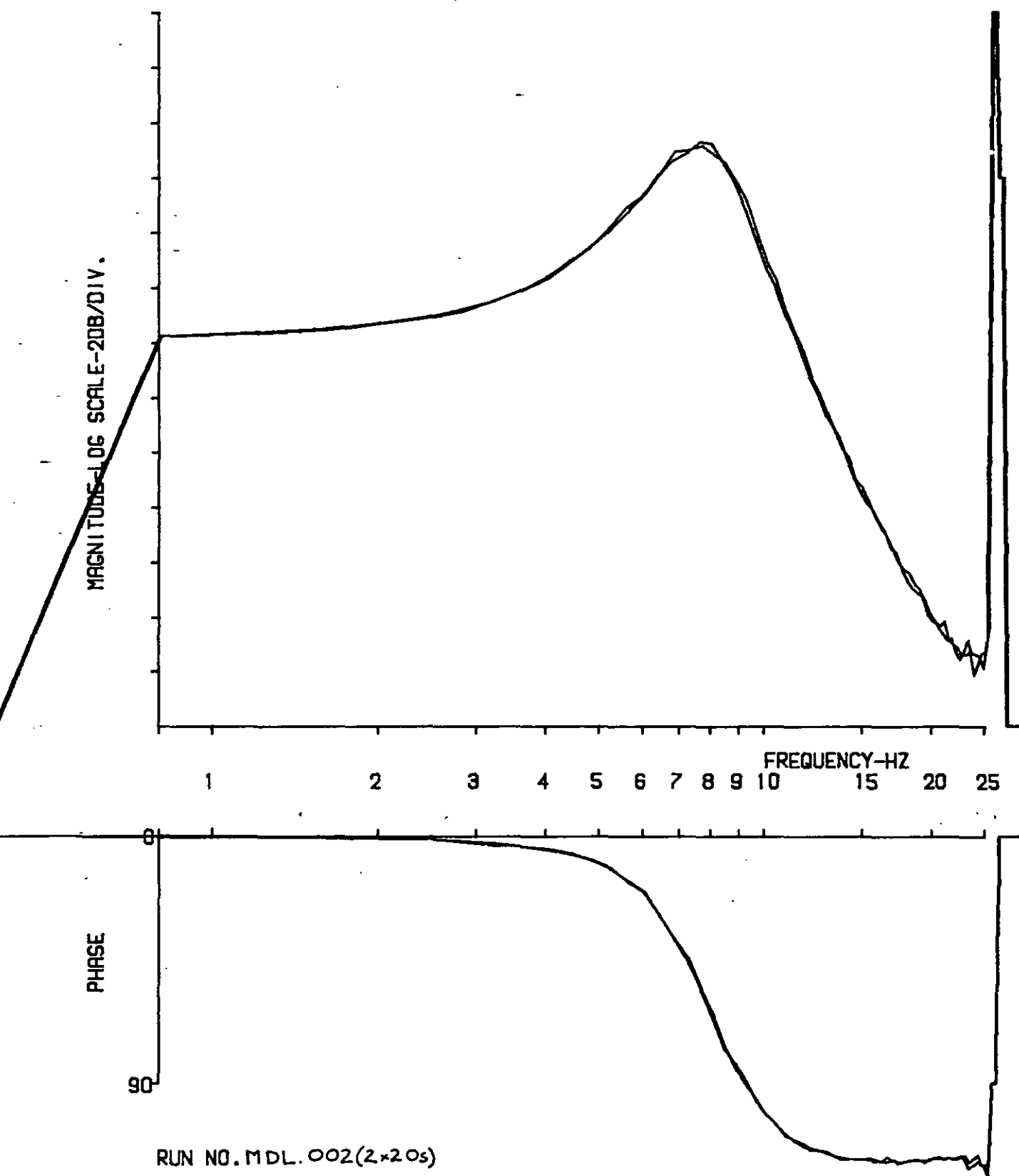


Fig. 5.12a Model response (2 plots, each 20 samples)

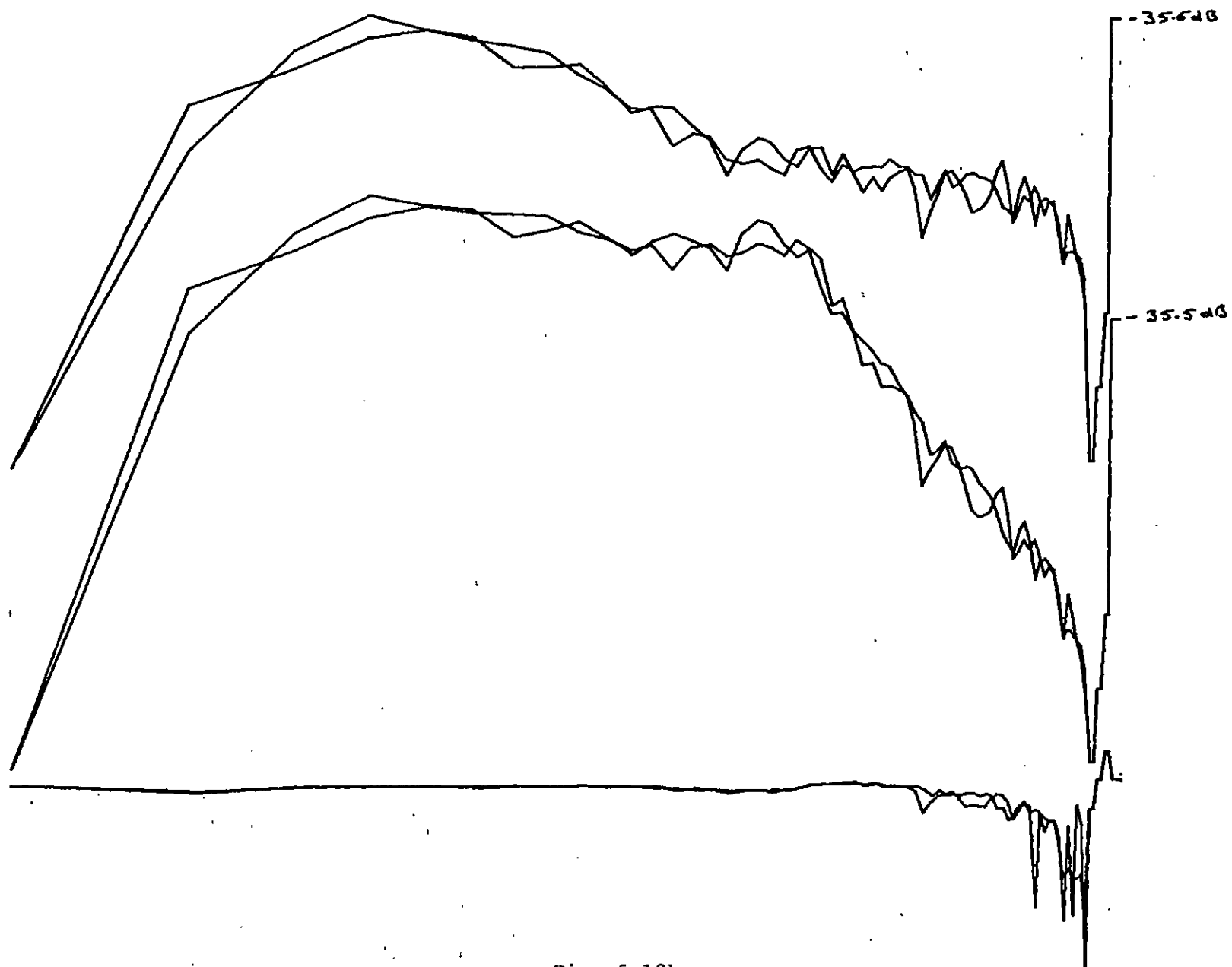


Fig. 5.12b

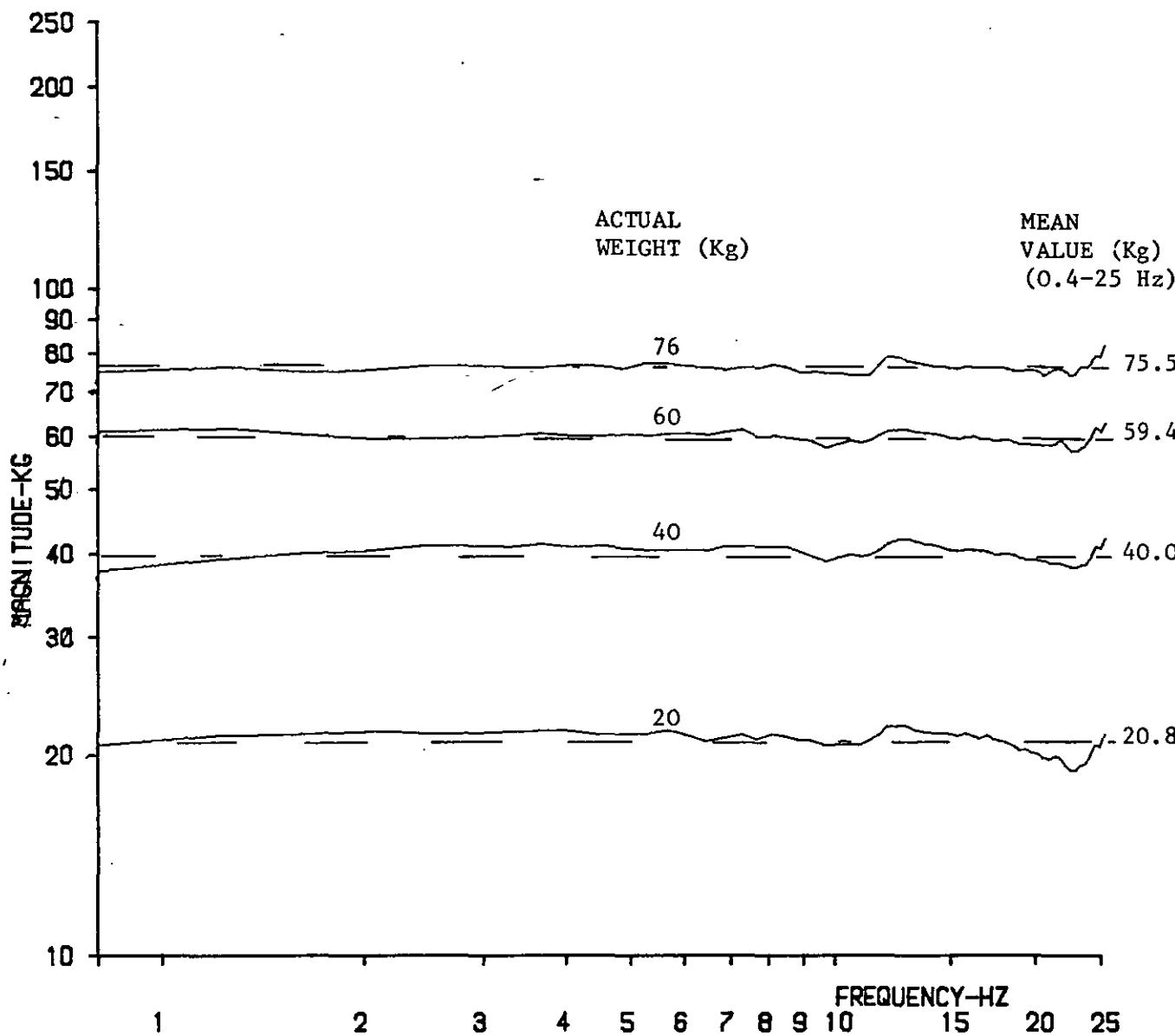
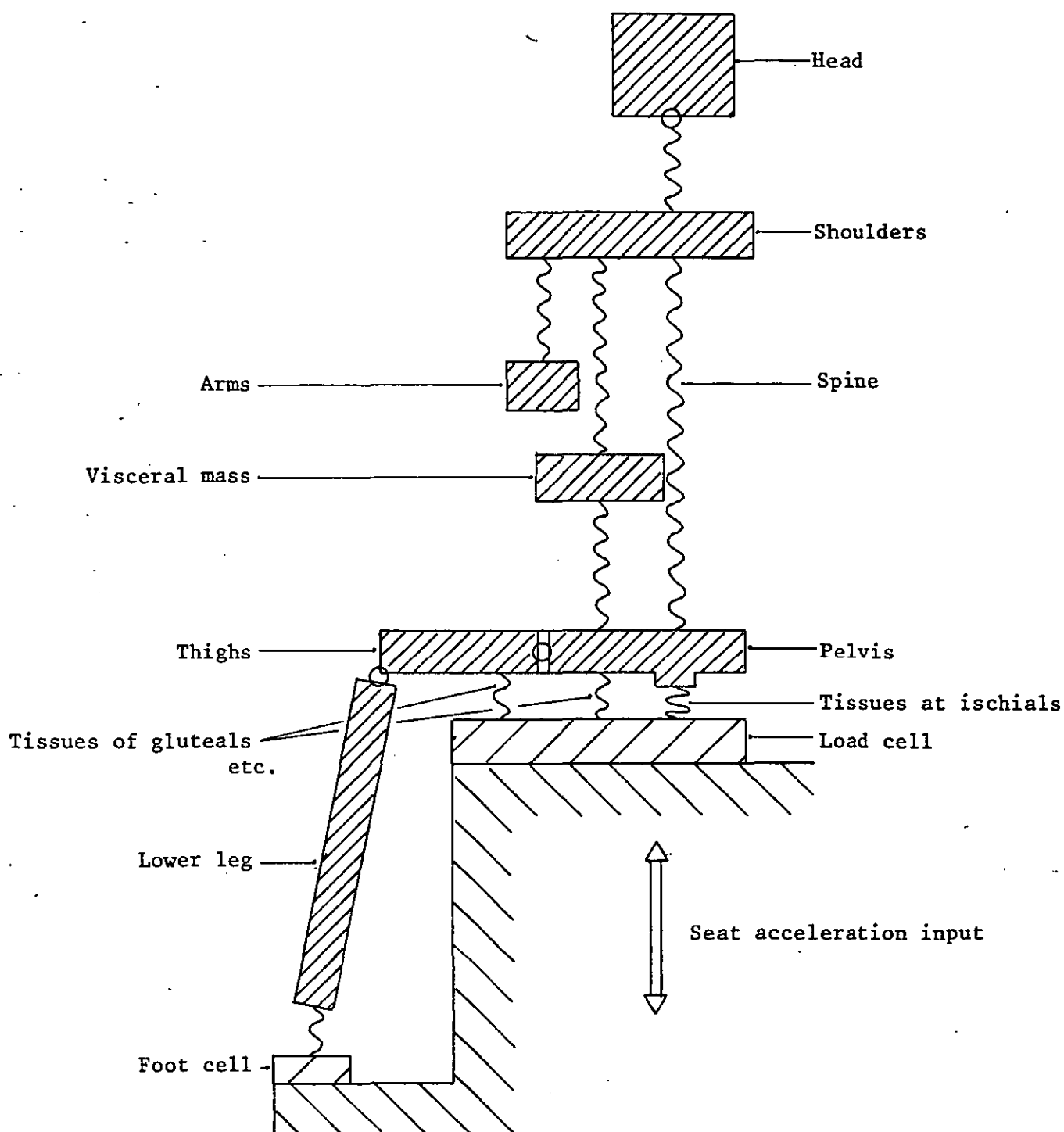


Fig. 5.13 Apparent mass of various weights (against 70 kg calibration)



Tissues considered rigid in the frequency range of interest



Tissues that may have resonance characteristics in the frequency range of interest.

Fig. 6.1 Conceptual model used to design experiments 1 to 4.

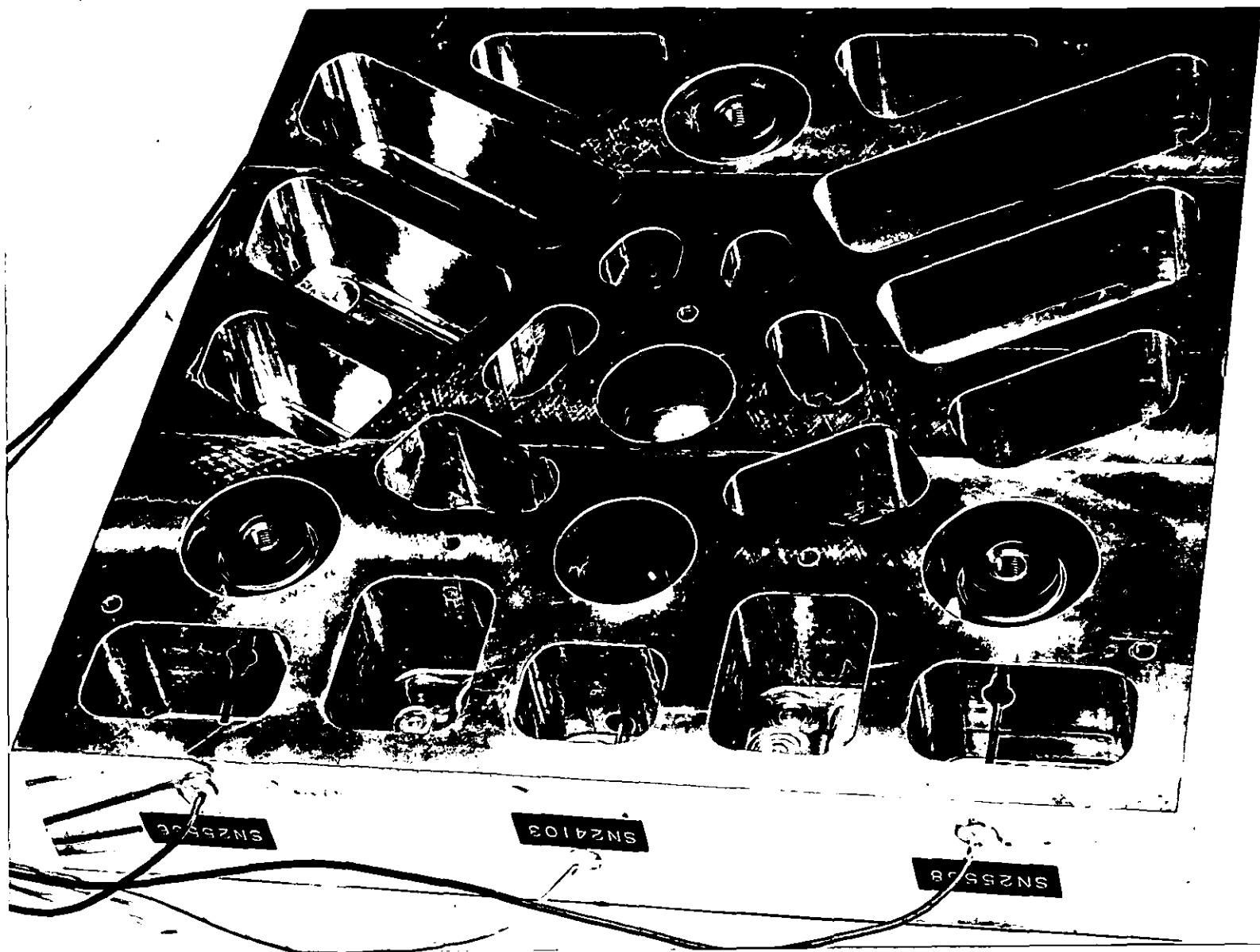


Fig. 6.2 Load cell - shown inverted with base-plate removed.

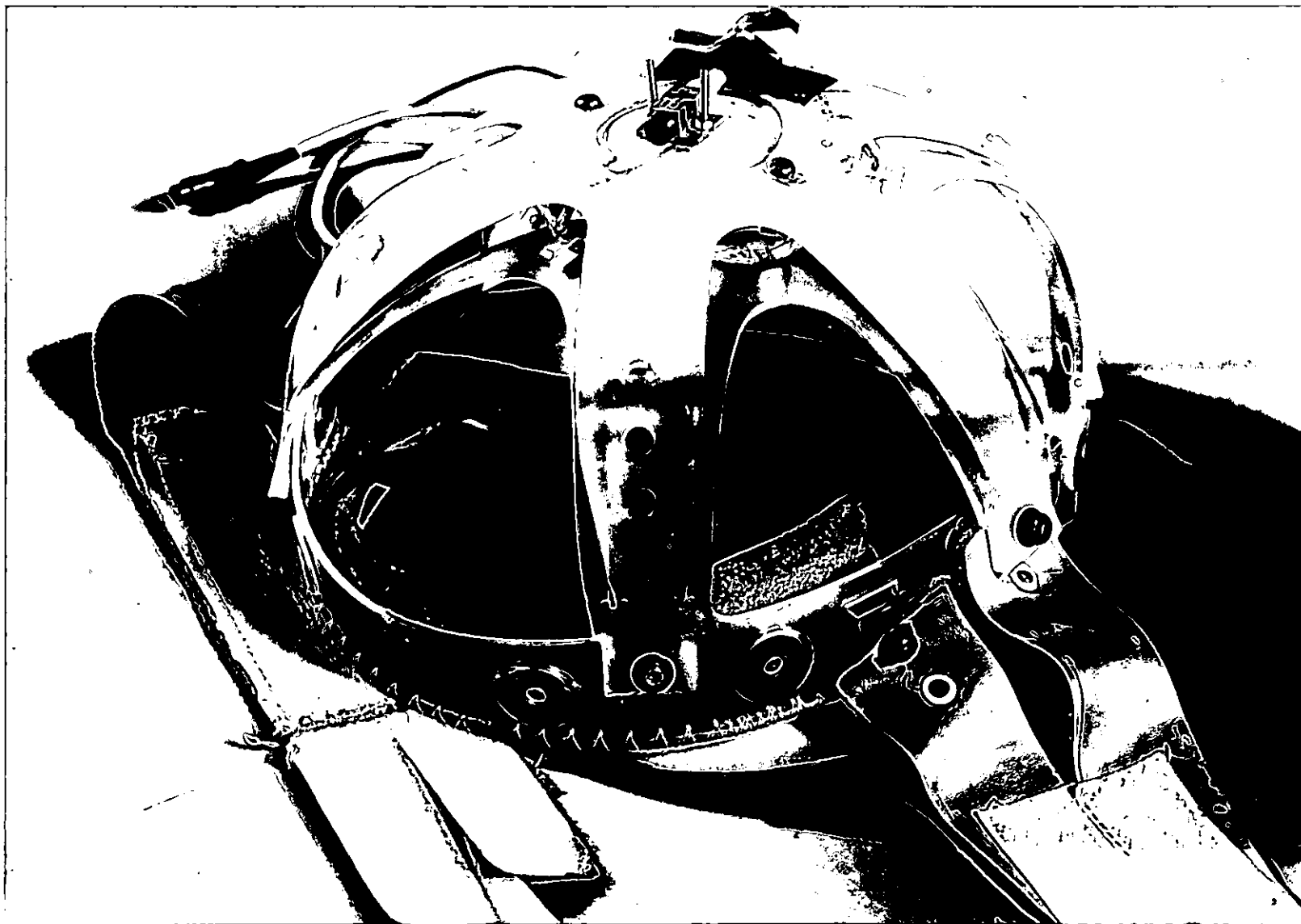


Fig. 6.3 Accelerometer head harness.

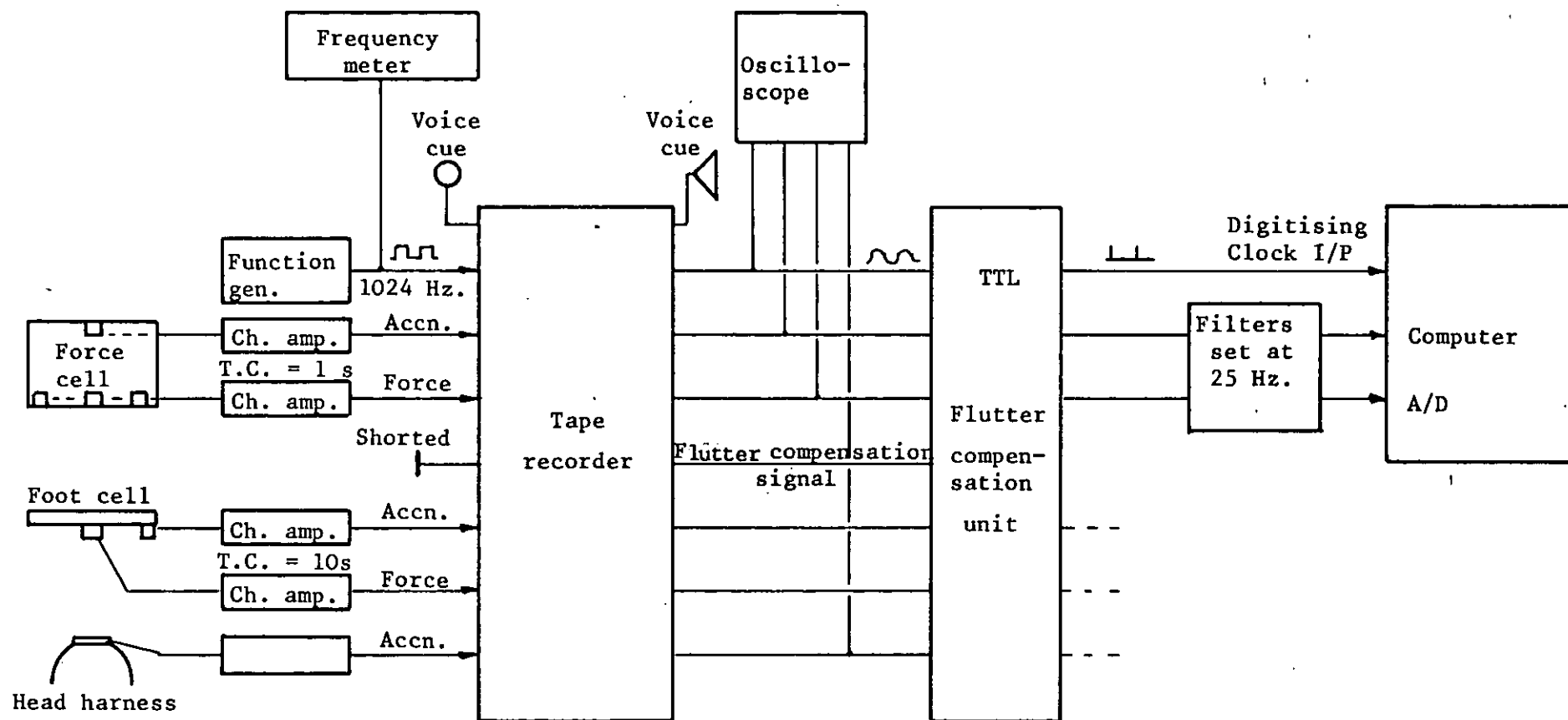


Fig. 6.4 Record and replay systems

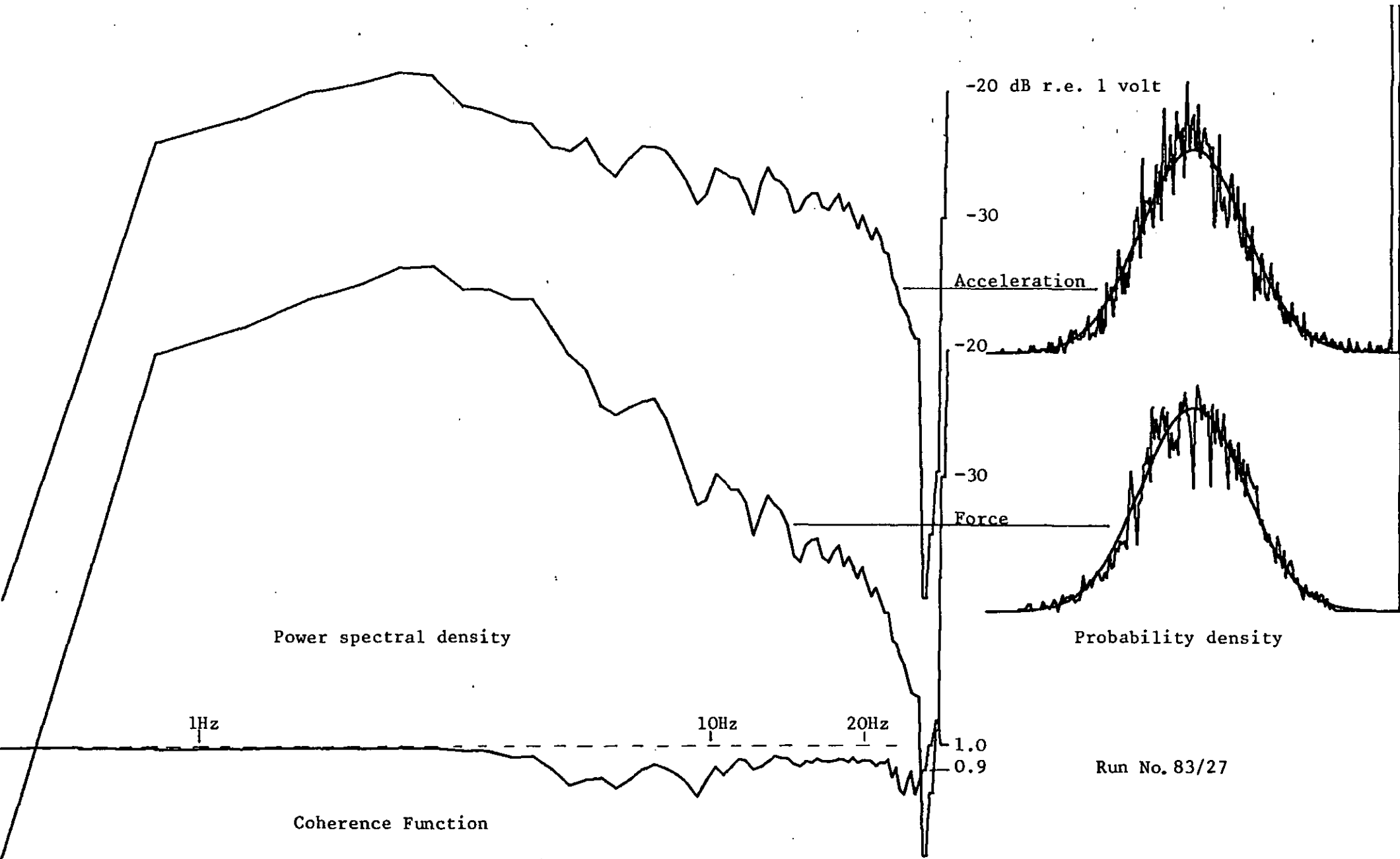
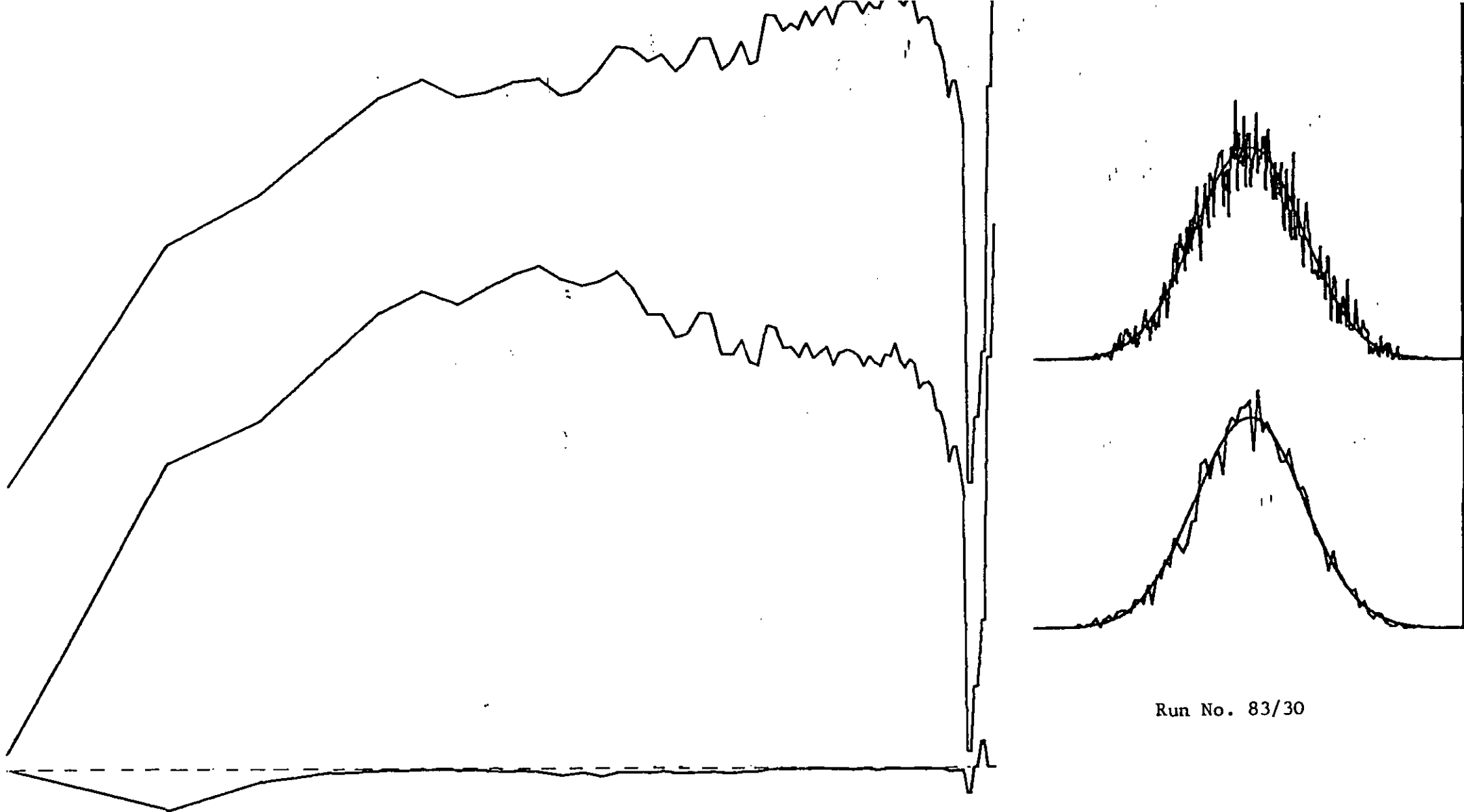


Fig. 7.1 Typical validation curves



Run No. 83/30

Fig. 7.2 Improvement in coherence function with spectral shaping of input

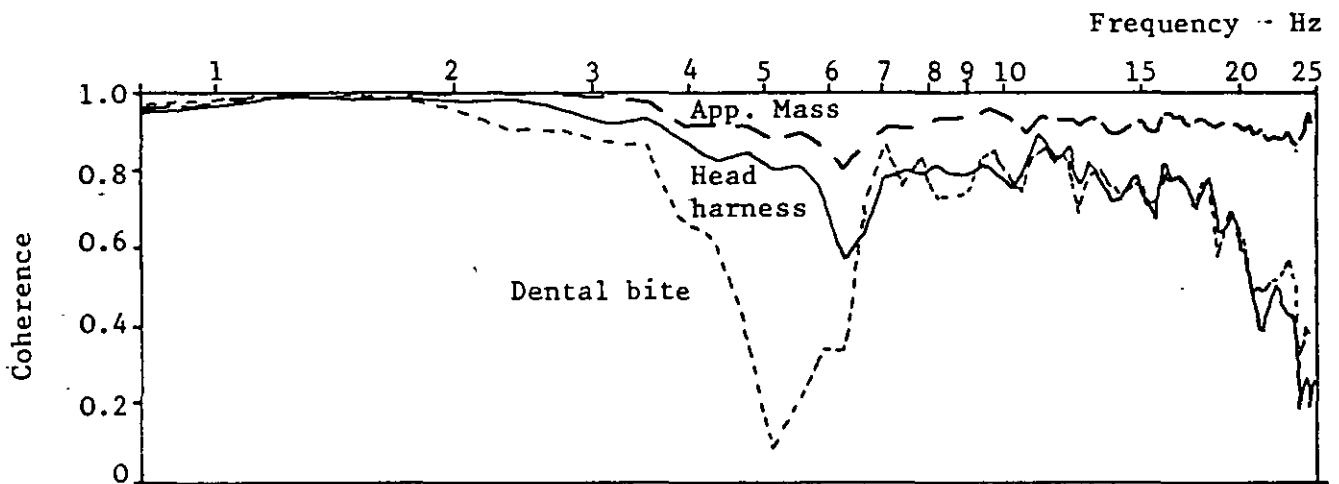
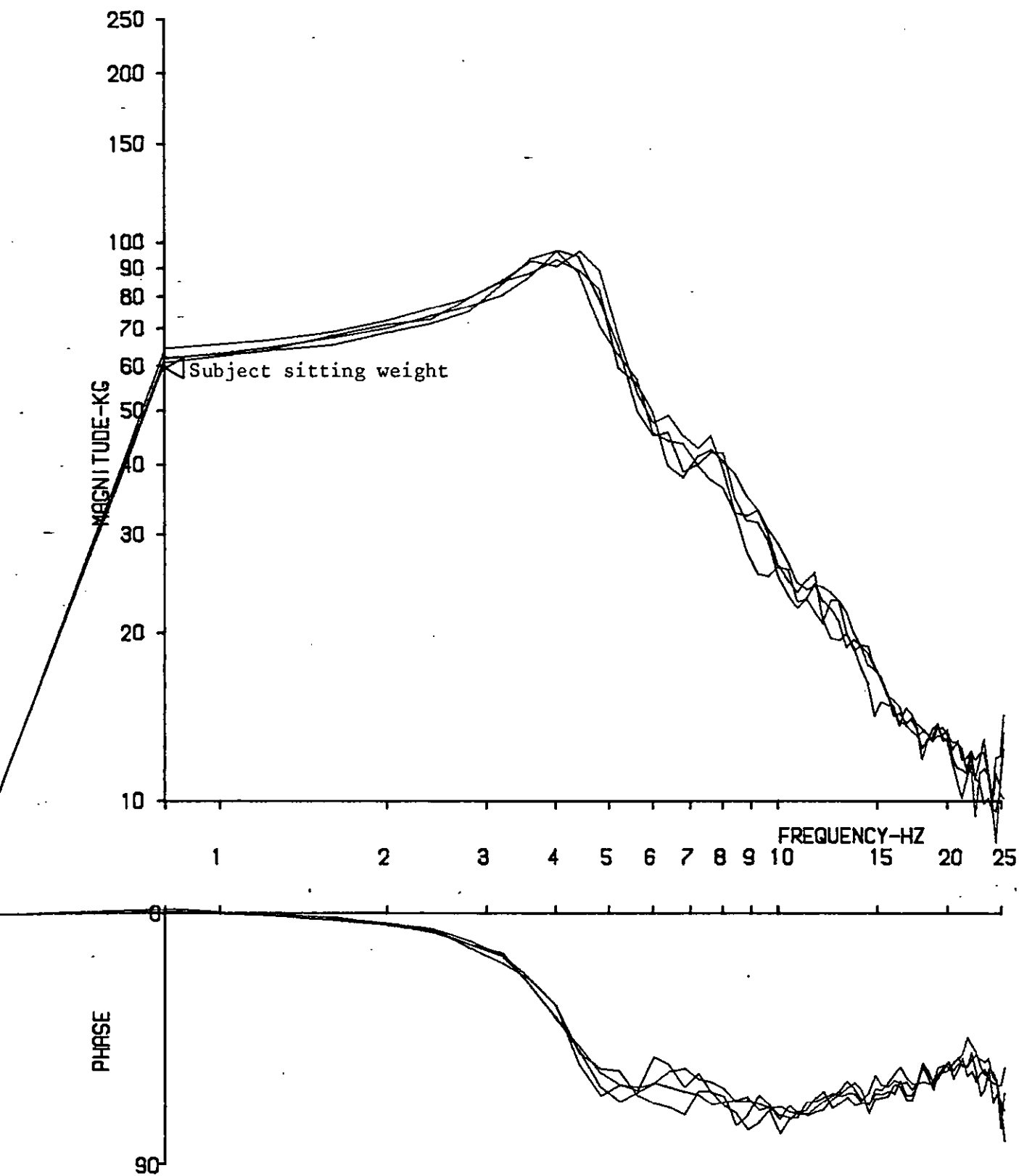


Fig. 7.3 Comparison of coherence functions for apparent mass and transmission to head harness and to dental bite.

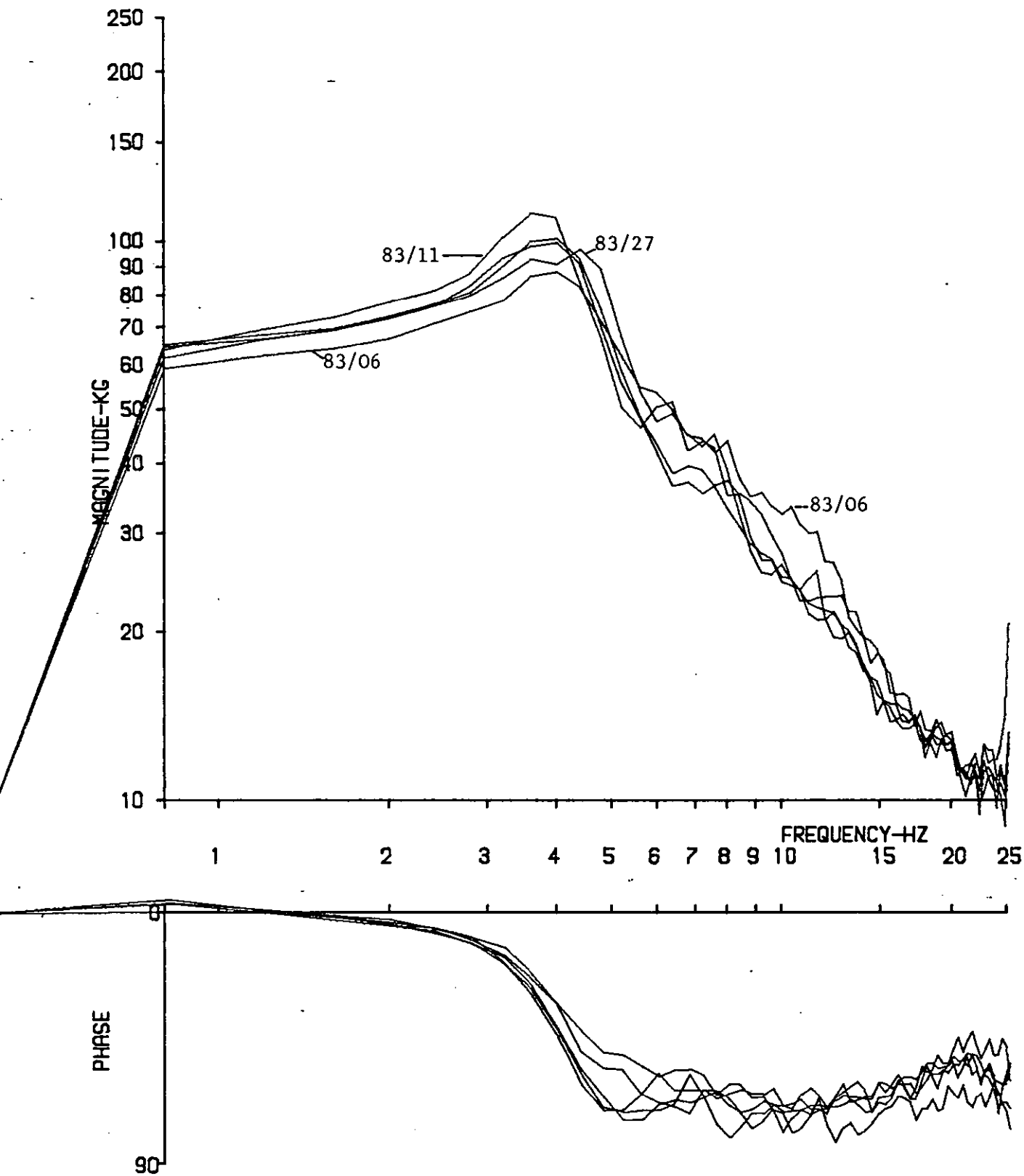
Run No. 83/07



RUN NO. 83/27

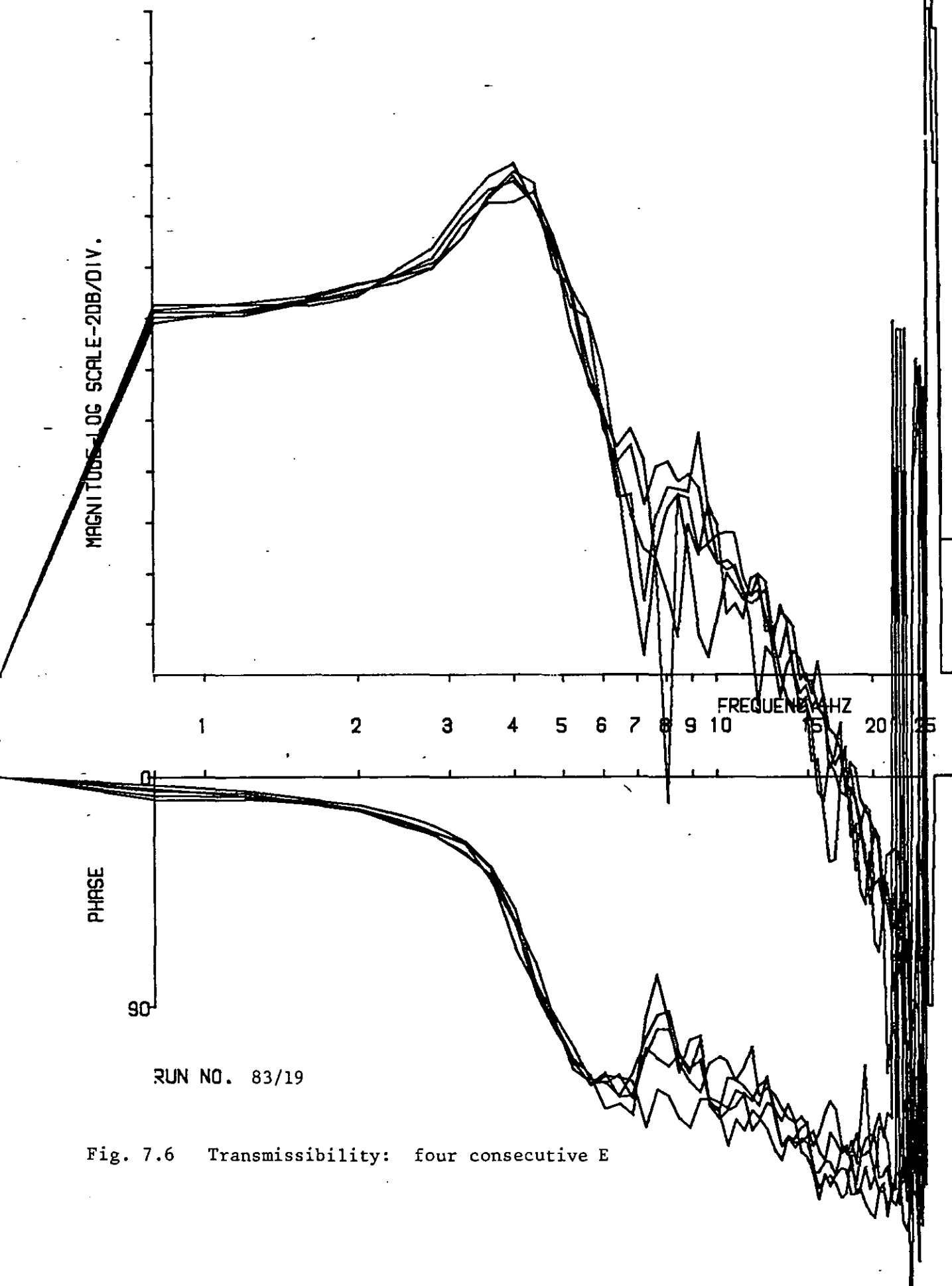
Fig. 7.4 Four consecutive measures E

Apparent Mass:



RUN NO. 83/06, 11, 19, 23, 27

Fig. 7.5 Apparent Mass. Five runs spread over 3 hrs. E



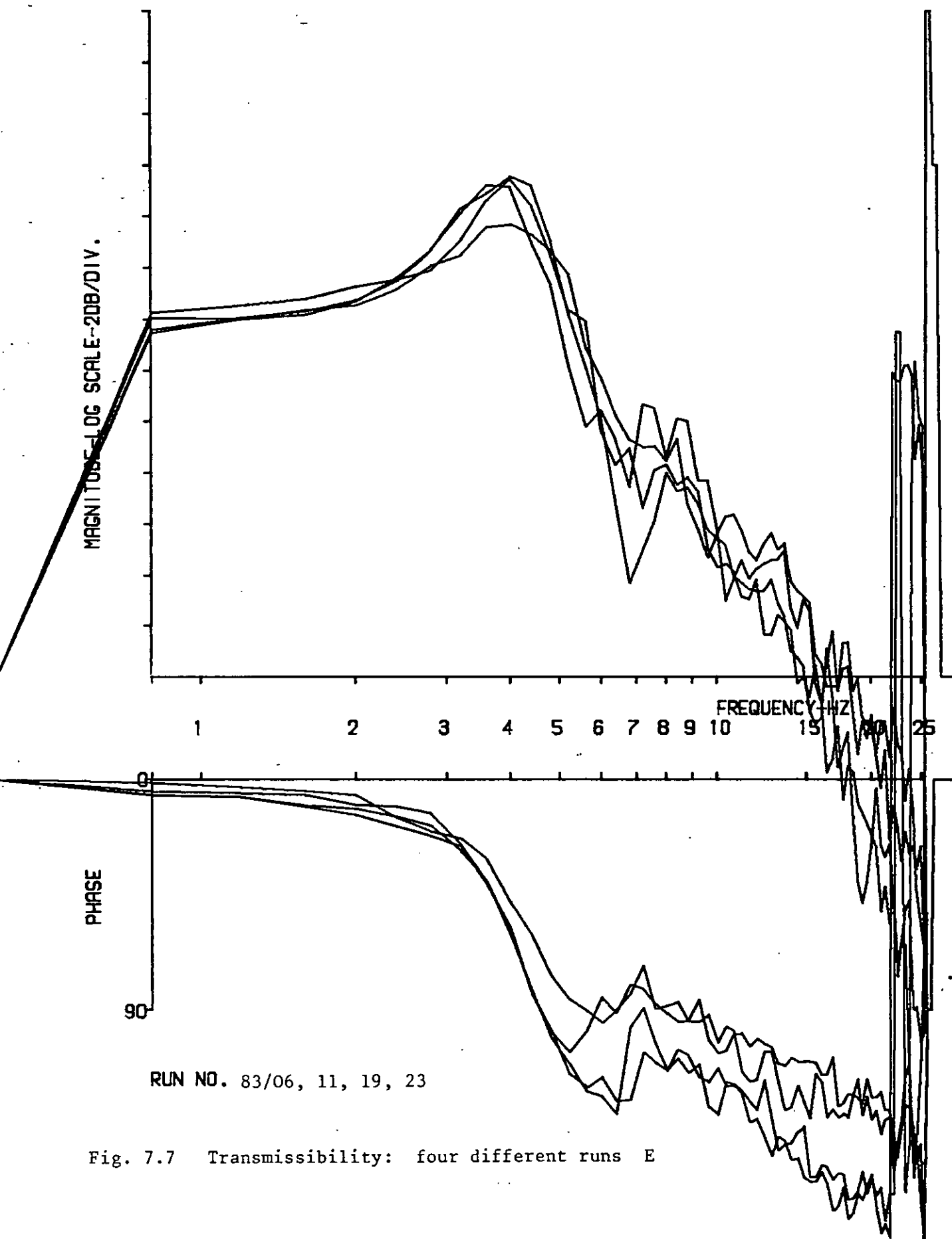


Fig. 7.7 Transmissibility: four different runs E

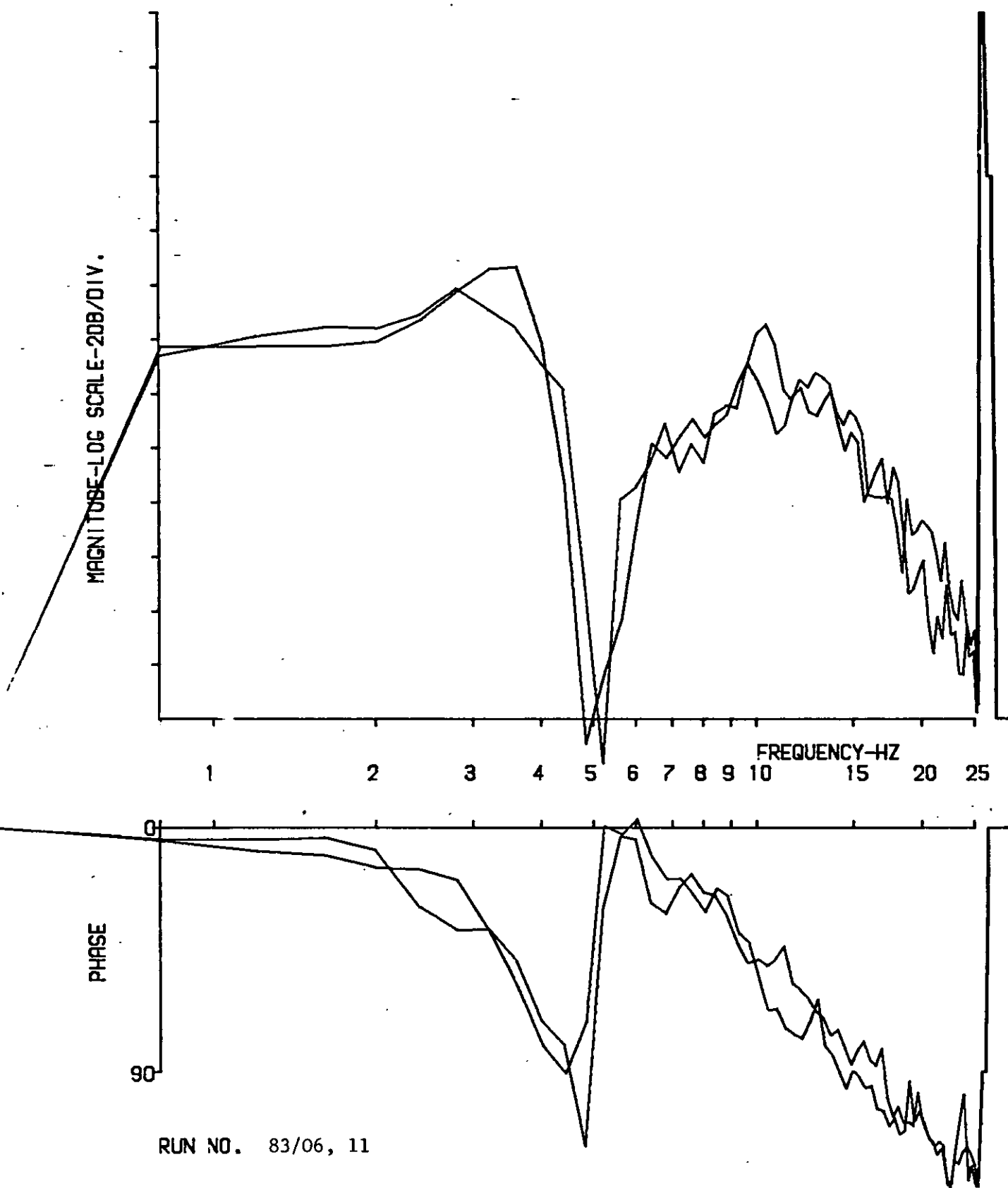
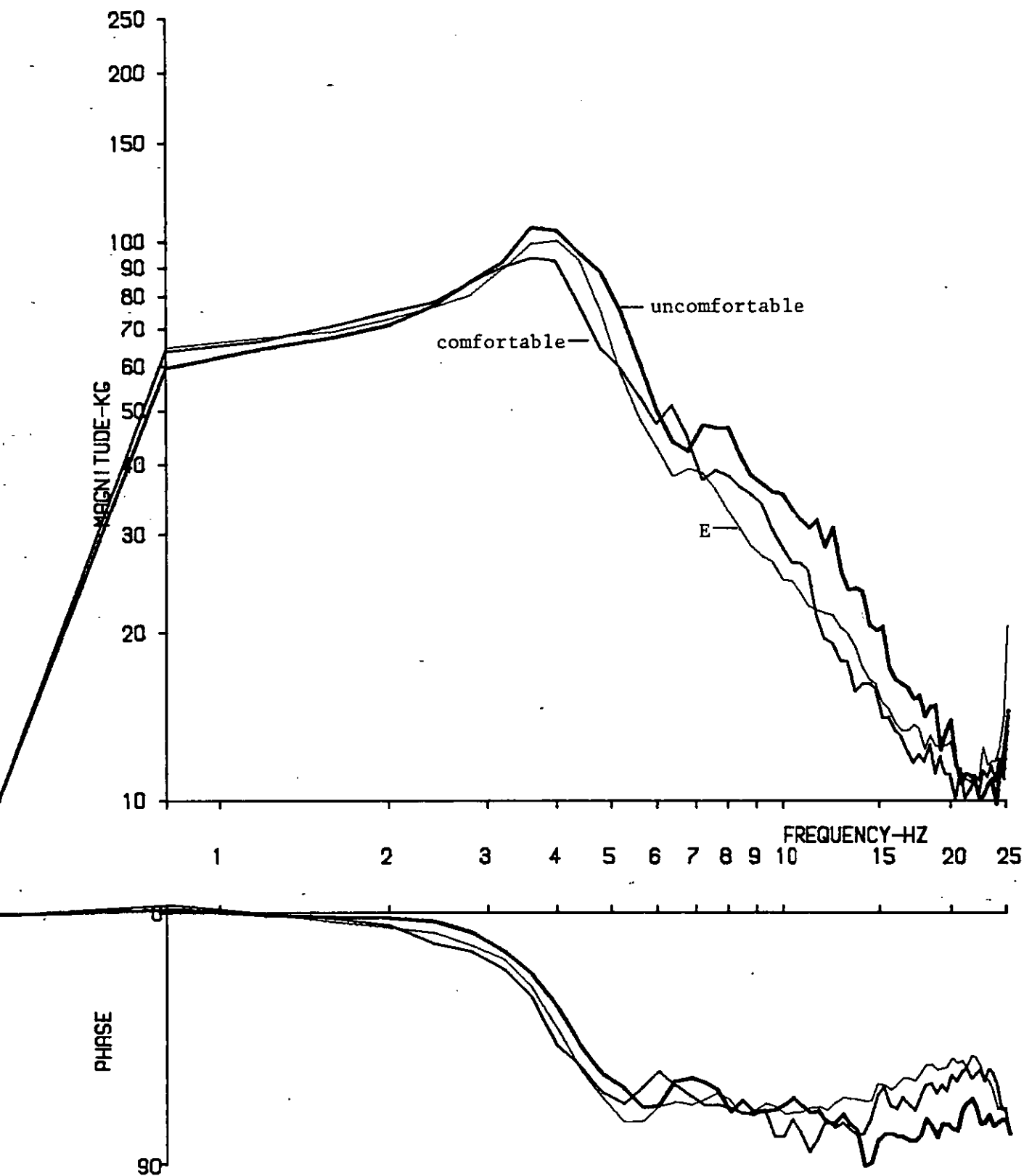


Fig. 7.8 Transmission to bite: 2 runs E



RUN NO. 83/19, 07, 08

Fig. 7.9 Apparent mass: E/most uncomfortable/most comfortable

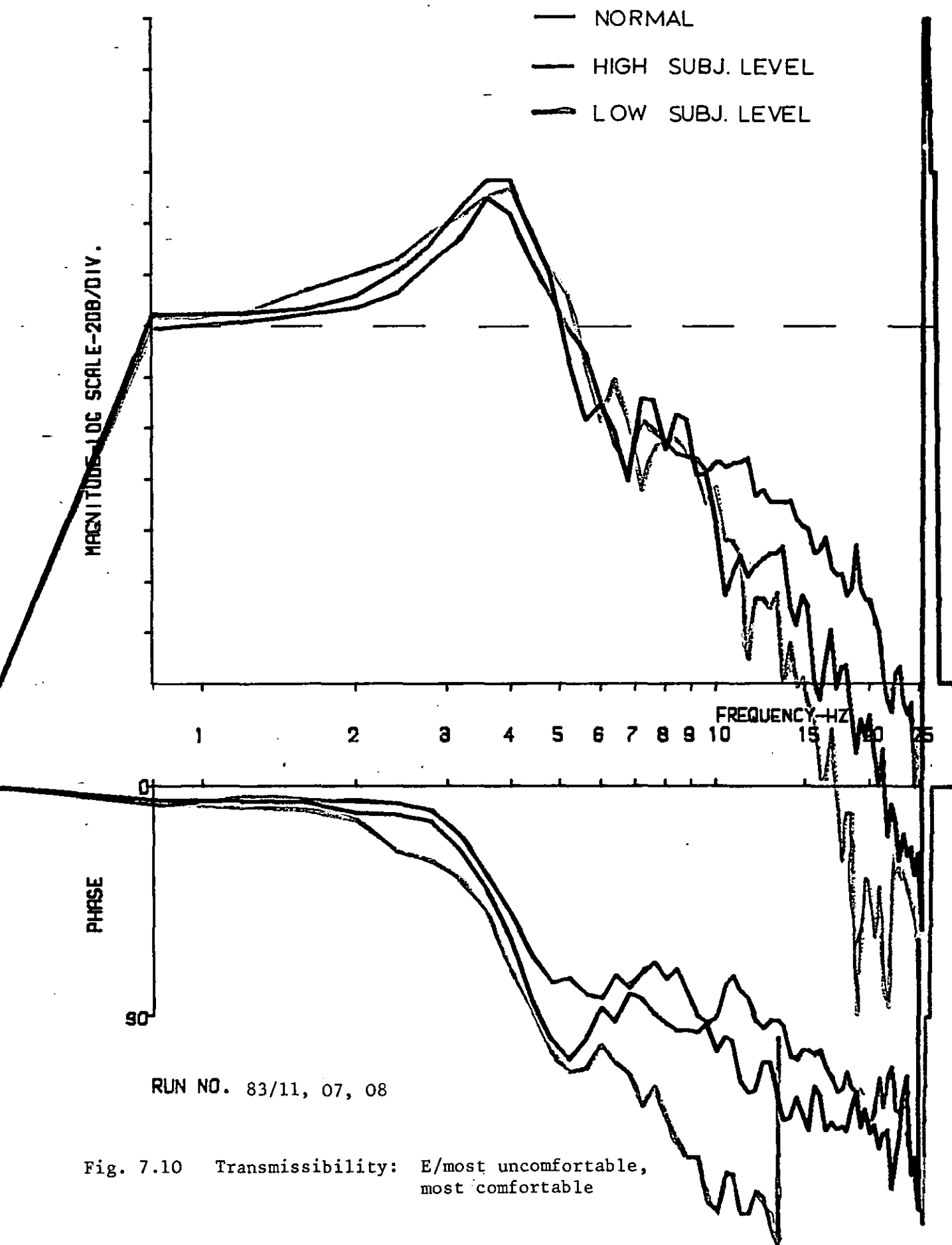
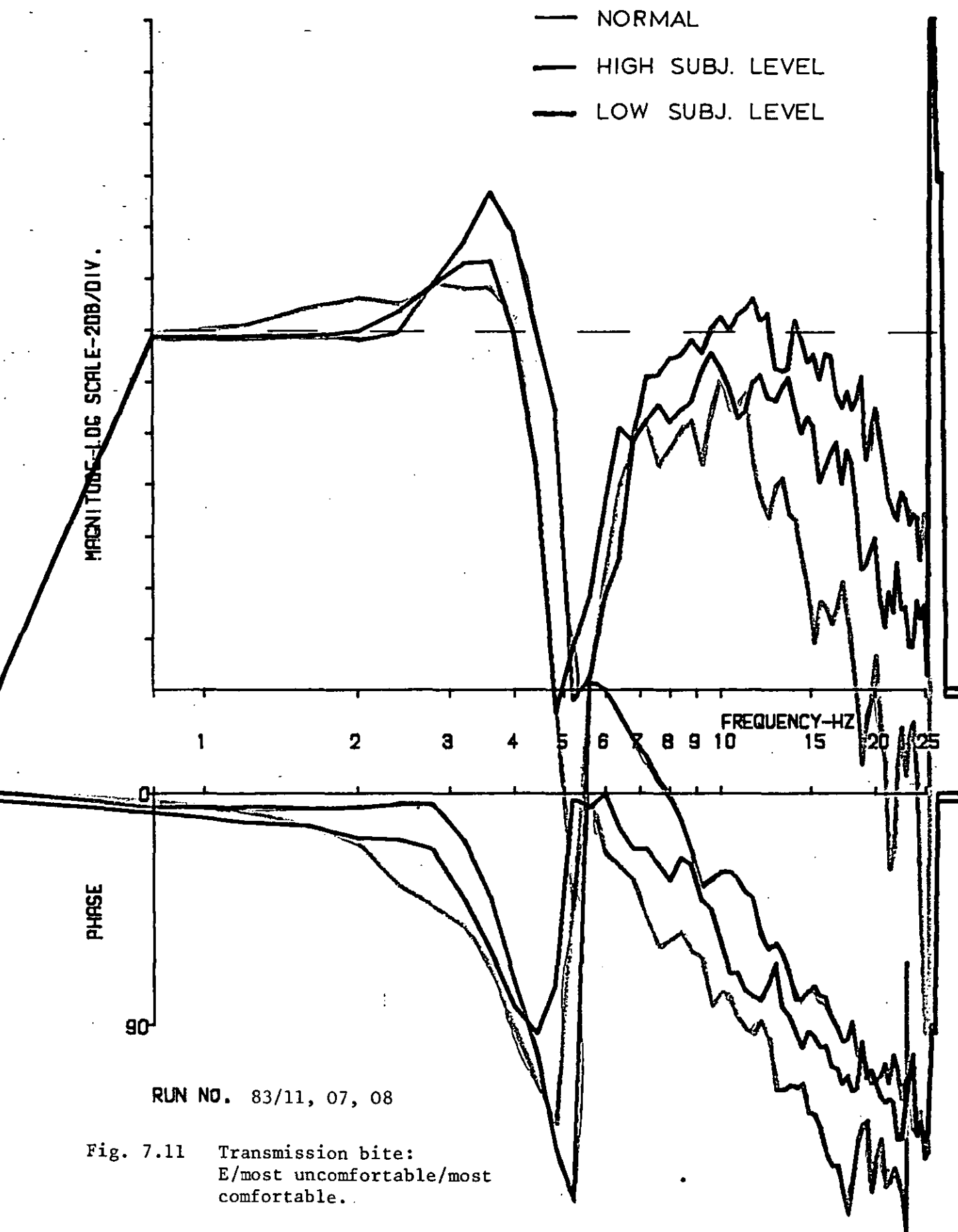
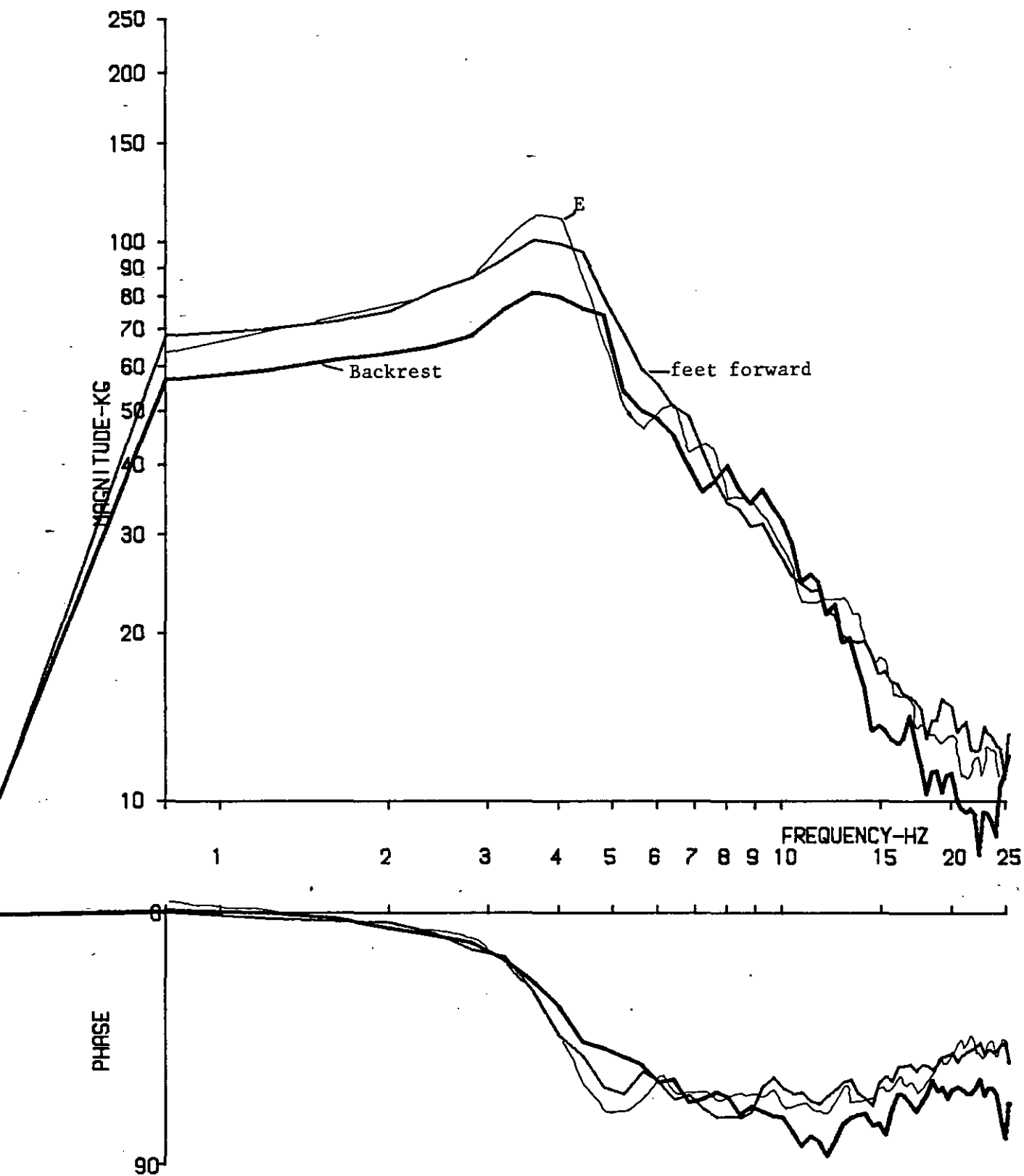


Fig. 7.10 Transmissibility: E/most uncomfortable,
most comfortable





RUN NO. 83/09, 10, 11

Fig. 7.12 Apparent mass: Backrest, feet forward, E

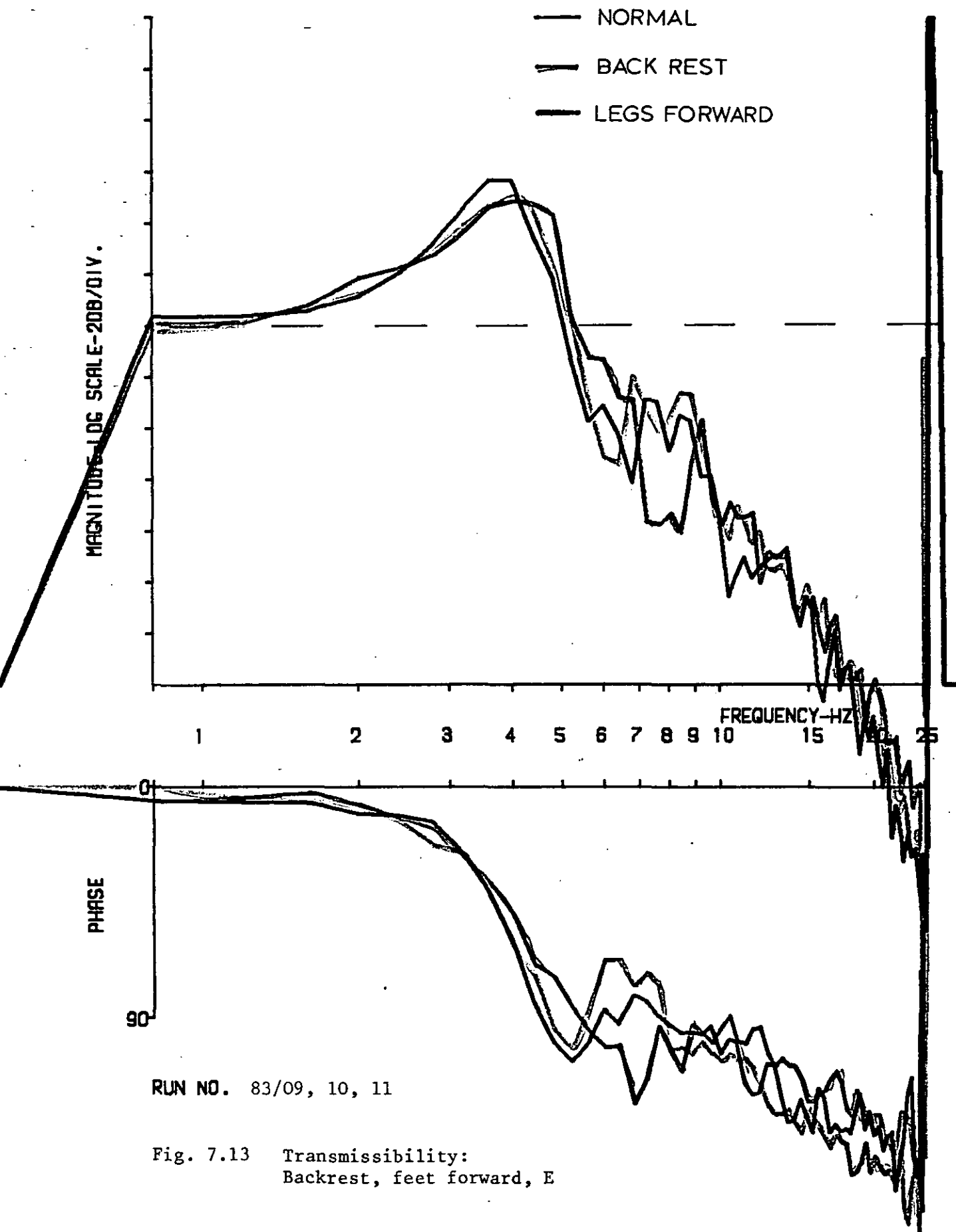


Fig. 7.13 Transmissibility:
Backrest, feet forward, E

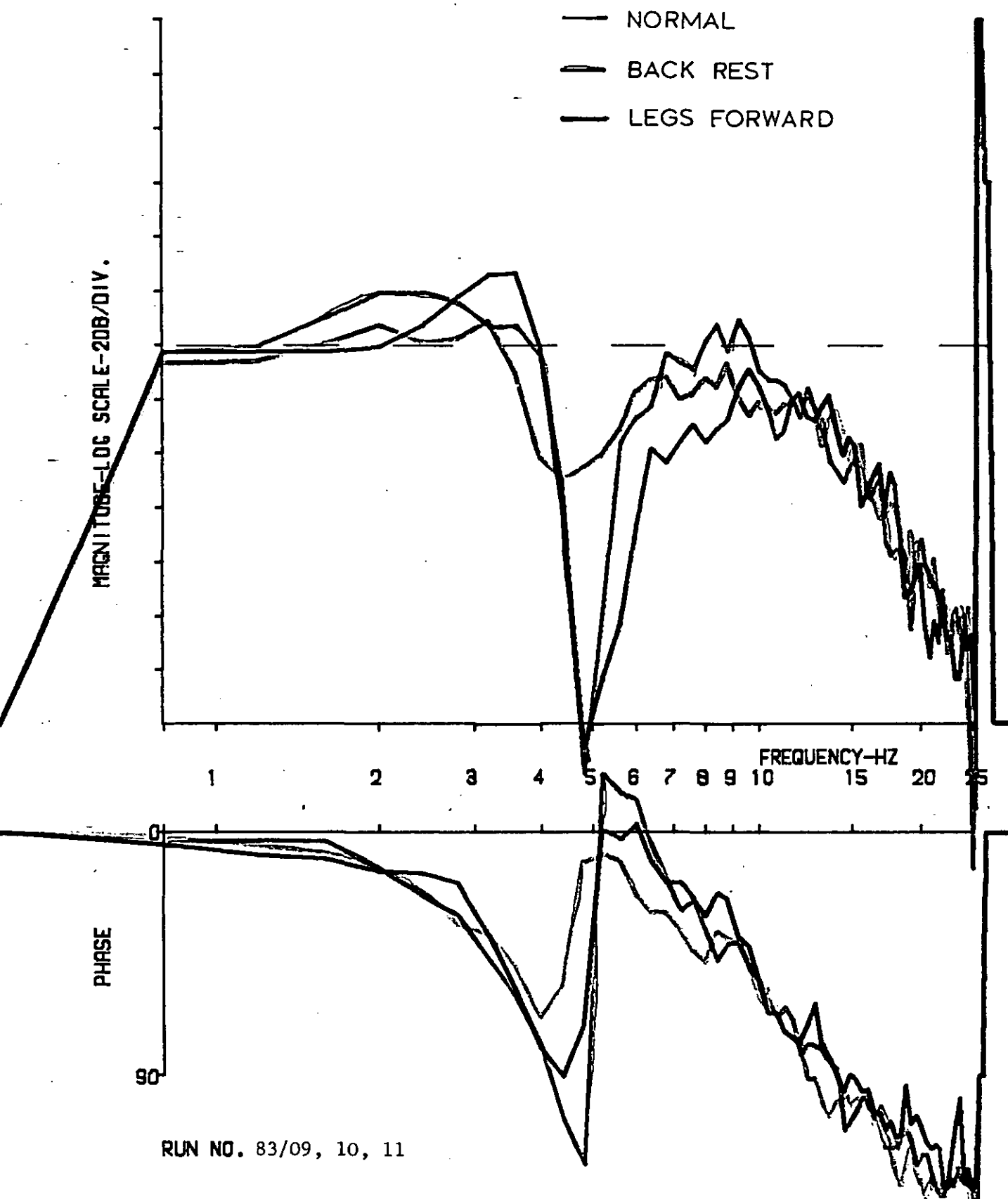
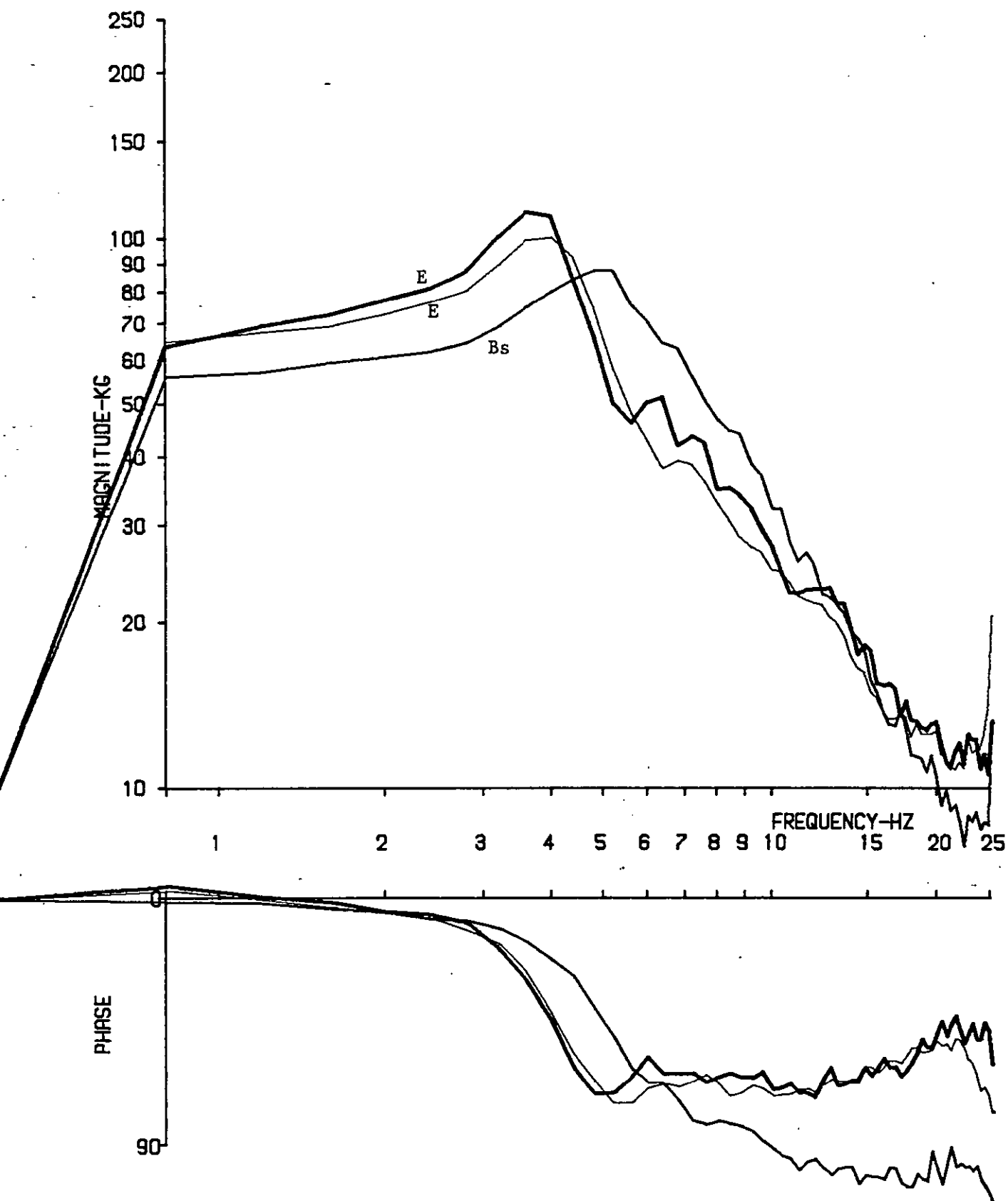
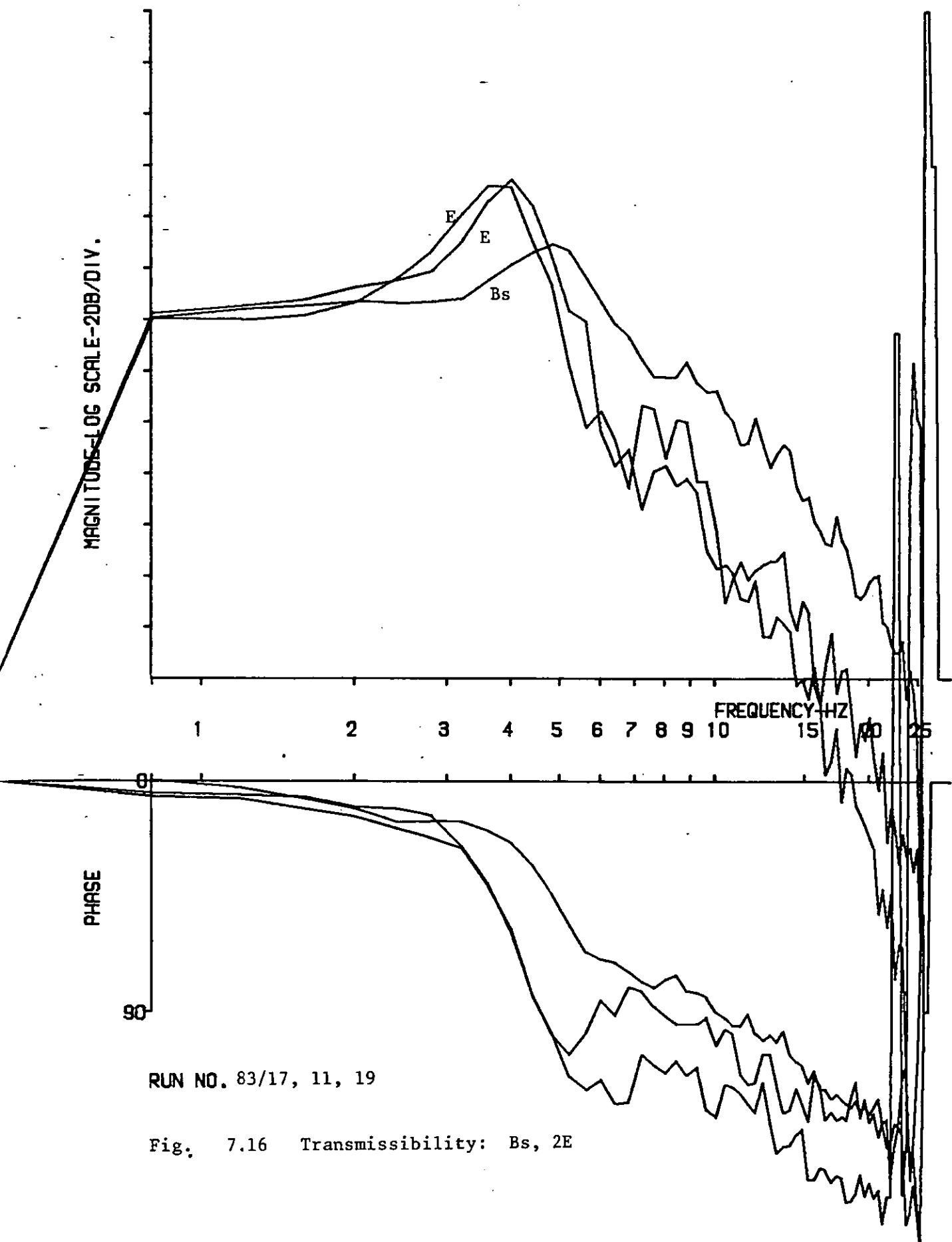


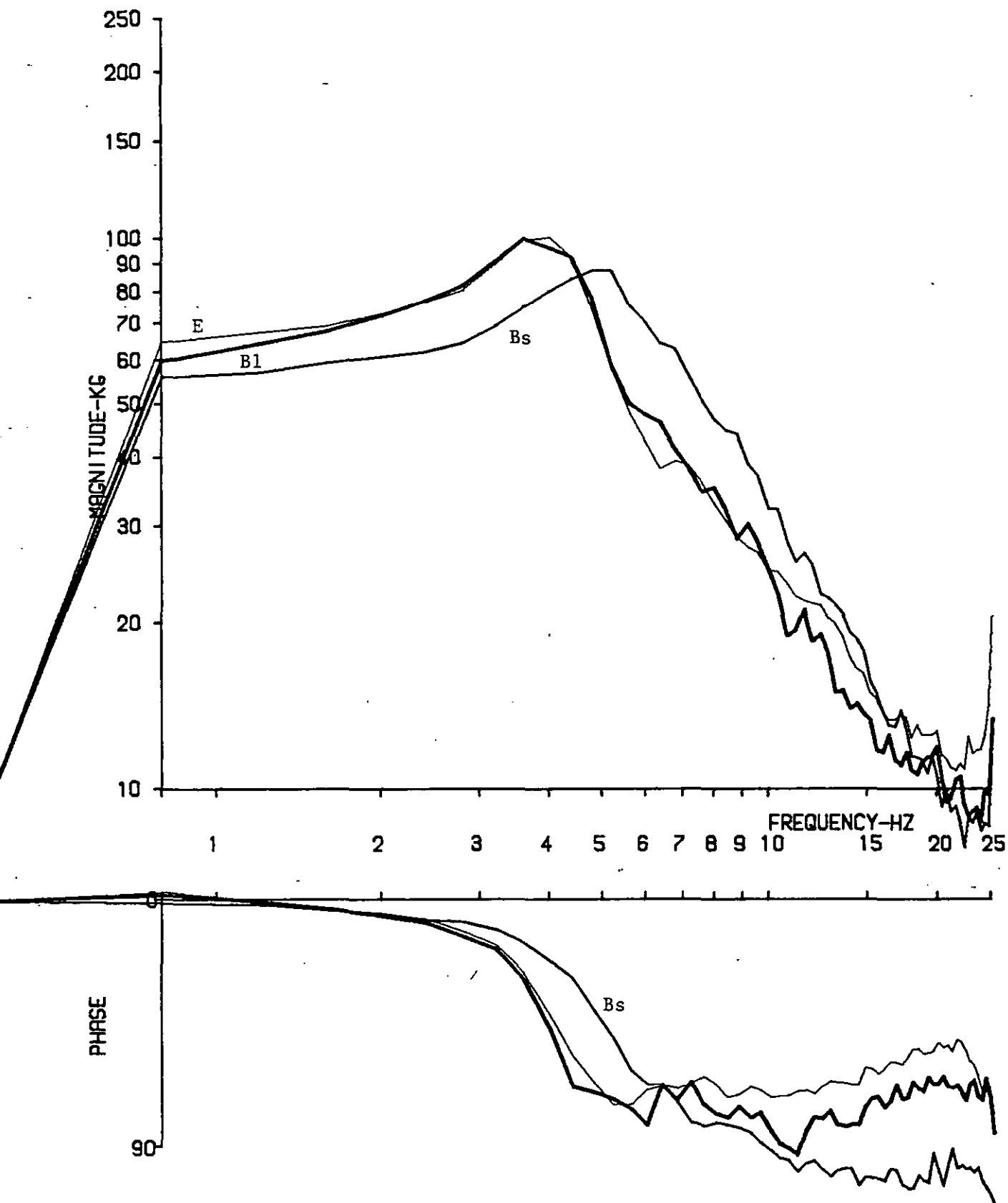
Fig. 7.14 Transmission bite: Backrest, feet forward, E



RUN NO. 83/12, 11, 19

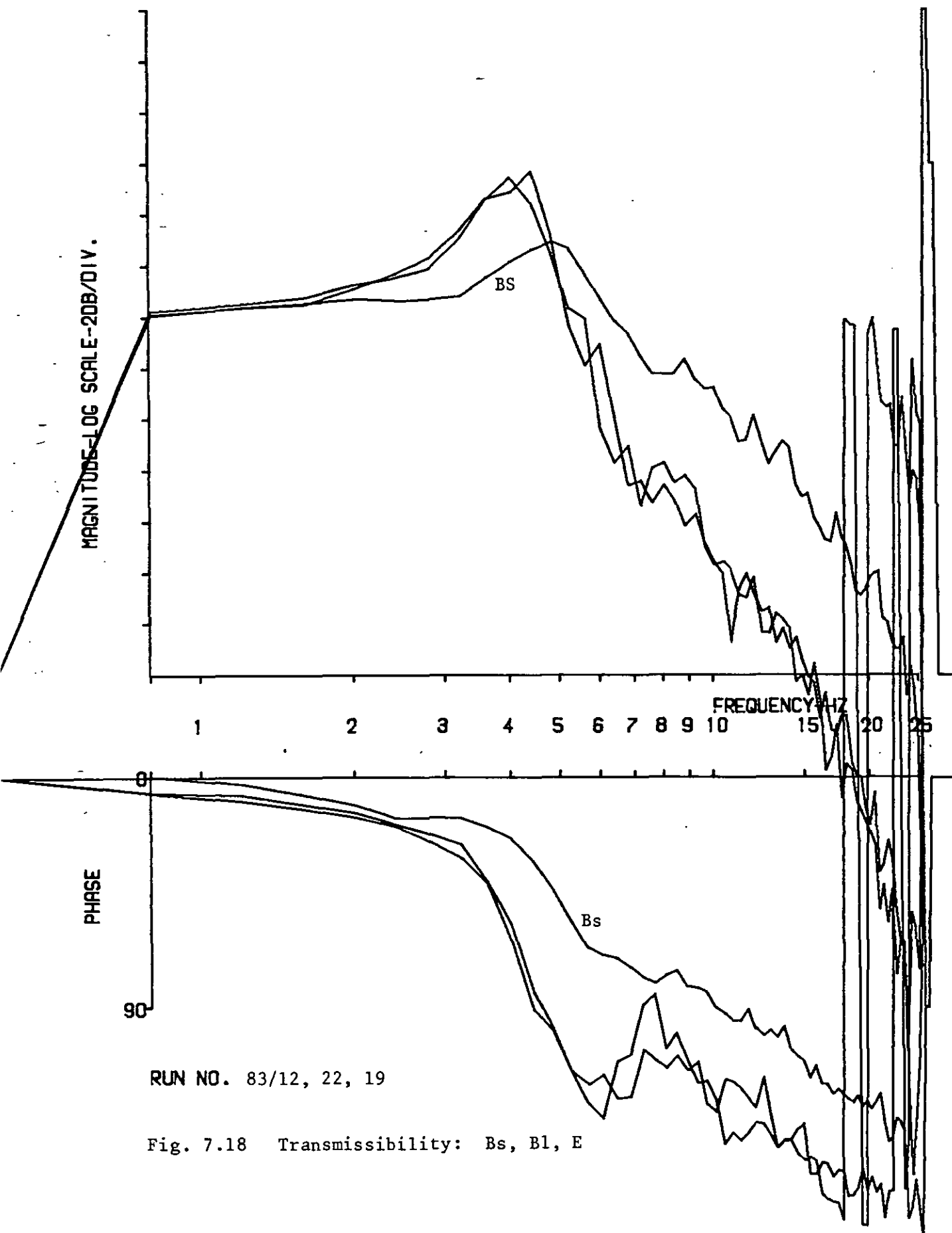
Fig. 7.15 Apparent mass: Bs, 2E

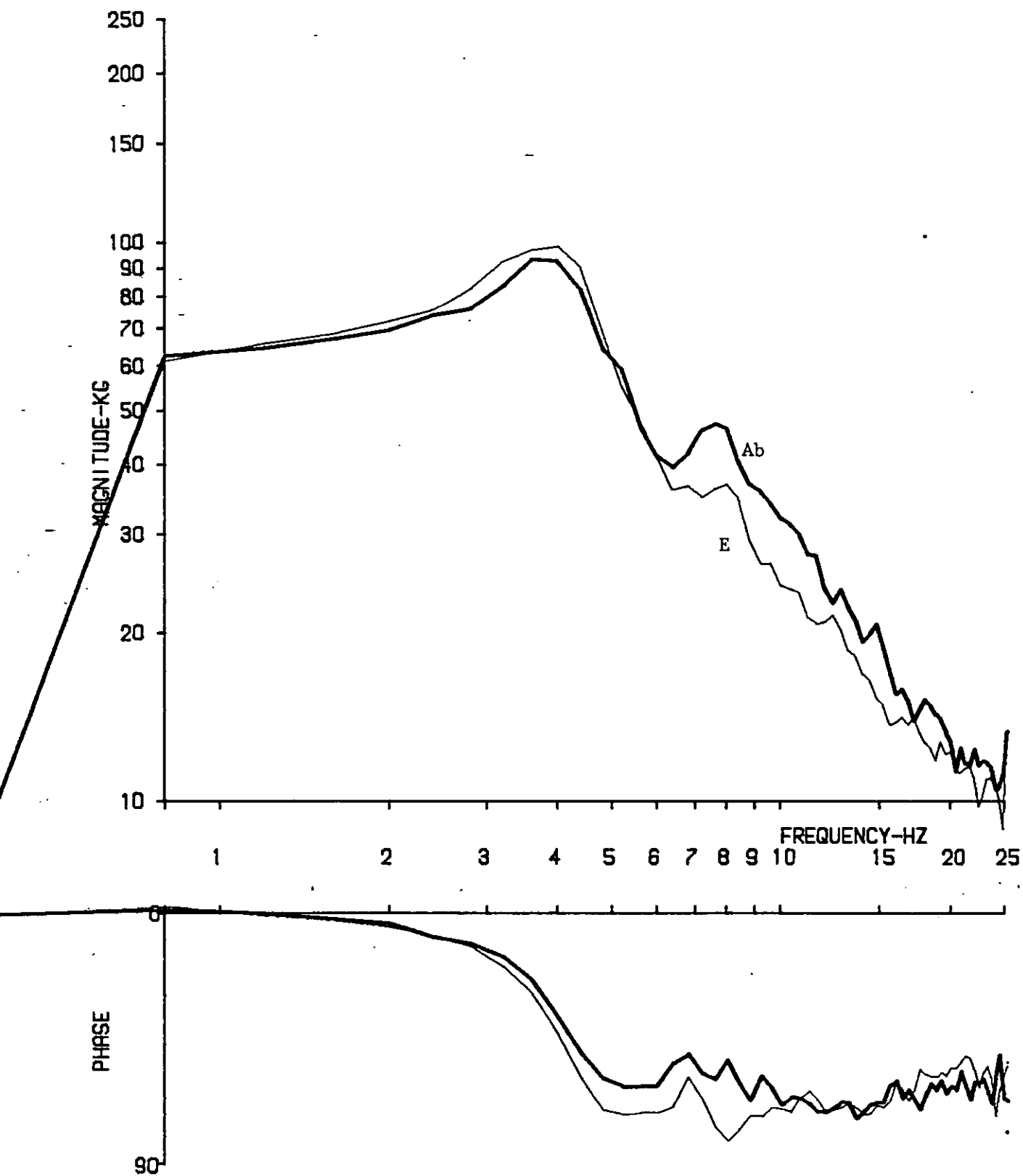




RUN NO. 83/12, 22, 19

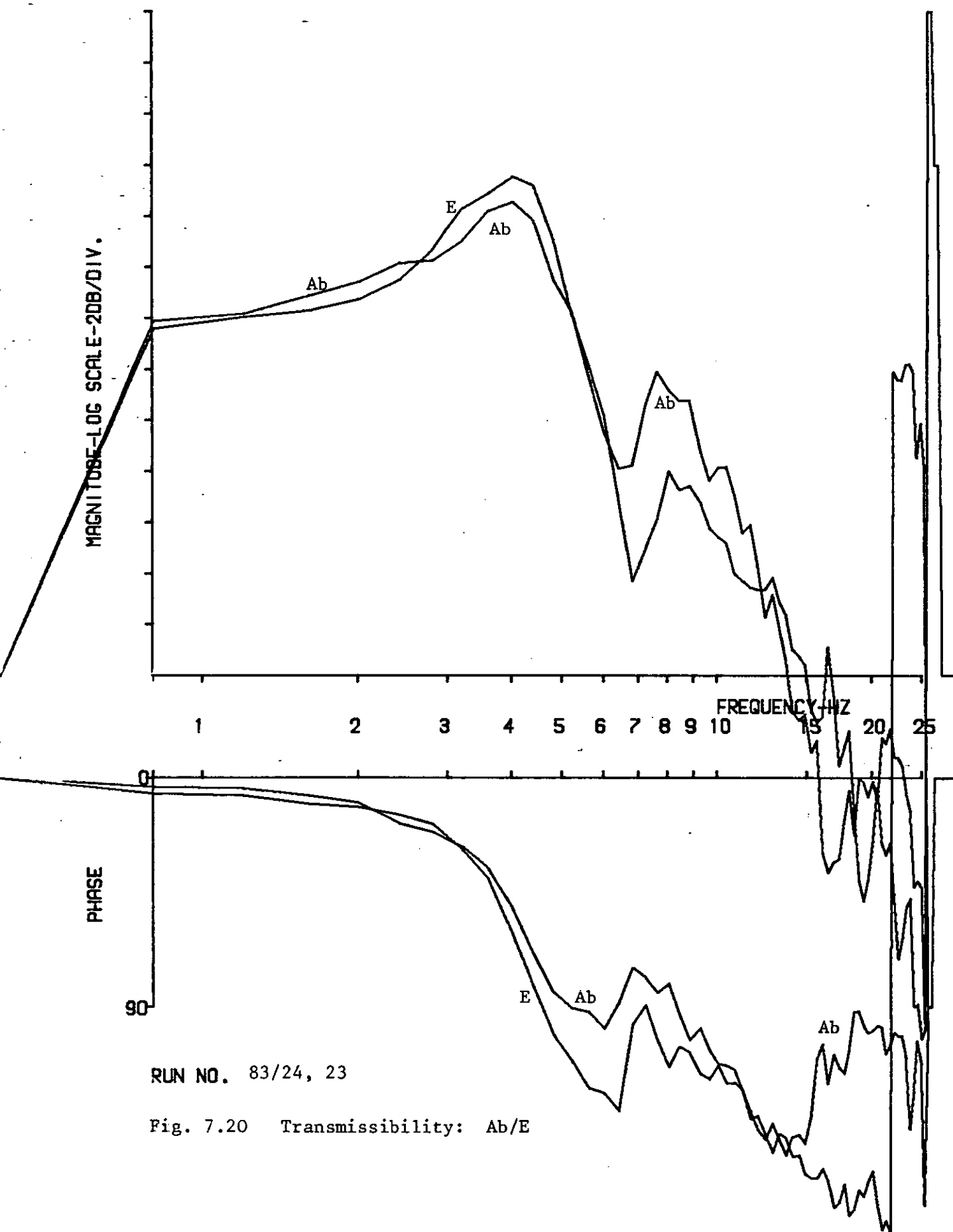
Fig. 7.17 Apparent mass: Bs, B1, E

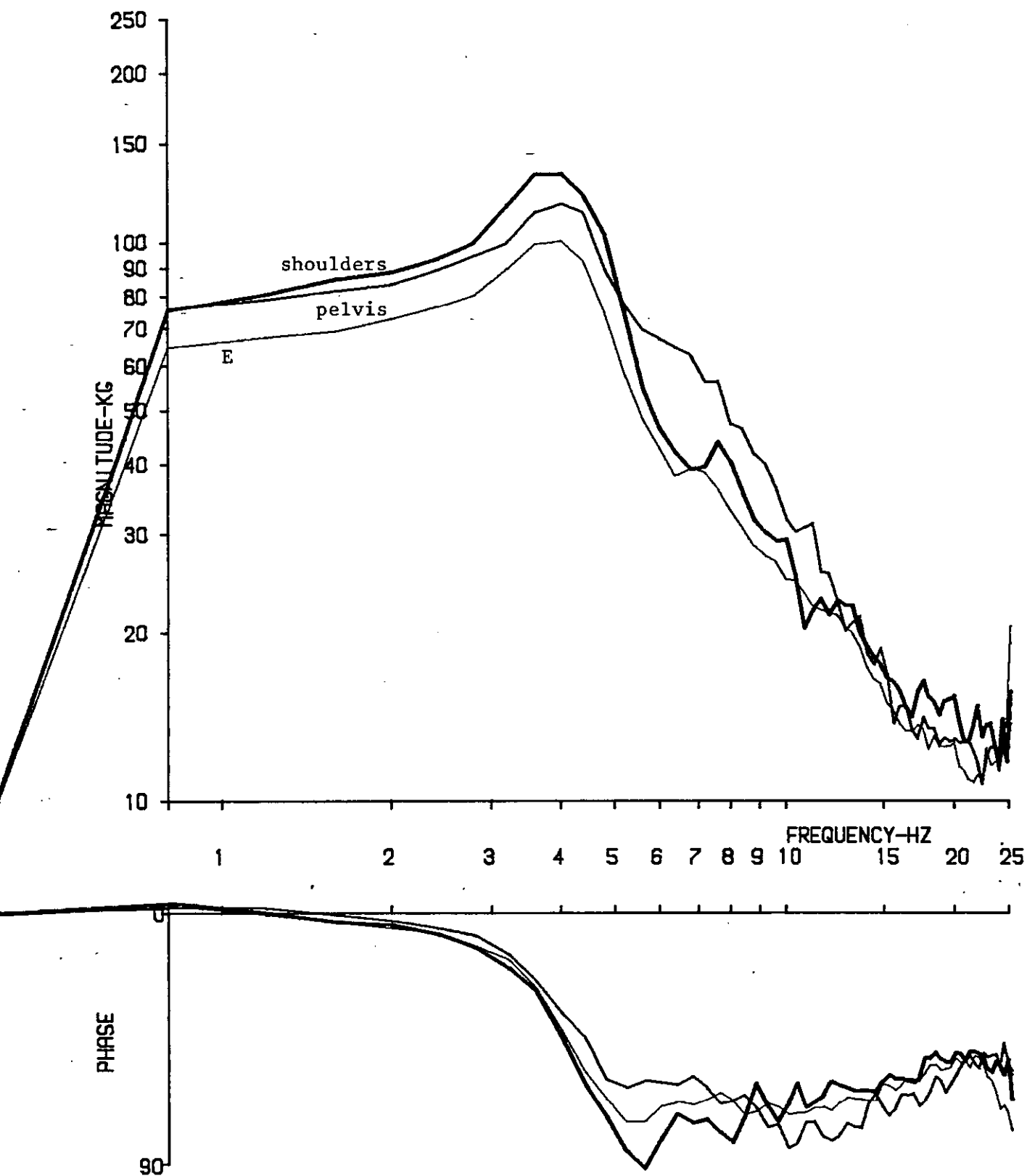




RUN NO. 83/24, 23

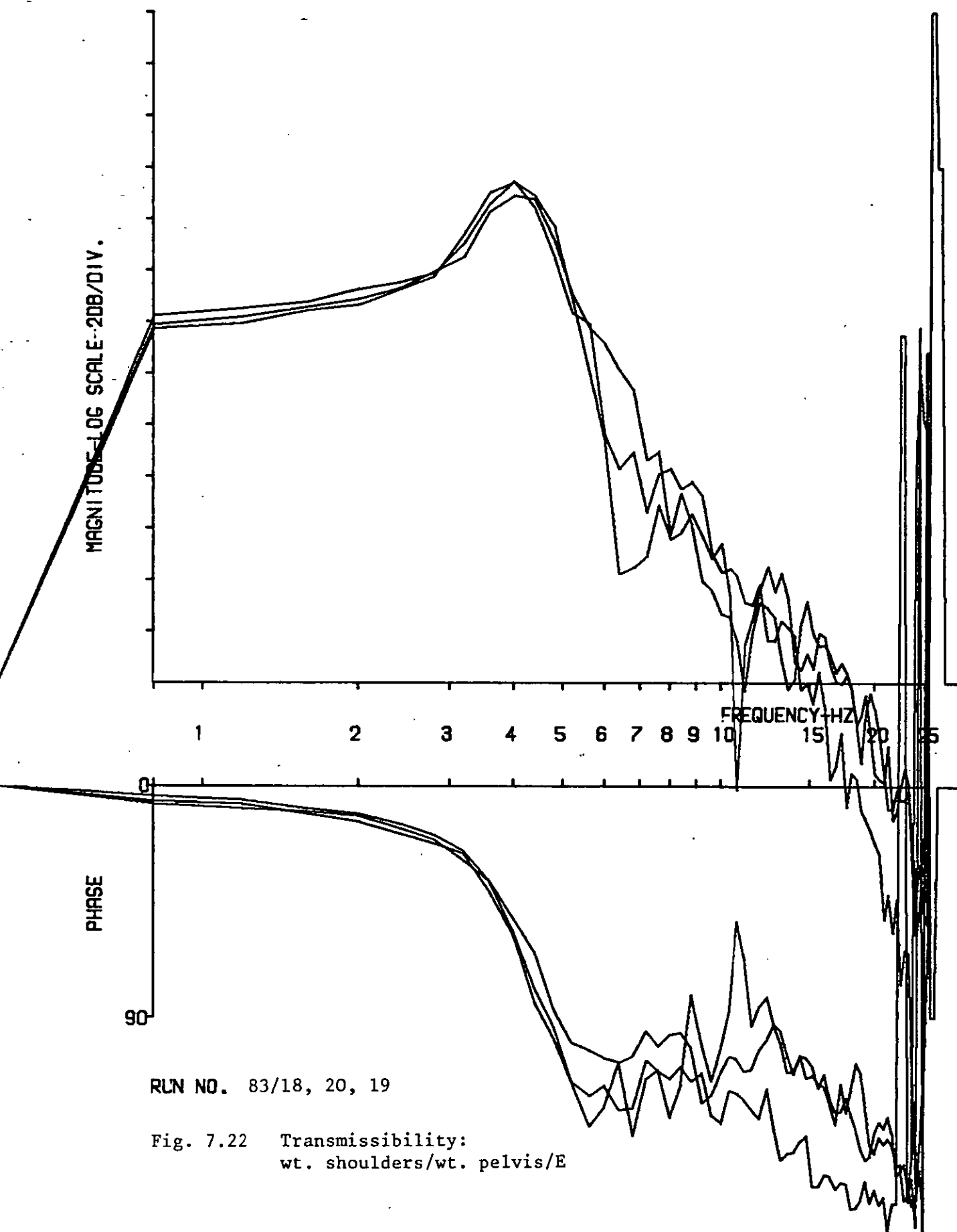
Fig. 7.19 Apparent mass: Ab/E

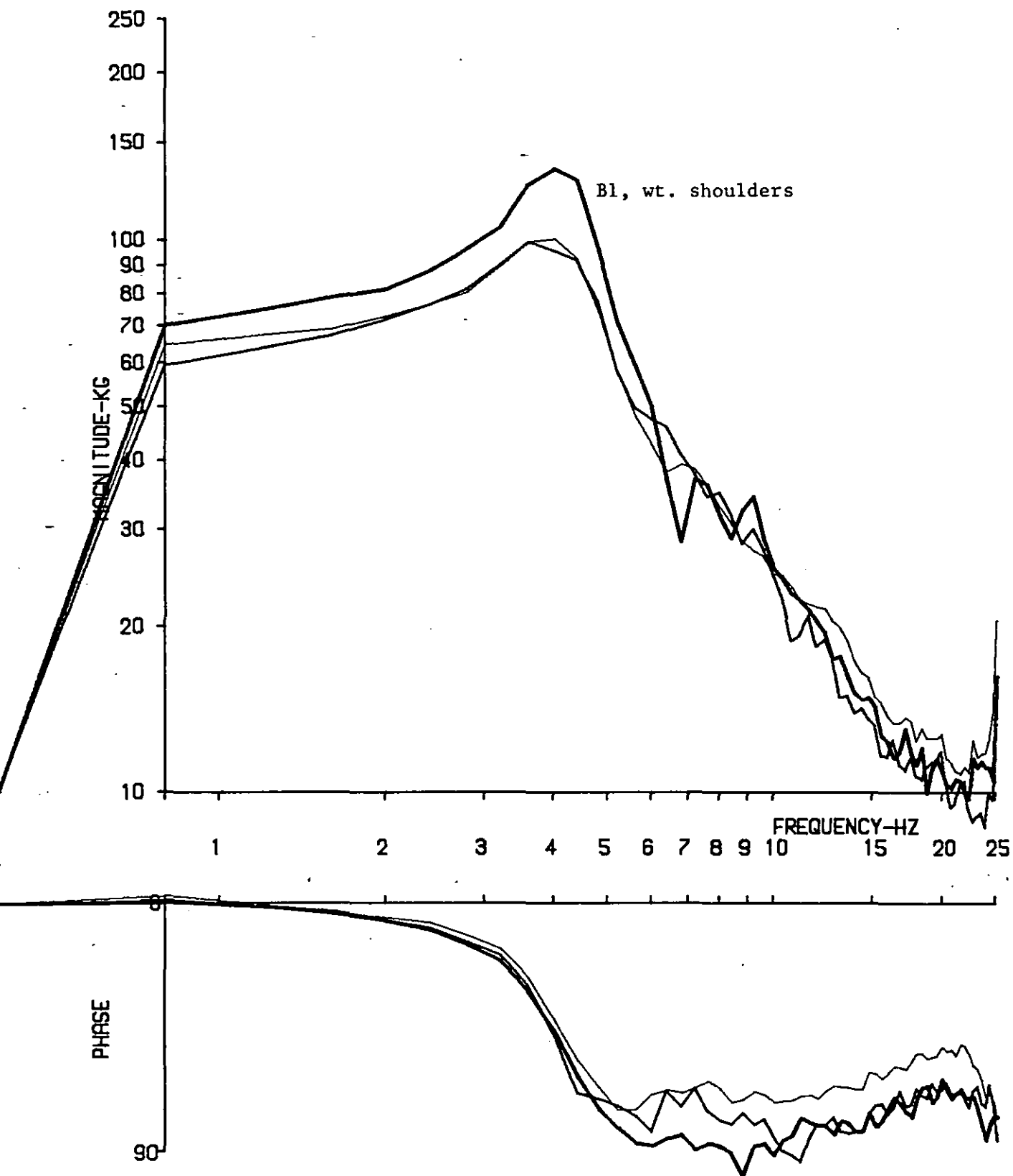




RUN NO. 83/18, 20, 19

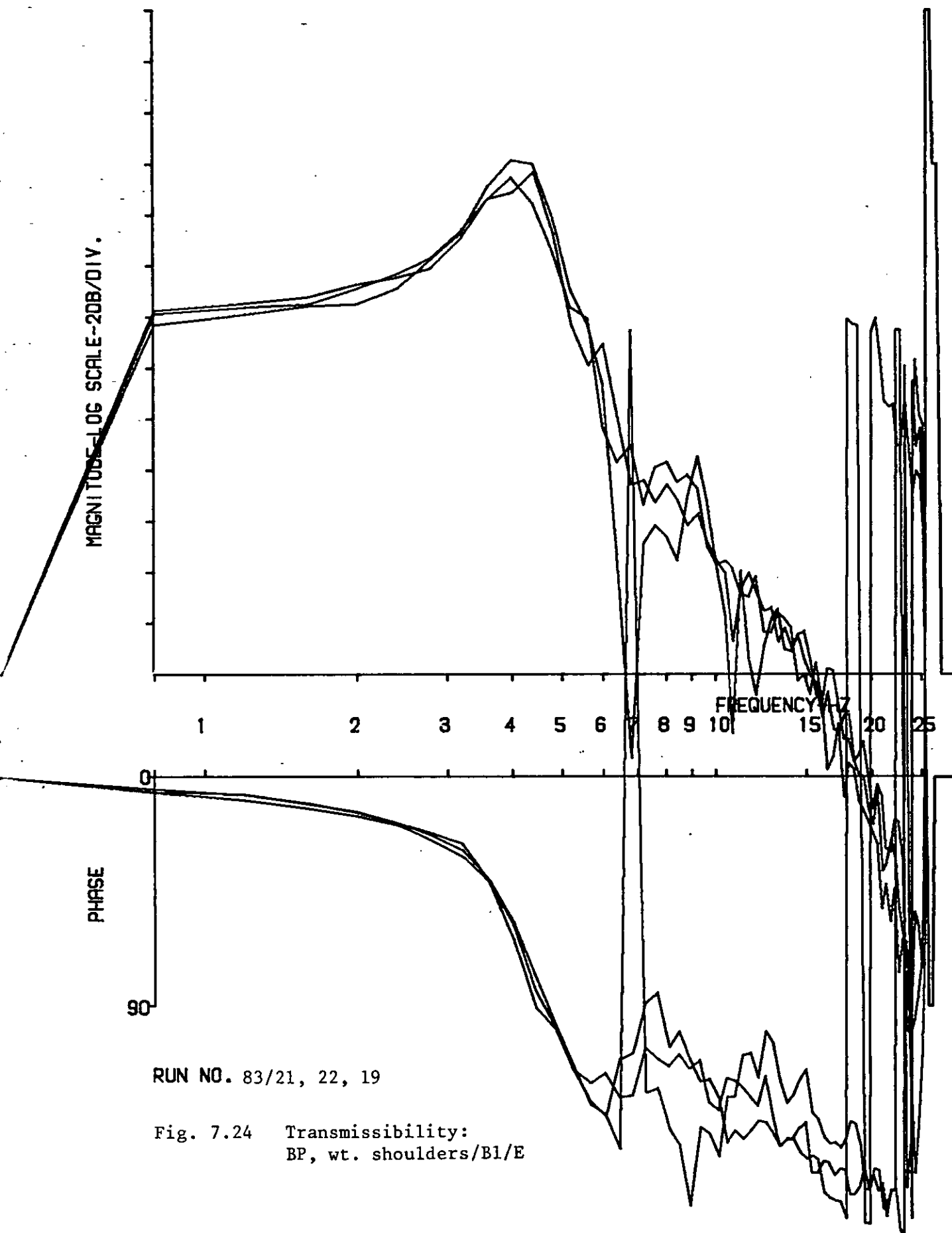
Fig. 7.21 Apparent mass: wt. shoulders/wt. pelvis/E

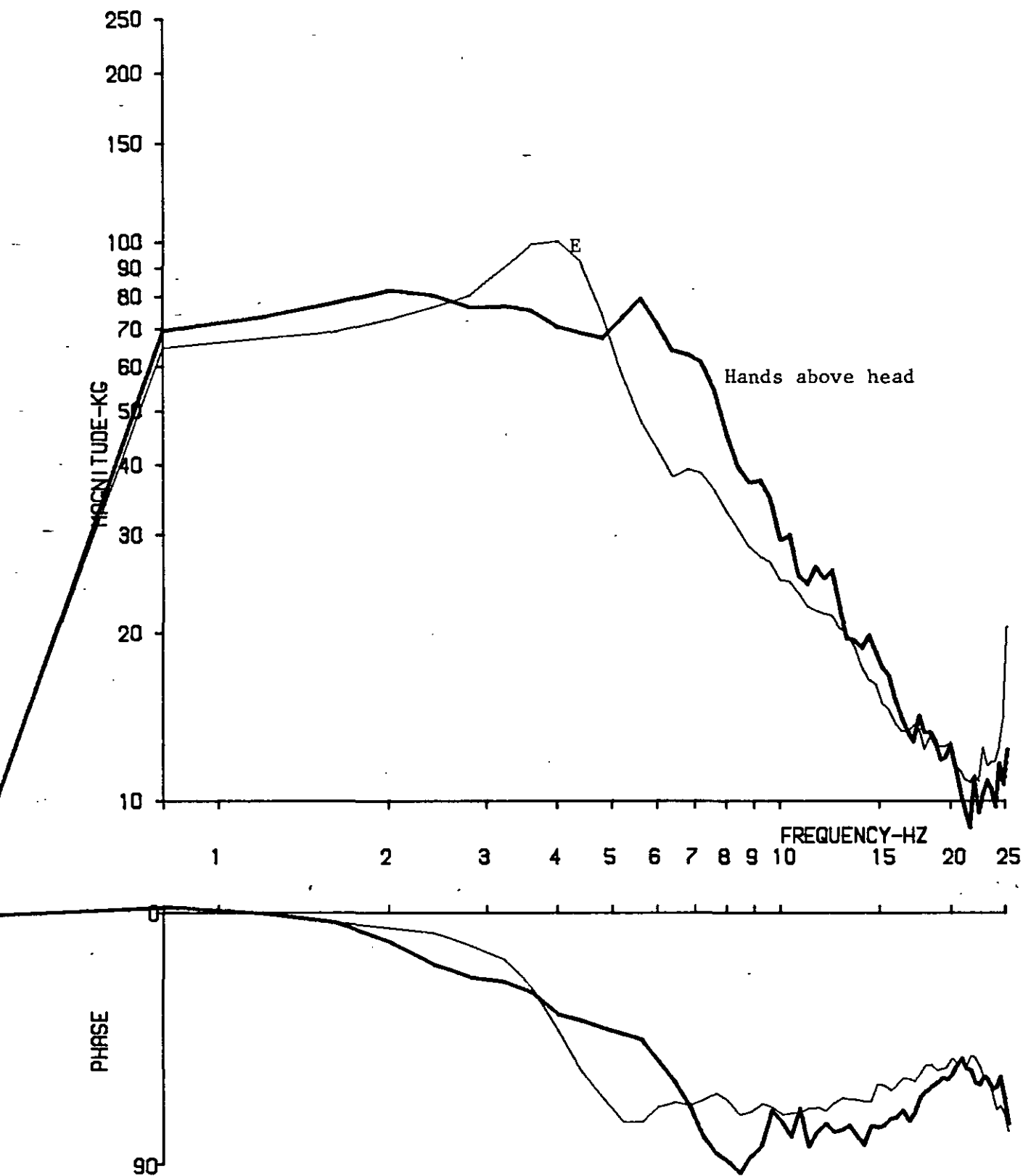




RUN NO. 83/21, 22 19

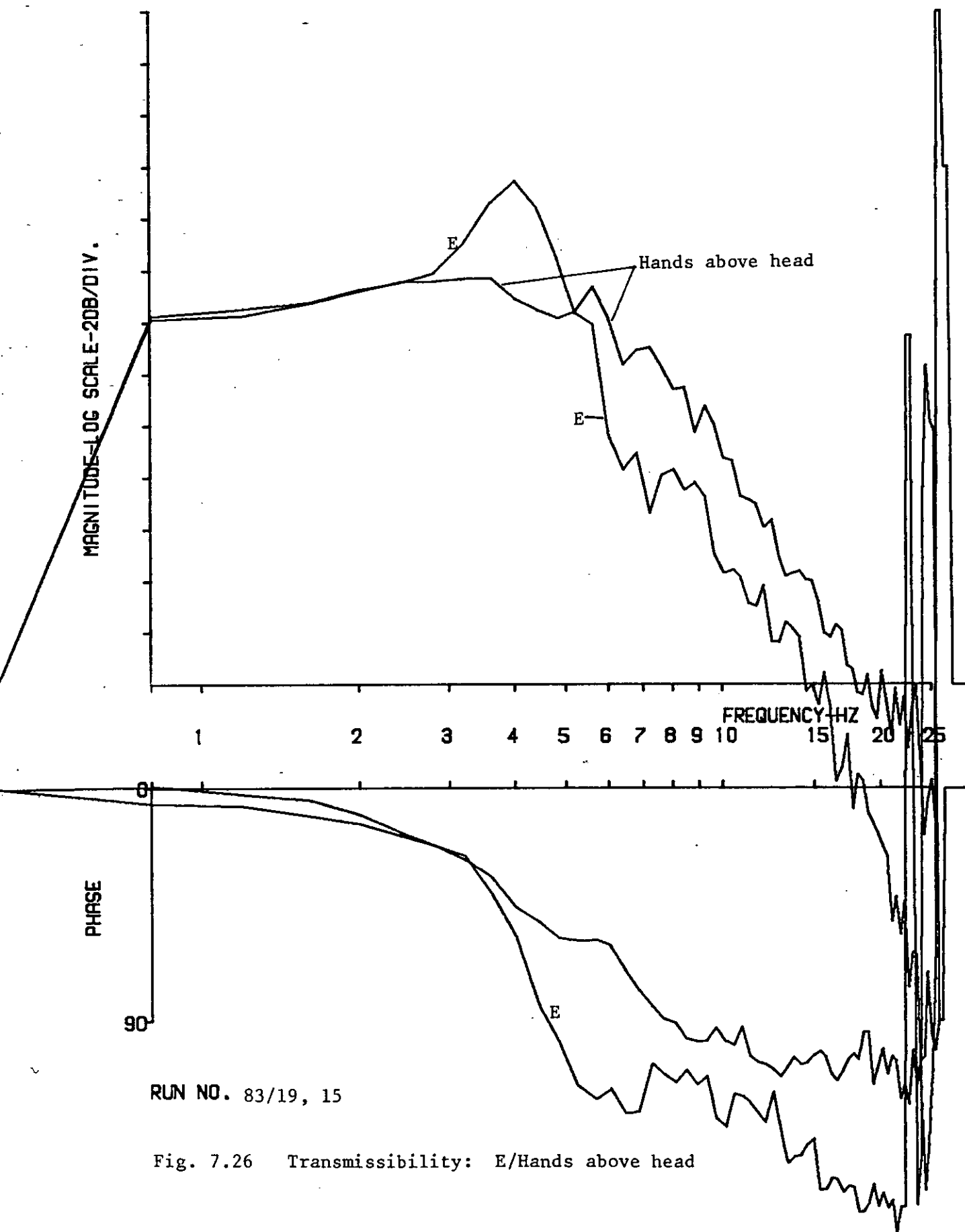
Fig. 7.23 Apparent mass: Bl, wt. shoulders/Bl/E

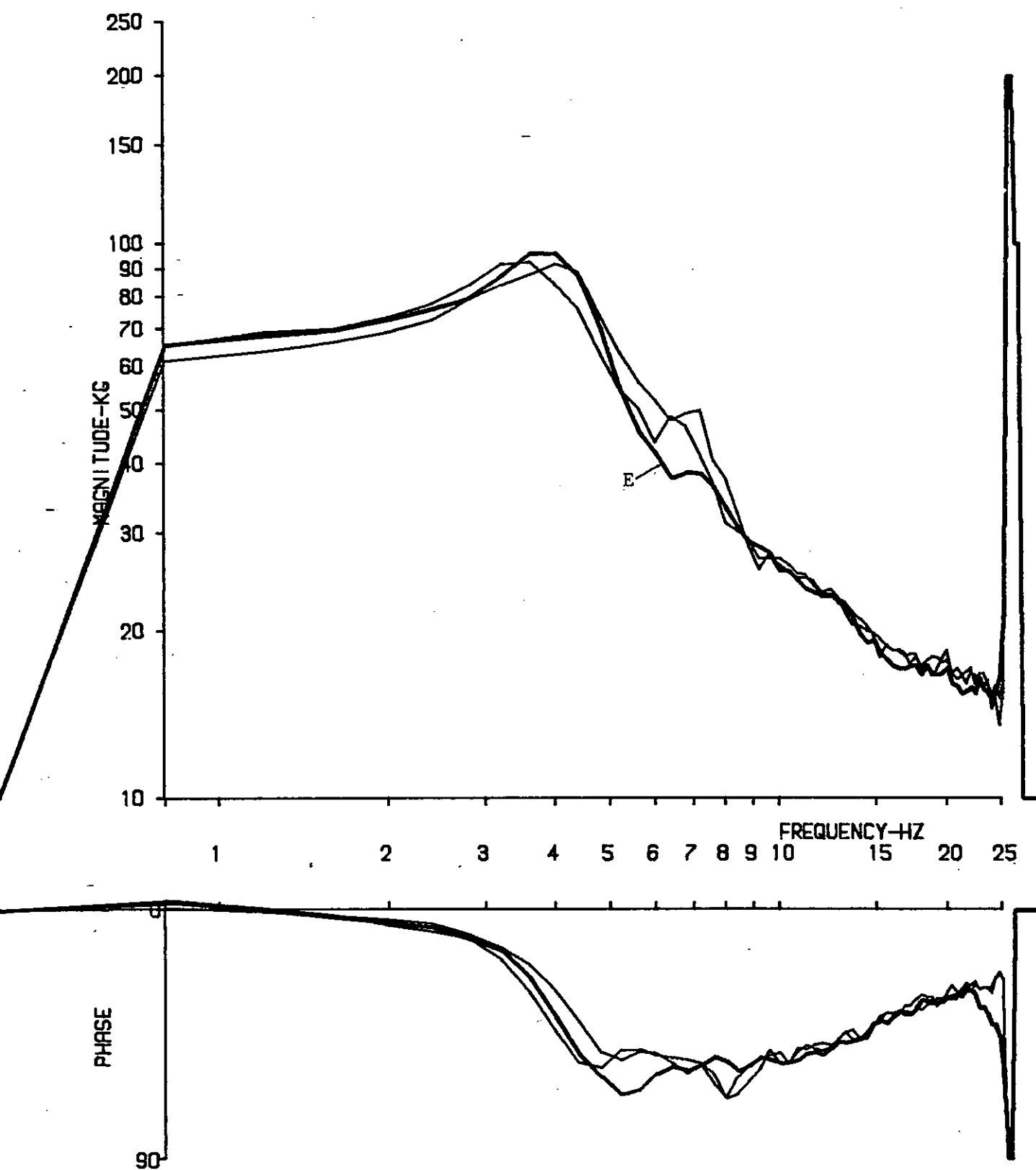




RUN NO. 83/19, 15

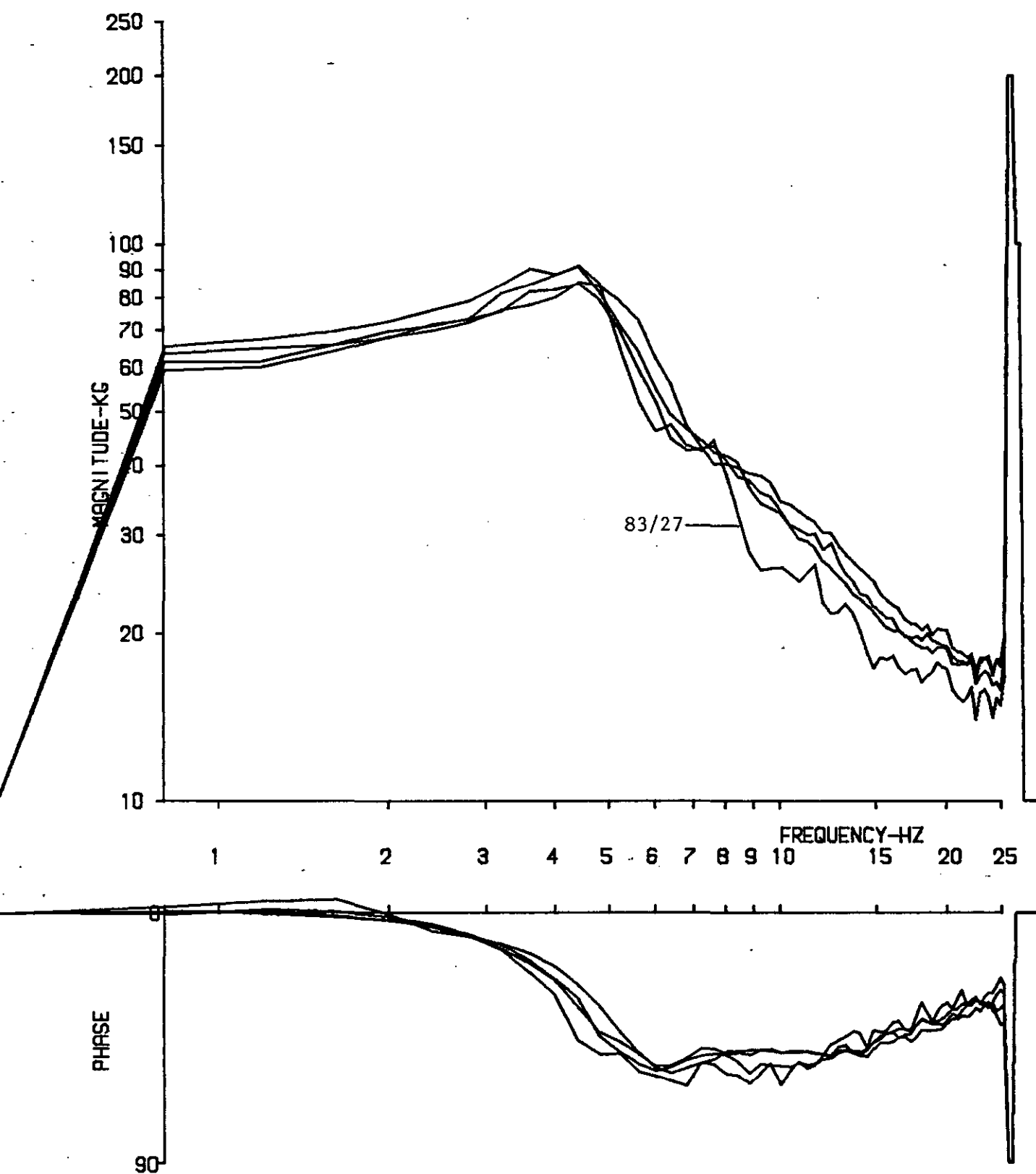
Fig. 7.25 Apparent mass: E/Hands above head





RUN NO. 83/19, 13, 14

Fig. 7.27 Apparent mass: E/Dr hands vibrated/Dr hands fixed
(NB. Not calibrated for cell unsprung mass: for comparison between spectra only)



RUN NO. 83/27, 28, 29, 30

Fig. 7.28 Apparent mass: Comparison of different stimuli E
 (NB. Not calibrated for cell unsprung mass: for comparison between spectra only)

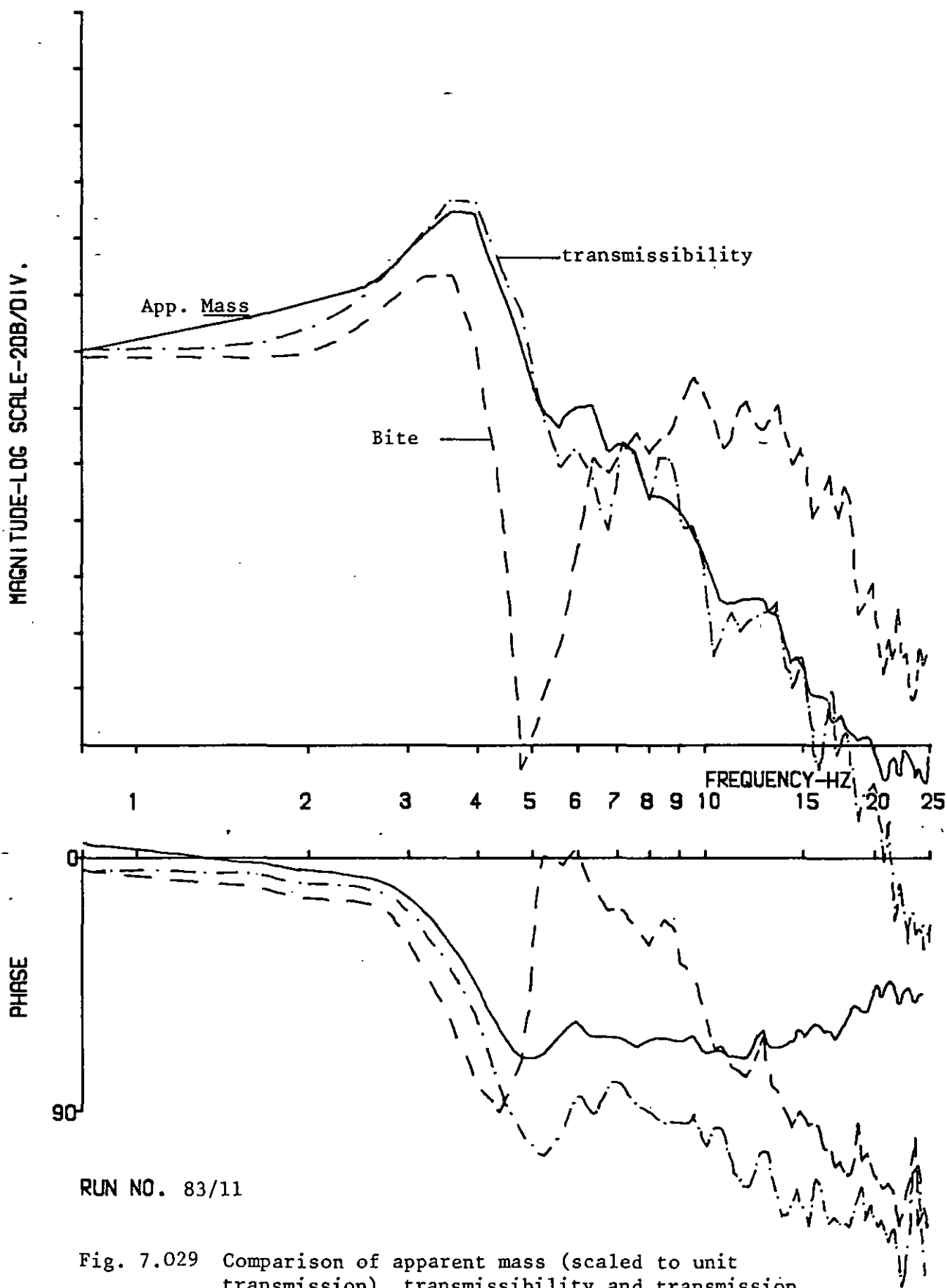
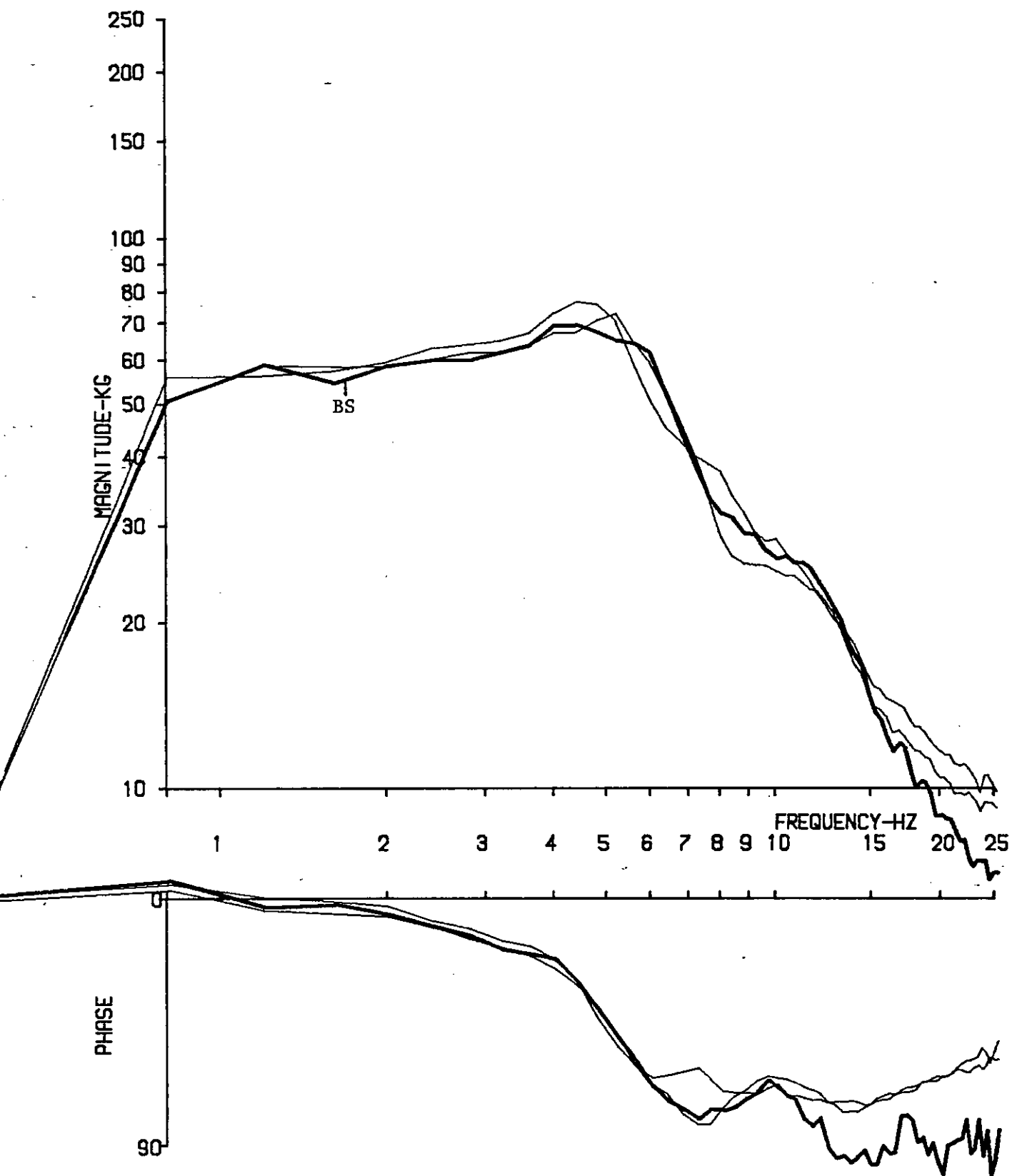
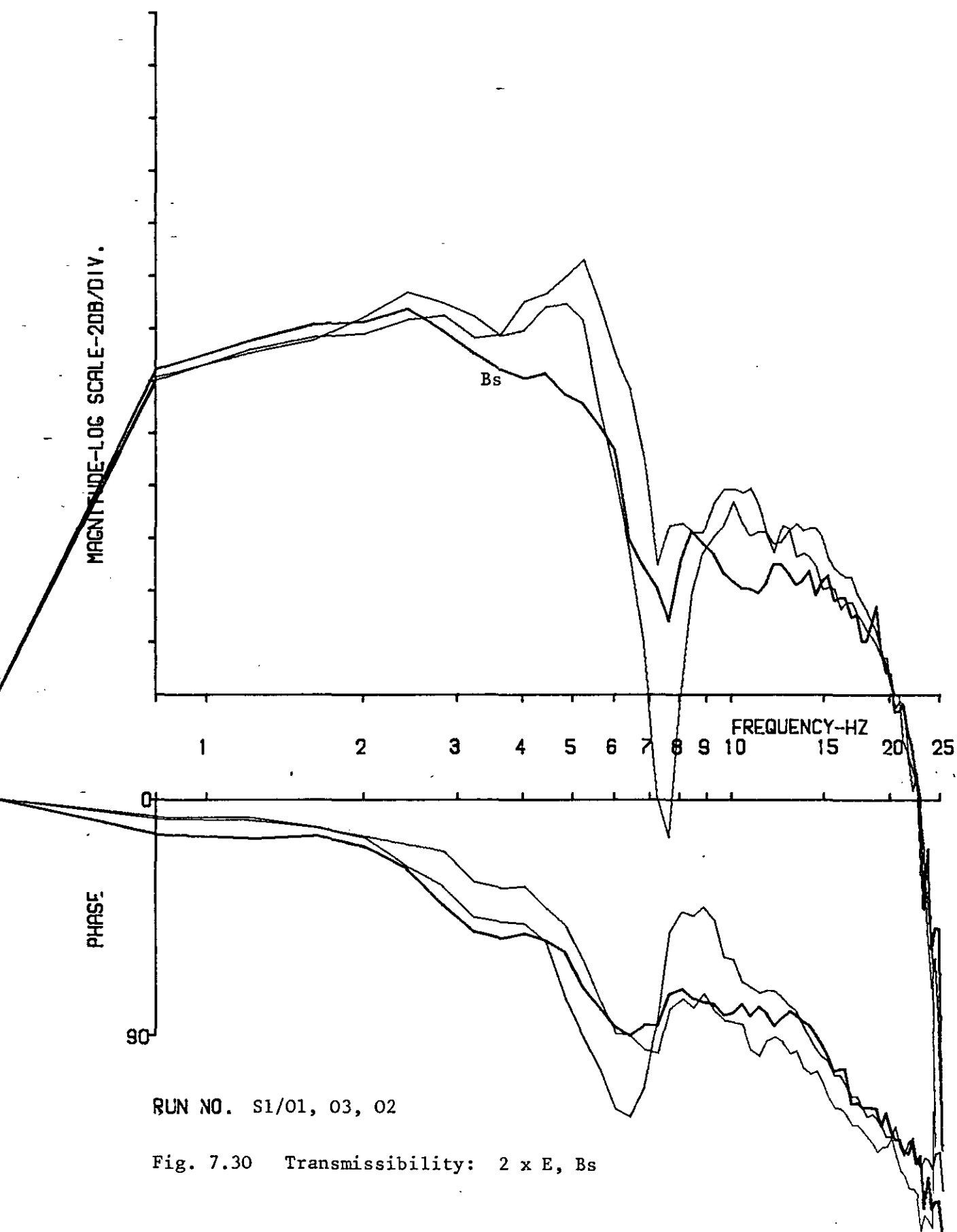


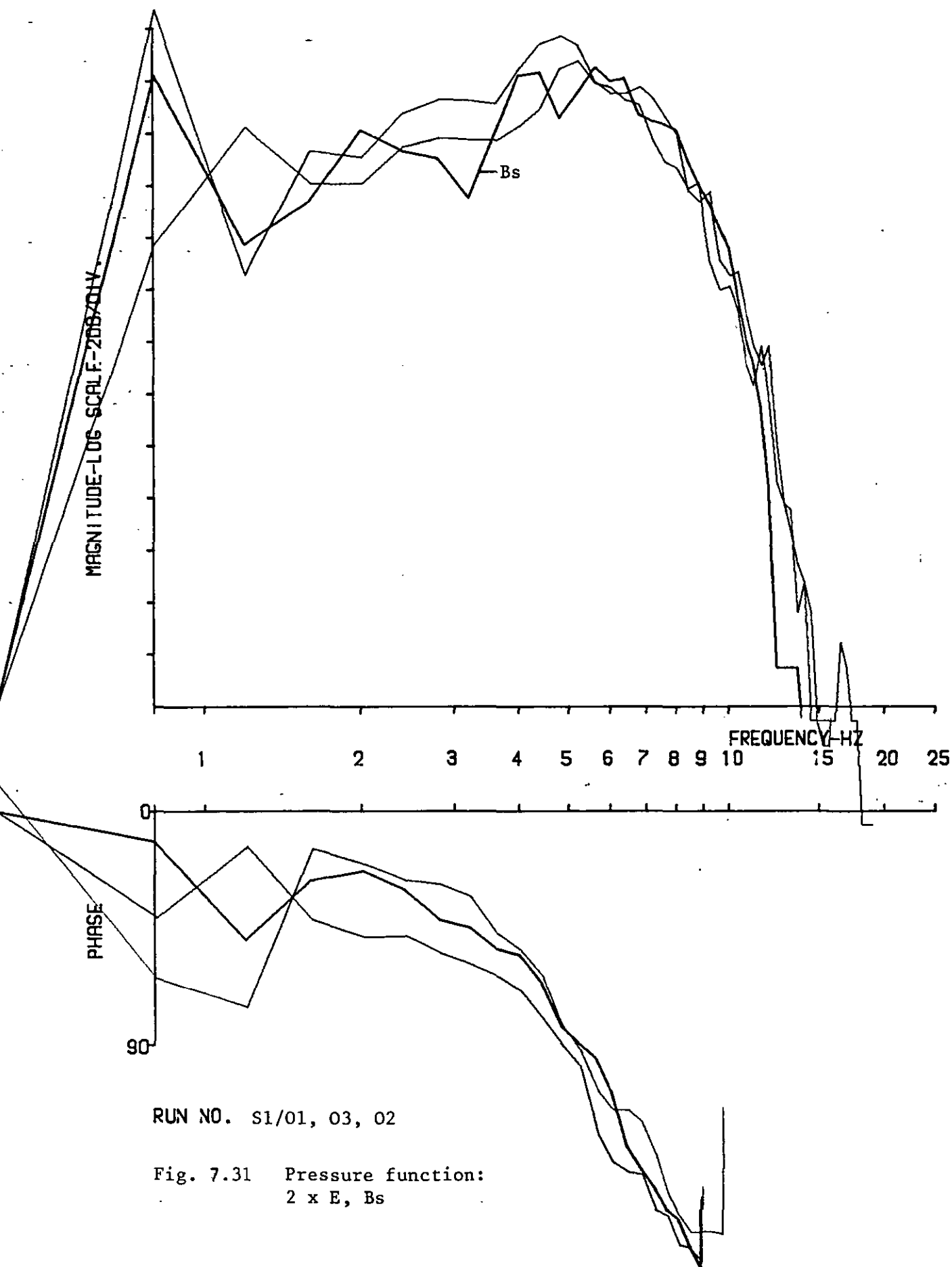
Fig. 7.029 Comparison of apparent mass (scaled to unit transmission), transmissibility and transmission to bite



RUN NO. S1/01, 03, 02

Fig. 7.29 Apparent mass: $2 \times E$, Bs





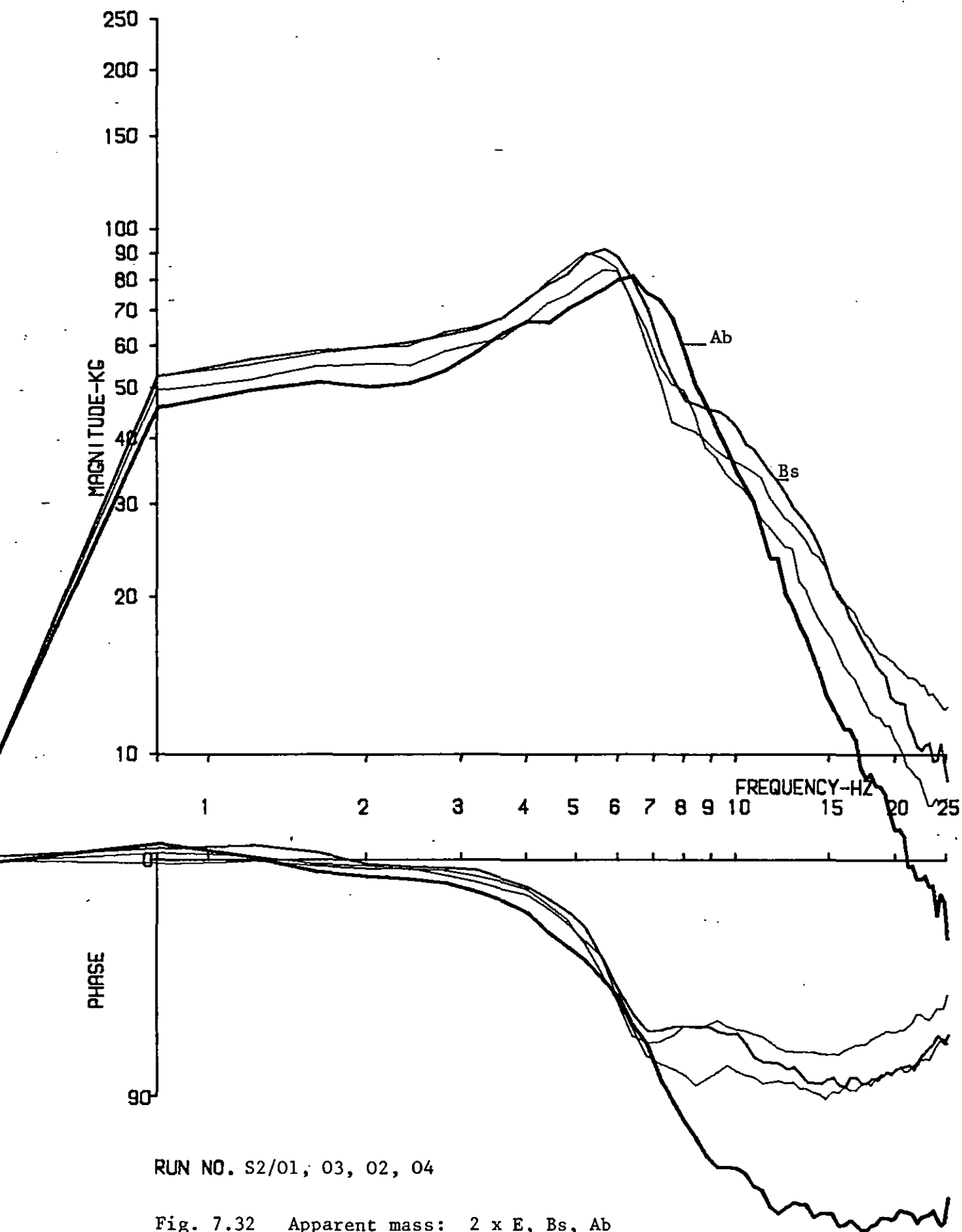
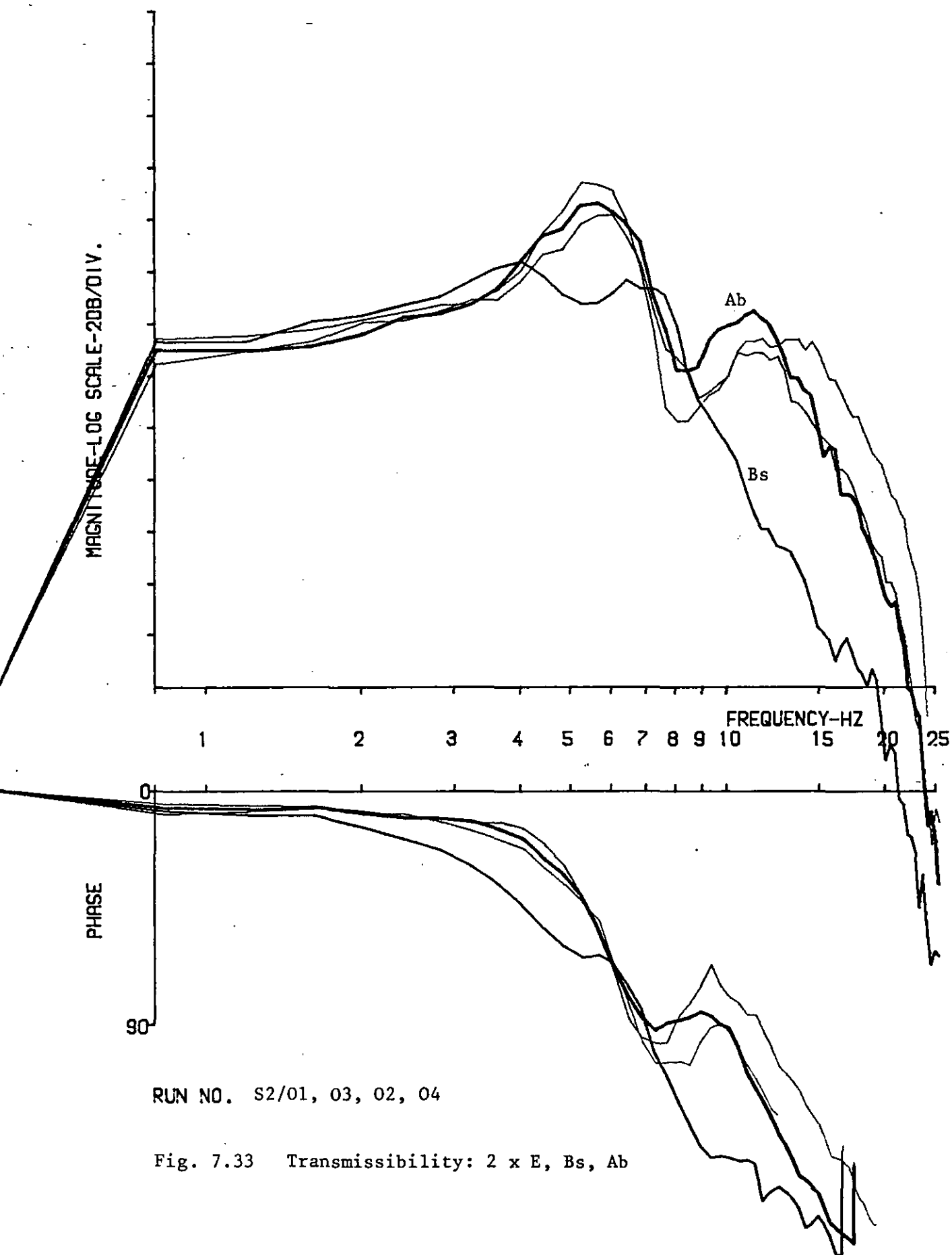
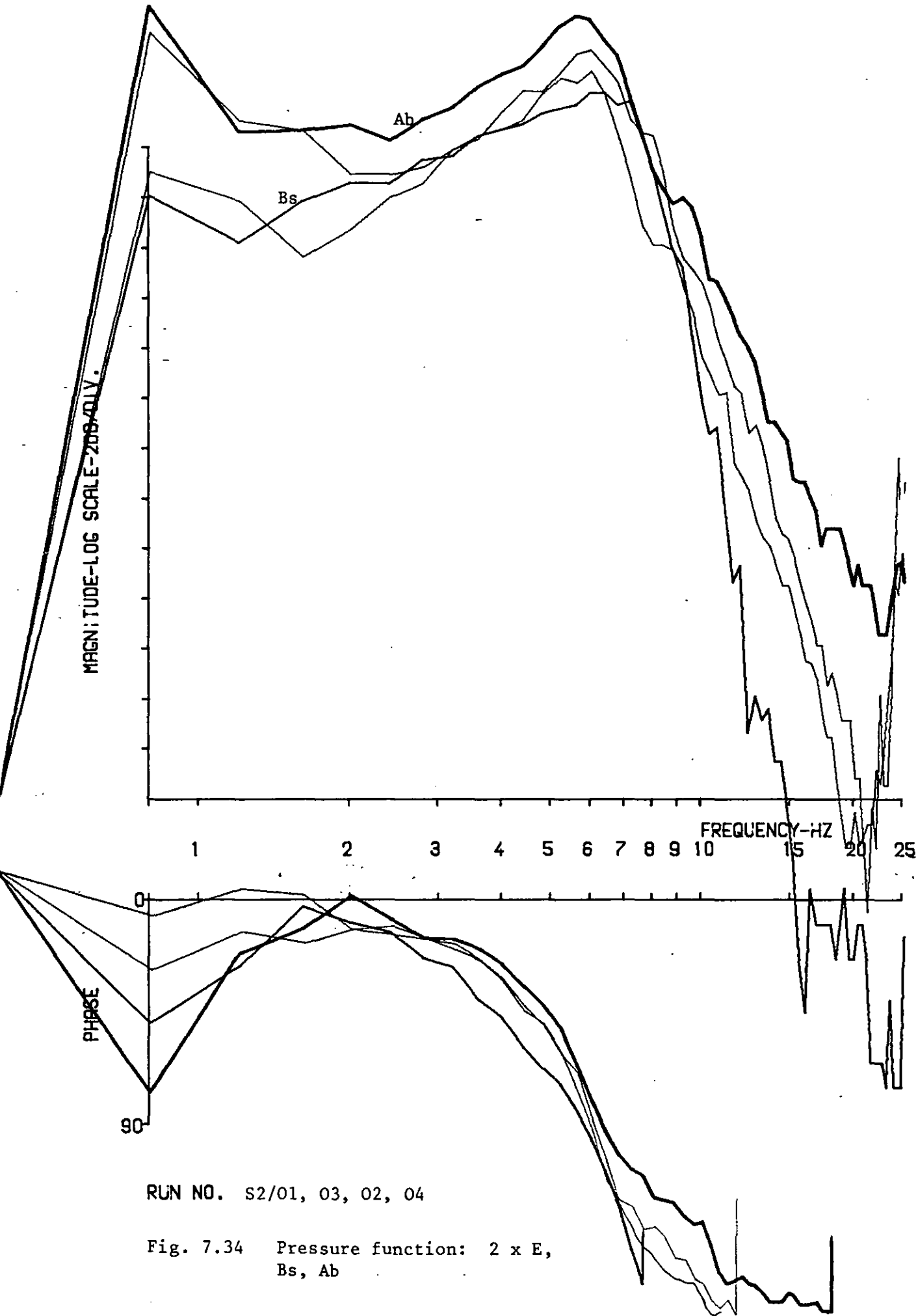
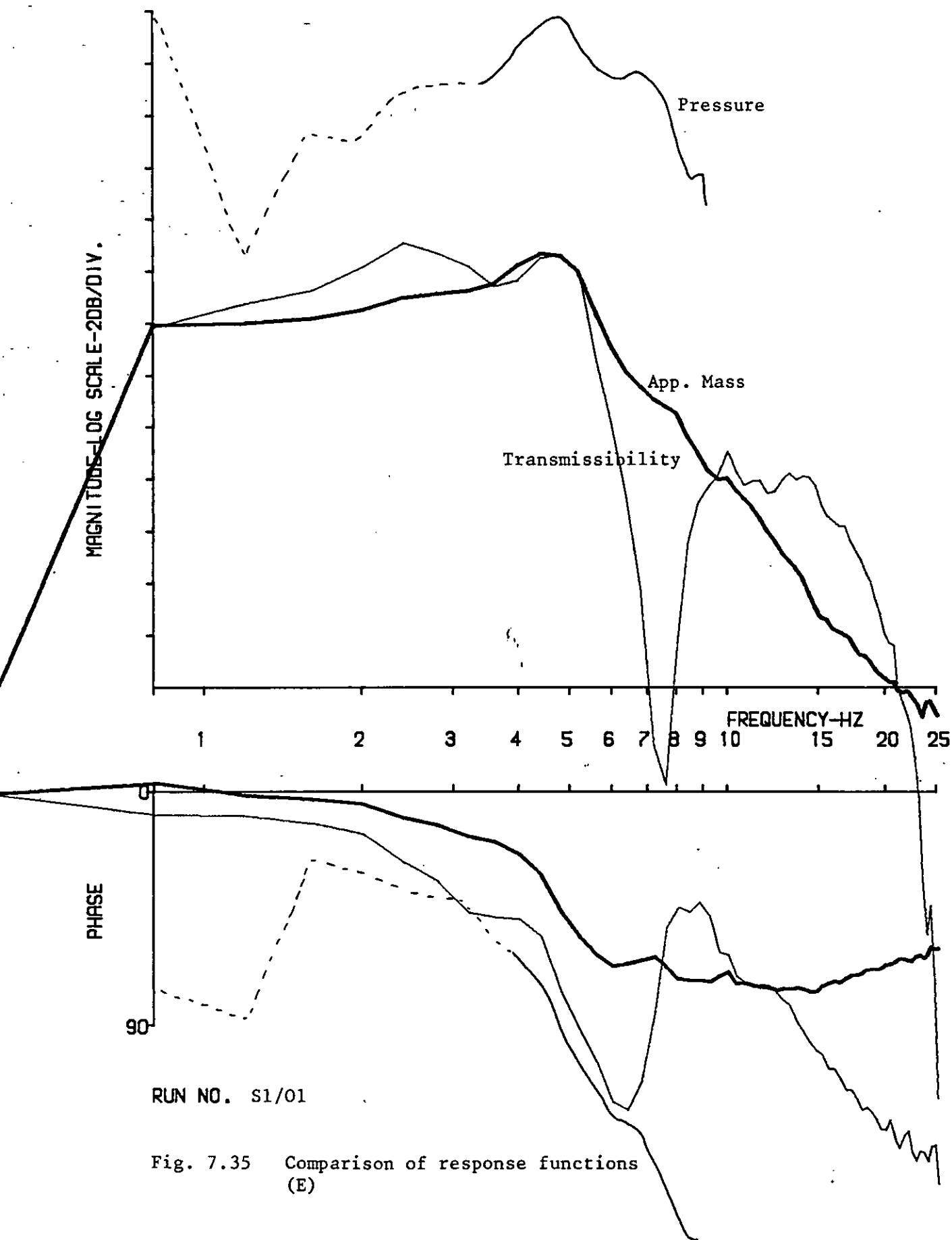


Fig. 7.32 Apparent mass: 2 x E, Bs, Ab







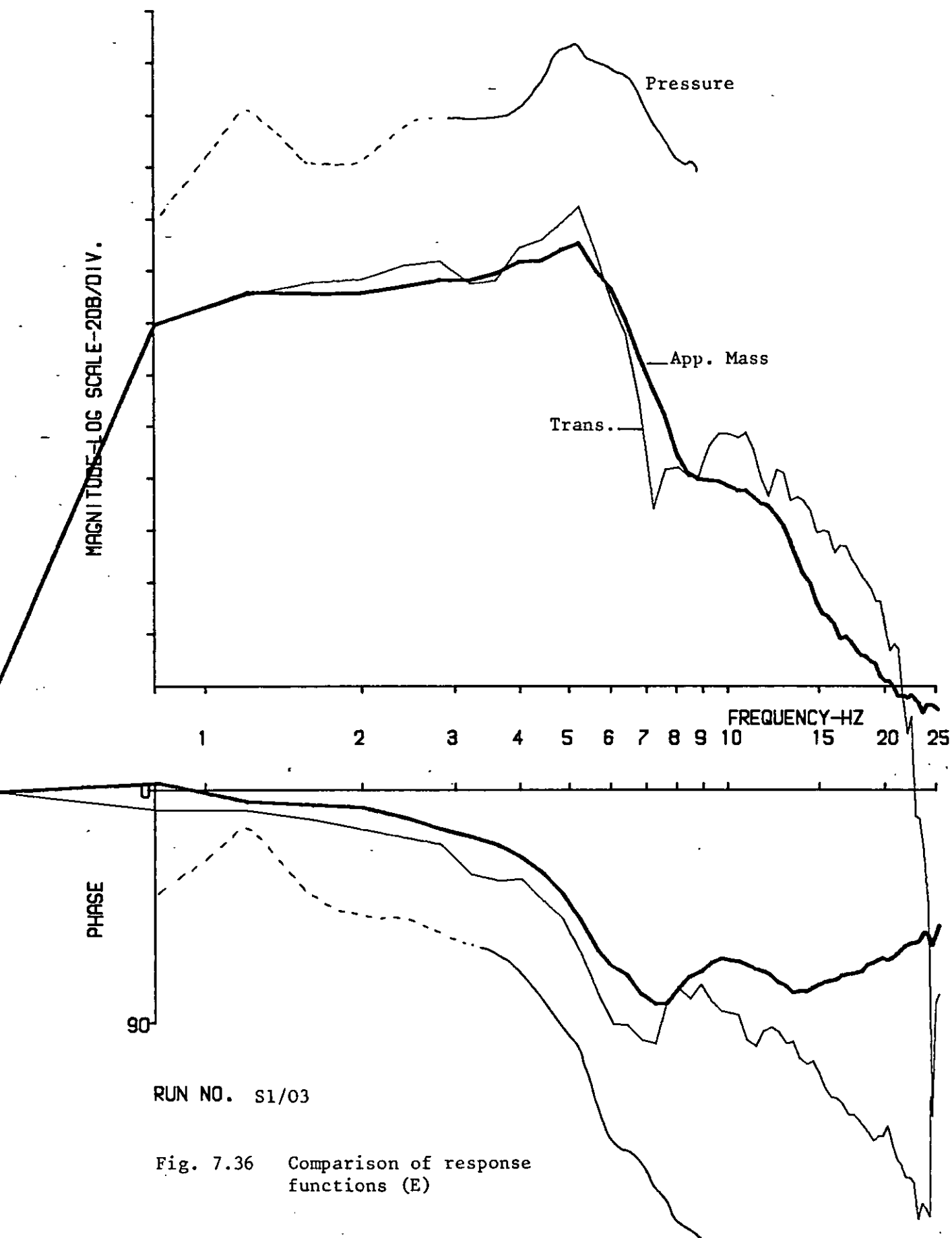


Fig. 7.36 Comparison of response functions (E)

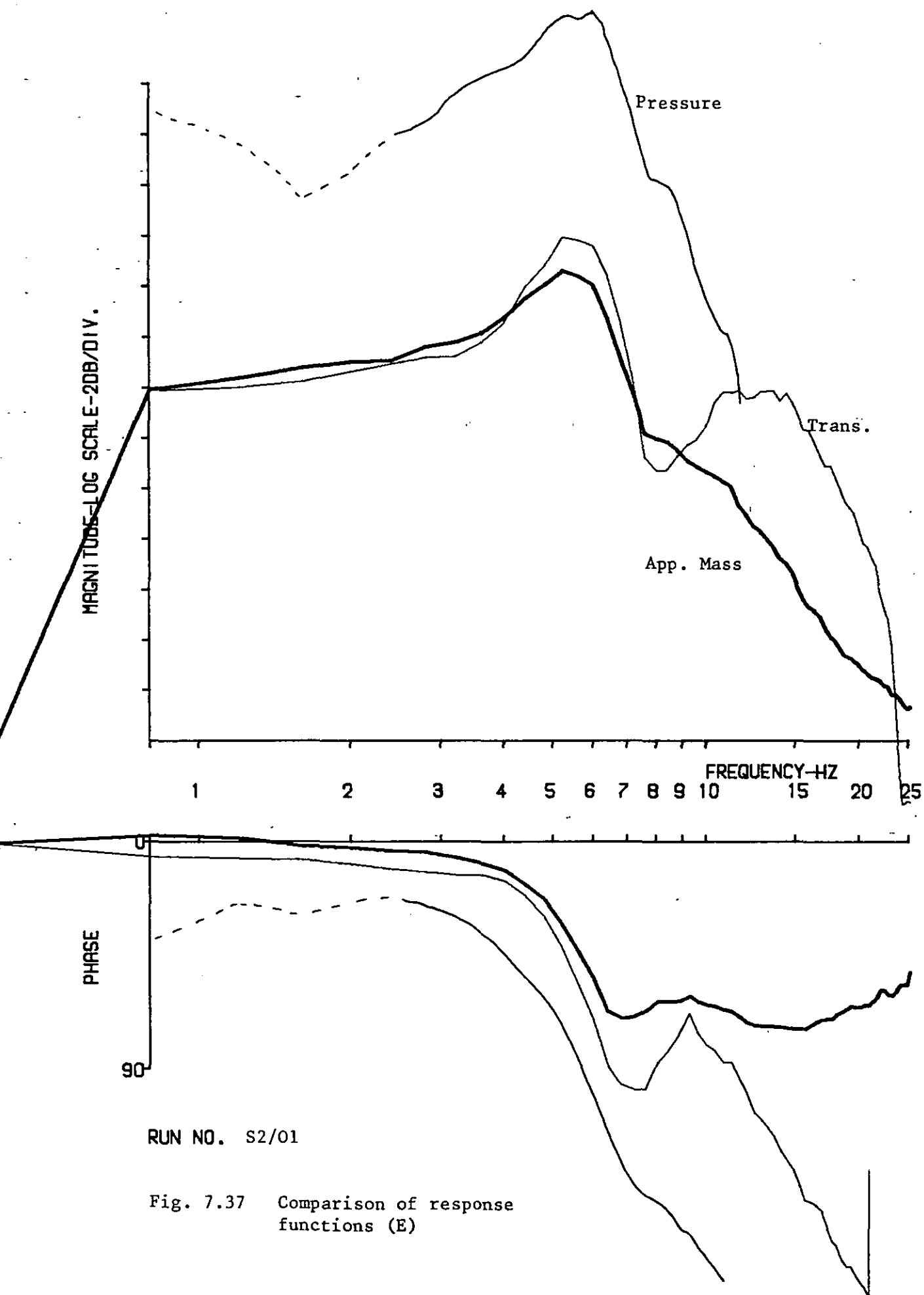
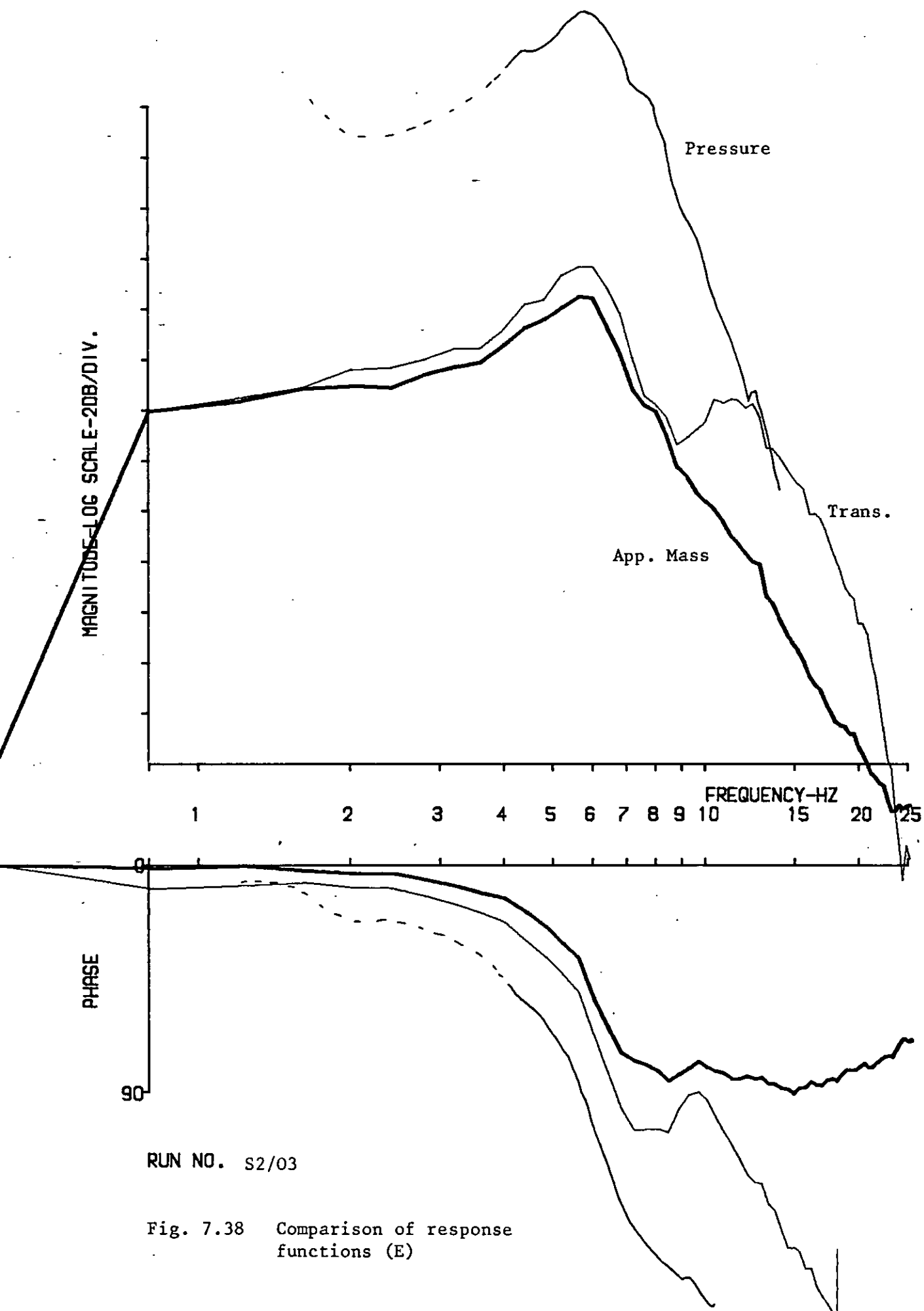
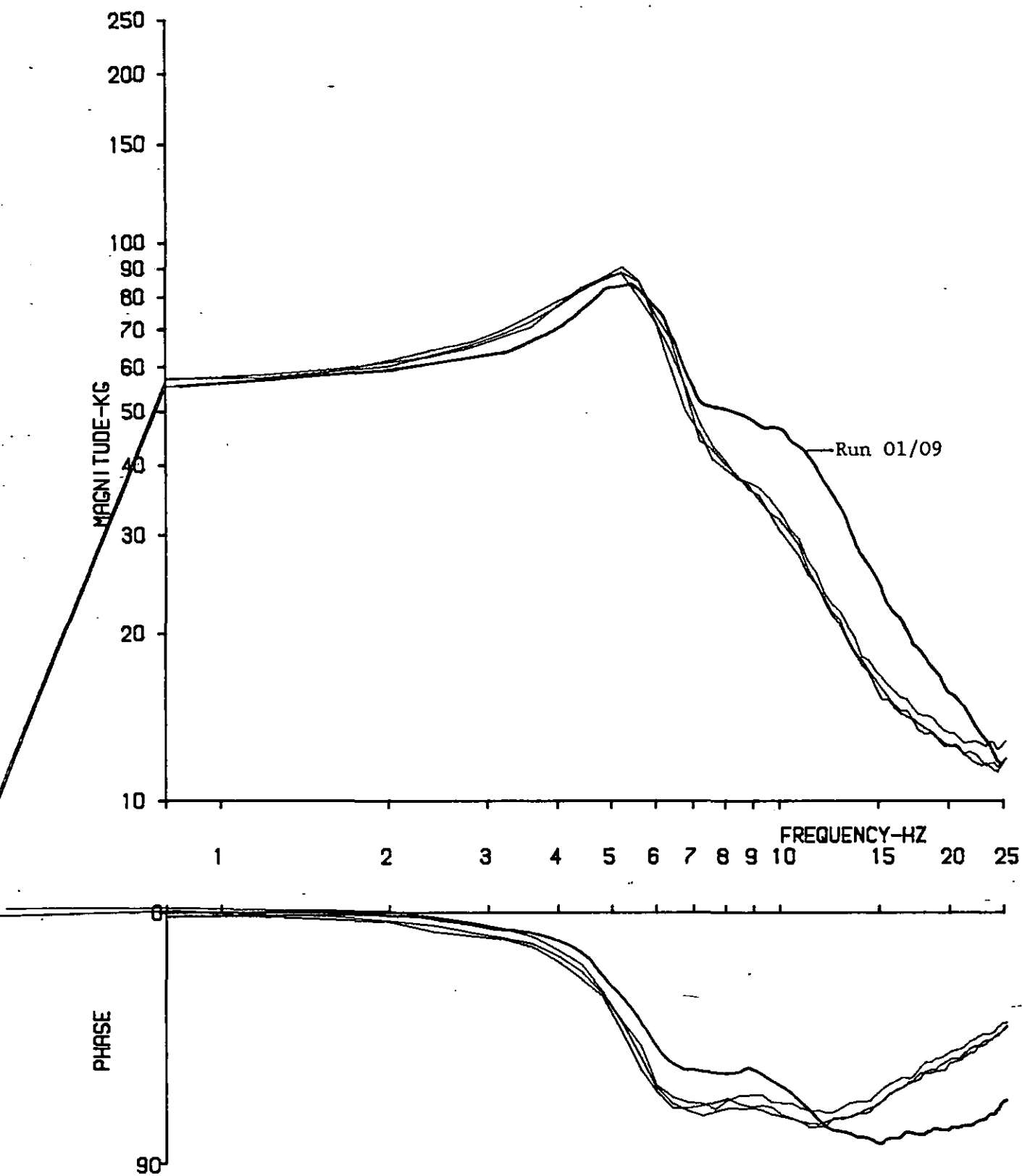


Fig. 7.37 Comparison of response functions (E)





RUN NO. 01/01, 07, 09, 13

Fig. 7.39 Apparent mass: $4 \times E$

MAGNITUDE-LOG SCALE-20dB/DIV.

Run 01/09

FREQUENCY-HZ

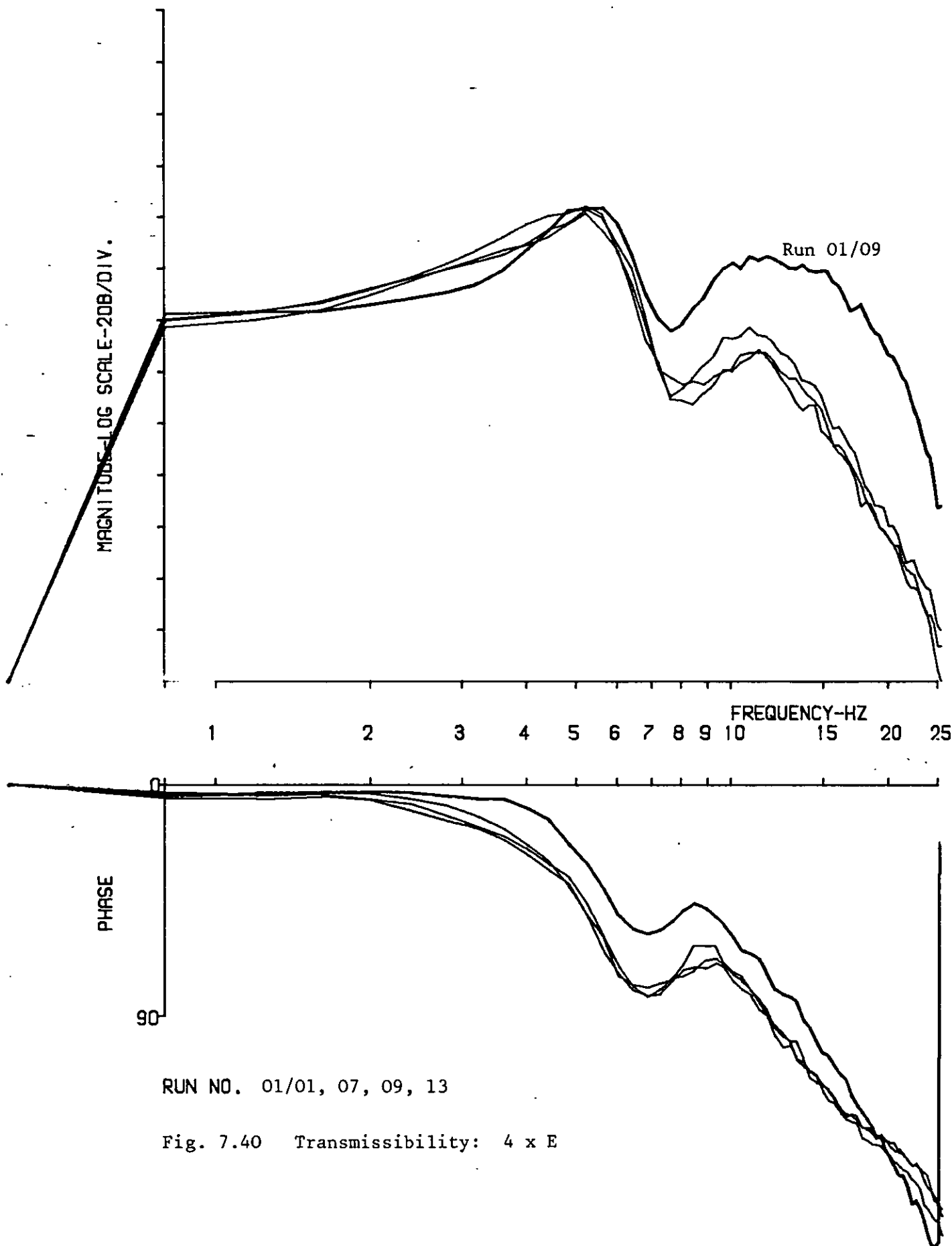
1 2 3 4 5 6 7 8 9 10 15 20 25

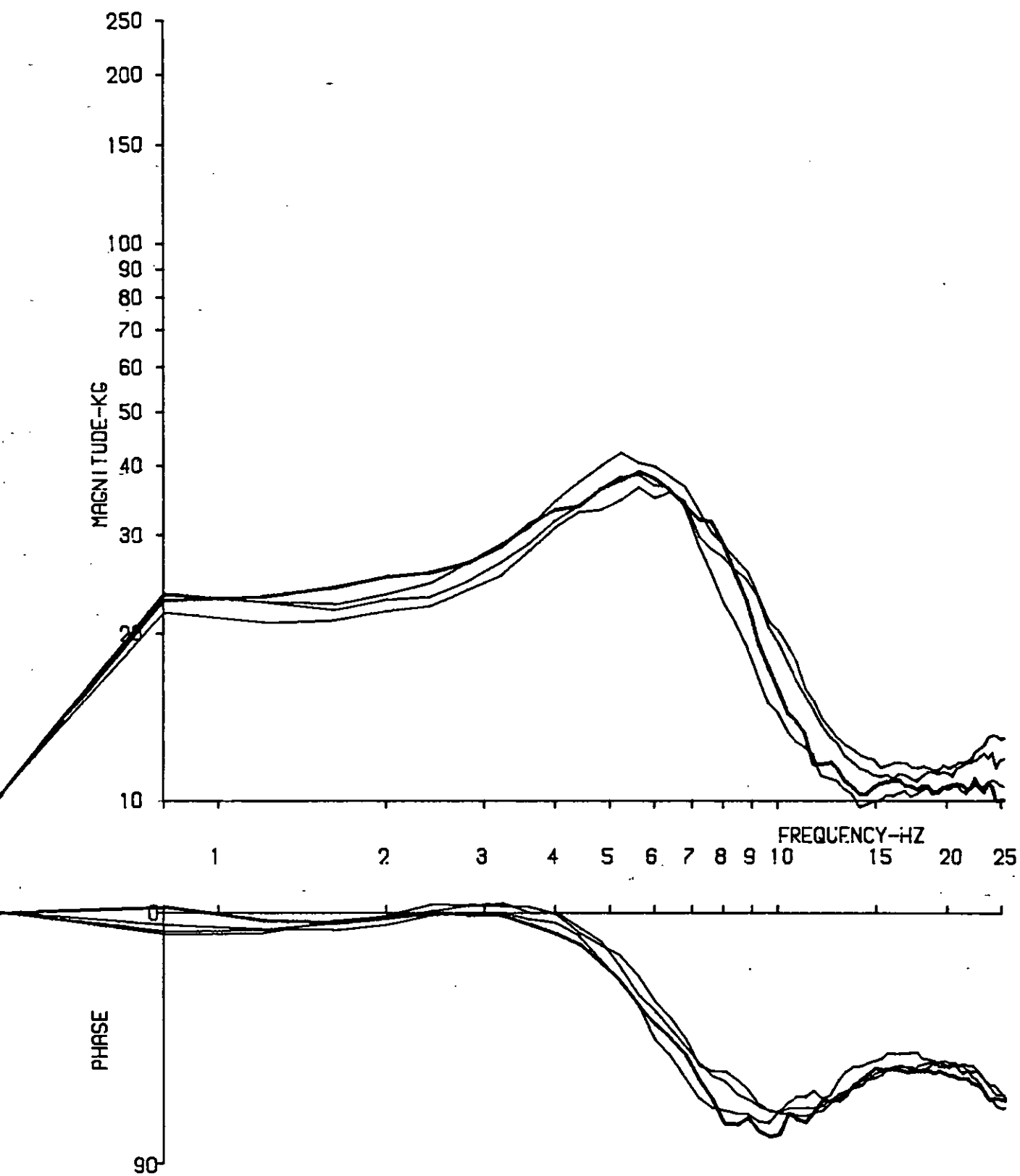
PHASE

90

RUN NO. 01/01, 07, 09, 13

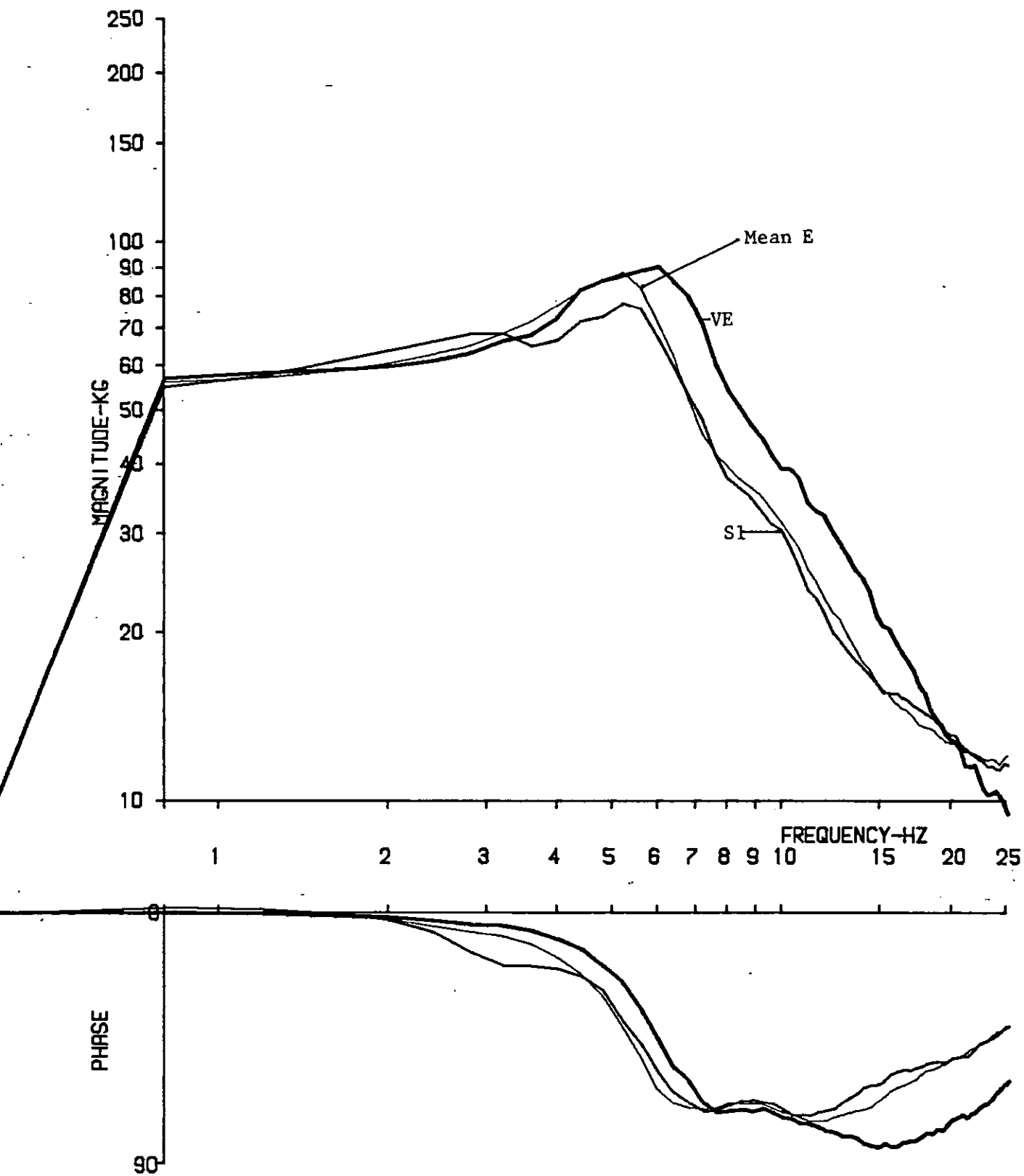
Fig. 7.40 Transmissibility: $4 \times E$





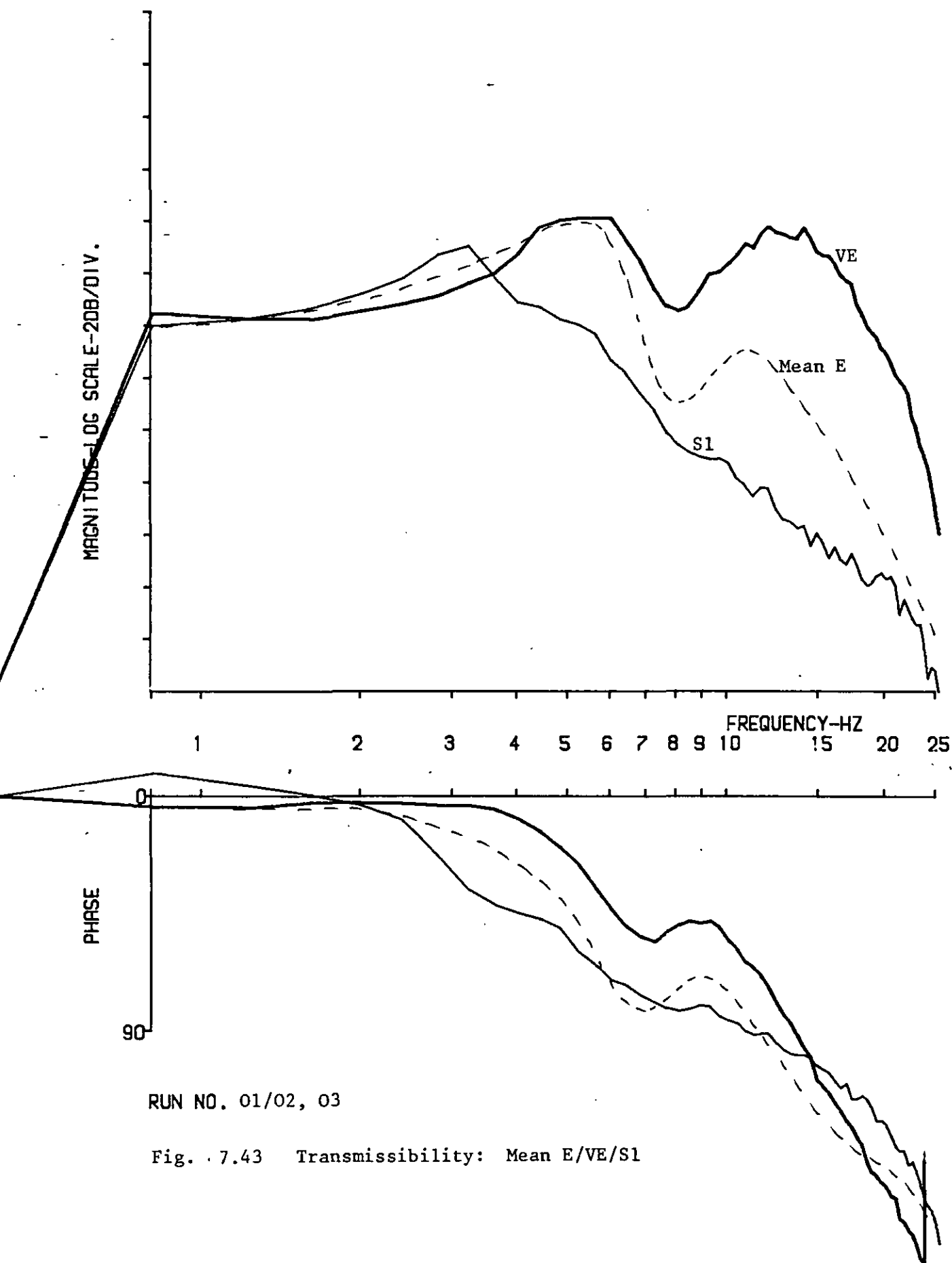
RUN NO. 01/01, 07, 09, 13

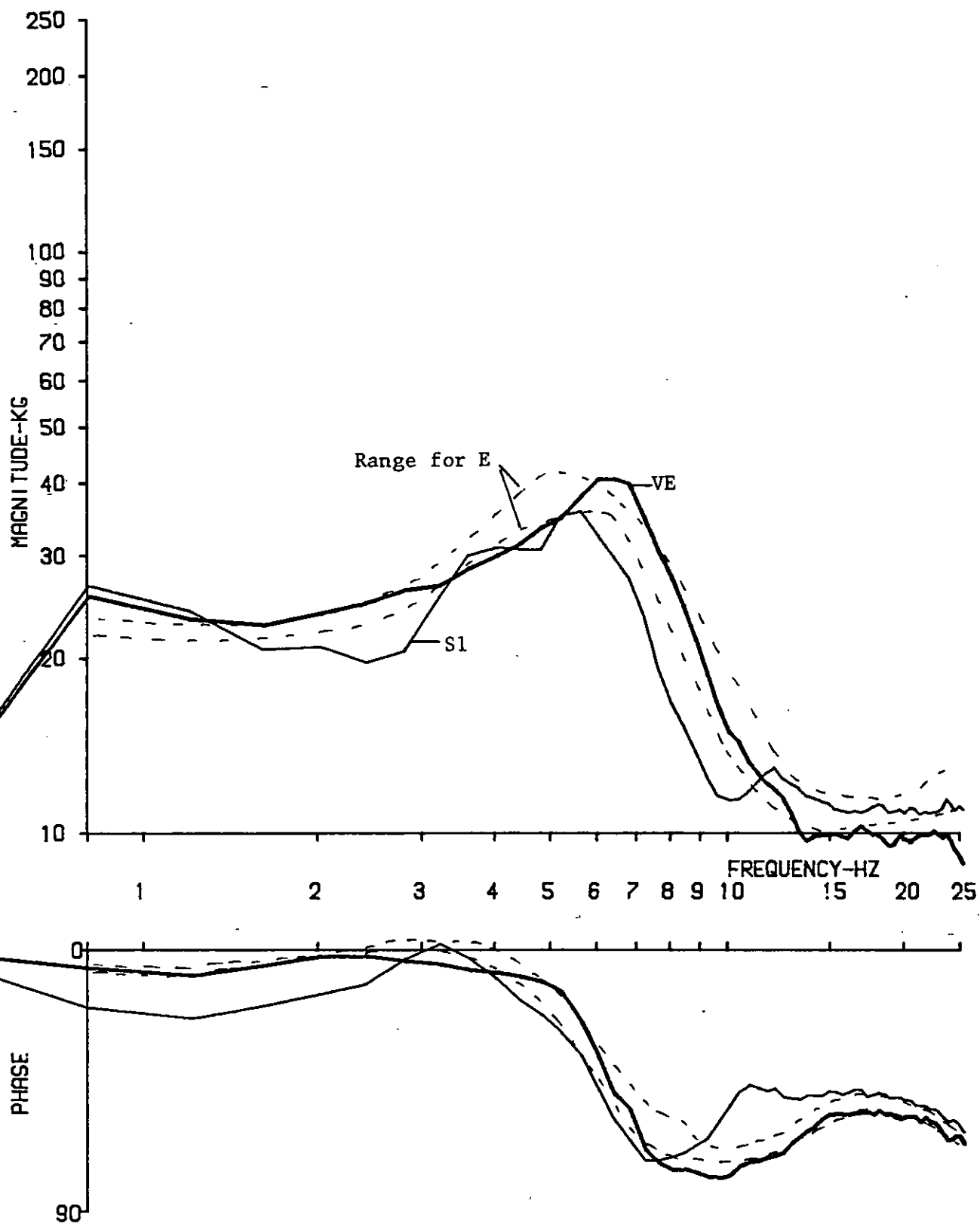
Fig. 7.41 Apparent mass feet: 4 x E



RUN NO. 01/02, 03

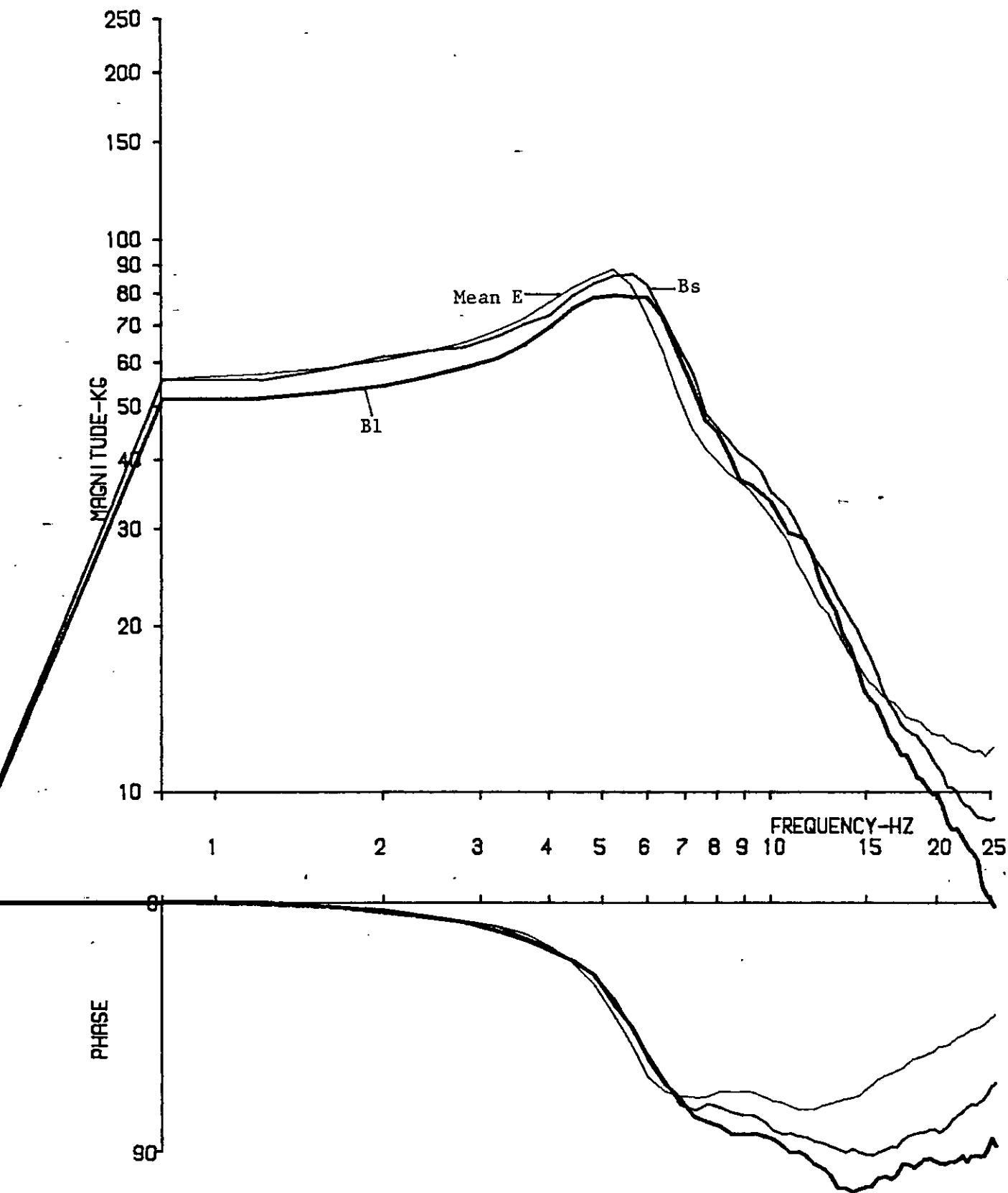
Fig. 7.42 Apparent mass: Mean E/VE/S1





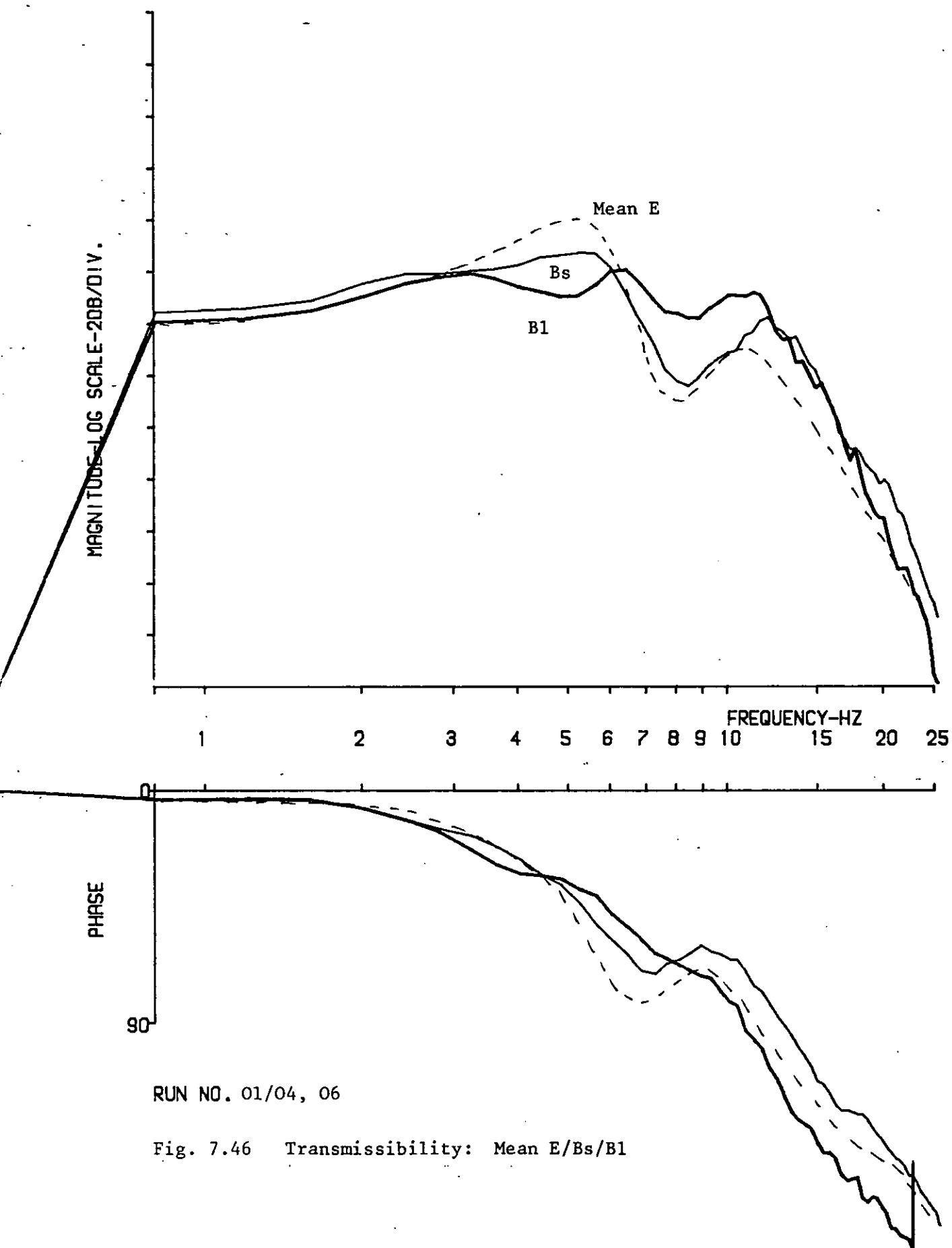
RUN NO. 01/02, 03

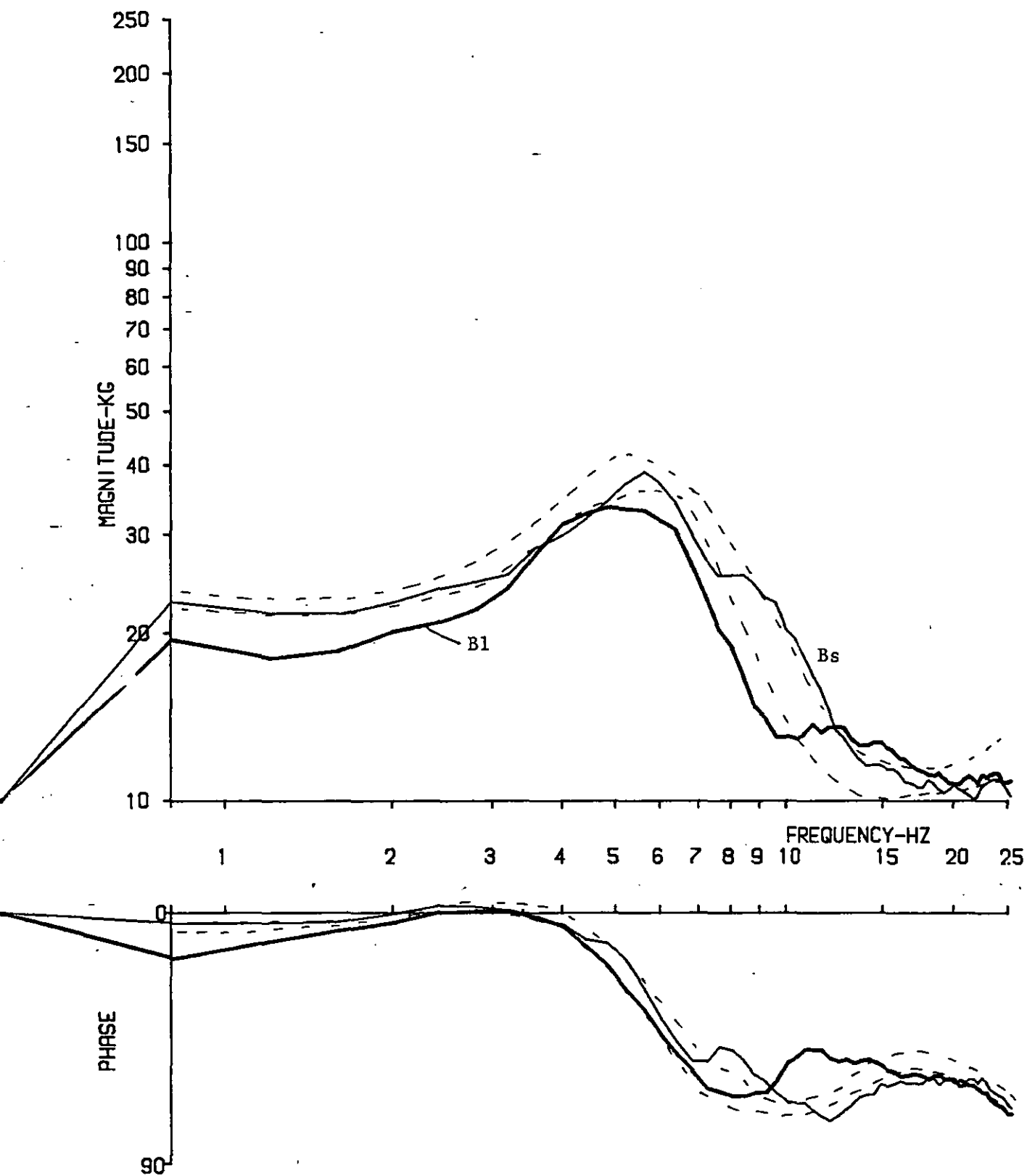
Fig. 7.44 Apparent mass feet: E/VE/S1



RUN NO. 01/04, 06

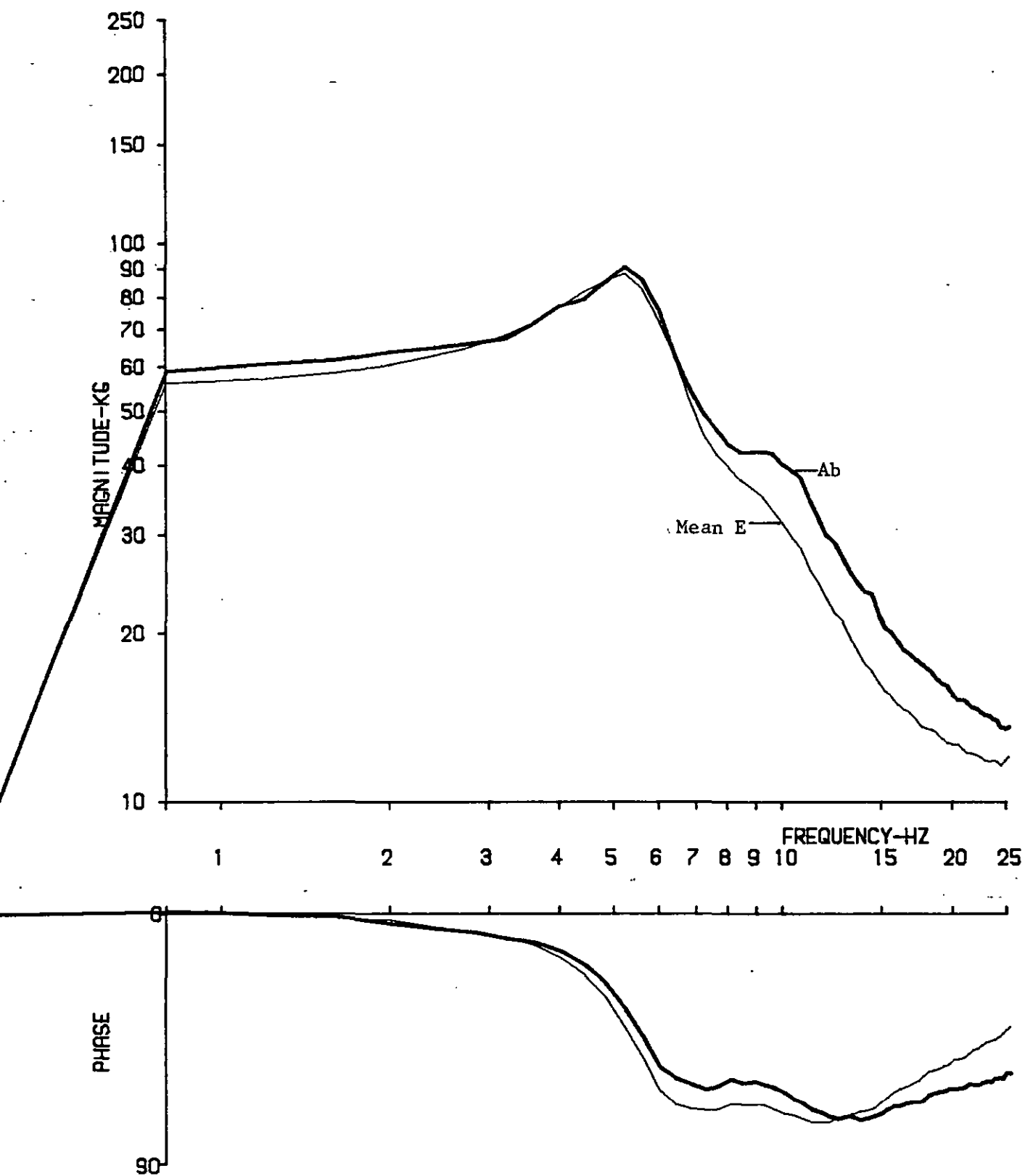
Fig. 7.45 Apparent mass: Mean E/Bs/B1





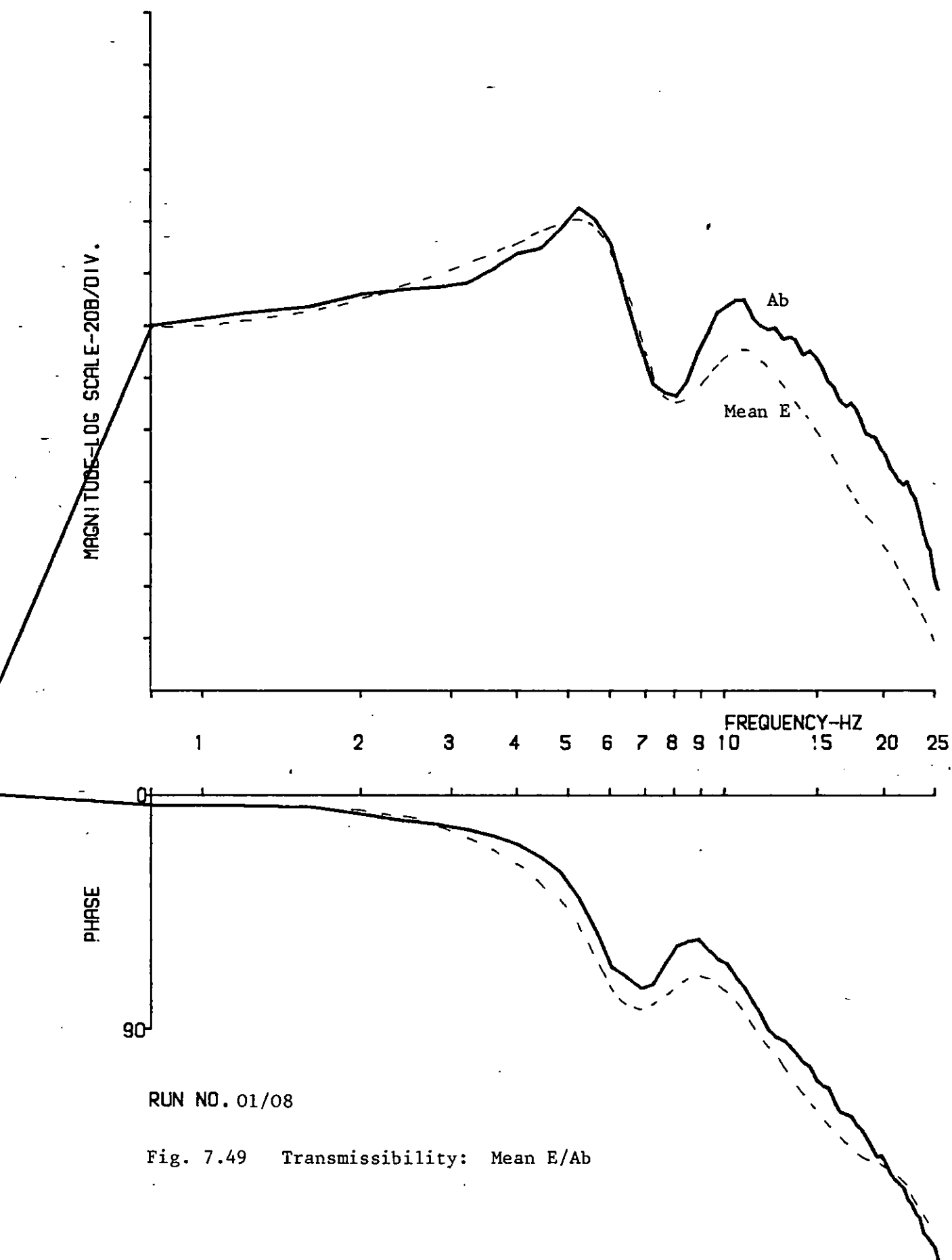
RUN NO. 01/04, 06

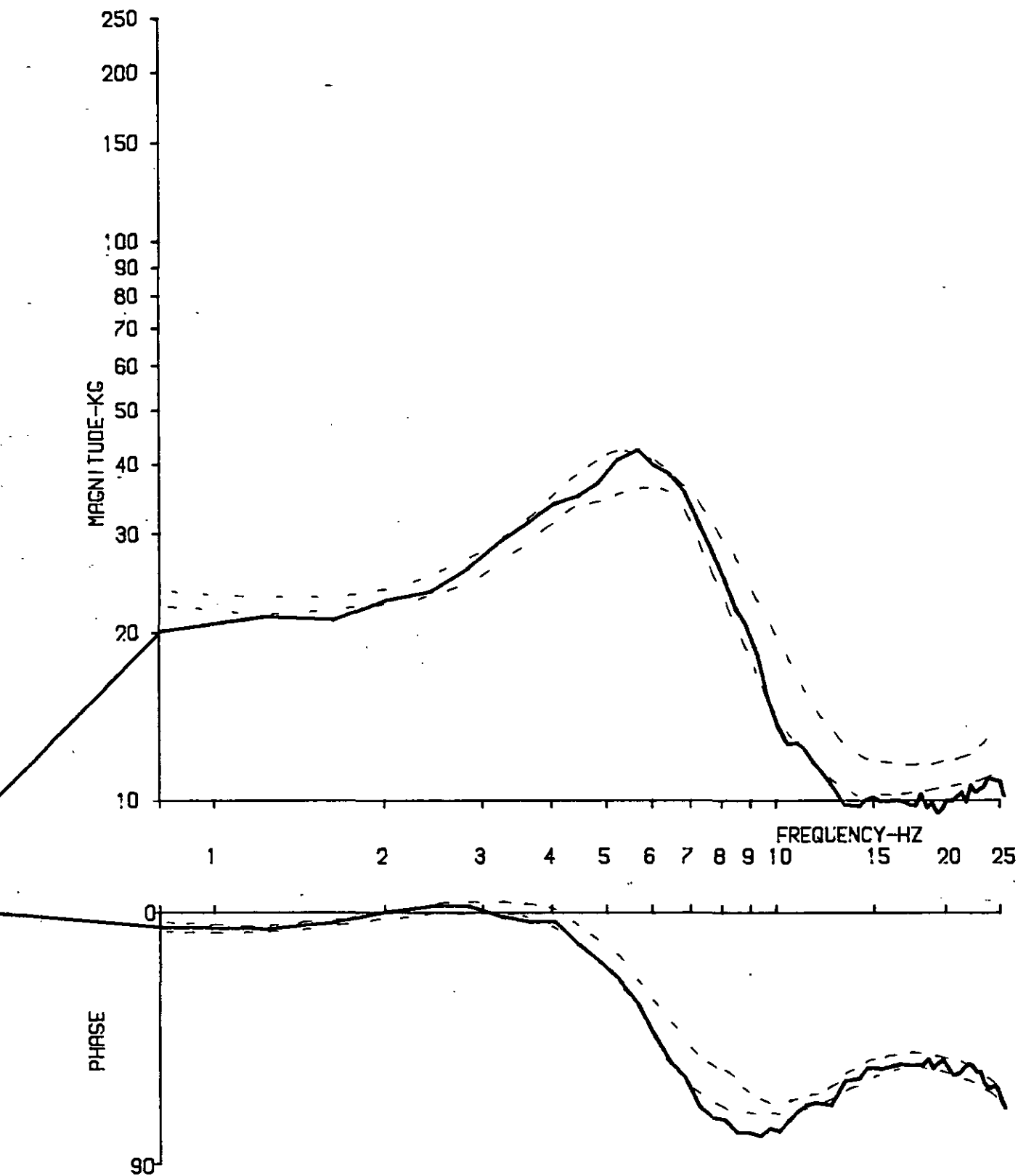
Fig. 7.47 Apparent mass feet: E/Bs/B1



RUN NO. 01/08

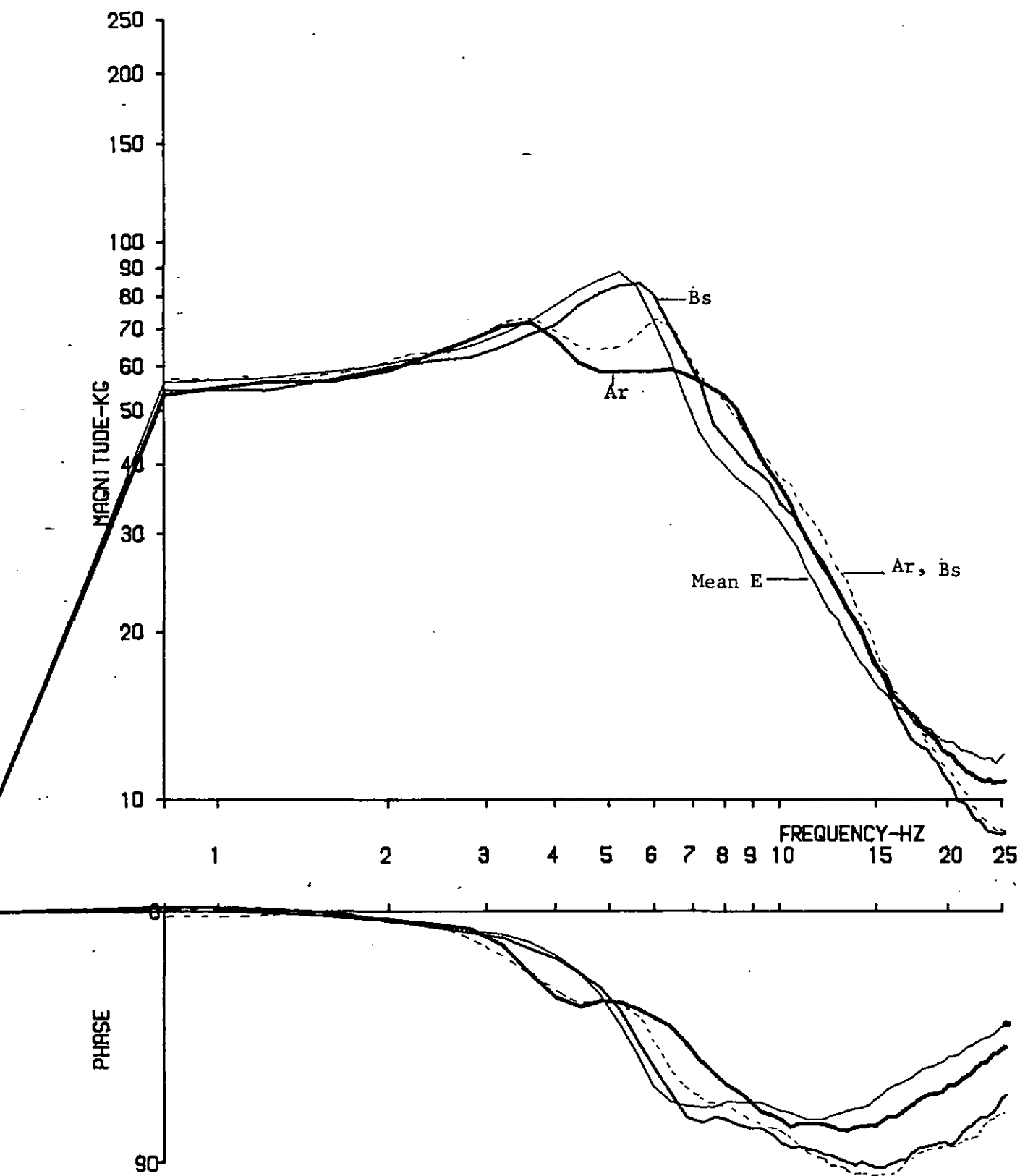
Fig. 7.48 Apparent mass: Mean E/Ab





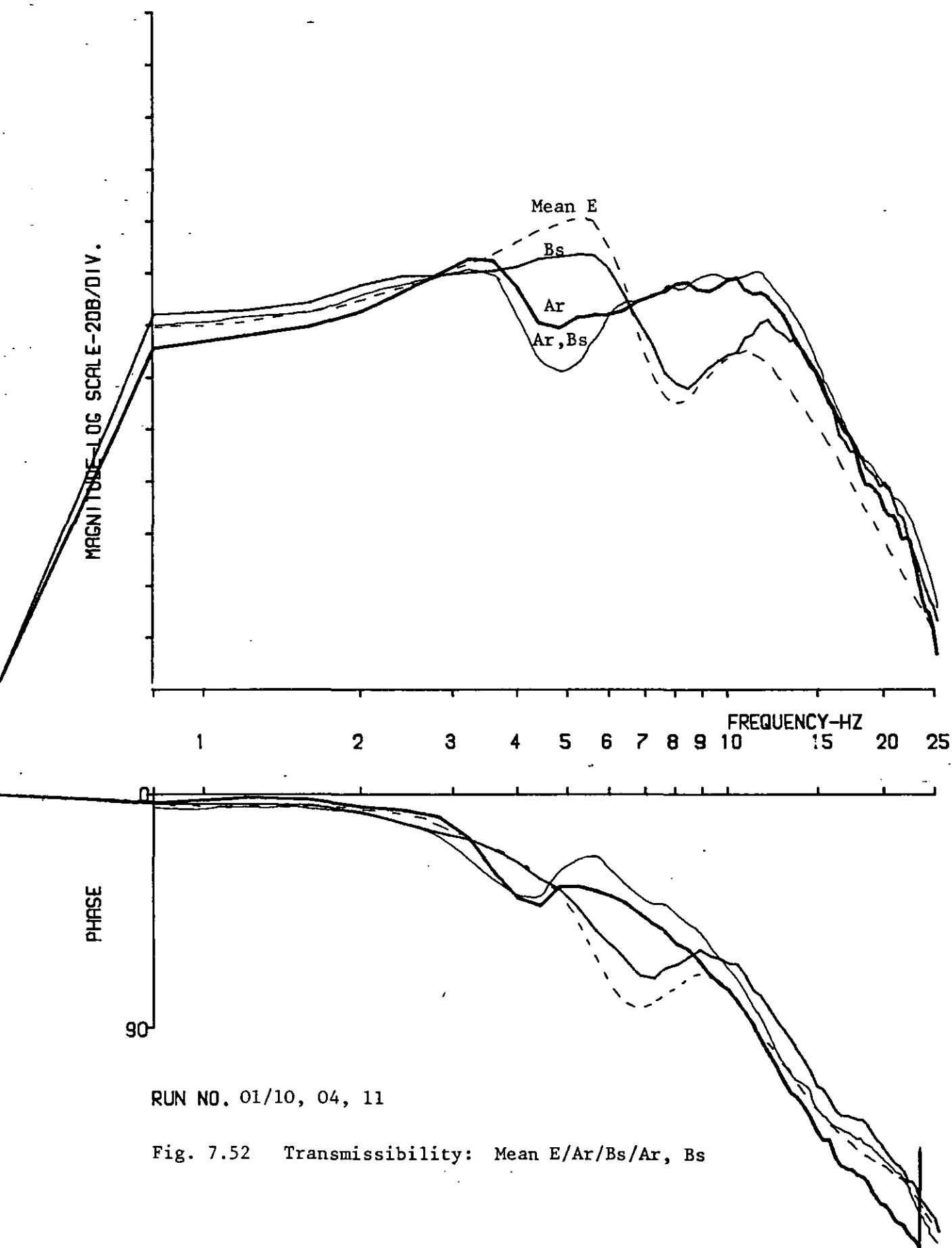
RUN NO. 01/08

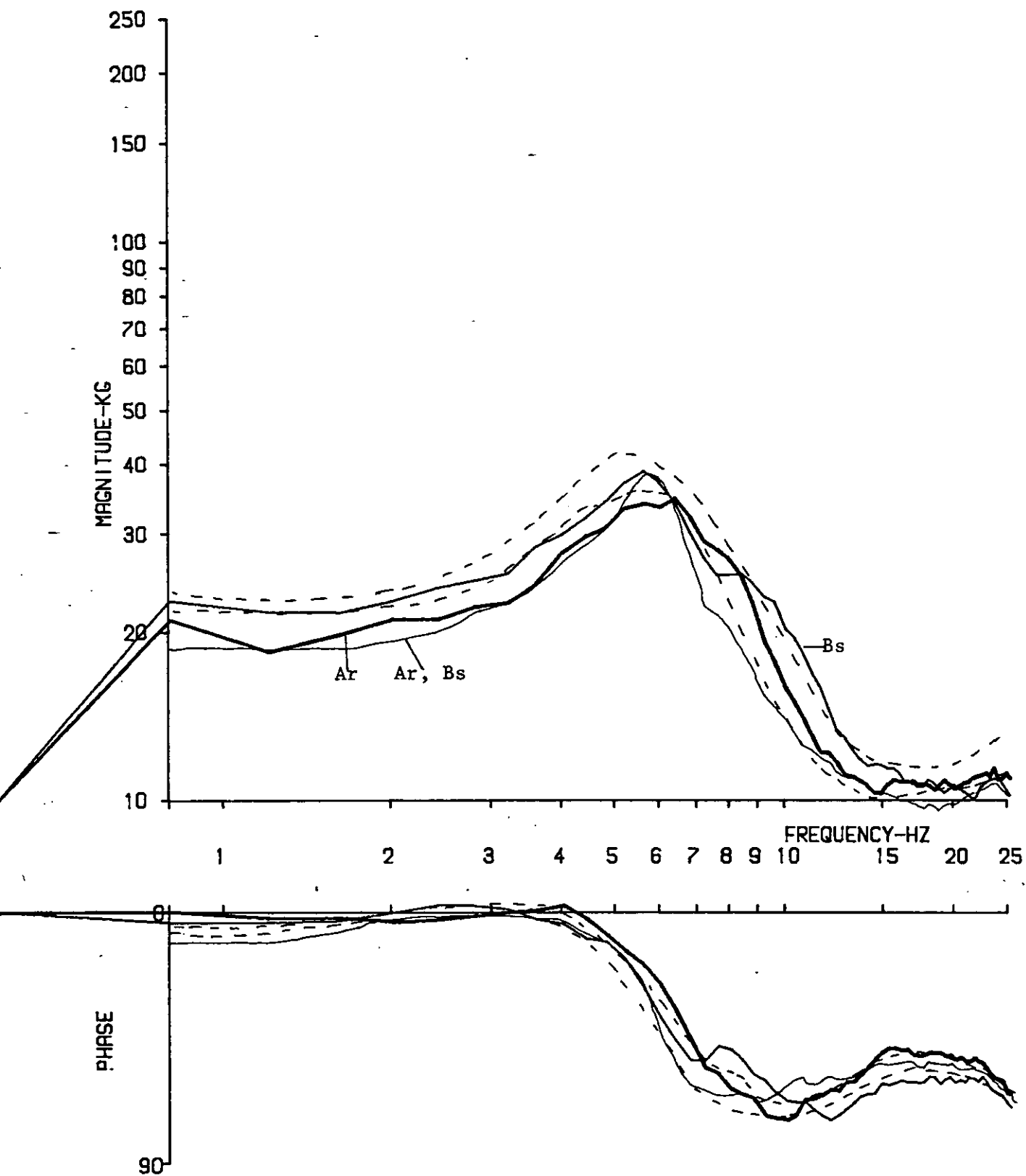
Fig. 7.50 Apparent mass feet: E/Ab



RUN NO. 01/10, 04, 11

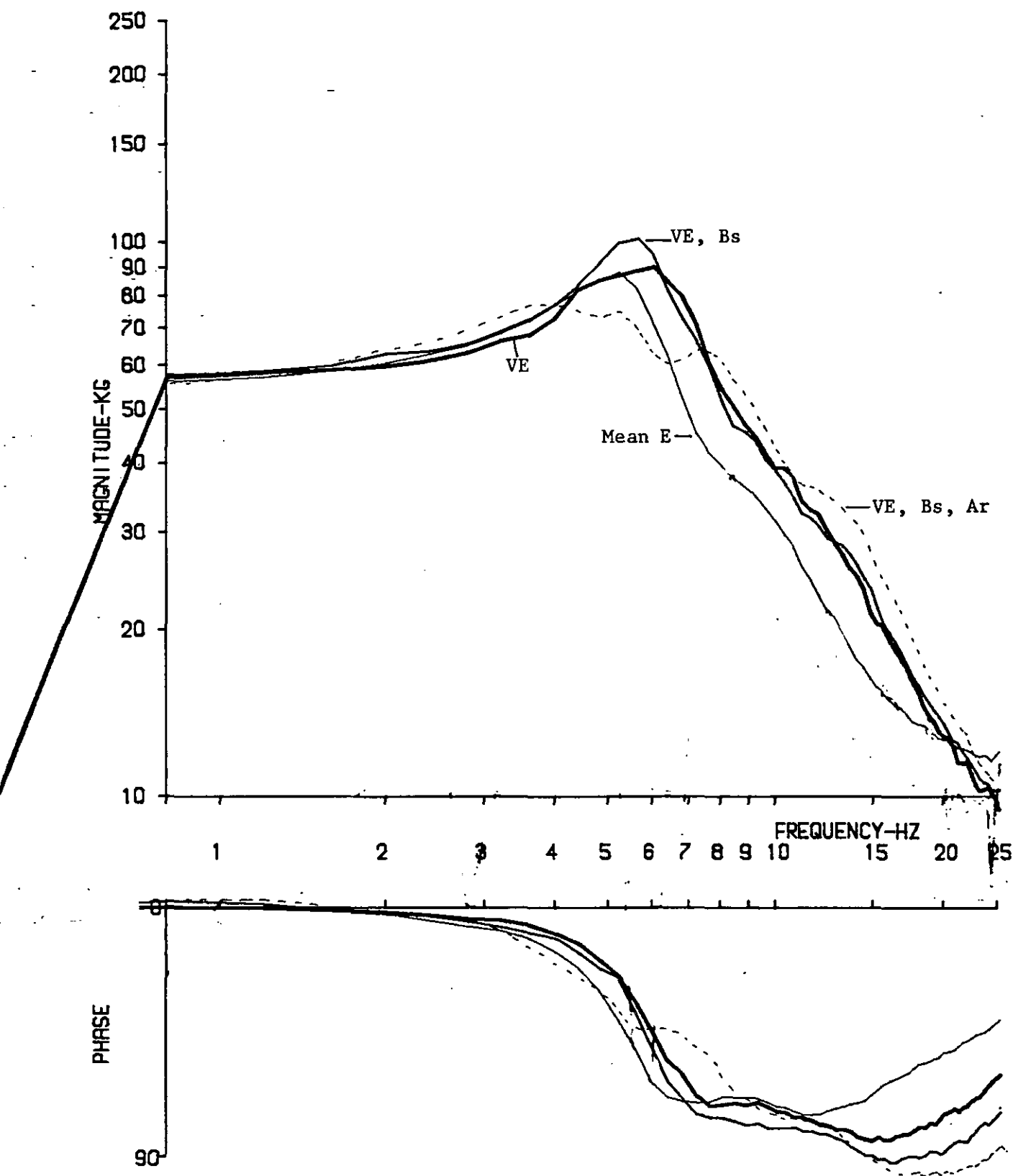
Fig. 8.51 Apparent mass: Mean E/Ar/Bs/Ar, Bs





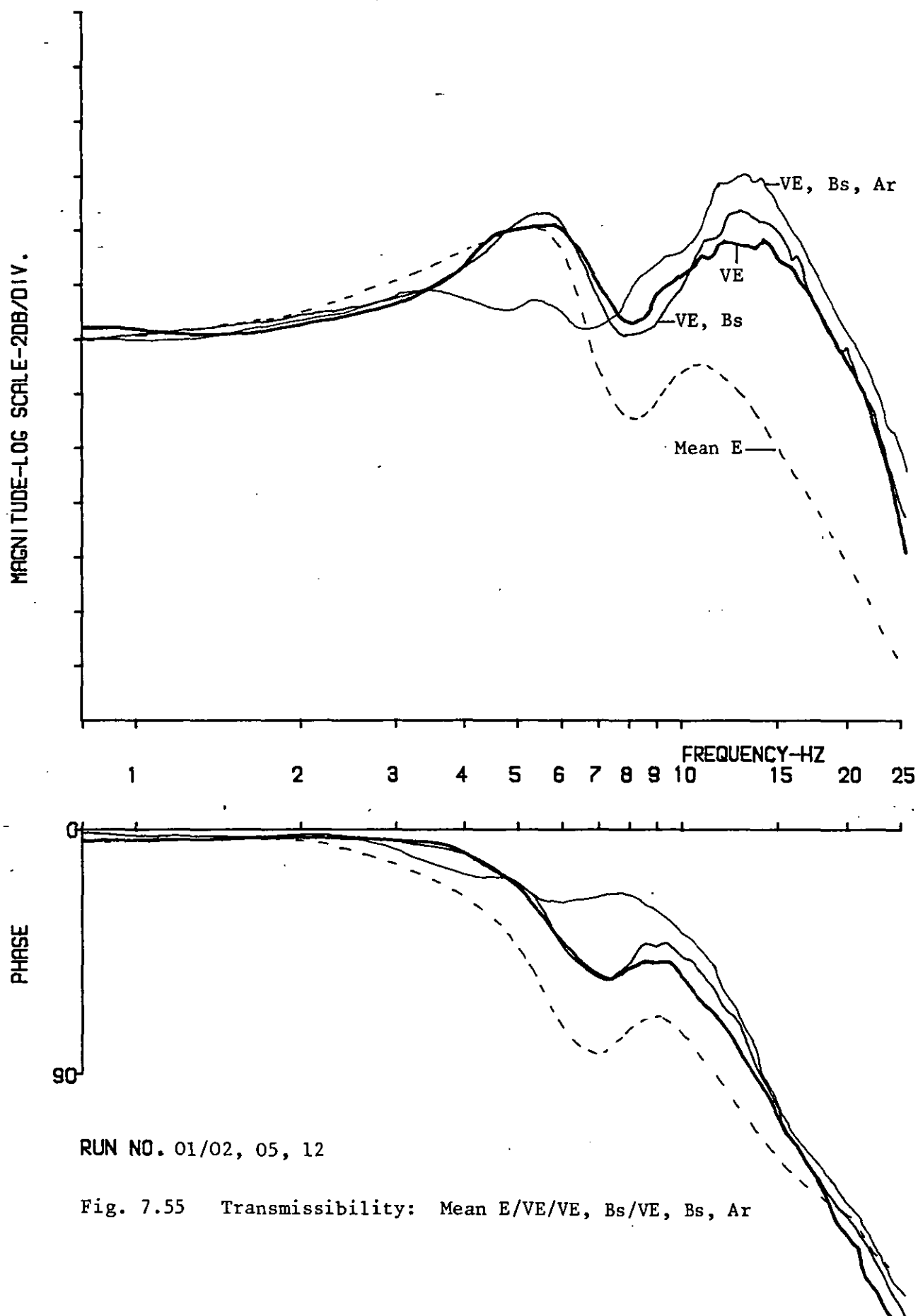
RUN NO. 01/10, 04, 11

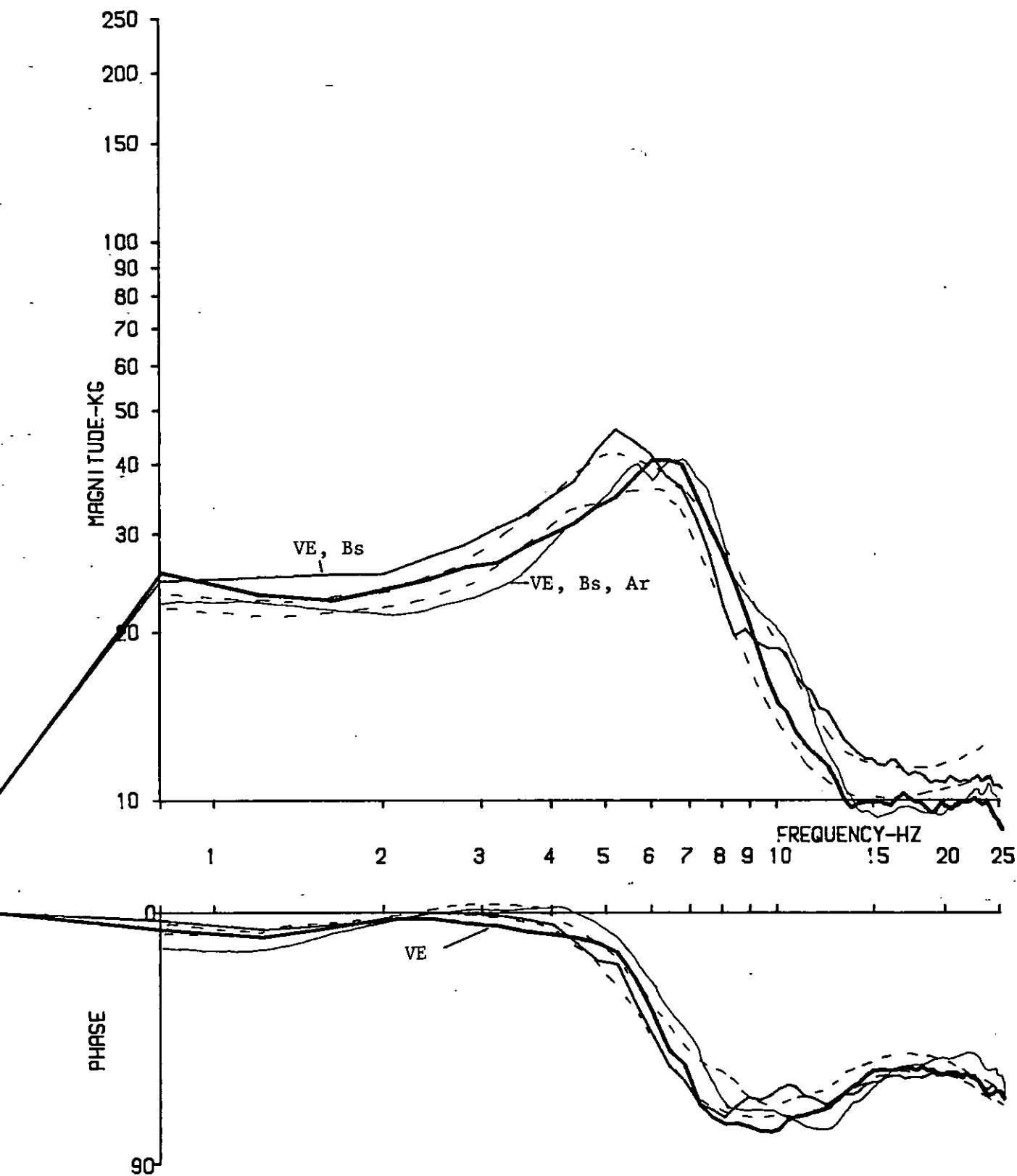
Fig. 7.53 Apparent mass feet: E/Ar/Bs/Ar, Bs



RUN NO. 01/02, 05, 12

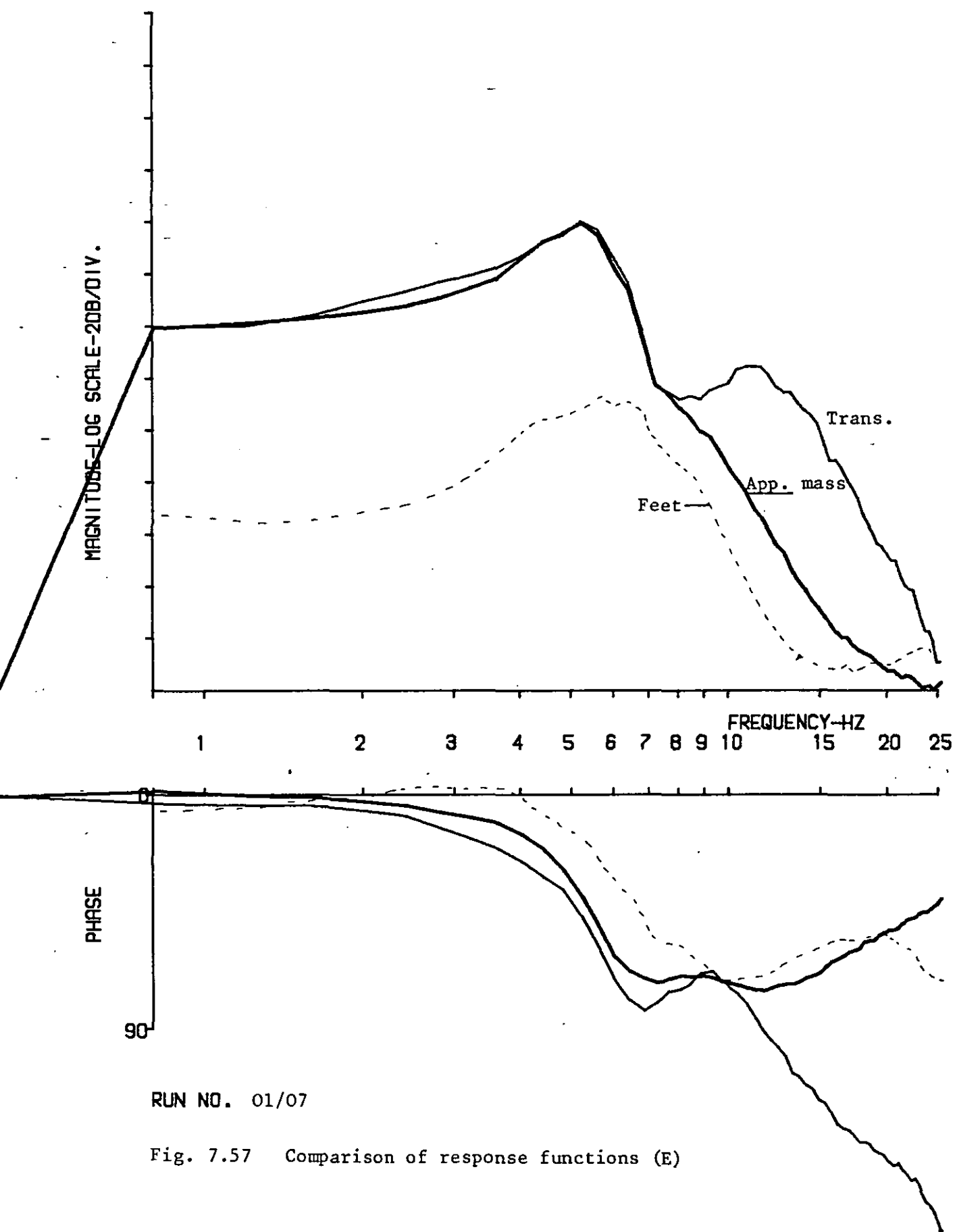
Fig. 7.54 Apparent mass: Mean E/VE/VE, Bs/VE, Bs, Ar





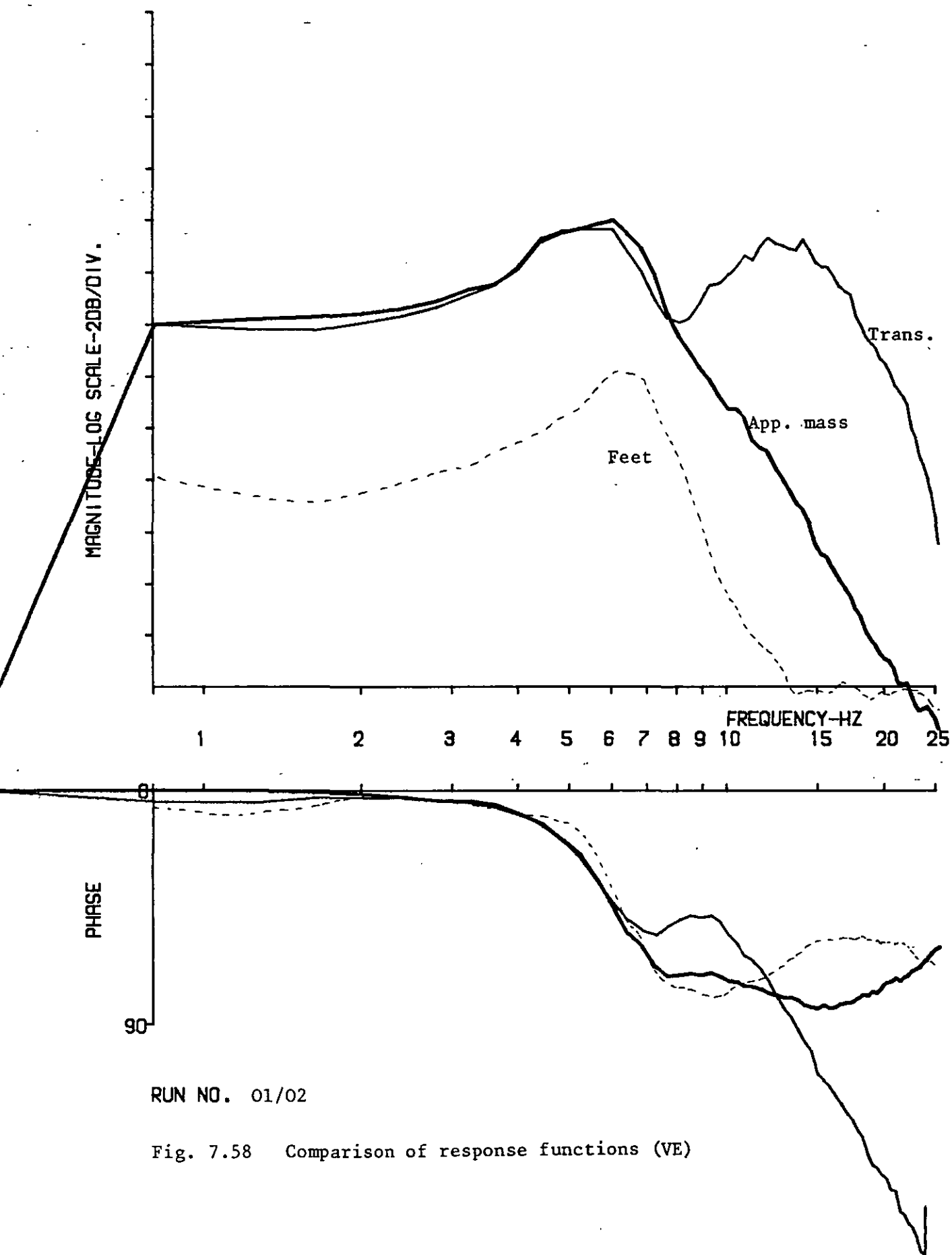
RUN NO. 01/02, 05, 12

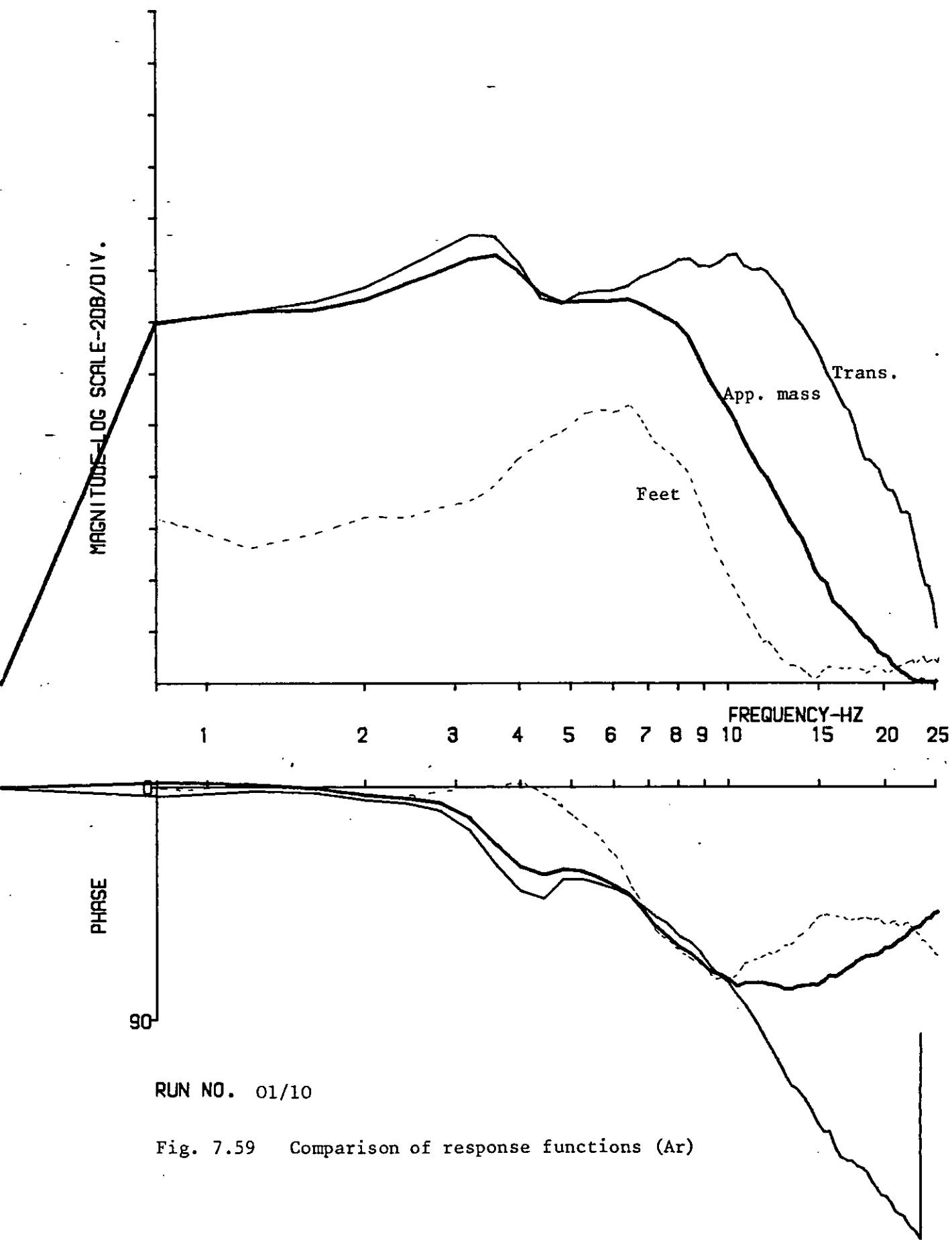
Fig. 7.56 Apparent mass feet: E/VE/VE, Bs/VE, Bs, Ar

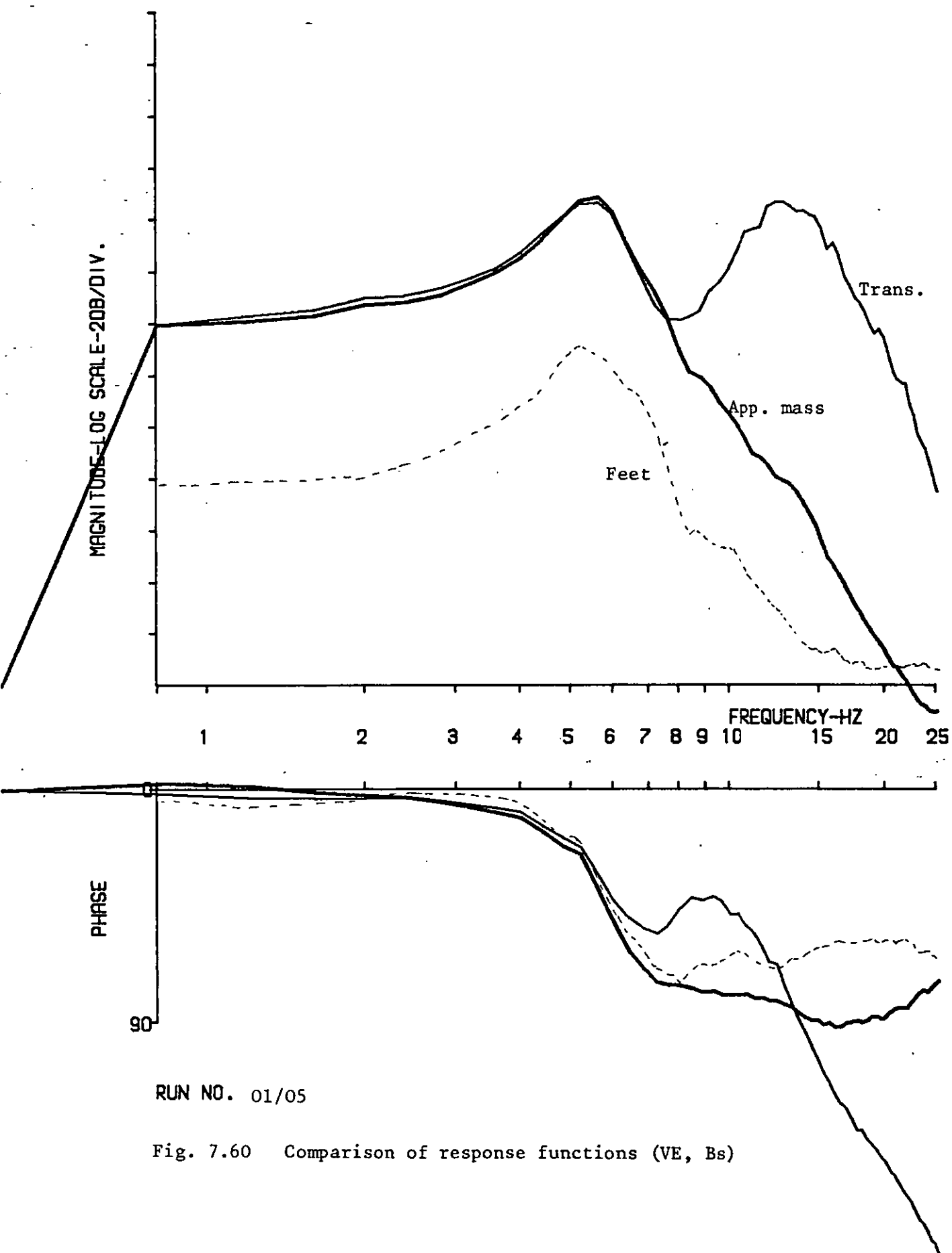


RUN NO. 01/07

Fig. 7.57 Comparison of response functions (E)

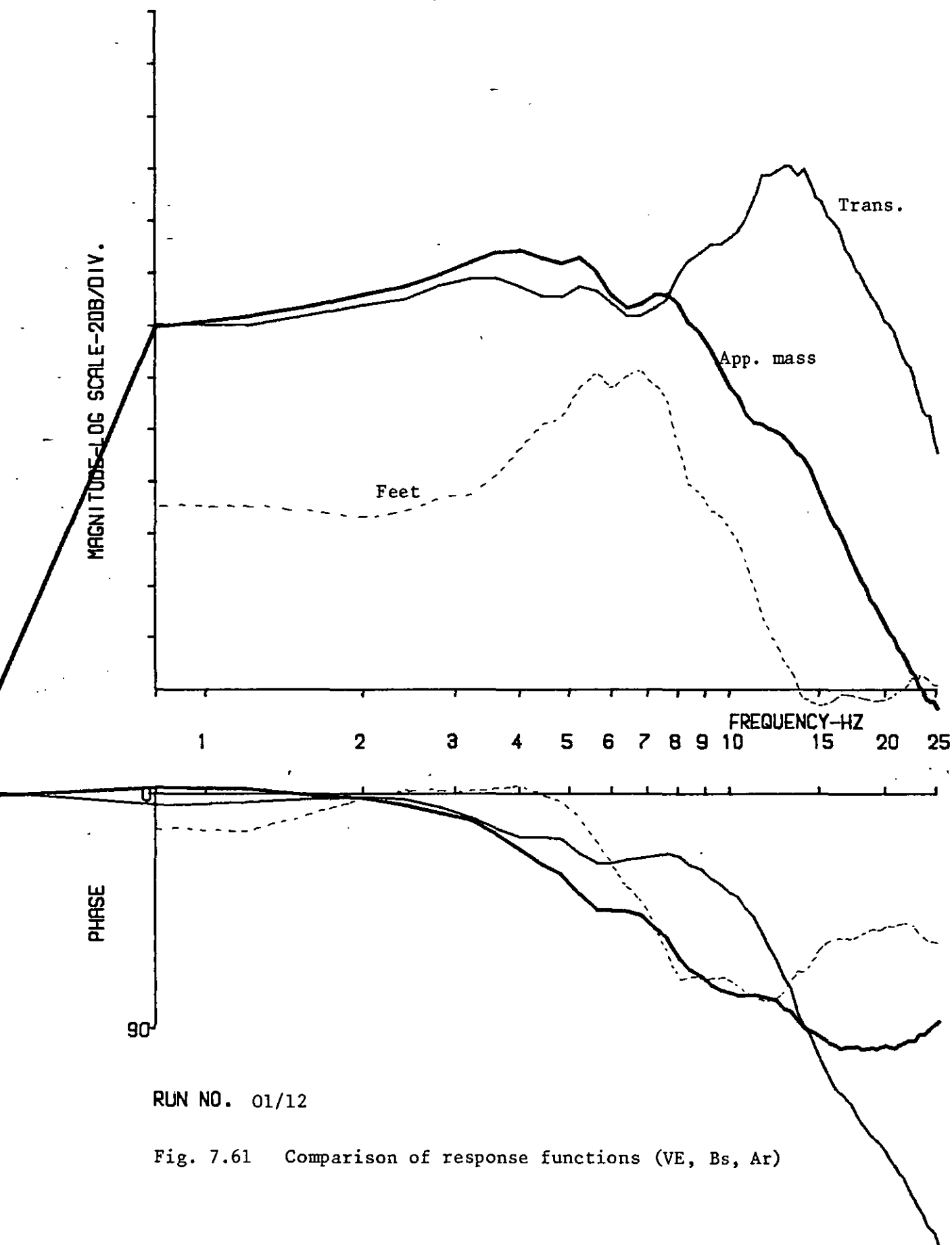


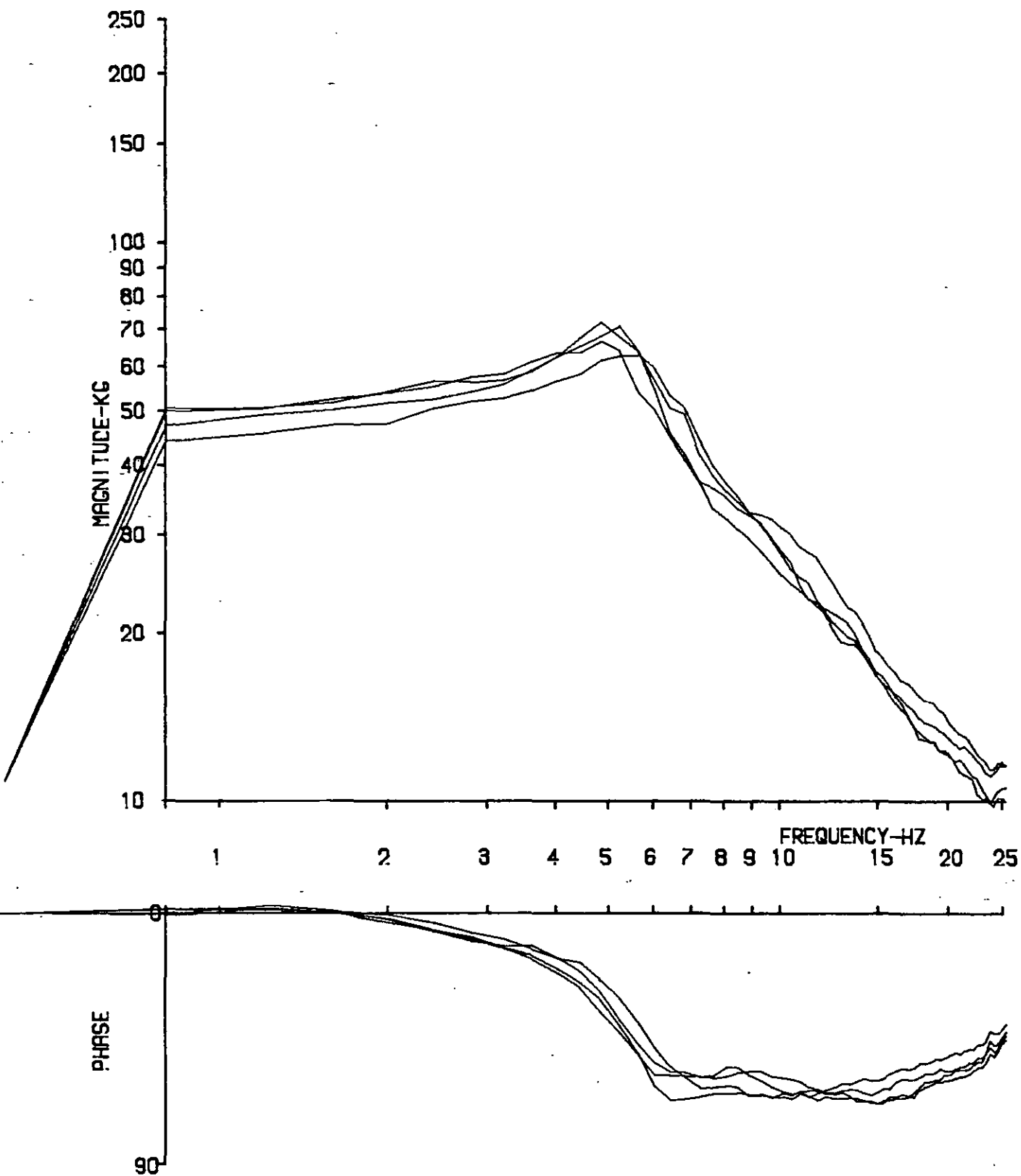




RUN NO. 01/05

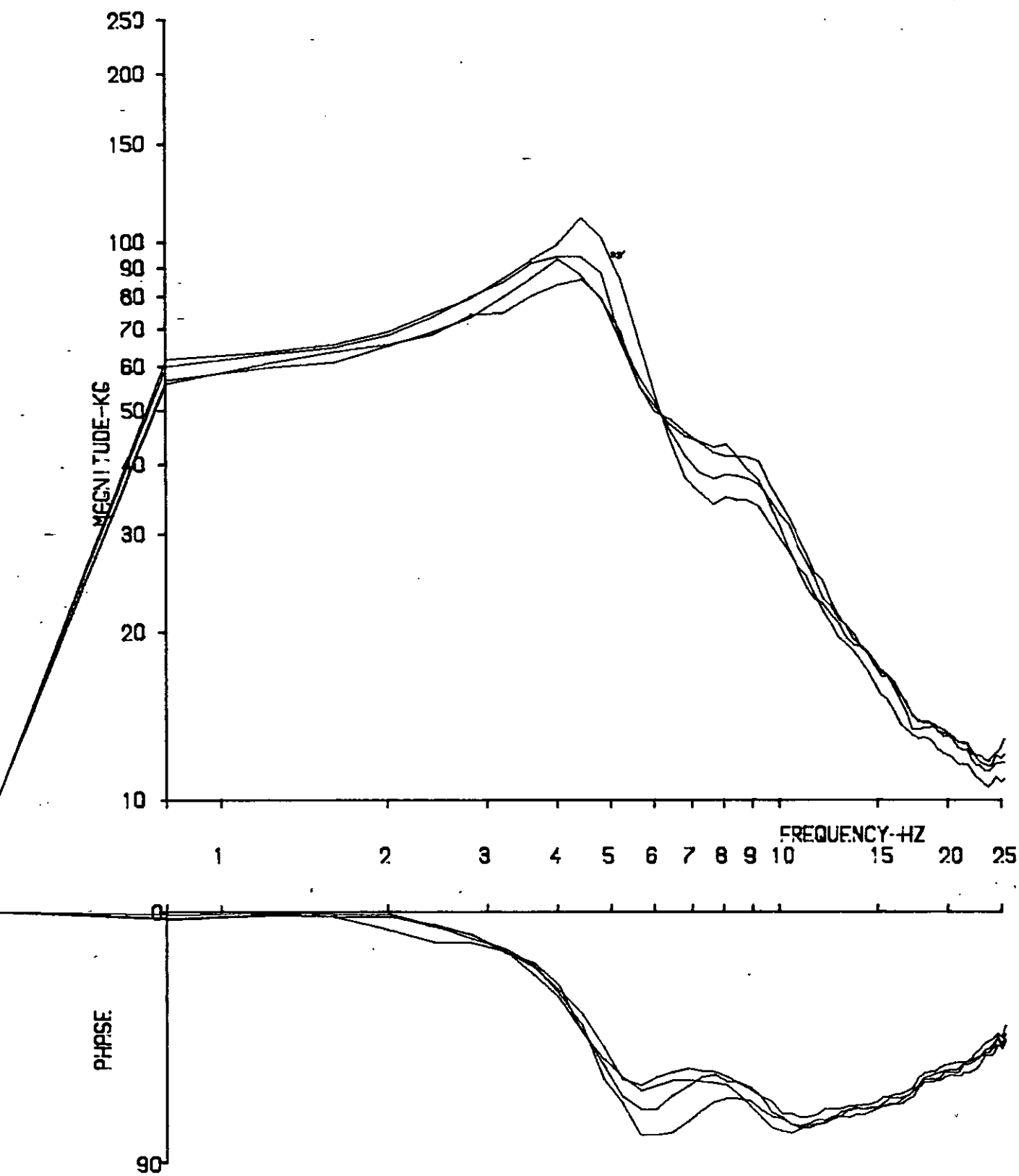
Fig. 7.60 Comparison of response functions (VE, Bs)





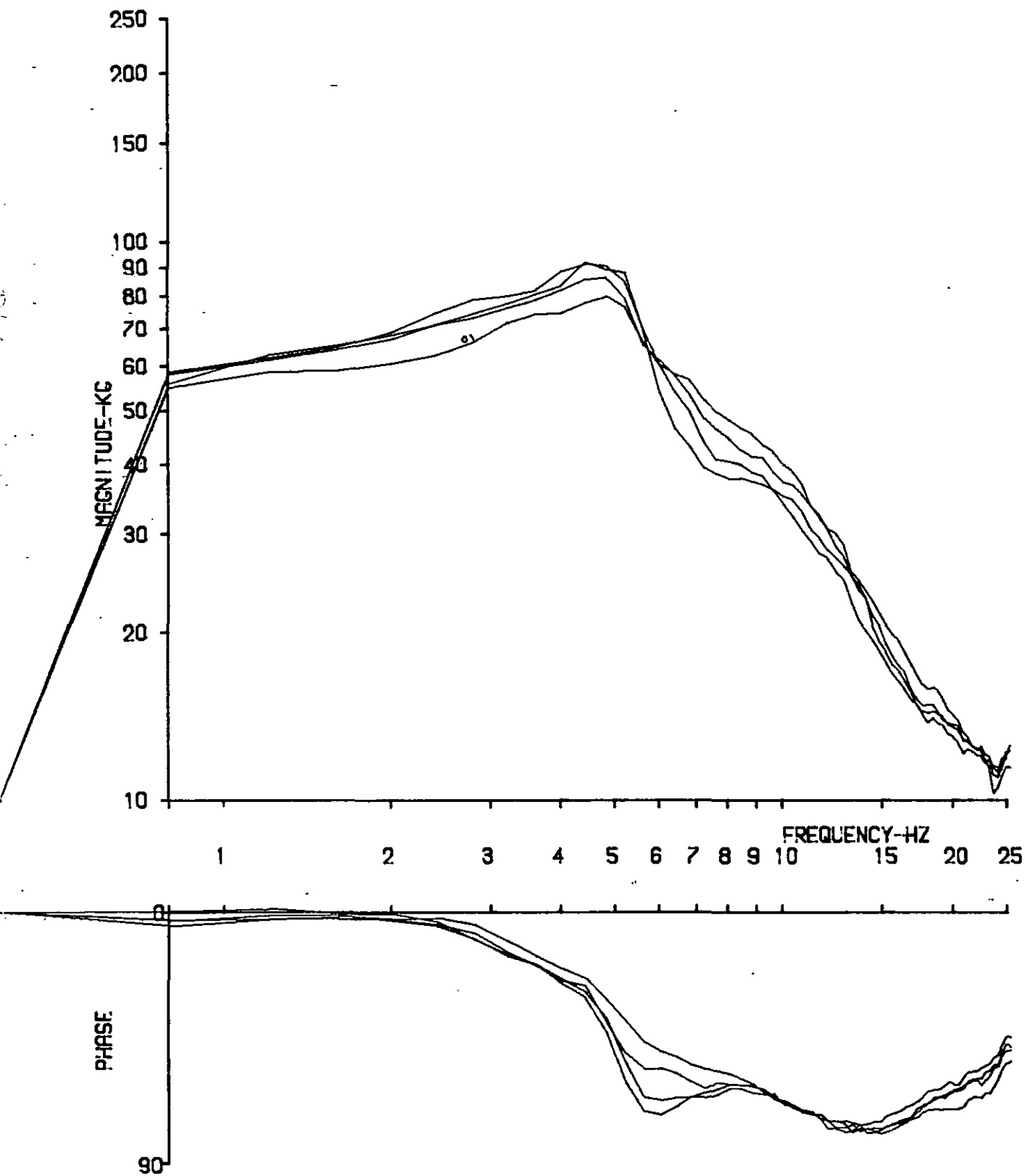
RUN NO.81/01, 06, 08, 11

Fig. 7.62 Apparent Mass: 4 x E



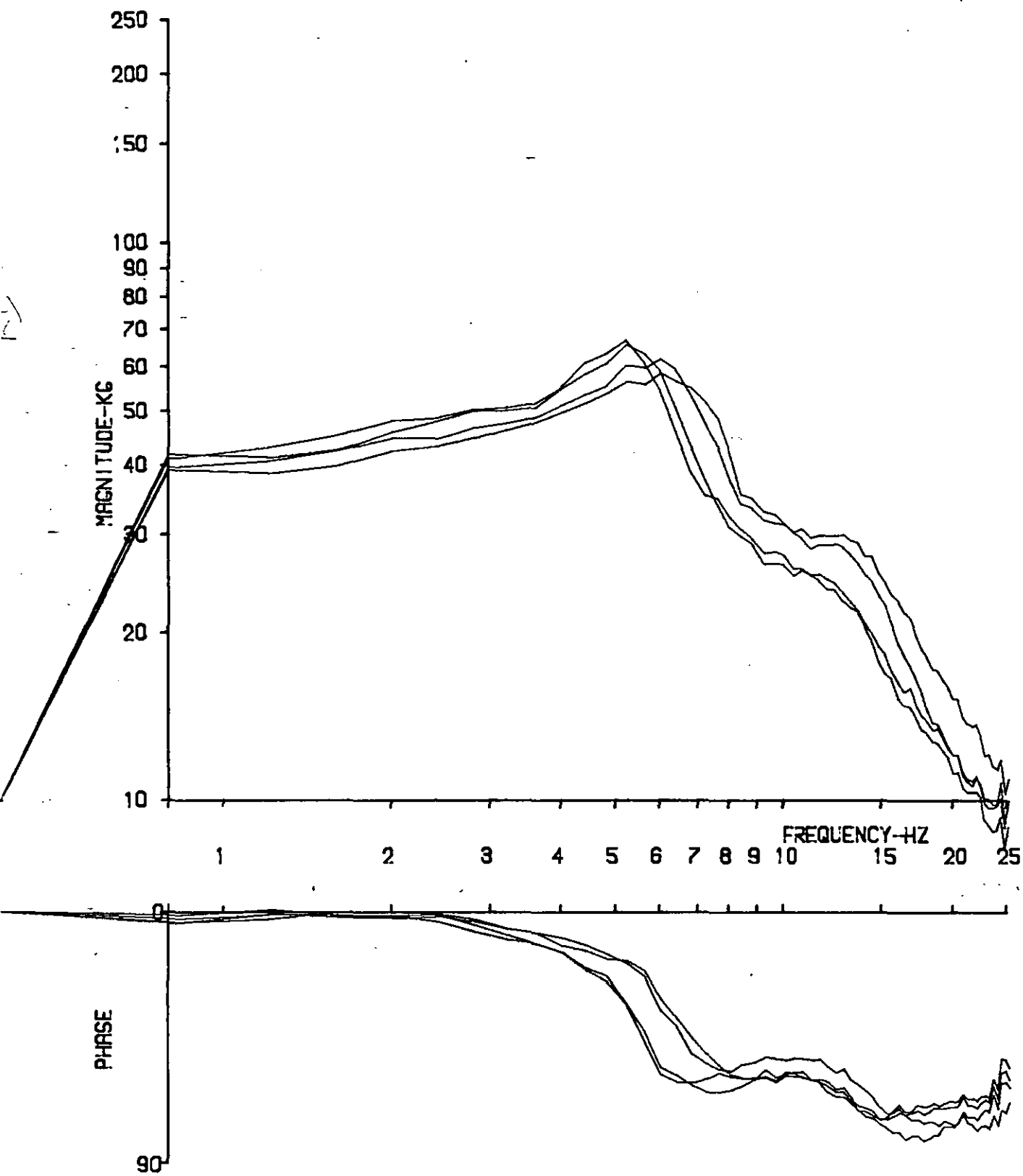
RUN NO. 82/03, 06, 08, 14

Fig. 7.63



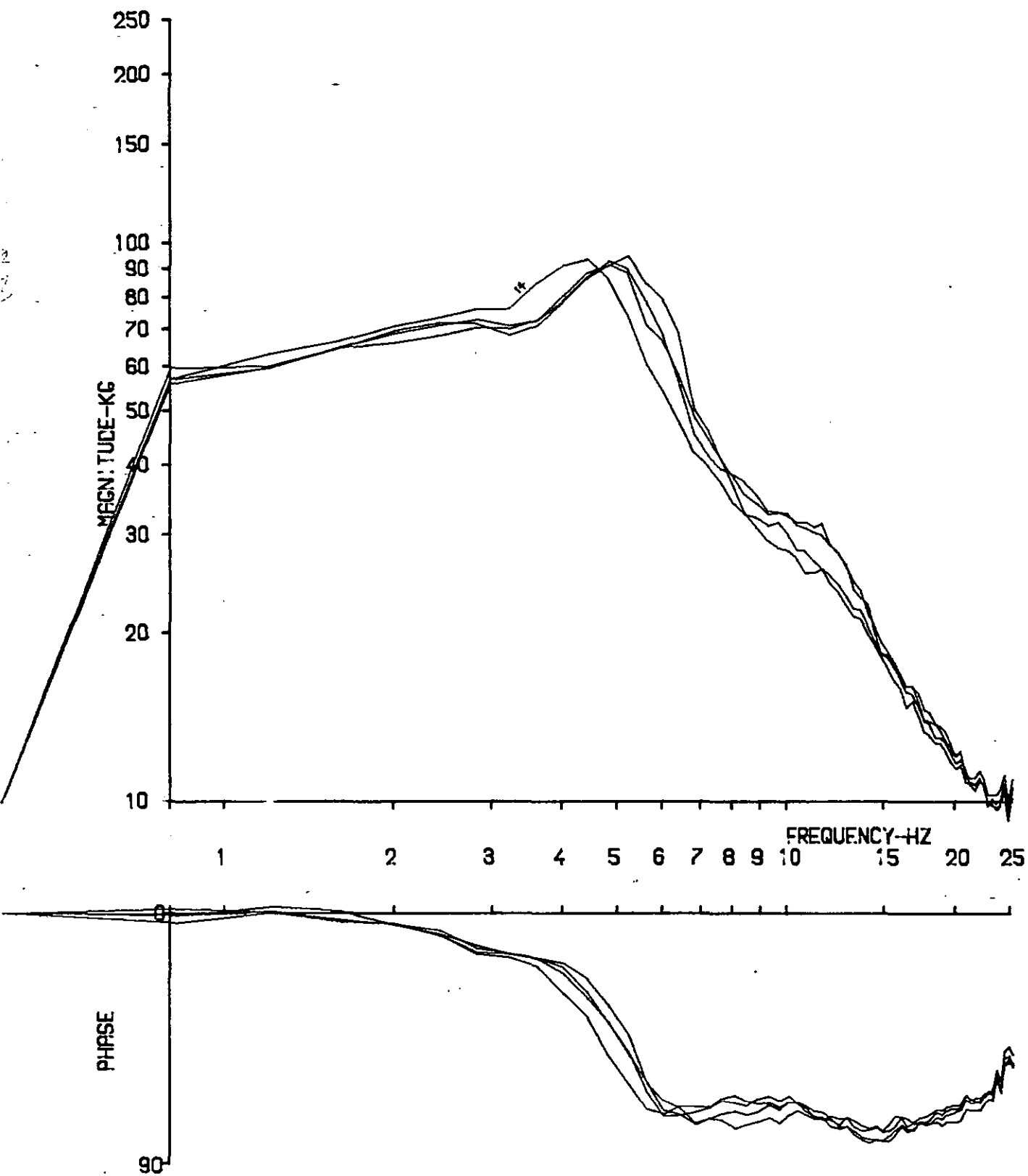
RUN NO. 85/01, 07, 09, 12

Fig. 7.64



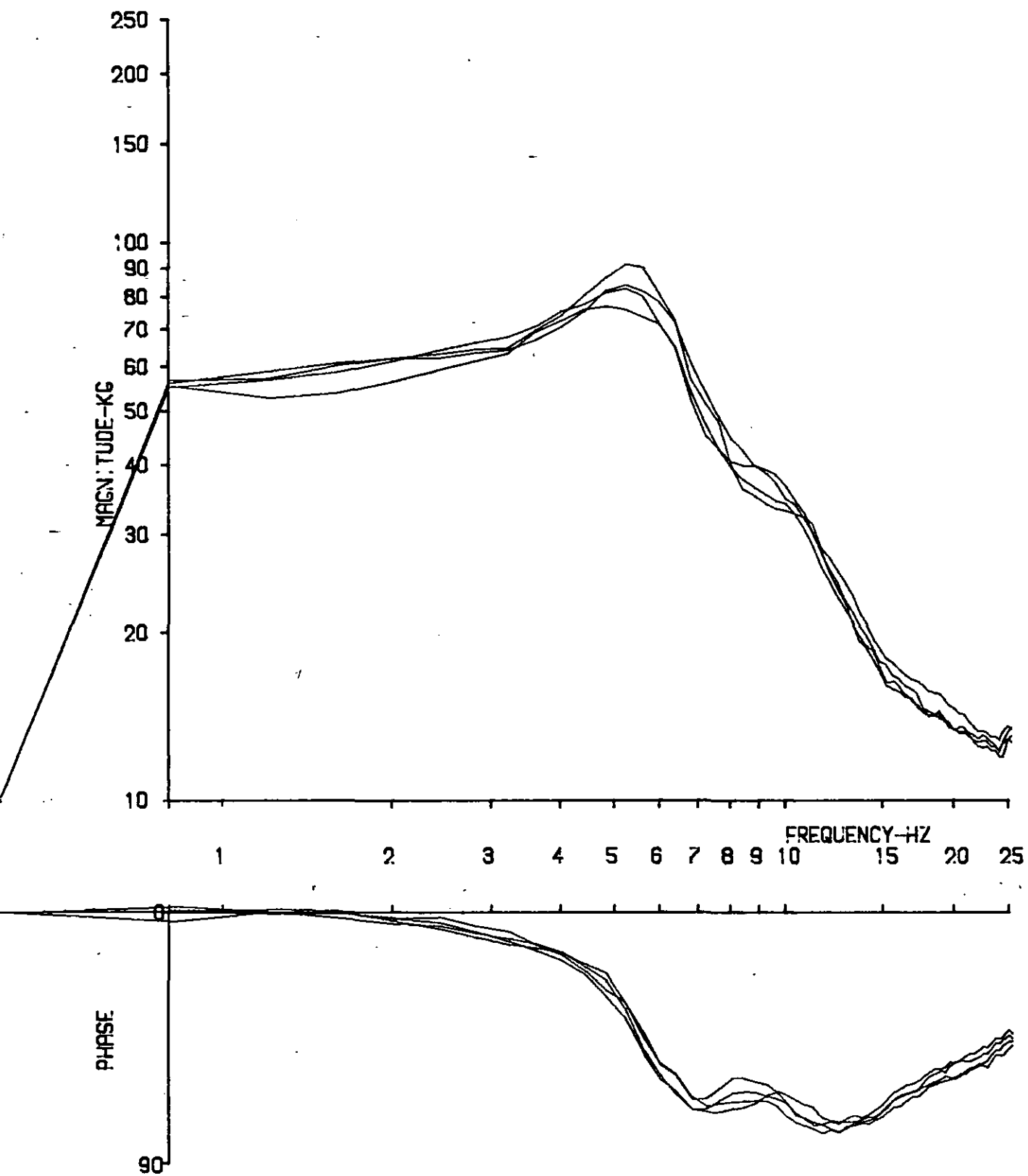
RUN NO. 84/03, 06, 08, 14

Fig. 7.65



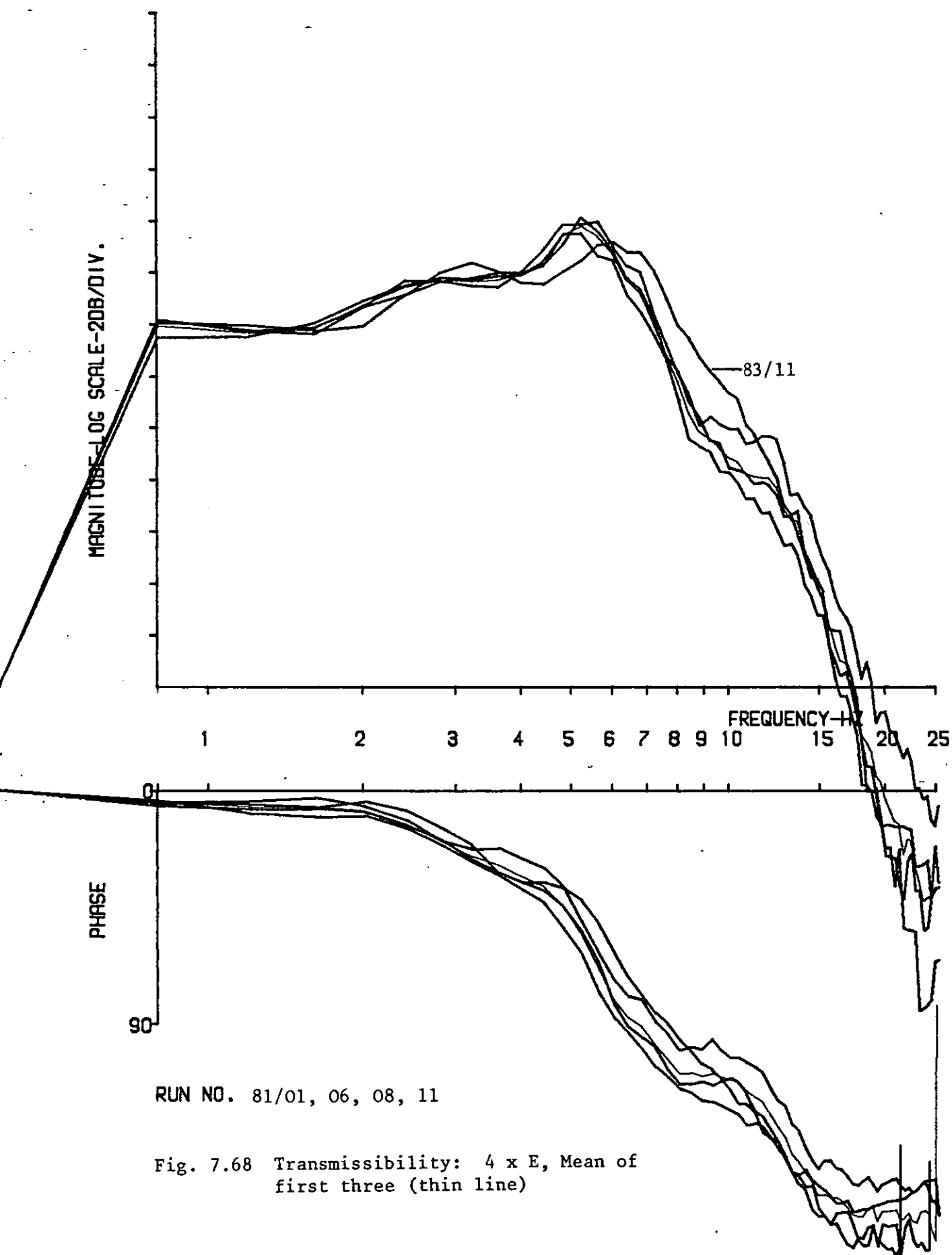
RUN NO. 83/02, 05, 08, 14

Fig. 7.66



RUN NO. 01/01, 07, 10, 13

Fig. 7.67



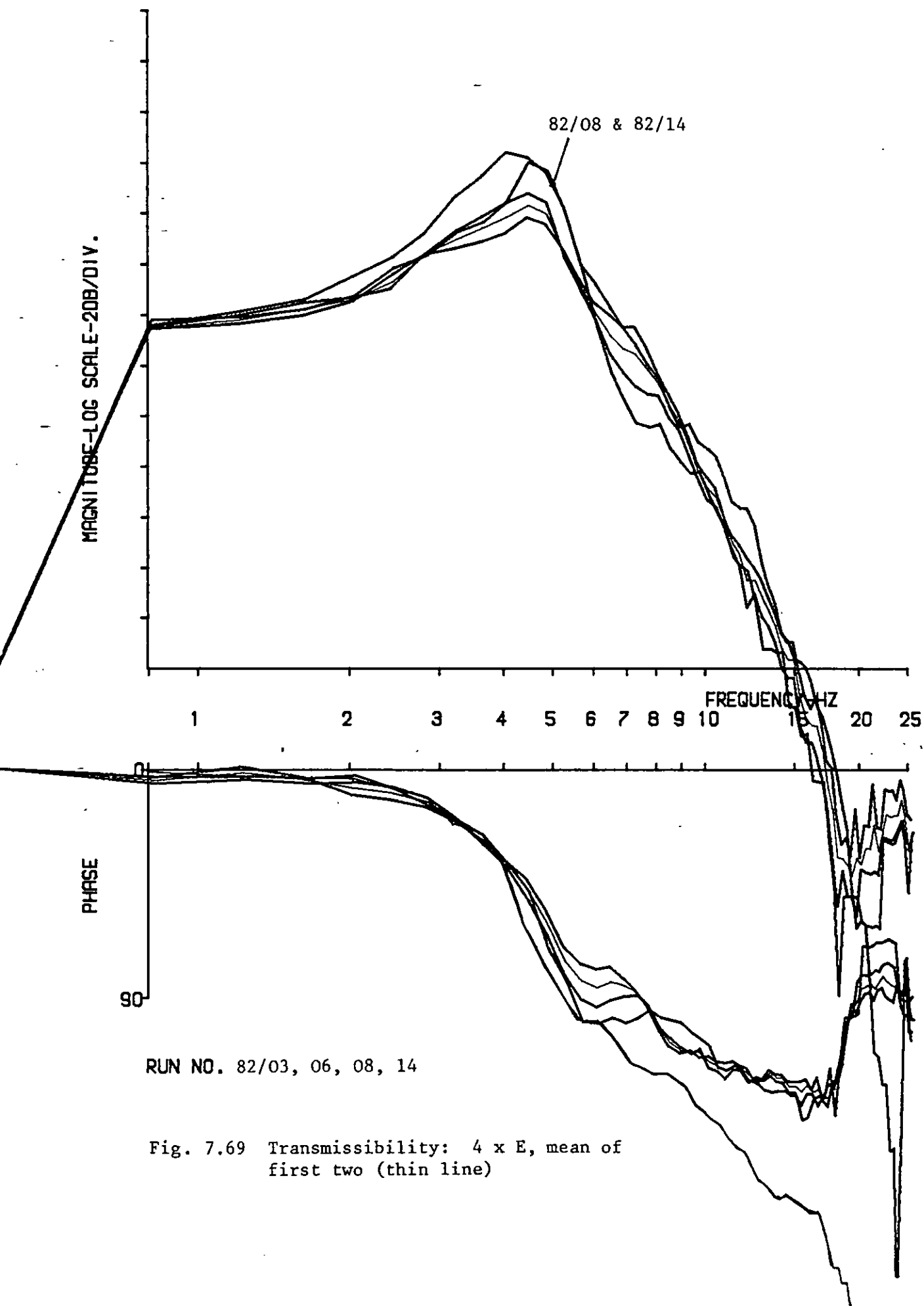
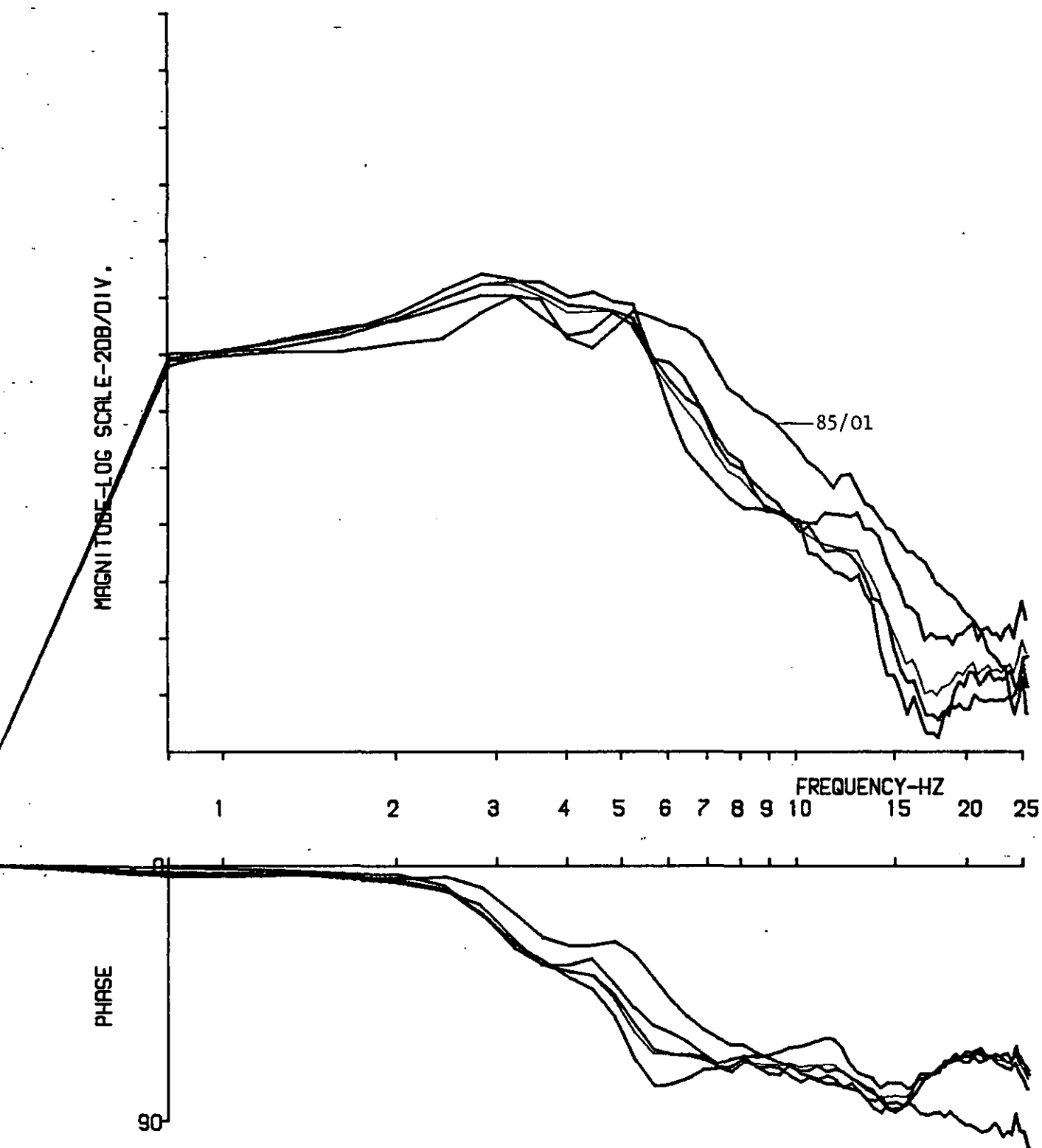
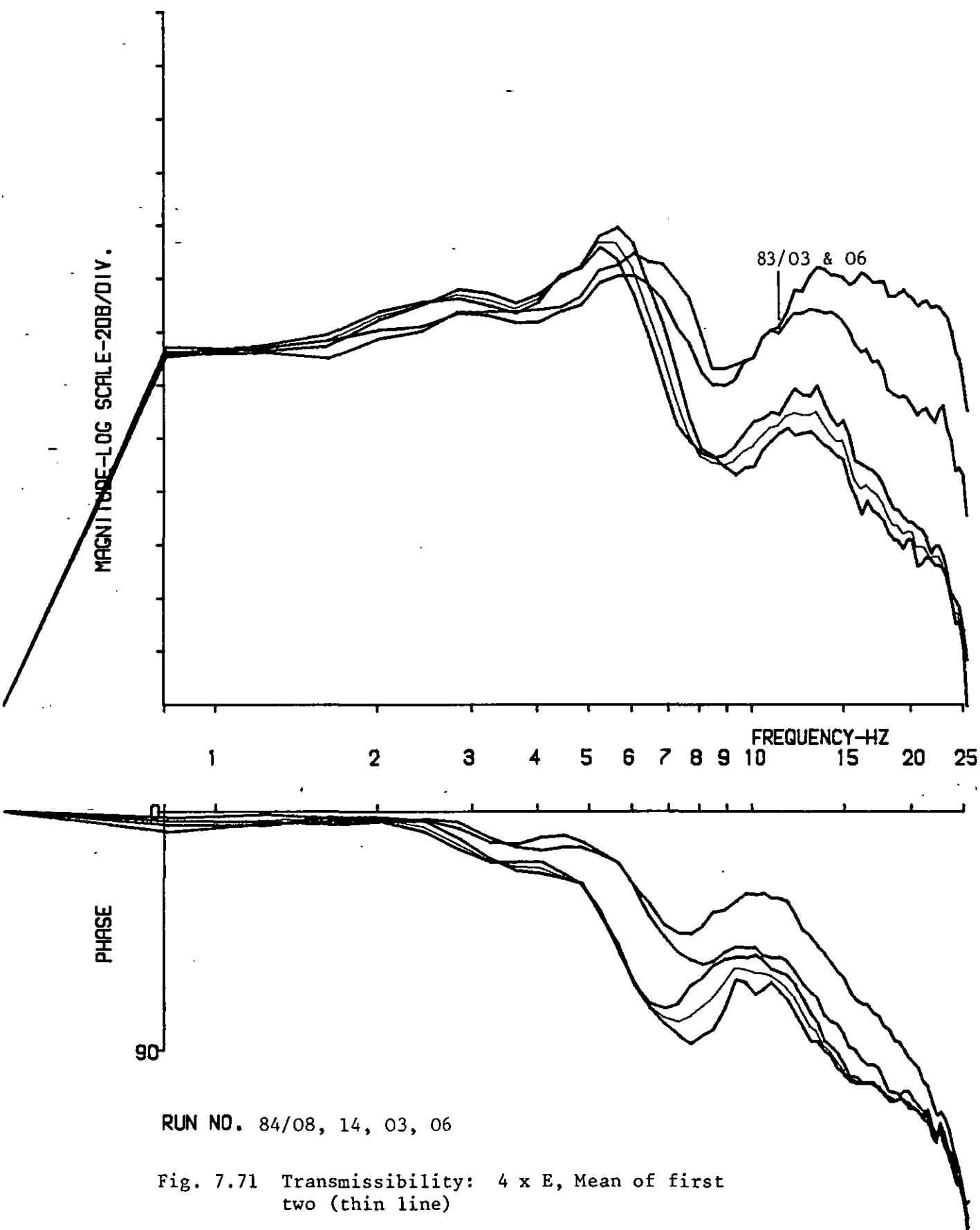


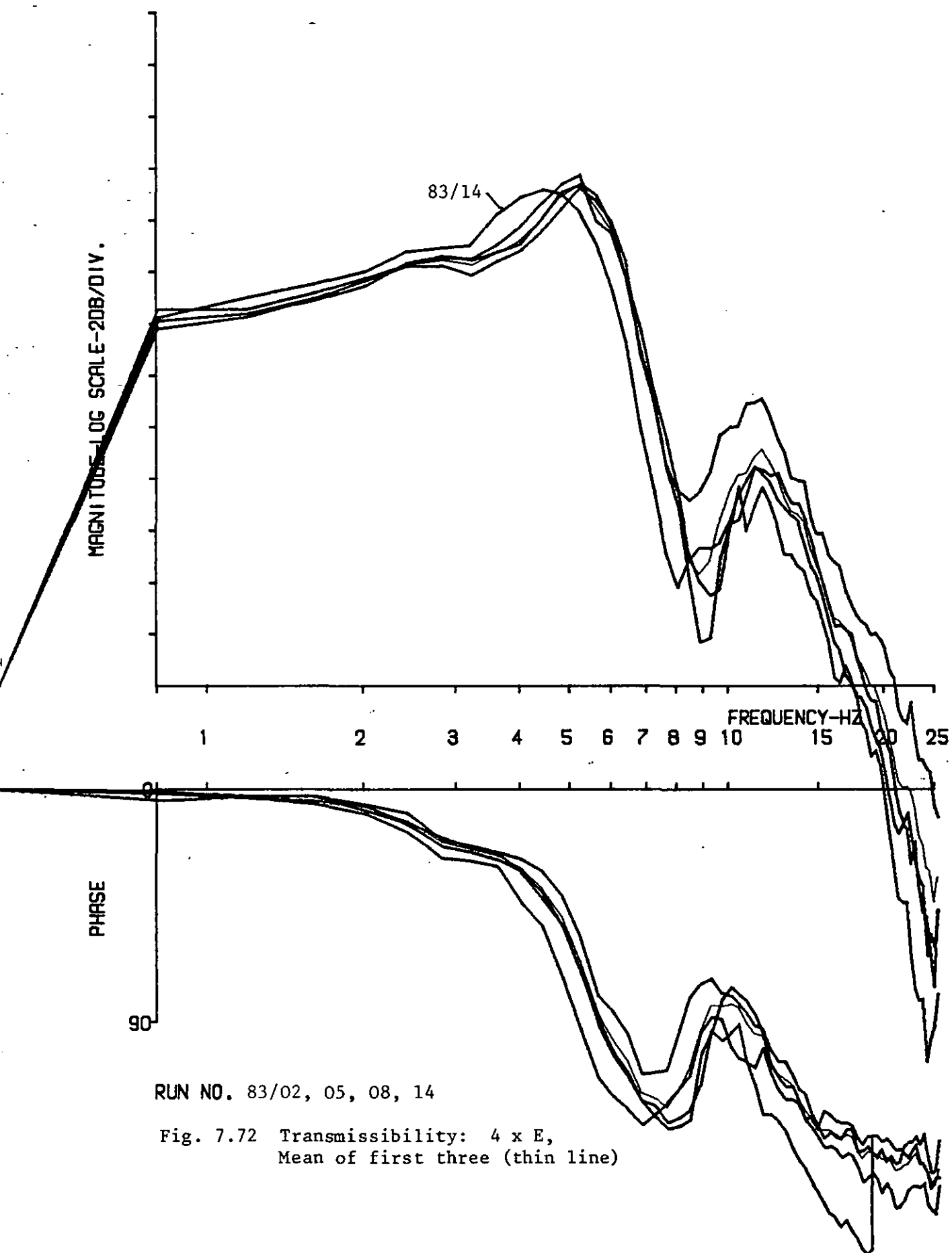
Fig. 7.69 Transmissibility: $4 \times E$, mean of first two (thin line)

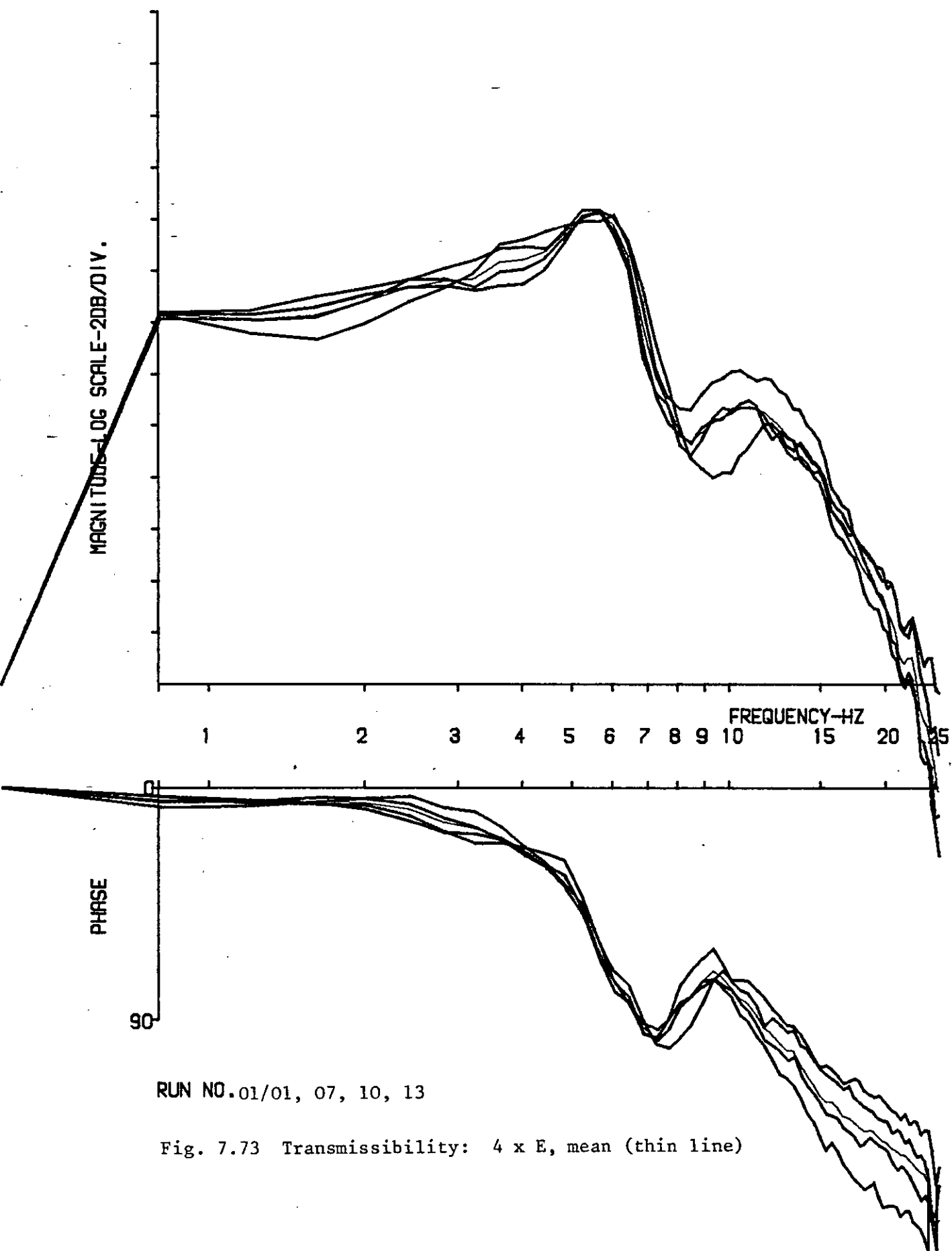


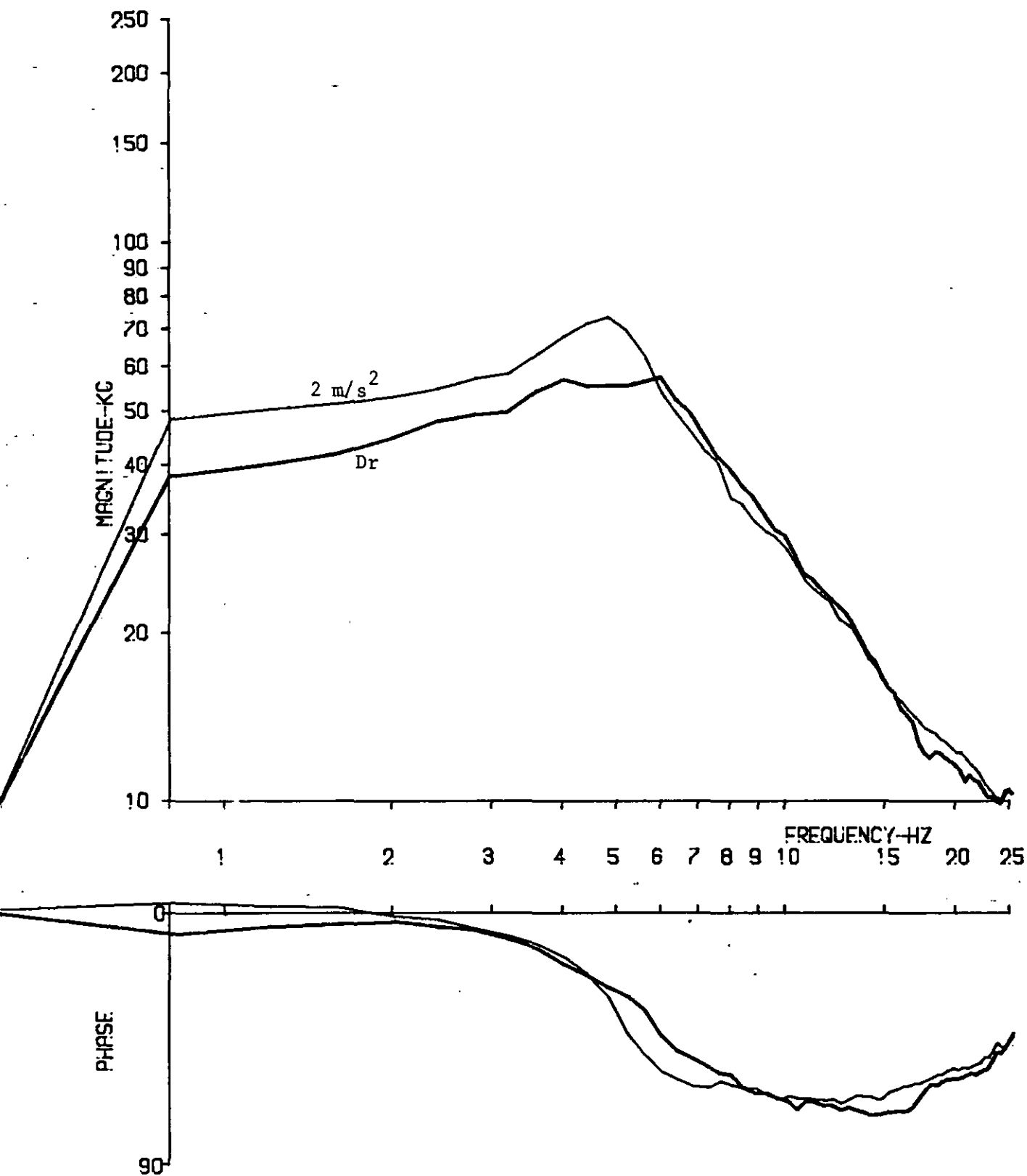
RUN NO. 85/07, 09, 12, 01

Fig. 7.70 Transmissibility: 4 x E, Mean of first three (thin line)



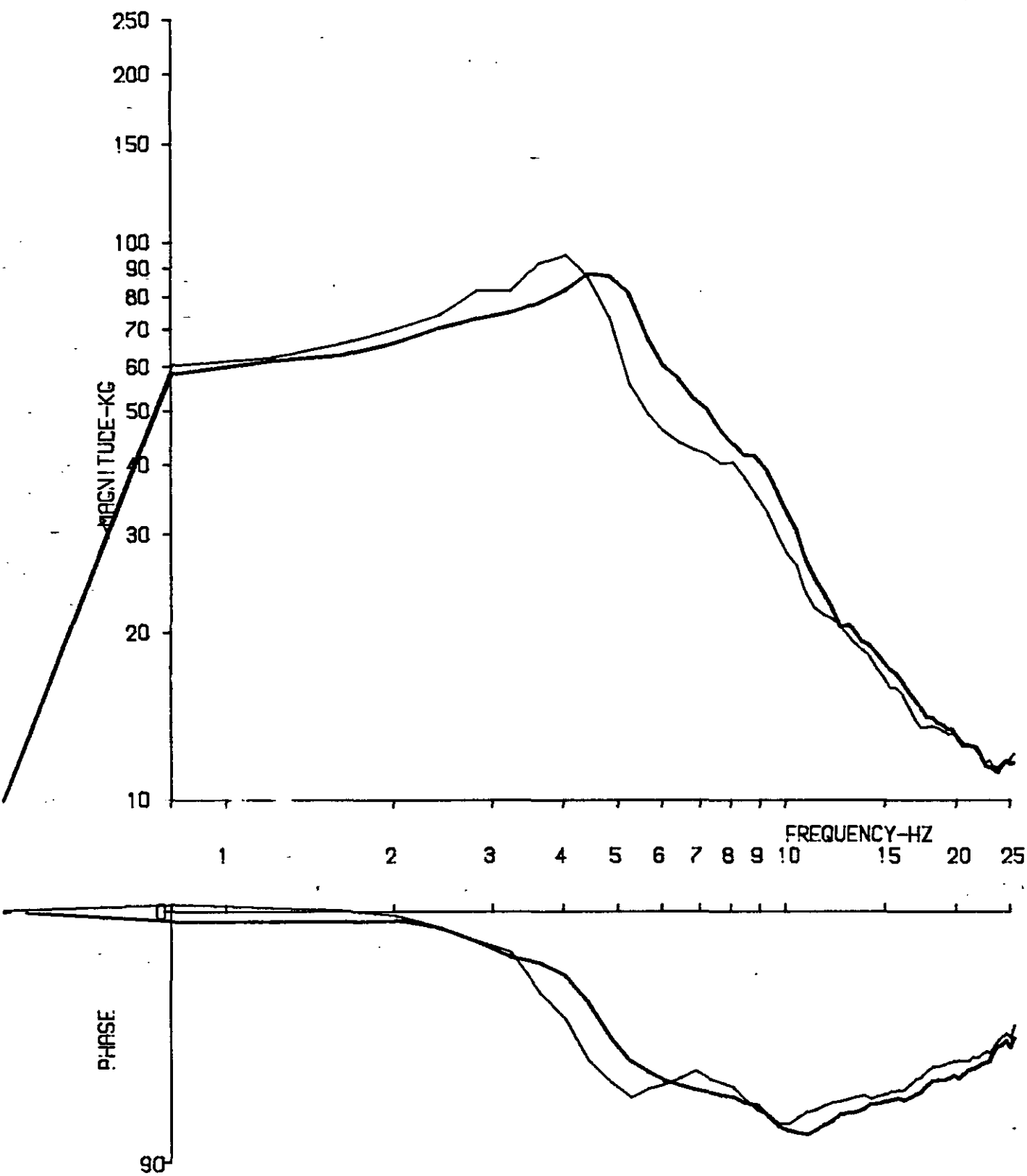






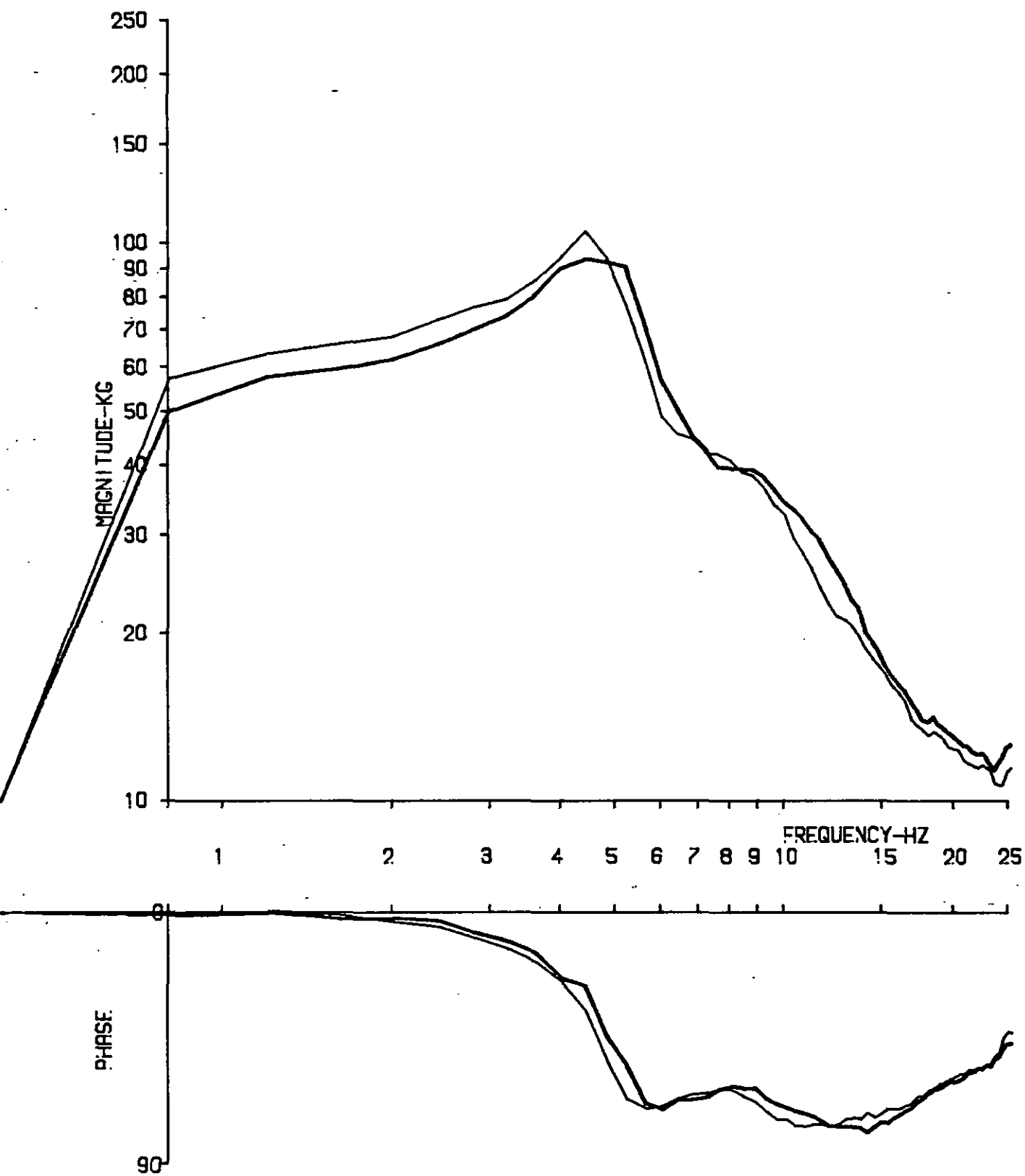
RUN NO. 81/12, 13

Fig. 7.74 Apparent Mass: Dr, E @ 2 m/s^2 r.m.s.



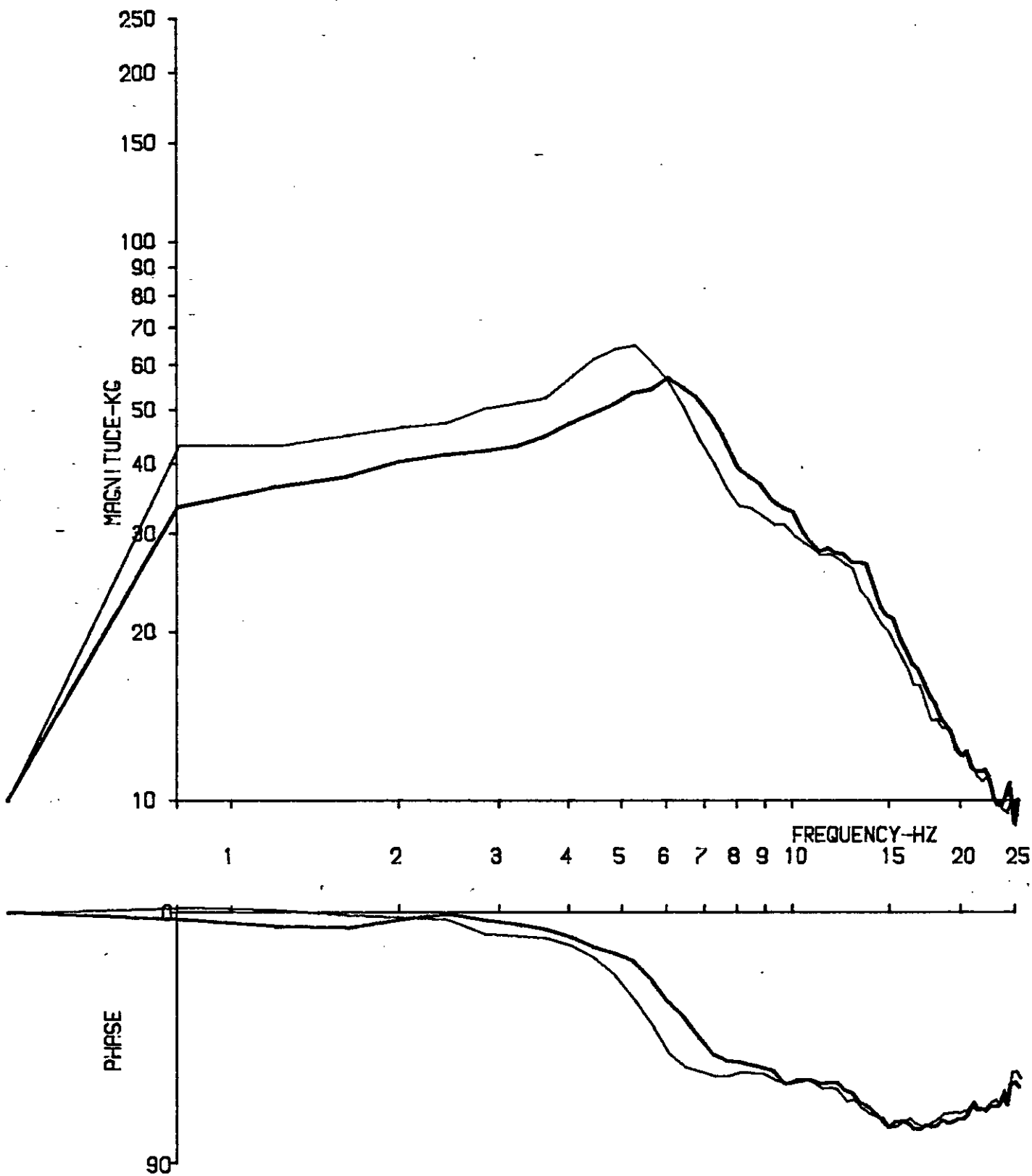
RUN NO. 82/02, 01

Fig. 7.75 Apparent Mass: Dr, E @ 2 m/s^2 r.m.s.



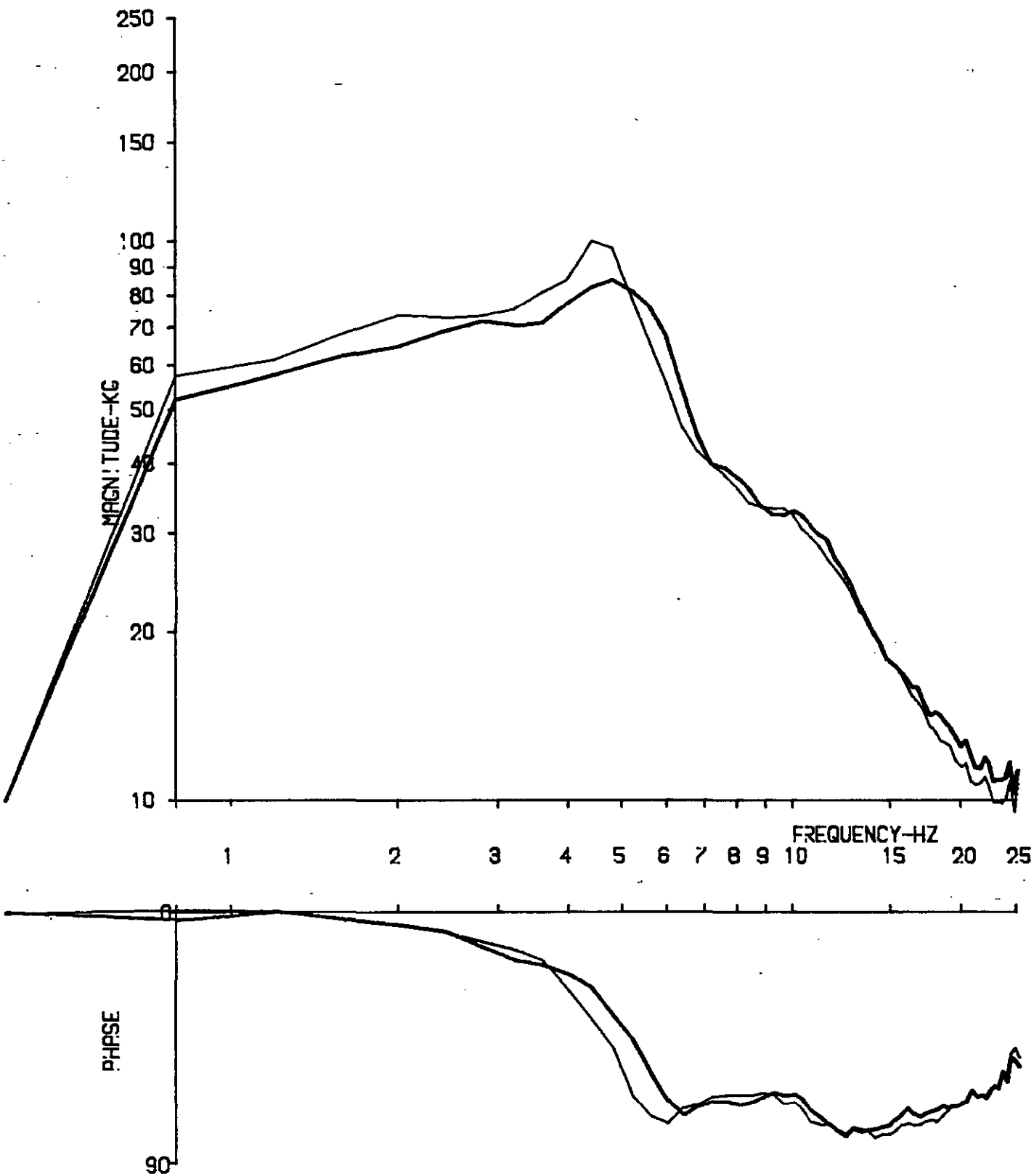
RUN NO. 85/13, 14

Fig. 7.76 Apparent Mass: Dr, E @ 2 m/s^2 r.m.s.



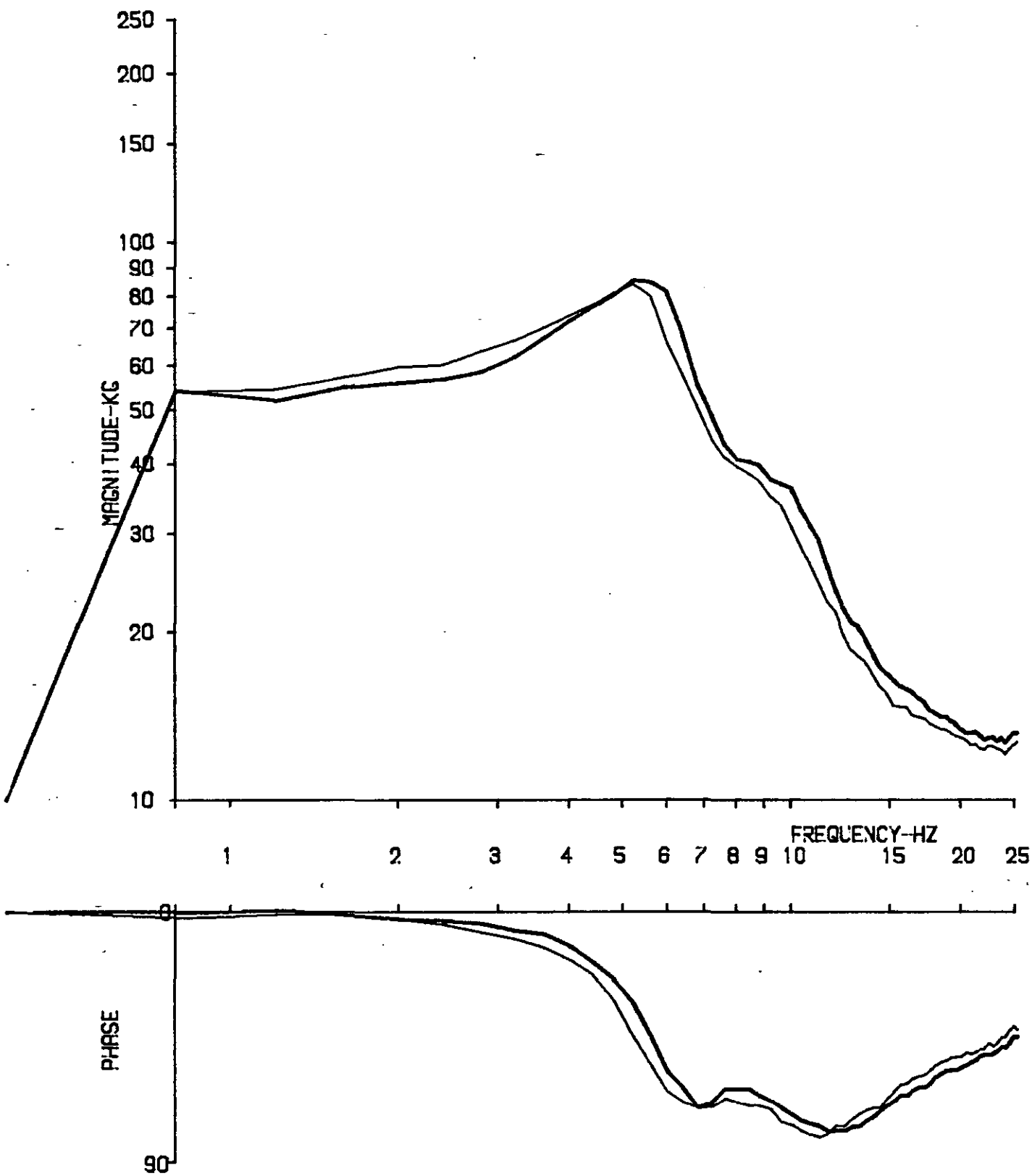
RUN NO. 84/02, 01

Fig. 7.77 Apparent Mass: Dr, E @ 2 m/s^2 r.m.s.



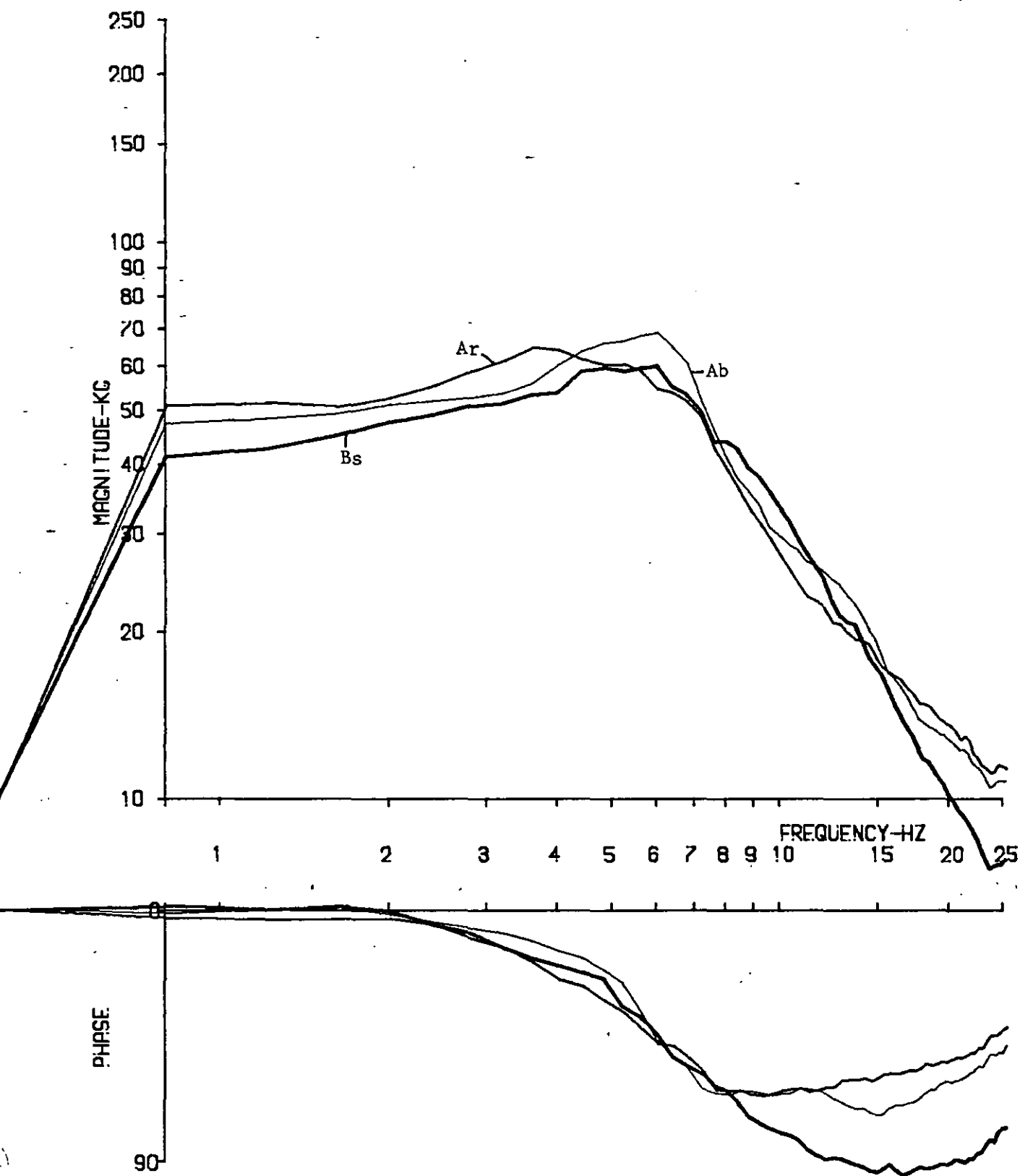
RUN NO. 83/06, 07

Fig. 7.78 Apparent Mass: Dr, E @ 2 m/s^2 r.m.s.



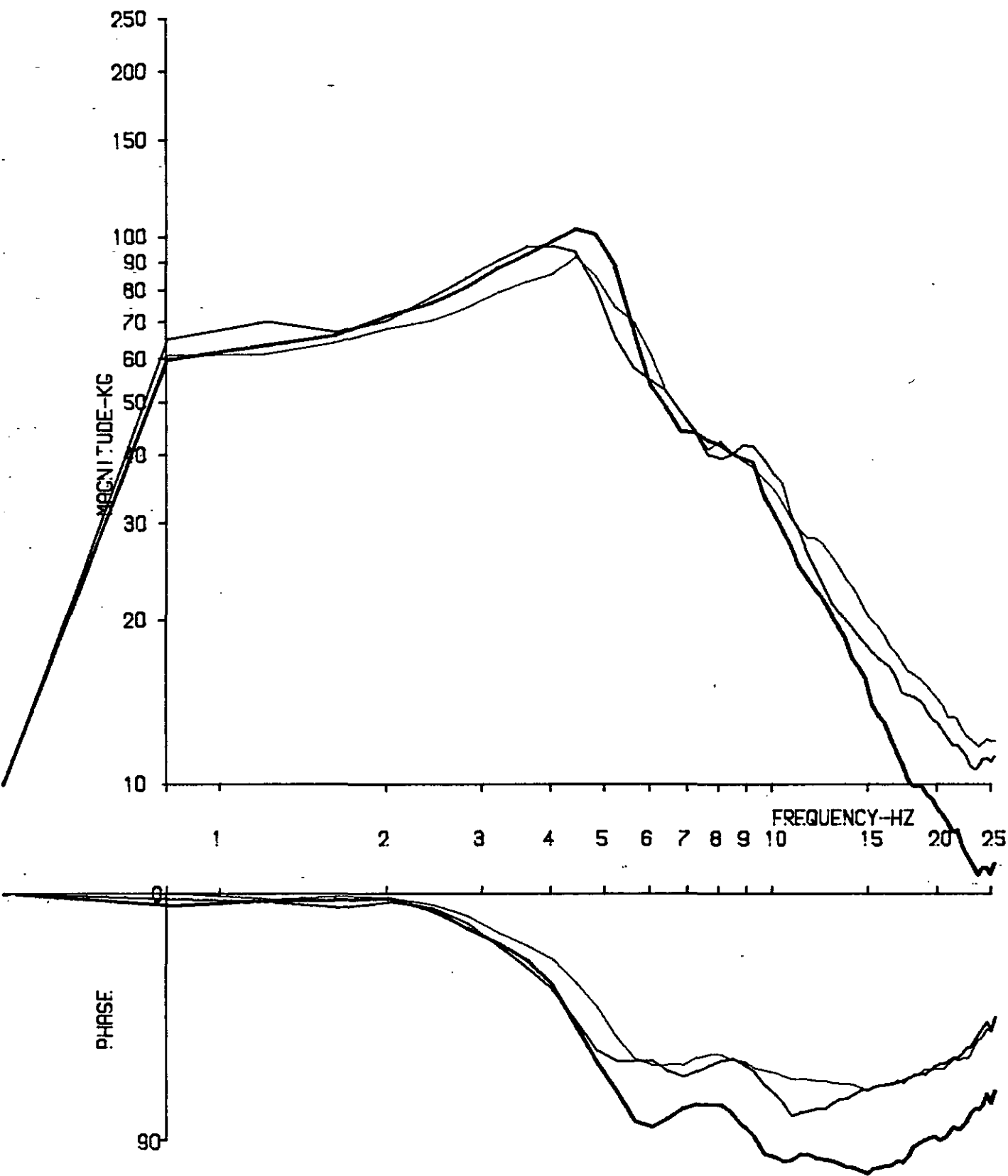
RUN NO. 01/09, 08

Fig. 7.79 Apparent Mass: Dr, E @ 2 m/s^2 r.m.s.



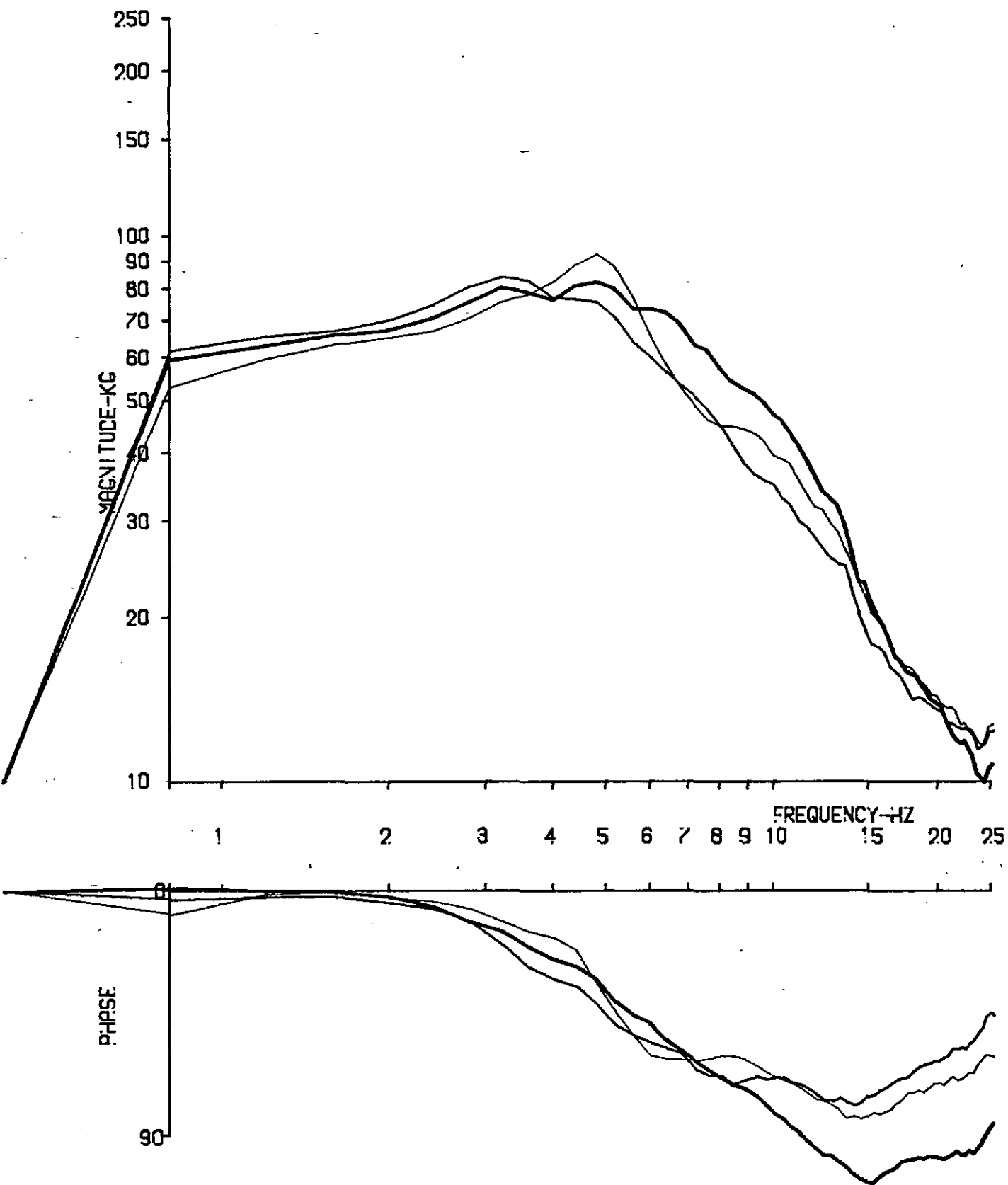
RUN NO. 81/07, 05, 10

Fig. 7.80 Apparent Mass: Bs/Ar/Ab



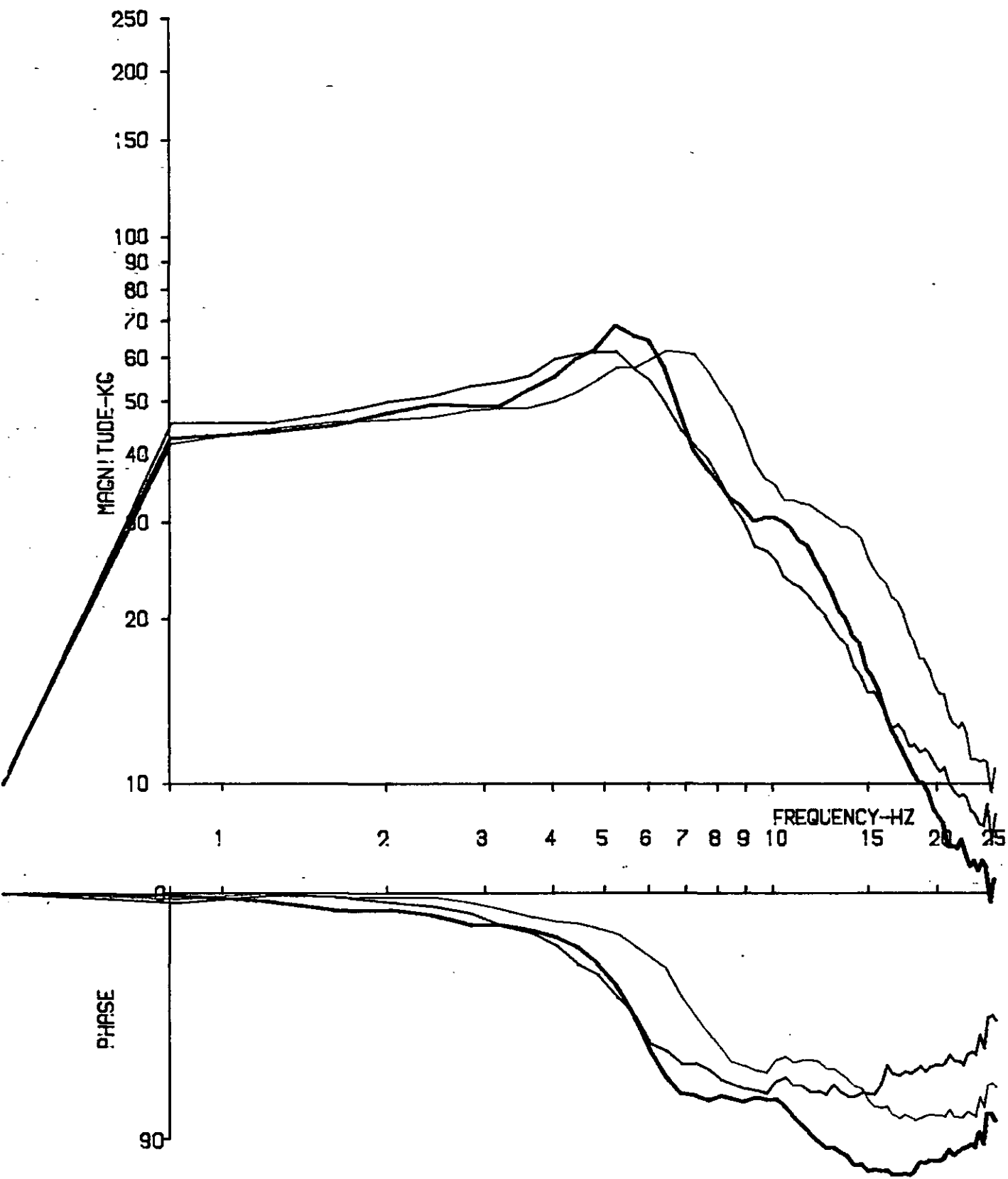
RUN NO. 82/07, 09, 04

Fig. 7.81 Apparent Mass: Bs/Ar/Ab



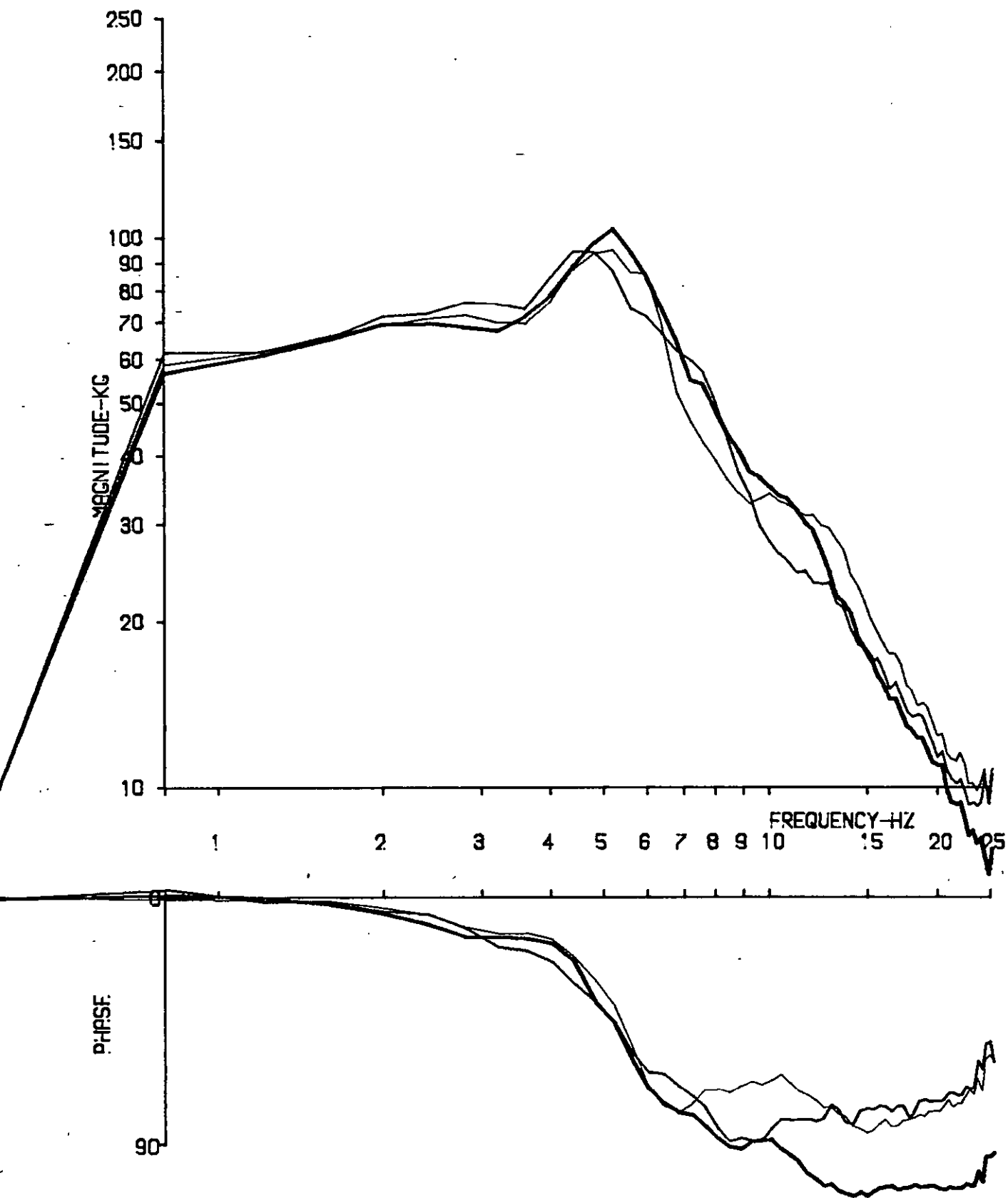
RUN NO. 85/08, 06, 11

Fig. 7.82 Apparent Mass: Bs/Ar/Ab



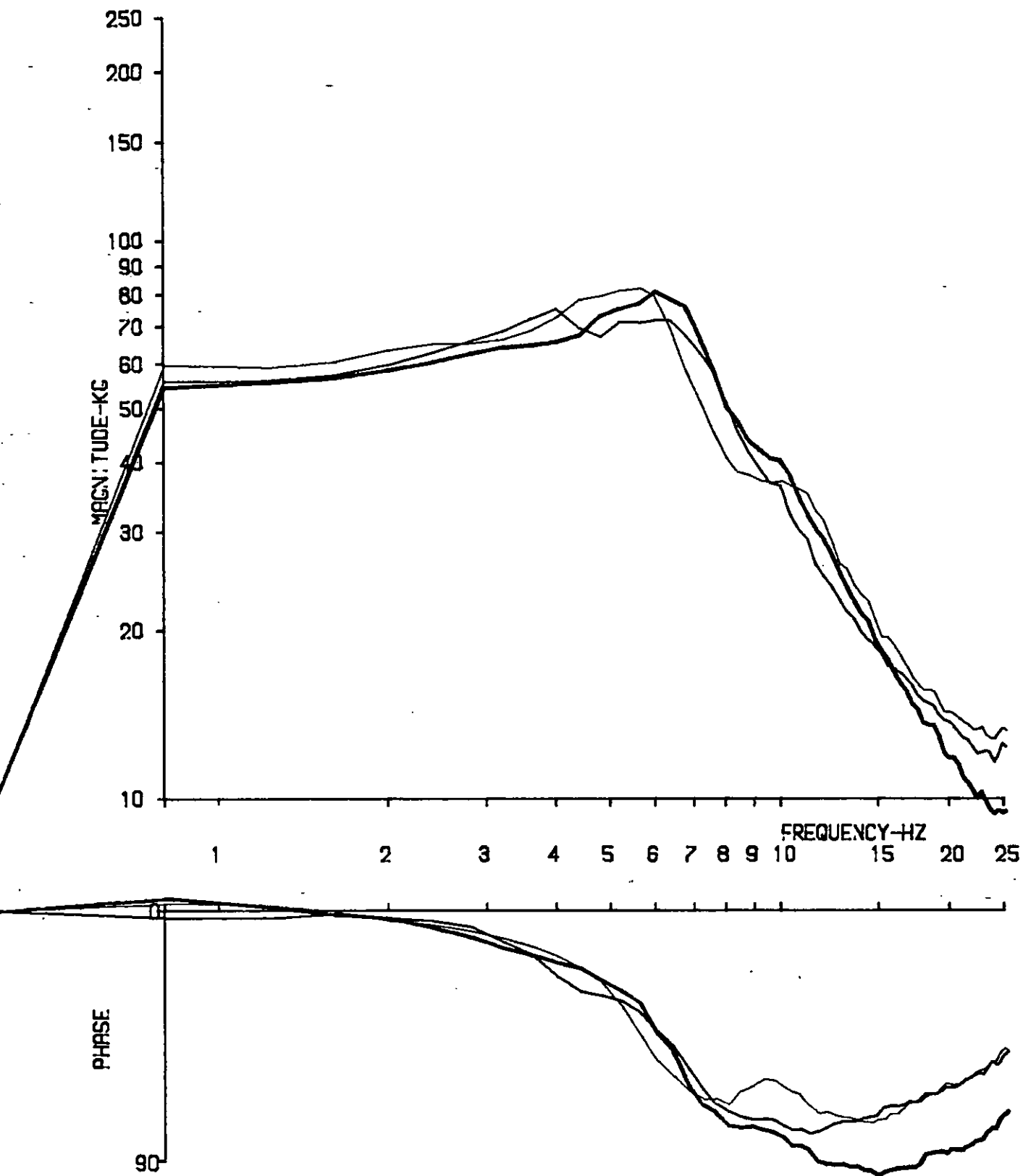
RUN NO. 84/07, 09, 04

Fig. 7.83 Apparent Mass: Bs/Ar/Ab



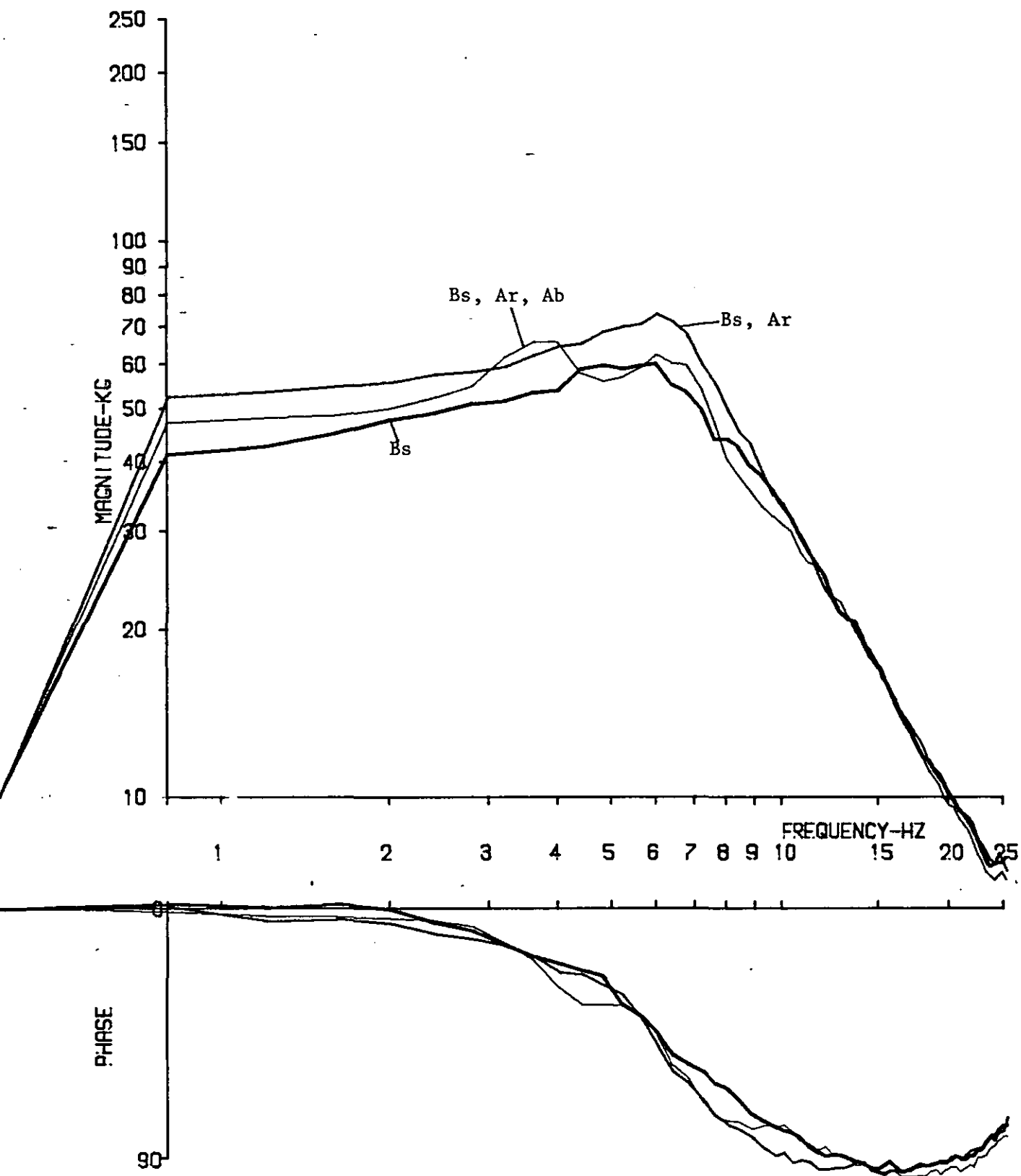
RUN NO. 83/01, 13, 04

Fig. 7.84 Apparent Mass: Bs/Ar/Ab



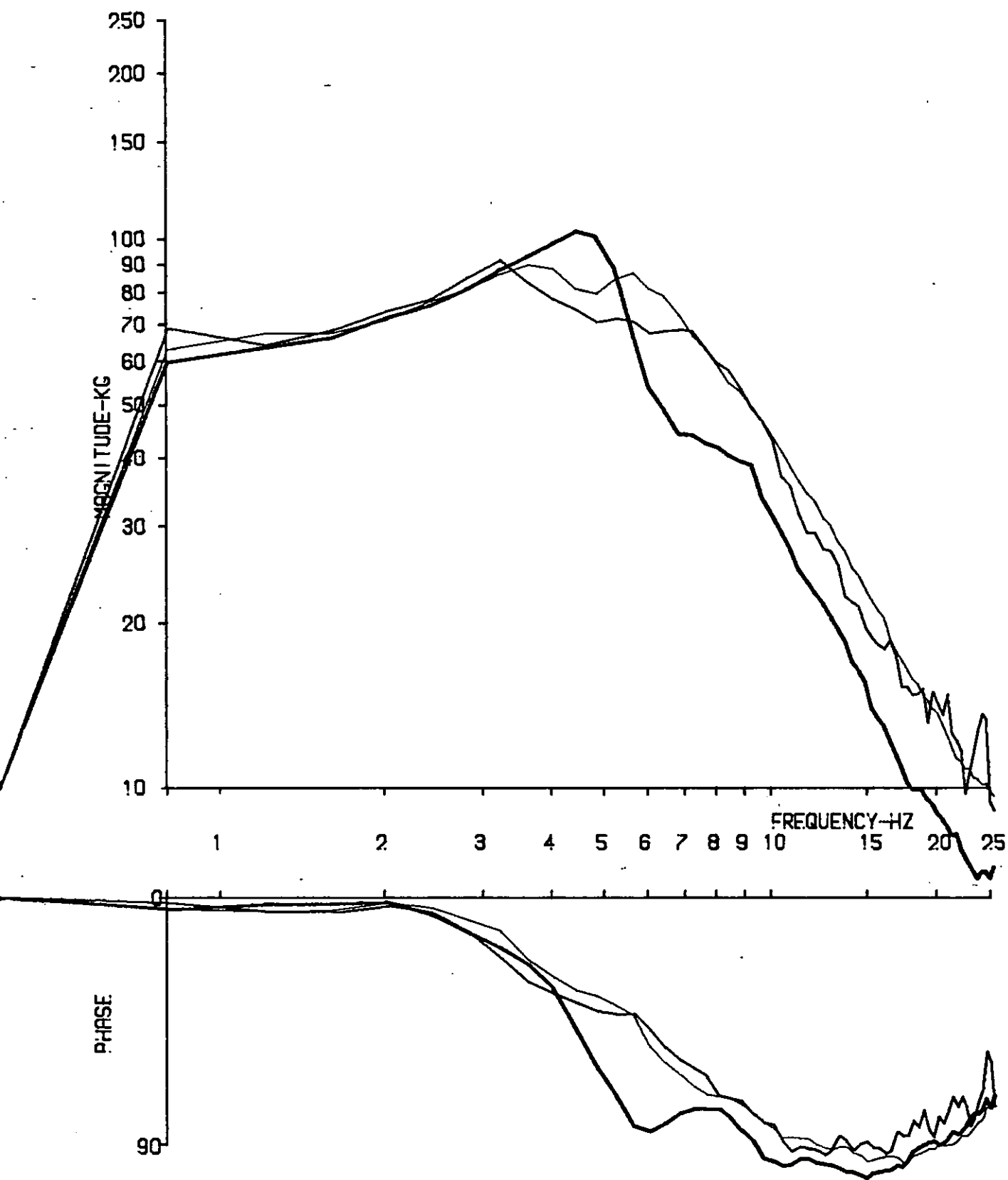
RUN NO. 01/14, 02, 11

Fig. 7.85 Apparent Mass: Bs/Ar/Ab



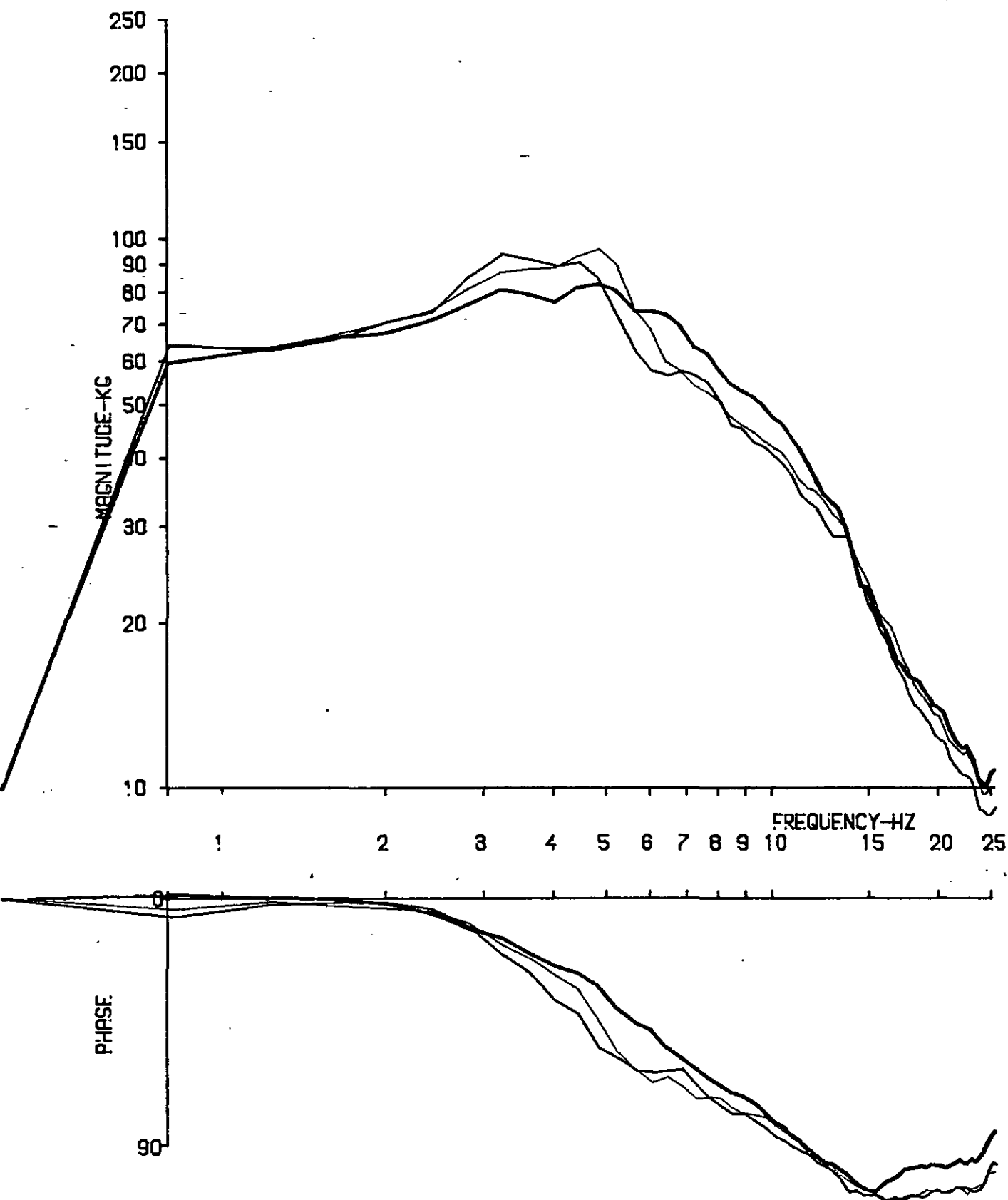
RUN NO. 81/07, 04, 02

Fig. 7.86 Apparent Mass: Bs/Bs, Ar/Bs, Ar, Ab



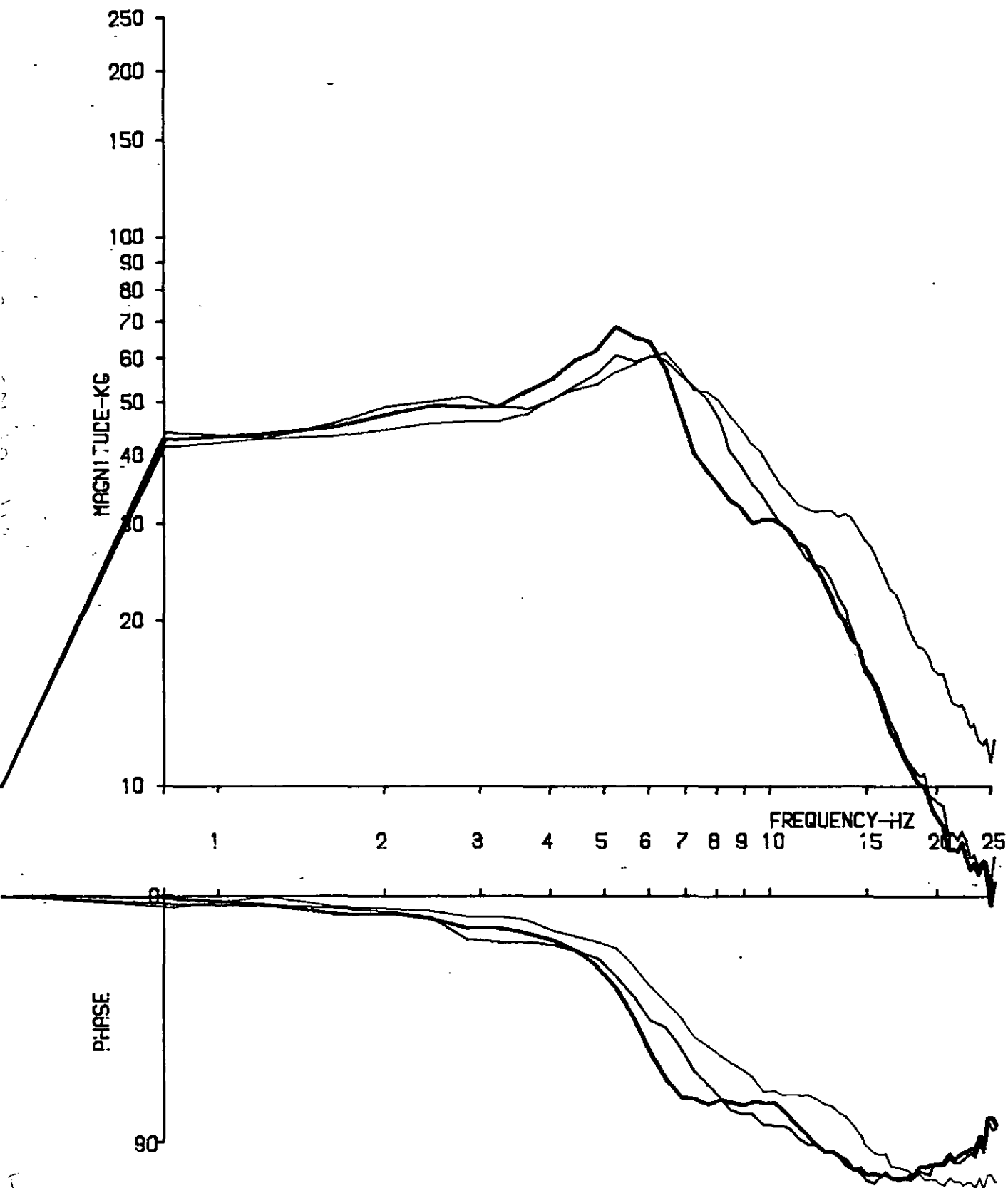
RUN NO. 82/07, 10 (poor δ), 12

Fig. 7.87 Apparent Mass: Bs/Bs, Ar/Bs, Ar, Ab



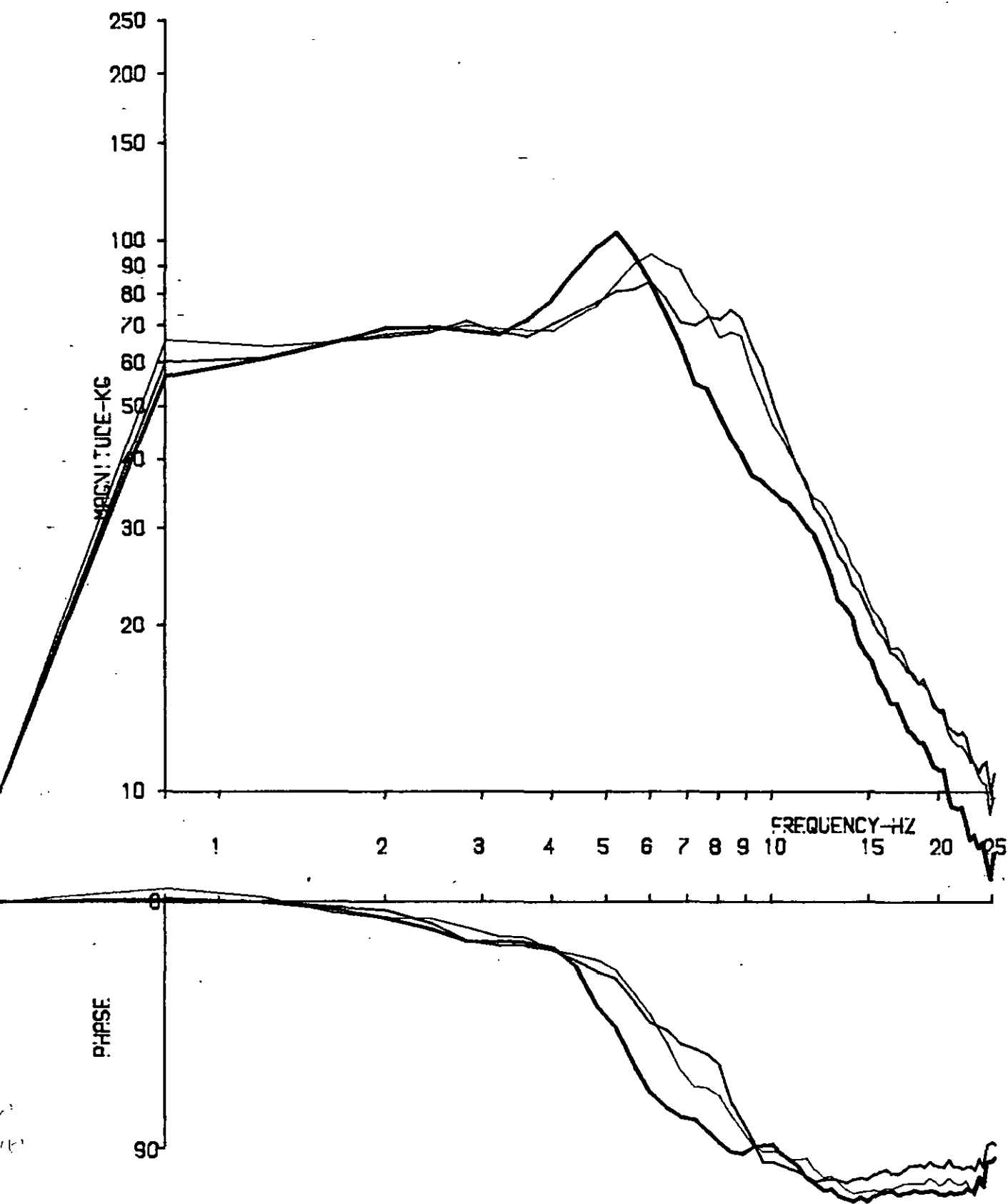
RUN NO. 85/08, 05, 03

Fig. 7.88 Apparent Mass: Bs/Bs, Ar/Bs, Ar, Ab



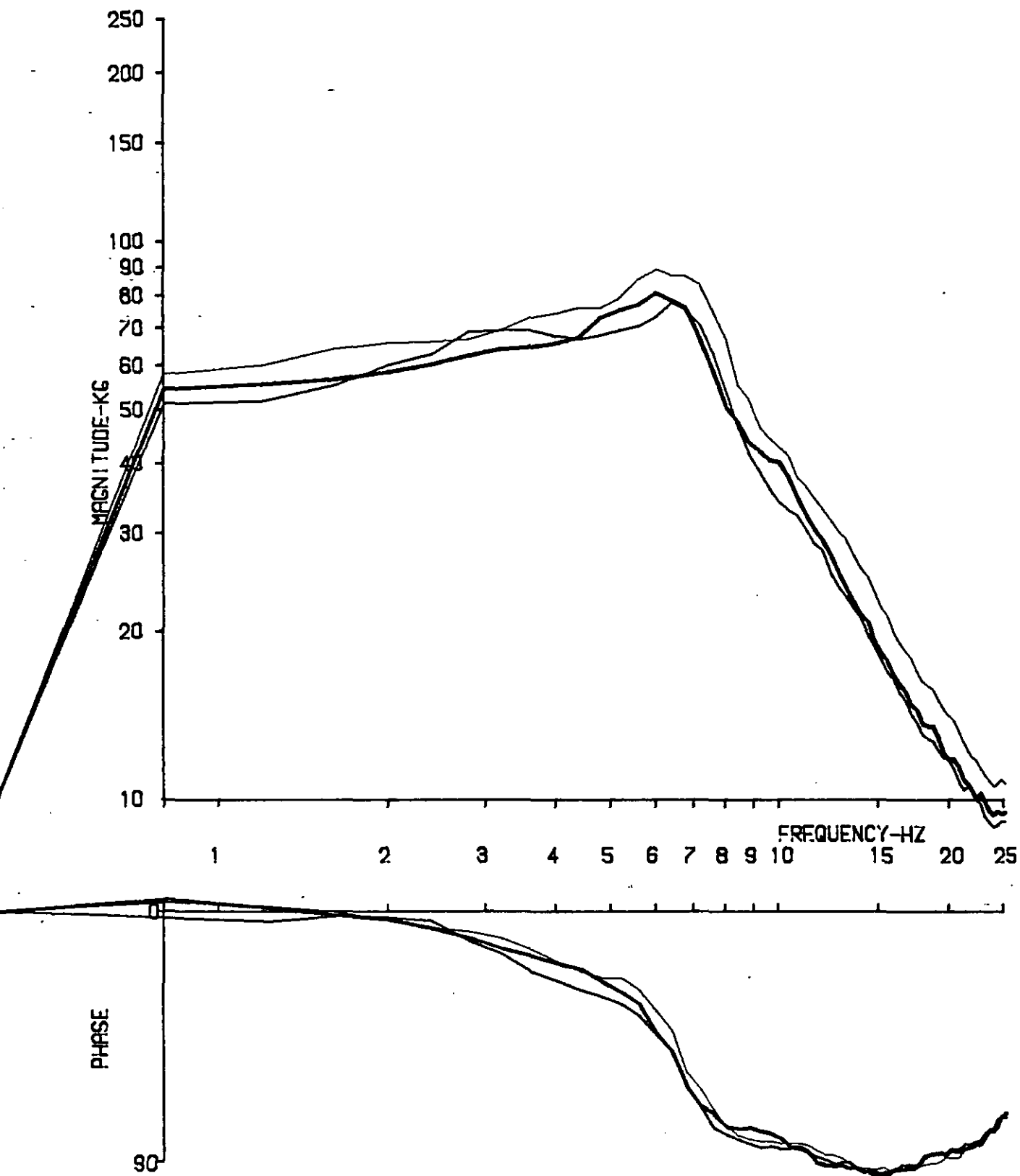
RUN NO. 84/07, 10, 12

Fig. 7.89 Apparent Mass: Bs/Bs, Ar/Bs, Ar, Ab



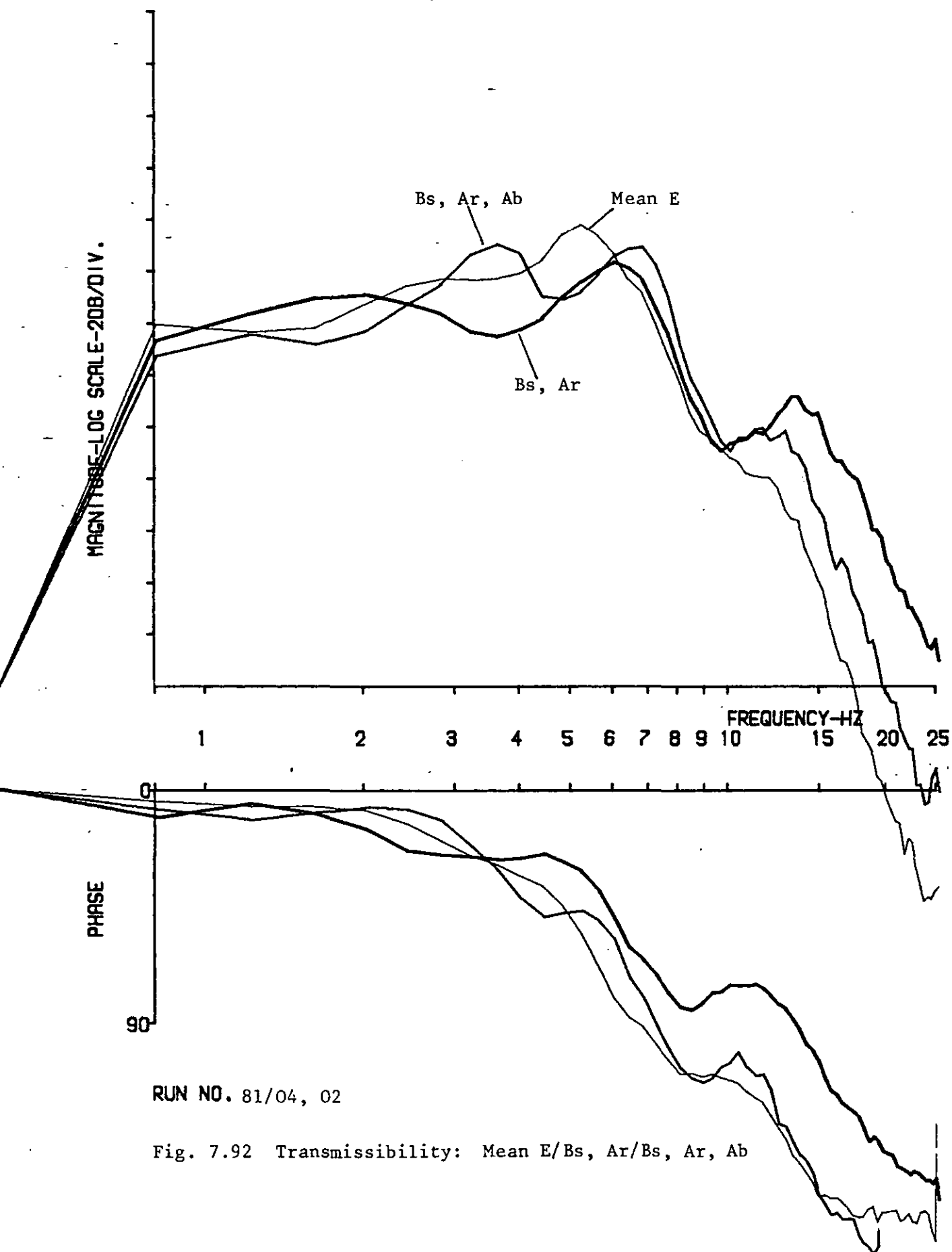
RUN NO. 83/01, 12, 10

Fig. 7.90 Apparent Mass: Bs/Bs, Ar/Bs, Ar, Ab



RUN NO. 01/14, 03, 05

Fig. 7.91 Apparent Mass: Bs/Bs, Ar/Bs, Ar, Ab



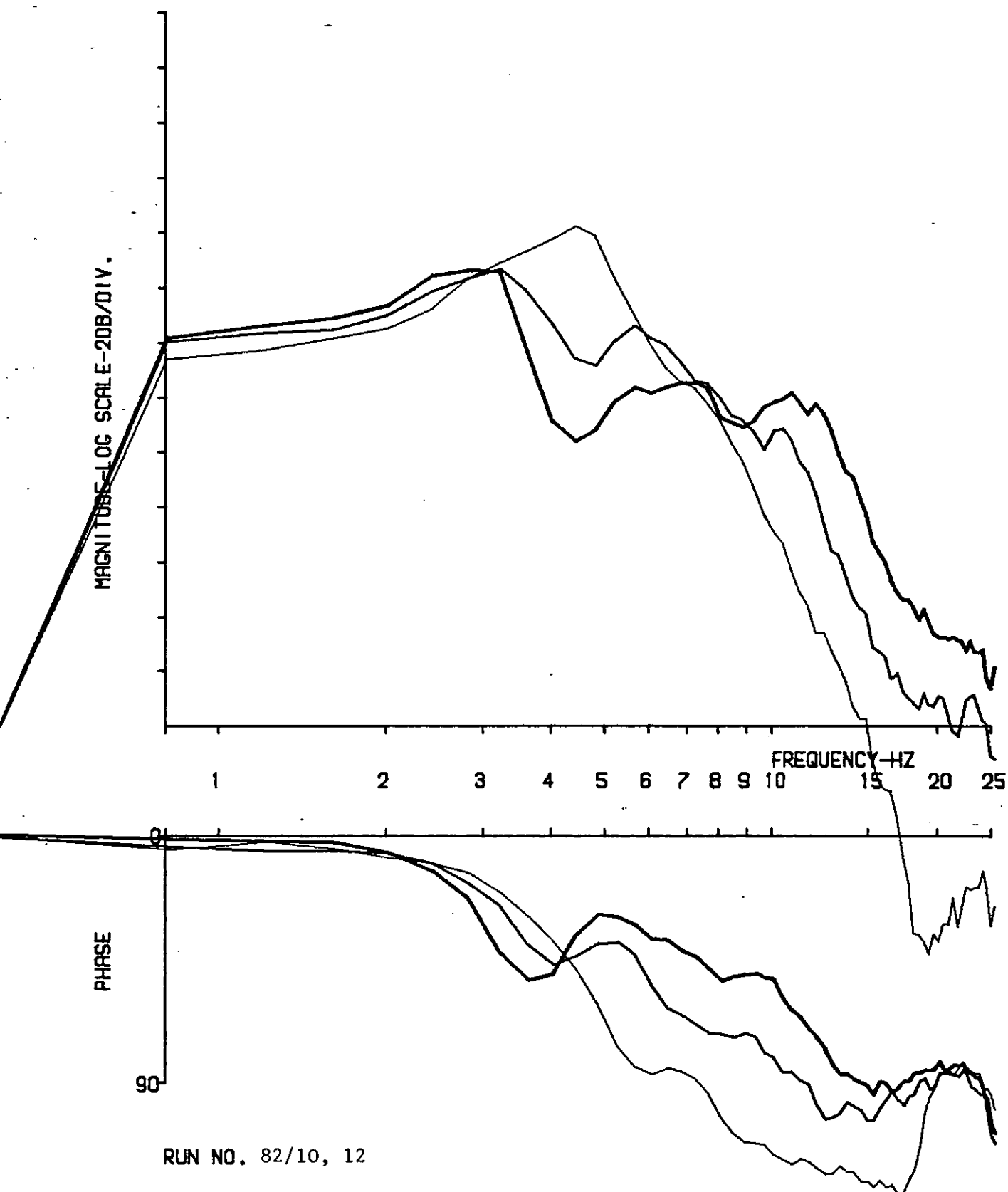
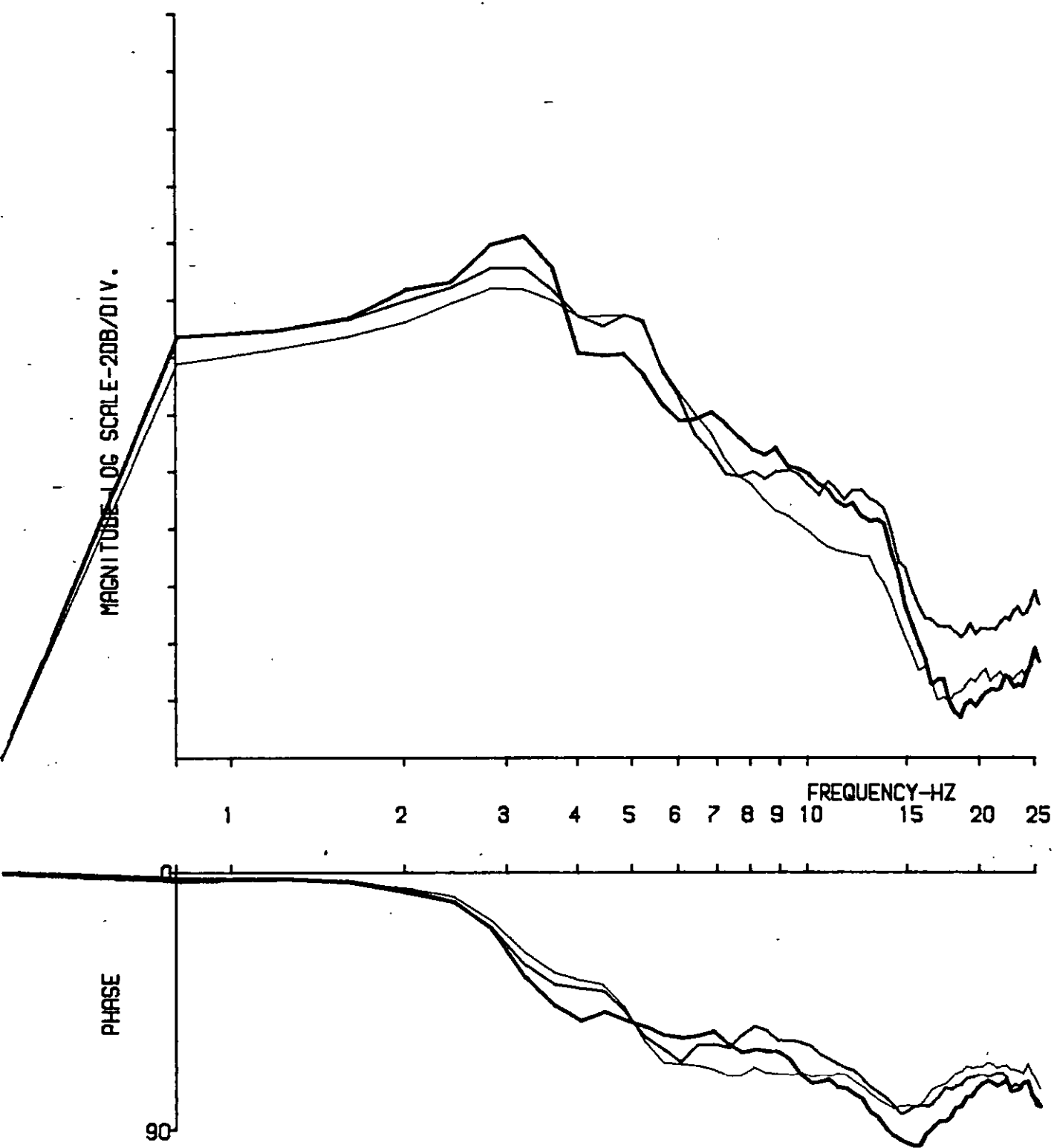
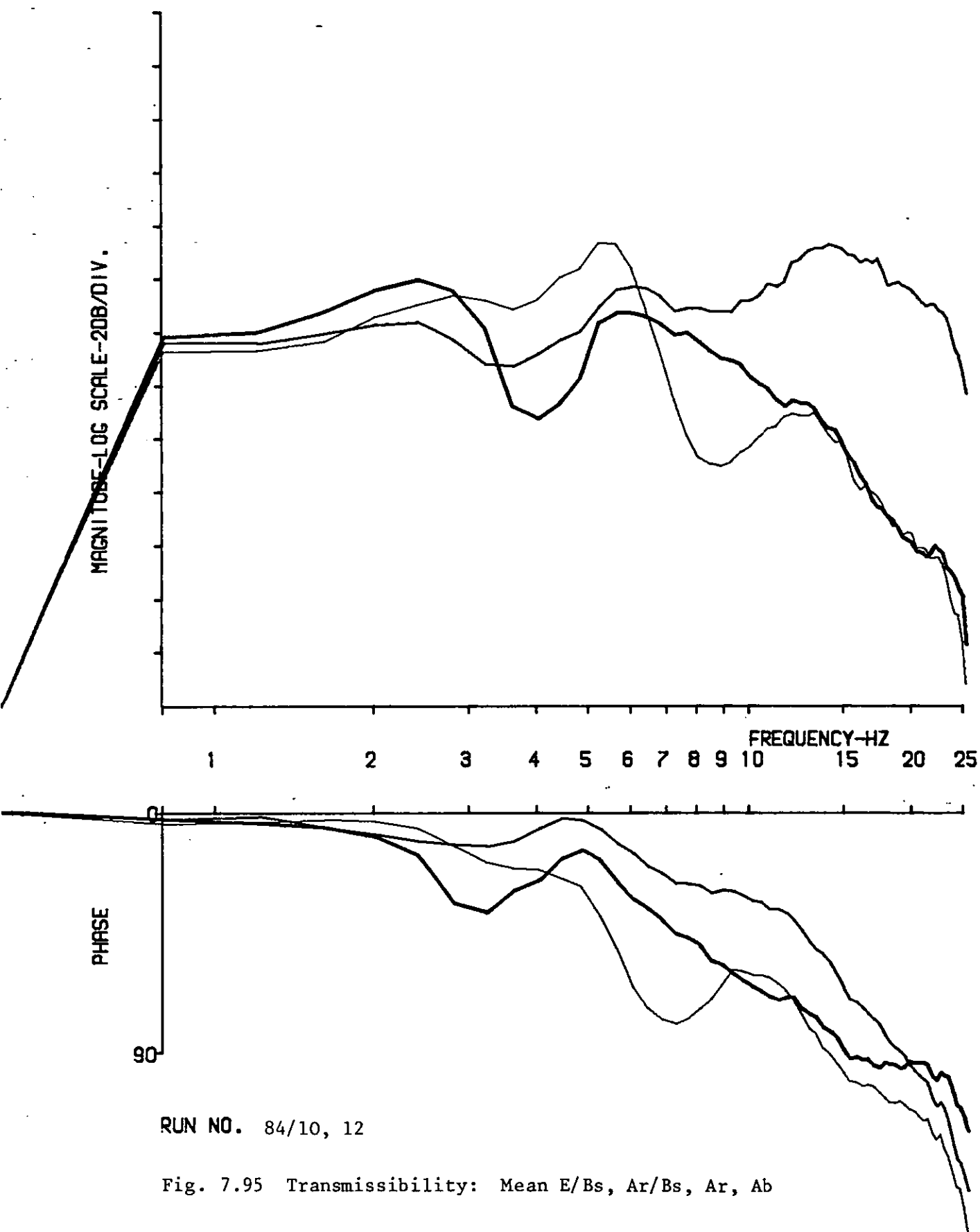


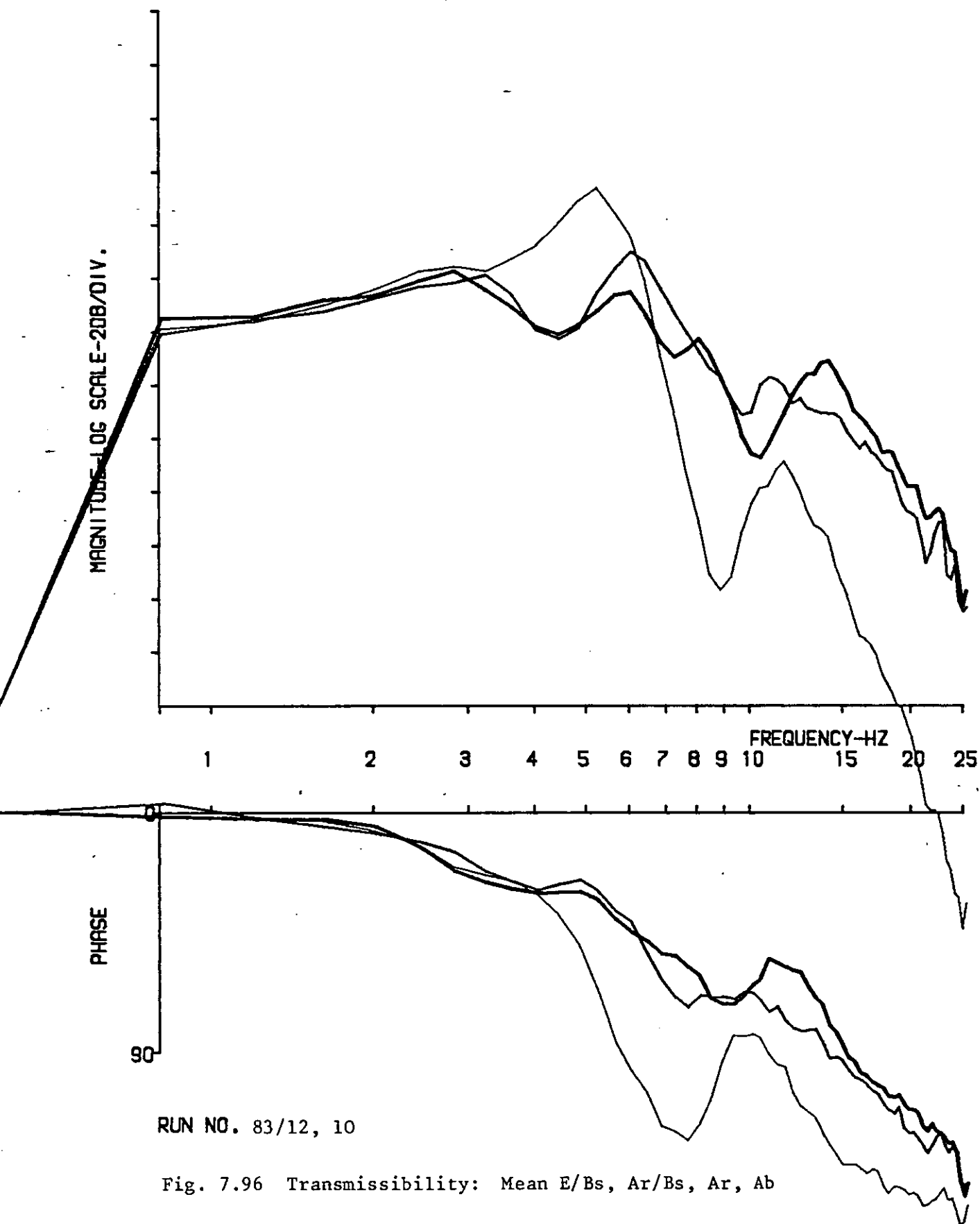
Fig. 7.93 Transmissibility: Mean E/Bs, Ar/Bs, Ar, Ab

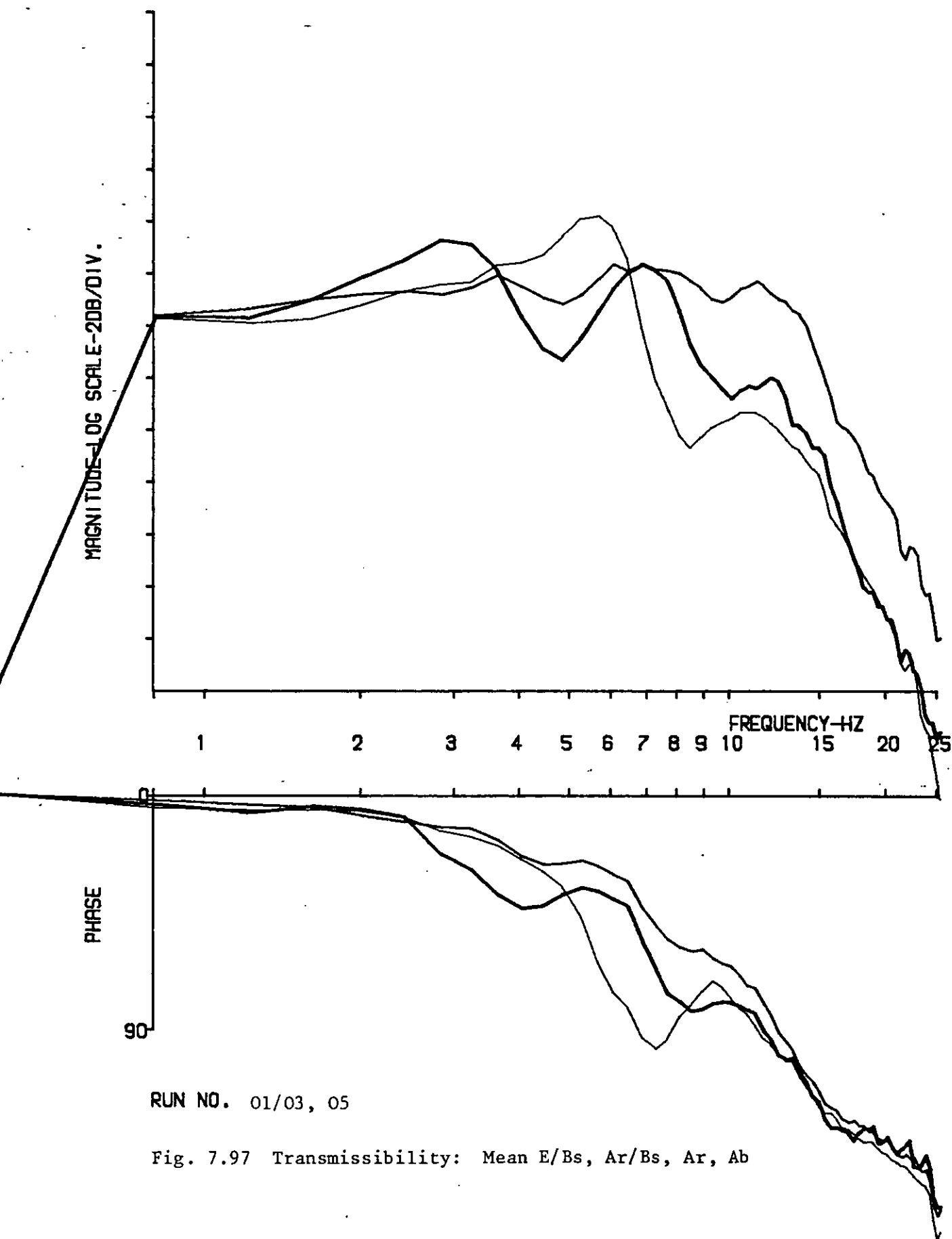


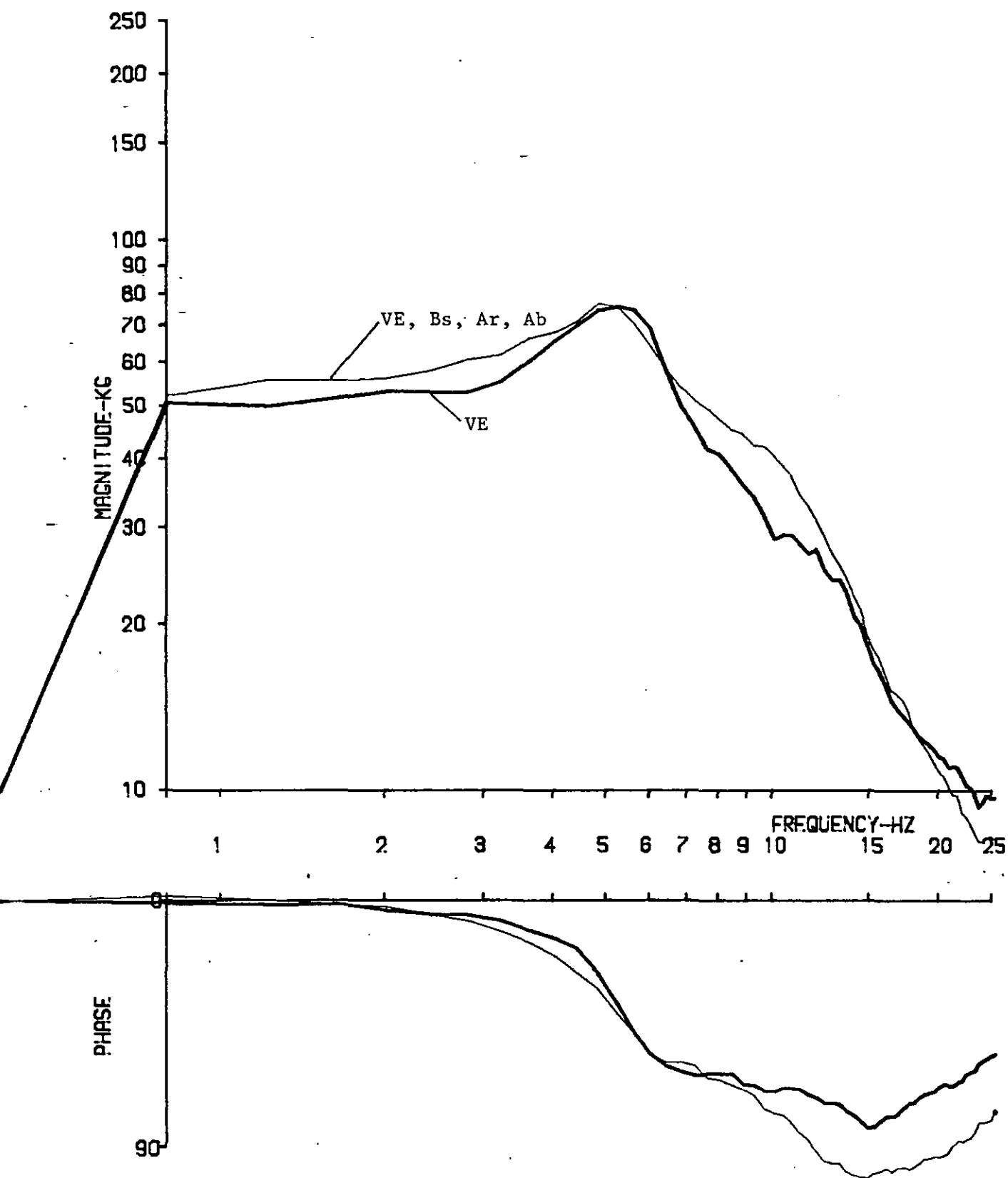
RUN NO. 85/05, 03

Fig. 7.94 Transmissibility: Mean E/Bs, Ar/Bs, Ar, Ab



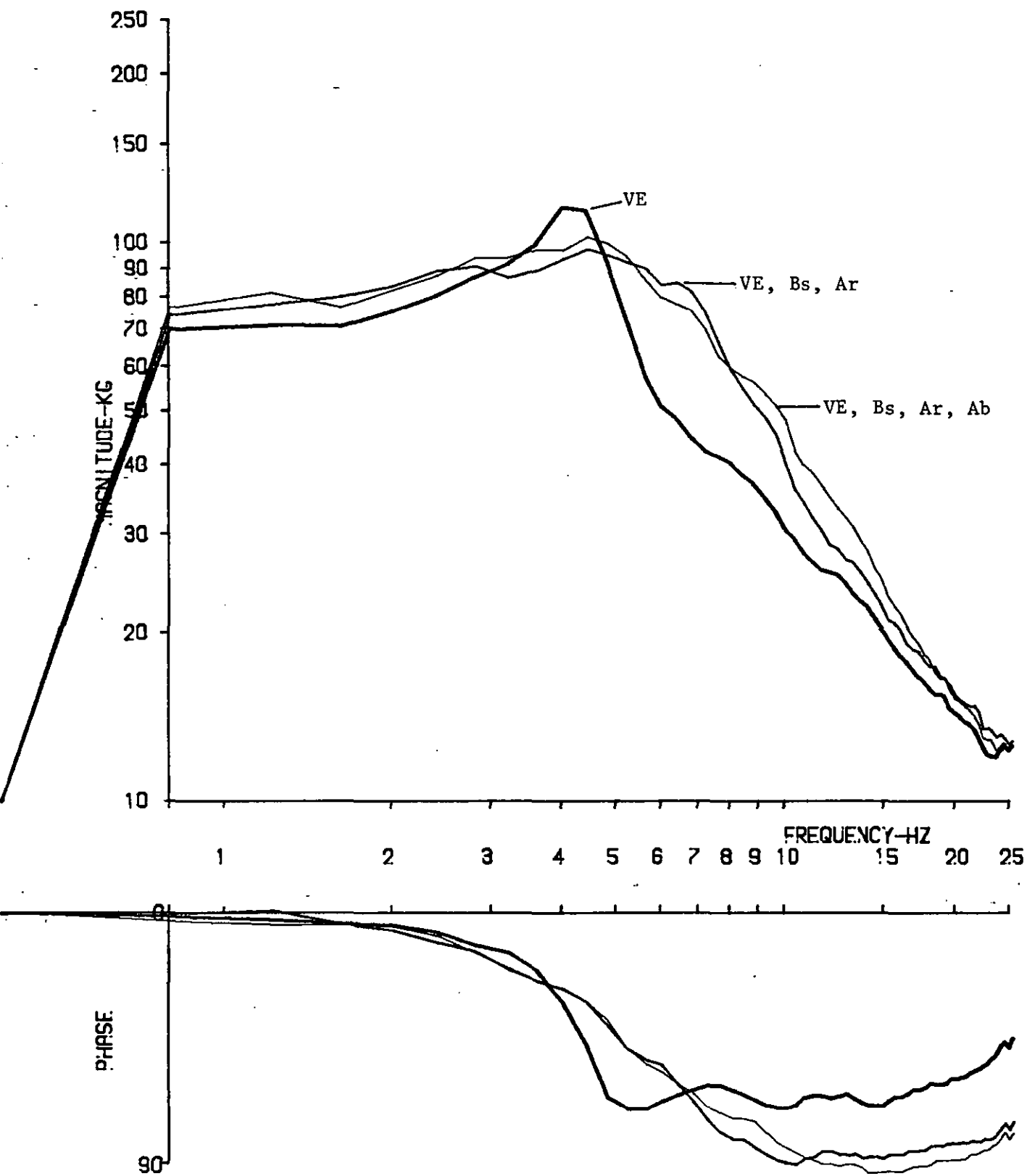






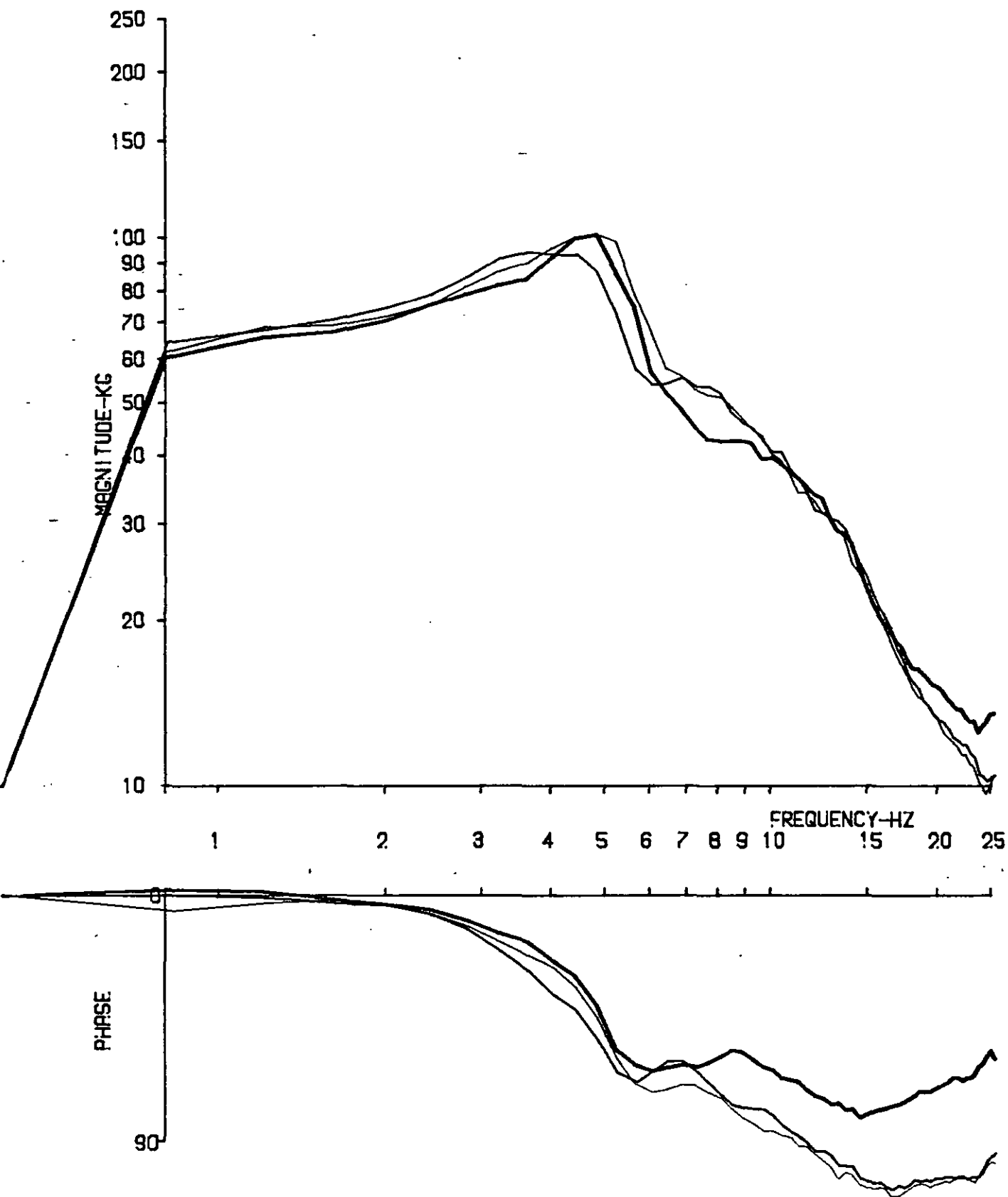
RUN NO. 81/09, 03

Fig. 7.98 Apparent Mass: VE/VE, Bs, Ar, Ab



RUN NO. 82/05, 11, 13

Fig. 7.99 Apparent Mass: VE/VE, Bs, Ar/VE, Bs, Ar, Ab



RUN NO. 85/10, 04, 02

Fig. 7.100 Apparent Mass: VE/VE, Bs, Ar/VE, Bs, Ar, Ab

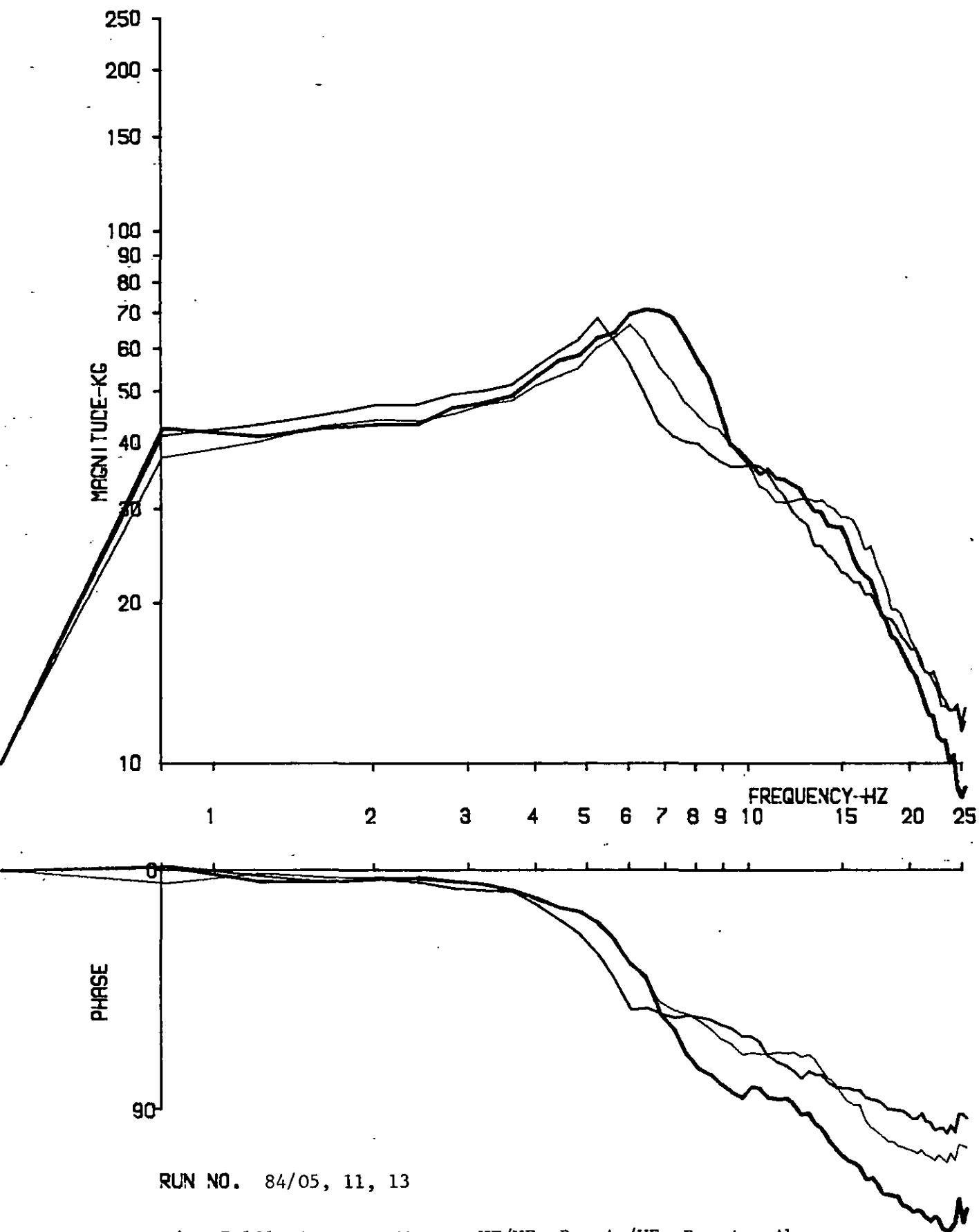
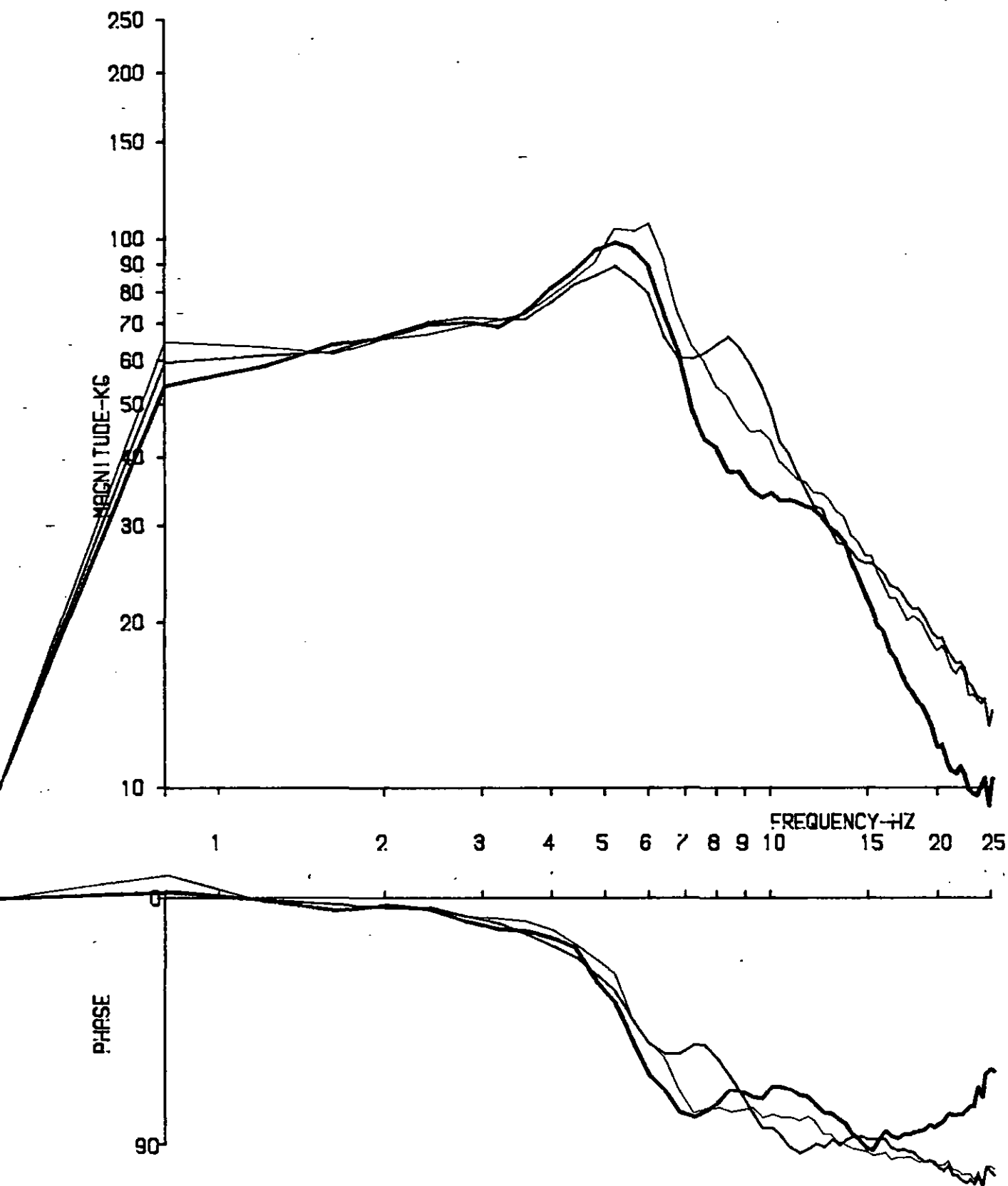
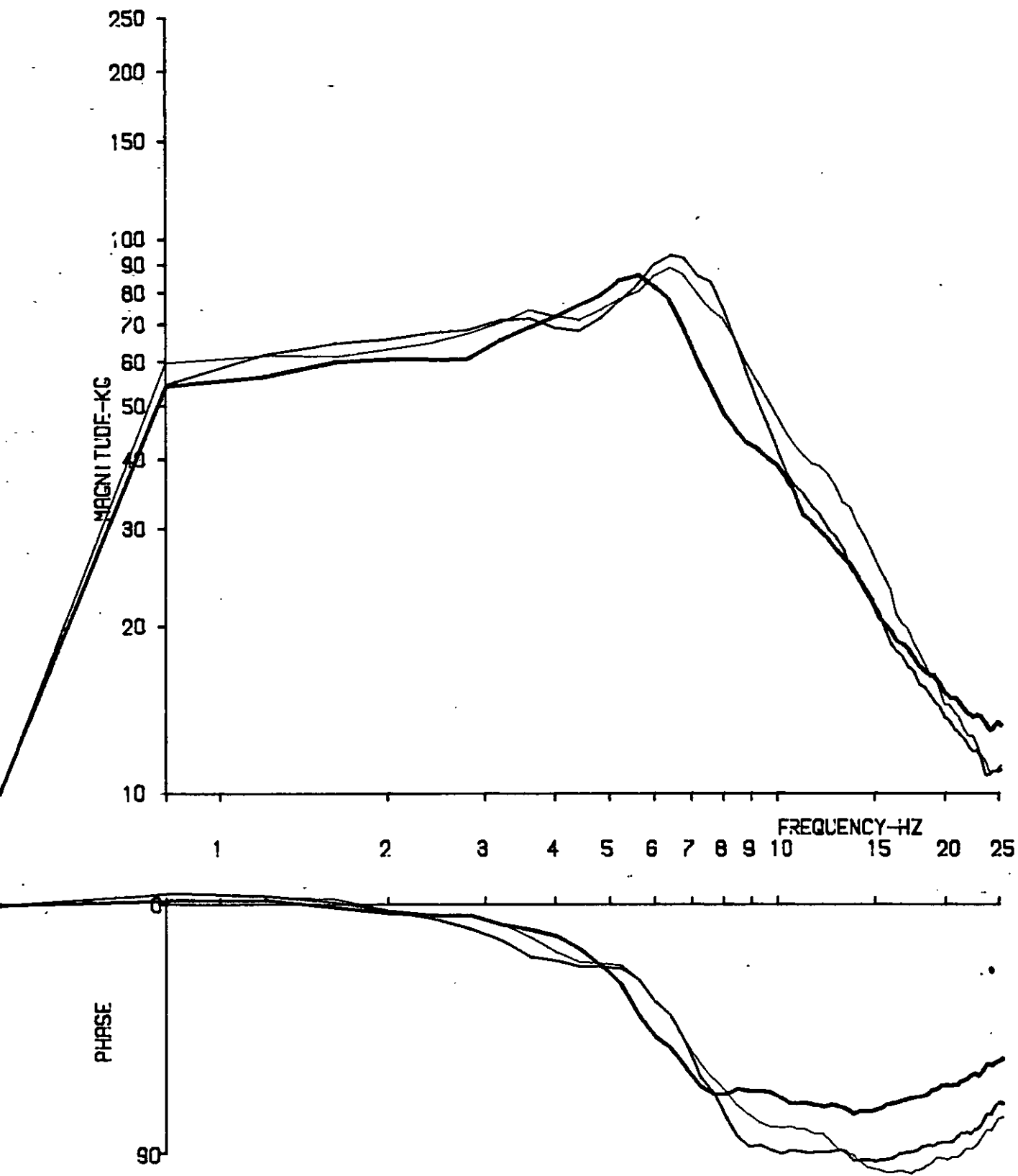


Fig. 7.101 Apparent Mass: VE/VE, Bs, Ar/VE, Bs, Ar, Ab



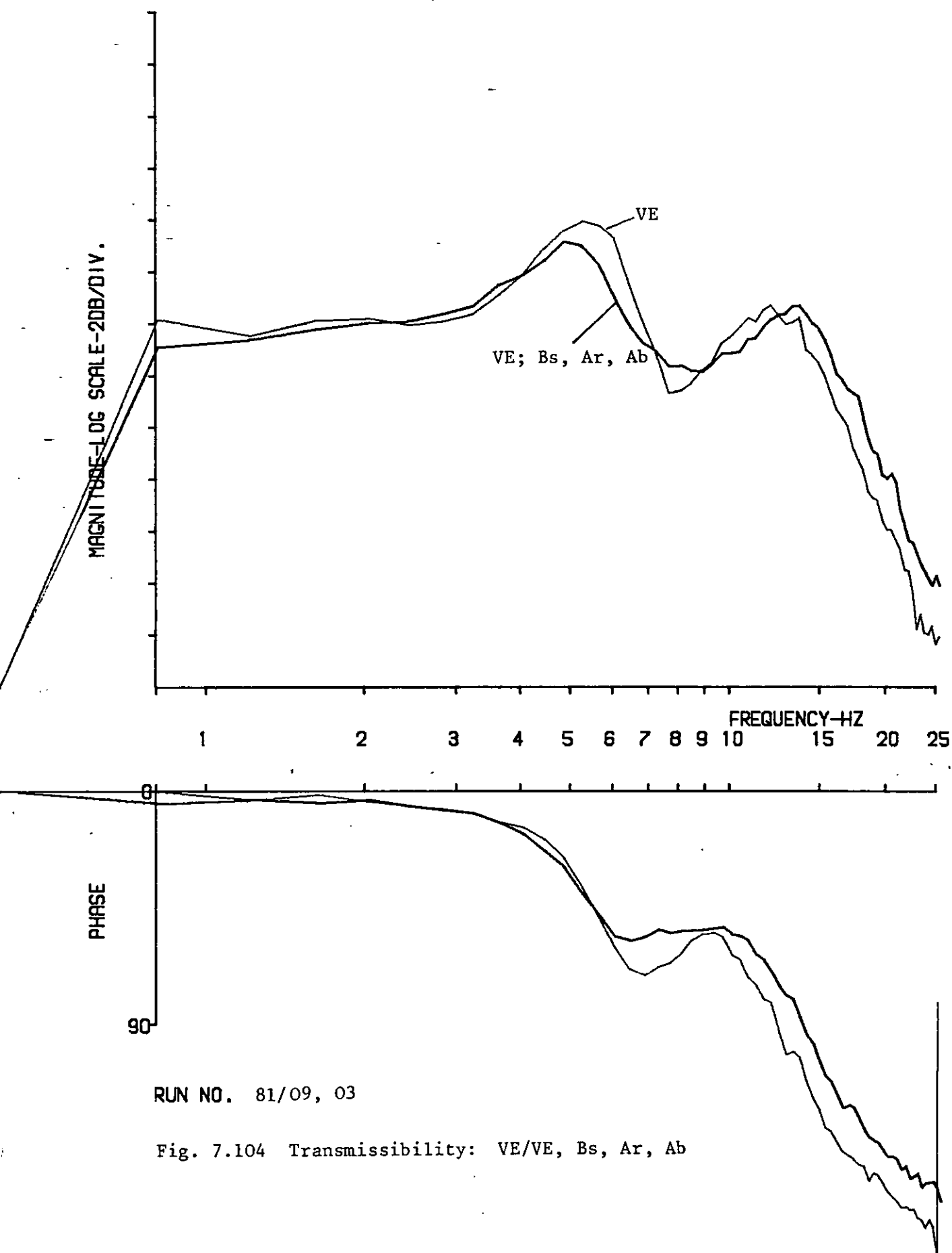
RUN NO. 83/03, 11, 09

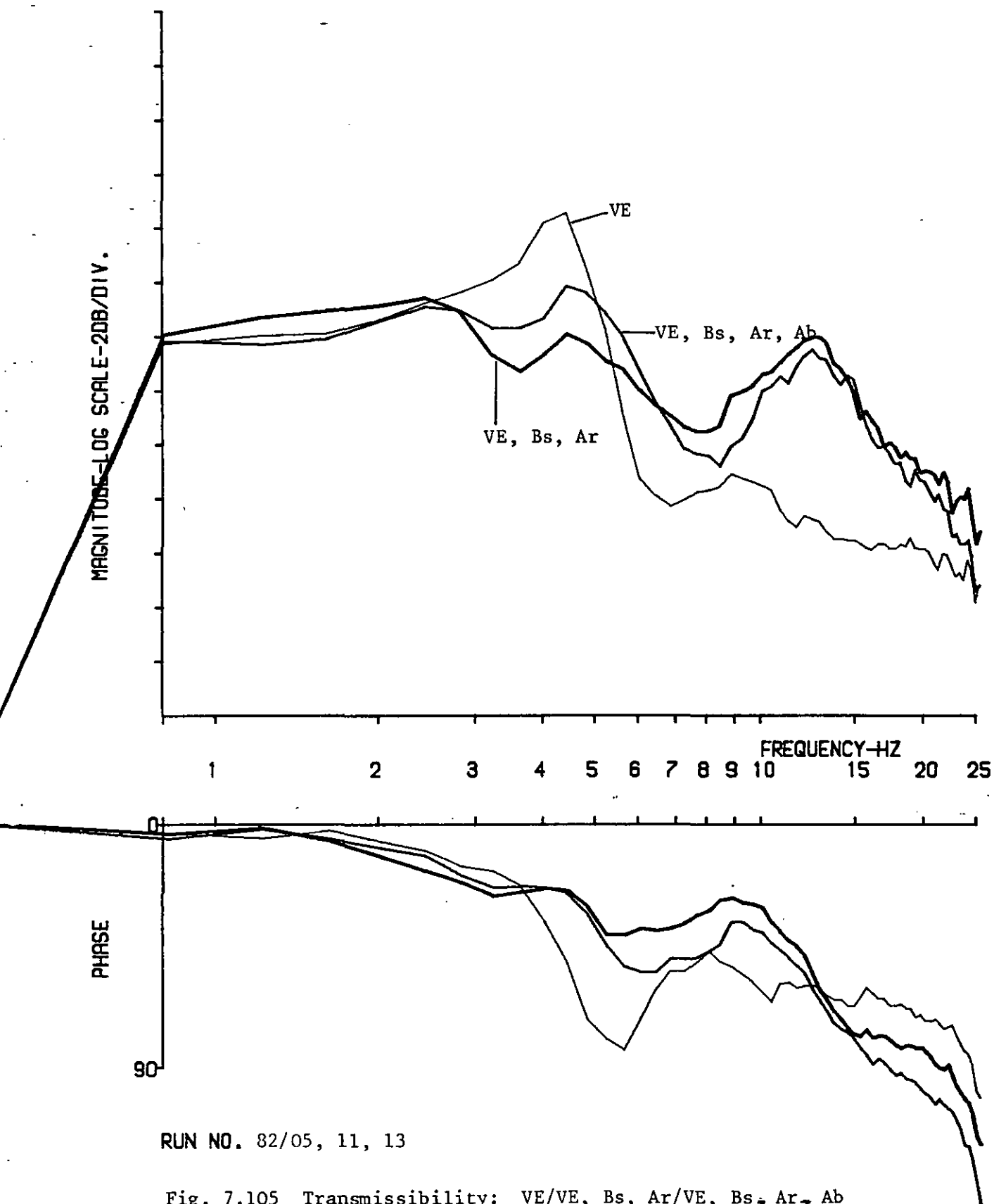
Fig. 7.102 Apparent Mass: VE/VE, Bs, Ar/VE, Bs, Ar, Ab

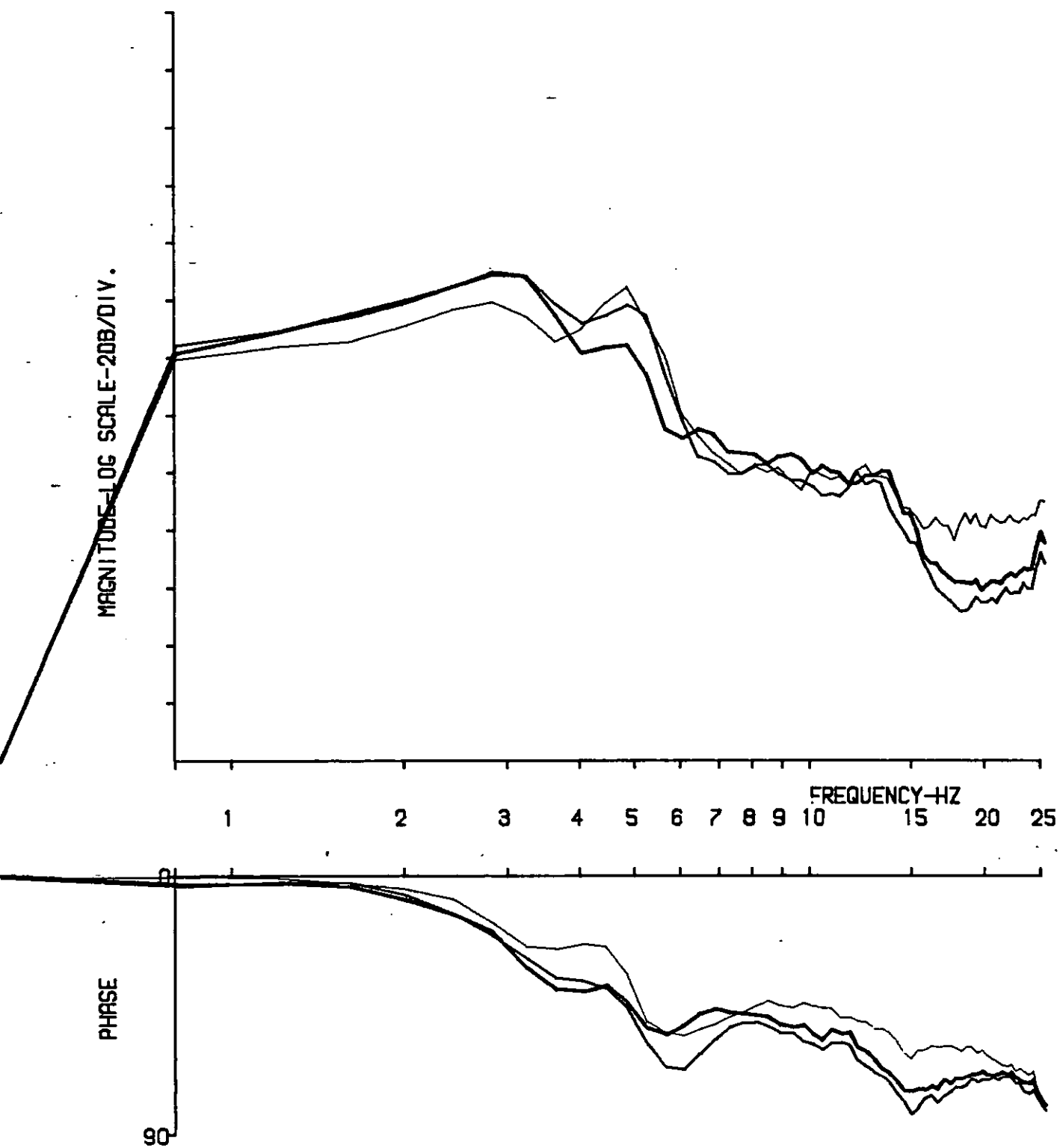


RUN NO. 01/12, 04, 06

Fig. 7.103 Apparent Mass: VE/VE, Bs, Ar/VE, Bs, Ar, Ab

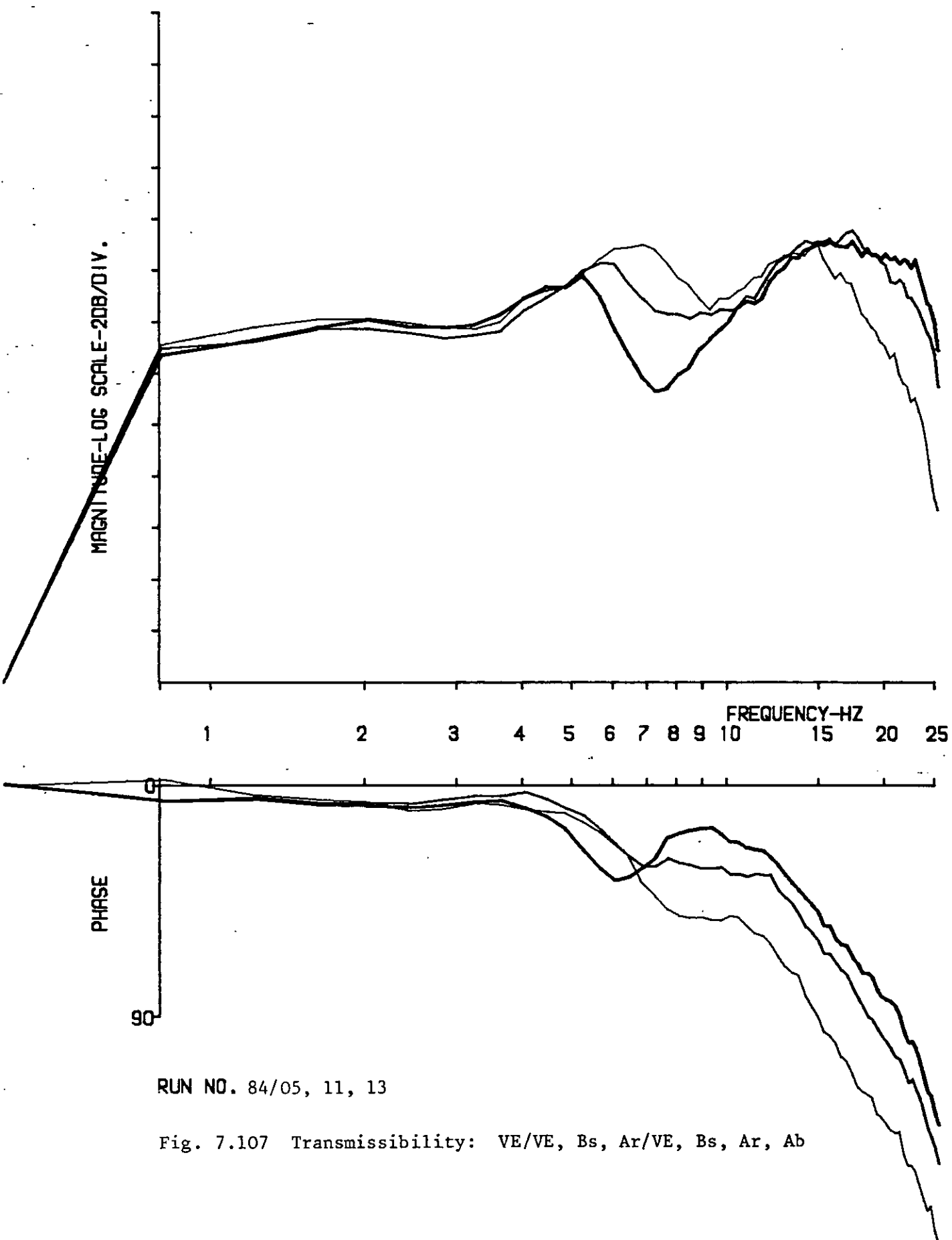






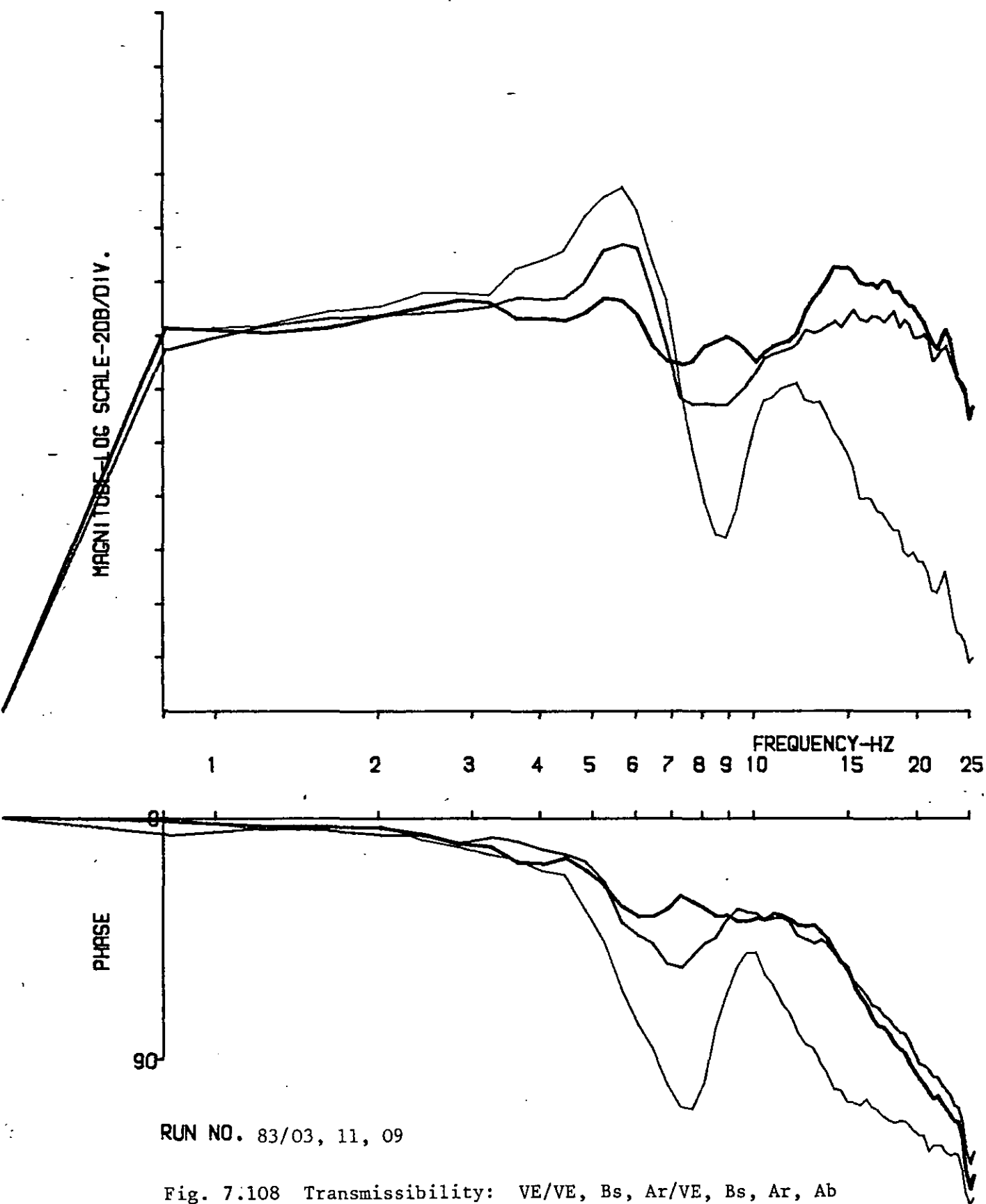
RUN NO. 85/10, 04, 02

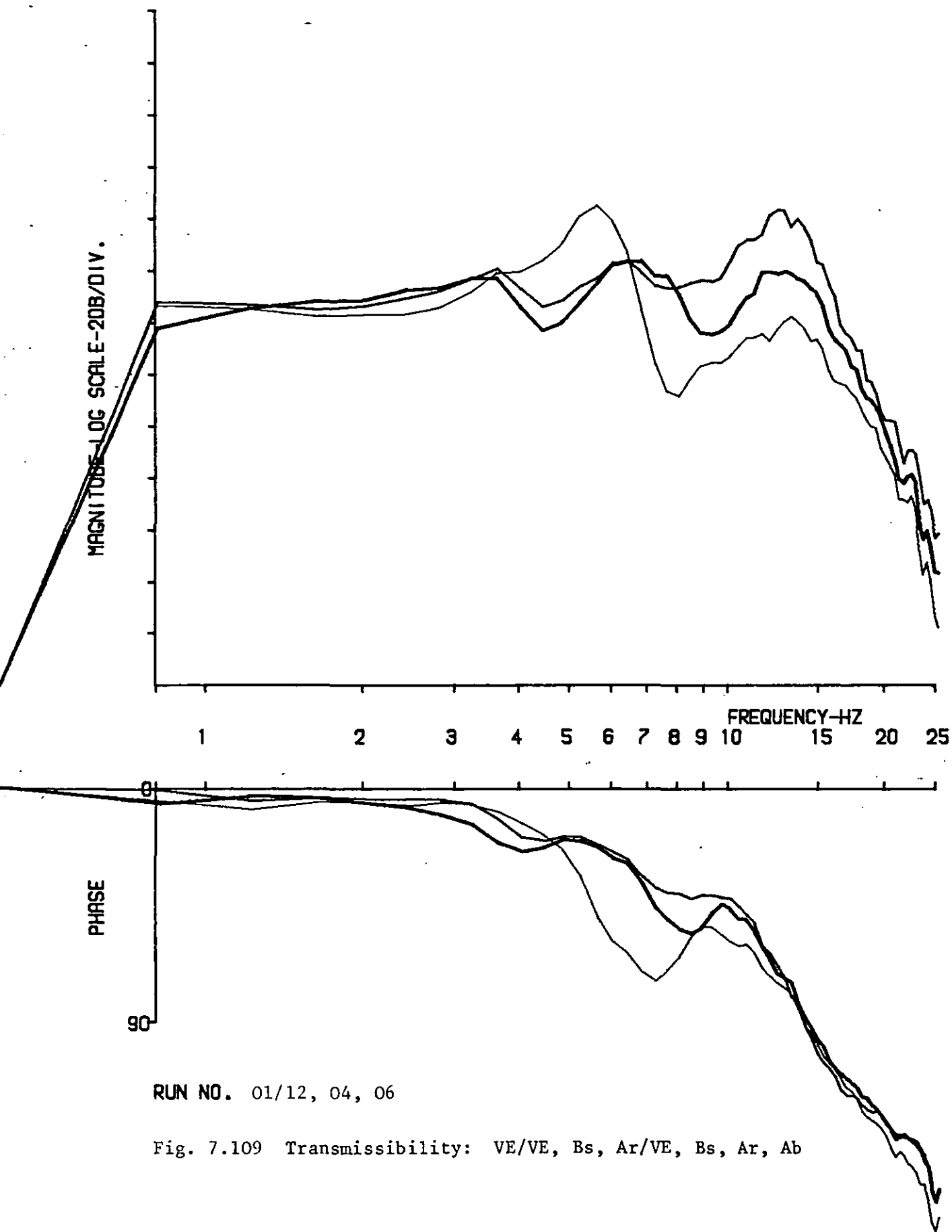
Fig. 7.106 Transmissibility: VE/VE, Bs, Ar/VE, Bs, Ar, Ab

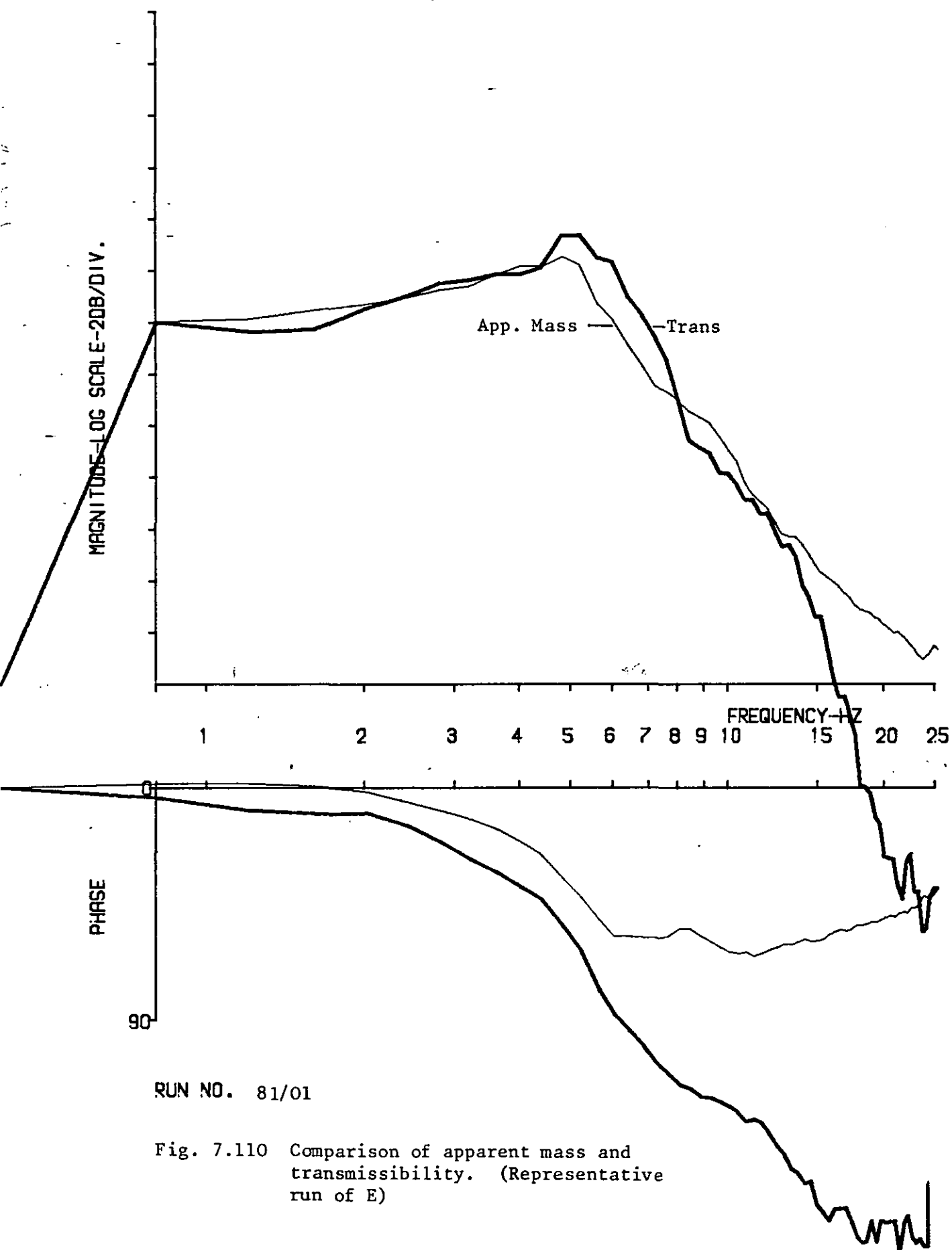


RUN NO. 84/05, 11, 13

Fig. 7.107 Transmissibility: VE/VE, Bs, Ar/VE, Bs, Ar, Ab







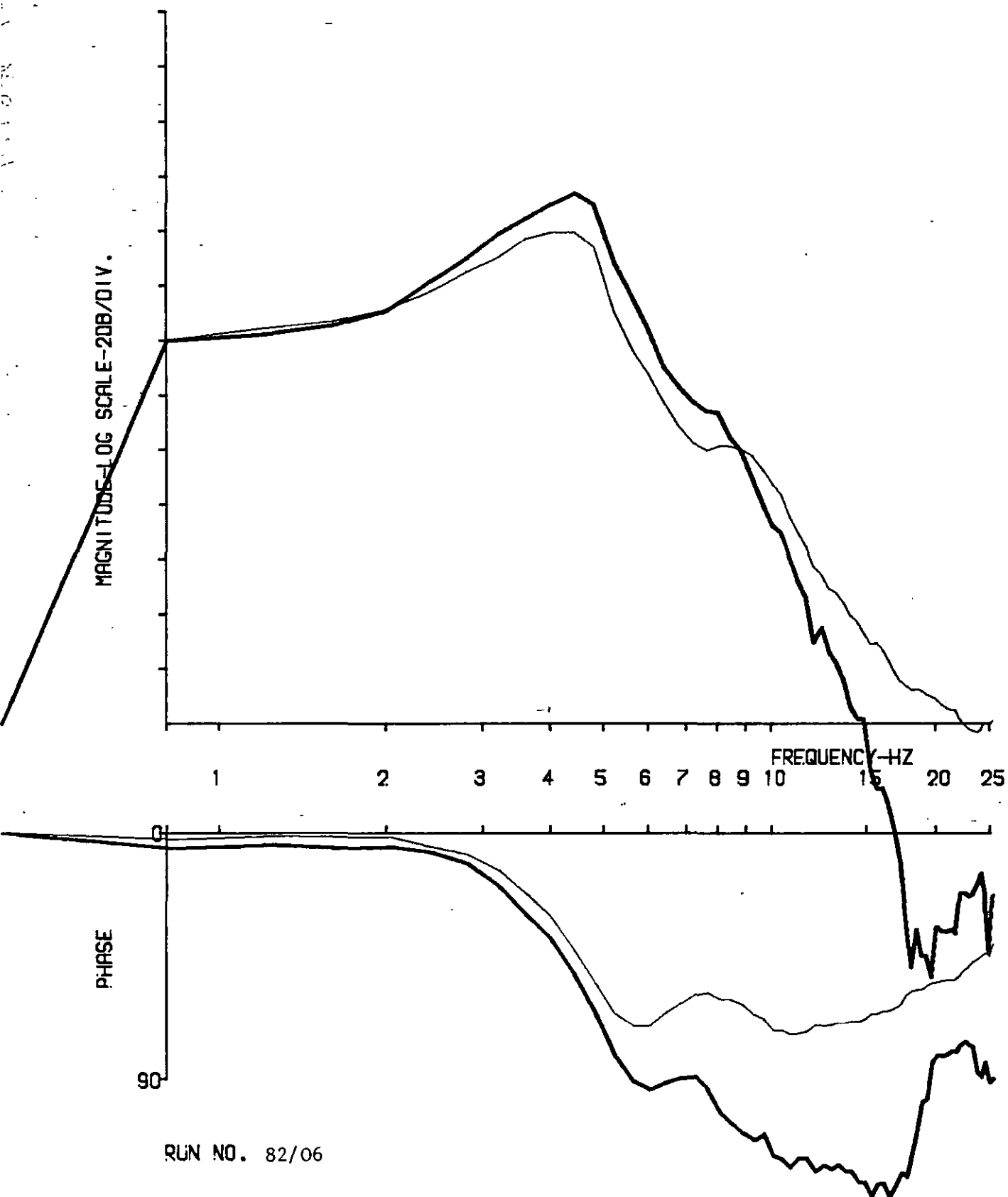
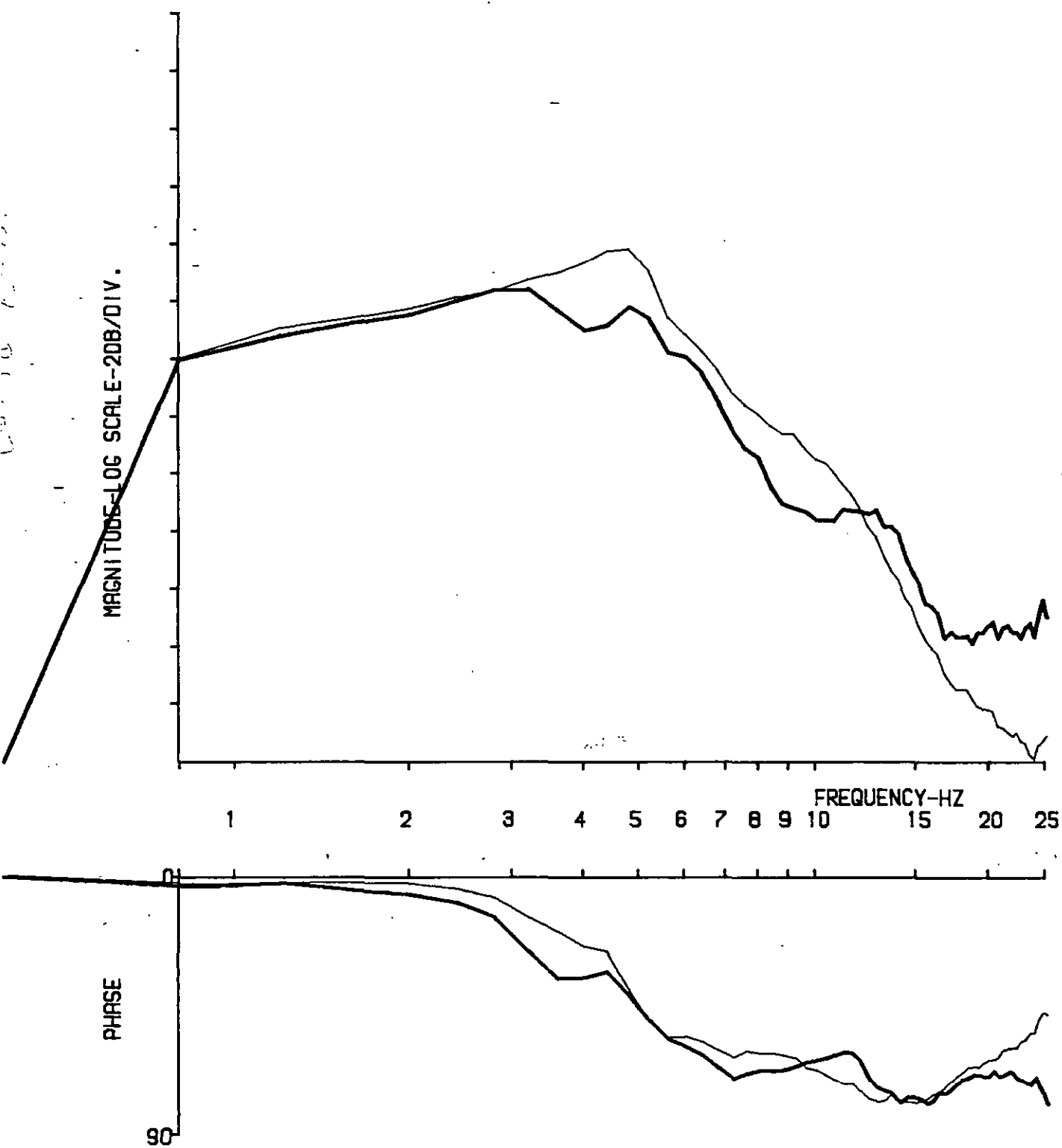
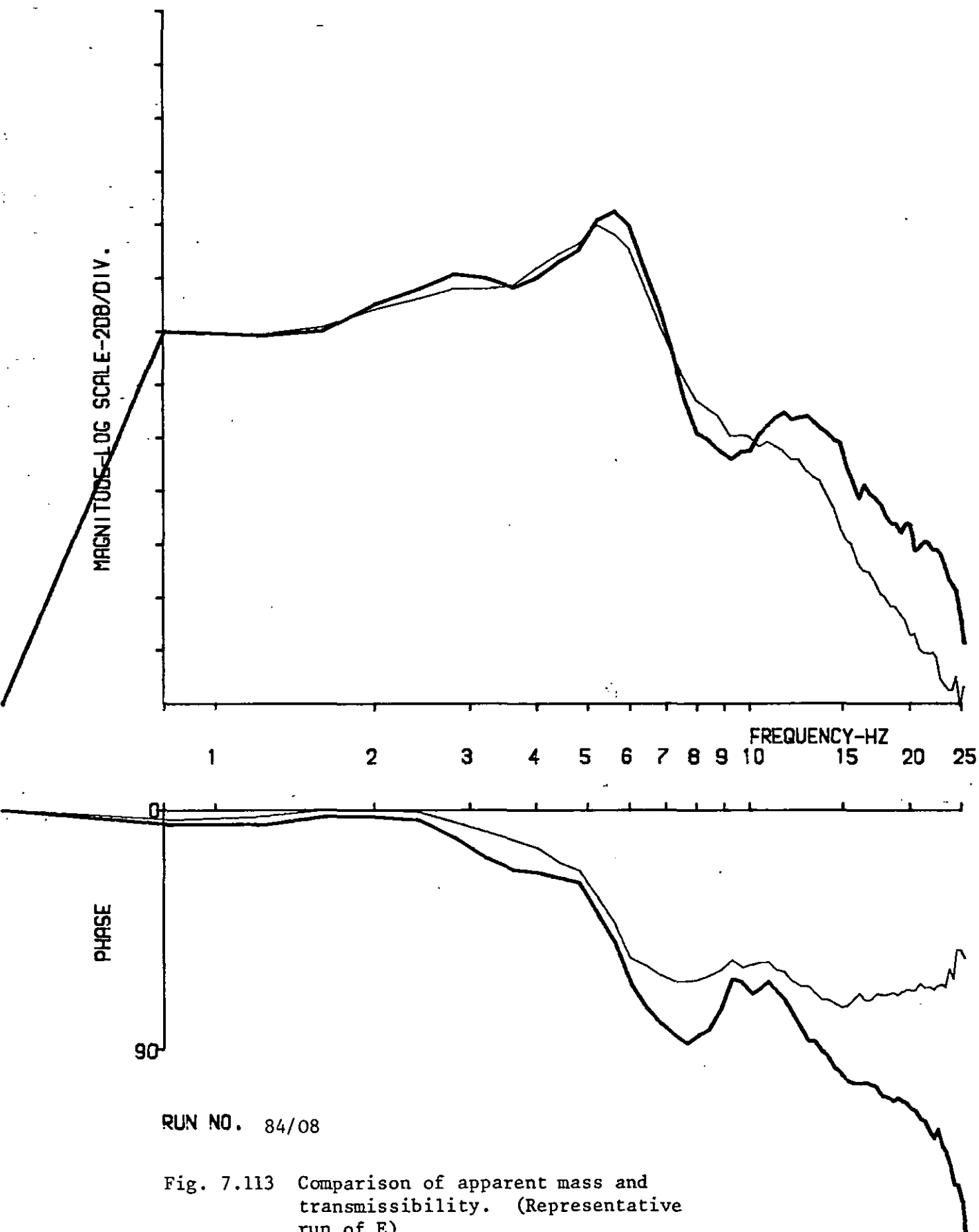


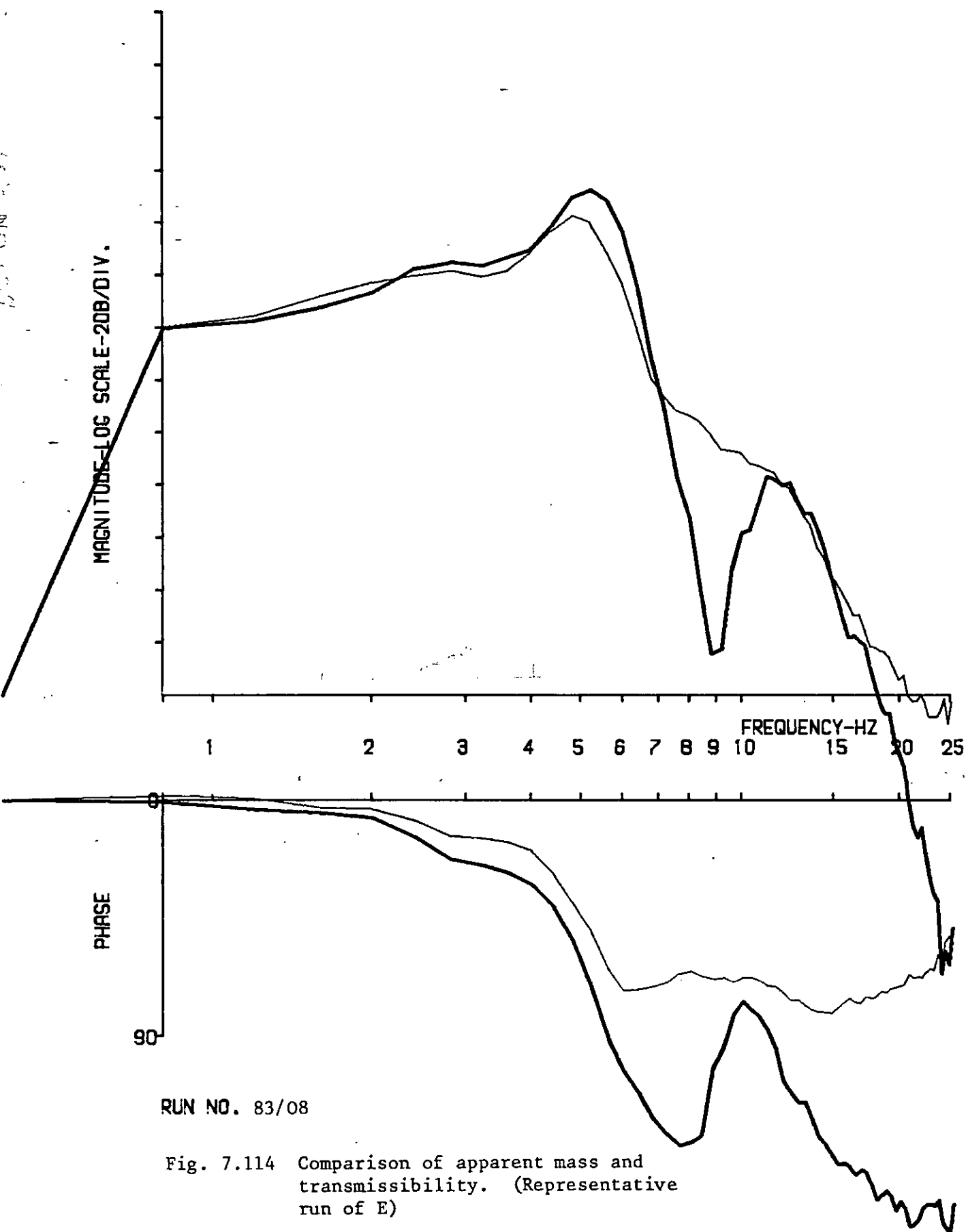
Fig. 7.111 Comparison of apparent mass and transmissibility. (Representative run of E)

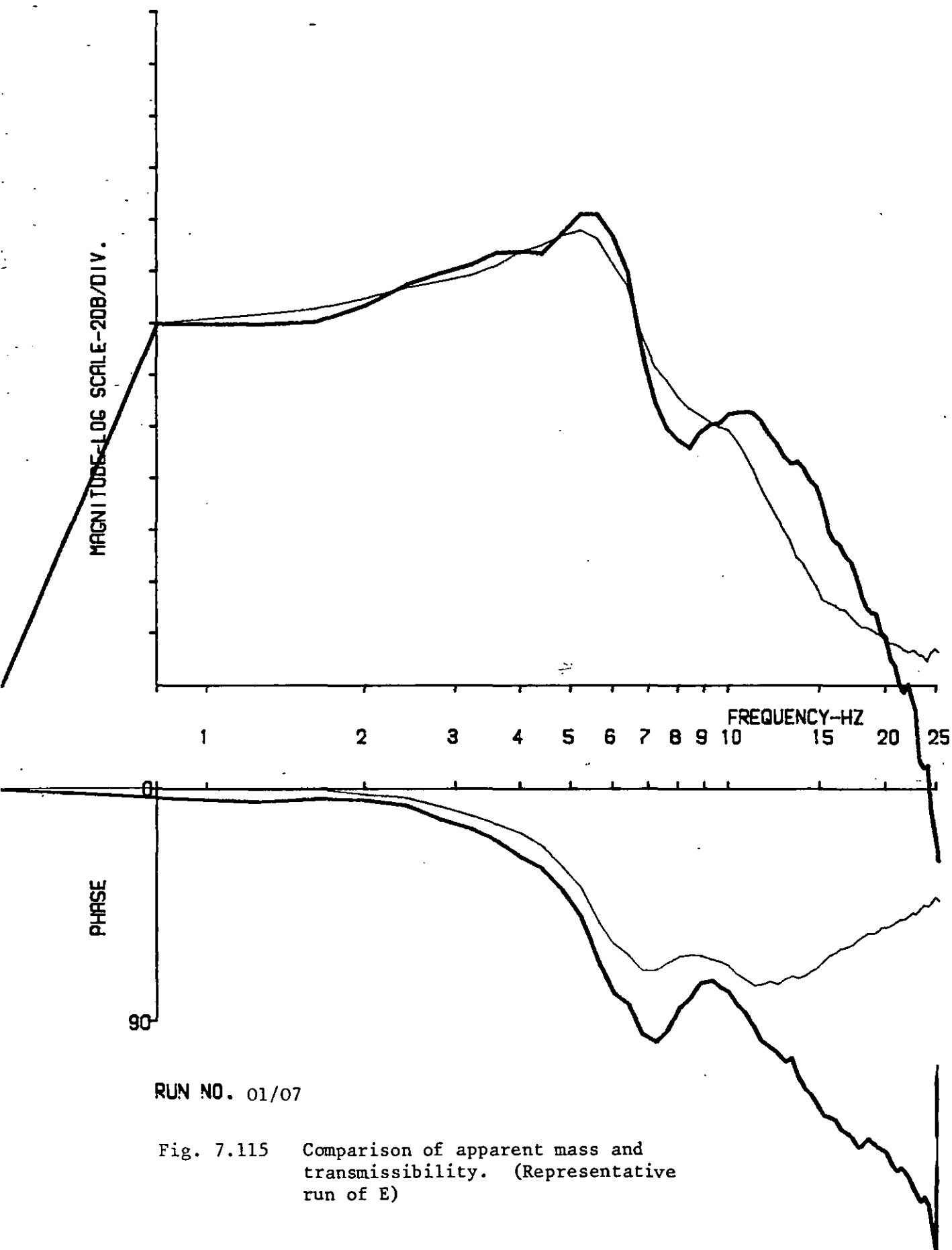


RUN NO. 85/07

Fig. 7.112 Comparison of apparent mass and transmissibility. (Representative run of E)

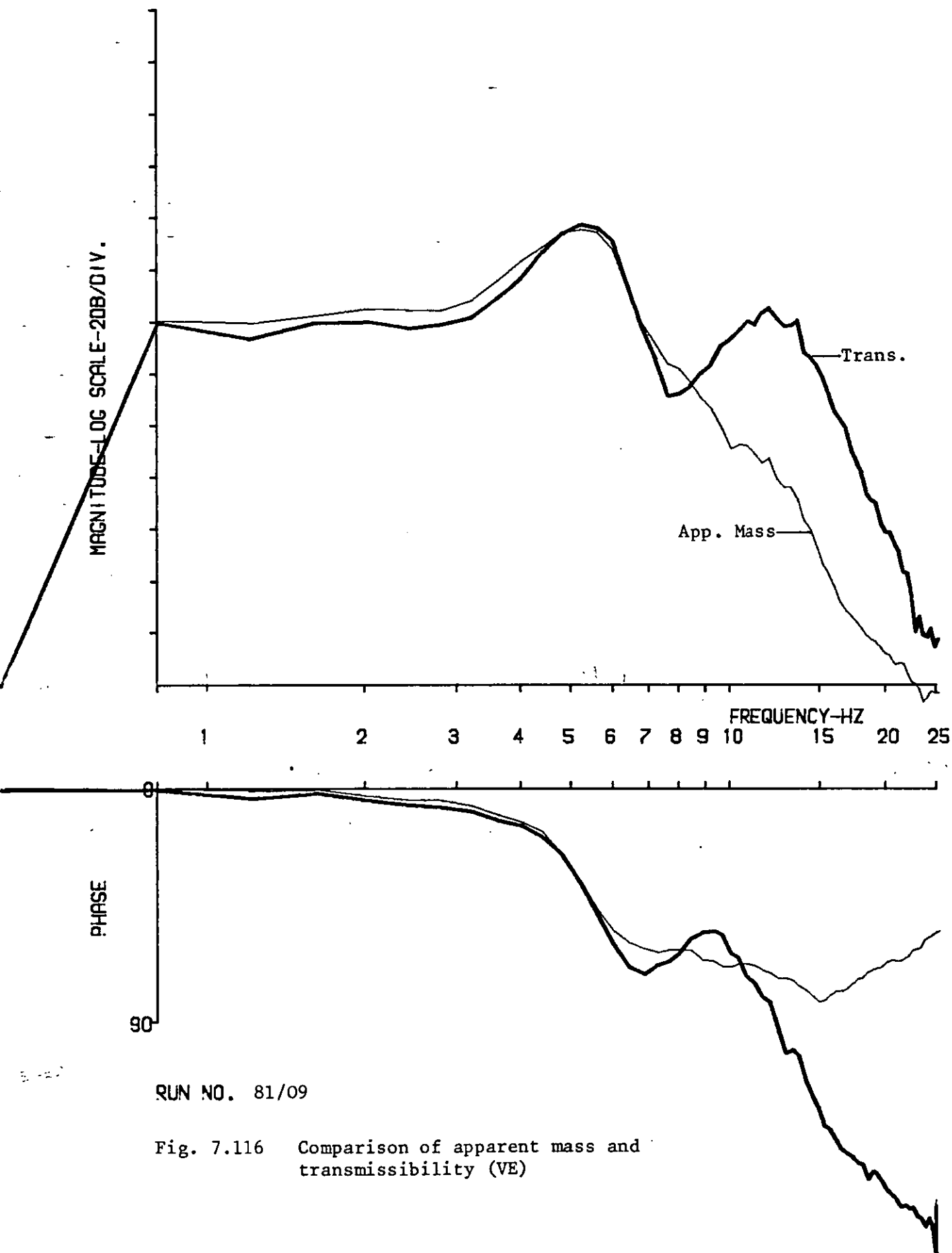


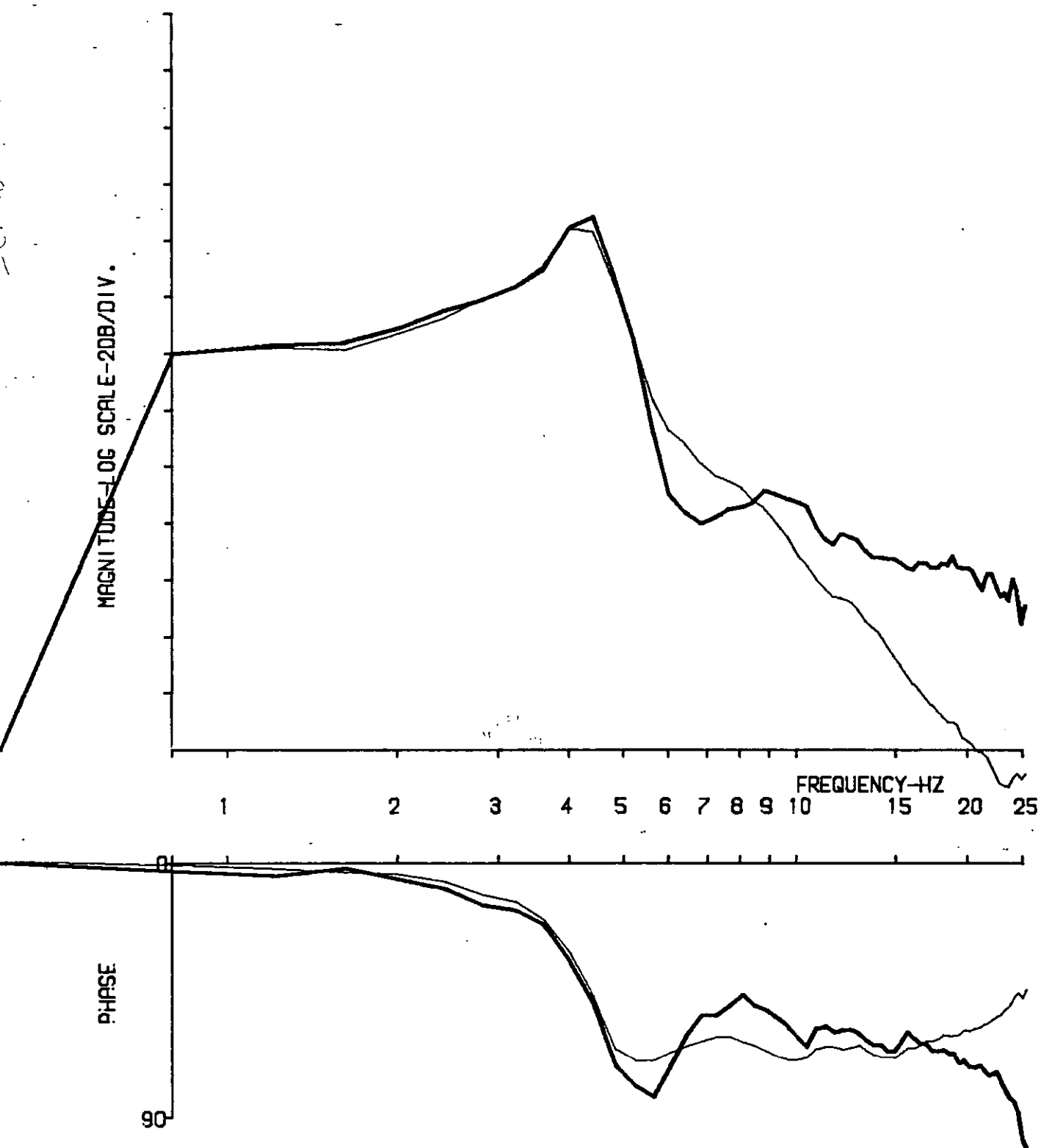




RUN NO. 01/07

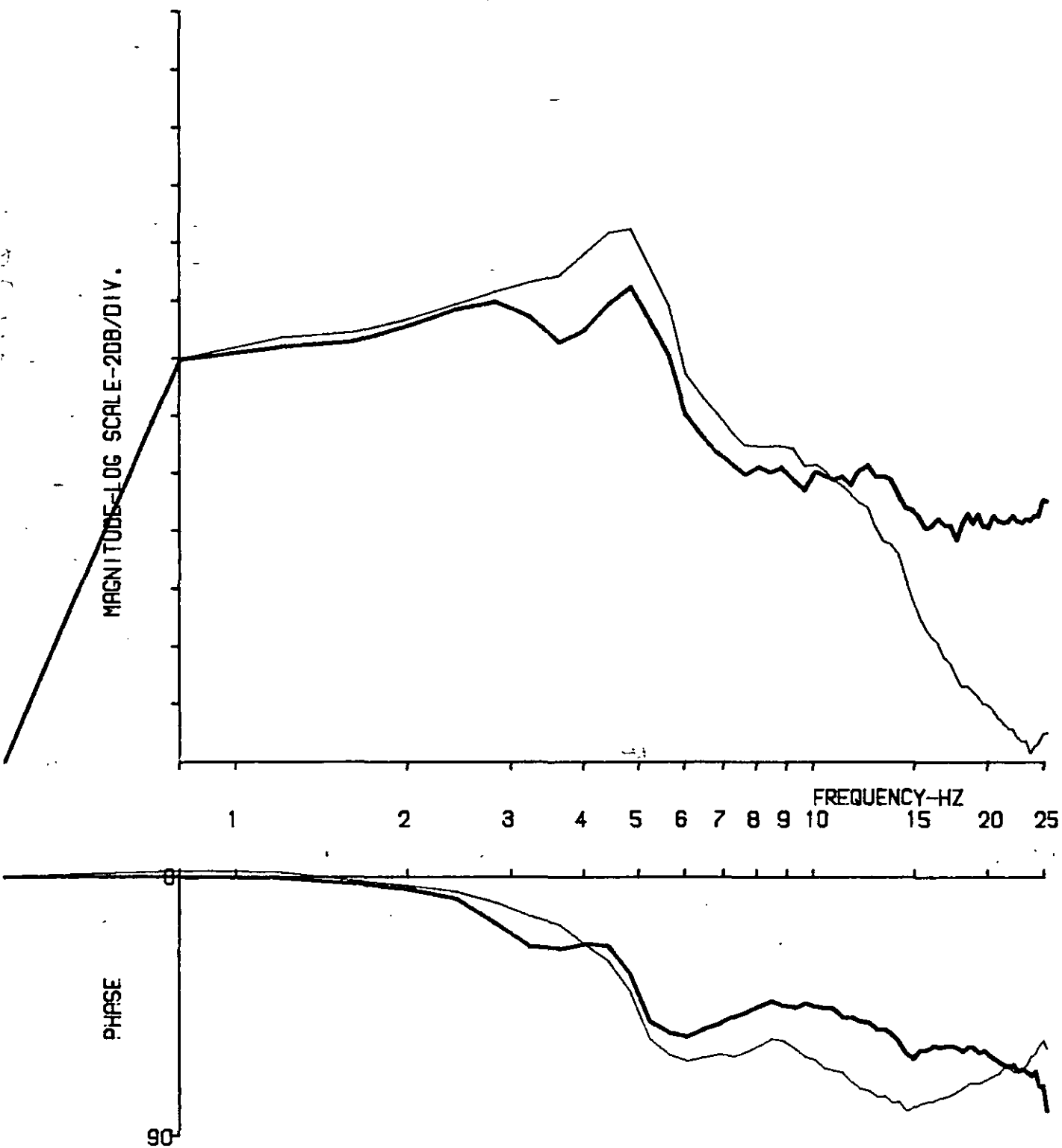
Fig. 7.115 Comparison of apparent mass and transmissibility. (Representative run of E)





RUN NO. 82/05

Fig. 7.117 Comparison of apparent mass and transmissibility (VE)



RUN NO. 85/10

Fig. 7.118 Comparison of apparent mass and transmissibility (VE)

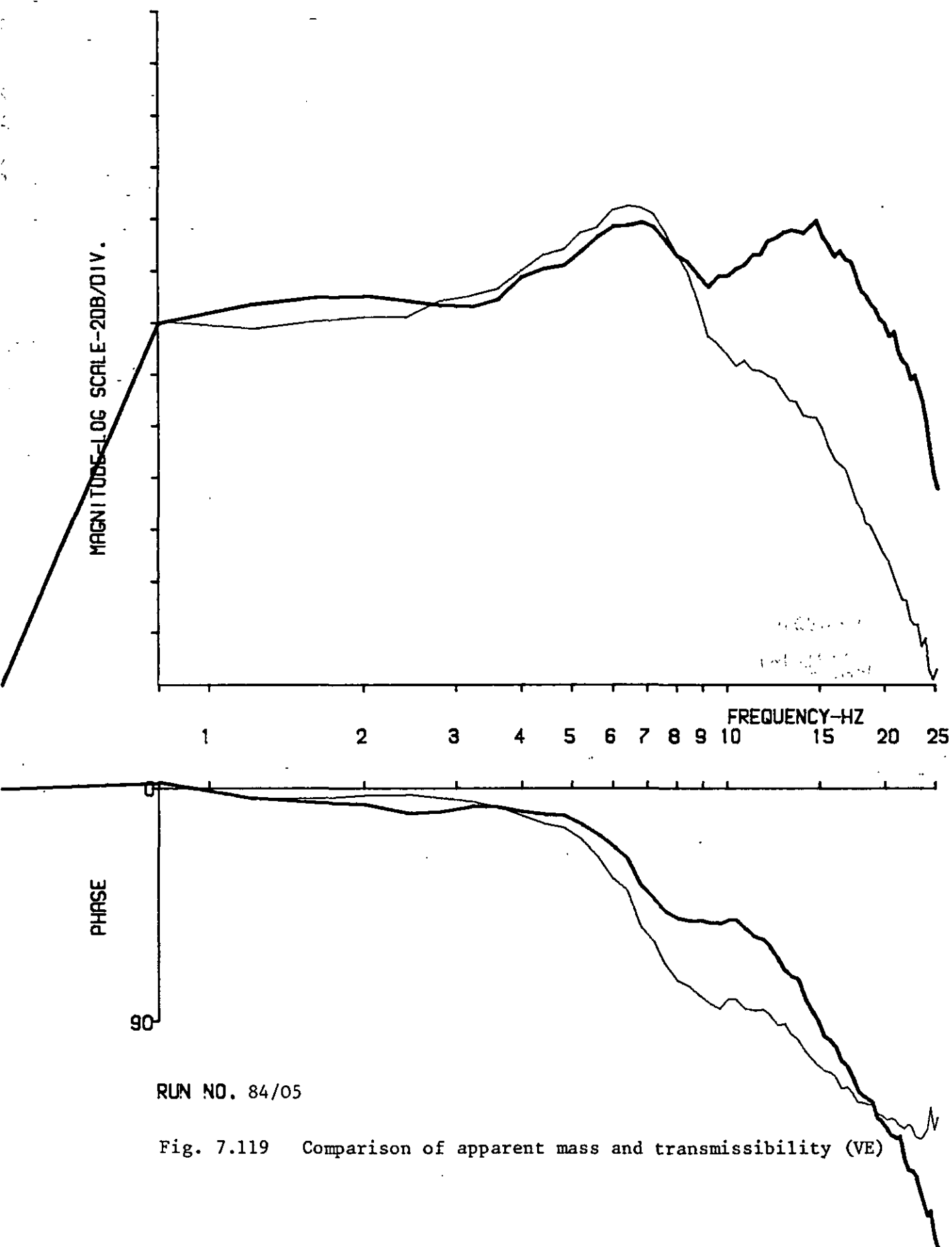
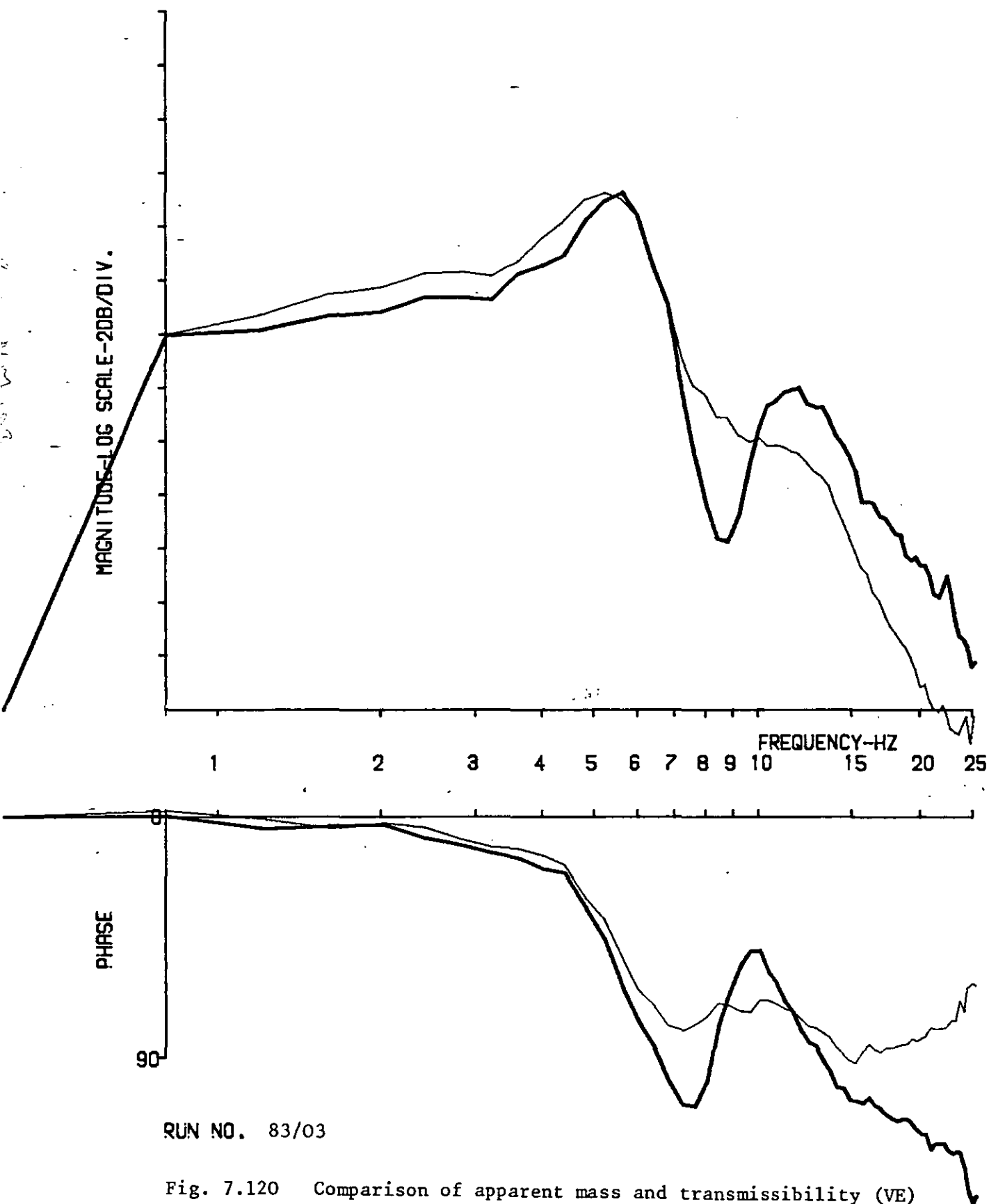
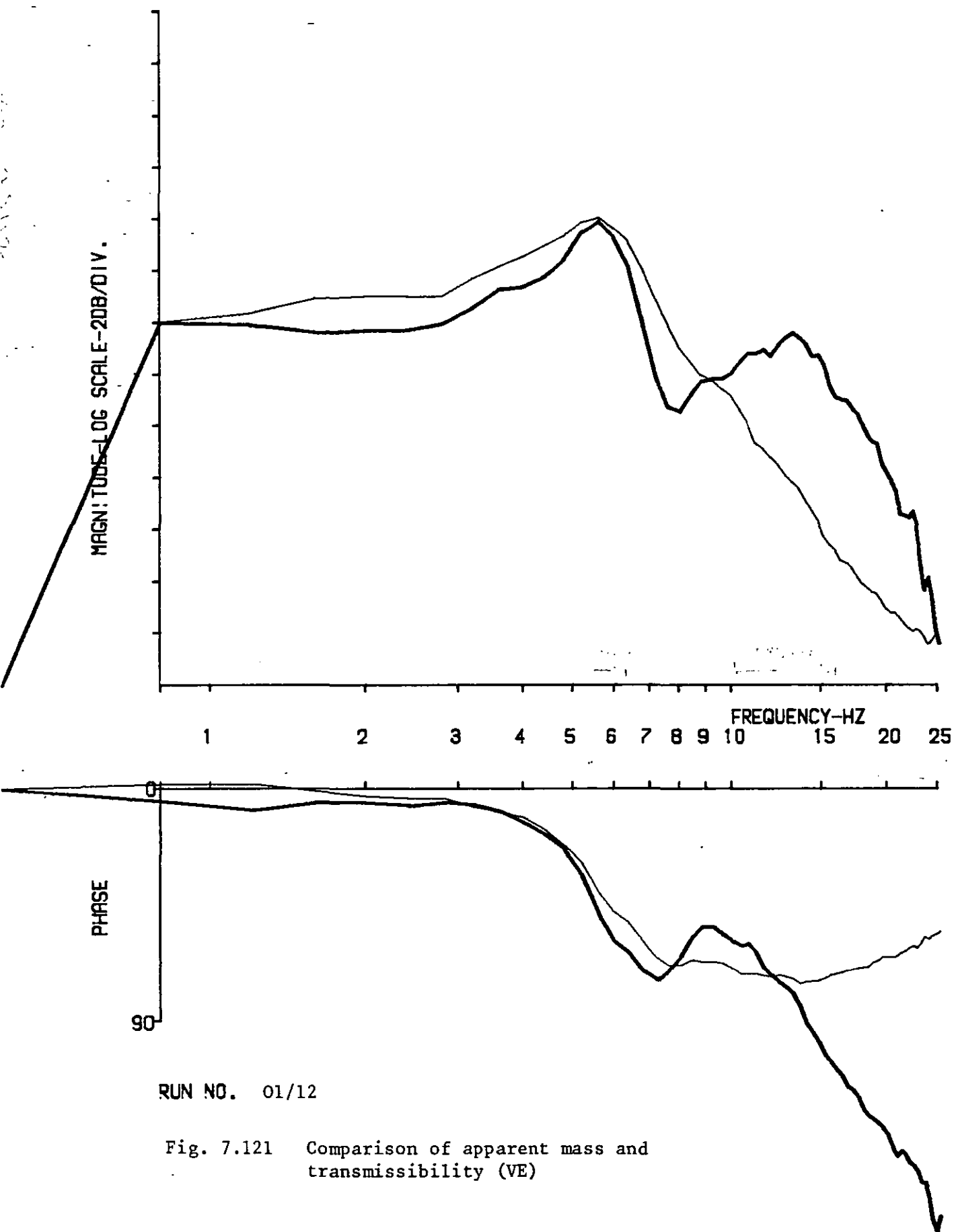
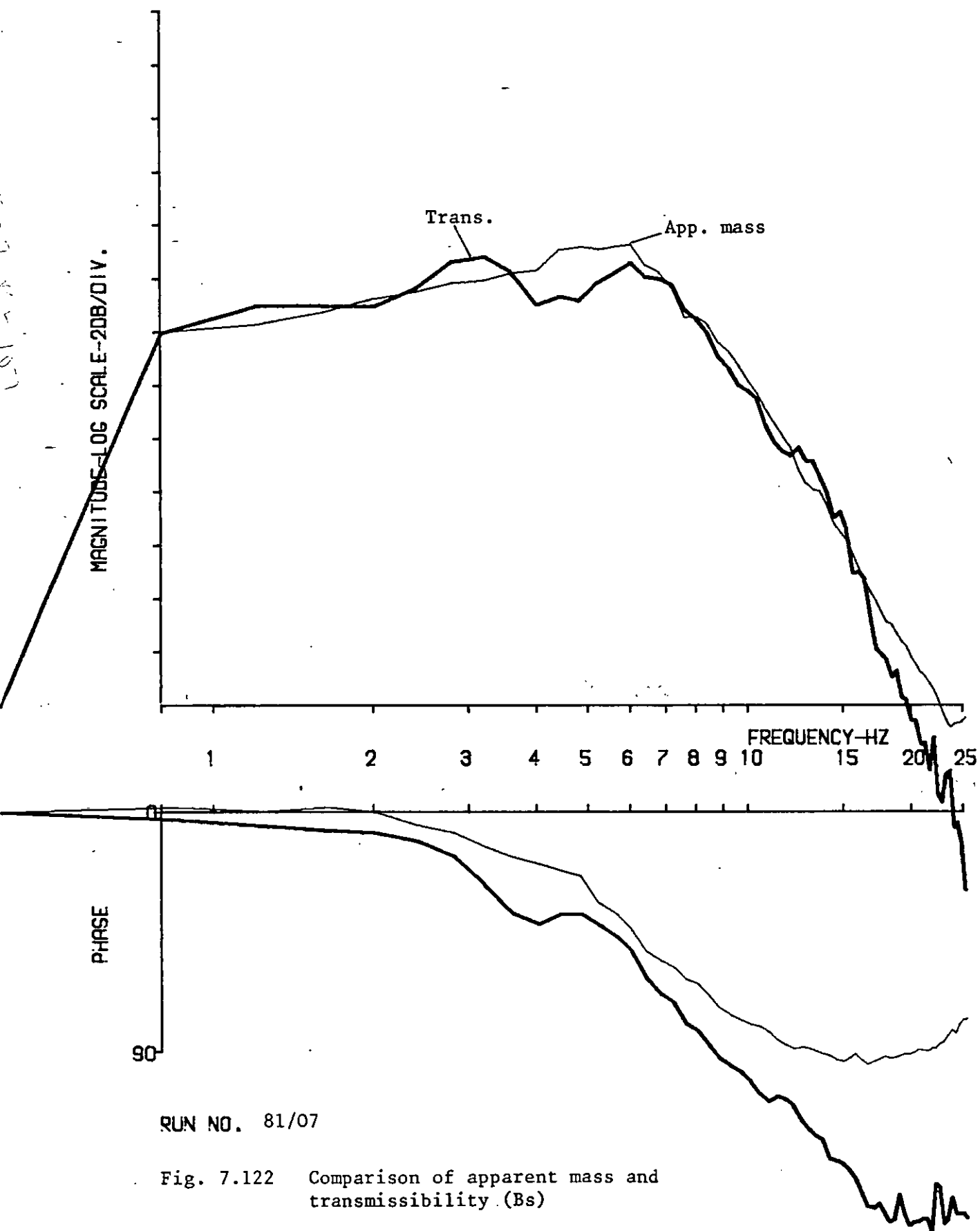


Fig. 7.119 Comparison of apparent mass and transmissibility (VE)







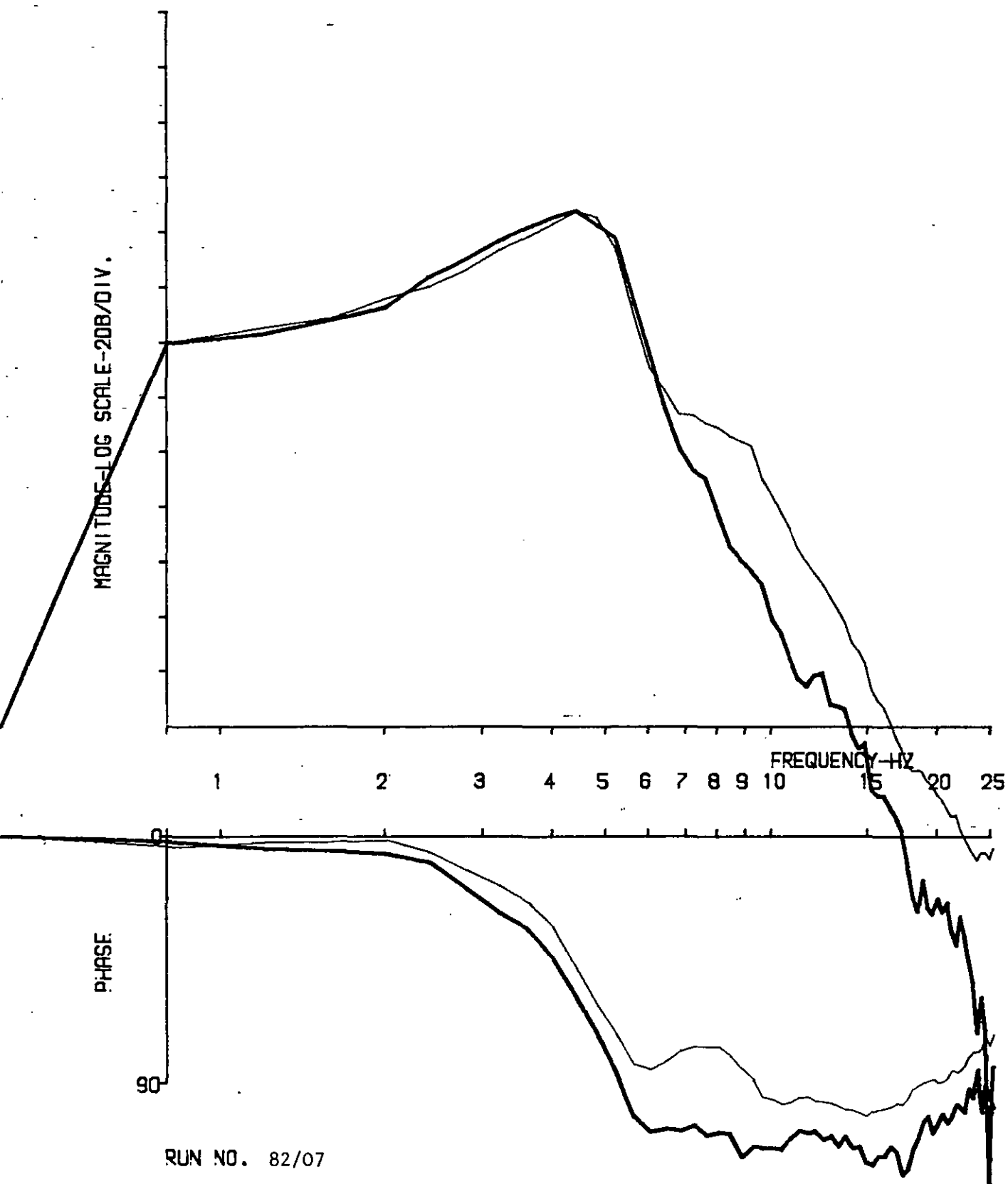
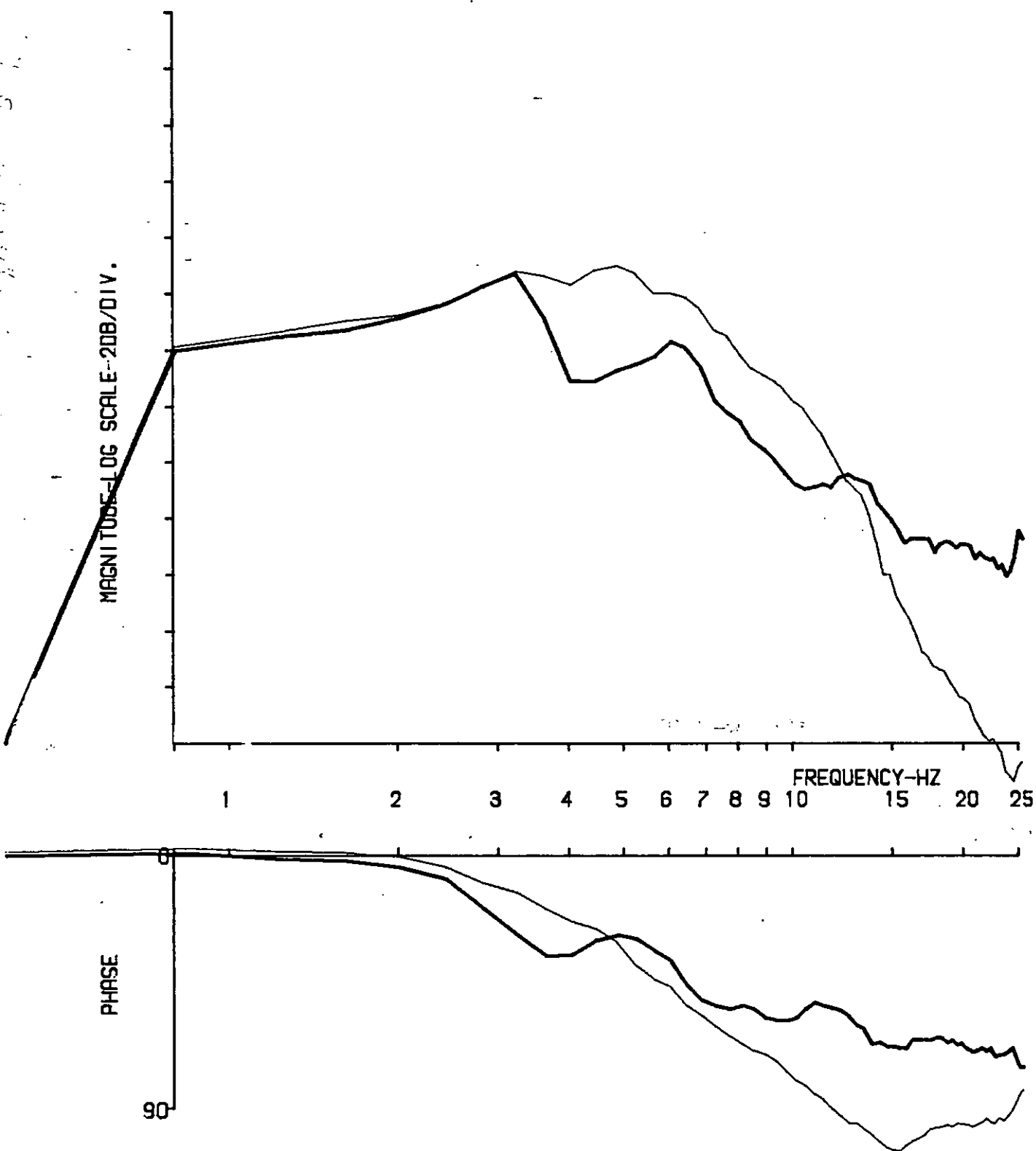
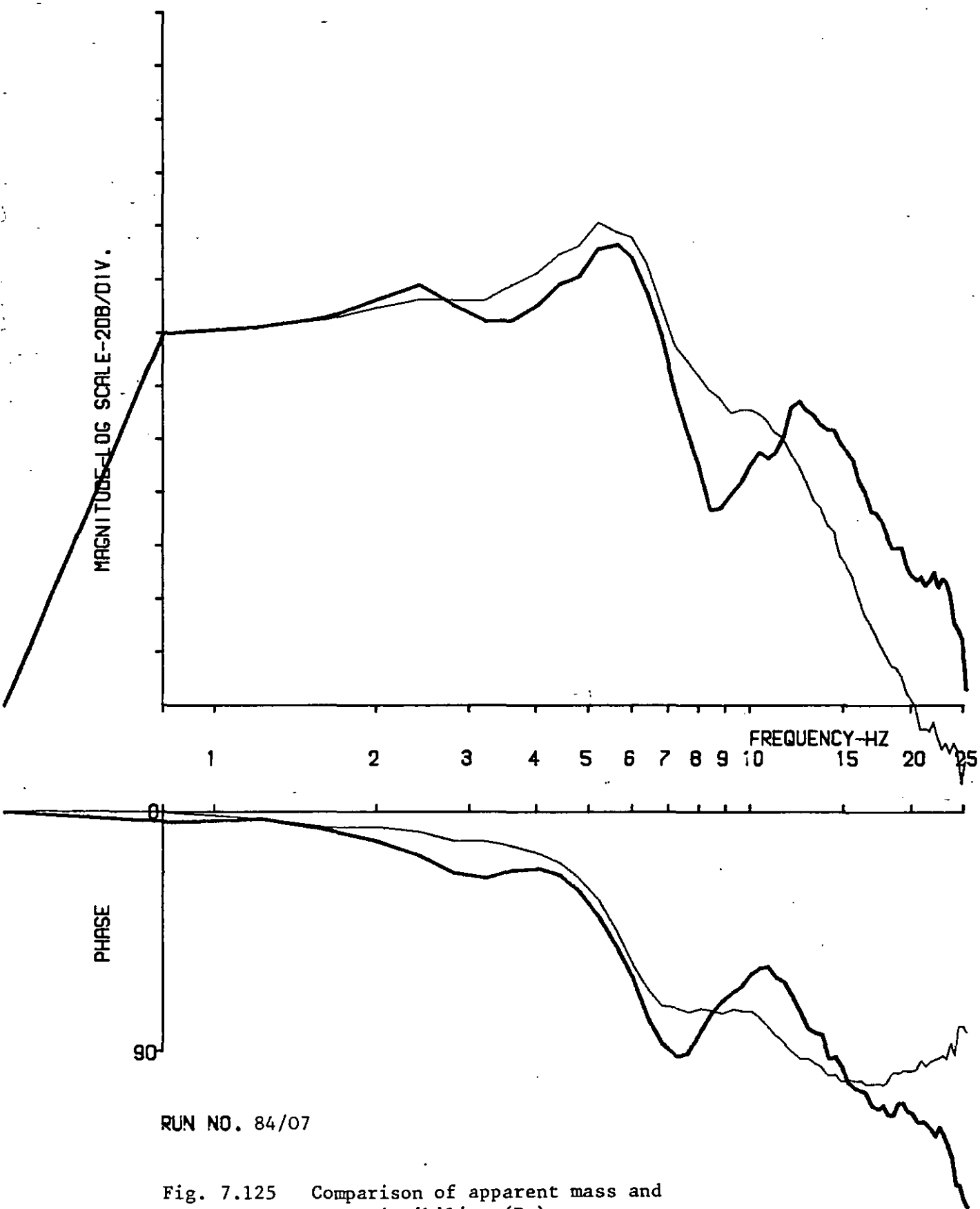


Fig. 7.123 Comparison of apparent mass and transmissibility (Bs)



RUN NO. 85/08

Fig. 7.124 Comparison of apparent mass and transmissibility (Bs)



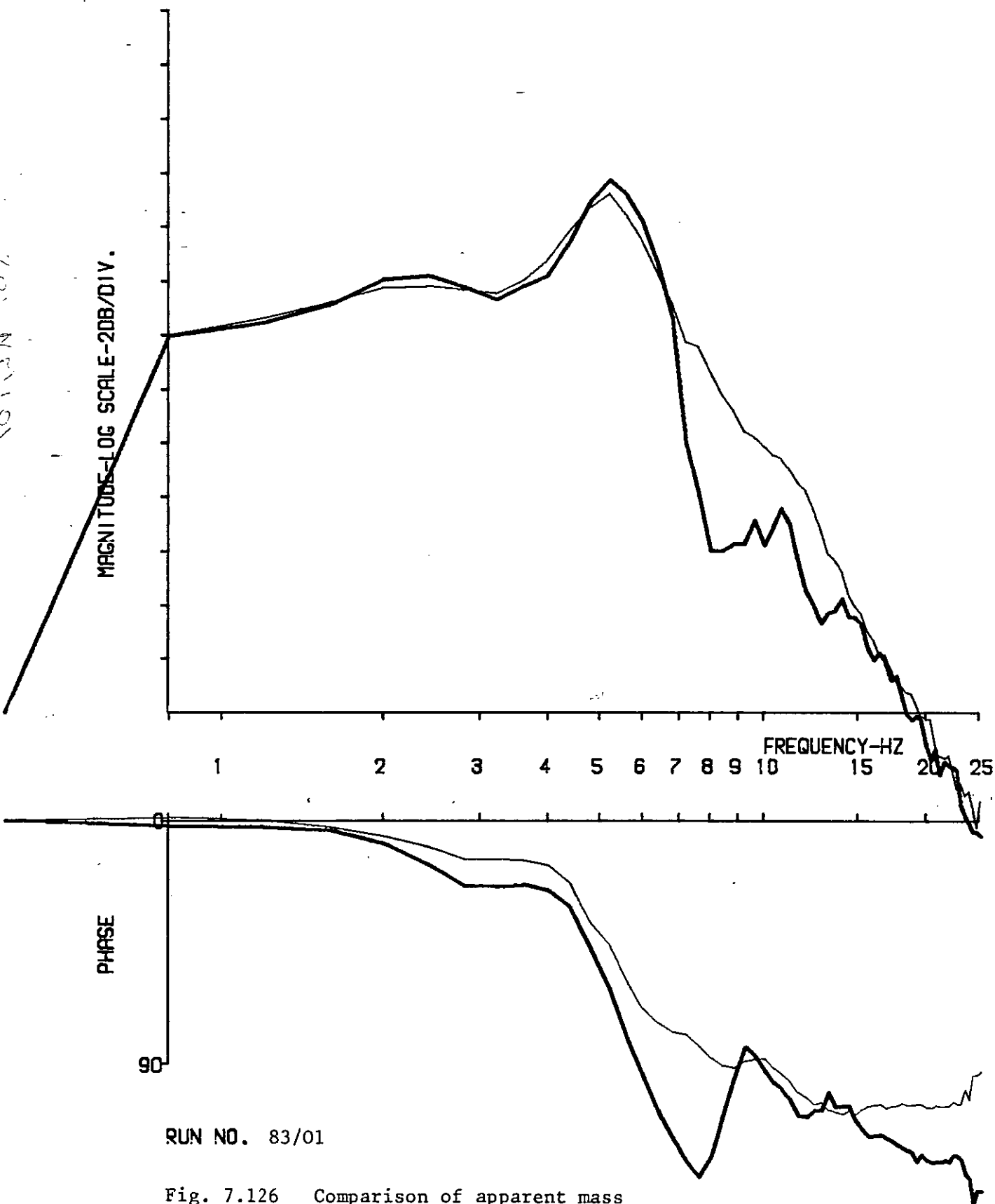
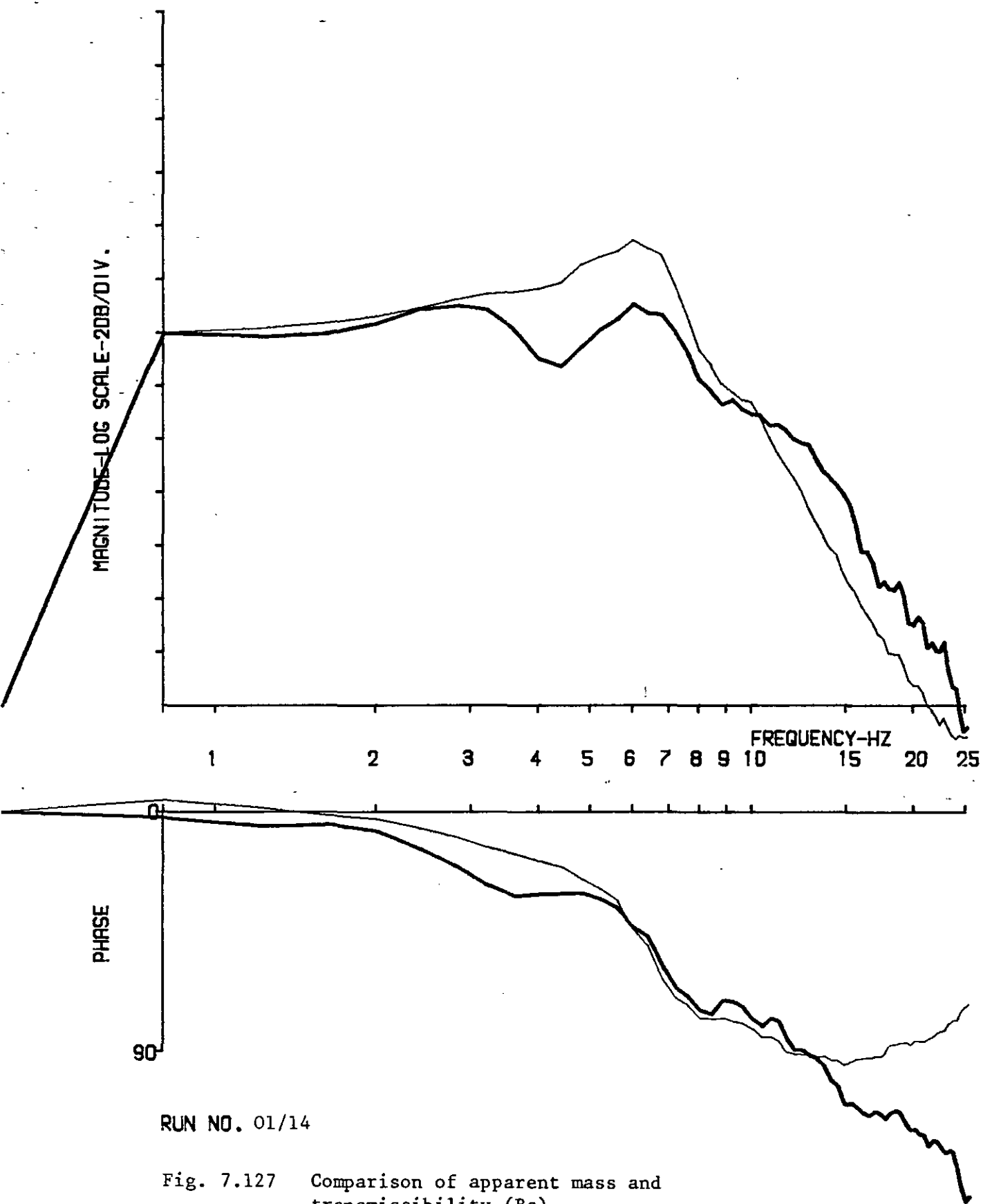
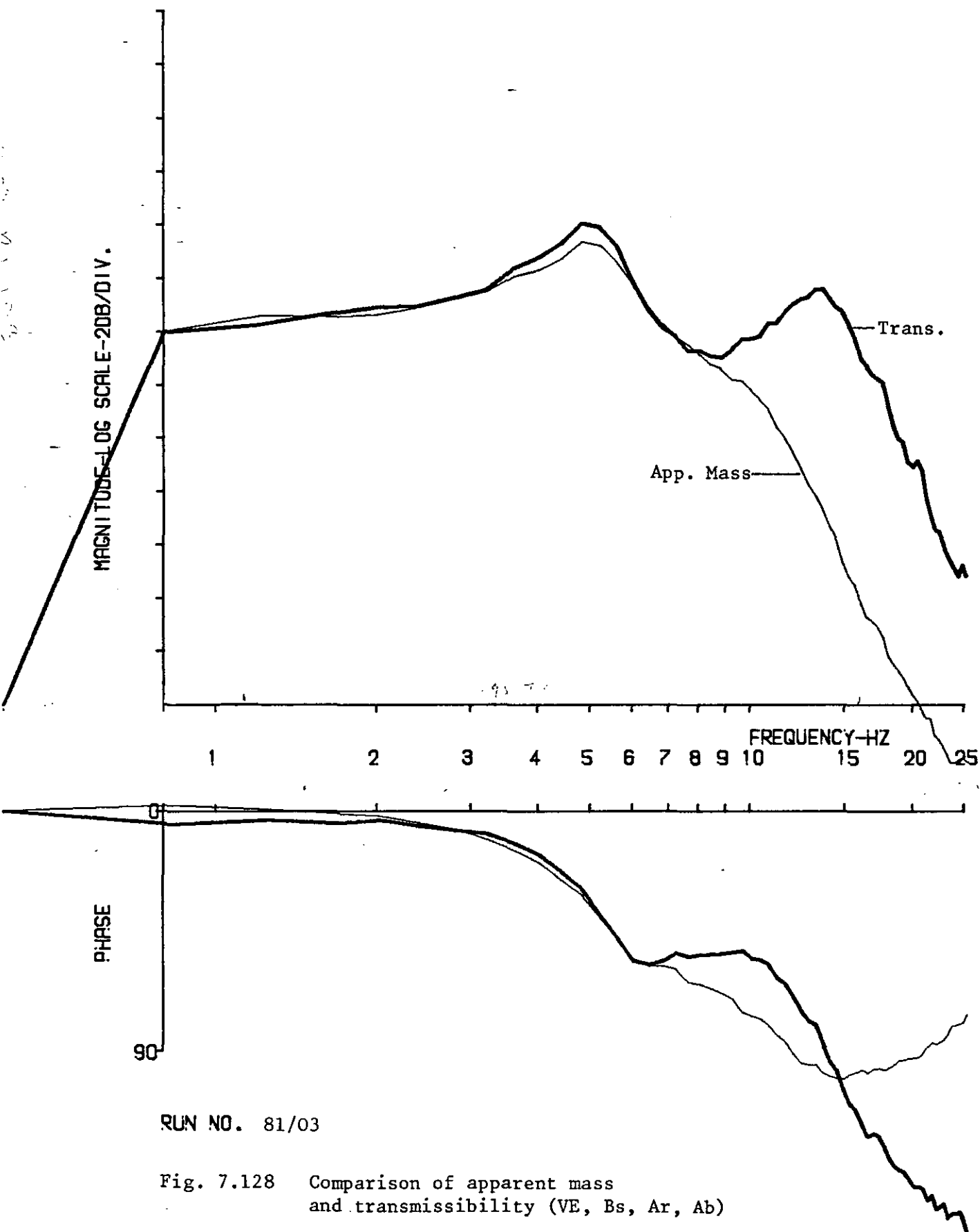
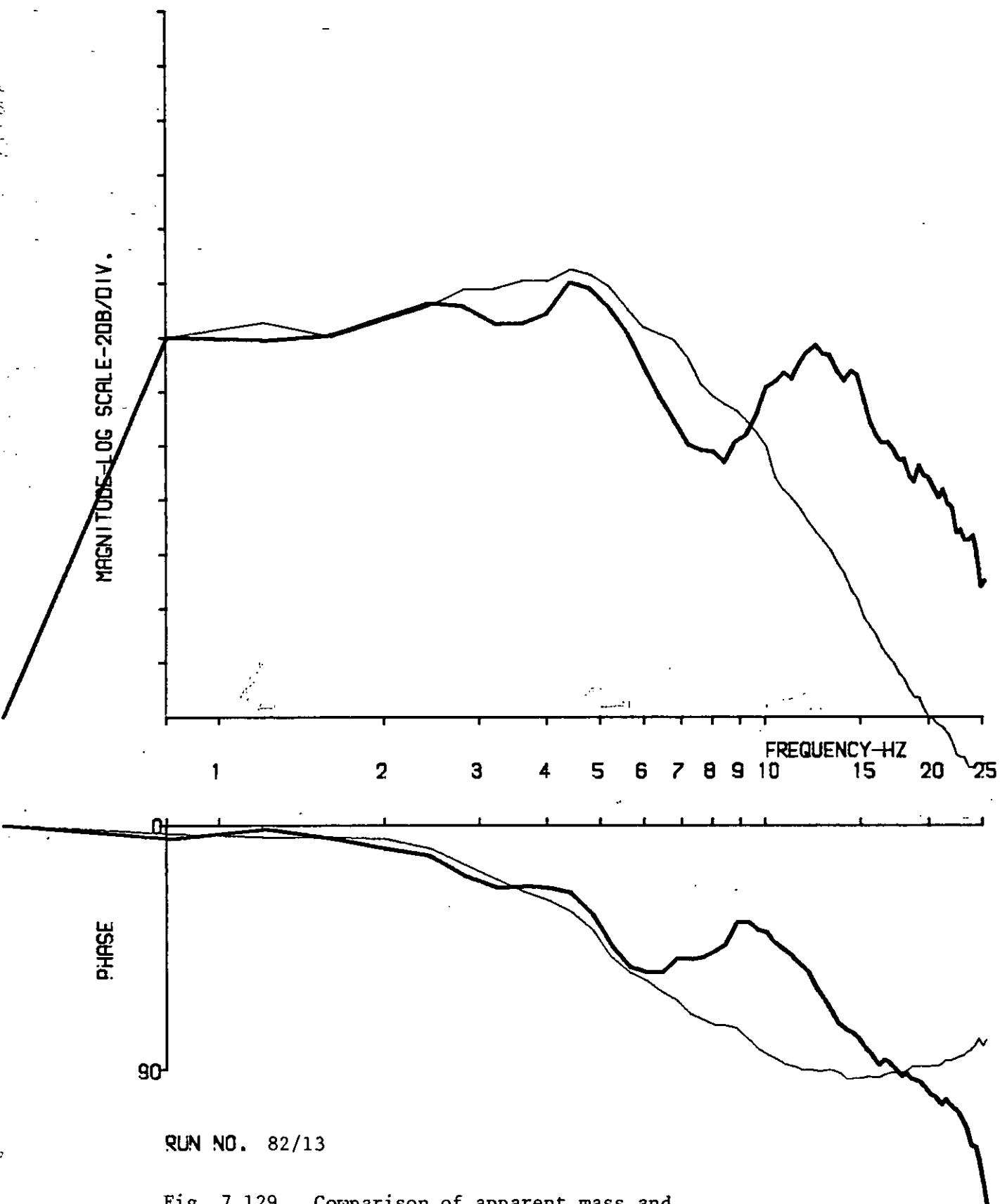


Fig. 7.126 Comparison of apparent mass and transmissibility (Bs)

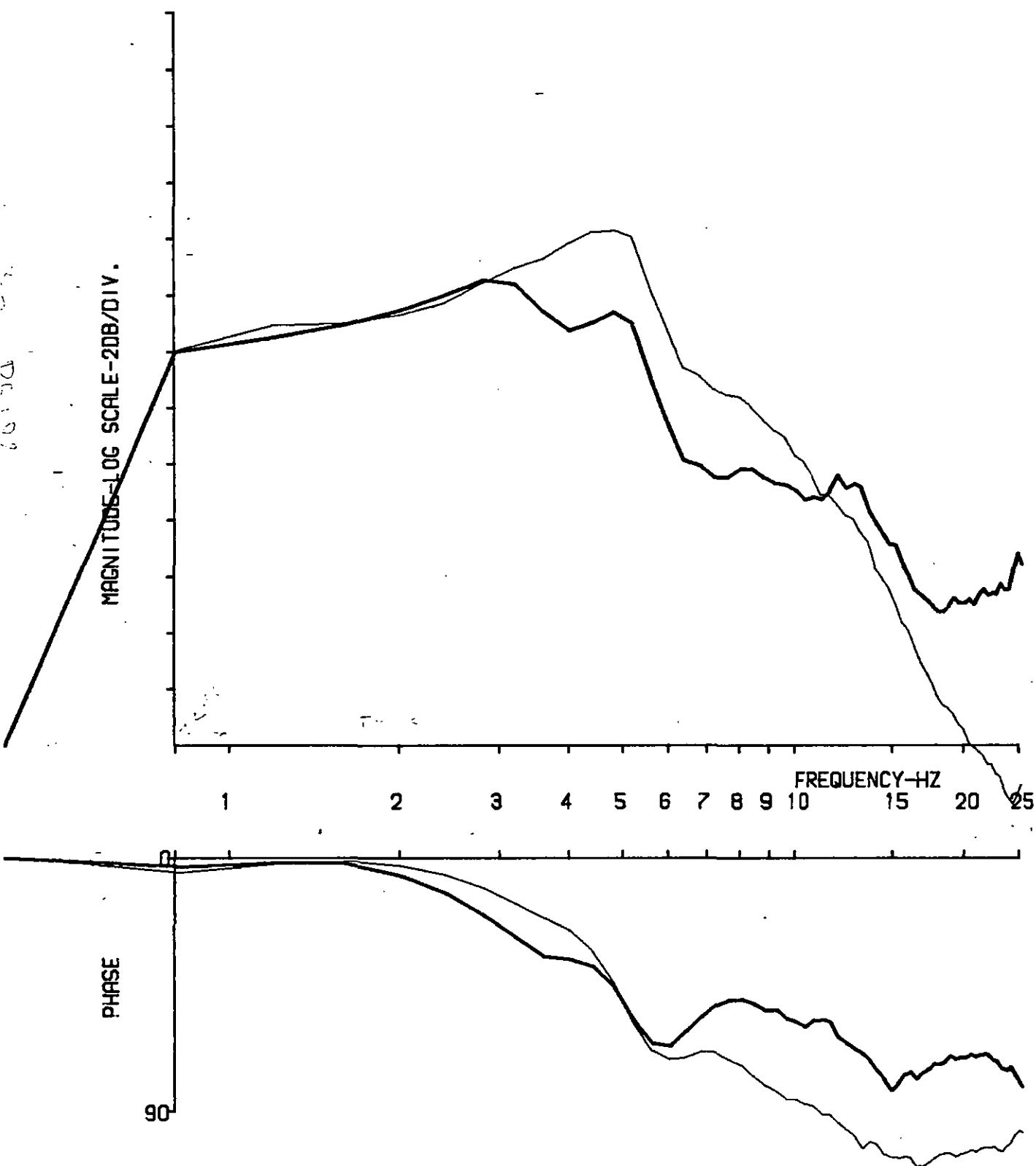






RUN NO. 82/13

Fig. 7.129 Comparison of apparent mass and transmissibility (VE, Bs, Ar, Ab)



RUN NO. 85/02

Fig. 7.130 Comparison of apparent mass and transmissibility (VE, Bs, Ar, Ab)

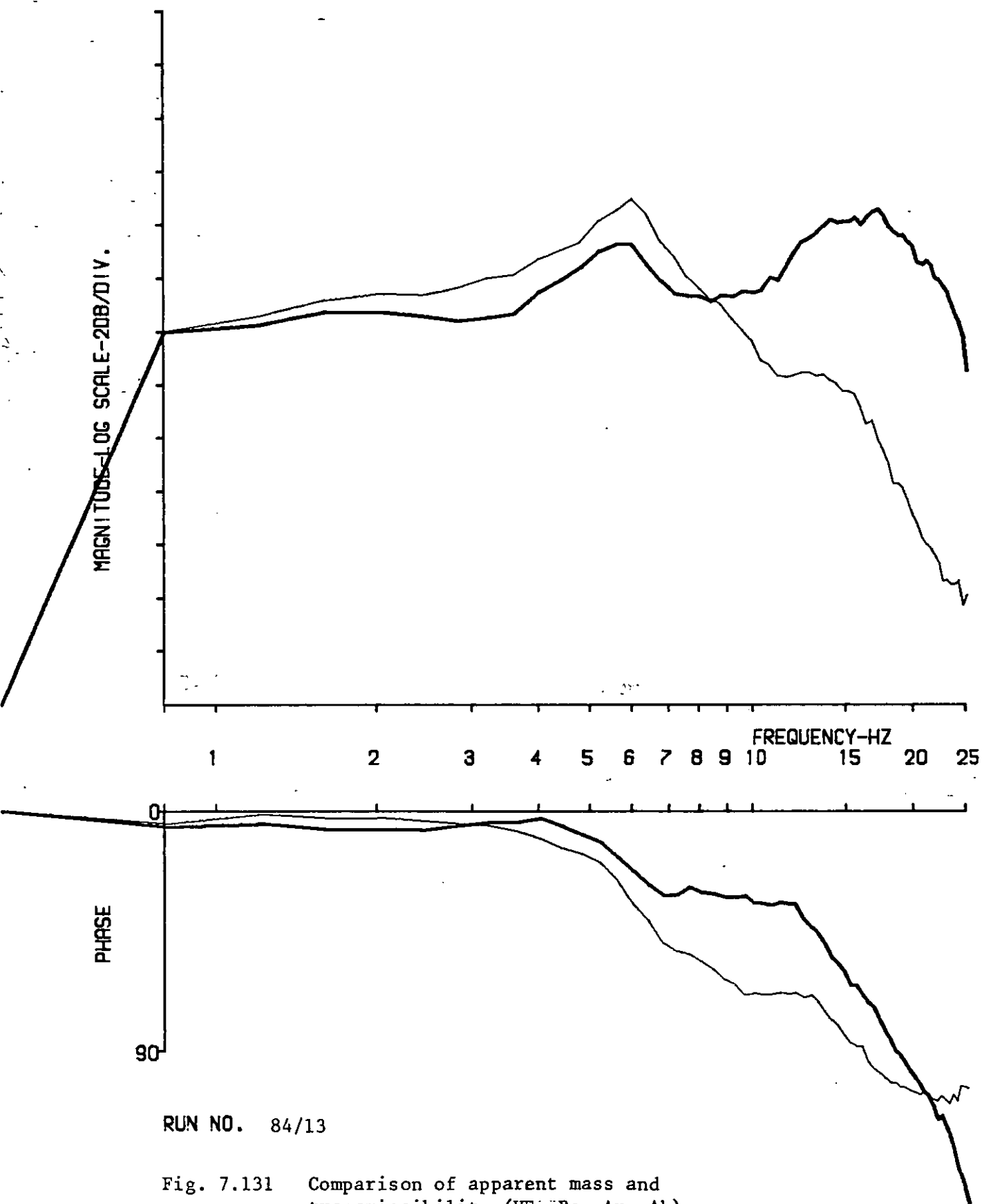


Fig. 7.131 Comparison of apparent mass and transmissibility (VE, Bs, Ar, Ab)

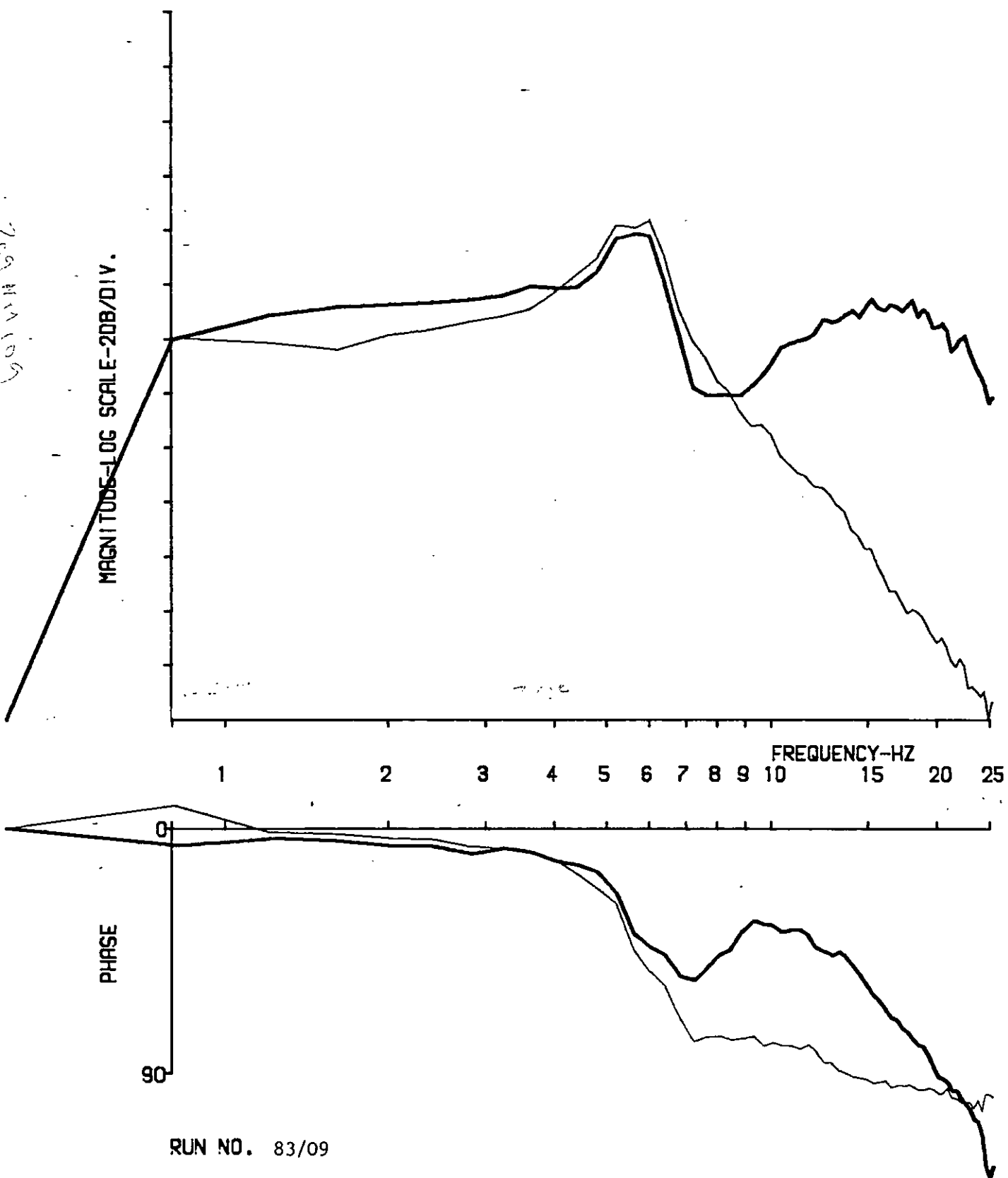
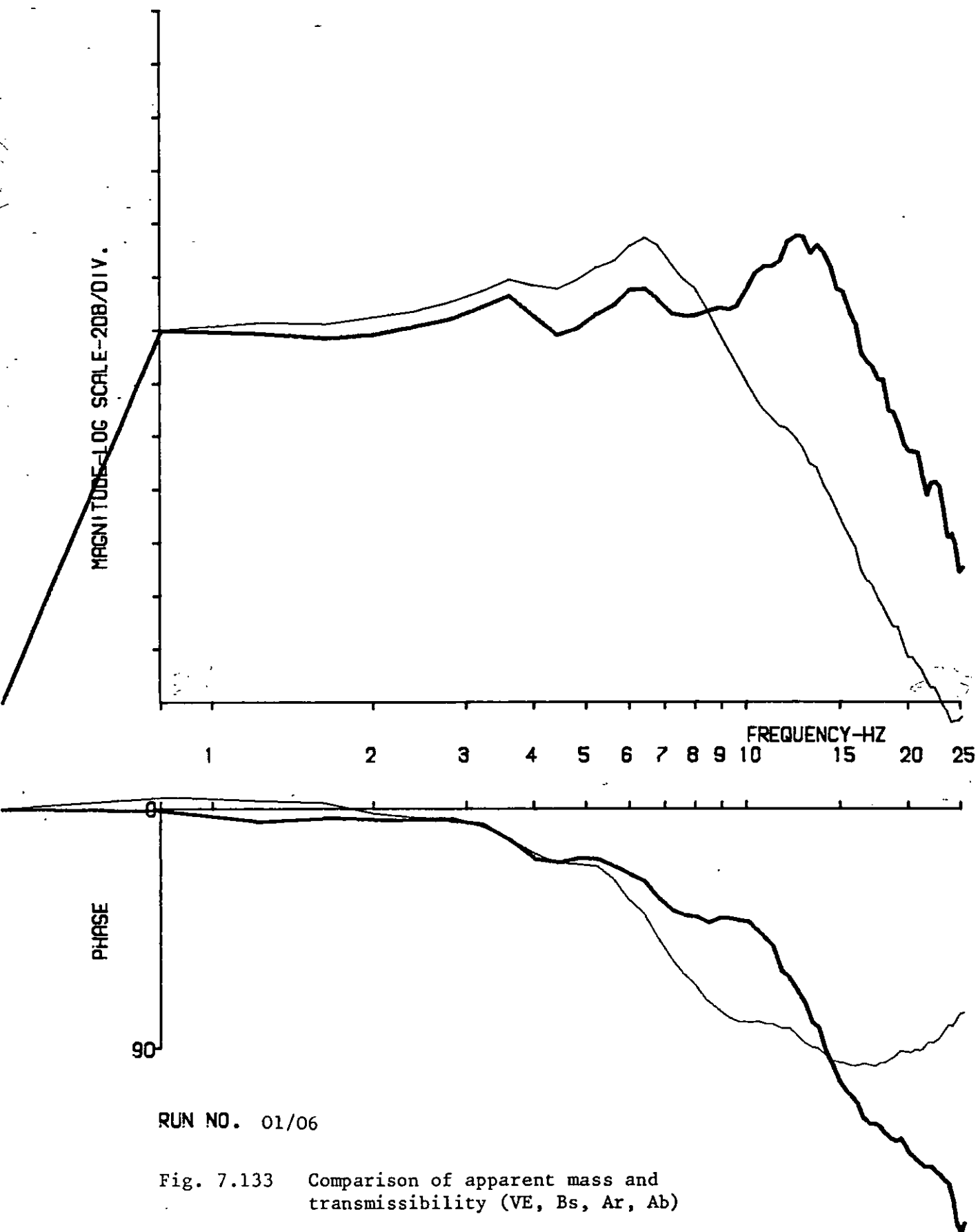
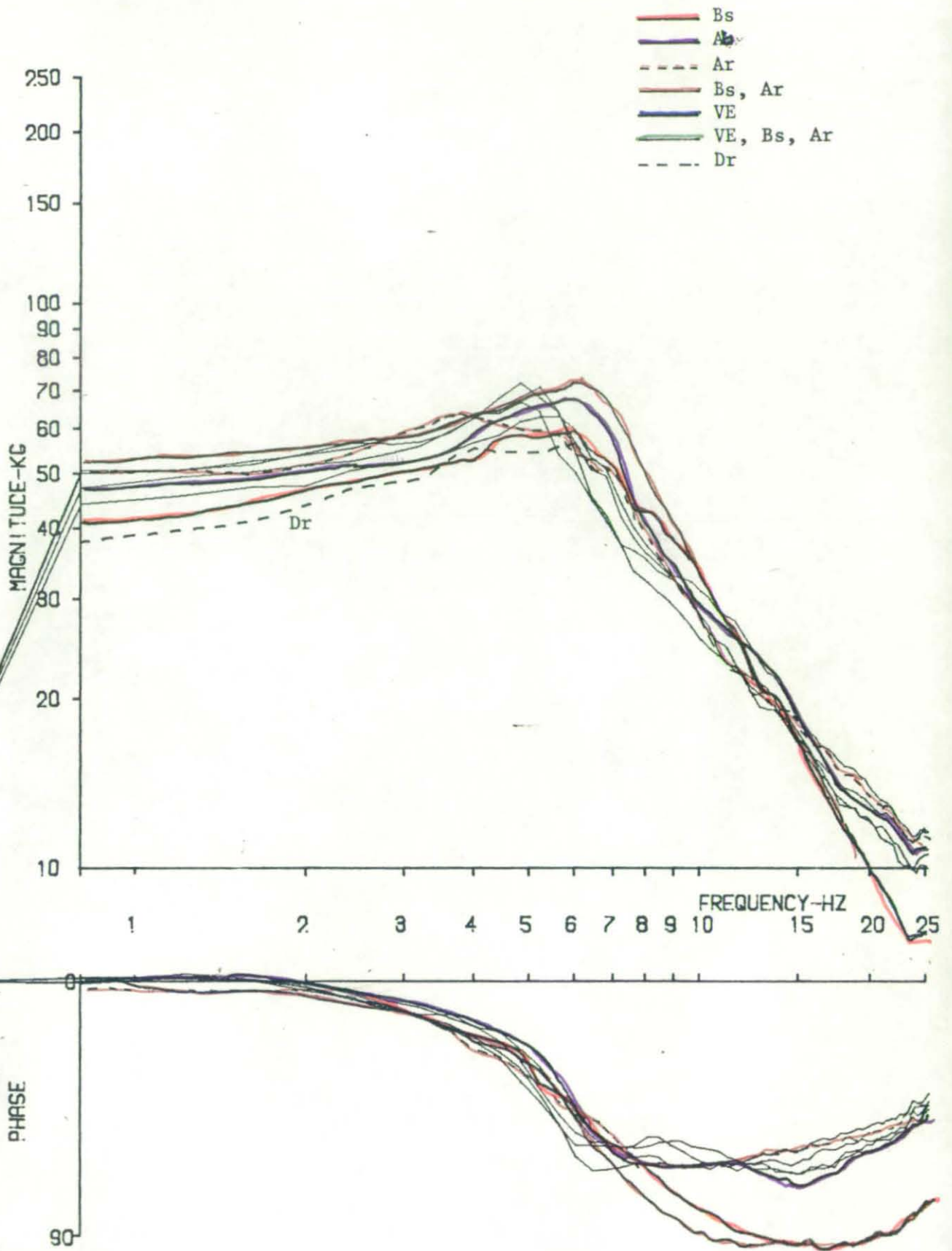


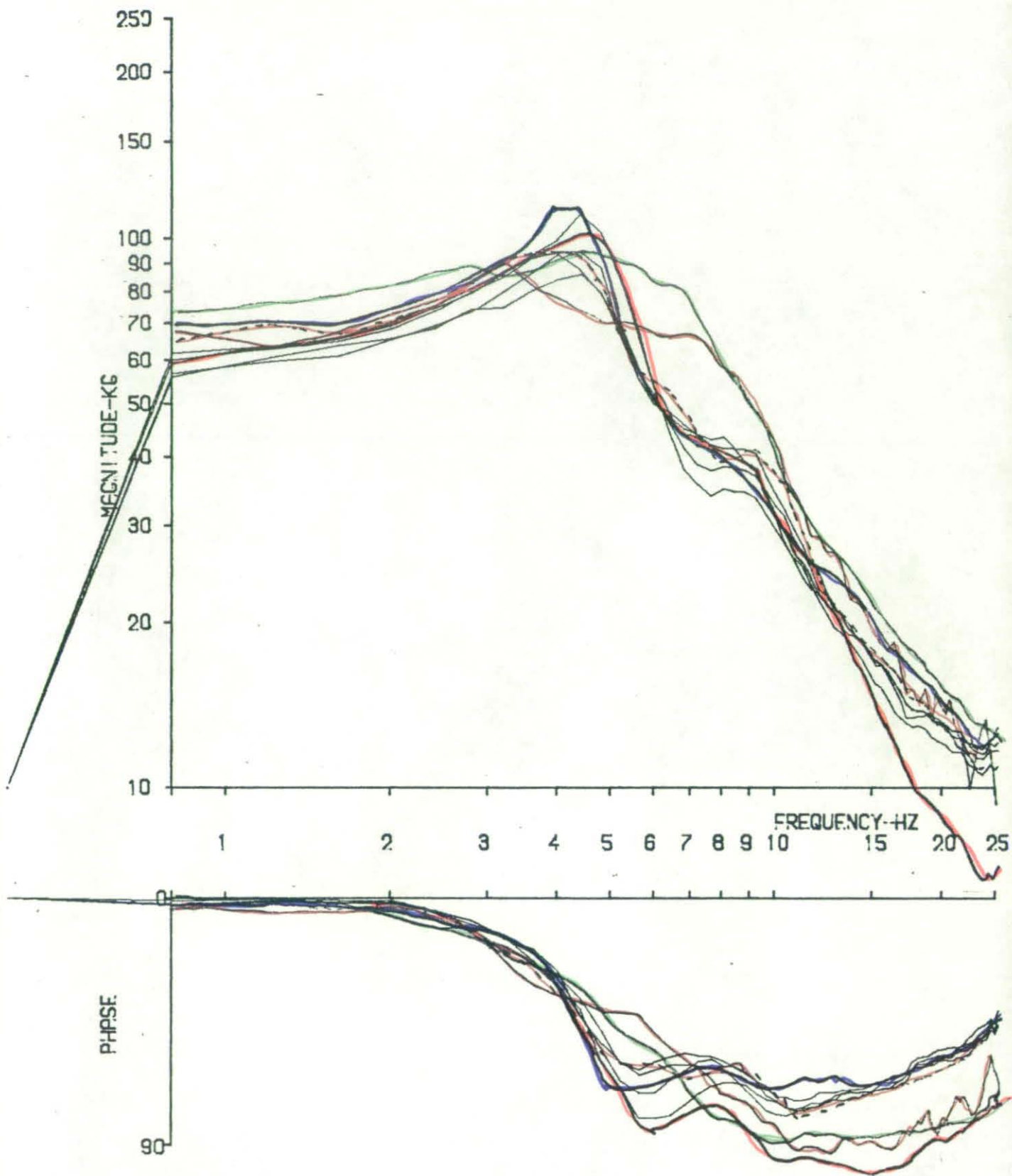
Fig. 7.132 Comparison of apparent mass and transmissibility (VE, Bs, Ar, Ab)





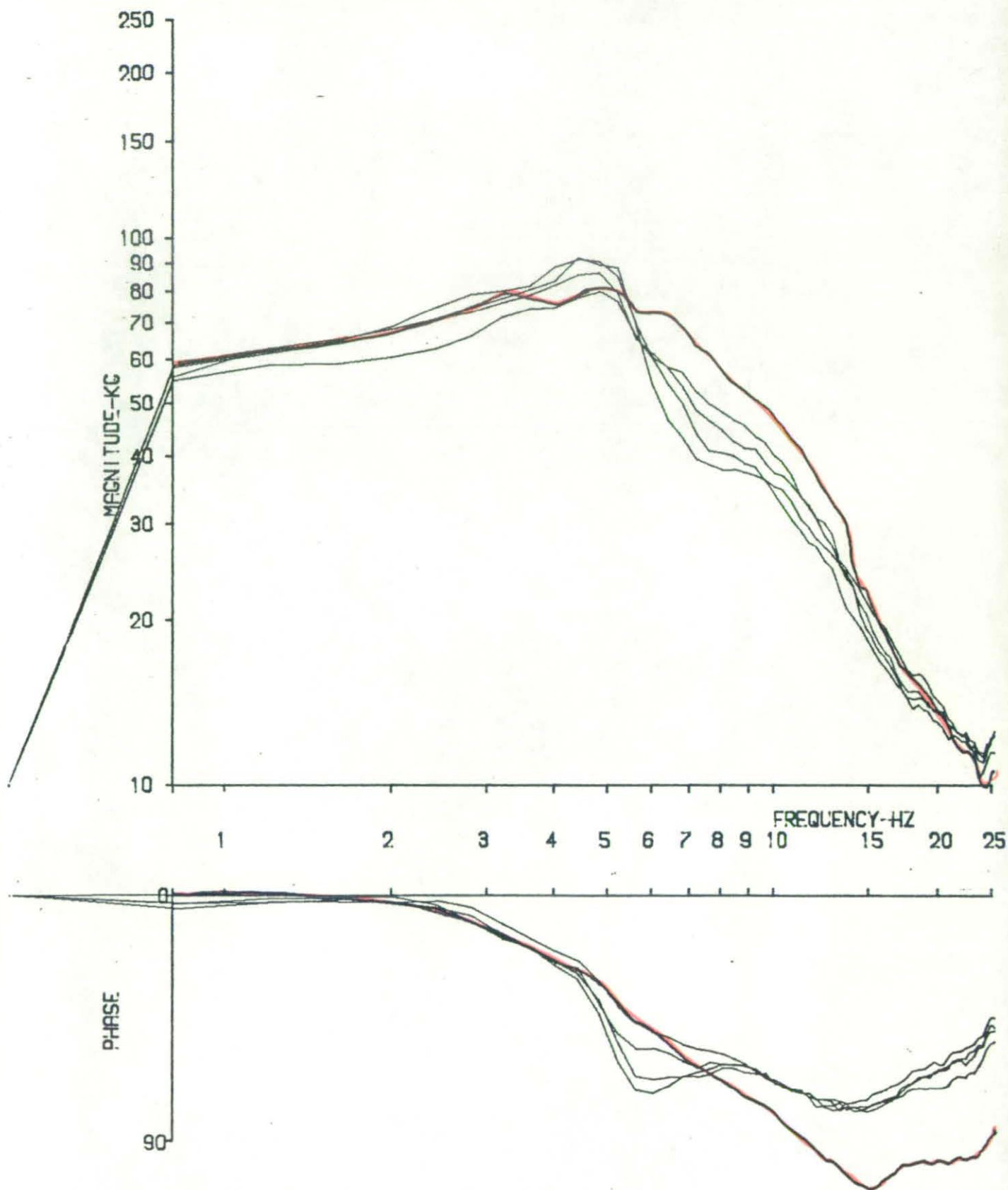
RUN NO. 81/

Fig. 7.134 Apparent mass. Effects of postural change



RUN NO. 82/

Fig. 7.135 Apparent mass. Effects of postural change



RUN NO. 857

Fig. 7.136 Apparent mass. Effects of postural change

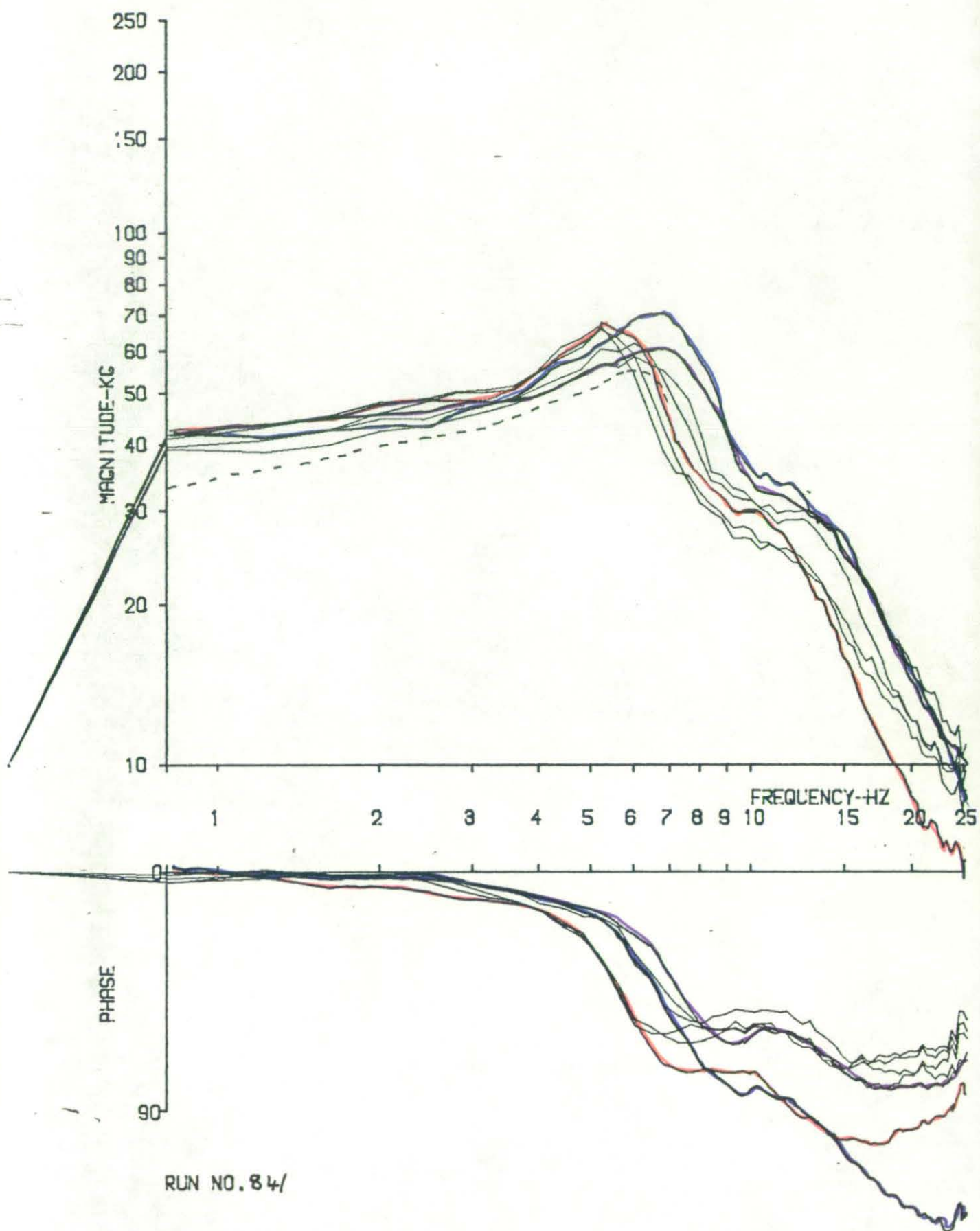
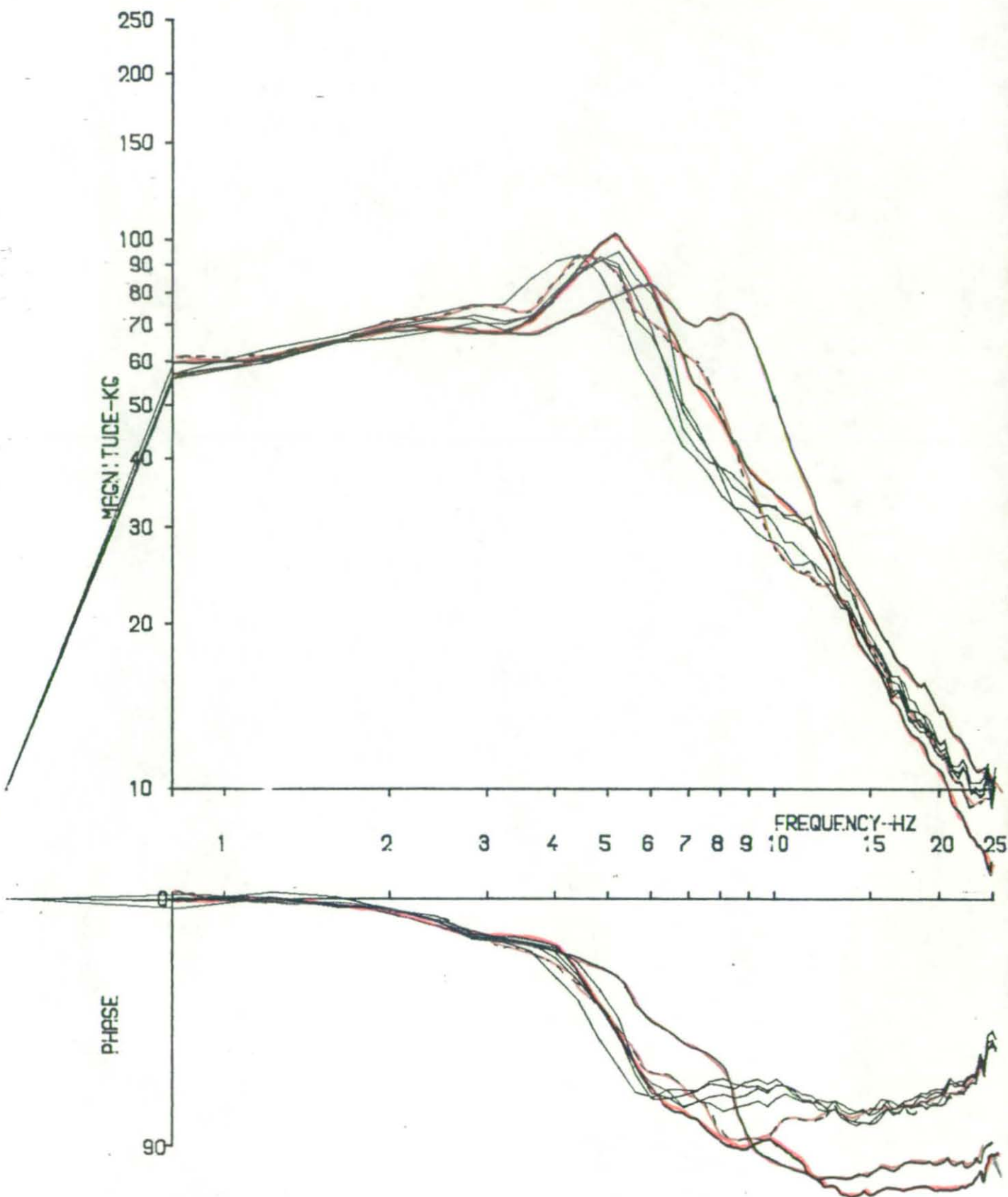
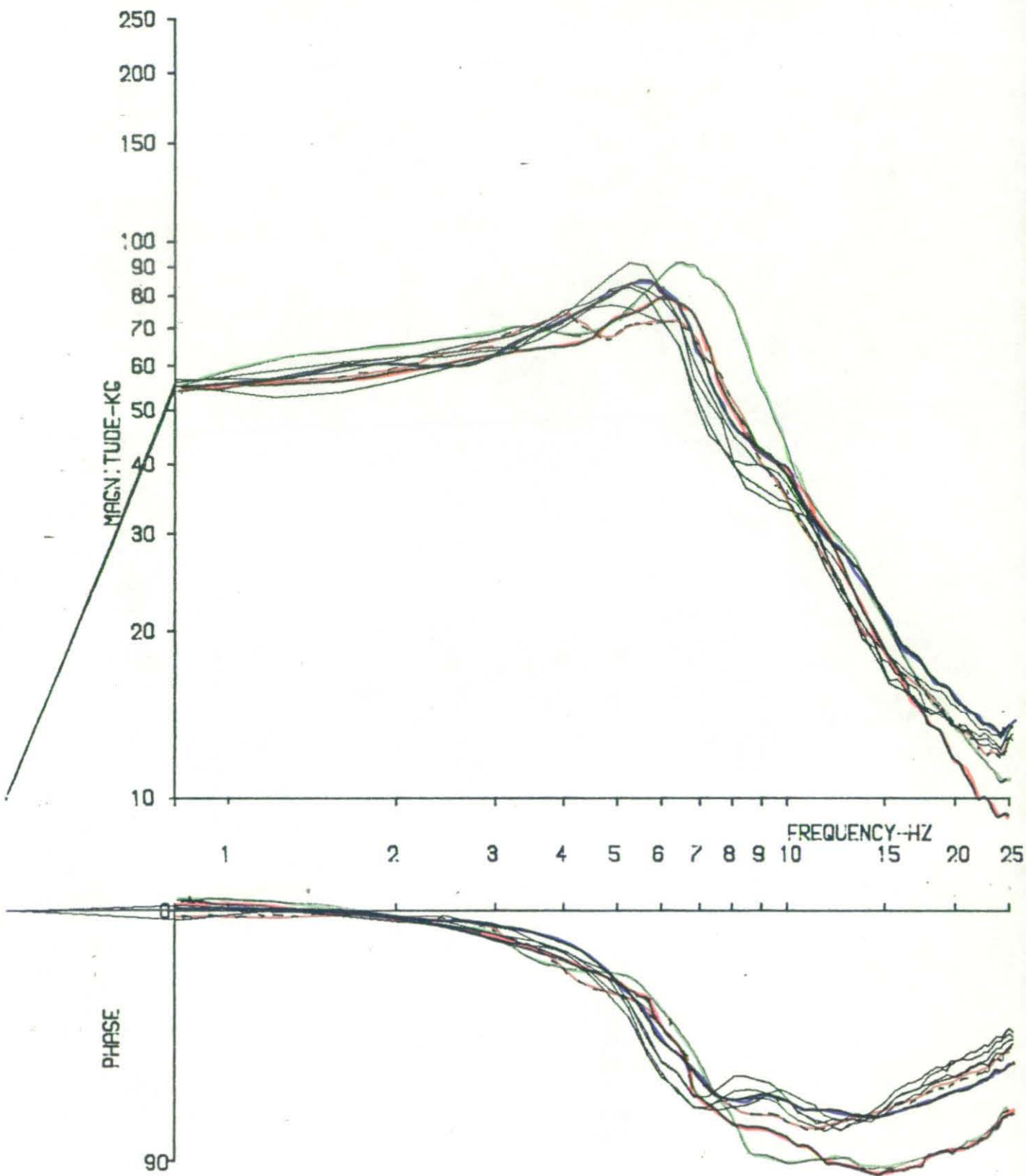


Fig. 7.137 Apparent mass. Effects of postural change



RUN NO. 83/

Fig. 7.138 Apparent mass. Effects of postural change



RUN NO. 01/

Fig. 7.139 Apparent mass. Effects of postural change

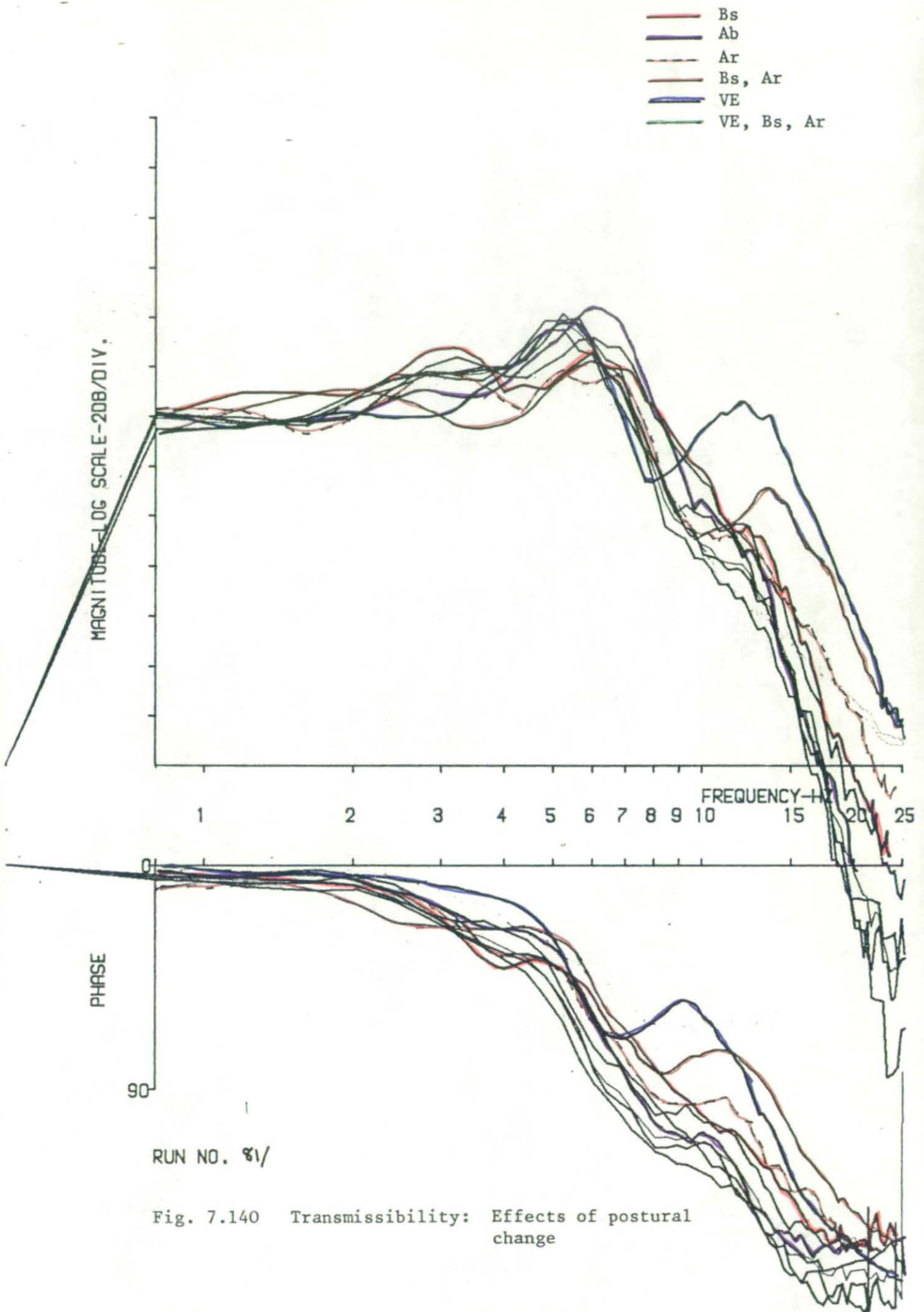


Fig. 7.140 Transmissibility: Effects of postural change

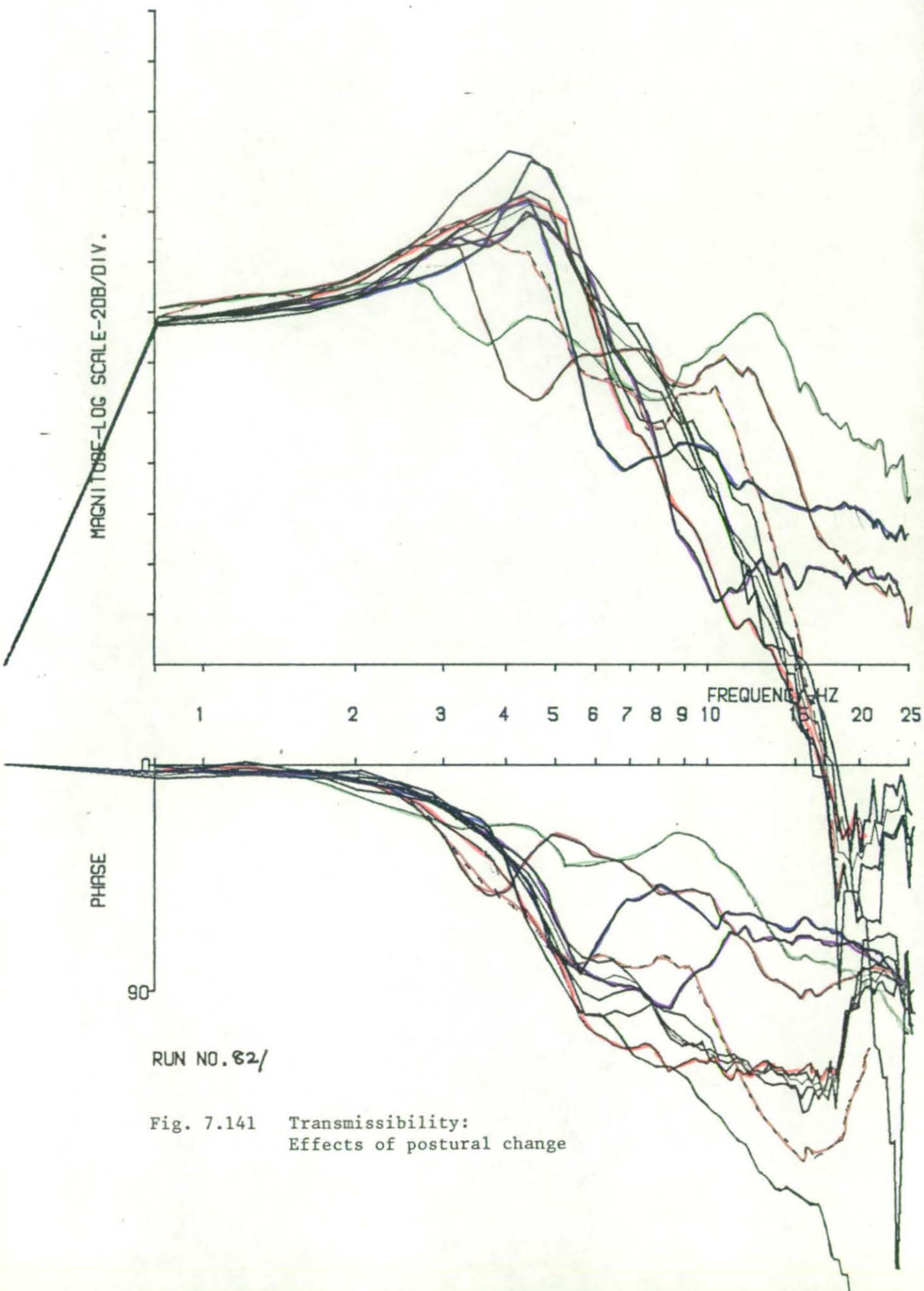
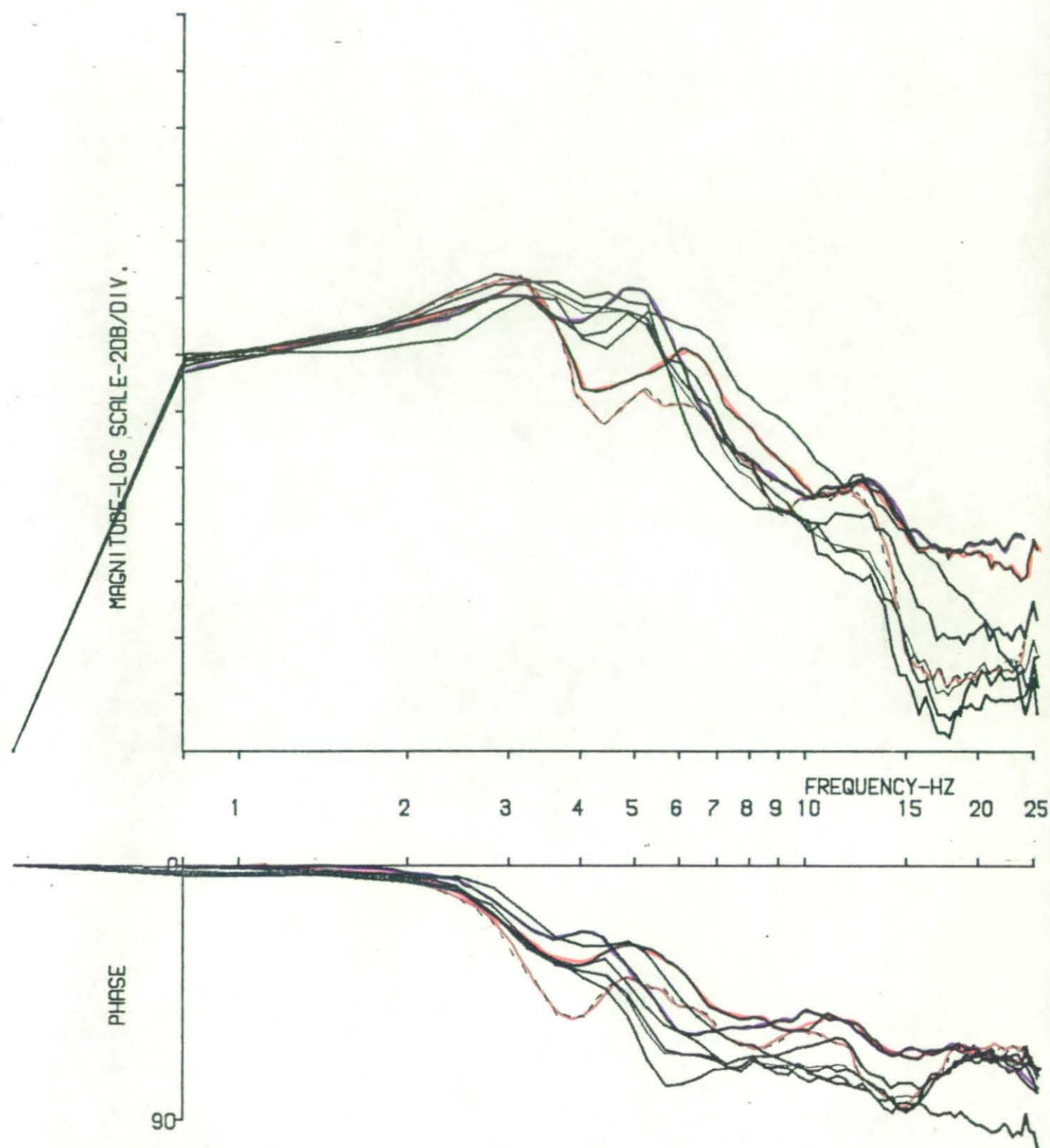


Fig. 7.141 Transmissibility:
Effects of postural change



RUN NO. 85/

Fig. 7.142 Transmissibility: Effects of postural change

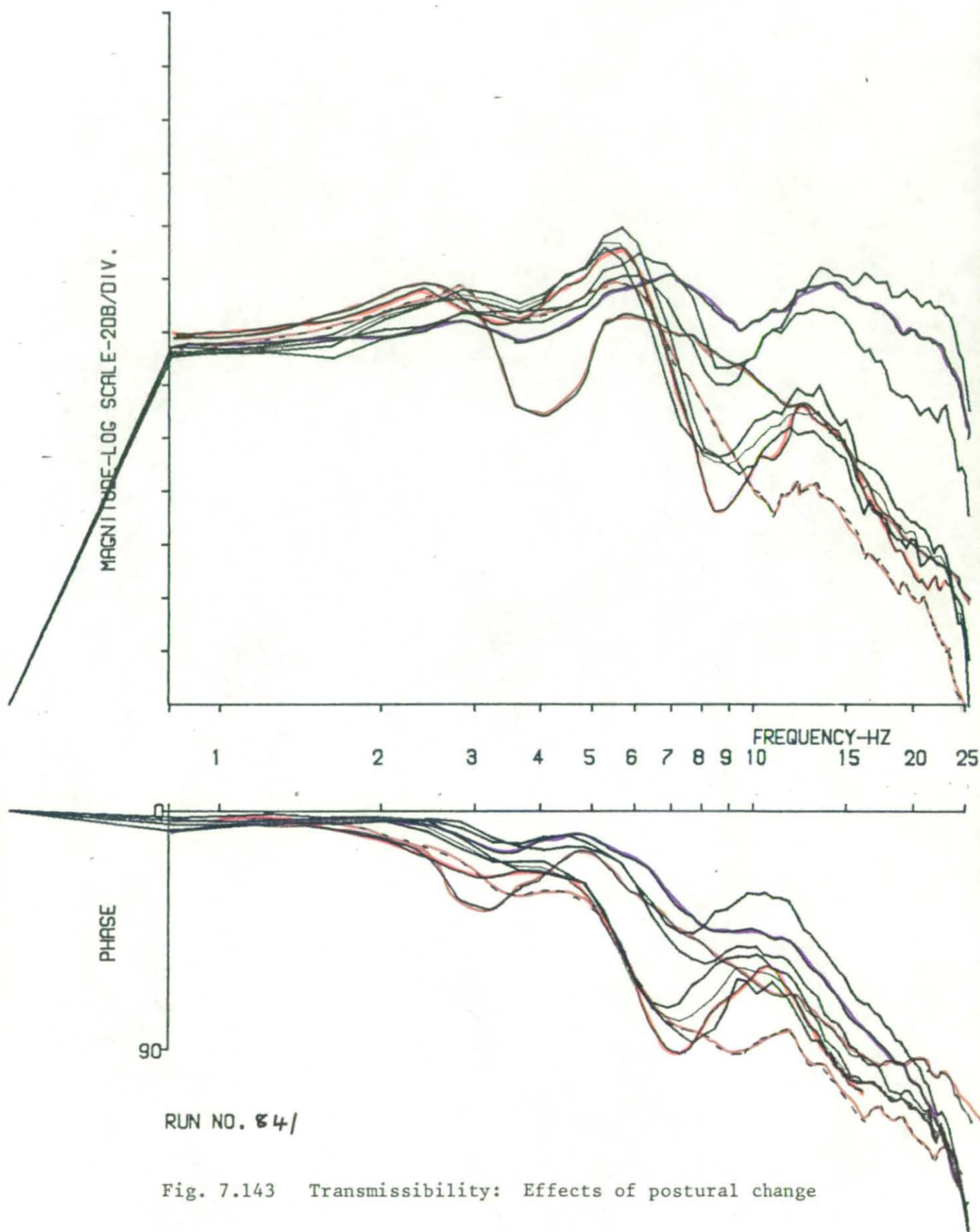


Fig. 7.143 Transmissibility: Effects of postural change

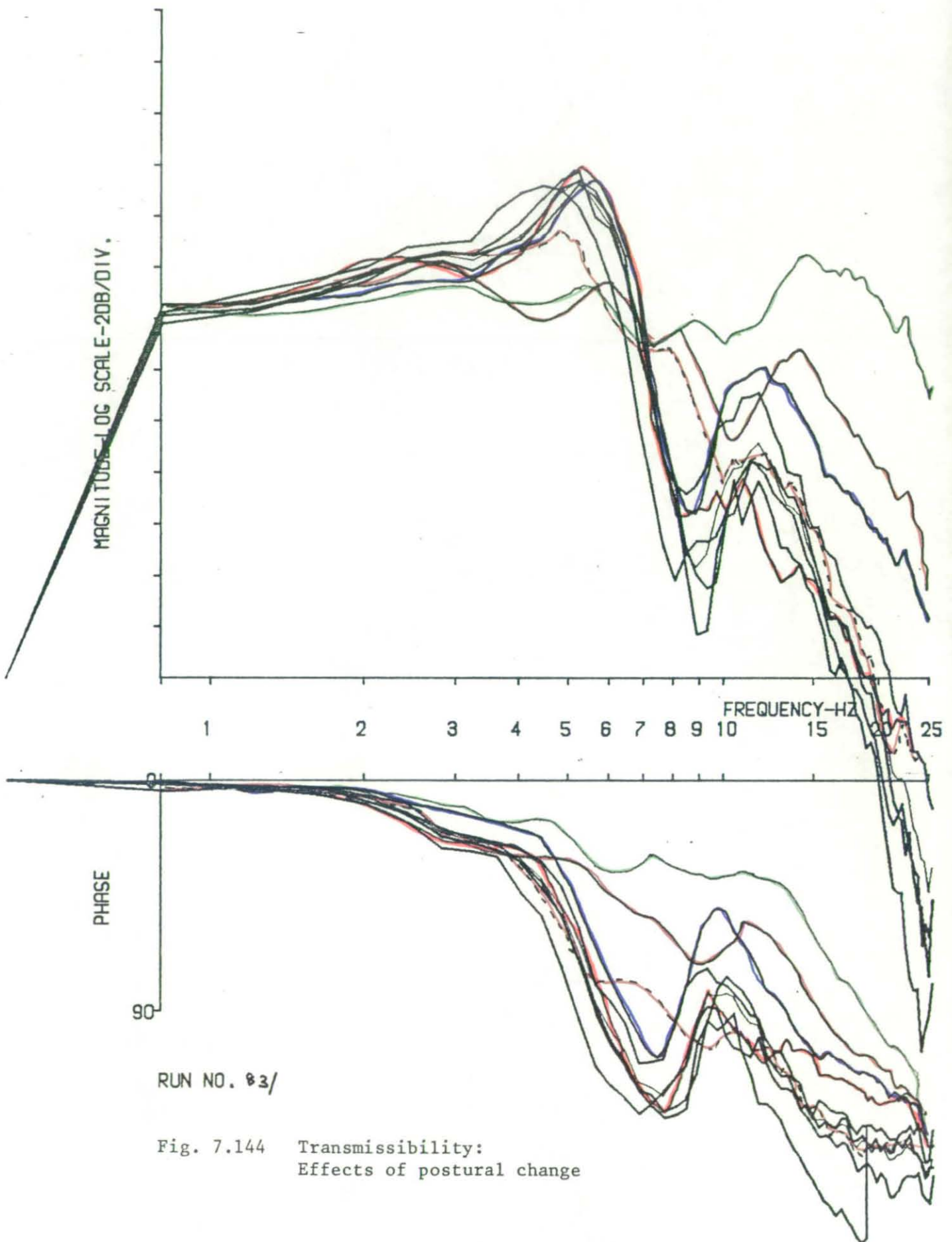


Fig. 7.144 Transmissibility:
Effects of postural change

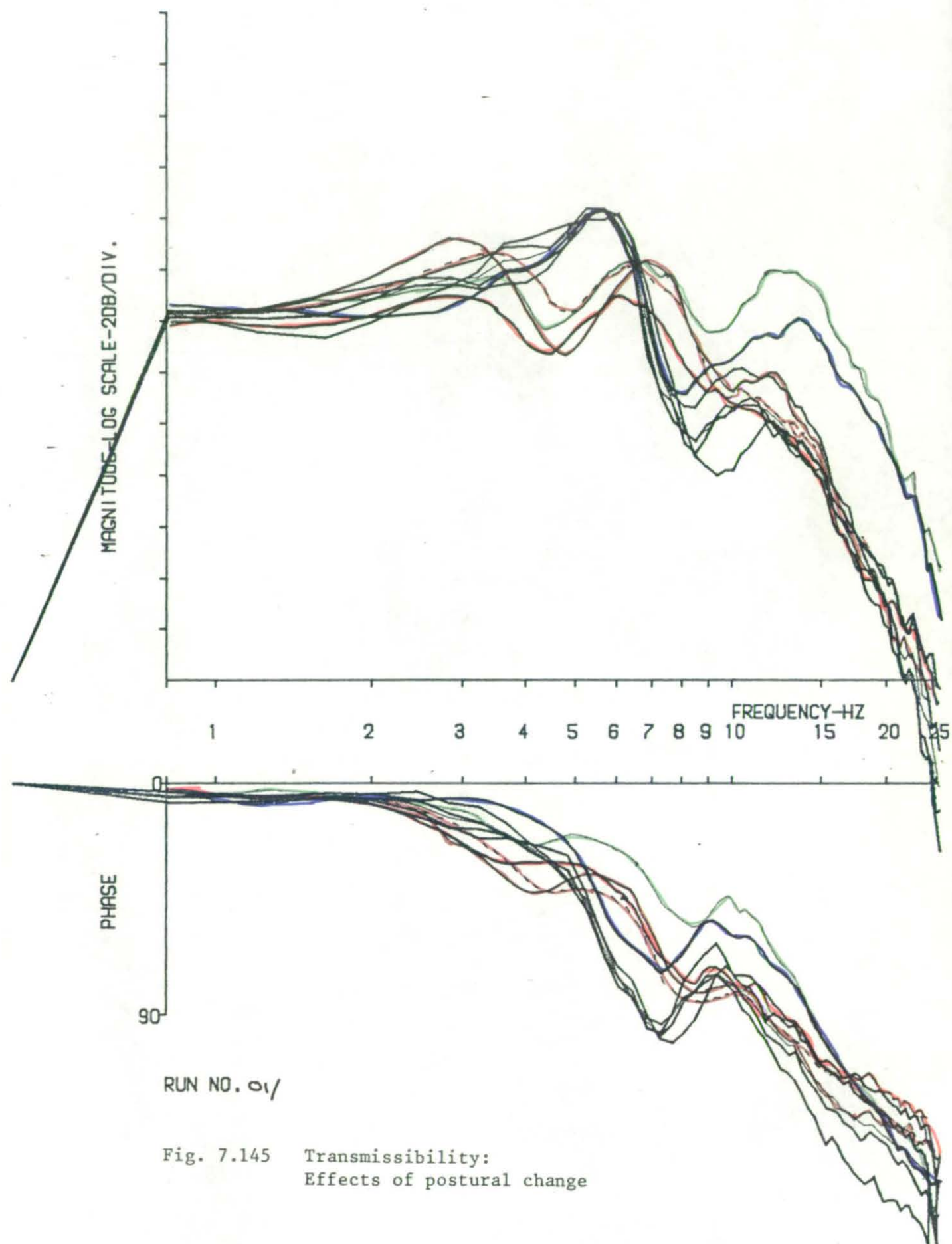
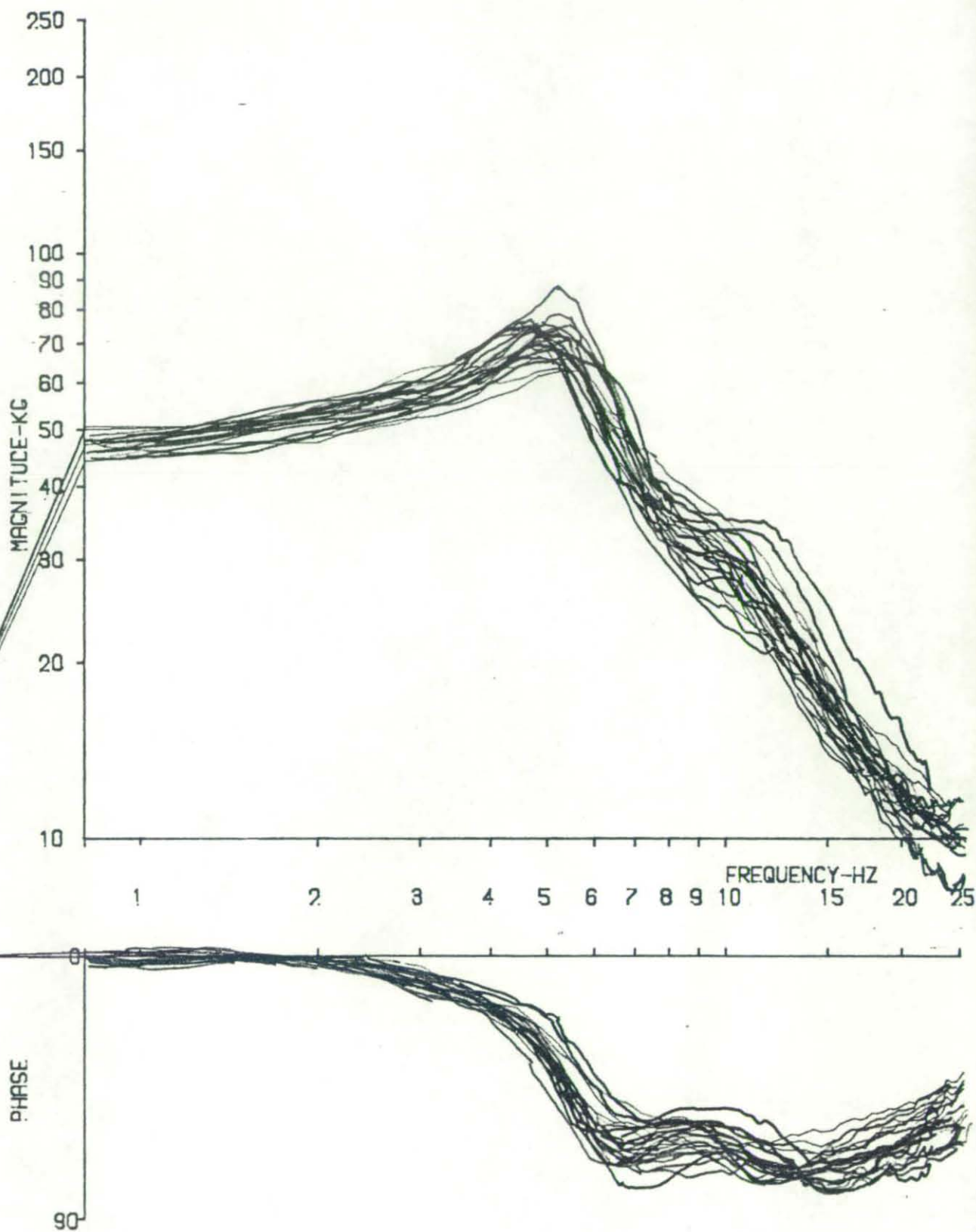


Fig. 7.145 Transmissibility:
Effects of postural change



RUN NO.

Fig. 9.1 Apparent mass: All subjects of exp. 4 (4E)
(Values shifted in magnitude and frequency - see text)

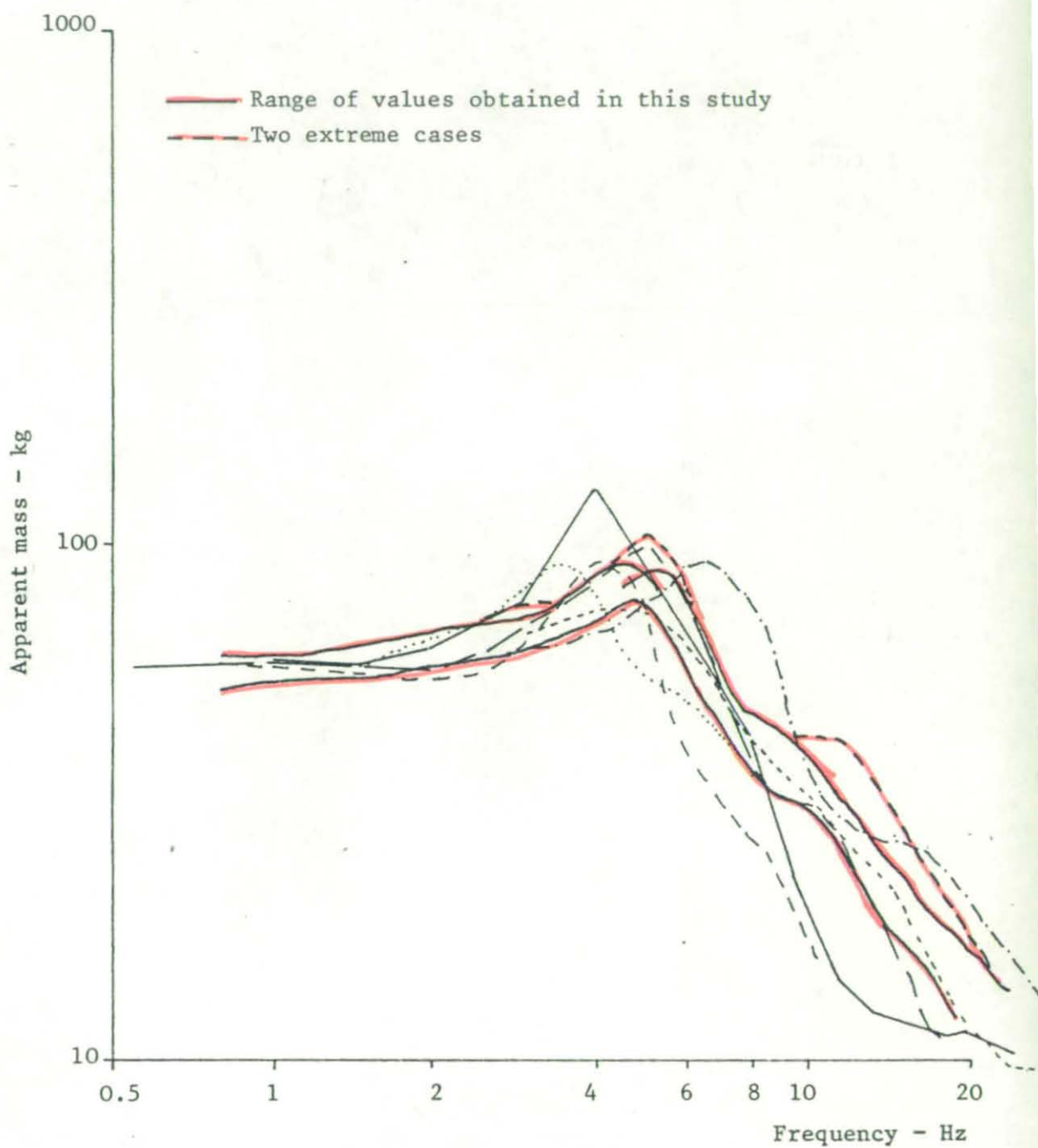


Fig. 9.2 Data of fig. 9.1 rescaled and superimposed on results of other authors (fig. 2.29). Graphs shifted in magnitude (to normalize to similar body weights), but not shifted in frequency.

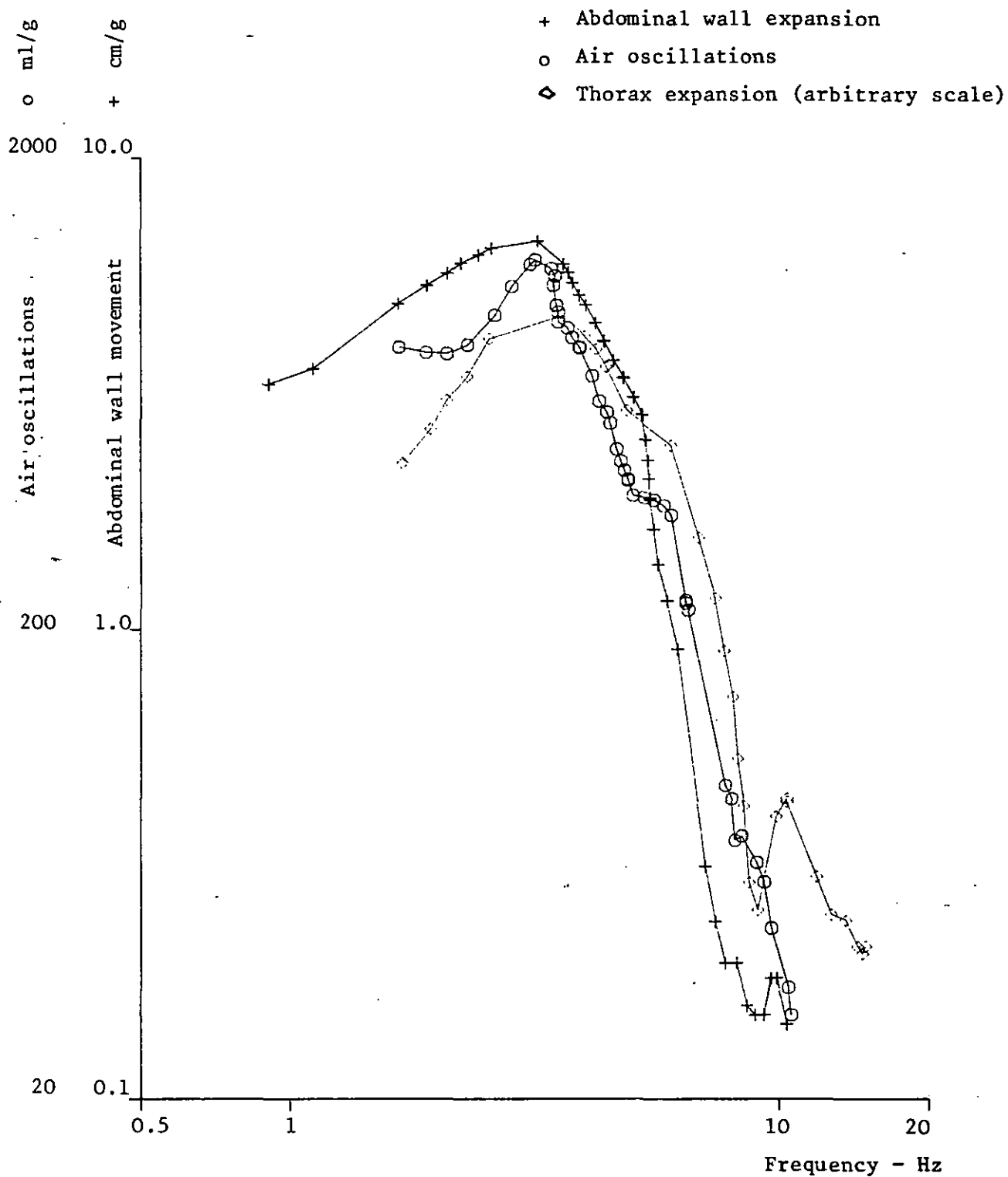


Fig. 9.3a Responses of supine subject vibrated in a_z direction
 (after Coermann et al 1960)

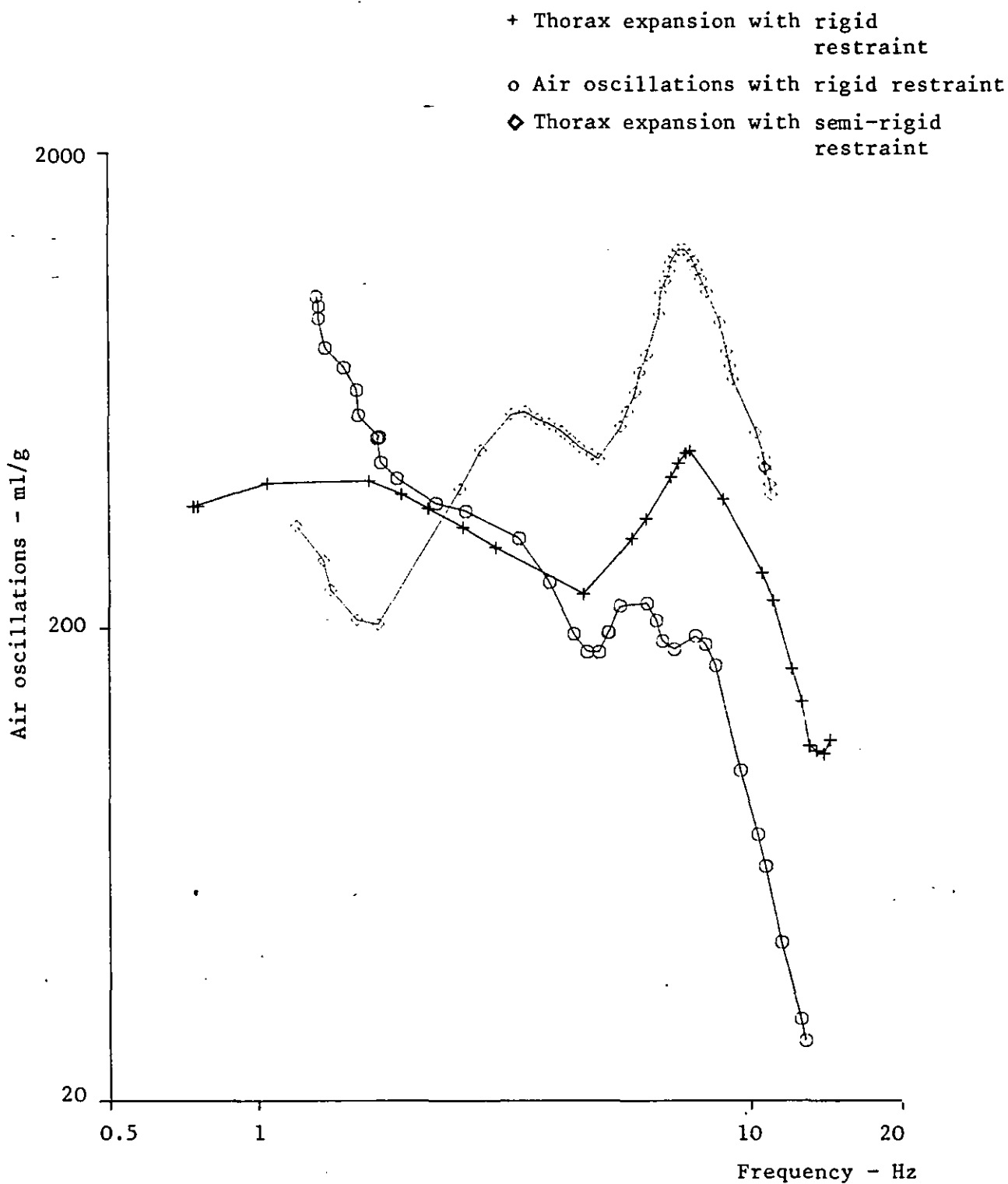


Fig. 9.3b As fig. 9.3a, but with rigid and semi-rigid restraints

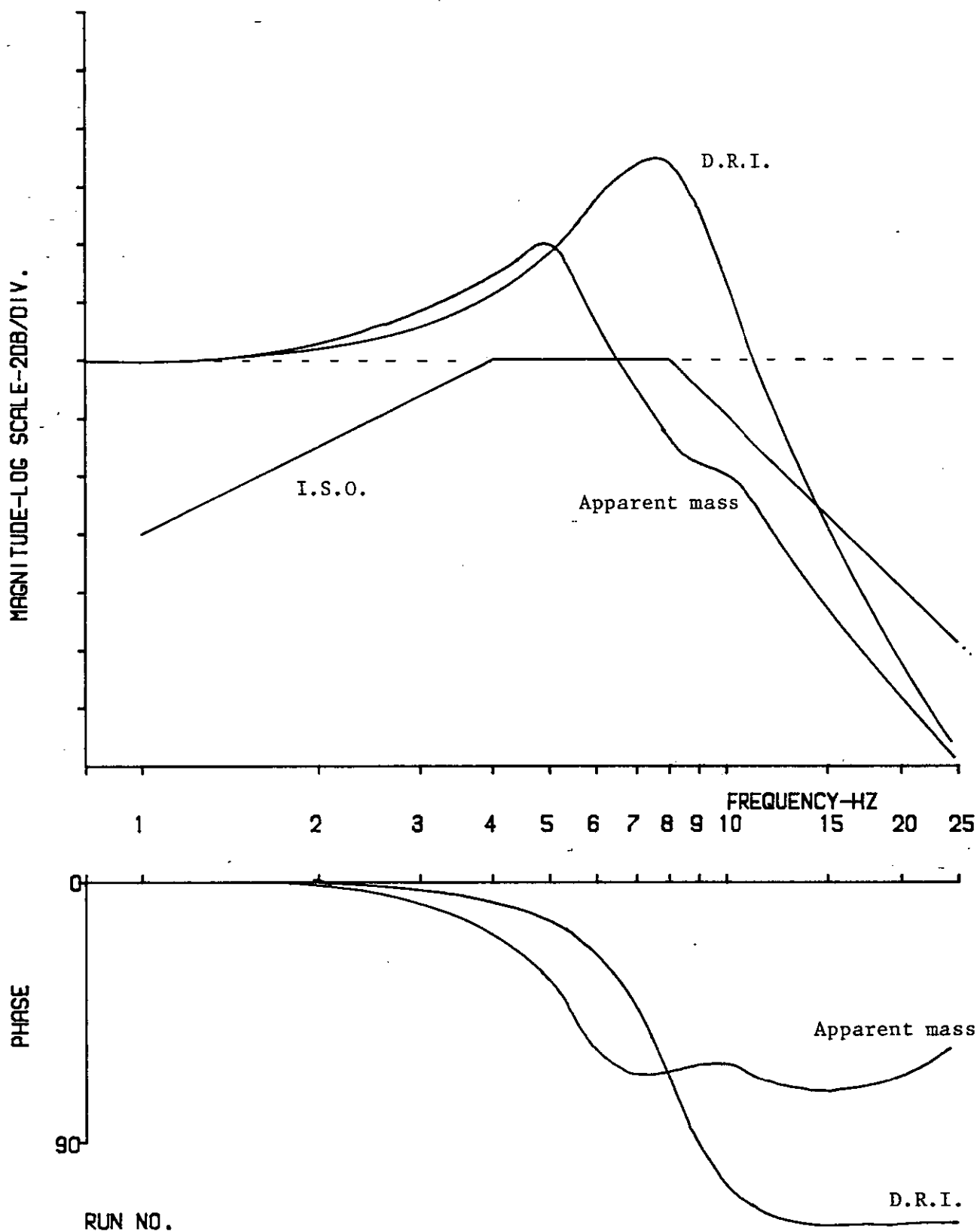


Fig. 10.1 Comparison of I.S.O. weighting function, D.R.I. analogue and typical apparent mass.

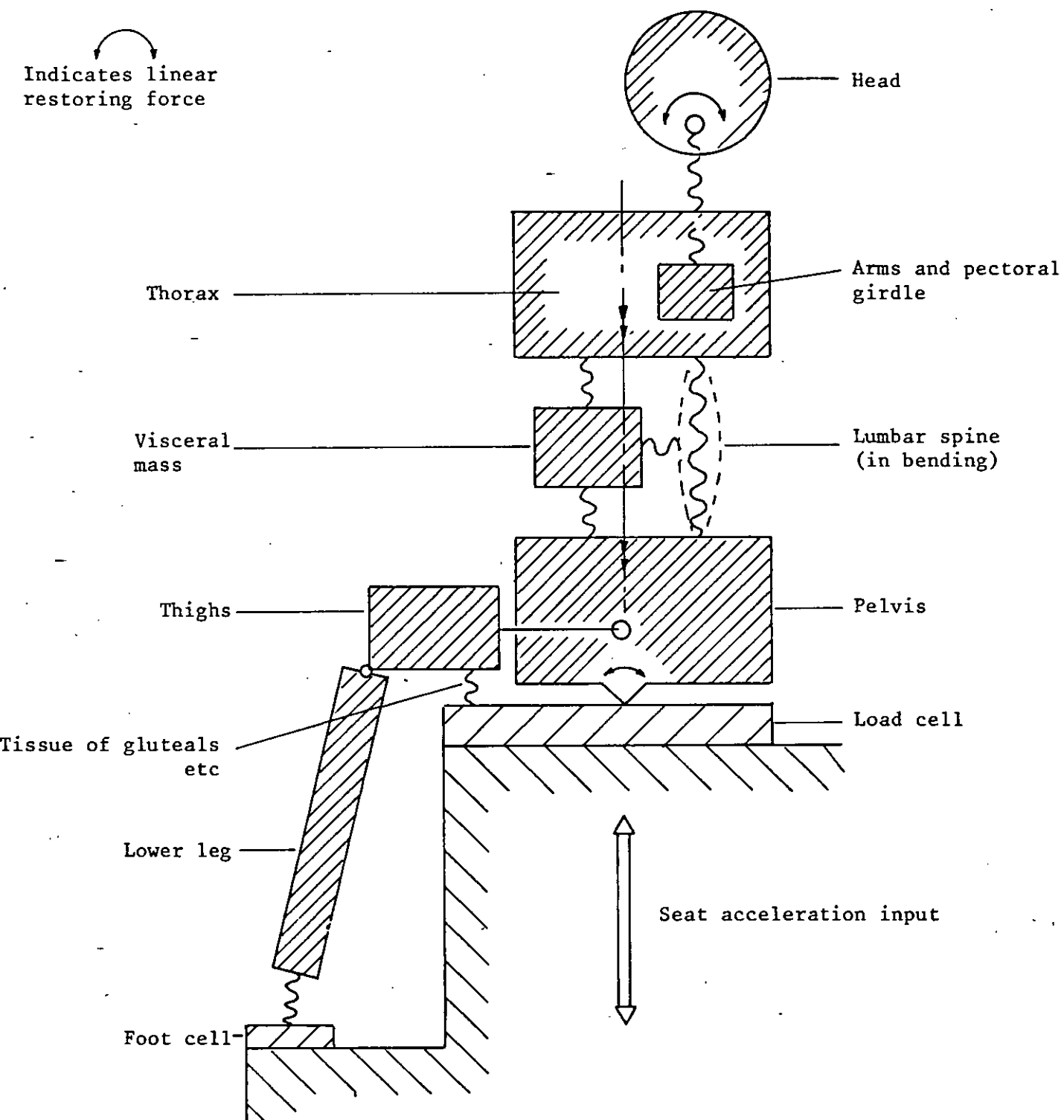


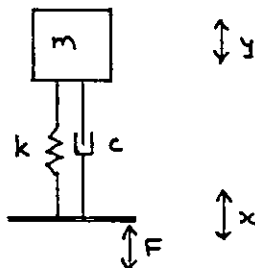
Fig. 10.2 Improved conceptual model.

APPENDIX 1: GLOSSARY OF SYMBOLS

f	Frequency
f_0	Natural frequency
Δf	Resolution bandwidth
$F_{n_1, n_2, \alpha}$	100 α percentage point of the F distribution
$G_x(f)$ (or $G_{xx}(f)$)	Power spectral density function
$G_{xy}(f)$	Cross power spectral density function
$H(f)$	Frequency response function
N	'Block size' in digital computation
n	Number of degrees of freedom
n_1	Number of sample records
$p(x)$	Probability density function
$\Delta \tau$	Half-power point bandwidth
t	Time variable
Δt	Increment in time. Inverse of digitising rate
T	Duration of observation
X, Y, Z	Denotes direction (according to I.S.O. 2631). - Z equivalent to the longitudinal axis of the trunk
$x(t), y(t)$	Time dependent variables
$X(t), Y(t)$	Fourier transform of $x(t)$ or $y(t)$ at frequency f
$X_k, Y_k,$	Discrete Fourier transform of $x(t)$ or $y(t)$ at frequency point k
z	Standardised normal variable
Z_α	100 α percentage point of the standardised normal distribution.
α	Level of significance
$\gamma_{xy}^2(f)$	Coherence function
E_b	Bias error
ξ	Damping ratio
\bar{x}	Mean value of time function $x(t)$
σ_x	Standard deviation, or r.m.s. value of time function $x(t)$
σ_x^2	Variance of time function $x(t)$
\bar{y}_x^2	Mean square value of time function $x(t)$
χ^2	Statistical Chi-square variable.
\wedge	Indicates an estimate
$ $	Indicates a modulus.

APPENDIX 2: BEHAVIOUR OF SINGLE DEGREE OF FREEDOM LINEAR SYSTEM

The behaviour of a simple linear system can be a useful guide to the behaviour of more complex systems. We take as an example the simple mechanical system shown below.



The system has mass m , spring constant k and damping constant c . It is excited by force F and displacement x and responds with displacement y .

It can be shown that the transmissibility T , the complex ratio of y to x is given by $T = \frac{(k + j\omega)}{(-m\omega^2 + k + cj\omega)}$ where ω is angular frequency.

The apparent mass Z , the complex ratio of F to \ddot{x} is given by

$$Z = \frac{m(k + j\omega)}{(-m\omega^2 + k + cj\omega)}$$

The relative displacement function D , the complex ratio of $y - x$ to \ddot{x} is given by $D = \frac{m}{(-m\omega^2 + k + cj\omega)}$

If we now let $\omega_0 = \sqrt{k/m}$, $\zeta = \frac{2c}{\sqrt{km}}$ ($\therefore k = m\omega_0^2$, $c = 2\zeta\sqrt{km} = 2\zeta m\omega_0$)

and $\alpha = \omega/\omega_0$

Then $T = \frac{(1 + 2j\alpha\zeta)}{(1 - \alpha^2 + 2j\alpha\zeta)}$

$$Z = mT = \frac{m(1 + 2j\alpha\zeta)}{(1 - \alpha^2 + 2j\alpha\zeta)}$$

$$D = \frac{1}{\omega_0^2(1 - \alpha^2 + 2j\alpha\zeta)}$$

or, in terms of magnitude and phase,

$$|T| = \sqrt{\frac{1 + (2\zeta\alpha)^2}{(1 - \alpha^2)^2 + (2\zeta\alpha)^2}} \quad \phi_T = \tan^{-1} \left[\frac{2\zeta\alpha^3}{1 - \alpha^2 + 4\zeta^2\alpha^2} \right]$$

$$|Z| = m \cdot |T| \quad \phi_Z = \phi_T$$

$$|D| = \frac{1}{\omega_0^2 \sqrt{(1 - \alpha^2)^2 + (2\zeta\alpha)^2}} \quad \phi_D = \tan^{-1} \left[\frac{-2\zeta\alpha}{1 - \alpha^2} \right]$$

If D is normalised to be relative to the relative displacement under normal gravity (i.e. when $W = 0$), then the W_0^2 term disappears and the ϕ_b term positive. The transmissibility and normalised relative displacement functions are clearly similar. They are plotted in fig. A2.1.

Note that as $\alpha \rightarrow 0$, $|T|$ and $|D| \rightarrow 1.0$

and ϕ_r and $\phi_b \rightarrow 0$

Note also that as $\alpha \rightarrow \infty$,

$$|T| \rightarrow \frac{2\zeta}{\alpha} \quad (\text{i.e.} - 6\text{dB/octave slope})$$

$$|D| \rightarrow \frac{1}{\alpha^2} \quad (\text{i.e.} - 12\text{dB/octave slope})$$

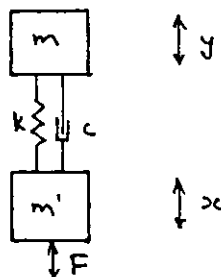
$$\phi_r \rightarrow \tan^{-1} \left[\frac{2\zeta\alpha}{4\zeta^2 - 1} \right] \rightarrow 90^\circ$$

$$\phi_b \rightarrow \tan^{-1} \left[\frac{2\zeta}{\alpha} \right] \rightarrow 0$$

Note also that in each case, the modulus is maximum not at $\alpha = 1$, but at some value less than one. The maxima are, in fact, at different frequencies. That for $|D|$ is at $\alpha = \sqrt{(1 - 2\zeta^2)}$, ($\zeta^2 \leq 0.5$)

$$\text{that for } |T| \text{ is at } \alpha^2 = \frac{\sqrt{(1 + 8\zeta^2)} - 1}{4\zeta^2}$$

A further system of interest is that containing an unsprung mass m' as below:



Although the transmissibility function remains the same, the apparent mass equations for this system are complex, as the curve shown in fig. A2.1 suggests. However, the extreme points are of interest.

As $\alpha \rightarrow 0$,

The modulus $\rightarrow m + m'$

The phase $\rightarrow 0$

As $\alpha \rightarrow \infty$,

The modulus $\rightarrow m'$

The phase $\rightarrow \frac{2\zeta}{(m'/m)\alpha} \rightarrow 0$

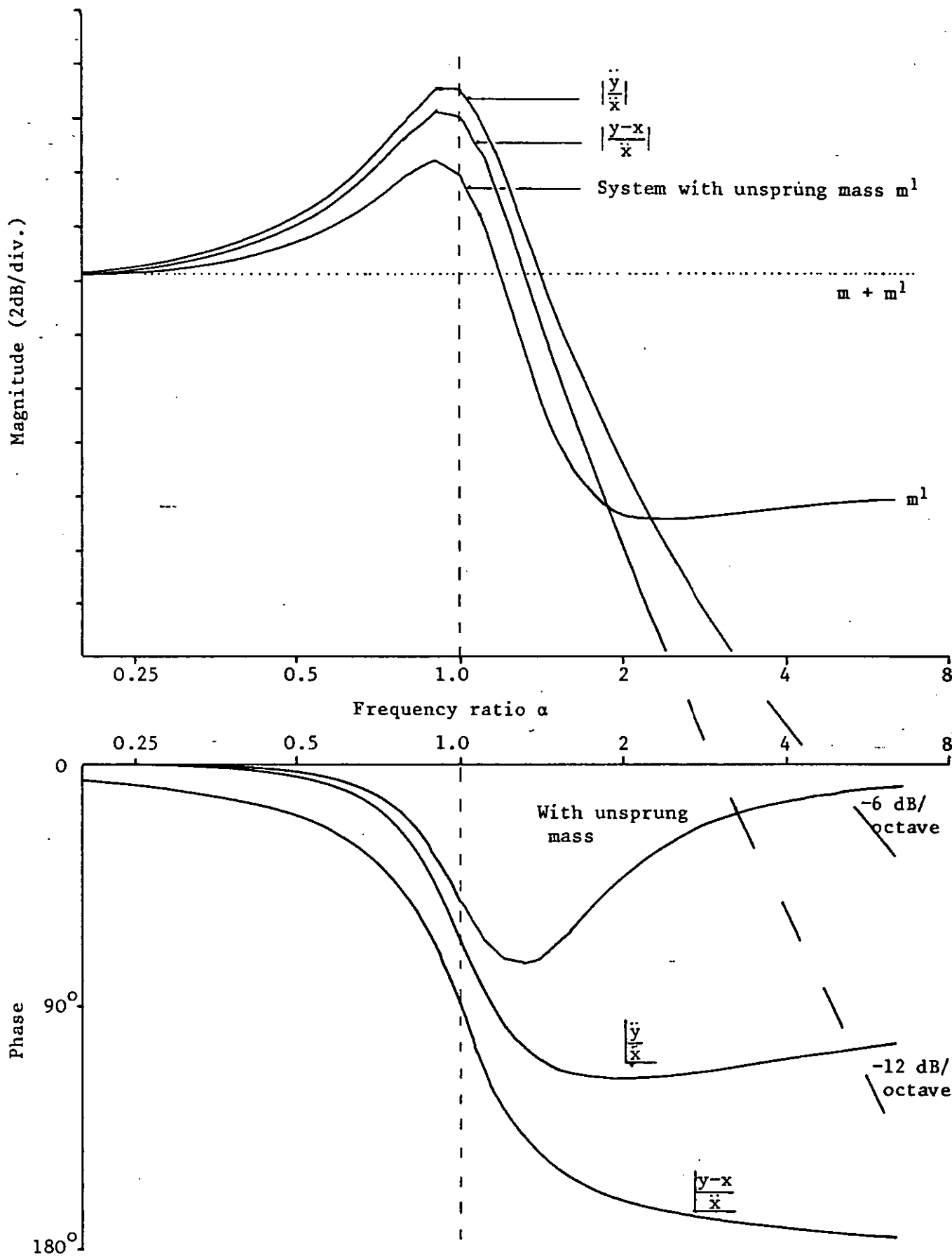


Fig. A2.1 Response functions for system with damping factor $\xi = 0.25$

APPENDIX 3: HEAD MOVEMENTS DURING Z VIBRATION

Introduction

When someone is exposed to whole body Z axis vibration, the head as well as moving in the Z direction exhibits a 'nodding' motion about a Y axis - Guignard & King 1972, Vogt et al. 1979. This combined motion leads to reduced visual performance and problems in measurement of seat to head vibration transmissibility.

In order to hold an image on the fovea, the eyeball rotates relative to the head so that one would expect rotational head motion to be important as regards vision (Rowlands & Allen, 1969). However, the vestibulo-ocular reflex leads to rapid eye movement to compensate for head rotation (Bizzi et al. 1972) and visual performance can be maintained up to 6Hz angular motion - Benson 1972. Griffin & Lewis 1978 suggest that translational head movements may not be compensated for, so that visual performance is dependant on both rotational and translational motion of the head. In addition, Dupuis & Hartung 1978 have observed translational resonance of the eyeball at frequencies of the order of 20 to 25 Hz, so that translational motion may have increased importance at high frequencies.

As the thorax is a relatively rigid structure, the transmission of vibration from the seat to the cervical region gives useful information on trunk biodynamics. Seat to head transmissibility in the Z direction is often used in this respect. However, due to the nodding motion, accelerometers fitted to the head may not give a true indication of az motion of the head.

Thus, to understand the effects of whole-body Z vibration on vision and to obtain reliable transmissibility measurements, one needs an understanding of both the rotational and translational movements of the head.

Problems

As a result of the danger of whiplash in vehicle accelerations, a great deal of experimental and theoretical informaton is available on the motion of the head resulting from high X accelerations applied to the

trunk, e.g. Ewing & Thomas 1972, King & Mertz 1973, Reber & Goldsmith 1979. However, there is little information on responses to Z vibration where the angular head and neck movements are likely to be large and muscular control may be significant.

Measurements of head accelerations are also made difficult as a result of tissue movement - a transducer may not reflect accurately the movement of the underlying skeletal structure. Most researchers have been well aware of this problem and transmissibility measurements are usually based on accelerometers fitted to a dental bite or very tight fitting head harness. However, within the accuracy of radiographic techniques, Sandover 1974 observed that relative accelerometer - skull movement in the Z direction was minimal with a tight fitting head harness. Also Ziegert & Lewis 1979 suggested that an accelerometer weighing some 30g strapped over thin tissues (they used the tissues over the tibia) with a force of 25N could be used for measurements up to about 200Hz. Sandover & Soames 1975 used photo-emitting diodes to investigate the geometry of head nodding, and Sandover 1974 concluded that the errors arising from not taking angular motion into account were likely to be greater than those resulting from tissue compression if one wished to measure Z head movements. Biggs 1975 found that the head rotated about points at the same level as the first cervical vertebra. She also noted that motion was different when the eyes were closed. This is to be expected if the vestibular reflex is part of a feedback loop which includes computation of retinal error and central involvement with anticipating muscle activity - Bizzi et al. 1972. Likewise, one might expect the use of a dental bite to lead to excess muscle activity in the neck and consequent abnormal patterns of head movement.

Transitional and rotational movements of the head can be calculated from measurements from several transducers firmly fixed to the cranium - Guignard et al 1979. However, Padgaonkar et al 1975 have shown that in practice nine linear accelerometers are needed to obtain a reliable measure of three dimensional motion of a rigid body. Affixation of several transducers is quite cumbersome as are the resultant calculations, and most researchers would prefer to use one, or at most two, transducers with minimal calculation.

Thus, little is known of the motion of the head resulting from whole body vibration and numerous problems can be expected when one attempts to

do so. A number of researchers have investigated transmissibility, but apart from Guignard et al, none have taken head movements into account in order to obtain reliable measures of translational or rotational head movements.

Aim

The aim of this note is to make use of available information and develop a simple model that might represent head movements during whole body Z vibration.

Development of the model

Even if the thorax is assumed rigid, the geometry of the head-neck system is clearly complex. However, it is unlikely that the neck flexes as much during low level Z vibration as during X impact. One would assume that human development would minimise muscle loading so that the centre of gravity of the head would be over the atlanto-occipital joint. The nodding during vibration would then have to arise from differences in the inertial properties of those parts of the head in front and behind the centre of gravity, or X movement as well as Z movement at the input to the head. However, if one takes the view of Jones & Gilley 1960 - that the head is in unstable equilibrium (to maintain muscle tonus) with the centre of gravity forward of the atlanto-occipital joint - then head nodding can be a direct consequence of the inability of the neck musculature to cope with the inertial forces of vibration.

Biggs 1975, found that the head rotated about points at the level of C1 during Z vibration, and Berthoz 1971 found the same for X vibration. It seems reasonable therefore, as a first approximation, to accept the usual assumption that the occipital condyles represent the anatomical and dynamic pivot point. The assumption of point application of forces results in rotation being about that point. Ewing & Thomas 1973 have investigated head geometry in some detail, and fig A3.1 shows their co-ordinate system with typical locations of the 'occipital condylar point' together with head centre of gravity locations from the data of Walker et al. 1973. Note that the centre of gravity is some 20 mm forward of the assumed pivot point.

To develop the approach further, it is assumed that the muscles act

- in a passive manner - simply as a restoring force proportional to the inertial forces of head movement. We now have a simple model of the head rotating about a point, similar to that of Barnes & Rance 1975, Melvin et al. 1973, and Anon. The model is illustrated in fig A3.2. Also indicated is a transducer location R.

The following assumptions have been made:

Assumption 1: The head behaves like a series of laminae in the XZ plane with centres of gravity all on the same axis in the YY direction, so that it can be considered as a single lamina.

Assumption 2: All motion and forces are in the XZ plane and all moments about a YY axis.

Assumption 3: Forces acting on the head are translational only, and applied at a single point O. Any moment is the result of the reaction to inertial forces.

Assumption 4: If the centre of gravity G moves away from its normal position with respect to O, then a restoring couple P about O results. In dynamic situations, damping may occur.

Using the nomenclature of fig. A3.2 we equate translational and rotational forces and accelerations:

Thus, in translation, the sum of translational forces is equal to the product of the head mass and the acceleration of the centre of gravity.

$$\text{i.e. } F_z = m \cdot \ddot{Z}_g = m \cdot (\ddot{Z}_0 - h \cdot \dot{\theta}^2 \cos \theta - h \cdot \ddot{\theta} \sin \theta) \quad \text{--- Eqn. I}$$

(Neglecting constant gravitational forces)

$$\text{and } F_x = m \cdot \ddot{X}_g = m (\ddot{X}_0 - h \cdot \dot{\theta}^2 \sin \theta + h \cdot \ddot{\theta} \cos \theta) \quad \text{--- Eqn. II}$$

In rotation, the sum of couples about the centre of gravity is equal to the product of the head moment of inertia about the centre of gravity and the angular acceleration.

$$\text{i.e. } F_z \cdot h \cdot \sin \theta - F_x \cdot h \cdot \cos \theta - P = I_{C_g} \cdot \ddot{\theta} \quad \text{--- Eqn. III}$$

To simplify matters further, two major assumptions are made:

Assumption 5: Rotational movements are relatively small so that terms in $\dot{\theta}^2$ tend to zero and the terms $h\sin\theta$ and $h\cos\theta$ can be regarded as constants. This assumption, in effect, states that the behaviour is linear.

Assumption 6: The neck can be regarded as rigid and rigidly attached to the thorax. During Z vibration, the trunk behaves like a two degree of freedom linear system as regards the Z movement of O relative to the seat, with insufficient feedback of the head angular motion to affect the behaviour of the trunk system.

If $\dot{\theta}^2 = 0$, and $h\cos\theta$ and $h\sin\theta$ are constant (denoted by z_g and x_g), then equations I to III reduce to

$$P + I_o \ddot{\theta} = m.x_g.\ddot{z}_o - m.z_g.\ddot{x}_o$$

(where I_o

is the moment of inertia about O)

Assumption 6 means that the point O is constrained to move in the a direction, so that $\ddot{x} = 0$ and the above equation becomes

$$P + I_o \ddot{\theta} = m.x_g.\ddot{z}_o \quad \text{--- Eqn. IV}$$

The couple P and resulting equations

We now consider two possibilities for the couple P.

a) Barnes & Rance assumed the behaviour to be like a single degree of freedom linear system, so that $P = k\theta + c\dot{\theta}$ where k and c are respectively stiffness and damping constants.

Using the 'D' operator, this becomes

$$P = [k + cD]\theta$$

b) An alternative is that the behaviour is similar to that of limb joints. For this situation, Moffatt et al 1969 found a series Maxwell system to be a good descriptor.

Then $P = k\theta = c\dot{\theta}$ and $\theta = \theta_k + \theta_c$
 so that $c\ddot{\theta}_c + k\theta_c = k\theta$

and hence, ..

$$c\dot{P} + kP = ck\dot{\theta}$$

Using the 'D' operator, this gives

$$P = c.k \left[\frac{D}{cD + k} \right] \theta$$

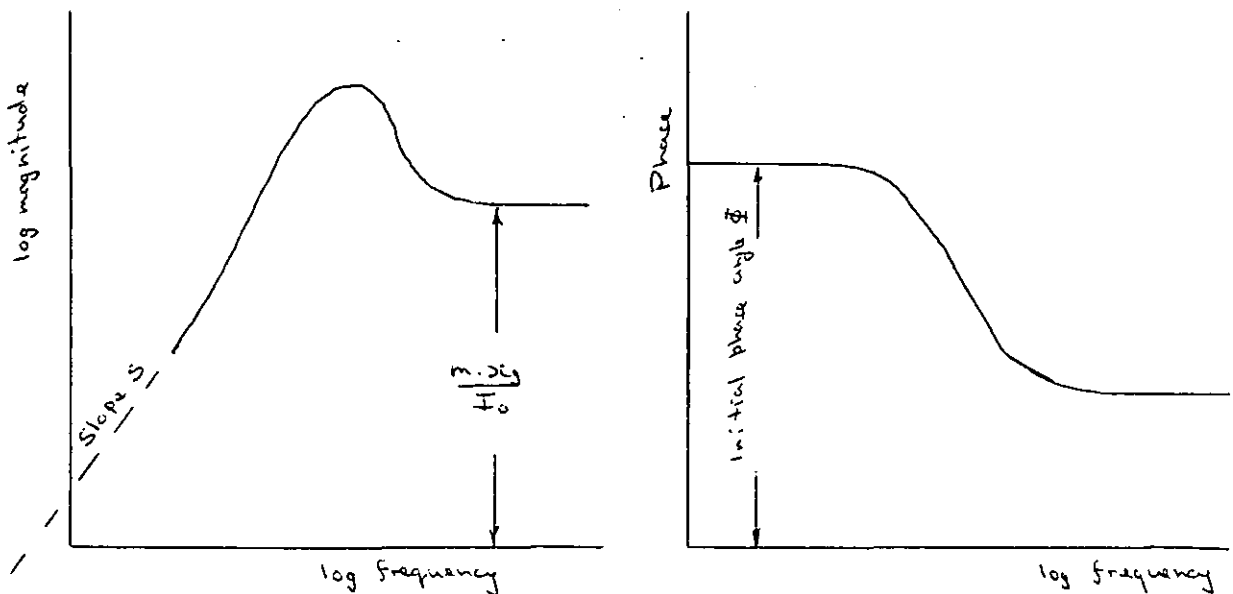
If these values are put in equation IV, it can be shown that the system equation becomes:

In case a) $\frac{\ddot{\theta}}{\ddot{Z}_0} = \frac{m.x_s}{I_0} \left[\frac{\frac{1}{\omega_0^2} \cdot D^2}{(1 + 2\frac{\eta}{\omega_0} D + \frac{1}{\omega_0^2} D^2)} \right] \quad \text{--- Eqn. V}$

In case b) $\frac{\ddot{\theta}}{\ddot{Z}_0} = \frac{m.x_s}{I_0} \cdot 2\eta' \left[\frac{\frac{1}{\omega_0} \cdot D \cdot (1 + \frac{1}{2\eta' \omega_0} D)}{(1 + 2\frac{\eta}{\omega_0} D + \frac{1}{\omega_0^2} D^2)} \right] \quad \text{--- Eqn. VI}$

where $\omega_0 = \sqrt{\frac{k}{I_0}}$, $\eta = \frac{c}{2\sqrt{k \cdot I_0}}$, $\eta' = \frac{1}{4\eta}$

Both equations V and VI give a transfer function as below:



For case a) the slope S tends to 12 dB/octave, and the initial phase angle ϕ is 180°

for case b) the slope S tends to 6 dB/octave and the initial phase angle ϕ is 90° .

However, the actual values found by Moffatt et al need consideration. They gave the following relationships:

$$c = a_1 |M|, \quad k = a_2 + a_3 |M|$$

where $|M|$ is the absolute value of the moment at the joint.

For a_1 their mode was about 0.45 sec/rad and range 0.3 to 0.76

For a_2 their mode was about 7 m.kg/rad and range 0.5 to 7.84

For a_3 their mode was about 7 rad⁻¹ and range 0.44 to 15.3

If one assumes (M) to be the moment to hold the head still under normal gravity, using typical head mass and centre of gravity position values (see below), (M) would be between 0.068 and 0.145 kgm. Thus c would be between 0.03 and 0.06 kg.m.sec/rad and k between 7.5 and 8 kg.m/rad. This would give $W = 6.2$ to 10.1 Hz

$$\text{and } \phi^0 = 0.8 \text{ to } 3.3$$

Although W is of the order expected, the damping ϕ^1 is exceptionally high. The assumption b) is therefore suspect. Experimental data (see later) did not agree with the 6dB/octave and 90° phase angle values, and this reinforced the decision to discount assumption b) and follow assumption a).

$$\text{In this case} \quad \frac{\ddot{\theta}}{z_0} = \frac{-m \cdot x_g}{I_0} \cdot \frac{\alpha^2}{((1-\alpha^2) + 2\kappa \cdot \beta \cdot j)}$$

$$\text{Modulus} \quad \left| \frac{\ddot{\theta}}{z_0} \right| = \frac{m \cdot x_g}{I_0} \cdot \frac{\alpha^2}{\sqrt{(1-\alpha^2)^2 + 4\kappa^2 \beta^2 \alpha^2}} \quad \text{--- Eqn. VII}$$

$$\text{Phase angle} = \tan^{-1} \left(\frac{-2\kappa \beta \alpha}{1-\alpha^2} \right)$$

and the maximum value is at $\alpha = \frac{1}{\sqrt{1-2\kappa^2 \beta^2}}$ where $\alpha = \frac{\text{excitation frequency}}{w_c}$

The magnitude constant

The value of the constant $\frac{m \cdot x_g}{I_o}$ is the first consideration as it controls the magnitude of rotational motion.

A reasonable estimate of these values can be made from available anatomical data of Walker et al 1973, and Ewing & Thomas 1973. The data below are presented with reference to the anatomical coordinate system of Ewing & Thomas 1972 (origin at superior edge of auditory meati, x axis through infra orbital notch line).

Walker et al (cadaveric material, similar data produced by Becker 1972, and Hodgson et al 1972):

Head mass	- 4.38 kg \pm 0.59	(\pm 1SD, N = 18)
Moment of inertia	- 0.238 N.m.s ² \pm 0.038	(\pm 1SD, N = 17)
Position of	- x: 8.8 mm \pm 7.1	(\pm 1SD, N = 17)
centre of gravity	z: 21.4 mm \pm 5.0	(\pm 1SD, N = 17)

Ewing & Thomas (from x-rays of subjects)

Position of		
occipital	x: -11.0 mm $\begin{pmatrix} +5.2 \\ -6.5 \end{pmatrix}$	(range, N = 12)
condylar point	z: -25.5 mm $\begin{pmatrix} +5.8 \\ -4.0 \end{pmatrix}$	(range, N = 12)

The actual data points for the two positions are given on Fig. A3.1.

To obtain the moment of inertia about the occipital condylar point (I_o) we need to add to the above value $m(o^2 - g^2)$, where g is the distance of the centre of gravity from the origin and o is the distance of the centre of gravity from the occipital condylar point. Using mean values, this gives $I_o = 0.33 \text{ N.m.s}^2$ and

$$\frac{m \cdot x_g}{I_o} = 1.15 \text{ r.m}^{-1}$$

The stiffness term

A further term is $w_o = \sqrt{\frac{k}{I_o}}$

Some data are available to give the order of magnitude of w_o . Melvyn et al 1973 calculated the moment at C1 during impact and their curves indicate that the angular flexibility in extension is of the order of $2.5^\circ/\text{Nm}$, and in flexion $0.6^\circ/\text{Nm}$. Schultz et al 1979 measured the behaviour of cadaveric lumbar motion segments (ligaments and discs only) and their graphs show that, for angles of the order of a degree, the flexibilities were of the order of $1.5^\circ/\text{Nm}$ in both flexion and extension. These values correspond to angular stiffnesses of 23, 95 and 38 Nm/rad respectively.

Using the mean value for I_o given above, this leads to values for w_o of 1.3, 2.7 and 1.7 Hz respectively.

The Damping term

No data could be found on damping characteristics, but during vibration, whole body damping is often of the order of 0.25.

Head movement as a result of seat vibration

We now make use of assumption 6 and consider the whole body system subject to a seat vibration Z_o and consider the motion of the point R. in

$$\text{Firstly, } \ddot{Z}_r = \ddot{Z}_o - x_r \ddot{\Theta} \text{ and secondly } \frac{\ddot{\Theta}}{\ddot{Z}_{in}} = \frac{\ddot{\Theta}}{\ddot{Z}_o} \cdot \frac{\ddot{Z}_o}{\ddot{Z}_{in}}$$

$$\text{so that } \frac{\ddot{Z}_r}{\ddot{Z}_o} = 1 - x_r \frac{\ddot{\Theta}}{\ddot{Z}_o} \quad \text{--- Eqn. VIII}$$

$$\text{and } \frac{\ddot{Z}_r}{\ddot{Z}_{in}} = \frac{\ddot{Z}_o}{\ddot{Z}_{in}} \left(1 - x_r \frac{\ddot{\Theta}}{\ddot{Z}_o} \right) \quad \text{--- Eqn. IX}$$

(i.e. $x_r \frac{\ddot{\Theta}}{\ddot{Z}_o}$ is an error term, with actual errors dependent on phase relationships).

These relationships are illustrated in Fig. A3.3 for systems with the following parameters

$$\frac{\ddot{Z}_o}{\ddot{Z}_{in}} : \text{ resonant frequency} = 4.8 \text{ Hz, damping} = 0.25$$

$\ddot{\theta}_z$: resonant frequency = 10 Hz, damping = 0.25, $\left(\frac{m\chi_y}{I_0}\right) = 1.0$,
 $\chi_r\left(\frac{m\chi_y}{I_0}\right) = 1.0$

The values for resonant frequency and $\chi_r\left(\frac{m\chi_y}{I_0}\right)$ for $\ddot{\theta}_z$ were purposely made larger than those estimated above to emphasise the effects of head nodding.

Model validation

The behaviour suggested by the model is supported by a small amount of experimental evidence.

Barnes & Rance (personal communication) measured head angular acceleration in response to a vibration at the seat. The mean values of their results for pitch motion (i.e. $\ddot{\theta}$) converted to r/s^2 per m/s^2 (i.e. $\frac{\ddot{\theta}}{\ddot{z}_0}$) is shown in Fig. A3.4. The similarity in form to the value in A3.3 is clearly apparent. Their peak values were of the order of $4.3 r/s^2/m/s^2$ @ 6 Hz.

In experiment 1 (section 7) transmissibility to a dental bite and head harness mounted accelerometers were measured simultaneously. The results (e.g. Fig. 8.29) showed the secondary peak expected when χ is large. It was assumed that the bite acceleration was equivalent to \ddot{z}_r , and that the head harness acceleration (accelerometer over occipital condylar point) was \ddot{z}_0 . Hence, $\frac{\ddot{z}_r}{\ddot{z}_0}$ and $\frac{\ddot{z}_0}{\ddot{z}_0}$ were known and $\chi_r \frac{\ddot{\theta}}{\ddot{z}_0}$ could be calculated from equation IX. This calculation was carried out on the raw data using block manipulation on the Hewlett Packard 5451A computer. Fig. A3.5 shows the resulting values for one trial. The curves for $\chi_r \frac{\ddot{\theta}}{\ddot{z}_0}$ are similar to those predicted by the model, although the phase change is much greater, and resonance effects are not clearly evident (although it was observed in other runs).

Further manipulation of the raw data allowed calculation of $\frac{\ddot{\theta}}{\ddot{z}_0}$ and resulting values are shown in Fig. A3.4 to compare with the data of Barnes & Rance. The similarity in form is remarkably high.

Some differences in amplitude between these results deserve comment. If χ_r is taken as 100 mm, the following may be obtained:

	Barnes & Rance	Experiment	Model
Max. Val. of $\frac{\ddot{\theta}}{\ddot{z}_{in}}$ r/s ² per m/s ²	4(2.5 to 5.8) @ 6 Hz	10 @ 5 Hz	1.0* @ 9 Hz
High frequency values for $\frac{\ddot{\theta}}{\ddot{z}_{in}}$		10 to 15	$\frac{m \cdot x_g}{I_o} = 1.2$

* Assuming $\frac{m \cdot x_g}{I_o} = 1.2$

Thus, estimates from the experimental data are of similar order and suggest that the model should use a higher value for $\frac{m \cdot x_g}{I_o}$ and a value for ω_o of about 6 Hz.

It must be emphasised here that the parameters used for the model were based on experimental data showing large variability. Thus the 3 S.D. ranges can be estimated as below

$$\begin{aligned} \omega_o &: 1.7 \text{ Hz} \pm 1.5 \text{ Hz} \\ \frac{m \cdot x_g}{I_o} &: 1.15 \pm 3.0 \end{aligned}$$

Likewise, the vibration data used were from experiments not designed for this purpose. The transmissibility data refer to one subject only and the accelerometers were not placed in the most suitable positions and errors must have arisen as a result. The energy available at some frequencies for Q were very low, and the data therefore unreliable.

It must be emphasised that the model used here is clearly simplistic to a degree, and the experimental evidence scanty. However, the modelling results and the experimental evidence have clear similarities and this suggests that in the absence of anything better, the model can at least be used to help understand the biodynamic behaviour of the head.

Discussion

If indeed this model is representative of head behaviour, then the following predictions are of interest

- If an accelerometer is positioned at R so that x_r is large, the apparent transmissibility measured is subject to error. For minimal error, $x_r \rightarrow 0$ i.e. the accelerometer should be mounted on the vertical

through the occipital condylar point. This error may be an explanation of the wide differences in transmissibility reported by different authors.

- b) The amplitude of the angular motion is related to $\frac{m x_g}{I_0}$. The values of m and I_0 are constant, but x_g increases as the subject leans the head forward. Thus posture is likely to affect the angular motion contribution to error considered above.
- c) The error in transmissibility is apparent as a second 'resonance' (in both magnitude and phase) at about the frequency of the maximum angular motion.
- d) Unfortunately, the accelerometer placed to maximise x_r , does not by itself give a good indication of angular motion ($\frac{\ddot{\theta}}{Z_{in}}$), although influenced by it.
- e) The function $\frac{\ddot{\theta}}{Z_{in}}$ shows maximum values between the resonant frequencies of the main body system and head angular motion system. At high and low frequencies, its value falls off rapidly.

If visual acuity relates to angular or translational velocity of the eye, then the velocity functions $\frac{\dot{\theta}}{Z_{in}}$ and $\frac{\dot{z}_r}{Z_{in}}$ are relevant. However, the acceleration functions $\frac{\ddot{\theta}}{Z_{in}}$ and $\frac{\ddot{z}_r}{Z_{in}}$ already fall off rapidly at high frequencies, so the velocity functions should fall off particularly rapidly. This suggests that visual impairment at high frequencies relates to resonance of the eyeball in the head, over-compensation of the vestibulo-ocular reflex, or more complex head or body resonant behaviour.

f) Berkson et al 1979 report large inter subject differences in the flexibility of cadaveric lumbar spines. One might therefore expect large differences in head neck flexibility and the effects predicted above. In addition, age may be an intervening variable - Lysell 1969 has suggested that the differences in disc degeneration before and after age about 30 years could be a cause of differences in neck flexion.

g) The model assumes the system to be linear. However, large movements of the head would lead to significant terms in θ^2 and consequent non-linearity. This may be a source of reduced coherence function in transmissibility estimates.

REFERENCES

ANON

Effets physiologiques des vibrations-No2. Etude biomechanique et electromyographique des mouvements de la tete.

Contrat DRME. 64-34-204-00-480-75-01.Lab.de physiologie du travail.

BARNES,G.R. & RANCE,B.H. (1975)

Head movement induced by angular oscillation of the body in the pitch and roll axes.

Av.Sp.Env.Med. 46(8),987-993

BECKER,E.B. (1972)

Measurement of mass distribution parameters of anatomical segments.

16th. Stapp Car Crash Conf. SAE NY 160-185.

BENSON,A.J. (1972)

Effect of angular oscillation in yaw on vision.

Mtg. UK Group on Human Response to Vibration.

Univ.Sheffield, Sept. 1972.

BERKSON,M.H.,NACHEMSON,A. & SCHULTZ,A.B. (1979)

Mechanical properties of human lumbar spine motion segments -Part II:Responses in compression and shear: influence of gross morphology.

ASME J.Biomech.Eng. 101(1),53-57.

BERTHOZ,A. (1971)

Biomechanics and neuromuscular responses to oscillating and transient forces in man and in the cat.

Biomechanics III. 3rd. Int.Sem. Rome 1971. (Karger, Basel, 1973).

BIGGS,G.J. (1975)

An investigation into head movements during whole body vibration.

Final Yr.Proj.Rept. Dept.Human Sci. Loughborough Univ.Tech. May 1975.

BIZZI,E., KALIL,R.E.,MORASSO,P. & TAGLIASCO,V. (1972)

Central programming and peripheral feedback during eye-head coordination in monkeys.

In:Dichgans & Bizzi (Eds).Cerebral control of eye movements and motion perception. Karger 1972.

CHOU,C.C. & SINHA,S.C. (1976)

On the kinematics of the head using linear acceleration measurements.

J.Biomechanics 9,607-613.

DUPUIS,H. & HARTUNG,E. (1978)

The biomechanical behaviour of the bulbous under vibration stress.

Ist.Int.Conf. on Mechanics in Med. & Biol., RWTH Aachen, Aug./Sept. 1978.

- EWING, C.L. & THOMAS, D.J. (1972)
Human head and neck response to impact acceleration.
NAMRL Monograph 21, USAMRL 73-1.
- EWING, C.L. & THOMAS, D.J. (1973)
Torque versus angular displacement response of human head to
-Gx impact acceleration.
17th Stapp Car Crash Conf. SAE NY, 309-342.
- GUIGNARD, J.C. et al (1979)
A method for studying human biodynamic responses to
whole-body z-axis vibration.
AGARD-CPP-267, Paper No. 10.
- HODGSON, V.R., MASON, M.W. & THOMAS, L.M. (1972)
Head model for impact.
16th Stapp Car Crash Conf. SAE NY, 1-13.
- ISO 2631
Guide for the evaluation of human exposure to whole-body
vibration.
International Standard ISO 2631, 1978-01-15.
- JONES, F.P. & GILLEY, F.M. (1960)
Head balance and sitting posture: An X-Ray analysis.
J. Physiol. 49, 289-293.
- KING, W.F. & MERTZ, H.J. (Eds) (1973)
Human impact response.
Plenum, NY.
- LYSELL, E. (1969)
Motion in the cervical spine.
Acta Orthop. Scand. Suppl. 123.
- MELVIN, J.W., McELHANEY, J.H. & ROBERTS, V.L. (1973)
Evaluation of dummy neck performance.
In: Human Impact Response (ed King & Mertz) Plenum NY.
- MOFFAT, C.A., HARRIS, E.H. & HASLAM, E.T. (1969)
An experimental and analytic study of the dynamic properties
of the human leg.
J. Biomech. 2(4), 373-387.
- PADGAONKAR, A.J., KRIEGER, K.W. & KING, A.I. (1975)
Measurement of angular acceleration of a rigid body using
linear accelerometers.
ASME J. Applied Mechanics, 552-556.
- REBER, J.G. & GOLDSMITH, W. (1979)
Analysis of large head-neck motions.
J. Biomech. 12, 211-222.
- ROWLANDS, G.F. & ALLEN, G.R. (1969)
The rotational eye movements needed to correct for vibration
of the head.
RAE Tech. Memo. EP427. Aug. 1969.

SCHULTZ, A.B., WARWICK, D.N., BERKSON, M.H. & NACHEMSON, A.L.
(1979)

Mechanical properties of human lumbar spine motion
segments-Part I: Responses in flexion, extension, lateral
bending and torsion.

ASME J. Biomechanical Eng. 101(1), 46-52.

VOGT, L., SCHWARTZ, E. & MERTENS, H. (1979)

Head movements induced by vertical vibrations.

AGARD-CPP-266/267.

WALKER, L.B., HARRIS, E.H. & PONTIUS, U.R. (1973)

Mass, volume, center of mass, and mass moment of inertia of the
head and head and neck of the human body.

17th. Stapp Car Crash Conf. SAE NY, 525-537.

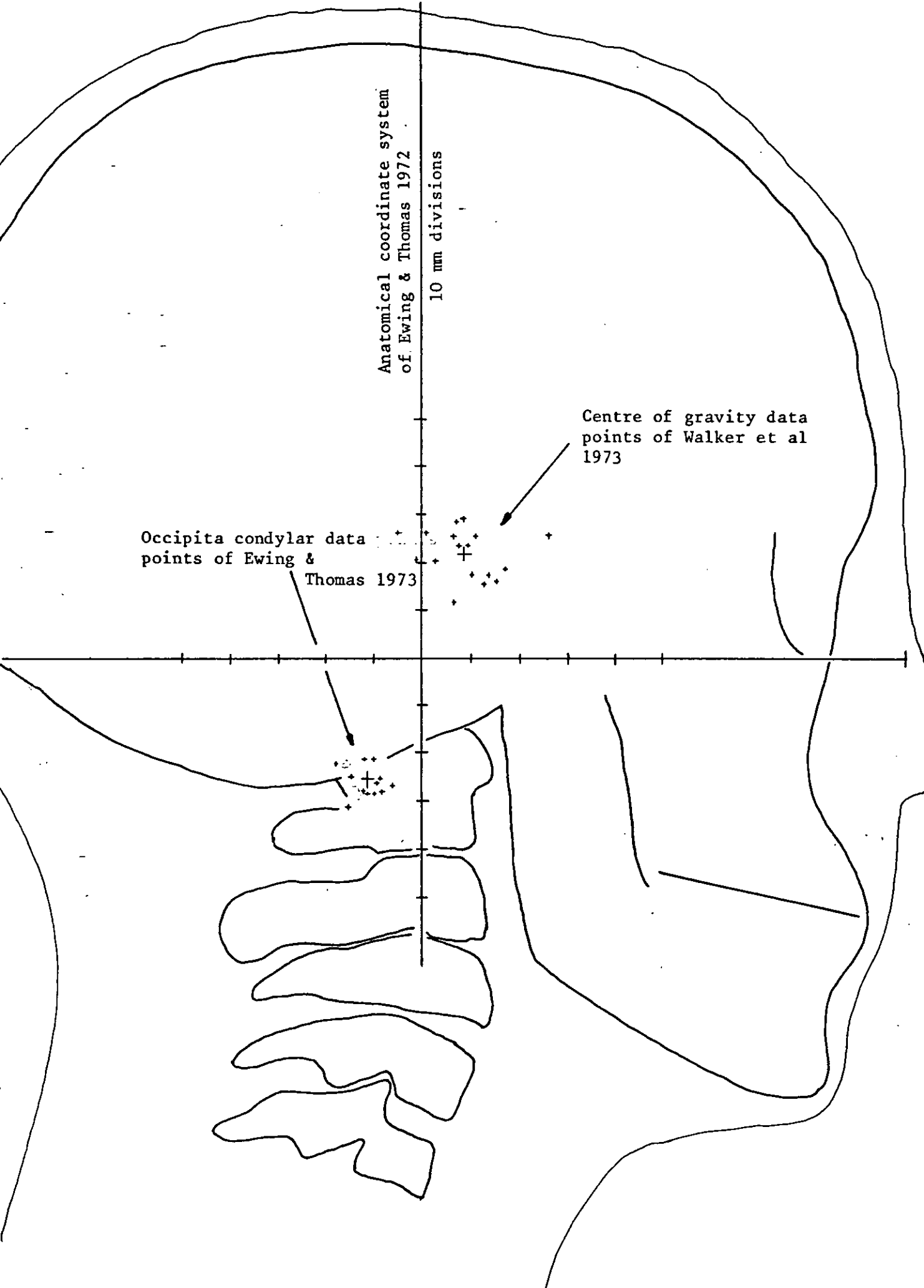


Fig. A3.1 Head geometry (drawn full scale)

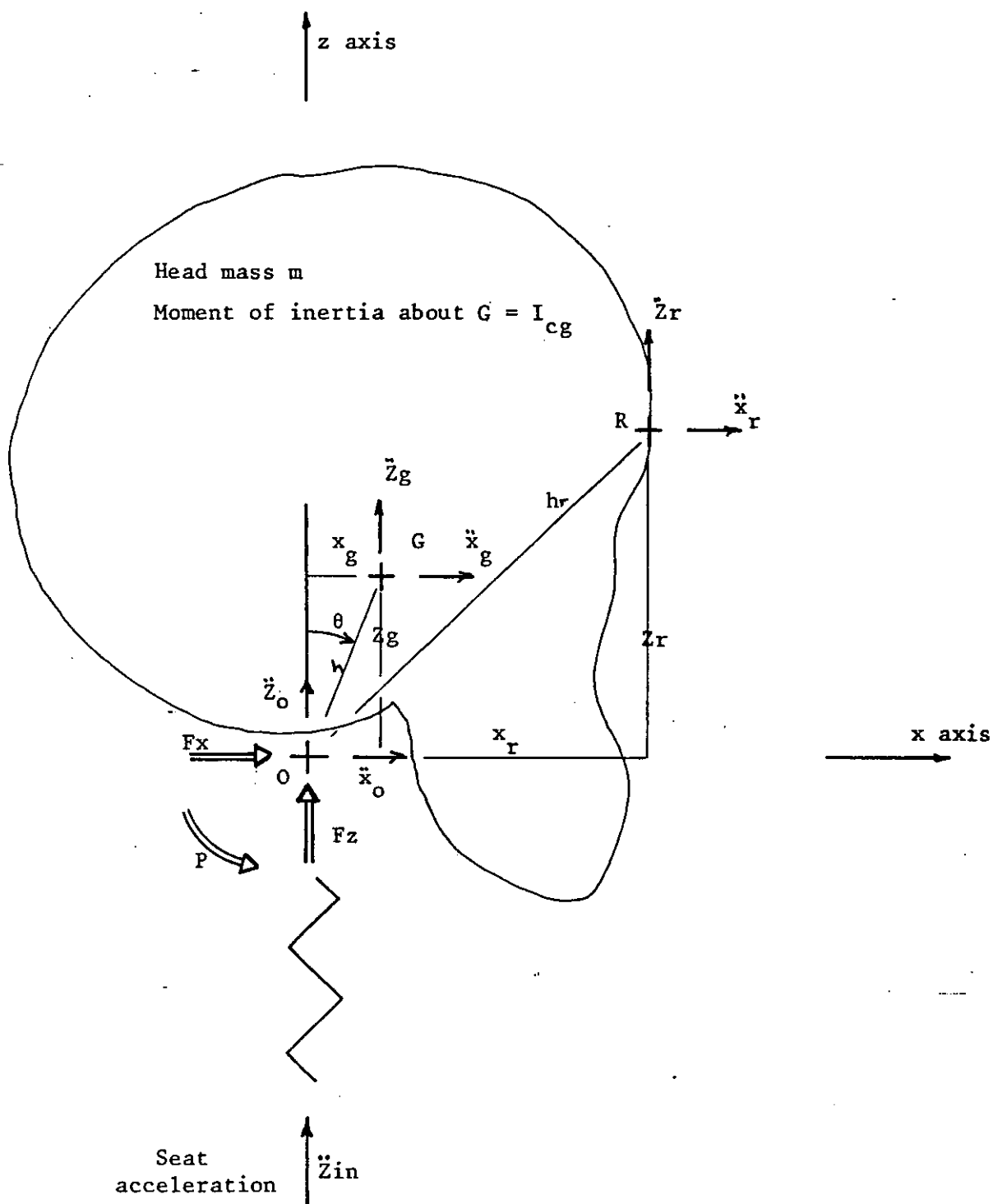


Fig. A3.2 Forces assumed to be acting on the head

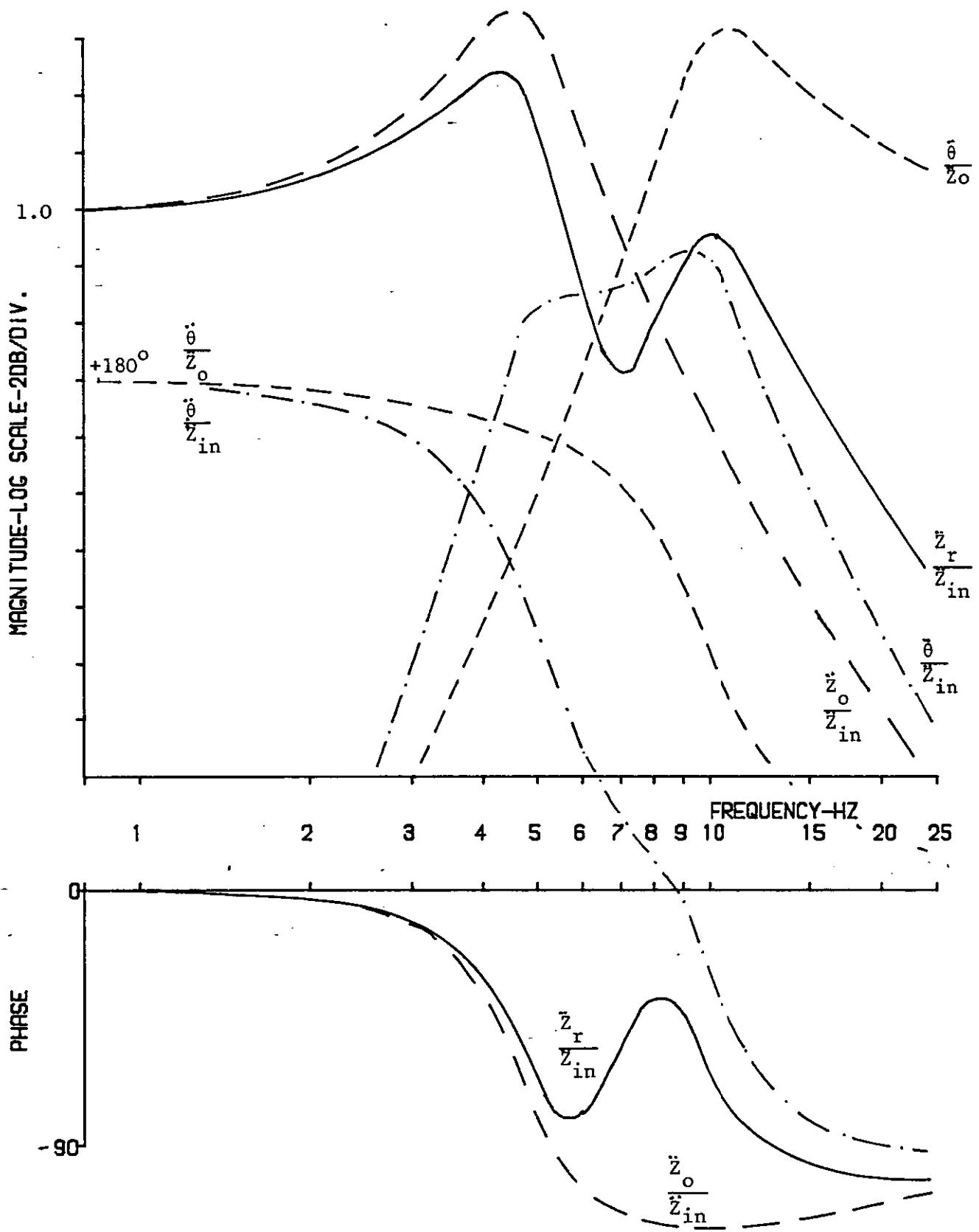


Fig. A3.3 Response of possible head model - see text

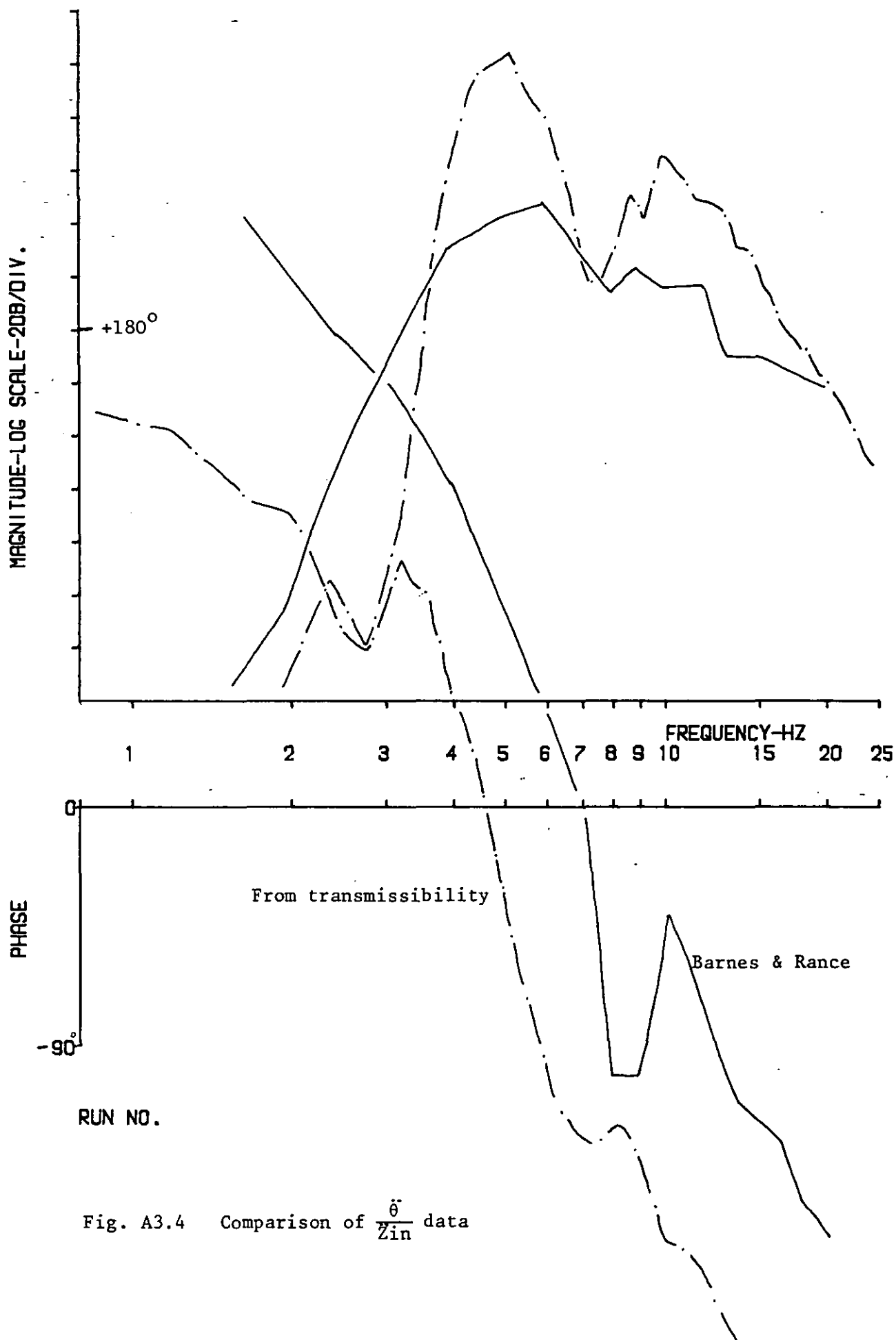
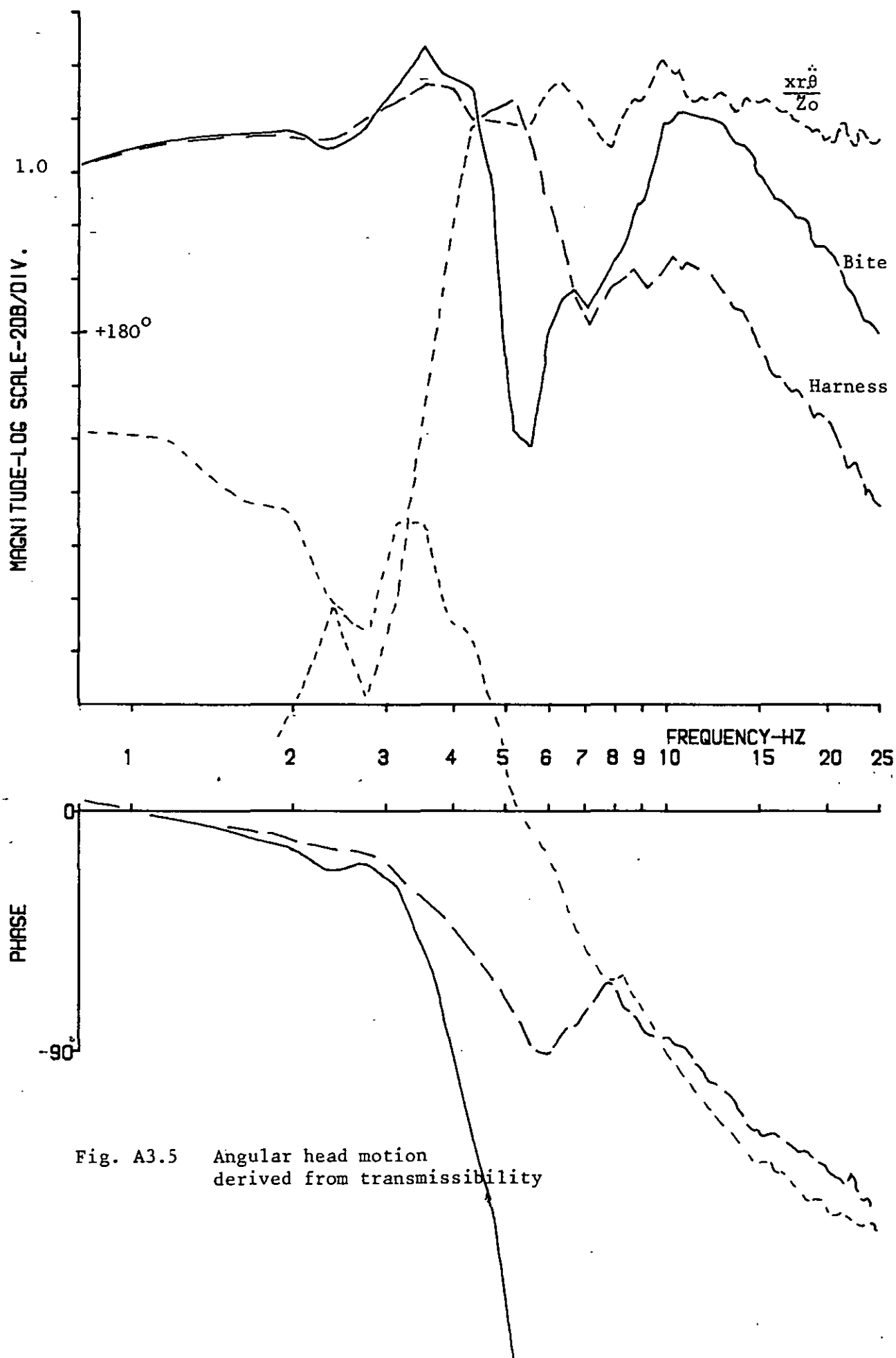


Fig. A3.4 Comparison of $\frac{\ddot{\theta}}{Z_{in}}$ data



APPENDIX 4 VIBRATION FACILITY

A4. Vibration facility

The vibration facility consisted of the vibration room, the vibrator and hydraulic power pack, signal conditioning equipment, and the control room, fig. A4.1. The control room served as a general instrumentation area and contained, as well as the vibrator control unit, all necessary tape-recorders, oscilloscopes etc. A fully screened, common earth, signal trunking system connected vibrator room and control room so that only a minimal amount of instrumentation encumbered the subject. There was audio and visual contact between the control room and vibration room.

A4.1 Vibration room

To make the surroundings as normal as possible for the subject, he was asked to sit on a vibrating chair mounted at normal sitting height in a room isolated from the activities of the laboratory. Internal room dimensions were 2.9m x 2.9m x 2.5m high, and the room (set 1.5m above the laboratory floor) was approached by a small flight of steps. One wall contained a 1.2m x 1.5m double glazed window. Glazing was 6mm float glass with minimal distortion, so that photography through the glass was satisfactory.

To reduce ambient noise levels as far as possible, the room was isolated from the actuator and the laboratory floor and ventilation was via sound treated ducting. Simple sound treatment of the room included heavy plaster-board walling, choice of carpeting to maximise sound absorption, moveable sound-absorbing panels within the room and location of fluorescent light controls outside of the room. With the vibrator and ventilation fan running, the ambient noise level at the subject's head was of the order of 40dB.A. The noise attenuation was of the order of 30dB over much of the frequency range - fig. A4.2.

The vibrating chair was similar to an office chair with extra members to add stiffness - fig. A4.3. The footrest was adjustable in height. The seat was horizontal, and consisted of 30mm plywood. The back-rest was composed of four horizontal strips of webbing so that the subject had back support with minimal friction or transfer of vibration direct to his back. With the vibrator at rest the seat was approx. 500mm from the floor. The

subject had at hand a push-button to halt the vibrator, and two wall-mounted push-buttons were available to the observer.

A4.2 Vibrator

The vibrator was an electrohydraulic vibrator designed for research with people (Servotest HV1). It had a total stroke of $\pm 150\text{mm}$ (including 25mm safety snubber at either end) and a dynamic thrust of 6.7 kN. The actuator was mounted on a 1.5m x 1.8m x 0.7m high concrete block, which was, in turn, mounted on 100mm cork. The vibrator table consisted of a milled duralumin plate 380mm x 380mm x 50mm, and, for normal use, carried a dead-weight consisting of approx. 160kg lead to reduce the effects of feedback of subject dynamics and the effects of 'stiction'. The actuator piston rod was mounted in hydrostatic bearings to minimise static friction and for operation with offset loading.

The vibrator control systems and hydraulic systems had been modified over a period of time to improve reliability, the ergonomics of operation and, in particular, to take into account a number of proposals (Lawes 1974) to improve safety. The electrical and hydraulic circuits are shown in block diagram form in figs. A4.4 and A4.5, and the control panel and hydraulic control panel in figs. A4.6 and A4.1.

The following were included to ensure safe operation as far as possible:

- a) Built in oscillator with damped, multi-turn frequency control (to avoid inadvertent decade switching)
- b) Signal not connected until amplitude control set to zero
- c) Displacement limits set on actuator movement - limit variable and set low for normal use.
- d) Feedback shared between displacement, pressure and acceleration so that the effects of transducer failure are reduced (this led unfortunately to some frequency response problems at low frequencies - fig. 4.7).

- e) Key required to operate both electronics and hydraulics. Two-man operation necessary at start-up.
- f) Electronics only operative when hydraulic pressure at satisfactory level.
- g) Mains failure protection.
- h) As far as possible, any electrical malfunction, emergency stop or inadvertent action results first of all in rapid but not sudden, reduction of signal to zero (time constant approx. 0.8 sec) followed by complete hydraulic shut-down (approx. 6 sec). After such action, start-up has to follow the normal procedure.
- i) Vibrator motion and hydraulic capacity minimal, so that available velocities and accelerations small.
- j) Hydraulic snubbers to avoid metal to metal contact in case of malfunction.
- k) Clear control layout and operational practices as far as possible.

Accidental failure simulated in various ways showed that the highest transient accelerations occurred when the actuator ran into the upper snubbers. In this case (with a 70kg. load) the peak acceleration value was 20m/s^2 ("Dynamic Response Index" also 20 m/s^2).

The feedback and loop gain controls allowed modification of system feedback to suit particular conditions. However, experience had shown it to be sufficient to set the controls in one position giving system characteristics suitable for most practical situations. In this condition, the system response (acceleration) was as in fig. A4.7. The non-linearity at low frequencies (indicated by the coherence function) probably relates to increased influence of displacement feed-back.

As expected with an electrohydraulic vibrator, significant distortion of low frequency sinusoidal signals occurred as a result of stiction. Rowlands 1974 designated a root sum of squares percentage error as below:

$$\text{Percentage error} = 100 \sqrt{\frac{A_1^2 + A_2^2 + \dots + A_{10}^2}{A_0^2}}$$

where A_1 , A_2 etc. are the amplitudes of the harmonics of the fundamental A_0 .

By using a Federal Scientific narrow band spectrum analyser, the amplitudes of all significant harmonics were obtained from the acceleration spectra and the percentage error calculated. Rowlands used the first ten harmonics, but in this case all harmonics of amplitude down to 1% of fundamental were included (this resulted in from 2 to 14 harmonics being included). Distortion tends to reduce as the vibration amplitude is increased and the analysis was carried out at two levels to represent the range of intensities expected for most experimental work with subjects. Significant distortion arose from the built-in oscillator and representative values are included in table I.

Frequency (Hz)	Acceleration level - m/s^2 r.m.s.		Oscillator Distortion
	0.5	2.0	
1	17.7%	11.0%	5.7%
3	18.6	7.1	
6	8.2	5.4	
10	10.1	4.3	
20	9.5	4.4	3.8

Table I. Acceleration distortion of vibration (using $\sqrt{\sum (\frac{A}{A_0})^2}$ %).

The relevant values obtained by Rowlands (for a larger vibrator) are given in table II for comparison.

Frequency - Hz	Acceleration level - m/s^2 r.m.s.			
	0.18	0.42	0.85	1.78
3	33.1%	18.3%	11.0%	7.1%
5	26.8	16.2	9.1	8.7
7	19.2	12.8	8.2	6.3

Table II. Acceleration distortion of large vibrator (Rowlands 1974).

A4.3 Hydraulic Power Pack

The power pack was designed to deliver 27 litre/min oil at 15MN/m^2 , filtered to 1 micron. The hydraulic circuit is shown in fig. A4.5. To reduce noise levels, the unit was converted to water cooling and acoustically isolated. The unit was housed in a multi-walled room (1.8m x 1.8m x 1.5m high), the wall components (from inside out) consisting of 25mm 'Revertex A4 (FR)' fire resistant sound absorbing foam mounted on an open mesh framework; 40mm air gap; 2mm S.D.S. steel sandwich; 100mm minimum air gap; 2mm S.D.S. steel sandwich. All joints of the room were separated by 12mm neoprene sponge and the room stood on a 150mm reinforced concrete slab with 100mm cork supporting the slab. The resulting sound attenuation characteristics and noise spectrum are shown in fig. A4.8. The noise level outside of the enclosure (1m distant), with power pack in operation, was of the order of 40 dBA - well less than the normal ambient level for the laboratory area. Unfortunately cooling water pipeline noises raised the level to approx. 55 dBA, although this was still below ambient.

A4.4 Signal conditioning

The signal conditioning unit (shown in fig. A4.6) allowed the shaping of signals supplied to the vibrator system and the weighting and measurement of table acceleration signals.

The following were available:

Vibrator Input signals

- a) High pass: all components below 0.1 Hz. (-3dB point) filtered out automatically to eliminate drift on the vibrator.
- b) $\pm 6\text{dB}$: the signal is 'integrated' or 'differentiated' at 6dB/octave over the whole band.
- c) Low pass: 12dB/octave from fixed frequencies of 5, 25, 50 and 100 Hz.
- d) Gain: gain of $\times 10$.

Vibrator output signals

- a) I.S.O. 2631 'Vertical' weighting network
- b) I.S.O. 2631 'Horizontal' weighting network.

Both networks conform to S.A.E. J1013.

- c) dB 'A' weighting network. .
- d) Switched frequency increase to allow use of a, b, c with data replayed at x8 normal speed.
- e) True r.m.s. measurement with choice of time constants and range - output in dB. Output available as 10mV/dB or at meter on vibrator control unit.

A4.5 Operation of vibrator

The operational procedures for both vibrator and signal conditioning unit are set out below:

OPERATION OF VIBRATOR

IN THE WRONG HANDS THIS EQUIPMENT CAN BE DANGEROUS. ON NO ACCOUNT SHOULD ANYONE ATTEMPT TO OPERATE IT UNTIL THEY HAVE RECEIVED INSTRUCTION AND ARE AWARE OF THE SAFETY PROCEDURES. CONFORMANCE WITH THE SAFETY PROCEDURES IS OBLIGATORY.

These notes are intended to serve as a reminder of the operational routine.

START UP

- 1) Check that the vibrator is free of obstruction, the room clear and no-one on or near the vibrator seat.
- 2) Plug in the control unit and switch on. The green light (A) should glow. Check that the red emergency stop button is out.
- 3) Ask the second operator to hold the 'reset' button (B).
- 4) Check the power pack controls.

PRESSURE BY -PASS VALVE OPEN (ANTICLOCKWISE)?

WATER VALVE OPEN AND WATER RUNNING?

- 5) Switch on at isolator.
- 6) Turn start key (If you put your ear to the power pack you should hear the motor start).
- 7) Bring the hydraulic pressure up by closing the pressure by -pass valve. The seat should rise, the oil should make a hissing noise until the valve is tight shut, and the pressure should rise to 2000 psi.
- 8) The second operator can now release the 'reset' button. The 'hydraulics' light should glow.

- 9) Check that the fan to the vibrator room is running.
- 10) This completes operations at the hydraulic unit. Until you switch off, the only attention required is an occasional check of the oil temperature. If this rises at all, increase the water flow. It is vital that the temperature should not rise to the red mark. High oil temperature will cause shut down and a long delay (2 days) before the oil cools sufficiently for operation.

RUNNING

- 1) Set up the input signal. There are three alternatives: Internal (sinusoidal) signal, External (displacement) signal, External (acceleration) signal.

- a) Internal

The frequency is set on the 10 turn dial (C). The nominal range is 0 to 100 Hz (actual minimum about 0.5 Hz). Set the switch (D) to 'internal'.

- b) External

Set the switch (D), to external, and switch (E) either to 'accl' or 'disp' and plug in the corresponding external signal at (F). There is a 'differentiating' circuit between the two sockets and this can be used to change the characteristics of the feed-back system. However, the system is intrinsically biased to acceleration control.

- 2) Set the chair position by the mean value control (G). It is not normally necessary to adjust this control. Its operation is dependent on the maximum displacement range settings (not available to the normal user).
- 3) Dependent on the type of overall control required, set the requisite 'outer loop control' button (H). This should normally be set at 'off'. Do not use the other settings without consultation with J.S.
- 4) Press the 'on' button (J). It will not accept the command unless the amplitude control (K) is set to zero.
- 5) Increase the vibration amplitude slowly to the required level by control (K). Check the required level on the meter (L). The scale is in m/s^2 r.m.s. Note that the operation of the meter is dependent on the operation of the signal conditioning unit next to the vibration control unit.
- 6) Four output signals are available for use at (M). The most useful are acceleration and displacement. The nominal scales are:-
Acceleration: 1 volt output equivalent to $10\text{m/s}^2 \pm 2\%$
Displacement: 1 volt output equivalent to 21 mm.

THE SUBJECT

- 1) Excepting in emergency, the subject should only get onto or leave the seat when the system is running and the amplitude at zero.
- 2) Make sure that he/she understands the operation of the subject stop button.

EMERGENCY SHUT DOWN

- 1) Press the subject stop button, either of the red stop buttons in the

vibrator room, or the red stop button at the vibrator controller.

- 2) The vibrator motion will be reduced rapidly to zero, and after a few seconds the chair will sink to its lower position as the oil pressure falls off. The subject can then dismount.
- 3) After emergency shut down, the whole start-up procedure has to be repeated. Note that you must open the pressure bye-pass valve before attempting to start again.

CLOSE DOWN

- 1) When the subject is away from the seat, press any of the emergency shut-down controls.
- 2) Switch off and unplug the control unit.
- 3) OPEN THE PRESSURE BYE-PASS VALVE. (anticlockwise).
- 4) Shut off the water valve.
- 5) Switch off at the isolator.
- 6) Record your run and the elapsed time in the vibrator log book.

TIDY UP

LEAVE EVERYTHING AS YOU FOUND IT.

OPERATION OF SIGNAL CONDITIONING UNIT

This unit can be used to shape signals intended to drive the vibrator, or condition and measure signals from the vibrator. There are three main sections - signal shaping, I.S.O. filtering, true r.m.s. measurement.

(1) Signal Shaping

- (i) High pass: All components below 0.1 Hz are filtered out automatically. This is to eliminate drift on the vibrator.
- (ii) ± 6 dB: The signal is 'integrated' or 'differentiated' at 6dB/octave over the whole band.
- (iii) Low pass: A 12dB/octave roll off from fixed frequencies of 5, 25, 50 and 100 Hz is available.
- (iv) Gain: A gain of $\times 10$ is available if required.

(2) I.S.O. Filtering

Besides an 'A' weighting network for noise, the tentative I.S.O. vibration weighting networks are available for vertical (a) and horizontal (c) vibration. If weighting is to be performed on recorded data, time can be saved by switching (at the back) to (b) or (d) which will increase all the vibration weighting frequencies by a factor of 8.

(3) True r.m.s.

This unit uses squaring and logging circuits to give a true r.m.s. value of the input signal.

The time constants can be changed by a switch (T_C), the two set positions being roughly for noise (out) and vibration (in), or by adding extra capacitors at the sockets at the back of the instrument. (A useful arrangement is $22\mu F$ and $470\mu F$ in the 'short' and 'long' positions respectively, to give suitable time constants (1.8sec and 30sec) for fast and slow moving vibration signals).

There are two range settings set by switch ($\times 10$) giving:

(in) : zero output equivalent to 0.01V r.m.s. at input ($0.1m/s^2$ @ 1 volt/g)

(out) : zero output equivalent to 0.1V r.m.s. at input ($1m/s^2$ @ 1 volt/g).

The output varies from 0.00 volts to about 0.30 volts, with 0.01 volts equivalent to 1dB. Small negative voltages apply as -dB, but they are not very accurate. The r.m.s. circuit can be checked by use of the 'cal' button at the back. Depression gives an output of 0.350 volts.

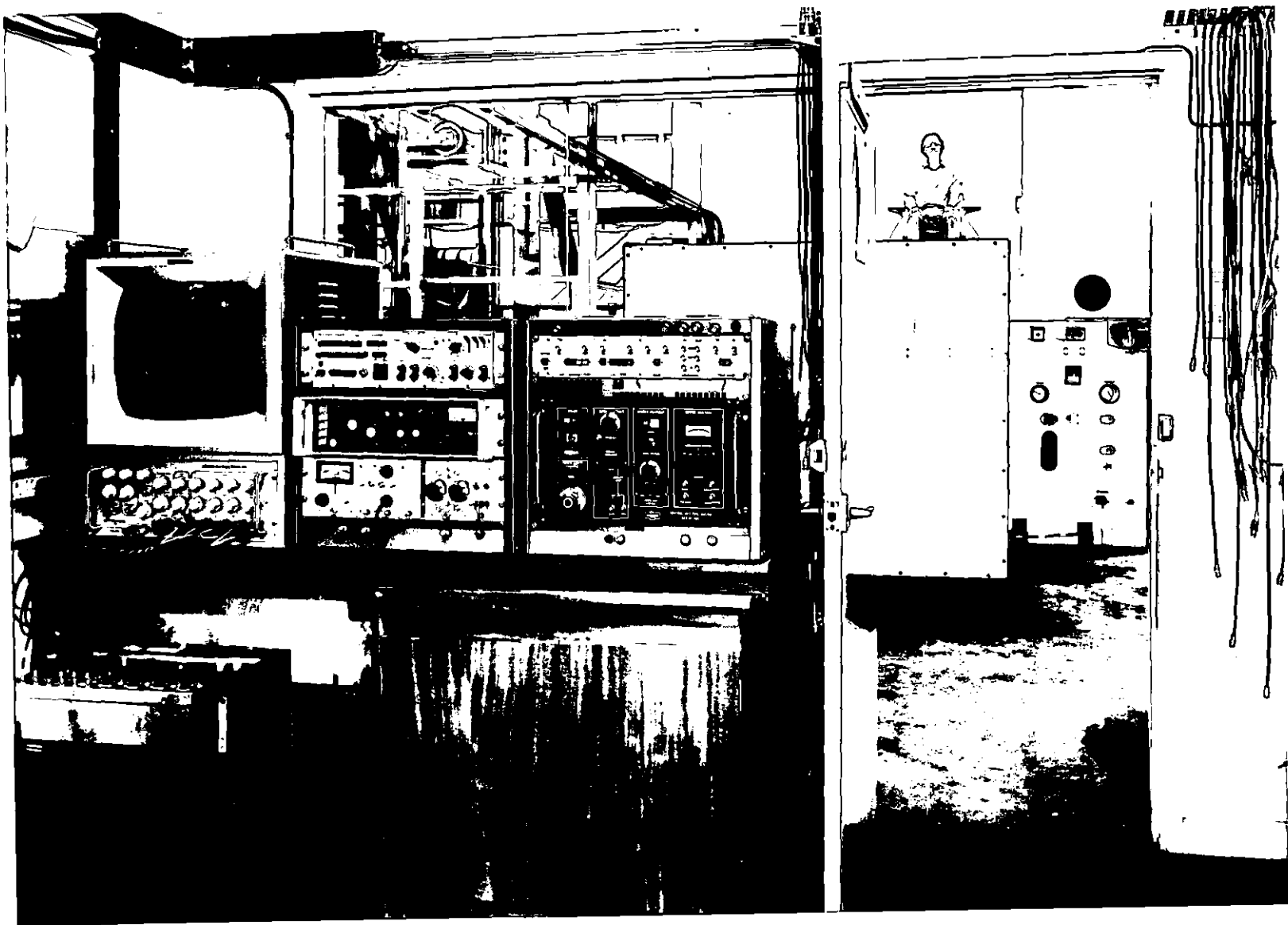


Fig. A4.1 Vibration facility

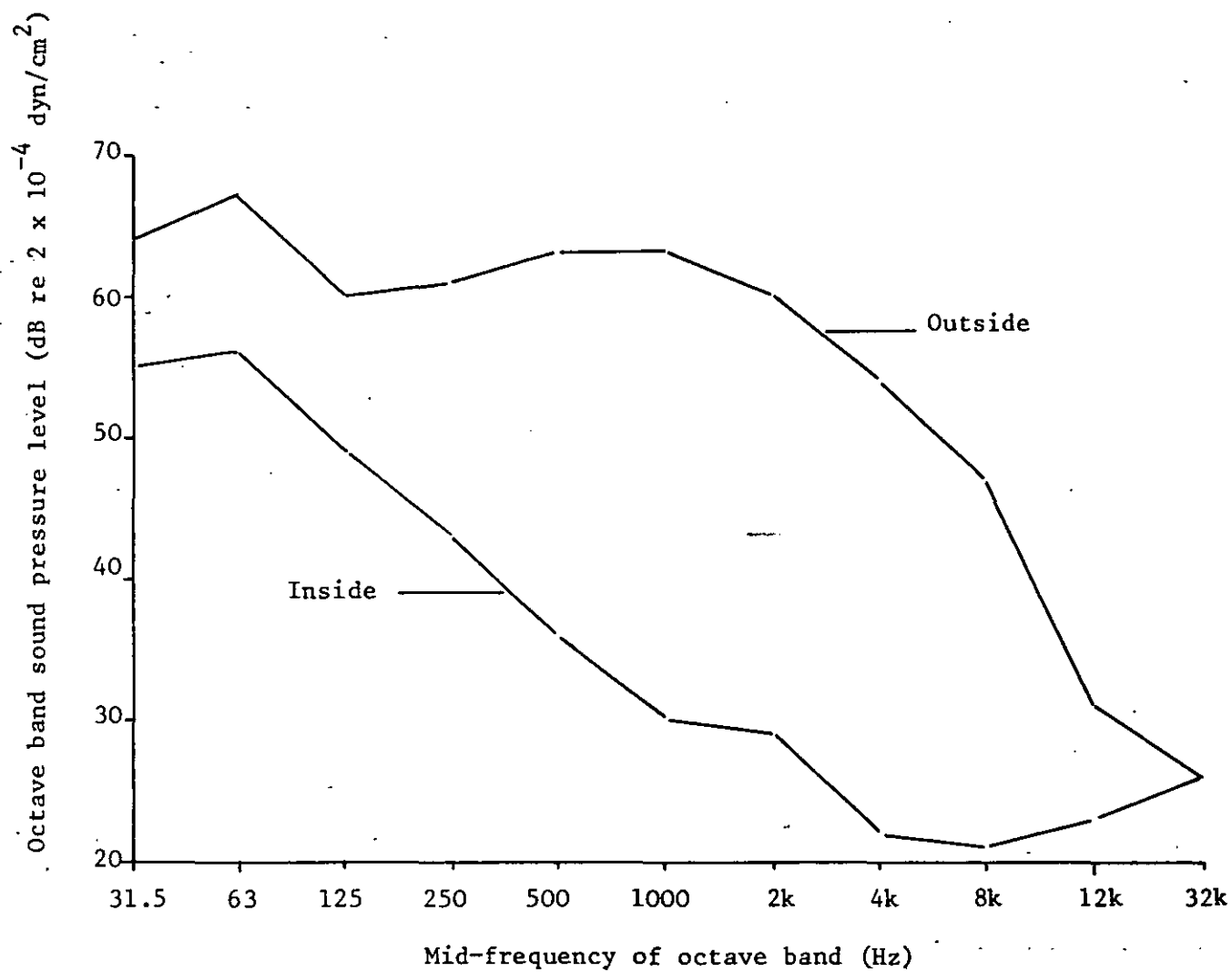


Fig. A4.2 Noise levels measured inside and outside of vibration room (vibrator in operation)



Fig. A4.3 Vibrating chair

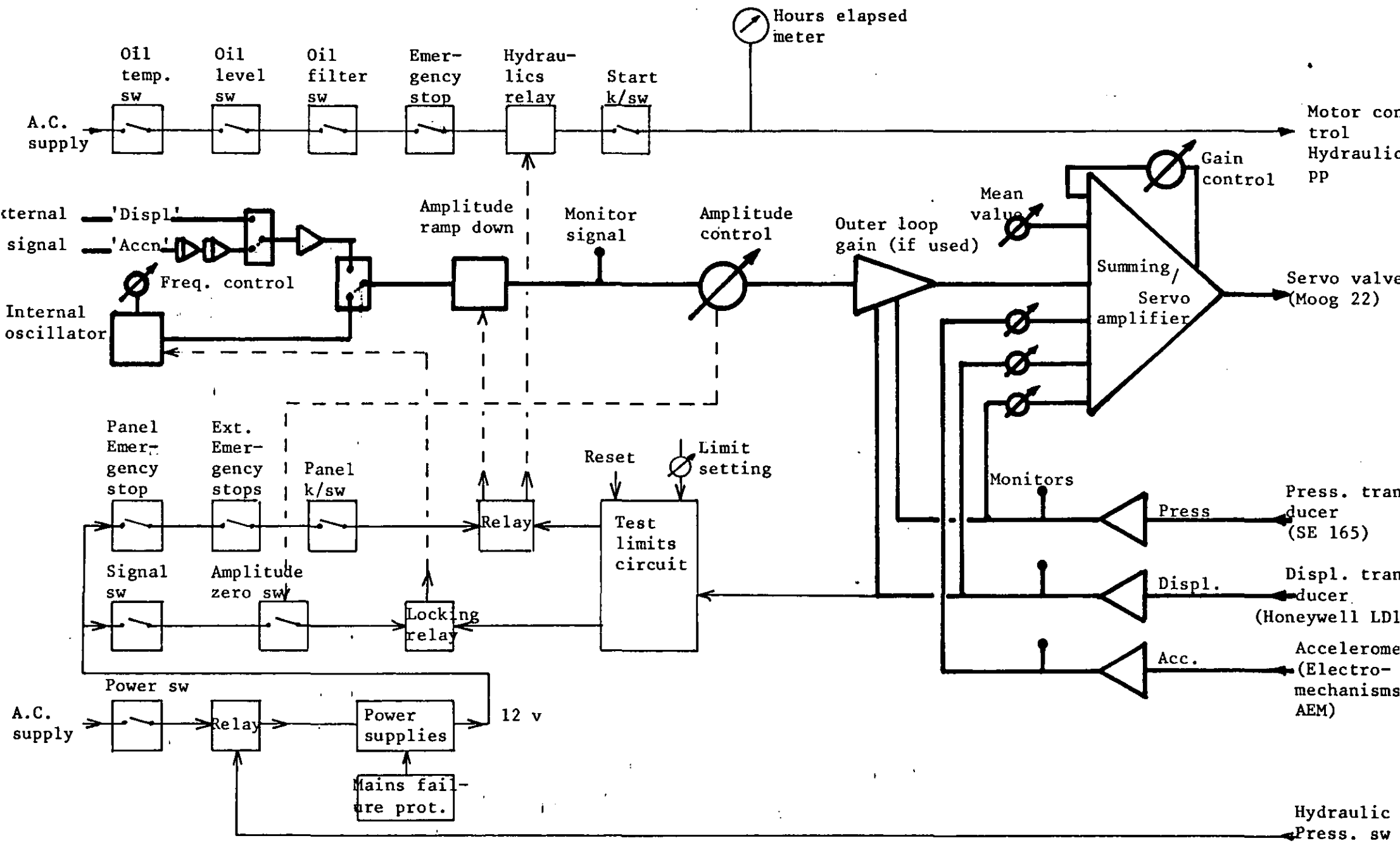


Fig. A4.4 Vibrator control circuits

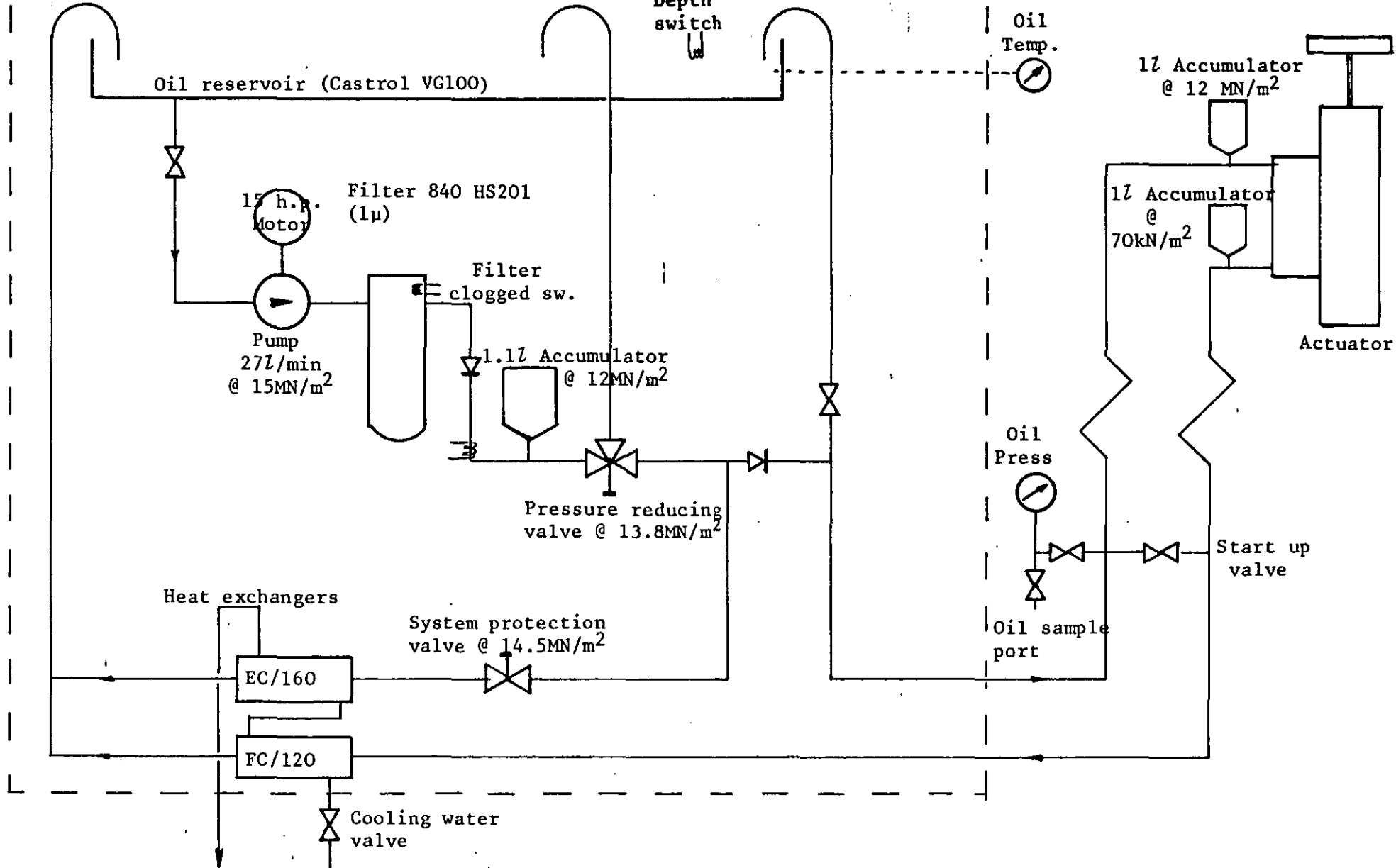


Fig. A4.5 Hydraulic Circuit

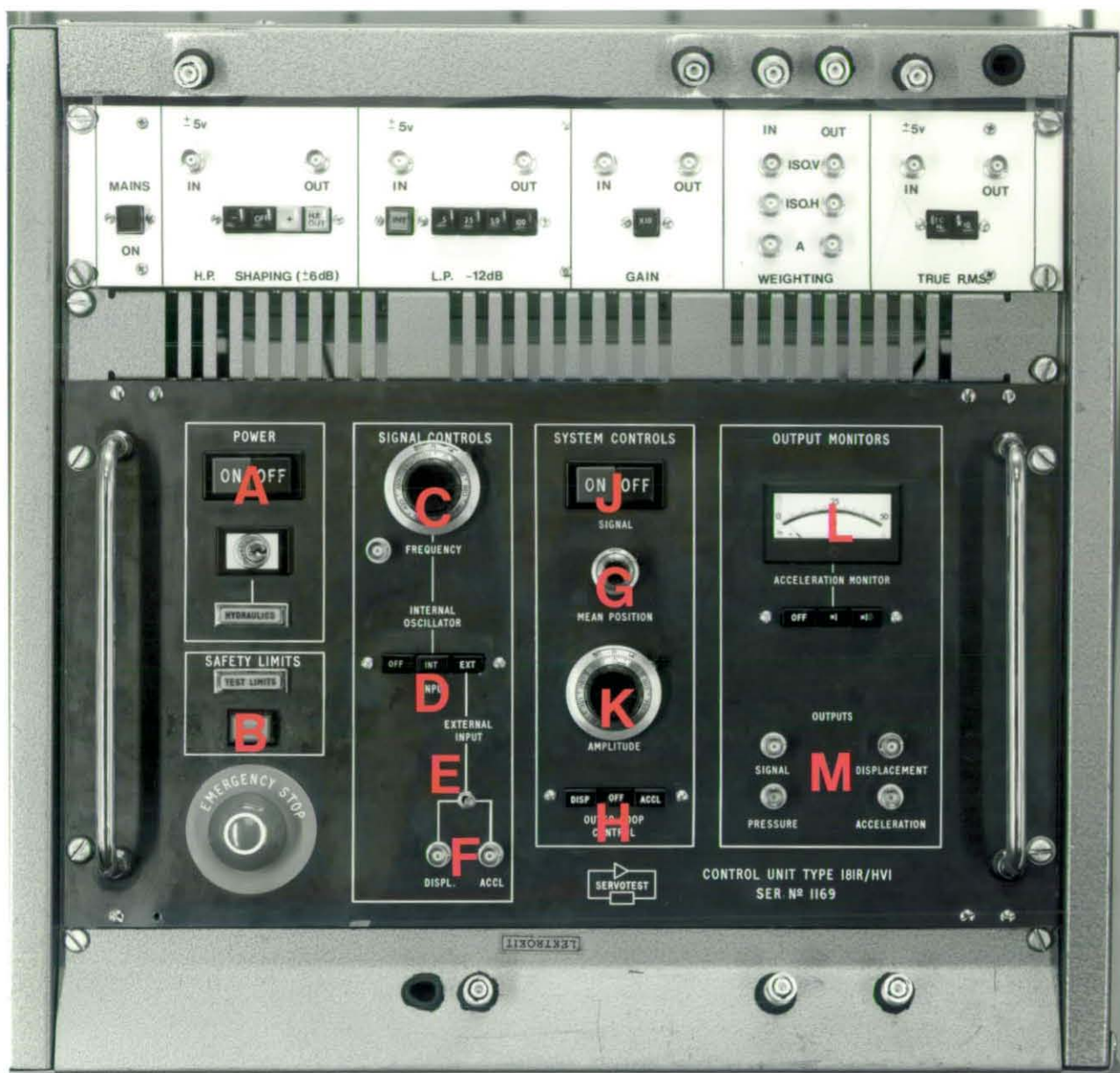


Fig. A4.6 Vibrator control panel and signal conditioning unit.

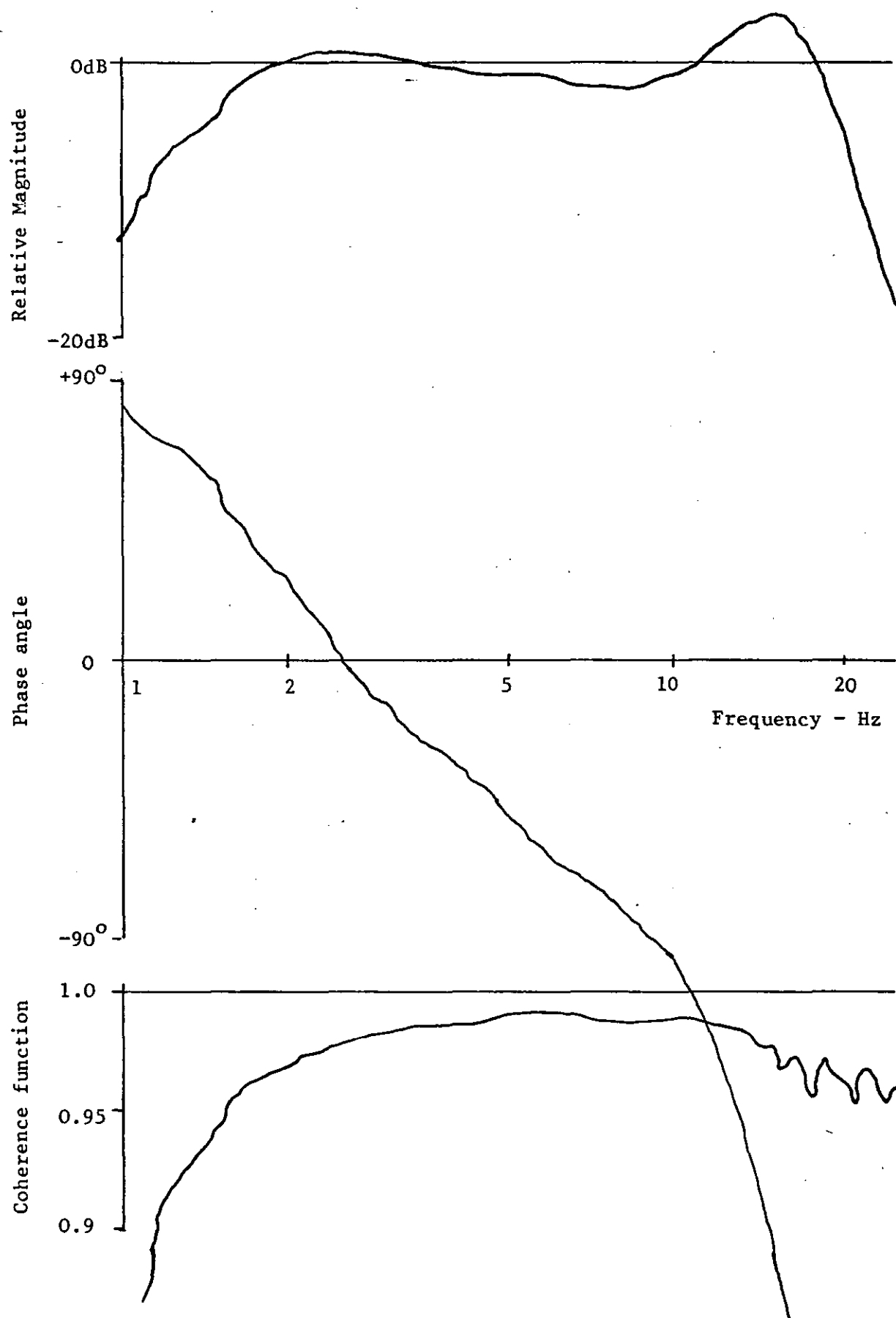


Fig. A.4.7 System (acceleration) response of vibrator..
 70kg mass on chair, acceleration level 1m/s^2 r.m.s. (ISO weighted)
 (Note non-linearity at low frequency)

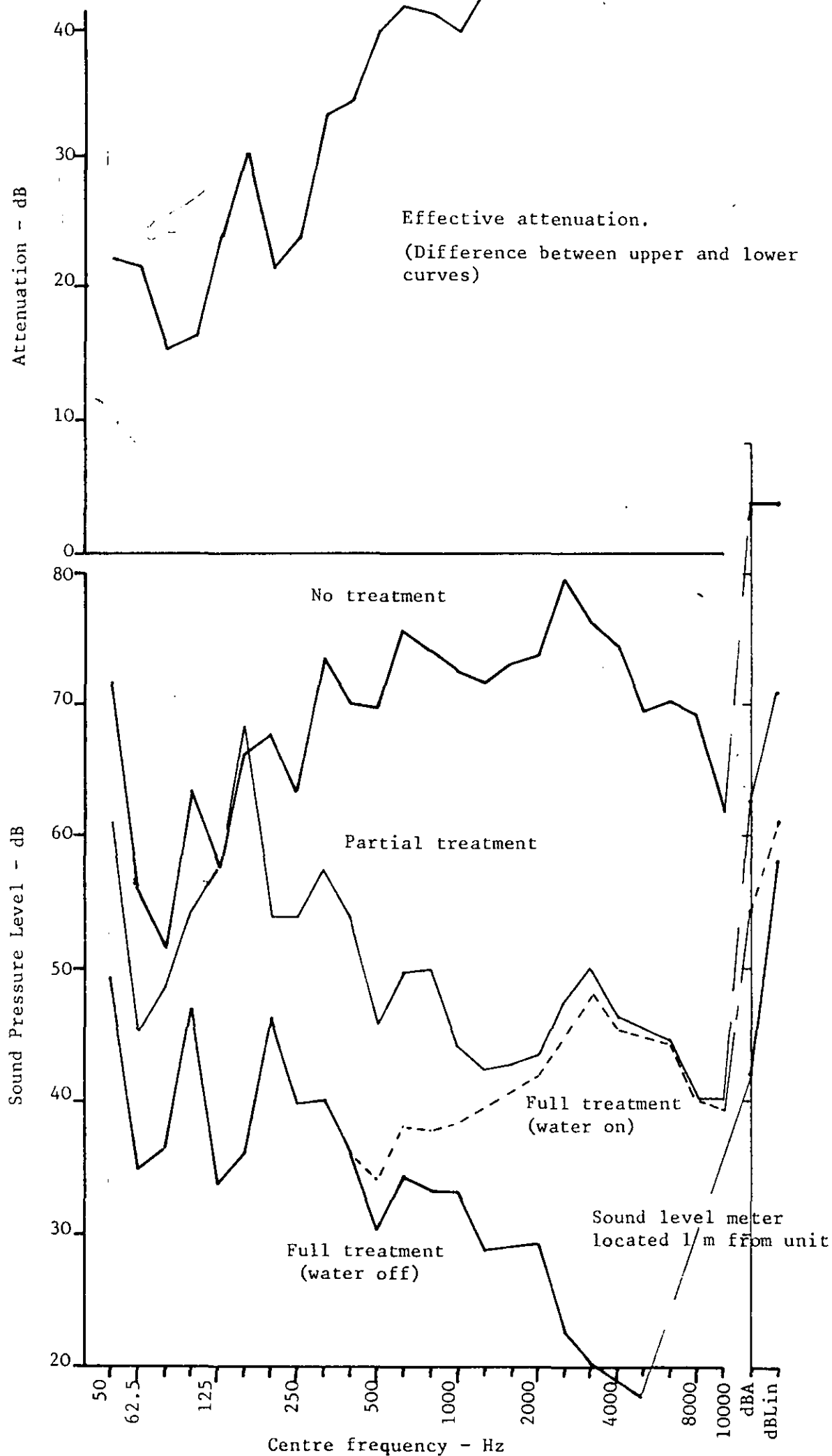


Fig. A4.8 Noise treatment of power pack - 1/3 Octave analysis

APPENDIX 5: EQUIPMENT SPECIFICATIONS

The manufacturers specifications are listed briefly below.

1. Analogue tape recorder

Philips 'Ana-log 7' $\frac{1}{2}$ " I.R.I.G. compatible

F.M. Recording:

<u>Speed</u>	<u>Freq. Range</u>	<u>S/N Ratio</u>	<u>Harmonic dist.</u>	<u>Wow & Flutter</u>
30 i.p.s.	0-10 kHz	45 dB	< 1%	0.15%
to				
15/16 i.p.s.	0-312 Hz	39 dB	< 1%	0.50%

Speed variation: within 0.15% of nominal value.

Amplifier characteristics:

Non-linearity < 1%

Drift < 1%

2. Load cell and foot rest accelerometers

Kistler type 816A:

Acceleration range $\pm 50,000 \text{ m/s}^2$

Sensitivity 0.5 pC/m/s^2

Nominal natural frequency 20 kHz

3. Head accelerometer

Endevco type 2265-20

Acceleration range $\pm 200 \text{ m/s}^2$

Sensitivity 2.3 mV/m/s^2

Nominal natural frequency 1.3 kHz

Linearity 2%

4. Force transducers

3 Kistler type 903A transducer connected in parallel in the load cell

1 Kistler type 903A transducer in the foot rest

Characteristics for each cell:

Range 0-60 kN

Sensitivity (Nominal) 4.4 pC/N

Nominal natural frequency 50 kHz

Deflection (Nominal) $15 \mu\text{m}$ at maximum load

Linearity better than 1%

The actual sensitivities for the three transducers used in the load cell were (in the range of loading in use) 44.2, 44.2, and 45.7 pC/N. The mean sensitivity of the three in parallel was therefore 44.7 pC/N.

Using the deflection indicated above, it was calculated that the natural frequency of the system consisting of the three transducers with a load of 100 kg was 1.7 kHz.

5. Charge amplifiers

Load cell: Vibrometer type TA/3/C:

Frequency range 0-50 kHz

Time constant (variable) $0.1/\mu$ s - 100 s

Linearity 0.05%

Absolute accuracy +0.3, - 0.2%

Included low pass filter variable from 1 kHz to 300 kHz

Foot rest: Kistler type 568:

Range $100-10^6$ pC to give -5V, +10V output

Frequency range 0.5 kHz at the settings used

Time constant 10s

Linearity $\pm 0.1\%$

Absolute accuracy $\pm 1\%$

6. Function generator

Prosser type A100

Max. output ± 10 V into 50 Ω

Frequency range 0.8 mHz - 100 kHz

Frequency accuracy $\pm 1\%$ of scale

Frequency stability $\pm 0.1\%/8$ hrs, $\pm 0.01\%/^{\circ}\text{C}$

i.e. reasonable practical range $\pm 0.2\%$

7. Display oscilloscope

LAN type 419B/4 channels

8. Ultraviolet Recorder

Honeywell 'Visicorder' 2106

Frequency range of galvanometers used: 0-3 kHz

Sensitivity 486 mV/cm

9. Driver Amplifier

Honeywell 'Accudata' 107:

Frequency response 0-20 kHz $\pm 5\%$ D.C. value

Drift $< \pm 30 \mu\text{V}/^\circ\text{C}$

Gain ranges 0.01 to 20

10. Random function generator

Solartron type JM 1861 with J X 1962 low pass filter

Pseudo random function generator

Clock frequency 10^{-3} Hz to 10^6 Hz

Maximum register length $\sim 2^{21}$

(Hence Repeat period @ 50 Hz max. frequency and 'inverse repeat' $\simeq 2000$ secs)

APPENDIX 6 FLUTTER COMPENSATION UNIT

During frequency modulated magnetic tape-recording, low frequency amplitude variations ('flutter') arise as a result of tape speed variations. Although tape-recorder speeds are well controlled, at the most suitable tape speed for this work ($3\frac{3}{4}$ i.p.s.) flutter variations lead to increased electrical noise levels at about 4 Hz which is within the frequency range of interest.

Flutter can be alleviated to some extent by shorting one tape-recorder channel (i.e. zero input) during recording, and biasing normal signals by the output of this channel on replay. This was demonstrated to be useful, by using the shorted channel output as the 'screen' for the other channels on replay. In the long-term, however, this method was not suitable as connections with other equipment required disconnection of the tape-recorder mains earth if 50 Hz noise were to be avoided - an unsafe procedure.

A simple unit was constructed so that signals could be biased by subtraction in operational amplifier circuits. This system proved quite suitable. Figs. A6.1 (a & b) show the reduction in signal noise obtained.

The unit was also designed to offer further signal conditioning found necessary. An increased gain on one operational amplifier channel was made available so that tape-recorded signals used for A/D conversion triggering could be increased to the order of 5-10 volts. The A/D conversion unit required a T.T.L. logic signal if external digitisation control were needed, whilst the tape-recorder frequency limitations reduced the rate of rise of recorded high-frequency square waves. A simple logic system was built into the unit so that it provided a T.T.L. output in step with an applied, relatively slowly rising, periodic voltage.

The unit is free-standing and proved simple in use as well as fulfilling its requirements. The circuit diagram is given in Fig. A6.2.

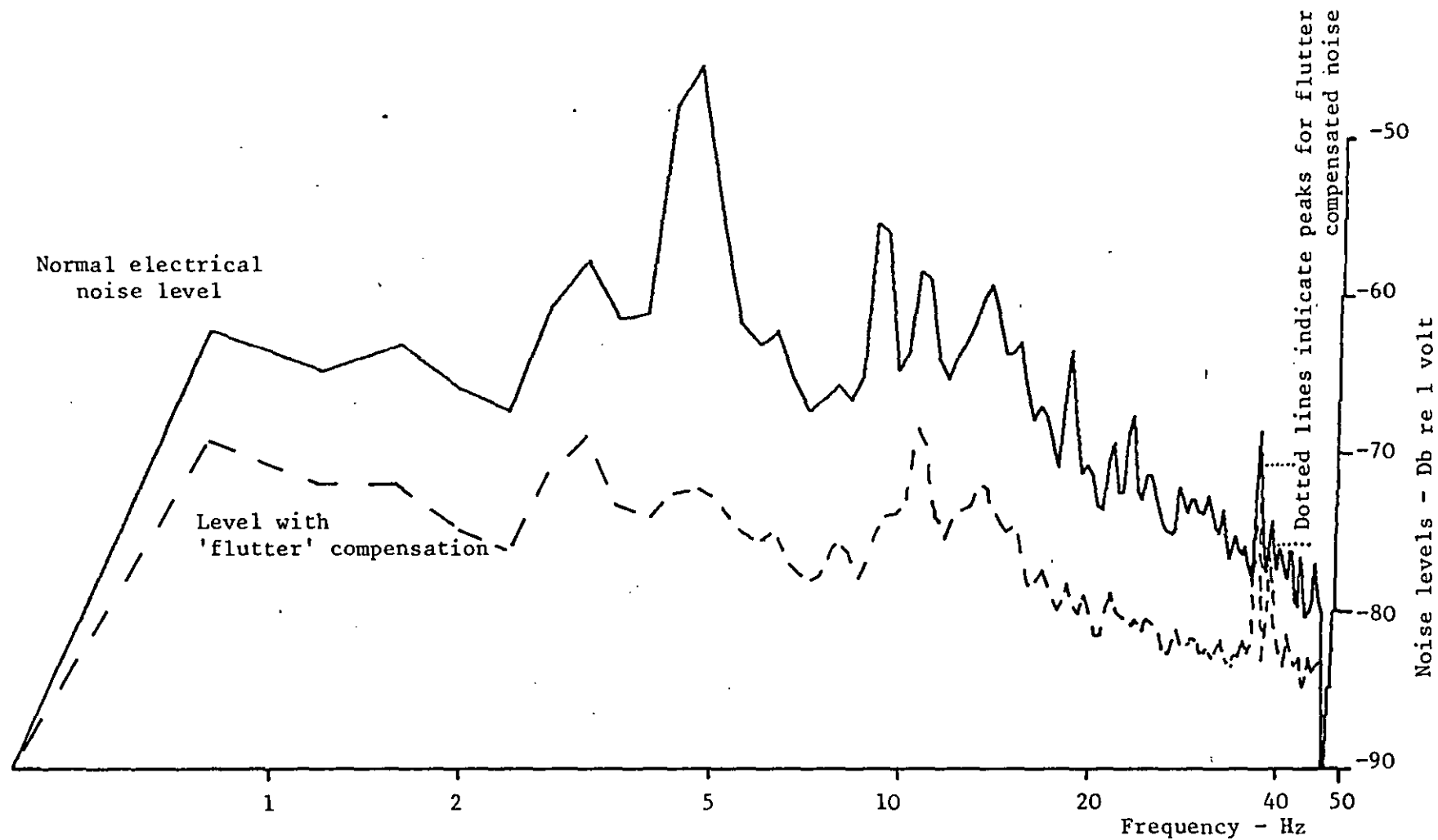


Fig. A6.1a Noise reduction by 'flutter' compensation

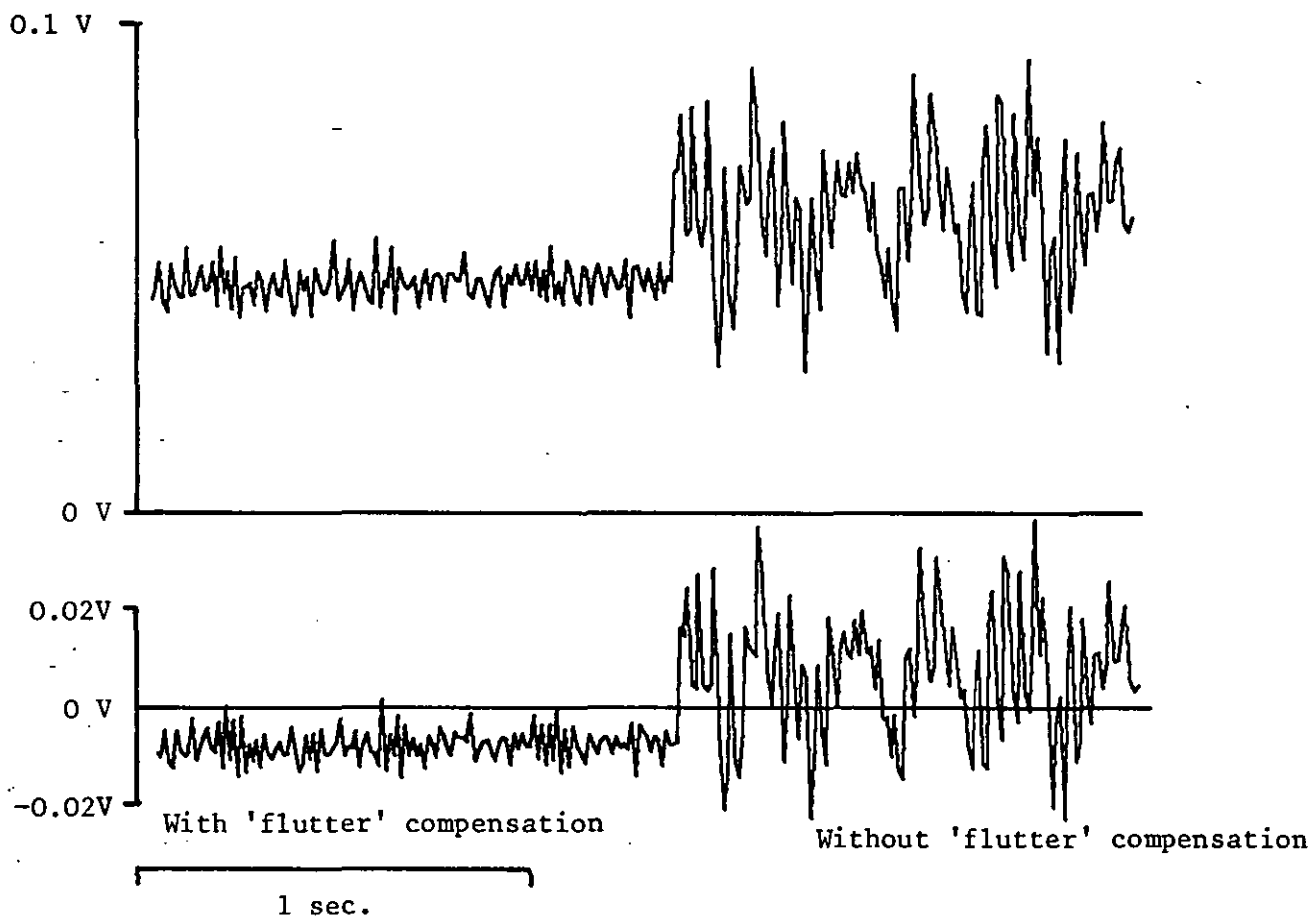


Fig. 6.1b Effects of 'flutter' compensation on noise in the time domain
(Low Pass Filter @ 250Hz).

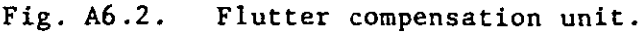


Fig. A6.2. Flutter compensation unit.

APPENDIX 7: ANT-ALIASING FILTERS

It is usually recommended (e.g. Chapman 1975) that for prevention of alias errors, the filter be of the Butterworth (i.e. 'maximally flat') type. The anti-aliasing filter unit used for this study was a 6 pole Butterworth (i.e. -36 dB/octave past the -3 dB point) based on a commercially available module (Barr & Stroud EF 10 and EF 14). The cut-off frequency of these modules is controlled by external capacitors and resistors. At each of the 4 available cut-off frequencies (25, 50, 100 or 250 Hz), these external elements were matched as far as possible so that the filter characteristics for the two channels were the same, both in magnitude and phase. The characteristics for operation at 25 Hz are shown in Figs. A7.1 a & b.

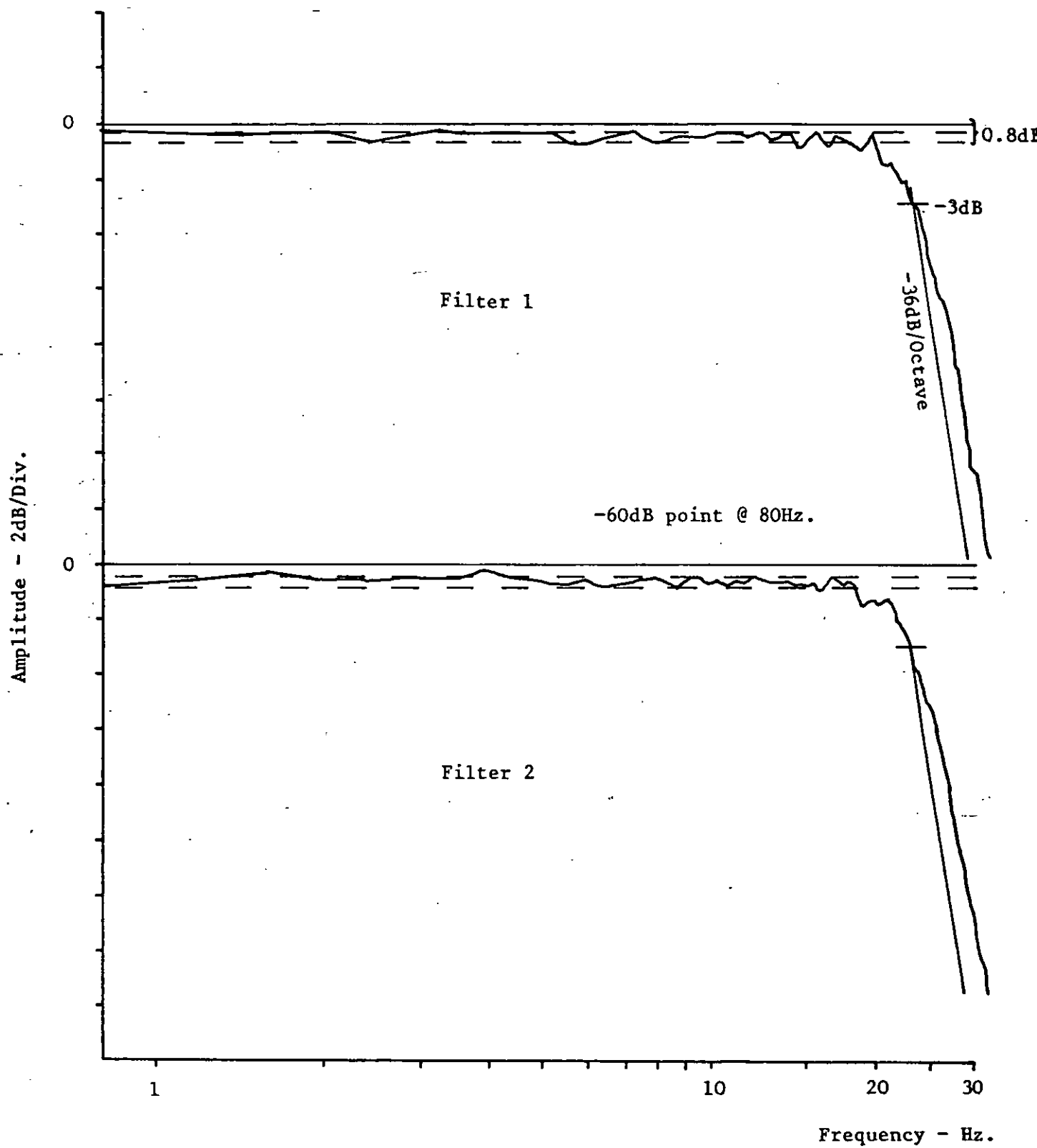


Fig. A7.1a Filter characteristics (magnitude)

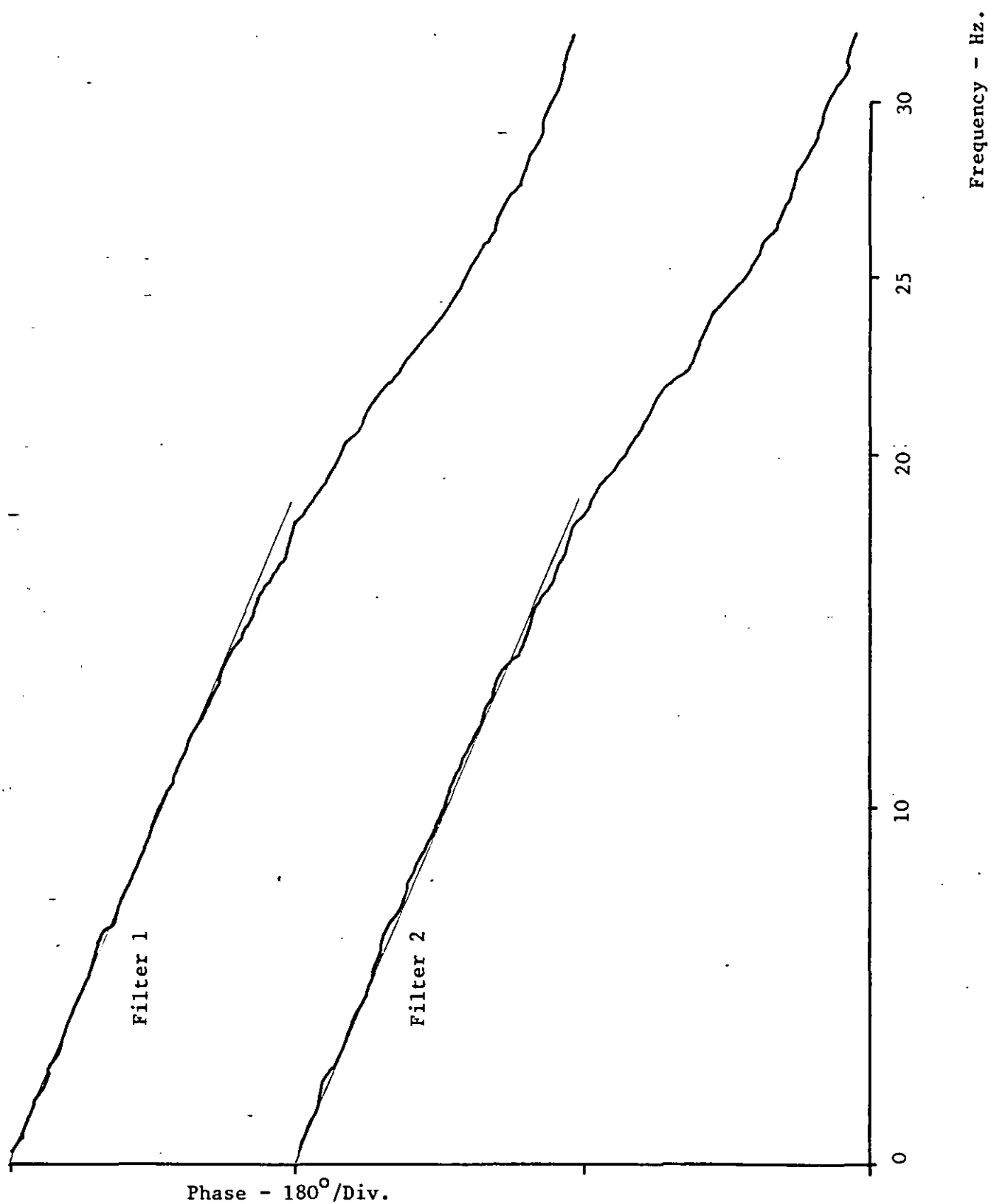
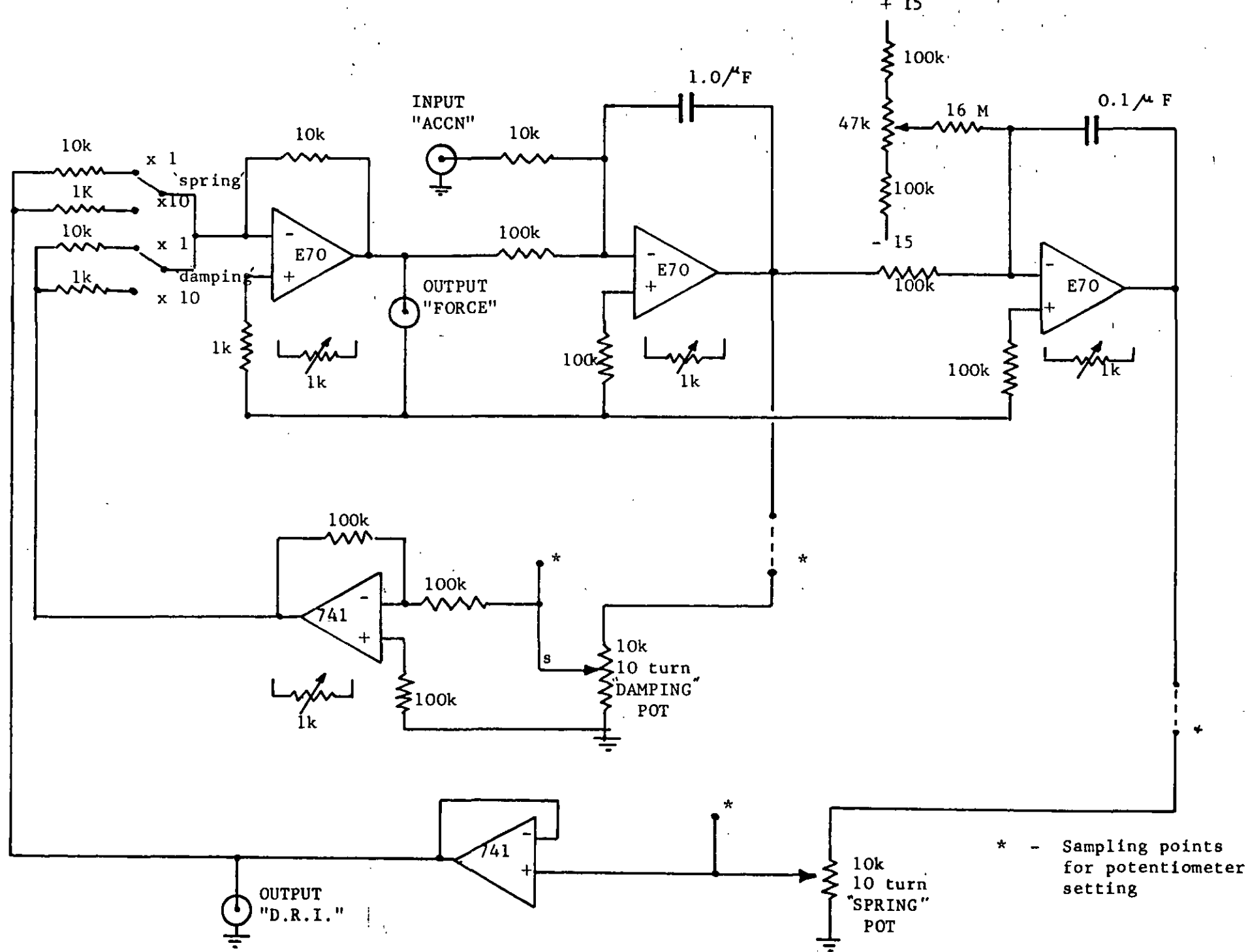


Fig. A7.1b Filter characteristics (phase)

APPENDIX 8: ELECTRICAL ANALOGUE

A single degree of freedom electrical analogue was available for the generation of the 'dynamic response index' during impacts (Sandover & Cole 1974). The circuit, based on analogue computer techniques, is illustrated in Fig. A8.1. The analogue characteristics are variable.

Fig. A8.1. Circuit diagram for D.R.I. unit.



* - Sampling points for potentiometer setting

